GENE THERAPY FOR THE CENTRAL AND PERIPHERAL NERVOUS SYSTEM

EDITED BY: Andrew P. Tosolini and George M. Smith
PUBLISHED IN: Frontiers in Molecular Neuroscience

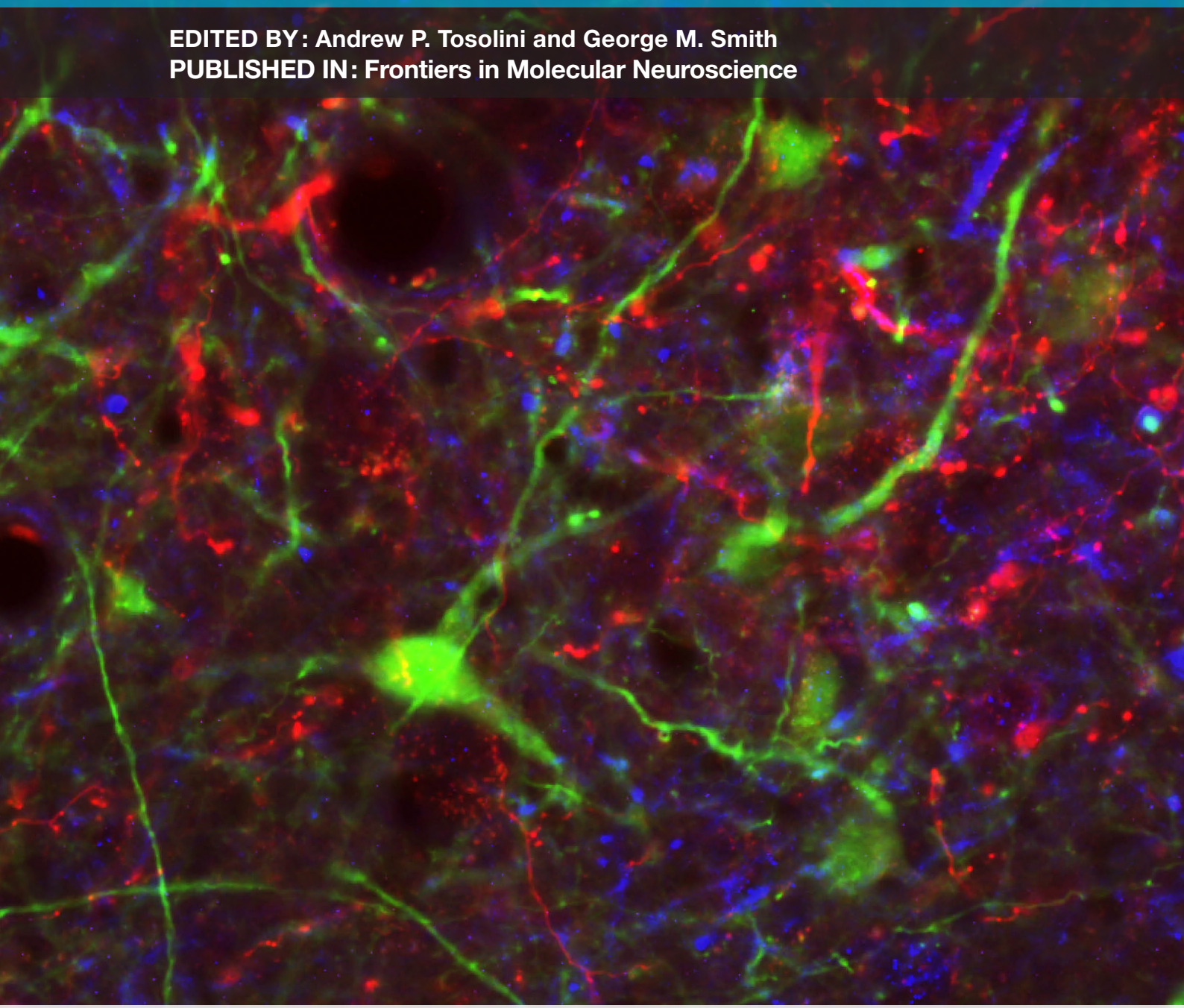

frontiers Research Topics

ISSN 1664-8714
ISBN 978-2-88945-475-4
DOI 10.3389/978-2-88945-475-4

About Frontiers

Frontiers is more than just an open-access publisher of scholarly articles: it is a pioneering approach to the world of academia, radically improving the way scholarly research is managed. The grand vision of Frontiers is a world where all people have an equal opportunity to seek, share and generate knowledge. Frontiers provides immediate and permanent online open access to all its publications, but this alone is not enough to realize our grand goals.

Frontiers Journal Series

The Frontiers Journal Series is a multi-tier and interdisciplinary set of open-access, online journals, promising a paradigm shift from the current review, selection and dissemination processes in academic publishing. All Frontiers journals are driven by researchers for researchers; therefore, they constitute a service to the scholarly community. At the same time, the Frontiers Journal Series operates on a revolutionary invention, the tiered publishing system, initially addressing specific communities of scholars, and gradually climbing up to broader public understanding, thus serving the interests of the lay society, too.

Dedication to Quality

Each Frontiers article is a landmark of the highest quality, thanks to genuinely collaborative interactions between authors and review editors, who include some of the world's best academicians. Research must be certified by peers before entering a stream of knowledge that may eventually reach the public - and shape society; therefore, Frontiers only applies the most rigorous and unbiased reviews.
Frontiers revolutionizes research publishing by freely delivering the most outstanding research, evaluated with no bias from both the academic and social point of view.
By applying the most advanced information technologies, Frontiers is catapulting scholarly publishing into a new generation.

What are Frontiers Research Topics?

Frontiers Research Topics are very popular trademarks of the Frontiers Journals Series: they are collections of at least ten articles, all centered on a particular subject. With their unique mix of varied contributions from Original Research to Review Articles, Frontiers Research Topics unify the most influential researchers, the latest key findings and historical advances in a hot research area! Find out more on how to host your own Frontiers Research Topic or contribute to one as an author by contacting the Frontiers Editorial Office: **researchtopics@frontiersin.org**

GENE THERAPY FOR THE CENTRAL AND PERIPHERAL NERVOUS SYSTEM

Topic Editors:
Andrew P. Tosolini, University College London, United Kingdom
George M. Smith, Temple University, United States

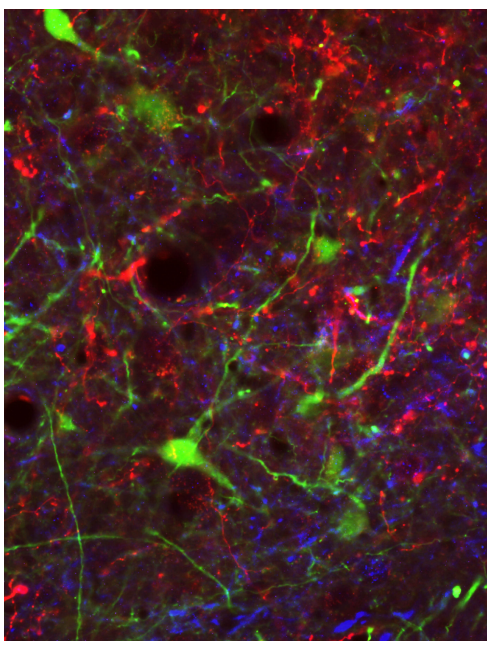

Cover image showing mCherry (red) labeled corticospinal tract axons extending amongst GFP positive propriospinal neurons (Green) within lamina VI and IV of the upper cervical spinal cord. For anterograde tracing of corticospinal tract axons AAV2/mCherry was injected into the somatomotor cortex of adult rats. To label propriospinal neurons, a high-retrograde transportable lentivirus (HiRet) encoding GFP was injected into the lower cervical spinal cord. Immunolabeling of vGlut1 positive terminals are label blue.

Image: George M. Smith Laboratory

Gene therapy is at the forefront of current techniques that aim to re-establish functional connectivity, after an insult to the brain, spinal cord or peripheral nerves. Gene therapy makes the most of the existing cellular machinery and anatomical networks to facilitate molecular changes in DNA, RNA and proteins aiming to repair these disrupted connections. For instance, gene therapy is currently being used to target genes in conditions including spinal cord injury, amyo-

trophic lateral sclerosis, spinal muscular atrophy, stroke and multiple sclerosis, amongst others. The various delivery routes include viral-vectors, genetically modified cellular implants, naked DNA/RNA, liposomes, Cre-Lox recombination, optogenetics and nanoparticles. In particular, gene therapy aims to restore function by augmenting the expression of neuroprotective/axonal growth-promoting neurotrophic factors (e.g., BDNF, CNTF, NGF and GDNF, etc.). Furthermore, the downstream intracellular signalling pathways after receptor activation can also be targeted (e.g., mTor, MAPK, etc.).

On the other hand, gene therapy can also be used to downregulate and/or remove faulty mutated genes, such as those contributing to disease progression or that inhibit axonal regeneration (e.g., SOD-1, TDP-43, Nogo-A, MAG, OmGP, etc.). Depending on the methodology, these genes, for instance, can be silenced, removed or replaced to alleviate the underlying pathology. As such, gene therapy can transform a largely toxic and inhibitory milieu surrounding a neuronal/axonal insult into a growth-permissive environment that will ultimately aid neuronal survival and functional regeneration. Moreover, gene therapy has the capacity to target non-neuronal cells and can be even used for neuroanatomical tract tracing. Ultimately, the principal outcome of gene therapy is to functionally restore damaged neuronal and/or axonal connections irrespective of the system it is being introduced in to.

This Research Topic is devoted to work using gene therapy for the both the central and/or peripheral nervous system.

Citation: Tosolini, A. P., Smith, G. M., eds. (2018). Gene Therapy for the Central and Peripheral Nervous System. Lausanne: Frontiers Media. doi: 10.3389/978-2-88945-475-4

Table of Contents

frontiers in Molecular Neuroscience

EDITORIAL
published: 22 February 2018
doi: 10.3389/fnmol.2018.00054

Editorial: Gene Therapy for the Central and Peripheral Nervous System

Andrew P. Tosolini[1]* *and George M. Smith*[2]*

[1] Sobell Department of Motor Neuroscience and Movement Disorders, Institute of Neurology, University College London, London, United Kingdom, [2] Department of Neuroscience, Shriners Hospitals Pediatric Research Center, Lewis Katz School of Medicine, Temple University, Philadelphia, PA, United States

Keywords: gene therapy, CNS, PNS, AAV, lentivirus, non-viral vectors, neurons, glia

Editorial on the Research Topic

Gene Therapy for the Central and Peripheral Nervous System

It is with great pleasure that we present the research topic dedicated to Gene Therapy for the Central (CNS) and Peripheral Nervous System (PNS). Gene therapy is at the cutting-edge of techniques utilized to develop novel therapeutics to treat insult(s) to the brain, spinal cord and/or peripheral nerves. Indeed, gene therapy can be applied via many different routes and as such can overcome the many obstacles facing oral and systemic delivery of synthetic drugs, thereby permit greater targeting of neural tissue. With this advantage, gene therapy has the potential to (1) correct disease-causing DNA mutations, (2) eliminate toxic RNA/proteins and/or (3) increase the expression of therapeutic proteins. Gene therapy can ameliorate aspects of debilitating neurological diseases and thus, can provide a platform for functional recovery.

Over the last few years, advances in basic science and technology have enabled enhanced pre-clinical strategies culminating in the emergence of sophisticated treatment options available for patients. The most recent gene therapy success is an FDA and EMA approved antisense oligonucleotide (ASO) that is the first and only treatment option available to treat spinal muscular atrophy. Moreover, ASOs have successfully reduced toxic protein levels in a phase 1/2a clinical trial to treat Huntington's Disease (HD). This treatment option was considered safe and well tolerated and was granted orphan drug designation by the FDA and EMA. These advances offer great hope to patients, their families, clinicians and basic scientists, and emphasizes the potential of gene therapy to treat "the incurable" neurological diseases/disorders.

In 2013, we launched this research topic to provide a platform to continue the discussion and amalgamate recent advances in gene therapy technology and strategies for the treatment of PNS and CNS disorders. In conclusion, we are proud to present an extremely productive discussion consisting of 18 articles in total comprised of eight original articles, five full-length reviews, three mini-reviews and one hypothesis and theory article and represents a world-wide collaboration with submissions received from USA, United Kingdom, Europe, Asia, New Zealand and Australia. This research topic discusses gene therapy strategies to treat neurological disorders including amyotrophic lateral sclerosis (ALS), spinal muscular atrophy (SMA), spinocerebellar ataxia (SCA), neuropathic pain, stroke, peripheral nerve injury and repair.

The novel studies presented in this research topic focus on improving transduction efficiency and gene transfer using adeno-associated virus (AAVs) and non-viral methods (**Table 1**). Tanguy et al compare the transduction efficiency between scAAV9 and AAVrh10 serotypes after systemic delivery. von Jonquieres et al. continue to demonstrate glial-specific transduction in the

Edited by:
Hermona Soreq,
Hebrew University of Jerusalem, Israel

Reviewed by:
Shai Berlin,
Technion Israel Institute of Technology, Israel

***Correspondence:**
Andrew P. Tosolini
a.tosolini@ucl.ac.uk
George M. Smith
george.smith@temple.edu

Received: *14 January 2018*
Accepted: *07 February 2018*
Published: *22 February 2018*

Citation:
Tosolini AP and Smith GM (2018) Editorial: Gene Therapy for the Central and Peripheral Nervous System. Front. Mol. Neurosci. 11:54. doi: 10.3389/fnmol.2018.00054

TABLE 1 | Highlights from the original research published in this research topic.

Article	Highlights	Model
Rogers et al.	• Established a non-viral, antibody-based delivery method to transduce motor neurons *in vivo* after intraperitoneal injection. • PEGylated polyethylenimine (PEI-PEG12) conjugated to a MRL2-antibody carrying DNA to the neurotrophin receptor p75 (p75NTR) targeted to motor neurons. • 72 h after injection, ∼25% of lumbar, ∼18% or thoracic and 17% of cervical motor neurons were transduced.	Wild-type mice
Smolny et al.	• Developed a non-viral, antibody-based delivery method for specific gene transfer in microglia *in vitro* and *in vivo*. • OX42-immunoporter can bind plasmid DNA, and is trafficked to lysosomes in microglia via CD11b receptor-mediated internalization. • OX42-immunogenes were specific to microglia and not astrocytes, but did not induce robust gene expression *in vitro* and *in vivo*.	*In vitro* and Wild-type mice
Tanguy et al.	• Compared transduction efficiencies of scAAV9 and AAVrh10 in the brain, spinal, cord and peripheral nervous tissue after intravenous delivery in neonatal mice. • AAVrh10 transduction was superior in the medulla, cerebellum, hippocampus, cortex, dorsal spinal cord, and spinal motor neurons. • Dose-related transduction efficiency differences were observed in the sciatic nerve.	Wild-type mice
Jackson et al.	• For the first time, AAV-PHP.B was demonstrated to transduce the rat CNS. • After intravenous delivery in neonatal rats AAV-PHP.B was demonstrated to have a higher transduction efficiency than AAV9 when using the same CBA promoter. • AAV-PHP.B with a synapsin promoter resulted in an enhanced transduction efficiency and neuronal specificity that induced TDP-43-like pathology and ALS-like phenotypes.	Wild-type rats
von Jonquieres et al.	• Three MAG promoter sizes (0.3, 1.5, and 2.2 kb) were packaged into AAV-cy5 vector and were delivered into the striatum in wild-type neonates. • All three promoter sizes exclusively transduced oligodendrocytes. • Robust and oligodendrocyte-specific long-term GFP expression was reported at 8 months after neonatal delivery.	*In vitro* and Wild-type mice
Oliván et al.	• Application of a non-toxic, tetanus toxin fragment (TTC) to spinal cord organotypic cultures increased SMN levels. • Intramuscular injections of TTC reduced mRNA of autophagy markers (*Becn1, Atg5, LC3,* and *p62*) and pro-apoptotic genes (*Bax* and *Casp3*) in the spinal cord and downregulated *LC3* and *Casp3* expression in skeletal muscle in SMA mice. • Intramuscular TTC application is suggested to show a compensatory effect in the expression of certain genes involved in muscle damage response, oxidative stress and calcium homeostasis in SMA mice.	*Ex vivo* and SMNΔ7 mice
Wu et al.	• Intraganglionic injections of AAV5-caRHEB into cervical DRGs transduced mainly large caliber DRG neurons. • ChABC treatment increased the number of regenerating axons through the DREZ irrespective of DRG-transduction, which resulted in sensory behavioral "responses." • caRHEB expression in DRGs after dorsal root crush enhances synaptic formation and/or functional regeneration into the spinal gray matter.	*In vitro* and Wild-type mice
Su et al.	• miR-30b agomir transfection down-regulated the voltage-gated sodium channel Nav1.3 mRNA that was stimulated with TNF-α in primary DRG neurons. • miR-30b overexpression reduced neuropathic pain after spinal nerve ligation, with demonstrated reduction in Nav1.3 mRNA and protein expression in both DRG neurons and spinal cord. • miR-30b antagomir activated the Nav1.3 voltage-gated sodium channel.	*In vitro* and wild-type rats

brain after injecting a chimeric AAV1/2 vector into neonatal striatum, despite using three differently sized MAG promoters. Jackson et al. combined an engineered AAV-serotype with a neuronal-specific promoter to increase transduction efficiency and reduce off-target effects after intravenous delivery. Wu et al. increase the intrinsic growth potential of injured sensory axons using combinatory treatment involving chondroitinase ABC and AAV-mediated constitutively active GTPase Rheb (Wu et al.).

In addition, Smolny et al. present a non-viral, antibody-based delivery method for microglia-specific gene transfer. Rogers et al. describe spinal motor neuron transduction after peripheral delivery of plasmid DNA as a PEGylated polyethylenimine conjugated antibody. Oliván et al. demonstrate that atoxic-tetanus neurotoxin fragment modifies expression of autophagy and pro-apoptotic genes in the spinal cord and skeletal muscle. Su et al. show miRNA-mediated suppression of

TABLE 2 | Highlights from the review, mini-review and hypothesis and theory articles published in this research topic.

Article	Highlights	Type
Murlidharan et al.	• Describes AAV-vector biology, their cellular entry mechanisms and axonal transport profiles of well-characterized AAV serotypes. • Discusses the implications of AAV-vector applications (e.g., direct application, intravenous injections, etc.). • Considers the safety aspects of AAV-mediated applications to the CNS.	Review
Parr-Brownlie et al.	• Describes lentiviral vector biology, including modified envelope glycoproteins and the expression of transgenes under the regulation of cell-selective and inducible promoters. • Deliberates on the benefit of lentiviral-vectors combined with other techniques such as anatomical tract-tracing, immunohistochemistry, confocal and electron microscopy. • Proposes limitations and future perspectives including ways that lentiviral-vectors can contribute to the gene therapy clinical trials.	Review
Tan et al.	• Explores the challenges facing non-viral nucleic acid delivery to the CNS and provides strategies to overcome them. • Discusses the advantages and disadvantages of different administration routes of nucleic acid delivery. • Considers how retrograde axonal transport can be used to deliver non-viral nucleic acids.	Review
Wagner et al.	• Describes the epidemiology, molecular pathology and mouse models related to spinocerebellar ataxia-1 (SCA-1). • Discusses the literature related to stem cell, gene and alternative therapies used to treat SCA-1. • Identifies the various challenges for gene, stem cell and alternative therapies for SCA-1.	Review
Tosolini and Sleigh	• Describes the epidemiology, genetics, classifications and mechanisms causing SMA and ALS/MND and deliberates on potential commonalities. • Provides an update on clinical gene therapies for both SMA and ALS/MND. • Identifies four key areas that ALS/MND gene therapies can learn from the recent success in the SMA gene therapies including therapeutic targeting, combinational treatment, considering the dose and drug concentration as well as optimizing the therapeutic timing.	Review
Craig and Housley	• Provides a summary of the viral-mediated gene therapy research used to treat stroke. • Highlights the key areas that gene therapy needs to address to ameliorate stroke including protein synthesis, delivery site and viral-vectors. • Identifies therapeutic protein candidates for stroke treatment.	Mini-review
Stoica and Sena-Esteves	• Summarizes the literature on AAV-mediated gene therapy studies that reduce SOD1 toxicity to treat SOD1-related ALS/MND. • Discusses the current hurdles to be addressed to advance the development of clinical gene therapies such as non-cell autonomous toxicity, cellular and anatomical targeting and the delivery methods. • Identifies RNA interference as a successful therapeutic target to ameliorate disease.	Mini-review
Yang et al.	• Summarizes the development and application of the CRISPR/CAS9 toolkit. • Describes the use of CRISPR/Cas9 to generate animal models of neurodegenerative diseases. • Discusses how CRISPR/Cas9 can be applied to treat animal models of Parkinson's and Huntington's Disease.	Mini-review
Hoyng et al.	• Summarizes the research on gene therapy in animal models of peripheral nerve repair and identify key future directions. • Provides a perspective on the path for clinical translation for PNS-gene therapy for traumatic nerve injuries. • Addresses efficacy and safety concerns for human applications and identify the ideal patient population for a proof-of-concept clinical study.	Hypothesis and theory

specific voltage-gated sodium channels can alleviate neuropathic pain.

This research topic also includes a number of full-length and mini-reviews (**Table 2**). Murlidharan et al. describe the biology of different AAV strains, including their transduction profiles, cellular tropisms and mechanisms of CNS transport, for increased translational application. Parr-Brownlie et al. review lentiviral-vector approaches to enhance transduction efficiency, mediate cell-specificity, restrict gene expression spatially and temporally, and discuss limitations and future prospects. Tan et al. critically analyse the advantages and disadvantages of strategies using non-viral nucleic acids to deliver therapeutic genes by circumventing the immune response and thus, appeasing safety concerns potentially associated with viral-mediated gene therapies. Wagner et al. examine the gene and stem cell pre-clinical therapeutic options that preserve Purkinje cell health to treat SCA, and suggest that RNA interference (RNAi) might have great promise. Finally, Tosolini and Sleigh discuss important considerations learned from the success of a recently FDA- and EMA-approved gene therapy for SMA to develop viable gene therapies and strategies to treat ALS.

For the mini-reviews, Yang et al. discuss the "hot topic" of CRISPR/Cas9 gene editing and how these tools can be applied to various research models and the development of treatments for neurodegenerative disease, such as HD and Parkinson's disease. Craig and Housley focus on gene therapy approaches for stroke and discuss injury mechanisms, appropriate timings for therapeutic intervention and deliberate on candidate therapeutic proteins as therapeutic options. Stoica and Sena-Esteves deliver a succinct mini-review of AAV-mediated SOD1-ALS amelioration strategies and describe the hurdles to overcome for CNS gene delivery.

The Hypothesis and theory submission by Hoyng et al. summarize the state-of-research for peripheral nerve repair, identify future targets and provide a translational perspective on PNS gene therapy.

This research forum describes many important characteristics of diverse gene therapy applications for the development of tangible treatment options for different CNS and PNS disorders. Indeed, the advances in gene therapy strategies discussed within this research topic give hope that treatment options for many incurable CNS and PNS disorders are closer to becoming a viable clinical option.

AUTHOR CONTRIBUTION

All authors listed have made a substantial, direct and intellectual contribution to the work, and approved it for publication.

FUNDING

AT holds a postdoctoral position supported by a Wellcome Trust Senior Investigator Award [107116/Z/15/Z] to Giampietro Schiavo (Institute of Neurology, University College London). This work was supported by National Institute of Health (R01NS103481), Shriners Hospitals for Pediatric Research (SHC-84050) and DOD (SC140089) to GS.

Conflict of Interest Statement: The authors declare that the research was conducted in the absence of any commercial or financial relationships that could be construed as a potential conflict of interest.

frontiers in
MOLECULAR NEUROSCIENCE

ORIGINAL RESEARCH ARTICLE
published: 14 October 2014
doi: 10.3389/fnmol.2014.00080

Non-viral gene therapy that targets motor neurons *in vivo*

Mary-Louise Rogers[1]*, Kevin S. Smith[1], Dusan Matusica[2], Matthew Fenech[1], Lee Hoffman[3], Robert A. Rush[1] and Nicolas H. Voelcker[4]

[1] *Department of Human Physiology, Centre for Neuroscience, Flinders University, Adelaide, SA, Australia*
[2] *Department of Anatomy and Histology, Centre for Neuroscience, Flinders University, Adelaide, SA, Australia*
[3] *Department of Chemistry and Biochemistry, South Dakota State University, Brookings, SD, USA*
[4] *Australian Research Council Centre of Excellence in Convergent Bio-Nano Science and Technology, Mawson Institute, University of South Australia, Adelaide, SA, Australia*

Edited by:
Andrew Paul Tosolini, University of New South Wales, Australia

Reviewed by:
Gong Chen, The Pennsylvania State University, USA
Giampietro Schiavo, UCL Institute of Neurology, UK

****Correspondence:***
Mary-Louise Rogers, Department of Human Physiology, Centre for Neuroscience, Flinders University, GPO Box 2100, Adelaide, SA 5001, Australia
e-mail: mary-louise.rogers@flinders.edu.au

A major challenge in neurological gene therapy is safe delivery of transgenes to sufficient cell numbers from the circulation or periphery. This is particularly difficult for diseases involving spinal cord motor neurons such as amyotrophic lateral sclerosis (ALS). We have examined the feasibility of non-viral gene delivery to spinal motor neurons from intraperitoneal injections of plasmids carried by "immunogene" nanoparticles targeted for axonal retrograde transport using antibodies. PEGylated polyethylenimine (PEI-PEG12) as DNA carrier was conjugated to an antibody (MLR2) to the neurotrophin receptor p75 (p75NTR). We used a plasmid (pVIVO2) designed for *in vivo* gene delivery that produces minimal immune responses, has improved nuclear entry into post mitotic cells and also expresses green fluorescent protein (GFP). MLR2-PEI-PEG12 carried pVIVO2 and was specific for mouse motor neurons in mixed cultures containing astrocytes. While only 8% of motor neurons expressed GFP 72 h post transfection *in vitro,* when the immunogene was given intraperitonealy to neonatal C57BL/6J mice, GFP specific motor neuron expression was observed in 25.4% of lumbar, 18.3% of thoracic and 17.0% of cervical motor neurons, 72 h post transfection. PEI-PEG12 carrying pVIVO2 by itself did not transfect motor neurons *in vivo*, demonstrating the need for specificity via the p75NTR antibody MLR2. This is the first time that specific transfection of spinal motor neurons has been achieved from peripheral delivery of plasmid DNA as part of a non-viral gene delivery agent. These results stress the specificity and feasibility of immunogene delivery targeted for p75NTR expressing motor neurons, but suggests that further improvements are required to increase the transfection efficiency of motor neurons *in vivo*.

Keywords: targeted gene delivery, PEI, PEGylation, retrograde transport, immunogenes, p75NTR

INTRODUCTION

Targeted gene therapy has the potential to be developed for diseases involving death of motor neurons such as amyotrophic lateral sclerosis (ALS). Motor neurons can be transfected by injecting every muscle innervated by spinal motor neurons. Transport of therapy is then by axonal pathways originating from, terminating in, or passing through the injection site. However, this requires many painful injections and even then, it may not be possible to reach all spinal motor neurons (Towne et al., 2011). Alternatively motor neurons can be difficult to access and transfect from the circulation or centrally through injections into the cerebrospinal fluid (CSF). Peripheral injections of viral gene therapy have not been successful at selectively targeting motor neurons (Towne et al., 2008). The blood brain barrier (BBB) is also effective at keeping toxins and infectious material out of the central nervous system (CNS; Pardridge, 2006). Our group has been developing targeted gene delivery agents called "immunogenes" with the aim of using them to deliver therapeutic genes to diseased motor neurons (Rogers and Rush, 2012). They are composed of antibodies that internalize after targeting cell surface receptors and are conjugated to cationic carriers, able to condense DNA/RNA, forming the immunogene. Cells that express the cognate cell-surface receptors of the targeting antibody can therefore be specifically transfected with immunogenes *in vivo* from the circulation (Rogers and Rush, 2012).

Antibodies that internalize into target cells are essential for immunogenes. We previously used an antibody (clone MC192) to the rat common neurotrophin receptor p75 (p75NTR) as a targeting agent (Barati et al., 2006). p75NTR is a receptor highly expressed on motor neurons during the embryonic period, down regulated in adulthood (Yan and Johnson, 1988), only to be re-expressed following neuronal injury, including ALS (Lowry et al., 2001). Past research has revealed that p75NTR is retrogradely trafficked in signaling endosomes in motor neurons when taken up by at distal terminals (Lalli and Schiavo, 2002), rendering this receptor ideally suited to deliver therapeutic genes for motor neurons. Transport from the periphery to motor neurons should be possible using antibodies that target rat p75NTR (Bronfman et al., 2003), i.e., MC192 and pan specific MLR2 (Rogers et al., 2006; Matusica et al., 2008). Both have been demonstrated to internalize with the receptor making them ideal targeting agents.

The development of immunogenes as targeted nanocarriers is particularly attractive for diseases such as ALS. In almost all cases of ALS, death occurs within 3–5 years of diagnosis due to the selective death of motor neurons and there are no effective therapies (Turner et al., 2013). We have previously used immunogenes to deliver therapeutic glial-derived growth factor (GDNF) to injured motor neurons *in vivo* in neonatal rats (Barati et al., 2006). The rat specific p75NTR antibody MC192 was conjugated to a cationic polymer poly(L-lysine; PLL) to condense plasmids expressing GDNF and the immunogene was given intramuscularly (Barati et al., 2006). Although GDNF rescued motor neurons that innervated injected muscles, this first generation immunogene could not be used in the circulation to access larger pools of motor neurons (Barati et al., 2006), making it vulnerable to rapid degradation. Cytotoxicity *in vivo* can be associated with the surface charge of the polymer (Chollet et al., 2002) and poor stability is associated with interactions with erythrocytes and serum components such as albumin, lipoproteins or IgG (Rogers and Rush, 2012). These issues can be overcome by masking the surface charge with agents such as polyethylene glycol (PEG). Forming a hydrophilic shell, PEG limits the hydrophobic or electrostatic interactions with the extracellular medium and prevents binding of the cationic polymer with erythrocytes and plasma proteins (Chollet et al., 2002; Rogers and Rush, 2012). Hence, such measures are required for stealth in the circulation.

After entering cells, non-viral gene delivery agents must be able to escape the endosome/lysosomal compartments to deliver their payload of DNA or RNA to the nucleus and RNA-induced silencing complex (RISC) complex, respectively, (Rogers and Rush, 2012). Our first generation immunogene used PLL that required fusogenic peptides to escape endosomal/lysososomal compartments of cells (Navarro-Quiroga et al., 2002). Other DNA/RNA condensing agents such as polyethylenimine (PEI) have more useful properties including a mechanism for endosomal escape. PEI possesses a high cationic charge density due to secondary amino groups that enables the endosomal/lysosomal release of complexes due to the so-called "proton sponge effect" (Boussif et al., 1995; Tang and Szoka, 1997; Lungwitz et al., 2005). PEI unlike PLL also facilitates the entry of plasmid DNA into the nucleus (Godbey et al., 1999).

Toxicity of intravenously administered cationic polyplexes cannot only be reduced by PEGylation (Merdan et al., 2003; Ogris et al., 2003; Malek et al., 2009) but also when nanoconstructs are also endowed with antibodies or other targeting moieties (Zhang et al., 2003; Luo et al., 2010; Höbel et al., 2011; Schaffert et al., 2011). This may be reflective of specificity in addition to lower toxicity because of reduction in charge after conjugation to for example an antibody. Besides systemic toxicities, cytotoxic effects are also observed upon polyplex internalization. Since polycations electrostatically bind and condense DNA, non-specific electrostatic binding to any kind of cellular polyanions (e.g., enzymes, mRNA, or genomic DNA) may deregulate the expression profile of housekeeping genes (Godbey et al., 2001) or induce activation of genes involved in apoptosis (Masago et al., 2007). Consequently, characteristics of cationic polyplex formulations such as molecular weight, cationic charge density and the presence of free polymer also influence their cytotoxicity (Kunath et al., 2003; Boeckle et al., 2004; van Gaal et al., 2011). Accordingly, we hypothesize that an ideal candidate for a safe non-viral gene delivery vector is a carrier with a neutral to slightly negative charge and the capability of being targeted to the cell type required.

In addition to targeting cells from the periphery, we also aimed to improve the expression of transgenes. Methods to improve nuclear import of plasmids are of particular importance in post mitotic cells such as motor neurons. Transfection rates can be poor in post mitotic cells as there is limited breakdown of the nuclear envelope (Zabner et al., 1995). Therefore, modifying plasmids to improve nuclear entry is required. One way of achieving this is to include in the plasmid design a DNA targeting sequence (DTS) that bind to endogenously expressed transcription factors that then act as nuclear localization sequences (NLSs) and improve nuclear import (Mandke and Singh, 2012). Plasmid vectors also often contain sites that can produce innate immune responses through unmethylated cytosine guanine bases separated by only one phosphate (CpGs; Magnusson et al., 2011). Removal of CpGs from the plasmid backbone has been shown to reduce immune reactions to plasmids and prolong expression *in vivo* (Magnusson et al., 2011; Davies et al., 2012). Hence, plasmids that are chosen for *in vivo* delivery should include DTS and minimal CpGs.

Here, we report on the development and evaluation of immunogenes capable of targeting motor neurons *in vitro* and *in vivo*. We demonstrate specificity of delivery to motor neurons can be achieved from peripheral injections using p75NTR antibody MLR2. We show that nanocarriers comprised of p75NTR antibody MLR2 conjugated to PEGylated PEI can deliver plasmids to mouse motor neurons *in vitro* and *in vivo*. In addition, we demonstrate gene expression in motor neurons *in vivo* using plasmids designed for improved nuclear entry and less immunogenicity. Hence, we explore the potential of using p75NTR-targeting immunogenes as gene therapy.

MATERIALS AND METHODS

PREPARATION OF NANOCONSTRUCTS

Branched PEI ($C_{24}H_{59}N_{11}$PEI, molecular weight 25 kDa; Sigma Aldrich, Australia) was made to 20 mg/ml in H_2O and deprotonated with HCl to pH 7.0. PEI was then buffer exchanged on PD10 columns (GE, Australia) with 20 mM 4-(2-hydroxyethyl)-1-piperazine ethane sulfonic acid (HEPES; Invitrogen, Aust), 250 mM NaCl, and pH 7.9. 50 mg of PEI was PEGylated with a branched PEG reagent (Methyl-$PEO_{12})_3$-PEO_4-NHS ester (Thermo Scientific, Rockford, IL, USA) with a molecular weight of 2421 g/mol, (**Figure 1**). This was achieved at a molar ratio of 10:1 PEG to PEI. The number of PEGs per PEI was analyzed by spectral analysis using a Varian 300 MHz NMR spectrometer NMR with deuterium oxide (D_2O) as the solvent indicating on average 12 PEG moieties conjugated per PEI, corresponding to 6% of amines on the PEI being PEGylated. Hybridoma MLR2 was grown and MLR2 purified on protein G column as previously described (Rogers et al., 2006). Conjugation of PEI-PEG12 or PEI to anti-p75NTR MLR2 was achieved using methods adapted from Blessing et al. (2001) and Germershaus et al. (2006). Briefly, the cross-linker *N*-succinimidyl 3-(2-pyridyldithio)propionate

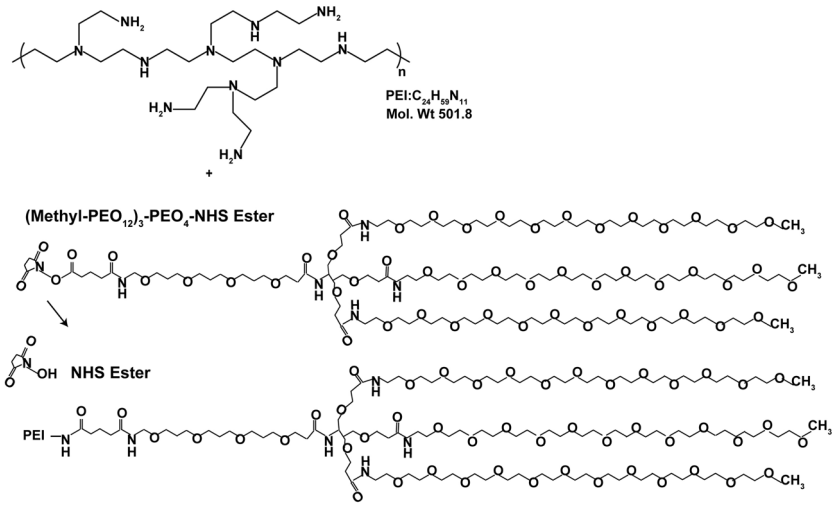

FIGURE 1 | Stepwise synthesis of PEGylated PEI.

(SPDP; Sigma Aldrich, Australia) was used to produce SPDP-activated PEI-PEG12, PEI, and MLR2 IgG. A molar ratio of 1.62 SPDP to PEI was found to generate one functional SPDP-activated PEI-PEG12. PEI without PEG12 was also functionalized using the same method but at a molar ratio of 1.3 SPDP to PEI to generate one SPDP activated PEI. Twenty molar excess DTT was used to generate a thiol-functionalized PEI-PEG12 and PEI. The reactions were all conducted for 1 h. MLR2 IgG was activated with SPDP (at a molar ratio of 4 SPDP: 1 IgG for 2 h), to produce 1 functional SPDP-activated MLR2. To produce the conjugate, thiol-functionalized PEI-PEG12 or PEI was mixed with SPDP-activated MLR2 at a molar ratio of 2:1, and reacted for 24 h under nitrogen gas atmosphere. The amount of PEI-PEG12 or PEI per IgG was calculated as 1.3 to 1 after measuring the release of pyridine-2-thione (343 nm). All reactions were in a reaction buffer of 20 mM HEPES, 250 mM NaCl, pH 7.9, and after each step constructs were purified by gel filtration on PD-10 columns. PEI concentration was calculated by TNBS (2,4,6-trinitrobenzene sulfonic acid) assay using a standard PEI dilution curve as previously described (Snyder and Sobocinski, 1975). The conjugate was purified using cation exchange on HiTrap SP Sepharose (GE, Australia) with stepwise NaCl elution of 1.0, 2.0, and 3.0 M NaCl in 20 mM HEPES pH 7.2. The MLR2-PEI-PEG12 conjugate was eluted with 2.0 M NaCl, and the construct MLR2-PEI with 3.0 M NaCl. A 100 kDa cut-off Ultra 4 (Millipore) centrifuge column was used to replace the high salt with isotonic buffer (20 mM HEPES, 0.15 M NaCl, pH 7.3.

PREPARATION OF PLASMID DNA

An enhanced green fluorescent protein (GFP) expressing plasmid was from Aldevron (pgWiZ; Fargo, ND, USA). This plasmid was used for some *in vitro* transfection experiments and although produces sustained GFP expression it can induce immune responses *in vivo* (Chamarthy et al., 2003; Grønevik et al., 2005; Rose et al., 2014). Hence for *in vivo* work a bicistronic pVIVO2 plasmid (9.6 kb) was purchased from Invivogen (San Diego CA, USA). pVIVO2 includes a SV40 DNA targeting signal (DTS) for improved nuclear entry with cytosine and guanine separated by only one phosphate (CpG) motifs removed from the plasmid backbone to reduce immune reactions *in vivo* (Davies et al., 2012). pVIVO2 also contains two human ferritin composite promoters, FerH (heavy chain) and FerL (light chain) combined with SV40 and CMV enhancers for GFP and LacZ expression, respectively. Competent *Escherichia coli* cells were transformed with pgWiZ or pVIVO2 plasmids and purified using Endotoxin Free Maxi Prep Kits (Qiagen) as per the manufacturer's instructions.

SIZE AND ZETA POTENTIAL AND GEL RETARDATION

Nanoconstructs were subject to size (nm) and charge measurements (zeta potential in mV) using a Malvern Zetasizer Nano. Zeta potential is a measure of the magnitude of particle charge in solution. Briefly, MLR2-PEI-PEG12 or PEI-PEG12 was mixed with plasmid (pgWiZ) at a nitrogen (amine) to phosphate (DNA) ratio (N/P) of 2, 5, 10, and 12 in sample buffer (20 mM HEPES, 0.15 M NaCl, pH 7.3). Samples were placed in a disposable capillary cell (DTS 1060) where both zeta potential and particle size were measured. The charge at each N/P ratio was analyzed in gel-retardation assays as described (Kircheis et al., 1997). Briefly, samples (10 μl) containing 400 ng pDNA and varying amount of conjugate at different N/P ratios were applied to 1% agarose gels made in Tris-Borate-EDTA buffer with GelRed^{TM} at 1/10,000 (Biotium, Hayward, CA, US) at 100 V for 60 min. The gel was then imaged on a using BioRad Gel Doc 2000 transilluminator (Bio-Rad Laboratories, Hercules, CA, USA).

CELL CULTURE AND CYTOTOXICITY ASSAYS

Primary motor neurons (PMN) were isolated from E12.5 embryonic mouse (C57BL/6J) spinal cords as previously described (Wiese et al., 2010) or as mixed motor neuron/glia cultures (Ford et al., 1994) and cells cultured on 48-well plates (Nunc) coated with poly-D-ornithine/laminin (Wiese et al., 2010). Motor neurons were grown in Neurobasal media (Invitrogen) supplemented with

10% horse serum, GlutaMAX, B27 supplement (Invitrogen) and 10 nM β-mercaptoethanol and BDNF and CNTF (10 ng/ml; Invitrogen, Aust) as previously described (Wiese et al., 2010). Plasmids used for transfection were pgWiZ or pVIVO2 (both expressing GFP). Motor neurons were transfected in cell culture media (without horse serum or β-mercaptoethanol) for 4 h using the polyplexes MLR2-PEI, MLR2-PEI-PEG12, PEI-PEG12, and 20 μg of plasmid (pGwiZ or pVIVO2). Transfectants were removed after 4 h before replacing with full culture media. Viable motor neurons were examined before and after transfection for a total of 7 days in five separate wells using a Leica IX70 inverted fluorescence microscope. Transfection was measured by counting motor neurons expressing GFP detected by microscopy as a percentage of motor neurons plated in at least five wells. Mouse NSC34 motor neuron-like cells, human SHSY5Y and fibroblast control cells were cultured as previously described (Rogers et al., 2010; Shepheard et al., 2014). Flow cytometry for determining labeled antibody specificity is exactly as described previously (Rogers et al., 2010) using an Accuri C6 Flow Cytometry (BD).

ANTIBODY AND GENE DELIVERY IN C57BL/6J MICE

Approval to undertake experiments using C57BL/6J mice described in this current study was by the Flinders University Animal Welfare Committee. Antibody to p75NTR (MLR2) was labeled with 4 fluorescent dye molecules (Atto-488-NHS-Ester; Sigma) per antibody molecule, as described by the manufacturer. The degree of labeling (DOL) was determined by absorbance of labeled antibody at 501 and 280 nm with the appropriate extinction coefficients and corrections for DOL. Intraperitoneal injections of labeled antibody or immunogenes were given to newborn C57BL/6J neonatal mice, always in two equal doses. After 3–4 days, mice were euthanized and transcardially perfused with PBS containing 1% sodium nitrite, followed by Zamboni's fixative (4% paraformaldehyde (w/v), 7.5% saturated picric acid (v/v), PBS, pH 7.4). Spinal cords and dorsal root ganglia (DRG) were removed and post fixed overnight in Zamboni's fixative at 4°C and then cryoprotected in PBS containing 30% sucrose (w/v). 30 and 10 μm sections were cut from spinal cords and DRGs embedded in OCT on a cryostat. Sections were blocked in blocking diluent (PBS with 10% donkey serum (Sigma-Aldrich), 0.2% Tween-20, 0.02% azide) and antibodies incubated in antibody diluent (PBS with 1% donkey serum (Sigma-Aldrich), 0.2% Tween-20, 0.02% azide). Primary antibodies used were rabbit anti homeobox transcription factor 9 (Hb9 used at 1:1000; Abcam, unavailable post 2012); rabbit anti-Choline Acetyltransferase (ChAT) P3YEB (a generous gift from Prof Dr. M. Schemann, Techn Univ Munich, 1:5000), and goat anti-mouse p75NTR (Sigma; 1 μg/ml) and chicken anti-GFP (Biosensis; 1/500). Secondary antibodies included donkey anti sheep-488, donkey anti rabbit-CY3, and donkey anti-chicken-488 (Jackson ImmunoResearch Laboratories). All secondary antibodies were diluted to 1:800. Imaging was carried out on an Olympus BX50 fluorescence microscope.

RESULTS

CONSTRUCTION AND CHEMICAL PROPERTIES OF NANOCONSTRUCTS

Branched PEI was used as a DNA condensing agent in the nanoconstructs. Each PEI molecule was PEGylated with 12 PEG moieties, each being 2.4 kDA in molecular weight (**Figure 1**). To engineer specificity of nanoconstructs for motor neurons expressing the cell surface receptor p75 neurotrophin receptor (p75NTR), PEI-PEG12 was conjugated to a monoclonal antibody p75NTR (MLR2; Rogers et al., 2006) using methods adapted from Blessing et al. (2001) and Germershaus et al. (2006) and shown in **Figure 2**. The final construct contains a disulfide bond between an amine on the antibody and an amine on the PEI.

Gel retardation was used to monitor electrostatic interactions between cationic amines (Nitrogen) in the PEI and the anionic phosphate group of the plasmid DNA (pgWiZ or pVIVO2). This procedure showed the PEI (N): plasmid (P) DNA ratio required to generate a neutral complex. **Figure 3** shows that an N/P of 10 (**lane 7**) and 12 (**lane 8**) retarded the complex MLR2-PEI-PEG12-pVIVO2 in the loading well. This is in contrast to PEI-PEG12-pVIVO2 where the complex was retarded with a N/P of 5 (**lane 3**), indicating that the full immunogene had a less positive charge than PEGylated PEI lacking the antibody. Exactly the same results were obtained if pVIVO2 was replaced with pgWiZ. The charge of the immunogene was confirmed by measuring zeta potential. **Table 1** shows that MLR2-PEI-PEG12 complexed to pgWiZ at N/P 12 had a zeta potential of -19.91 ± 1 mV, in contrast to PEI-PEG12 complexed to pgWiZ with a zeta potential of 4.8 ± 0.9 mV at N/P 12. The size of the MLR2-PEI-PEG12 complexed to plasmid at N/P 12 was 95.3 ± 11 nm, indicating that the DNA was condensed. PEI-PEG12 was 101.1 ± 16.1 nm in size at N/P 12.

CYTOTOXICITY AND *IN VITRO* SPECIFICITY OF NANOCONSTRUCTS

We next examined the cytotoxicity and transfection ability of immunogenes for motor neurons *in vitro*. PMN were isolated from embryonic mice as previously described (Wiese et al., 2010) in 48-well plates and 4 days later transfected with plasmids (pgWiZ or pVIVO2) expressing GFP, using MLR2-PEI or MLR2-PEI-PEG12. We counted viable motor neurons before and after transfection (**Figure 4A**) for a total of 7 days ($n = 3$ motor neuron isolations in five separate wells). The viability of cells transfected with MLR2-PEI-PEG12-pgWiz was not significantly different than for non-transfected cells over this time period. 48 h and 72 h post transfection with MLR2-PEI-PEG12-pGwiZ there were 46.4 ± 3.5 and 41.1 ± 0.7% of the original viable motor neurons present. This was not significantly different from control non-transfected cells where there were 57.7 ± 2.4 and 51.2 ± 2.7% of original viable motor neurons present at that same time period. However, when PEI was not PEGylated, the number of live motor neurons was significantly ($p < 0.001$) reduced to 14.2 ± 2.6% then 1.1 ± 0.35%, 48 and 72 h post transfection with MLR2-PEI-pGwiZ (**Figure 4A**). There was no significant difference in the percentage of live motor neurons if pVIVO2 was used in place of pgWiZ (results not shown).

GFP expression in pure motor neurons 48 h after transfection is demonstrated with pVIVO2 (**Figure 4B**) or pgWiZ (**Figures 4C,D**) carried by MLR2-PEI-PEG12. **Figure 4C** shows GFP expression in the cell body and processes of a motor neuron and **Figure 4D** shows GFP-containing transfected neuronal processes over a bed of non-transfected cells. GFP expression was also observed in motor neurons after transfection with pVIVO2 carried by PEI-PEG12 (**Figures 4E,G**), and again there is cell bodies and processes

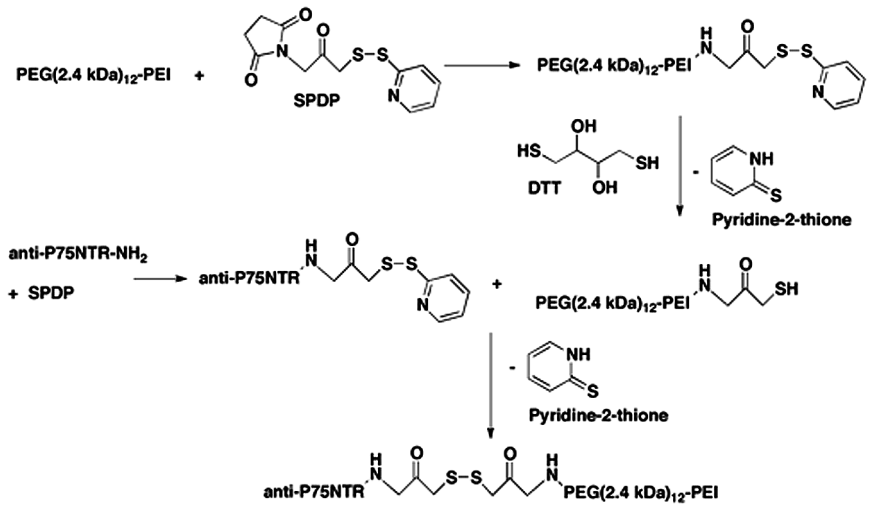

FIGURE 2 | Stepwise synthesis of the targeted nanoconstructs.

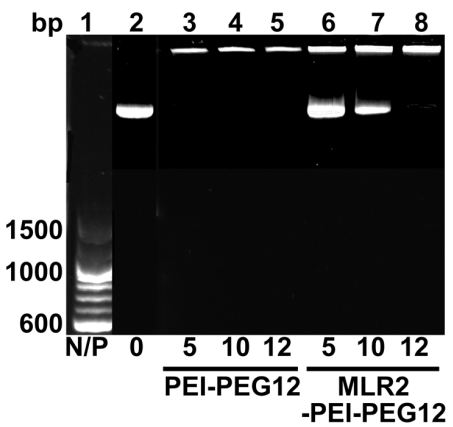

FIGURE 3 | Agarose gel retardation assay of MLR2-PEI-PEG12-pVIVO2 and PEI-PEG12-pVIVO2. Lane 1, 100 bp ladder; lane 2, naked pVIVO2 (400 ng); lane 3–5 400 ng pVIVO2 with PEI-PEG12 at N/P 5, 10, and 12; lanes 6–8 400 ng pVIVO2 with MLR2-PEI-PEG12 at N/P 5, 10, and 12.

Table 1 | Size and zeta potential of nanoconstructs.

Complex	N/P Ratio	Zeta potential (mV)	Particle size (nm)
PEI-PEG12	2	−14.4 ± 4.7	88.7 ± 13.2
PEI-PEG12	5	−0.5 ± 2.9	78.0 ± 15
PEI-PEG12	10	0.7 ± 3.1	75.8 ± 14
PEI-PEG12	12	4.8 ± 0.9	101.1 ± 16.1
MLR2-PEI-PEG12	5	−42.0 ± 0.4	78.3 ± 14
MLR2-PEI-PEG12	10	−32.5 ± 1.3	82.7 ± 10
MLR2-PEI-PEG12	12	−19.9 ± 1.3	95.3 ± 11

with GFP and also non-transfected cells. The percentage of motor neurons expressing GFP was determined 48 and 72 h post transfection with MLR2-PEI-PEG12-pgWiz and PEI-PEG12-pgWiz and MLR2-PEI-pgWiz (**Figure 4H**). Notably, MLR2-PEI-pgWiz did not produce any GFP possibly because few live motor neurons were present after 48 h. However, 8.0 ± 0.8% of motor neurons expressed GFP 48 h after transfection by MLR2-PEI-PEG12-pgWiz and this did not increase significantly by 72 h (8.3 ± 1.8%). Similarly, 7.0 ± 1.15% of motor neurons expressed GFP 48 h post transfection with PEI-PEG12-pgWiz and this rose to 8.1 ± 1.5% by 72 h post transfection (**Figure 4H**).

Mixed cultures of motor neurons and astrocytes were isolated from embryonic mice spinal cords (Ford et al., 1994) and transfected with MLR2-PEI-PEG12-pgWiz or PEI-PEG12-pgWiz. The percentage of motor neurons transfected after 48 h was 6.7 ± 0.32% for MLR2-PEI-PEG12-pGWIZ and 8.0 ± 1.6% for PEI-PEG12-pgWiz. However, 8.0 ± 1.6% of astrocytes were transfected with PEI-PEG12-pgWiz and significantly ($p < 0.001$) less (0.3 ± 0.3%) with MLR2-PEI-PEG12-pgWiz (**Figure 4I**). This demonstrates the selectivity of MLR2-PEI-PEG12 for motor neurons. **Figure 4F** shows GFP expression in astrocytes 48 h post transfection with PEI-PEG12-pgWiz.

SPECIFICITY OF ANTI-p75NTR (MLR2) AND RETROGRADE TRANSPORT *IN VIVO*

A key requirement for *in vivo* gene therapy is specificity to the target cell population. We used an antibody to p75NTR to target motor neurons and sought to demonstrate specificity and usefulness in neonatal mice where high numbers of motor neurons that express p75NTR occur. MLR2 was fluorescently labeled with Atto-488) and the specificity of the labeled antibody for p75NTR determined by flow cytometry. Cells expressing mouse p75NTR (**Figure 5A**) and human p75NTR (**Figure 5C**) were incubated with and without 20 μg/ml labeled MLR2 and subjected to flow cytometry analysis. The shift in mean fluorescence intensity to the right indicates an increase in the antibody binding to the cells. However, there was no change in fluorescence intensity after control fibroblasts

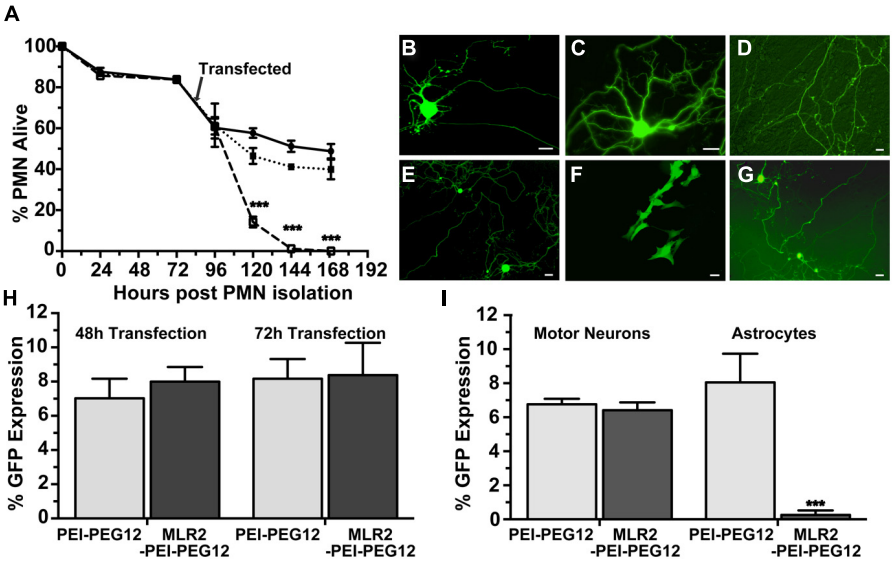

FIGURE 4 | Transfection of mouse primary motor neurons (PMN) with plasmid DNA using targeted nanoconstructs. (A) PMN were isolated from E12.5 embryos and transfected 3 days later with pGwiZ carried by MLR2-PEI (open squares) or MLR2-PEI-PEG12 (closed squares). The number of alive and dead motor neurons for each treatment or no treatment (closed circles) were counted every 24 h and the % of neurons that were alive calculated from the original 3000 neurons plated per well in 48-well plates ($n = 5$). There was significantly (***$p < 0.001$) less PMN alive after treatment with MLR2-PEI-pGwiZ. **(B)** Green fluorescent protein (GFP) expression in live pure motor neurons 48 h after transfection with by MLR2-PEI-PEG12-pVIVO2. **(C,D)** GFP expression after transfection with MLR2-PEI-PEG12-pGwiZ. **(E,G)** GFP expression in motor neurons or **(F)** Astrocytes after transfection with PEI-PEG12-pVIVO2. (scale bar: 20 μm). **(H)** The % of original (3000) motor neurons expressing GFP was determined 48 and 72 h post transfection of pure motor neurons with MLR2-PEI-PEG12-pGwiZ and PEI-PEG12-pGwiZ. **(I)**. Mixed cultures of motor neurons and astrocytes were isolated from embryonic mice spinal cords and 3000 cells plated per well in 48-well plates. The % of transfected motor neurons and astrocytes were determined 72 h after transfection with MLR2-PEI-PEG12-pGwiZ and PEI-PEG12-pGwiZ. There was significantly (***$p < 0.001$) less astrocyte transfection with MLR2-PEI-PEG12-pGwiZ, compared to PEI-PEG12-pGwiZ.

lacking p75NTR were incubated with 20 μg/ml labeled antibody (**Figure 5B**), indicating that the antibody indeed specifically targets p75NTR-expressing cells. Unlabeled MLR2 (with secondary anti-mouse antibody labeled with Alexia-Fluor-488) bound to human SHSY5Y cells as expected (**Figure 5D**). Unlabeled MLR2 was not tested on mouse NSC34 cells because the secondary antibody binds non-specifically to mouse derived cells.

Having demonstrated the specificity of the MLR2 antibody for p75NTR, we next tested the ability of MLR2 to be retrogradely transported to spinal cord motor neurons in neonatal mice from the circulation. Two doses of 75 μg of Atto-488 labeled MLR2 (150 μg total) were injected into neonatal B6 mice (average weight was 2 g; $n = 3$) and 36 h later, mice were perfused and spinal cords excised. Lumbar, thoracic and cervical sections were examined for motor neuron marker homeobox transcription factor 9 (Hb9; Red; nuclear stain) and labeled MLR2 (green). Representative micrographs show MLR2 and Hb9 in lumbar (**Figure 5E** i,ii), thoracic (**Figure 5E** iv,v) and cervical (**Figure 5E** vii,viii) sections. Merged images (**Figure 5E** iii,vi,ix) show that the majority of motor neurons identified by Hb9 also contained MLR2. The extent of retrograde transport was assessed for lumbar, thoracic and cervical regions by counting the number of motor neurons labeled with Hb9 and MLR2 and with both labels. **Figure 5F** shows pooled results from three mice; 88.6 ± 1.0% lumbar, 95.7 ± 0.5% thoracic and 87.3 ± 3.8% of cervical motor neurons identified by Hb9 label contained MLR2. Hence, MLR2 is efficiently transported to motor neurons from the circulation in neonatal mice. As expected the motor neurons from mice injected with MLR2-488 also contained p75NTR (**Figure 5G** i,ii, and iii) and MLR2-488 was also found in the p75NTR-expressing neurons of the dorsal root ganglia (DRGs; **Figure 5G** iv).

RETROGRADE TRANSPORT AND DELIVERY OF MLR2-PEI-PEG12-PVIVO2 TO MOTOR NEURONS *IN VIVO*

Given that MLR2 can be retrogradely delivered to the majority of motor neurons in neonatal mice, we then sought to determine the extent of gene delivery after injection of our immunogene in neonatal mice. Initially, neonatal B6 mice (average weight of 2 g) were injected with two doses of 75 μg MLR2-PEI-PEG12 carrying 58 μg of pgWiZ that expresses GFP and spinal cords examined 72 h later. However, no GFP was observed in spinal motor neurons or elsewhere (data not shown). We then used pVIVO2 that is designed specifically to enhance *in vivo* transfection through DTS and minimal CpGs. Cells transfected with pVIVO2 were identified by GFP expression. Neonatal B6 mice ($n = 5$; average weight was 2 g) were injected intraperitonealy twice with 75 μg of MLR2-PEI-PEG12 carrying 58 μg of pVIVO2, and 72 h later mice were perfused and spinal cords excised. In addition 75 μg of PEI-PEG12 carrying 77.3 μg of pVIVO2 was injected twice into three mice and 72 h later mice were perfused and spinal cords excised. Every 10th section was stained with the motor neuron marker rabbit anti-ChAT (since anti-Hb9 was not available) and chicken

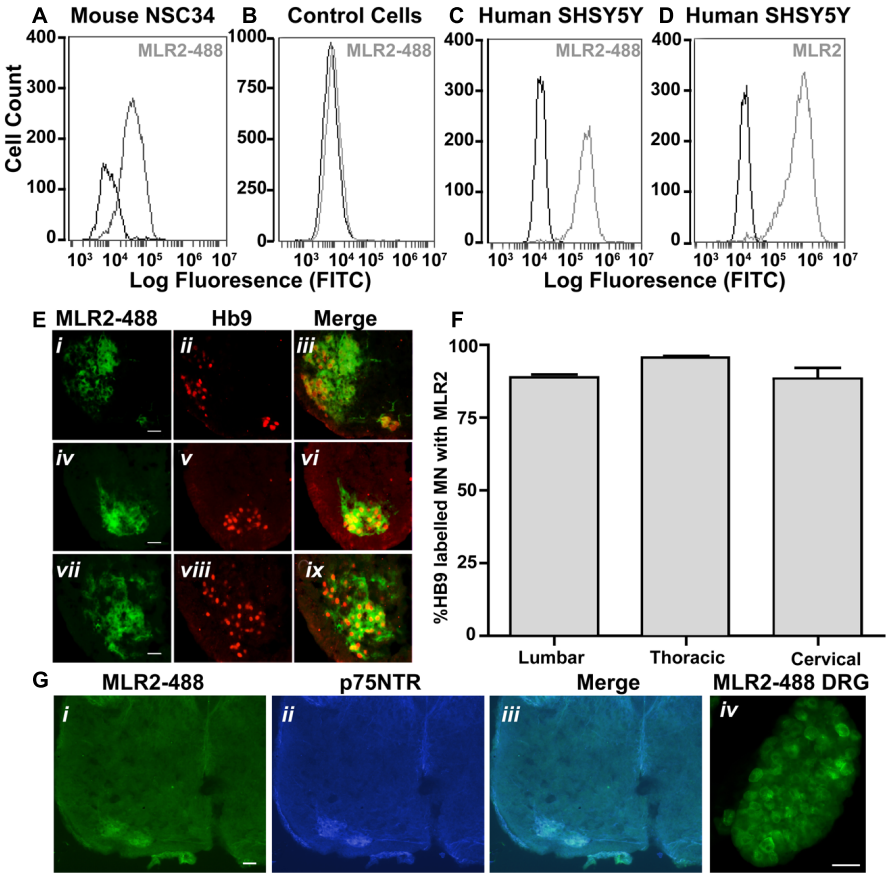

FIGURE 5 | MLR2 is specific for p75NTR and is transported to the majority of spinal motor neurons after intraperitoneal delivery into neonatal mice (A–D) Flow cytometry histograms demonstrating specificity of MLR2-488. Mouse motor neuron-like cells **(A)**, control fibroblasts **(B)**, human SHSY5Y neuroblastoma cells **(C)** were incubated with and without 20 μg of fluorescently labeled anti-p75NTR (MLR2-488) and fluorescence measured by flow cytometry. X-axis is FITC fluorescence intensity; Y-axis is number of cells displaying FITC fluorescence. Flow cytometry histogram from human SHSY5Y **(D)** incubated with 20 mg unlabeled MLR2 and then anti-mouse 488 (1/100) is included as control for MLR2. **(E)** 488-Fluoresecence observed in lumbar (i), thoracic (iv), and cervical (vii) regions of spinal cord sections of neonatal C57BL/6J spinal cord 36 h after two intraperitoneal injections of 75 μg of MLR2-488; scale bar: 90 μm. Motor neurons identified by anti-Hb9 (1/1000; ii,v,viii); also contained MLR2-488 (iii,vi,xi). **(F)** The majority of Hb9 labeled motor neurons also contained MLR2-488. The % of motor neurons containing MLR2-488 was calculated by counting neurons with Hb9 staining and neurons with MLR2-488 for 30 μm sections from the lumbar, thoracic and cervical regions ($n = 3$ mice with SEM). Motor neurons with MLR2-488-Fluoresecence also contained p75NTR (**G** i,ii,iii; scale bar 50 μm). MLR2-488 was also found in Dorsal root ganglion (from L2-L4; scale bar 80 μm) after intraperitoneal injections of MLR2-488.

anti-GFP. Representative micrographs show GFP expression in lumbar, thoracic and cervical spinal cord (**Figure 6A** i,iv,vii) and motor neurons identified by ChAT (**Figure 6A** ii,v,viii). Merged images (**Figure 6A** iii,vi,ix) show that motor neurons identified by ChAT also express GFP. Sections taken from control non-injected animals had no motor neuron staining after being subject to anti-GFP (**Figure 6A** x,xi,xii), demonstrating the specificity of the anti-GFP. In addition, lumbar sections from mice injected with PEI-PEG12-pVIVO2 did not have any GFP staining (**Figure 6B** i,ii,iii). The GFP expressing neurons from mice injected with MLR2 PEI-PEG12-pVIVO2 also contained p75NTR (**Figure 6C** i,ii,iii). DRGs were also transfected with GFP (**Figure 7A**). Cells expressing GFP contained p75NTR (**Figures 7B,C**). DRGs from PEI injected animals did not contain GFP (**Figures 7D,F**) even though they expressed p75NTR (**Figure 7E**). As shown in control sections p75NTR is expressed in a high number of large diameter cells (**Figure 7H**) and as expected there was no GFP staining (**Figure 7G**). The extent of retrograde transport and gene expression was assessed for lumbar, thoracic and cervical spinal cord regions of mice injected with MLR2-PEI-PEG12-pVIVO2 by counting the number of motor neurons labeled with ChAT and GFP and with both labels. **Figure 6D** shows pooled results from six mice; 25.4 ± 2% lumbar, 18.3 ± 3.4% thoracic and 17 ± 1.7% of cervical motor neurons from the spinal cord identified by ChAT label contained GFP.

DISCUSSION

Despite the fact that a wide range of non-viral gene delivery agents have been proposed, none have been developed that target motor neurons from the periphery. Here, we described nanoparticles that can deliver genes to motor neurons *in vivo* by an intraperitoneal route. We were able to specifically target motor neurons

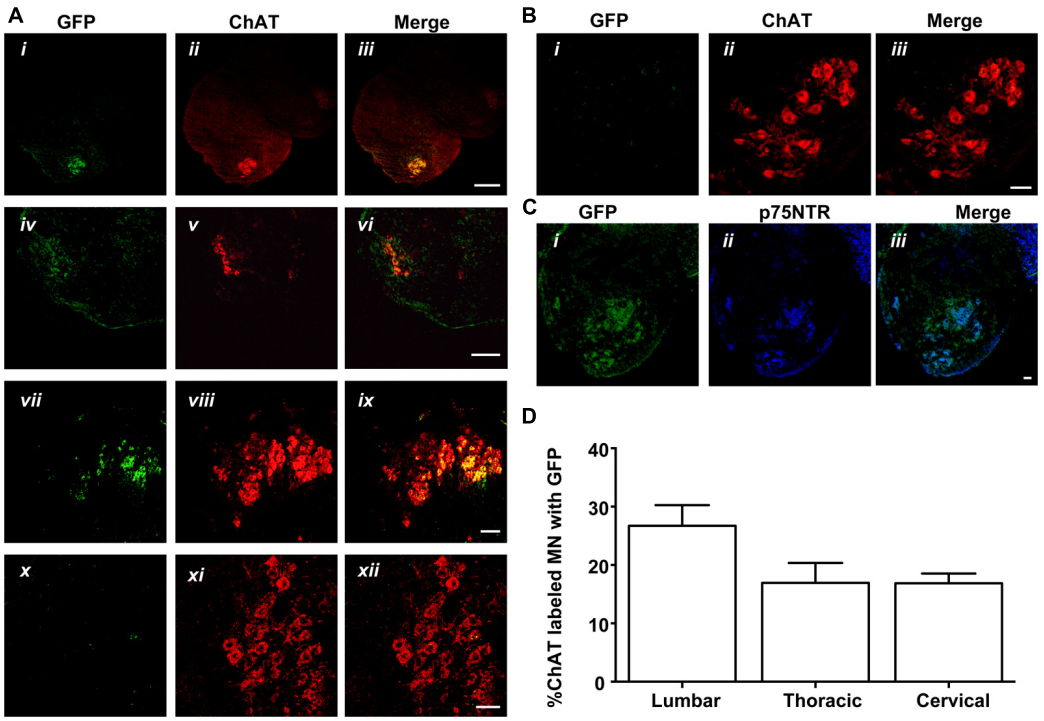

FIGURE 6 | MLR2-PEI-PEG12-pVIVO2 but not PEI-PEG12-pVIVO2 is retrogradely transported to motor neurons in neonatal mice and GFP expressed. (A) Two doses of 75 μg of MLR2-PEI-PEG12-pVIVO2 carrying 58 μg pVIVO2 (N/P 12) was injected into neonatal mice and 72 h later spinal cords excised and examined for GFP expression ($n = 5$). Motor neurons in the lumbar (ii), thoracic (iv), and cervical (vii) regions were identified by staining with ChAT (1/5000) and GFP expression identified with chicken anti-GFP (1/500). Motor neurons that expressed GFP (i,iv,vii) always contained ChAT (iii scale bar: 100 μm; vi scale bar: 100 μm; ix scale bar: 50 μm). Motor neurons from control sections of untreated mice identified by ChAT (xi), did not contain GFP fluorescence (x) after treatment with chicken anti-GFP (1/500) scale bar: 50 μm. **(B)** Two doses of 75 μg of PEI-PEG12-pVIVO2 carrying 77.3 μg pVIVO2 (N/P 5) was injected into neonatal mice and 72 h later spinal cords excised and examined for GFP expression ($n = 3$). Lumbar sections did not contain GFP fluorescence (i) after treatment with chicken anti-GFP (1/500) and motor neurons were identified by ChAT (ii), scale bar: 50 μm. **(C)** Motor neurons expressing GFP observed in mice injected with MLR2-PEI-PEG12-pVIVO2 (i) also expressed p75NTR (1 μg/ml goat anti-p75NTR; ii) scale bar: 50 μmm. **(B,C)** M. **(D)** Percentage of lumbar, thoracic and cervical motor neurons labeled with GFP and ChAT 48 h after MLR2-PEI-PEG12-pVIVO2 given, i.p. ($n = 5$ mice with SEM).

by including in our nanoparticle an antibody to p75NTR (MLR2) that binds and internalizes into motor neurons (Matusica et al., 2008).

The ability of p75NTR antibody MLR2 to target our nanoparticles to motor neurons from the periphery was shown by labeled MLR2 being observed in the majority of spinal motor neurons following intraperitoneal administration. MLR2 was labeled with an Atto-488 fluorophore and observed in the majority (near to 90%) of motor neurons identified by Hb9 staining, which is specific to the nucleus of developing spinal motor neurons (Arber et al., 1999). These observations indicate that MLR2 is retrogradely transported to most of the motor neurons after intraperitoneal delivery. The similar percentage of labeling across the lumbar, thoracic and cervical regions is not surprising, since motor neurons in all segments of the rodent neonatal spinal cord are known to express p75NTR (Yan and Johnson, 1988). We also observed labeled antibody in dorsal root ganglia (DRG). Previous work has shown the majority of motor neurons and sensory fibers in the spinal tract can be accessed in an identical manner by intravenous or intraperitonealy delivered agents that travel retrogradely in motor neurons and sensory fibers. Hence, intraperitoneal routes to motor neurons and dorsal root ganglia (DRG) that contain cell bodies of sensory fibers are from the circulation to terminals in the periphery. This was clearly shown by Alisky et al. (2002) where both intraperitoneal and intravenous injections of retrograde tracing agent cholera toxin subunit B (CTB) accessed all spinal motor neurons and produced identical staining. Hence, labeled MLR2 probably travels to the neuromuscular junctions via the circulation after intraperitoneal injections.

The nanoparticle comprising MLR2 conjugated to PEGylated PEI, and the GFP expressing plasmid pVIVO2 transfected motor neurons 72 h post intraperitoneal injections into 5 neonatal mice. 25.4% of lumbar, 18.3% of thoracic, and 17.0% of spinal motor neurons were transfected with pVIVO2 identified by GFP expression. When we injected PEGylated PEI carrying pVIVO2, there were no motor neurons transfected, demonstrating again that MLR2 antibody is an important component for retrograde transport to motor neurons in the spinal cord. This is also demonstrated by the fact there was no transfection in any other type of spinal cord cells when PEGylated PEI carrying pVIVO2 was injected into neonatal mice. Specificity and retrograde transport of the immunogene to motor neurons is by MLR2. Motor neurons were

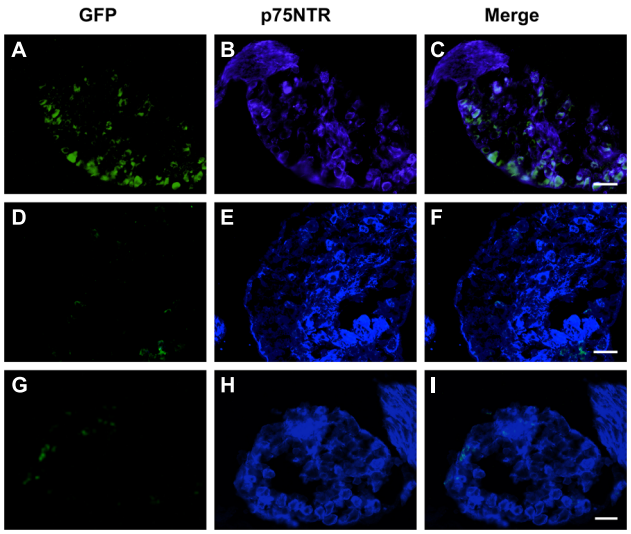

FIGURE 7 | MLR2-PEI-PEG12-pVIVO2 is retrogradely transported to dorsal root ganglia (DRG)s in neonatal mice and GFP expressed. Two doses of 75 μg of MLR2-PEI-PEG12-pVIVO2 carrying 58 μg pVIVO2 (N/P 12) was injected into neonatal mice and 72 h L2-L4 DRGs excised and examined for GFP expression ($n = 5$). GFP expression was identified with chicken anti-GFP (1/500) and p75NTR with goat anti-p75NTR (1 μg/ml). GFP fluorescence in DRG sections was detected after treatment with chicken anti-GFP (1/500; **A**) that also contained p75NTR (**B**,**C** scale bar: 50 μm). Two doses of 75 μg of PEI-PEG12-pVIVO2 carrying 77.3 μg pVIVO2 (N/P 5) was also injected into neonatal mice and 72 h later spinal cords excised and examined for GFP expression ($n = 3$). DRG sections did not contain GFP fluorescence **(D)** in neurons that also contained p75NTR **(E,F**; scale bar: 50 μm **E,F**). Control mice non-injected DRG sections did not contain GFP **(G)** but did contain p75NTR (**H,I**; scale bar: 50 μm).

identified by ChAT. Since motor neurons identified by ChAT overlap with Hb9 staining in neonatal mice, this was a valid analysis (Shneider et al., 2009). The low level of transfection observed in motor neurons *in vivo* may be explained by the reported inefficiency of non-viral gene delivery (Mintzer and Simanek, 2009; Rogers and Rush, 2012). In regards to dosage, we used the same dosage of nanoparticle as we did labeled antibody (75 μg/g body weight). Hence since the same amount of antibody (when labeled) can access all the motor neurons, other areas of the nanoparticle delivery may not be optimal. Further improvements to transfection efficiency *in vivo* can be made. We already have a large payload for our nanoparticle, and although PEI is PEGylated, the whole IgG (MLR2) was not. A way to reduce interactions of the IgG with the immune system is to use the antibody binding fragments. For example, antibody fragments that lack Fc domains (FAb, Fv, scFv), have reduced interactions with the immune system and non-targeted cells through Fc receptors (Peer and Lieberman, 2011). Indeed, previous work with antibody fragments for tumor targeting using immunoliposomes carrying plasmid DNA has produced less immune reaction than whole antibodies and more sustained expression *in vivo* (Zhou et al., 2011). Hence, further improvements to transfection efficiency may be made by using FAb or scFV of MLR2 instead of the whole IgG.

This is the first report of specific gene delivery to motor neurons via the circulation. Previous viral gene delivery attempts to transfect neonatal mouse motor neurons did not have the specificity to transfect mouse motor neurons via the circulation (Towne et al., 2008). Towne et al. (2008) tested intravenous delivery of recombinant adeno-associated virus (rAAVs) expressing small hairpin RNAs targeting mutant SOD1 in the ALS mouse model. Although the AAV virus could transfect mouse motor neurons from the circulation it was not specific, it also transfected most other cell types. Towne et al. (2011) then went on to serotype their AAV viral delivery for retrograde transport and gave multiple injections to muscle groups innervated by motor neurons in neonatal SOD1 mice. Unfortunately, they could not down regulate mutant SOD1 enough to improve outcomes in ALS mice. This was suggested to be because not all motor neurons were accessed by intramuscular injections resulting in inconsistent of levels of transfection across the spinal cord. Notably, approximately 28% of lumbar, 12% of thoracic, and 18% of cervical motor neurons were transfected in neonatal mice (Towne et al., 2011). It was concluded that the lack of improvement after their viral gene therapy might be because it is difficult to access all motor neurons by intramuscular injections. In contrast, we were able to achieve motor neuron transfection after intraperitoneal injections of immunogene. We did not need to inject every muscle group to get specific transfection of motor neurons. To our knowledge we are the first group to do so. We have shown that you can transfect 25.4% of lumbar, 18.3% of thoracic, and 17.0% of spinal motor neurons after delivery of our immunogene Considering our nanoconstruct may not still be optimal, our results are hopeful for developing targeted therapy.

PEI was used to condense plasmid DNA for gene delivery *in vitro* and *in vivo*. However, PEI was modified by PEGylation to make it "stealth-like" in the circulation. Our data indicates that PEGylation reduces the toxicity branched PEI has to pure motor neurons. The viability of motor neurons *in vitro* subject to PEI conjugated to p75NTR targeting antibody MLR2 was significantly poorer than PEGylated PEI conjugated to MLR2. This result was not surprising since previous work has shown PEI without modification is toxic (Moghimi et al., 2005) causing cell stress and apoptosis (Godbey et al., 1999; Moghimi et al., 2005). Other work has shown modifying PEI by PEGylation reduces cellular toxicity (Ogris et al., 1999; Malek et al., 2009), presumably by reduction in positive charge (Merdan et al., 2003; Hoskins et al., 2012) and the formation of a hydrophilic corona around the PEI/DNA core (Merdan et al., 2005). Grafting of PEI with PEG chains thus reduces the zeta potential of PEI-based polyplexes even at high N/P ratio (Merdan et al., 2005). The zeta potential of our immunogene were negative at the N/P ratio of 12 used *in vitro* and *in vivo* (Hoskins et al., 2012). Therefore, our results showing that PEGylated PEI reduces the zeta potential and toxicity of our immunogene *in vitro* are consistent with the literature.

Although we were able to transfect motor neurons *in vivo*, our immunogene produced a low percentage (∼8%) of transfection *in vitro*. This was significantly lower than the 17–25% of motor neurons transfected throughout the spinal cord *in vivo*. This disparity between *in vitro* and *in vivo* transfection is not unusual for stable cationic constructs containing grafted stealth agents and targeting agents. For example, Höbel et al. (2011) showed that despite their relatively low *in vitro* efficacy, PEI grafted with sugars

showed better *in vivo* than *in vitro* profiles and reduced toxicity. Most testing of non-viral gene delivery agents *in vitro* employs cell lines cell that rapidly divide with cell culture reagents that do not accurately mimic the *in vivo* situation (van Gaal et al., 2011). Furthermore, transfection is often undertaken without serum in the media, which does not mimic the high perecentage of serum in the circulation. Cationic polyplexes can interact with negatively charged blood components (e.g., proteins, erythrocytes), followed by the formation of aggregates. Under these conditions, precipitation can enhance the association of the delivery system with the cell surface, which can artificially elevate transfection rates with agents that are not stable in physiological media. Conversely, non-viral agents that are stable in physiological media often do not transfect efficiently in cell culture, leading to the conclusion that such systems are not worthy of further consideration. Another confounding factor with cell culture experiments is that the nuclear membrane breaks down during cell division, allowing efficient translocation of DNA into the nucleus of rapidly dividing cells that greatly facilitates transfection (Pérez-Martínez et al., 2011). We chose to test our nanoconstructs on PMN which do not divide. Our stable nanoparticle was not only PEGylated but also cross-linked to an antibody to p75NTR. Previous research has found that cross-linking amines in PEI increased the stability of PEGylated PEI and improved *in vivo* stability (Neu et al., 2007; Höbel et al., 2011). Therefore, our results producing significant *in vivo* transfection is probably reflective of the difficulty simulating *in vivo* environments *in vitro*.

PEGylation of PEI decreases the number of amines available for condensing plasmid DNA. The size of our immunogene complex at neutral charge was small (near 100 nm). This is in contrast to previous reports where branched PEI nanoconstructs complexed with DNA can be above 300 nm (Ewe et al., 2014). Conjugation to antibody MLR2 via a disulfide bridge, where amines were further reduced in the PEGylated PEI did not significantly increase the size of the complex. Previous work has shown that positively charged particles with sizes above 200 nm may be recognized and removed by the reticuloendothelial system (RES; Dash et al., 1999; Malek et al., 2009). PEGylation reduces this interaction (Ogris et al., 1999; Merdan et al., 2005; Malek et al., 2009) and also the size of the complex.

We observed no obvious off-target effects in the spinal cord and transfection of cells other than motor neurons in the spinal cord with our immunogene. Indeed, we did not observe transfection in any other cell types except for motor neurons. However, some of the p75NTR expressing cells were transfected the DRGs. p75NTR is known to be expressed in DRG cells (Yan and Johnson, 1988) and transfection of some of these cells by our immunogene again highlights the immunogene travels by receptor mediated retrograde transport to p75NTR expressing cells. The bicistronic pVIVO2 plasmid we used is specifically designed for *in vivo* transfection. The GFP reporter plasmid (pgWiZ) we used for *in vitro* transfections contains CpGs in its backbone that are known to induce immune response *in vivo* (Davies et al., 2012). pgWiZ is often used to improve humoral immune response to plasmid vaccination *in vivo* (Chamarthy et al., 2003; Grønevik et al., 2005; Rose et al., 2014). In contrast, pVIVO2 has minimal CpGs in its plasmid backbone and high levels of constitutive transgene expression has been reported for this plasmid *in vivo* (Mandke and Singh, 2012). In addition, pVIVO2 has DTS to improve nuclear entry into post mitotic cells such as motor neurons. We tried delivering pgWiZ to motor neurons by intraperitoneal injections with our immunoporter MLR2-PEI-PEG12, but found no significant expression *in vivo*. This has led us to us to conclude that plasmid design is an important component of effective non-viral gene delivery agents.

Specific delivery of genes to motor neurons is highly relevant to therapy of ALS and spinal muscular atrophy (SMA), where currently no effective therapy exists (Sreedharan and Brown, 2013). Our results show that motor neurons can be specifically transfected with peripherally administered immunogenes. Targeting motor neurons by use of the p75NTR is not surprising as this receptor is highly expressed in the embryonic period and early neonatal life (Yan and Johnson, 1988). Lentivirus that expressed heavy and light chains of rat p75NTR antibody (MC192) were recently shown transported retrogradely from the axonal tip to the cell body in an *in vitro* microfluidic culture model (Eleftheriadou et al., 2014). This is in agreement with our *in vivo* data where p75NTR antibody was found throughout the spinal cord after intraperitoneal delivery, indicating retrograde transport from terminals to ventral motor neurons throughout the spinal cord. Caution has to be taken with immunogenes use in ALS. p75NTR is down regulated in adulthood and re-expressed in injury, including ALS (Lowry et al., 2001). However, the level of p75NTR re-expression and health of the motor neurons must be sufficient for retrograde transport in the majority of motor neurons. A previous study (Copray et al., 2003) indicated 5% of L4 Lumbar motor neurons re-express p75NTR in adult ALS mice at symptomatic age. Further work is needed to determine if sufficient therapeutic genes can be delivered in adult ALS animal models via p75NTR targeting immunogenes. Since SMA is a disease often occuring in childhood (Arnold and Burghes, 2013), p75NTR targeting immunogenes could be trialed in SMA mice.

CONCLUSION

Our current research demonstrates the suitability of p75NTR targeting immunogenes to transfect motor neurons from the periphery in neonatal mice, but further work is required for use in adult animals.

ACKNOWLEDGMENTS

This project was funded by the Motor Neuron Disease Research Institute of Australia (Mary-Louise Rogers, Robert A. Rush), the Flinders Medical Centre Foundation (Mary-Louise Rogers, Robert A. Rush) and Flinders University Research Scholarship (Kevin S. Smith). We thank Prof Neil Cashman (University of British Columbia, Canada) for use of the NSC34 cell line. Funding was also provided by the Australian Research Council Centre of Excellence in Convergent Bio-Nano Science and Technology (project number CE140100036, Nicolas H. Voelcker).

REFERENCES

Alisky, J. M., Van De Wetering, C. I., and Davidson, B. L. (2002). Widespread dispersal of cholera toxin subunit b to brain and spinal cord neurons following systemic delivery. *Exp. Neurol.* 178, 139–146. doi: 10.1006/exnr.2002.8031

Arber, S., Han, B., Mendelsohn, M., Smith, M., Jessell, T. M., and Sockanathan, S. (1999). Requirement for the homeobox gene Hb9 in the consolidation of motor neuron identity. *Neuron* 23, 659–674. doi: 10.1016/S0896-6273(01)80026-X

Arnold, W. D., and Burghes, A. H. M. (2013). Spinal muscular atrophy: development and implementation of potential treatments. *Ann. Neurol.* 74, 348–362. doi: 10.1002/ana.23995

Barati, S., Hurtado, P. R., Zhang, S. H., Tinsley, R., Ferguson, I. A., and Rush, R. A. (2006). GDNF gene delivery via the p75(NTR) receptor rescues injured motor neurons. *Exp. Neurol.* 202, 179–188. doi: 10.1016/j.expneurol.2006.05.027

Blessing, T., Kursa, M., Holzhauser, R., Kircheis, R., and Wagner, E. (2001). Different strategies for formation of pegylated EGF-conjugated PEI/DNA complexes for targeted gene delivery. *Bioconjug. Chem.* 12, 529–537. doi: 10.1021/bc0001488

Boeckle, S., Von Gersdorff, K., Van Der Piepen, S., Culmsee, C., Wagner, E., and Ogris, M. (2004). Purification of polyethylenimine polyplexes highlights the role of free polycations in gene transfer. *J. Gene Med.* 6, 1102–1111. doi: 10.1002/jgm.598

Boussif, O., Lezoualc'h, F., Zanta, M., Mergny, M., Scherman, D., Demeneix, B., et al. (1995). A versatile vector for gene and oligonucleotide transfer into cells in culture and in vivo: polyethylenimine. *Proc. Natl. Acad. Sci. U.S.A.* 92, 7297–7301. doi: 10.1073/pnas.92.16.7297

Bronfman, F., Tcherpakov, M., Jovin, T., and Fainzilber, M. (2003). Ligand-induced internalization of the p75 neurotrophin receptor: a slow route to the signaling endosome. *J. Neurosci.* 23, 3209–3220.

Chamarthy, S. P., Kovacs, J. R., Mcclelland, E., Gattens, D., and Meng, W. S. (2003). A cationic peptide consists of ornithine and histidine repeats augments gene transfer in dendritic cells. *Mol. Immunol.* 40, 483–490. doi: 10.1016/j.molimm.2003.08.001

Chollet, P., Favrot, M. C., Hurbin, A., and Coll, J.-L. (2002). Side-effects of a systemic injection of linear polyethylenimine-DNA complexes. *J. Gene Med.* 4, 84–91. doi: 10.1002/jgm.237

Copray, J., Jaarsma, D., Kust, B., Bruggeman, R., Mantingh, I., Brouwer, N., et al. (2003). Expression of the low affinity neurotrophin receptor p75 in spinal motoneurons in a transgenic mouse model for amyotrophic lateral sclerosis. *Neuroscience* 116, 685–694. doi: 10.1016/S0306-4522(02)00755-8

Dash, P. R., Read, M. L., Barrett, L. B., Wolfert, M. A., and Seymour, L. W. (1999). Factors affecting blood clearance and in vivo distribution of polyelectrolyte complexes for gene delivery. *Gene Ther.* 6, 643–650. doi: 10.1038/sj.gt.3300843

Davies, L. A., Hyde, S. C., Nunez-Alonso, G., Bazzani, R. P., Harding-Smith, R., Pringle, I. A., et al. (2012). The use of CpG-free plasmids to mediate persistent gene expression following repeated aerosol delivery of pDNA/PEI complexes. *Biomaterials* 33, 5618–5627. doi: 10.1016/j.biomaterials.2012.04.019

Eleftheriadou, I., Trabalza, A., Ellison, S., Gharun, K., and Mazarakis, N. (2014). Specific retrograde transduction of spinal motor neurons using lentiviral vectors targeted to presynaptic NMJ receptors. *Mol. Ther.* 22, 1285–1298. doi: 10.1038/mt.2014.49

Ewe, A., Schaper, A., Barnert, S., Schubert, R., Temme, A., Bakowsky, U., et al. (2014). Storage stability of optimal liposome-polyethylenimine complexes (lipopolyplexes) for DNA or siRNA delivery. *Acta Biomater.* 10, 2663–2673. doi: 10.1016/j.actbio.2014.02.037

Ford, T., Graham, J., and Rickwood, D. (1994). Iodixanol: a nonionic iso-osmotic centrifugation medium for the formation of self-generated gradients. *Anal. Biochem.* 220, 360–366. doi: 10.1006/abio.1994.1350

Germershaus, O., Merdan, T., Bakowsky, U., Behe, M., and Kissel, T. (2006). Trastuzumab-polyethylenimine-polyethylene glycol conjugates for targeting Her2-expressing tumors. *Bioconjug. Chem.* 17, 1190–1199. doi: 10.1021/bc0601119

Godbey, W. T., Wu, K. K., and Mikos, A. G. (1999). Tracking the intracellular path of poly(ethylenimine)/DNA complexes for gene delivery. *Proc. Natl. Acad. Sci. U.S.A.* 96, 5177–5181. doi: 10.1073/pnas.96.9.5177

Godbey, W. T., Wu, K. K., and Mikos, A. G. (2001). Poly(ethylenimine)-mediated gene delivery affects endothelial cell function and viability. *Biomaterials* 22, 471–480. doi: 10.1016/S0142-9612(00)00203-9

Grønevik, E., Von Steyern, F. V., Kalhovde, J. M., Tjelle, T. E., and Mathiesen, I. (2005). Gene expression and immune response kinetics using electroporation-mediated DNA delivery to muscle. *J. Gene Med.* 7, 218–227. doi: 10.1002/jgm.650

Höbel, S., Loos, A., Appelhans, D., Schwarz, S., Seidel, J., Voit, B., et al. (2011). Maltose- and maltotriose-modified, hyperbranched poly(ethylene imine)s (OM-PEIs): physicochemical and biological properties of DNA and siRNA complexes. *J. Control. Release* 149, 146–158. doi: 10.1016/j.jconrel.2010.10.008

Hoskins, C., Wang, L., Cheng, W. P., and Cuschieri, A. (2012). Dilemmas in the reliable estimation of the in-vitro cell viability in magnetic nanoparticle engineering: which tests and what protocols? *Nanoscale Res. Lett.* 7, 77. doi: 10.1186/1556-276X-7-77

Kircheis, R., Kichler, A., Wallner, G., Kursa, M., Ogris, M., Felzmann, T., et al. (1997). Coupling of cell-binding ligands to polyethylenimine for targeted gene delivery. *Gene Ther.* 4, 409–418. doi: 10.1038/sj.gt.3300418

Kunath, K., Von Harpe, A., Fischer, D., Petersen, H., Bickel, U., Voigt, K., et al. (2003). Low-molecular-weight polyethylenimine as a non-viral vector for DNA delivery: comparison of physicochemical properties, transfection efficiency and in vivo distribution with high-molecular-weight polyethylenimine. *J. Control. Release* 89, 113–125. doi: 10.1016/S0168-3659(03)00076-2

Lalli, G., and Schiavo, G. (2002). Analysis of retrograde transport in motor neurons reveals common endocytic carriers for tetanus toxin and neurotrophin receptor p75NTR. *J. Cell Biol.* 156, 233–239. doi: 10.1083/jcb.200106142

Lowry, K., Murray, S., Mclean, C., Talman, P., Mathers, S., Lopes, E., et al. (2001). A potential role for the p75 low-affinity neurotrophin receptor in spinal motor neuron degeneration in murine and human amyotrophic lateral sclerosis. *Amyotroph. Lateral Scler.* 2, 127–134. doi: 10.1080/146608201753275463

Lungwitz, U., Breunig, M., Blunk, T., and Göpferich, A. (2005). Polyethylenimine-based non-viral gene delivery systems. *Eur. J. Pharm. Biopharm.* 60, 247–266. doi: 10.1016/j.ejpb.2004.11.011

Luo, X., Pan, S., Feng, M., Wen, Y., and Zhang, W. (2010). Stability of poly(ethylene glycol)-graft-polyethylenimine copolymer/DNA complexes: influences of PEG molecular weight and PEGylation degree. *J. Mater. Sci. Mater. Med.* 21, 597–607. doi: 10.1007/s10856-009-3903-1

Magnusson, T., Haase, R., Schleef, M., Wagner, E., and Ogris, M. (2011). Sustained, high transgene expression in liver with plasmid vectors using optimized promoter-enhancer combinations. *J. Gene Med.* 13, 382–391. doi: 10.1002/jgm.1585

Malek, A., Merkel, O., Fink, L., Czubayko, F., Kissel, T., and Aigner, A. (2009). In vivo pharmacokinetics, tissue distribution and underlying mechanisms of various PEI(-PEG)/siRNA complexes. *Toxicol. Appl. Pharmacol.* 236, 97–108. doi: 10.1016/j.taap.2009.01.014

Mandke, R., and Singh, J. (2012). Cationic nanomicelles for delivery of plasmids encoding interleukin-4 and interleukin-10 for prevention of autoimmune diabetes in mice. *Pharm. Res.* 29, 883–897. doi: 10.1007/s11095-011-0616-1

Masago, K., Itaka, K., Nishiyama, N., Chung, U.-I., and Kataoka, K. (2007). Gene delivery with biocompatible cationic polymer: pharmacogenomic analysis on cell bioactivity. *Biomaterials* 28, 5169–5175. doi: 10.1016/j.biomaterials.2007.07.019

Matusica, D., Fenech, M., Rogers, M., and Rush, R. (2008). Characterization and use of the NSC-34 cell line for study of neurotrophin receptor trafficking. *J. Neurosci. Res.* 86, 553–565. doi: 10.1002/jnr.21507

Merdan, T., Callahan, J., Petersen, H., Kunath, K., Bakowsky, U., Kopecková, P., et al. (2003). Pegylated polyethylenimine-Fab & apos; antibody fragment conjugates for targeted gene delivery to human ovarian carcinoma cells. *Bioconjug. Chem.* 14, 989–996. doi: 10.1021/bc0340767.

Merdan, T., Kunath, K., Petersen, H., Bakowsky, U., Voigt, K. H., Kopecek, J., et al. (2005). PEGylation of poly(ethylene imine) affects stability of complexes with plasmid DNA under in vivo conditions in a dose-dependent manner after intravenous injection into mice. *Bioconjug. Chem.* 16, 785–792. doi: 10.1021/bc049743q

Mintzer, M. A., and Simanek, E. E. (2009). Nonviral vectors for gene delivery. *Chem. Rev.* 109, 259–302. doi: 10.1021/cr800409e

Moghimi, S. M., Symonds, P., Murray, J. C., Hunter, A. C., Debska, G., and Szewczyk, A. (2005). A two-stage poly(ethylenimine)-mediated cytotoxicity: implications for gene transfer/therapy. *Mol. Ther.* 11, 990–995. doi: 10.1016/j.ymthe.2005.02.010.

Navarro-Quiroga, I., Antonio Gonzalez-Barrios, J., Barron-Moreno, F., Gonzalez-Bernal, V., Martinez-Arguelles, D. B., and Martinez-Fong, D. (2002). Improved neurotensin-vector-mediated gene transfer by the coupling of hemagglutinin HA2 fusogenic peptide and Vp1 SV40 nuclear localization signal. *Mol. Brain Res.* 105, 86–97. doi: 10.1016/S0169-328X(02)00396-0

Neu, M., Germershaus, O., Behe, M., and Kissel, T. (2007). Bioreversibly crosslinked polyplexes of PEI and high molecular weight PEG show extended circulation times in vivo. *J. Control. Release* 124, 69–80. doi: 10.1016/j.jconrel.2007.08.009

Ogris, M., Brunner, S., Schüller, S., Kircheis, R., and Wagner, E. (1999). PEGylated DNA/transferrin-PEI complexes: reduced interaction with blood components, extended circulation in blood and potential for systemic gene delivery. *Gene Ther.* 6, 595–605. doi: 10.1038/sj.gt.3300900

Ogris, M., Walker, G., Blessing, T., Kircheis, R., Wolschek, M., and Wagner, E. (2003). Tumor-targeted gene therapy: strategies for the preparation of ligand-polyethylene glycol-polyethylenimine/DNA complexes. *J. Control. Release* 91, 173–181. doi: 10.1016/S0168-3659(03)00230-X

Pardridge, W. (2006). Molecular Trojan horses for blood-brain barrier drug delivery. *Curr. Opin. Pharmacol* 6, 494–500. doi: 10.1016/j.coph.2006.06.001

Peer, D., and Lieberman, J. (2011). Special delivery: targeted therapy with small RNAs. *Gene Ther.* 18, 1127–1133. doi: 10.1038/gt.2011.56

Pérez-Martínez, F. C., Guerra, J., Posadas, I., and Ceña, V. (2011). Barriers to non-viral vector-mediated gene delivery in the nervous system. *Pharm. Res.* 28, 1843–1858. doi: 10.1007/s11095-010-0364-7

Rogers, M., Atmosukarto, I., Berhanu, D., Matusica, D., Macardle, P., and Rush, R. (2006). Functional monoclonal antibodies to p75 neurotrophin receptor raised in knockout mice. *J. Neurosci. Methods* 158, 109–120. doi: 10.1016/j.jneumeth.2006.05.022

Rogers, M. L., Bailey, S., Matusica, D., Nicholson, I., Muyderman, H., Pagadala, P. C., et al. (2010). ProNGF mediates death of Natural Killer cells through activation of the p75NTR-sortilin complex. *J. Neuroimmunol.* 226, 93–103. doi: 10.1016/j.jneuroim.2010.05.040

Rogers, M.-L., and Rush, R. A. (2012). Non-viral gene therapy for neurological diseases, with an emphasis on targeted gene delivery. *J. Control. Release* 157, 183–189. doi: 10.1016/j.jconrel.2011.08.026

Rose, L., Mahdipoor, P., Kucharski, C., and Uludağ, H. (2014). Pharmacokinetics and transgene expression of implanted polyethyleniminebased pDNA complexes. *Biomater. Sci.* 2, 833–842. doi: 10.1039/c3bm60200a

Schaffert, D., Kiss, M., Rodl, W., Shir, A., Levitzki, A., Ogris, M., et al. (2011). Poly(I:C)-mediated tumor growth suppression in EGF-receptor overexpressing tumors using EGF-polyethylene glycol-linear polyethylenimine as carrier. *Pharm. Res.* 28, 731–741. doi: 10.1007/s11095-010-0225-4

Shepheard, S. R., Chataway, T., Schultz, D. W., Rush, R. A., and Rogers, M. L. (2014). The extracellular domain of neurotrophin receptor p75 as a candidate biomarker for amyotrophic lateral sclerosis. *PLoS ONE* 9:e87398. doi: 10.1371/journal.pone.0087398

Shneider, N. A., Brown, M. N., Smith, C. A., Pickel, J., and Alvarez, F. J. (2009). Gamma motor neurons express distinct genetic markers at birth and require muscle spindle-derived GDNF for postnatal survival. *Neural Dev.* 4, 42. doi: 10.1186/1749-8104-4-42

Snyder, S. L., and Sobocinski, P. Z. (1975). An improved 2,4,6-trinitrobenzenesulfonic acid method for the determination of amines. *Anal. Biochem.* 64, 284–288. doi: 10.1016/0003-2697(75)90431-5

Sreedharan, J., and Brown, R. H. (2013). Amyotrophic lateral sclerosis: problems and prospects. *Ann. Neurol.* 74, 309–316. doi: 10.1002/ana.24012

Tang, M. X., and Szoka, F. C. (1997). The influence of polymer structure on the interactions of cationic polymers with DNA and morphology of the resulting complexes. *Gene Ther.* 4, 823–832. doi: 10.1038/sj.gt.3300454

Towne, C., Raoul, C., Schneider, B. L., and Aebischer, P. (2008). Systemic AAV6 delivery mediating RNA interference against SOD1: neuromuscular transduction does not alter disease progression in fALS mice. *Mol. Ther.* 16, 1018–1025. doi: 10.1038/mt.2008.73

Towne, C., Setola, V., Schneider, B. L., and Aebischer, P. (2011). Neuroprotection by gene therapy targeting mutant SOD1 in individual pools of motor neurons does not translate into therapeutic benefit in fALS mice. *Mol. Ther.* 19, 274–283. doi: 10.1038/mt.2010.260

Turner, M. R., Hardiman, O., Benatar, M., Brooks, B. R., Chio, A., De Carvalho, M., et al. (2013). Controversies and priorities in amyotrophic lateral sclerosis. *Lancet Neurol.* 12, 310–322. doi: 10.1016/S1474-4422(13)70036-X

van Gaal, E. V. B., Van Eijk, R., Oosting, R. S., Kok, R. J., Hennink, W. E., Crommelin, D. J. A., et al. (2011). How to screen non-viral gene delivery systems in vitro? *J. Controll. Release* 154, 218–232. doi: 10.1016/j.jconrel.2011.05.001

Wiese, S., Herrmann, T., Drepper, C., Jablonka, S., Funk, N., Klausmeyer, A., et al. (2010). Isolation and enrichment of embryonic mouse motoneurons from the lumbar spinal cord of individual mouse embryos. *Nat. Protoc.* 5, 31–38. doi: 10.1038/nprot.2009.193.

Yan, Q., and Johnson, E. M. Jr. (1988). An immunohistochemical study of the nerve growth factor receptor in developing rats. *J. Neurosci.* 8, 3481–3498.

Zabner, J., Fasbender, A. J., Moninger, T., Poellinger, K. A., and Welsh, M. J. (1995). Cellular and molecular barriers to gene transfer by a cationic lipid. *J. Biol. Chem.* 270, 18997–19007. doi: 10.1074/jbc.270.32.18997

Zhang, Y., Schlachetzki, F., and Pardridge, W. M. (2003). Global non-viral gene transfer to the primate brain following intravenous administration. *Mol. Ther.* 7, 11–18. doi: 10.1016/S1525-0016(02)00018-7

Zhou, Q. H., Fu, A., Boado, R. J., Hui, E. K., Lu, J. Z., and Pardridge, W. M. (2011). Receptor-mediated abeta amyloid antibody targeting to Alzheimer's disease mouse brain. *Mol. Pharm.* 8, 280–285. doi: 10.1021/mp1003515

Conflict of Interest Statement: Author Robert A. Rush is now retired from Flinders University and holds the position of Managing Director at Biosensis Pty. Ltd. which has commercial interest involving the MLR2 antibody used in this study. No other authors have conflicting interest.

Received: 03 July 2014; paper pending published: 07 August 2014; accepted: 18 September 2014; published online: 14 October 2014.

*Citation: Rogers M-L, Smith KS, Matusica D, Fenech M, Hoffman L, Rush RA and Voelcker NH (2014) Non-viral gene therapy that targets motor neurons in vivo. Front. Mol. Neurosci. **7**:80. doi: 10.3389/fnmol.2014.00080*

This article was submitted to the journal Frontiers in Molecular Neuroscience.

frontiers in
MOLECULAR NEUROSCIENCE

ORIGINAL RESEARCH ARTICLE
published: 09 October 2014
doi: 10.3389/fnmol.2014.00079

Development of non-viral vehicles for targeted gene transfer into microglia via the integrin receptor CD11b

Markus Smolny[1]*†, Mary-Louise Rogers[2]†, Anthony Shafton[3], Robert A. Rush[2] and Martin J. Stebbing[1]

[1] School of Medical Sciences and Health Innovations Research Institute, Royal Melbourne Institute of Technology University, Bundoora, VIC, Australia
[2] Department of Human Physiology, Centre for Neuroscience, Flinders University, Adelaide, SA, Australia
[3] The Florey Institute of Neuroscience and Mental Health, The University of Melbourne, Parkville, VIC, Australia

Edited by:
Andrew Paul Tosolini, University of New South Wales, Australia

Reviewed by:
Björn Spittau, Albert-Ludwigs-University Freiburg, Germany
Wenxin Wang, University College Dublin, Ireland

***Correspondence:**
Markus Smolny, Biosensis Pty Ltd., 39 Winwood Street, Thebarton, SA 5031, Australia
e-mail: markus@biosensis.com

†*Markus Smolny and Mary-Louise Rogers have contributed equally to this work.*

Microglial activation is a central event in neurodegeneration. Novel technologies are sought for that specifically manipulate microglial function in order to delineate their role in onset and progression of neuropathologies. We investigated for the first time whether non-viral gene delivery based on polyethyleneglycol–polyethyleneimine conjugated to the monoclonal anti-CD11b antibody OX42 ("OX42-immunogene") could be used to specifically target microglia. We first conducted immunofluorescence studies with the OX42 antibody and identified its microglial integrin receptor CD11b as a potential target for receptor-mediated gene transfer based on its cellular specificity in mixed glia culture and *in vivo* and found that the OX42 antibody is rapidly internalized and trafficked to acidic organelles in absence of activation of the respiratory burst. We then performed transfection experiments with the OX42-immunogene *in vitro* and in rat brain showing that the OX42-immunogene although internalized was degraded intracellularly and did not cause substantial gene expression in microglia. Investigation of specific barriers to microglial gene transfer revealed that aggregated OX42-immunogene polyplexes stimulated the respiratory burst that likely involved Fcγ-receptors. Transfections in the presence of the endosomolytic agent chloroquine improved transfection efficiency indicating that endosomal escape may be limited. This study identifies CD11b as an entry point for antibody-mediated gene transfer into microglia and takes important steps toward the further development of OX42-immunogenes.

Keywords: microglia, CD11b, OX42, non-viral vectors, polyethyleneimine (PEI), phagocytosis, respiratory burst

INTRODUCTION

Microglia are the primary immune cells of the central nervous system (CNS) and exert many of their important functions through changes in morphology and gene expression termed "microglial activation" (reviewed in Ransohoff and Cardona, 2010; Schafer et al., 2012). It is unclear if activated microglia are neuroprotective, neurotoxic or neuromodulatory in neuropathology (Saijo and Glass, 2011; Aguzzi et al., 2013). Thus, methods are being sought for that allows specific manipulation of microglial function in order to gain more insight into their role.

Viruses have been used to manipulate gene expression in microglial cells. Nevertheless, the development of a virus-based transgene carrier specifically targeting microglia has been proven difficult, because most viruses display broad tropism and therefore require extensive modification to increase specificity (Burke et al., 2002; Cucchiarini et al., 2003; Pfrieger and Slezak, 2012). Further, the application of viral vectors *in vivo* was shown to bear risk of insertional mutagenesis. This was found especially with lentiviral vectors (Burke et al., 2002; Bokhoven et al., 2009) that are often used to transfect microglia and other glial cells *in vitro* and *in vivo* (Wrzesinski et al., 2000; Balcaitis et al., 2005; Meunier et al., 2007, 2008; McCoy et al., 2008; Dominguez et al., 2010; Lee et al., 2011; Jiang et al., 2012; Kim et al., 2012; Liu et al., 2013; Maiorino et al., 2013) and thus limits their use for other purposes than basic research such as gene therapy.

Non-viral vehicles have emerged as an alternative for gene delivery with advantages such as ability to target specific populations of cells and low immunotoxicity compared to viruses (reviewed in Lv et al., 2006 and Raety et al., 2008). The cationic polymer polyethyleneimine (PEI) has been frequently used to bind and condense plasmid DNA (pDNA), to protect it from degradation and facilitate endosomal escape (Akinc et al., 2005; Neu et al., 2005; Yue et al., 2011). Further, modification of PEI with polyethyleneglycol (PEG) was demonstrated to add stability to PEI complexes by decreasing aggregation (Tang et al., 2003; Mishra et al., 2004; Millili et al., 2010), reducing PEI-mediated toxicity (reviewed in Lungwitz et al., 2005), diminishing non-specific interaction of positively charged PEI with negatively charged proteoglycans on off-target cells (Ogris et al., 2001) and improving *in vivo* gene delivery (Germershaus et al., 2006; Duan et al., 2010).

Non-viral bioconjugates based on PEI–PEG and chemically linked to monoclonal antibodies for receptor targeting (herein referred to as "immunogenes") may be a promising tool for specific modulation of microglial function. Antibodies may confer increased specificity compared to other ligands such as polysaccharides (Aouadi et al., 2009) and mannose receptor ligands (Ferkol

et al., 1996, 1998; Kawakami et al., 2000; Markovic et al., 2009) which bind to receptors that are more ubiquitously expressed. Such antibody-based vehicles have been successfully applied previously to deliver genes to several cell lines *in vitro* (Kircheis et al., 1997) and motor neurons (Barati et al., 2006) and cholinergic basal forebrain neurons (Berhanu and Rush, 2008) *in vivo*.

Antibodies to the integrin receptor CD11b, also known as complement receptor 3 (CR3), have the potential to be used for targeting immunogenes to microglia. The CD11b receptor is involved in the immune response of microglia and macrophages of the CNS and the peripheral immune system, respectively (Akiyama and McGeer, 1990; Berton and Lowell, 1999; Milner and Campbell, 2002). CD11b expression is up-regulated in activated microglia in a variety of neuropathological conditions, for instance in the hypothalamic paraventricular nucleus (PVN) following myocardial infarction (Rana et al., 2010). While immune receptors may trigger strong pro-inflammatory immune responses such as reactive oxygen species (ROS) production and the respiratory burst (Nimmerjahn and Ravetch, 2008) which are unwanted side-effects of gene transfer, CD11b is interestingly involved in both, pro-inflammatory (Block et al., 2007; Pei et al., 2007; Zhang et al., 2007; Hu et al., 2008; Davalos et al., 2012) and anti-inflammatory (Griffiths et al., 2009; Amarilyo et al., 2010; Ricklin et al., 2010) immune functions in microglia that seem to depend on the receptor binding site (Větvička et al., 1996; Xia et al., 1999; Ross, 2000) and interactions with other co-receptors such as Fcγ-receptors (Huang et al., 2011). More importantly, parasites and bacteria utilize CD11b to infect host cells and to avoid intracellular degradation (Mosser and Edelson, 1987; Hajishengallis and Lambris, 2011) indicating that CD11b may be also an entry point for antibody-mediated delivery of transgenes into microglia. The monoclonal antibody OX42 targets CD11b (Robinson et al., 1986) and is suggested to bind at or close to a site of CD11b related to its anti-inflammatory properties (Klegeris and McGeer, 1994; Sohn et al., 2003). Thus, OX42 may be suitable as a targeting ligand for microglial-specific gene delivery combined with the ability of PEI–PEG to bind, protect and transfer DNA into cells.

We thus propose to determine the specificity and suitability of the monoclonal antibody OX42 as a targeting agent for immunogenes for microglia and whether a targeting bioconjugate ("OX42-immunoporter") could be used for specific microglial transfection. Immunofluorescence studies with labeled OX42 antibody were conducted in cultured glia cells as well as *in vivo* to determine the specificity of CD11b for microglia, the ability of CD11b to internalize the antibody and its intracellular localization. Subsequent transfection experiments with the targeting bioconjugate were then conducted *in vitro* and *in vivo* utilizing immunohistochemistry (IHC) to determine successful microglial transfection. The activation of the respiratory burst by aggregated polyplexes as measured by dynamic light scattering (DLS) and an assay for ROS as well as limited endosomal escape as determined by transfections in presence of the endosomolytic agent chloroquine was then investigated to identify potential microglia-specific barriers to non-viral gene transfer. This study is the first to describe CD11b as a target on microglia for receptor-mediated gene transfer and to identify microglia-specific barriers that will lead to further development of targeting non-viral gene vehicles for microglial gene transfer.

MATERIALS AND METHODS

ANIMAL ETHICS

All procedures performed on animals were approved by the RMIT University Institutional Animal Experimentation Ethics Committee or the Alfred Medical Research and Education Precinct Animal Ethics Committee and conformed to the National Health and Medical Research Council of Australia code of practice for the care and use of animals for scientific purposes.

EXPERIMENTAL OVERVIEW

In vitro experiments for specificity and internalization of the OX42 antibody as well as transfections were performed in mixed cultures and isolated microglia obtained from 1 to 3 day old Sprague-Dawley rat brains as outlined in Section "Primary Cell Culture." A total of five brains of 9–10 weeks old male Sprague-Dawley rats (300–350 *g*) were used to test specificity of CD11b for microglia and for *in vivo* transfections. Studies on barriers to microglial transfections *in vitro* utilized mixed glia cultures and isolated microglia.

PRIMARY CELL CULTURE

Mixed glia cultures were prepared from neonatal Sprague-Dawley rat brains (days 1–3) based on the method developed by Nakajima et al. (1989). Briefly, a cell suspension was obtained by combination of mechanical and enzymatical (0.16% trypsin/0.01% deoxyribonuclease I, Sigma) dissociation of brain tissue. Mixed glia cultures were maintained in Dulbecco's Modified Eagle Medium with high glucose (DMEM, Gibco^{TM}) supplemented with 10% fetal bovine serum (FBS, Bovogen) and 2% penicillin-streptomycin (Gibco^{TM}) in poly-D-lysine (PDL, Sigma)-coated tissue culture flask (25 cm^2, TPP) exchanging half of the cell culture medium twice a week. Microglial cells appeared on top of an astrocytic layer after a few days and were available in sufficient amounts for isolation after 8–12 days. For immunofluorescence studies and transfections that involved mixed glia cultures, mixed cultures were prepared as above, but plated on PDL-coated coverslips in 24-well plates. Mixed cultures were used for experiments 3–4 days thereafter.

Microglial cells were isolated from mixed cultures by shaking the cell culture flasks at 37°C for 60 min (120 rpm). Dependent on the experiment, isolated microglia (>98% pure, determined by CD11b-immunoreactivity with OX42 antibody, data not shown) were either plated on PDL-coated coverslips (2×10^4 cells/well), onto PDL-coated fluorodishes (World Precision Instruments, 5×10^4 cells/dish) or in PDL-coated black 96-well plates (Greiner, 1×10^4 cells/well).

ANTIBODY PURIFICATION AND LABELING

OX42 and X63 antibody secreting hybridoma cell lines were grown in RPMI-1640 GlutaMax medium supplemented with 10% FBS, 1× penicillin-streptomycin-glutamine and 1× hypoxanthine-thymidine (Gibco^{TM}). The antibody X63 has no known antigen and was used as non-specific control IgG. Monoclonal antibodies

were purified from supernatant using protein G (Millipore) according to the manufacturer's instructions.

Antibodies were labeled according to manufacturer's instructions with either *N*-hydroxysuccinimide (NHS)-activated fluorescein or Alexa 488 sulfodichlorophenol (SDP) ester (Molecular Probes®). Tagged antibodies were purified on PD10 desalting columns (GE Healthcare). The fluorophore to protein (F/P) ratios obtained were F/P = 9 for OX42-FITC, 5 for OX42-Alexa488, and 4 for X63-Alexa488.

IMMUNOCYTOCHEMISTRY AND IMMUNOHISTOCHEMISTRY

Double-labeling experiments in mixed glia culture and in brain slices were performed to either determine specificity of OX42 antibody for microglia or assess transfections *in vitro* and *in vivo*. Cultures were fixed [4% paraformaldehyde (PFA), Merck] and then blocked for 30 min (10% normal horse serum, 0.1% Triton-X100, Sigma), while brain sections were blocked in 10% normal horse serum containing 0.5% Triton-X100 (1 h, room temperature). Antibodies against cell markers (**Table 1**) were used to detect astrocytes [anti-glial fibrillary acidic protein (GFAP)] and microglia [ionized calcium binding adapter molecule 1, (Iba1); or CD11b]. Green fluorescent protein (EGFP) expression in transfected cells was confirmed with a monoclonal mouse anti-EGFP antibody. Labeled secondary antibodies were applied to visualize primary antibody binding.

All antibody incubations in mixed culture were performed for 1 h at room temperature. For IHC, primary antibodies were incubated for 3 days at 2–8°C in a humidifying chamber and secondary antibodies applied thereafter for 2 h at room temperature followed by 1 h incubation with extravidin-Cy3 conjugate. Cell nuclei were counter-stained with Hoechst dye (1:500, 10–25 min).

Specific staining by primary antibodies was demonstrated *in vitro* by following the same immunostaining methods but omitting the primary antibodies (data not shown). Each condition was run on duplicate coverslips in each experiment and at least three experiments were performed.

CELLULAR DISTRIBUTION OF CD11b *IN VIVO*

Male Sprague-Dawley rats (300–350 *g*) were stereotactically injected under isoflurane anesthesia with 250–300 nL of Alexa 488-labeled OX42 antibody (right side) or Alexa 488-labeled X63 antibody (left side) into the PVN of the hypothalamus of the same animal (0.6 mm lateral from midline, 8.0 mm depth, –2.1 mm posterior from Bregma). Animals were kept anesthetized and perfused (4% PFA, Merck) 3 h after injections before brains were collected and post-fixed for 4 h. After 3–4 days of storage in 30% sucrose, 30 μm brain sections were cut on a cryostat, placed on gelatin-coated microscope slides and IHC performed. Two animals were injected and localization of OX42 antibody was assessed qualitatively by IHC.

INTERNALIZATION OF OX42 ANTIBODY

Isolated microglial cells on coverslips were incubated with 2 μg/mL FITC-tagged OX42 antibody at 37°C, fixed after 5, 10, 20, and 60 min and nuclei stained with Hoechst 34580 (Molecular Probes® 1:500, 10 min). Control cells were incubated for 30 min on ice. Non-specific internalization of antibody was examined by incubating microglia with Alexa 488-labeled X63 antibody (60 min, 37°C). The average green fluorescence was measured in the perinuclear region of each cell after background subtraction. Three independent experiments were performed ($n \geq 77$ cells per condition). Antibody internalization was quantified (ImageJ) as the increase in intracellular fluorescence by accumulated OX42 antibody in the perinuclear region. One-way analysis of variance (one-way ANOVA) and *post hoc* one-sample *t*-tests with Bonferroni correction were used to assess significance.

TRAFFICKING OF OX42 ANTIBODY

Isolated microglial cells on fluorodishes were incubated with 2 μg/mL OX42-Alexa 488 for 30 min on ice to saturate membrane CD11b. Cells were washed to remove unbound antibody and internalized antibody chased for further 60 min at 37°C. Cell nuclei (Hoechst) and acidic vesicles (Lysotracker Red, 50 nM, Molecular

Table 1 | Antibodies and reagents used for immunostaining.

Target	Antibody	Tag	Host	Use	c/DF	Source
CD11b	OX42	–	Mouse	ICC	1.25 μg/mL	RMIT
Iba1	α-Iba1	–	Goat	ICC	400	Abcam
				IHC	100	
GFAP	α-GFAP	–	Rabbit	ICC/IHC	150	Life Technologies
EGFP	α-GFP	–	Mouse	ICC	400	Roche
				IHC	200	
Mouse IgG	α-mouse	Alexa488	Donkey	ICC	400	Life Technologies
Mouse IgG	α-mouse	Biotin	Horse	ICC	400	Vector Labs
Goat IgG	α-goat	Biotin	Horse	ICC	400	Vector Labs
Rabbit IgG	α-rabbit	Alexa594	Donkey	ICC/IHC	400	Life Technologies
Biotin	Extravidin	Cy3	–	ICC/IHC	600	Sigma

c, concentration; DF, dilution factor; ICC, immunocytochemistry; IHC, immunohistochemistry; GFAP, glial fibrillary acidic protein; Iba1, ionized calcium binding adapter molecule 1.

Probes®) were stained for 5 min at 37°C, extracellular fluorescence quenched with 0.2% trypan blue and cells imaged. Two experiments were performed and results assessed qualitatively.

OX42-IMMUNOPORTER CONJUGATION

OX42 antibody in HEPES-buffered saline (HBS), pH 7.9, was modified with 10 mM *N*-Succinimidyl 3-(2-pyridyldithio)-propionate NHS ester (SPDP, ThermoFisher) at a ratio of 1.3 μL SPDP/mg OX42 for 2 h at room temperature. SPDP-modified antibody was desalted on PD-10 columns, protein positive fractions identified (DC-Protein Assay, Bio-Rad), pooled and antibody concentration estimated on a spectrophotometer (280 nm). Absorbance of the leaving group pyridine-2-thione was measured at 343 nm to calculate conjugation efficiency at the end of the immunoporter synthesis.

Branched 25 kDa PEI (Sigma) was dissolved in ultrapure water, neutralized with concentrated HCl, and desalted and buffer exchanged on PD-10 columns to HBS, pH 7.9. PEI-containing fractions were pooled and the PEI-concentration estimated with a TNBS-assay (2,4,6-trinitrobenzene sulfonic acid, Sigma) described by Snyder and Sobocinski (1975) and adapted for 96-well microplates.

Neutralized PEI was engrafted with PEG by incubating PEI with a 7.5 molar excess of 125 mM NHS-activated TMS$(PEG)_{12}$ (ThermoFisher) for 1 h at room temperature under nitrogen atmosphere. Under these reaction conditions, 12 PEG molecules bind to 1 molecule of PEI (data not shown). PEI–PEG was then purified on a PD-10 desalting column and PEI content estimated with a TNBS-assay.

PEI–PEG was modified with SPDP by incubating PEI–PEG in HBS (pH 7.9) with 5 μL of 10 mM SPDP per milligram PEI–PEG for 1 h at room temperature. SPDP-modified PEI–PEG was desalted on a PD-10 column and an excess of 150 μL of 25 mg/mL dithiothreitol (DTT, Sigma) added to activate SPDP-modified PEI–PEG. The mixture was incubated for 1 h at room temperature under nitrogen atmosphere. After reaction, the mixture was desalted to remove cleaved pyridine 2-thione and DTT. PEI-concentration was estimated with a TNBS-assay. Activated SPDP-modified PEI–PEG were prepared immediately before conjugation to avoid extended exposure to air and oxidization of the reactive sulfhydryl-group.

SPDP-modified OX42 antibody and activated SPDP-modified PEI–PEG were incubated overnight at a molar ratio of OX42 to PEI–PEG of 1:3. Incubation was done at room temperature under nitrogen in presence of 0.1 mM ethylenediaminetetraacetic acid (EDTA, Sigma). After incubation, the reaction mixture was desalted and protein-positive (280 nm) as well as pyridine-2-thione positive fractions (343 nm) pooled separately.

Conjugated OX42-immunoporter was purified in a first step with a HiTrap SP/HP cation exchange column (GE Healthcare) using increasing molarities of salt (0.5–3 M NaCl). The eluted OX42-immunoporter conjugate was then purified in a second step on a HiLoad 16/60 Superdex 200 gel filtration column (GE Healthcare) connected to a FPLC (BioLogic DuoFlow, Bio-Rad). The final bioconjugate was concentrated with 100 kDa ultrafiltration spin columns (Millipore) to 2–3 mg/mL in HBS, pH 7.3.

The average molar ratio of conjugated OX42 antibody and PEI–PEG was calculated based on the release of pyridine-2-thione according to the manufacturer's instructions and found to be $n = 1.1$. The yield of conjugated OX42-immunoporter was 40%.

PLASMID DNA CLONING AND PURIFICATION

Plasmid DNA was cloned and subcultured in competent DH5α *Escherichia coli* cells (Life Technologies) using standard procedures. An enhanced EGFP-expressing plasmid (pEGFP-N1, 4.7 kb) was a gift from Dr. W. Kruger (RMIT University, Melbourne) and was purified with NucleoBond® PC 2000 Kit (Macherey-Nagel) according to the manufacturer's instructions. The purity of plasmid preparations was $A_{260/280} \geq 1.9$ for all preparations and the integrity of sub-cloned pEGFP-N1 was confirmed by restriction enzyme analysis. A control vector pcDNA3.1/Zeo(+; 5.0 kb) which lacks the EGFP gene was a gift from Dr. H. Cuny (RMIT University, Melbourne).

GEL RETARDATION ASSAYS

The ability of PEI polyplexes to bind DNA (400 ng/well) was tested at nitrogen/phosphate (N/P) ratios of 2–10. The N/P-ratio was calculated by taking into account the molar concentration of nitrogen residues (23.2 mmol/L) of 25 kDa branched PEI and a phosphate content of 3 nmol per 1 μg nucleic acid. PEI-conjugates and pDNA (0.1 mg/mL in HBS, pH 7.3) were mixed to form PEI-pDNA complexes and incubated at room temperature for 30 min. Gel loading buffer (10X BlueJuice™, Life Technologies) was added and samples run on a 0.8% agarose gel (Promega) for 40–60 min at 100 V. Images were acquired on a fluorometer after DNA staining (SYBR® Safe DNA, Life Technologies).

POLYPLEX PREPARATION AND TRANSFECTION EXPERIMENTS

PEI–PEG and OX42-immunogene polyplexes were prepared at an N/P-ratio of 4. Transfectants (0.5 mg/mL in HBS) were added slowly to pDNA (0.5 mg/mL in HBS) and incubated for 15 min without vortexing. For *in vitro* transfections (20 μg DNA per well), complete cell culture medium (DMEM with 10% FBS) was then added to a total volume of 0.5 mL and the solution mixed by pipetting up and down. After removing the astrocyte-conditioned medium, mixed glia cultures were incubated with polyplexes for 16–24 h. For transfections performed in the presence of 100 μM chloroquine (Sigma), transfection medium was removed after 4 h. After removal of transfectants, a 1:1 mixture of fresh complete medium and astrocyte conditioned medium was added and cells were fixed (4% PFA, 10 min) after a total of 72 h and immunostaining performed.

Polyplexes were injected into three different brain regions of individual Sprague-Dawley rats (300–350 *g*). PEI–PEG and OX42-immunogene polyplexes were injected into the PVN (200 ng DNA; left side: PEI–PEG, right side: OX42-immunogene) or dorsal striatum (300 ng DNA). Three microgram of DNA were injected with the OX42-immunogene into the right lateral ventricle. Rats were perfused after 72 h and brain sections obtained as outlined in Section "Cellular Distribution of CD11b *In Vivo*" and IHC performed.

Transfection efficiency and specificity of PEI–PEG and OX42-immunogene *in vitro* was assessed by cell counting and was

based on cell type specific markers. Values were expressed as mean ± standard error of mean (SEM) and significance assessed with either a Student's *t*-test or one-way ANOVAs with *post hoc* *t*-tests with Bonferroni correction or *post hoc* one-sample *t*-tests with Bonferroni correction.

STUDY OF OX42-IMMUNOGENE AGGREGATION BY DYNAMIC LIGHT SCATTERING

The size-distribution profile of the OX42-immunogene polyplexes was investigated by adding complete cell culture medium (DMEM with 10% FBS), OX42-immunoporter (10.3 μg) and pDNA (20 μg, to form OX42-immunogene) in this order to the measurement vial used for DLS. The effect of diluents on OX42-immunogene aggregation was determined by adding HBS, DMEM (+FBS) or DMEM (–FBS) after polyplex maturation in HBS or DMEM (+FBS).

Raw data was acquired for 30 s for each measurement (three measurements per experiment) with a Fast DLS analyser (ALV GmbH, Germany). Intensity weighted size-distribution profiles were obtained from correlation functions using ALV-Correlator Software (ALV GmbH). The hydrodynamic diameter with the highest intensity for each experiment was obtained by averaging the values from the three separate measurements. Polyplexes were prepared twice for each experimental condition.

MEASUREMENT OF REACTIVE OXYGEN SPECIES PRODUCTION

A 96-well plate assay was developed to measure ROS production using the ROS-sensitive dye CM-H_2DCFDA [5-(and-6)-chloromethyl-2′,7′-dichloro-dihydro-fluorescein diacetate, acetyl ester; Molecular Probes®] which responds to intracellular oxidation with increase in fluorescence of its product DCF. Microglia were loaded with 5 μM dye in Krebs-HEPES-buffer (KHB) and incubated for 30 min (37°C). One microgram of OX42 antibody and non-viral vehicles (N/P = 4) were added to the wells and incubated at 37°C. Particulate zymosan A (Sigma, 1.5 μg/well) was used as positive control to trigger the respiratory burst and the NADPH oxidase inhibitor diphenyliodonium (DPI, Sigma) was used at 1 μM to abolish ROS production. Fluorescence was read on a plate reader (FlexStation 3) after 60 min. Baseline fluorescence values (KHB only) were subtracted and results expressed as percentage of the response to 100 ng/mL of the protein kinase C (PKC) activator phorbol-12,13-dibutyrate (PDBu, Enzo Life Sciences) which was used to normalize the responsiveness of different batches of isolated microglial cells. Results were expressed as mean ± SEM (n = 4–7 experiments in quadruplicate measurements) and significant ROS production was assessed with a one-way ANOVA test using *post hoc* one-sample *t*-tests with Bonferroni correction.

RESULTS

INTEGRIN CD11b IS EXPRESSED IN MICROGLIA BUT NOT IN ASTROCYTES

In order to develop microglia-specific vehicles for gene delivery with the OX42 antibody, we first investigated the cellular distribution of the target receptor CD11b. CD11b-immunreactive cells in mixed culture stained positive for Iba1 protein (**Figure 1A**). However, cells that expressed GFAP protein were not positive for CD11b (**Figure 1B**). This confirmed that CD11b expression is specific for microglia *in vitro* and that OX42 antibody binds to microglial cells only.

When Alexa 488-tagged OX42 and X63 antibodies where injected into rat brain, OX42-Alexa 488 showed strong green fluorescence and labeled many cells that appeared to be non-activated microglia with small cell bodies and long, fine processes (**Figures 1C,D**). However, X63-Alexa 488 fluorescence was only visible along the needle track and this control antibody did not bind to cells distant to the injection site (data not shown). Immunohistochemistry for microglia and astrocytes showed that the injected OX42 antibody specifically bound to microglial cells, because CD11b-positive cells also immunostained for Iba1 (**Figure 1C**). However, CD11b-IR did not co-localize with GFAP-positive astrocytes (**Figure 1D**). Thus, the *in vivo* data confirmed the specificity of CD11b for microglia, consistent with results obtained from immunofluorescence studies in cultured cells.

OX42 IS INTERNALIZED INTO MICROGLIA VIA CD11b RECEPTOR AND TRAFFICKED TO LYSOSOMES

While specificity of an antibody is an important aspect for non-viral gene delivery, internalization of OX42 is required to deliver genes into the cell. Live cell experiments demonstrated that strong vesicle-like fluorescence accumulated in the perinuclear region of isolated microglial cells (**Figure 2A**). As a control, microglia were incubated with OX42-FITC on ice to halt internalization. Microglia exhibited CD11b-IR only in the cell membrane under this condition (**Figure 2A**) confirming that OX42 binds to an extracellular epitope of CD11b. Alexa 488-tagged X63 antibody did not bind nor was internalized into microglia after 60 min (**Figure 2A**) suggesting that the uptake of OX42 antibody is mediated by the CD11b receptor and does not occur via other receptors, for instance Fcγ-receptors, or other non-specific mechanisms such as pinocytosis.

Internalization of OX42 antibody was further investigated in a time-lapse experiment. After the initial 5 min incubation period, OX42-FITC fluorescence in the perinuclear region increased rapidly and significantly (10 min: 163 ± 18 AU; 20 min: 232 ± 26 AU; 60 min: 448 ± 50 AU; $P < 0.0001$; **Figure 2B**).

In order to investigate the intracellular fate of internalized OX42 antibody, internalization experiments were repeated with Alexa 488-tagged OX42 antibody due to the pH-dependence of FITC fluorescence. Microglial cells were co-labeled with Lysotracker Red, a dye that accumulates in acidic vesicles and is often used to visualize lysosomes. OX42-Alexa 488 antibody accumulated in perinuclear vesicles after 60 min (**Figure 2C**) as observed in previous internalization assays. Antibody-containing vesicles were essentially all positive for Lysotracker Red staining demonstrating that internalized OX42 antibody is trafficked to acidic organelles that most likely represent late endosomes and lysosomes. Quenching the extracellular fluorescence further confirmed that the observed perinuclear fluorescence originates from intracellular vesicles (**Figure 2C**).

In summary, these experiments demonstrated that the OX42 antibody may be a suitable ligand for non-viral gene delivery into

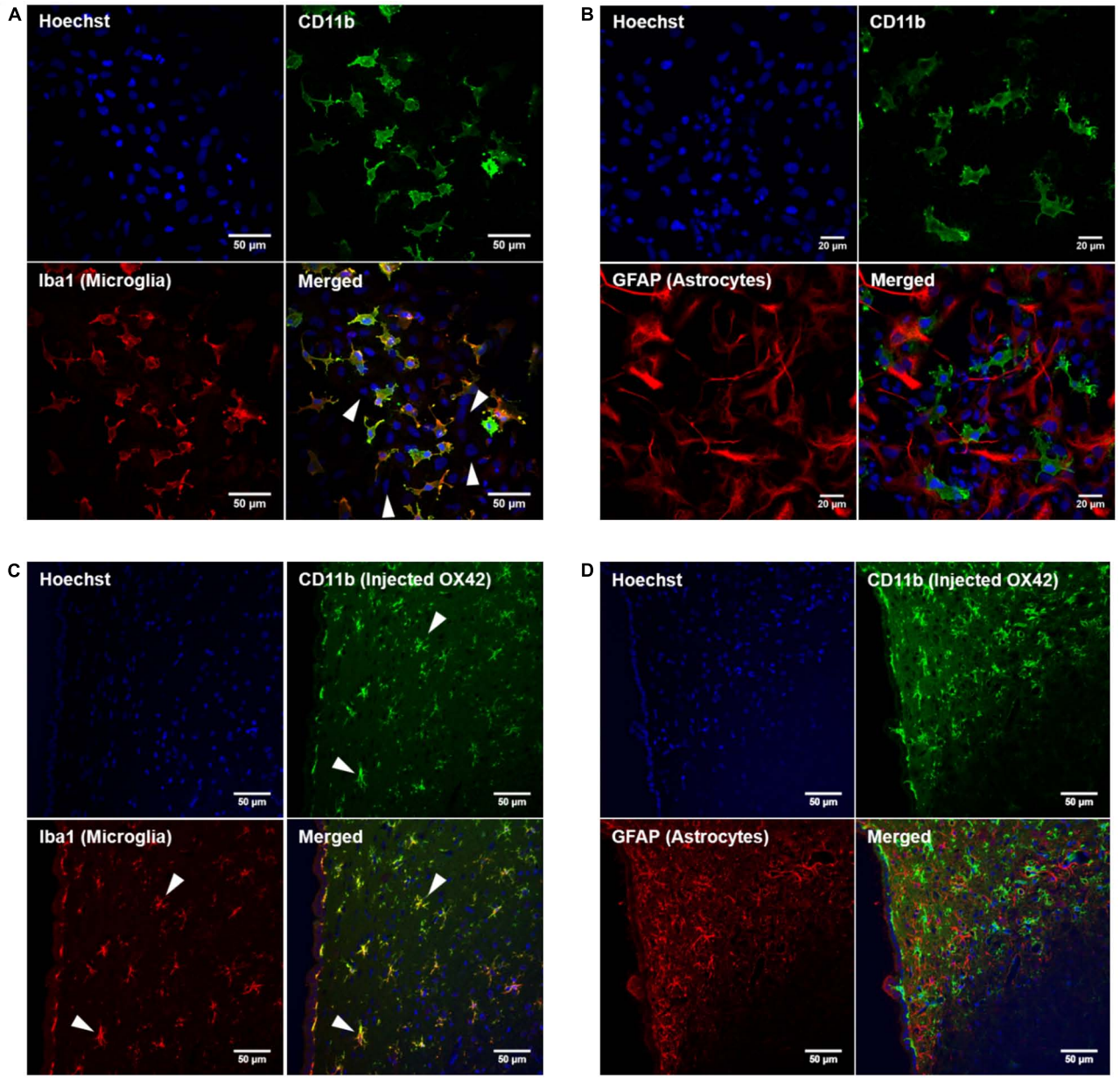

FIGURE 1 | Integrin receptor CD11b is specific for microglia *in vitro* and *in vivo*. (A) CD11b-positive cells (green) in mixed glia culture stained for the selective microglia marker Iba1 (red). Many cells that stained for the nuclear dye Hoechst were negative for CD11b and Iba1 (white arrow heads). **(B)** GFAP-positive cells (red) did not immunostain for CD11b (green) *in vitro*. **(C)** Immunohistochemistry of rat brains injected with OX42-Alexa 488 (green) demonstrated co-labeling with microglial marker Iba1 (red, white arrow heads). **(D)** GFAP-IR (red) and CD11b-IR (green) did not co-localize showing that astrocytes do not express CD11b or take up OX42 antibody.

microglia. Thus, a microglia-targeting OX42-immunoporter was developed by conjugating the OX42 antibody to PEG-engrafted PEI (PEI–PEG) via the hetero-bifunctional linker SPDP.

THE OX42-IMMUNOPORTER BINDS PLASMID DNA

The ability of the OX42-immunoporter bioconjugate to bind pDNA and form the OX42-immunogene was tested in gel retardation assays. OX42-immunoporters as well as PEI and PEI–PEG were able to bind plasmid DNA with increasing Nitrogen (PEI) to Phosphate (plasmid DNA; N/P) ratios (**Figure 3**). The OX42-immunoporter vehicle completely retarded pDNA at N/P = 5.

THE OX42-IMMUNOGENE REDUCES OFF-TARGET TRANSFECTION *IN VITRO*

Transfection efficiency and specificity of the targeting OX42-immunogene vs. non-targeting PEI–PEG were then compared in mixed glia culture. PEI–PEG transfected Iba1-IR microglia (yellow arrow heads) and GFAP-IR astrocytes (white arrow heads)

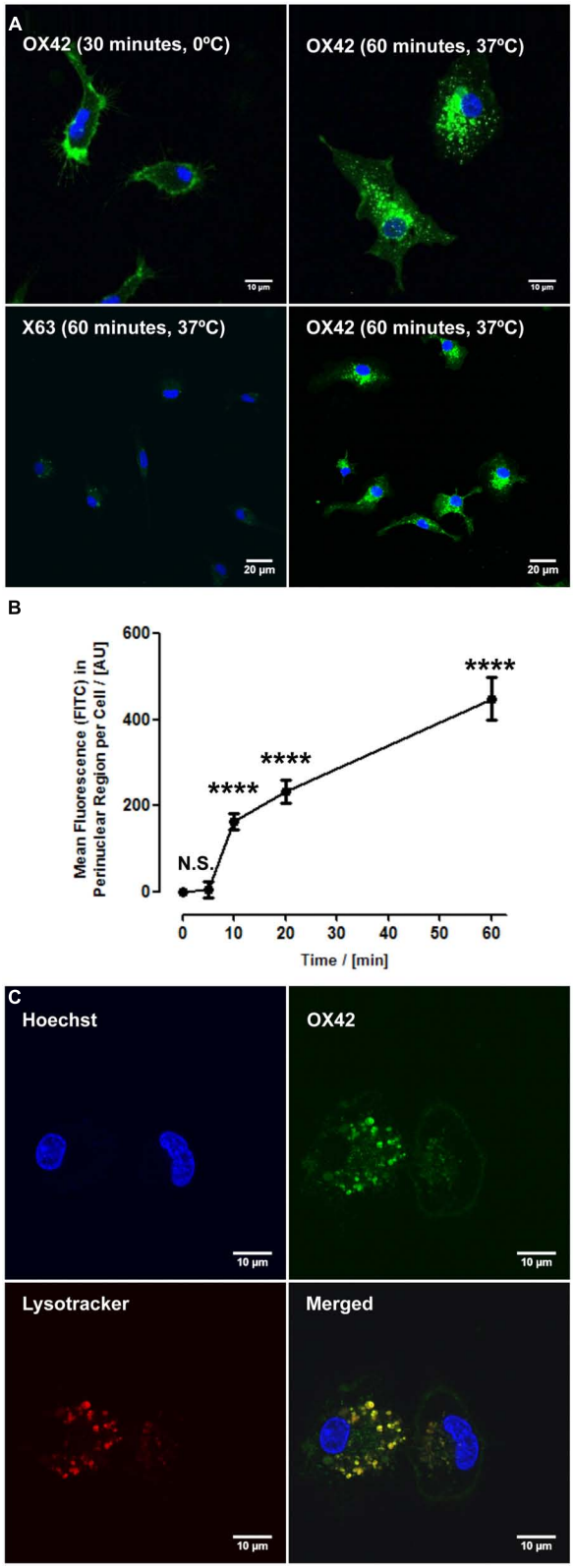

FIGURE 2 | OX42 antibody is internalized into microglia and accumulates in perinuclear acidic vesicles. (A) Microglial cells incubated *(Continued)*

FIGURE 2 | Continued
on ice with OX42-FITC (green) immunostained for CD11b in the membrane only. Microglia incubated with OX42-FITC at 37°C showed green fluorescent vesicles close to the cell nucleus (Hoechst-dye, blue) indicating the uptake of OX42 antibody into microglia. The negative control antibody X63 did not bind and internalize in microglia. **(B)** Quantification of FITC fluorescence demonstrated a rapid increase and accumulation of OX42 antibody in the perinuclear region of microglia. **(C)** The internalization of OX42 antibody was confirmed by quenching the extracellular fluorescence with trypan blue. Confocal images revealed that OX42 antibody accumulates in perinuclear acidic vesicles in microglial cells as observed by the co-localization of the acidic organelle marker Lysotracker Red. Values are plotted as Mean ± SEM. $n \geq 77$ cells per time-point. $^{****}P < 0.0001$ vs. control; N.S., not significant; AUs, arbitrary units.

as shown by EGFP-specific green fluorescence (**Figure 4A**, upper panel). The OX42-immunogene transfected very few cells *in vitro* and only some of them were potentially GFAP-negative microglia (yellow arrow heads), others were GFAP-positive astrocytes (white arrow heads, **Figure 4B**, lower panel). Quantification revealed that PEI–PEG transfected significantly more cells per coverslip than the OX42-immunogene (214 ± 37 vs. 5 ± 2, $P < 0.005$, **Figure 4B**). However, 80–90% of PEI–PEG-transfected cells were GFAP-IR astrocytes and not microglia (data not shown). Through incorporation of the OX42 antibody into the non-viral vehicle, the OX42-immunogene decreased the number of transfected cells significantly, but approximately 4 out of 5 transfected cells were still GFAP-IR astrocytes. Thus, the OX42-immunogene reduced off-target gene delivery into astrocytes, but did not cause substantial gene expression in microglia.

INGESTION OF THE OX42-IMMUNOGENE IS ASSOCIATED WITH INCREASE OF NON-SPECIFIC FLUORESCENCE

The low number of cells that were transfected with the OX42-immunogene prompted an investigation of the cause of the lack of EGFP expression in microglia. Confocal images at lower magnification demonstrated that PEI–PEG caused green fluorescence of different intensities (yellow and blue arrow heads, **Figure 5A**). In OX42-immunogene treated cells, mainly green fluorescence of low intensity was observed (blue arrow heads, **Figure 5A**) and this fluorescence was almost exclusively seen in GFAP-negative microglia (**Figure 5A**).

At higher magnification and increased laser power and gain (**Figure 5B**), cells that exhibited high intensity of green fluorescence were also IR for an anti-EGFP antibody (**Figure 5B**). EGFP-specific fluorescence was distributed within the cytoplasm and cell nucleus in PEI–PEG transfected cells. In contrast, the green fluorescence of low intensity was vesicle-like, concentrated around the cell nucleus and EGFP-IR was absent (**Figure 5B**). This indicated that the non-specific fluorescence is unrelated to EGFP expression. CD11b-immunoreactive microglia were the predominant cell type that displayed non-specific fluorescence upon treatment of mixed cultures with non-viral vehicles (yellow arrow heads, **Figure 5B**).

In order to firmly establish that the non-specific fluorescence was unrelated to EGFP-expression, mixed cultures were transfected as previously but delivering an empty control vector that lacked the EGFP reporter gene. After 3 days, PEI–PEG and

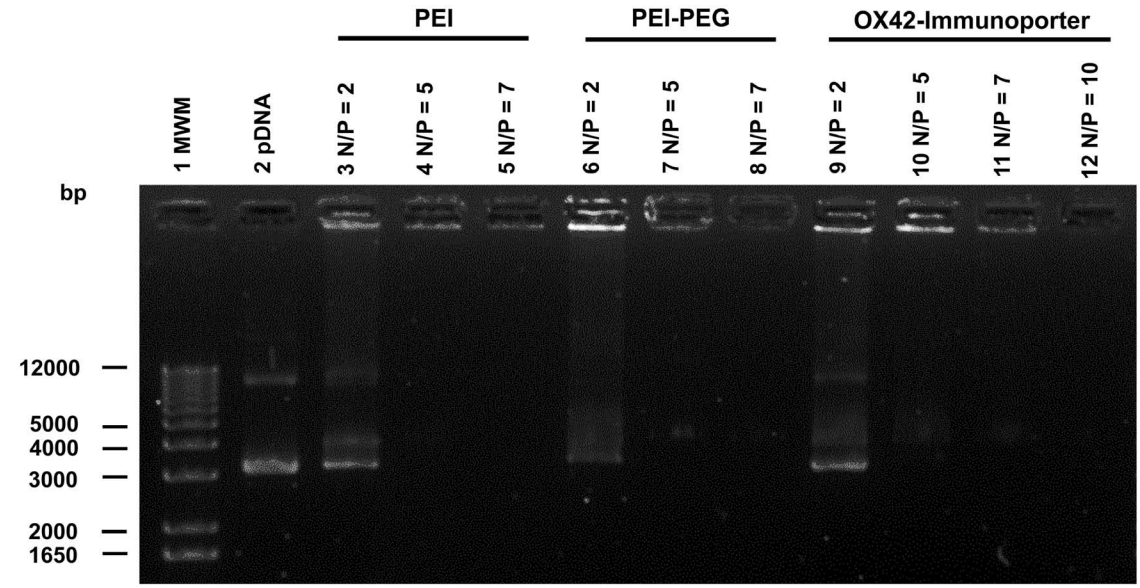

FIGURE 3 | Gel retardation assay demonstrates the ability of the OX42-immunoporter in binding and retarding plasmid DNA. Non-linearized pDNA alone (lane 2) migrated in two main bands. PEI (lanes 3–5) and PEI–PEG (lanes 6–8) completely retarded plasmid DNA at N/P-ratios of ≥5. The OX42-immunoporter (lanes 9–12) bound and retarded DNA with increasing N/P-ratios forming an OX42-immunogene. PEI, polyethyleneimine; PEG, polyethylene glycol; IP, immunoporter; bps, base pairs; pDNA, plasmid DNA.

OX42-immunogene treated cultures exhibited the same pattern of non-specific fluorescence (**Figure 6**) as observed in cultures treated with the transfectants carrying the EGFP-expressing plasmid (**Figures 5A,B**). This non-specific fluorescence was localized in GFAP-negative microglia, while untreated control cells had only a very low level of non-specific background fluorescence (**Figure 6**). Thus, the increase in intracellular, non-specific fluorescence was due to treatment of mixed cultures with PEI–PEG and the OX42-immunogene and it indicated that PEI–PEG and the OX42-immunogene were internalized but failed to cause gene expression in microglia

THE OX42-IMMUNOGENE DOES NOT TRANSFECT MICROGLIA *IN VIVO*

Whether the inability of the OX42-immunogene to cause EGFP expression in microglia was an artifact of the *in vitro* test system or reflected the actual inability of the OX42-immunogene to transfect microglia was investigated *in vivo* by injecting PEI–PEG and the OX42-immunogene into different brain areas.

PEI–PEG and the OX42-immunogene injected into the PVN (data not shown) caused an increase in green fluorescence as observed after injections of the OX42-immunogene into the right lateral ventricle (**Figure 7A**) and the dorsal striatum (**Figure 7B**). The majority of cells displaying green fluorescence were Iba1-IR microglial cells (yellow arrow heads, **Figure 7A**) that acquired a round amoeboid or phagocytic shape. Astrocytes did not exhibit green fluorescence (data not shown). The green fluorescence seen in microglia appeared to be non-specific as judged by the vesicle-like structure and absence of fluorescence in the nucleus as observed in EGFP-transfected cells *in vitro* (**Figure 5B**). After OX42-immunogene injection into the dorsal striatum, absence of EGFP-expression was demonstrated in brain sections either imaged directly without performing IHC or immunostaining with a mouse anti-EGFP antibody (**Figure 7B**). In absence of cell type specific markers, the fluorescence observed was non-specific and also seen in the red filter. Further, EGFP-IR was not observed either (**Figure 7B**) demonstrating that EGFP was not expressed *in vivo*. Further, the absence of an increased red fluorescence due to the secondary anti-mouse antibody also suggested that the OX42-immunogene was degraded, because the secondary antibody did not cross-react with the OX42 antibody component of the immunogene. Thus, the absence of EGFP-expression in microglia *in vivo* was consistent with the lack of EGFP-expression *in vitro*.

OX42-IMMUNOGENE AGGREGATES TRIGGER THE RESPIRATORY BURST IN MICROGLIA

The uptake of the non-viral vehicles into microglia, the apparent intracellular degradation concomitant with increase in non-specific fluorescence and the absence of widespread gene expression in microglia prompted an investigation into the reasons of this phenomenon. Initial experiments aimed at determining the size-distribution profiles for the OX42-immunogene formed in complete cell culture medium (DMEM with 10% FBS, **Figure 8A**). Complete cell culture medium contained small aggregates of <100 nm in diameter (**Figure 8A**). There was no marked difference in the size-distribution profile when the OX42-immunoporter was added suggesting that the vehicle had not substantially aggregated. However, when pDNA was added to form the OX42-immunogene complex (N/P = 4), large OX42-immunogene aggregates formed over a wide diameter range (≈50–1300 nm, **Figure 8A**). Based on the aggregate sizes observed, this suggested that the OX42-immunogene could potentially

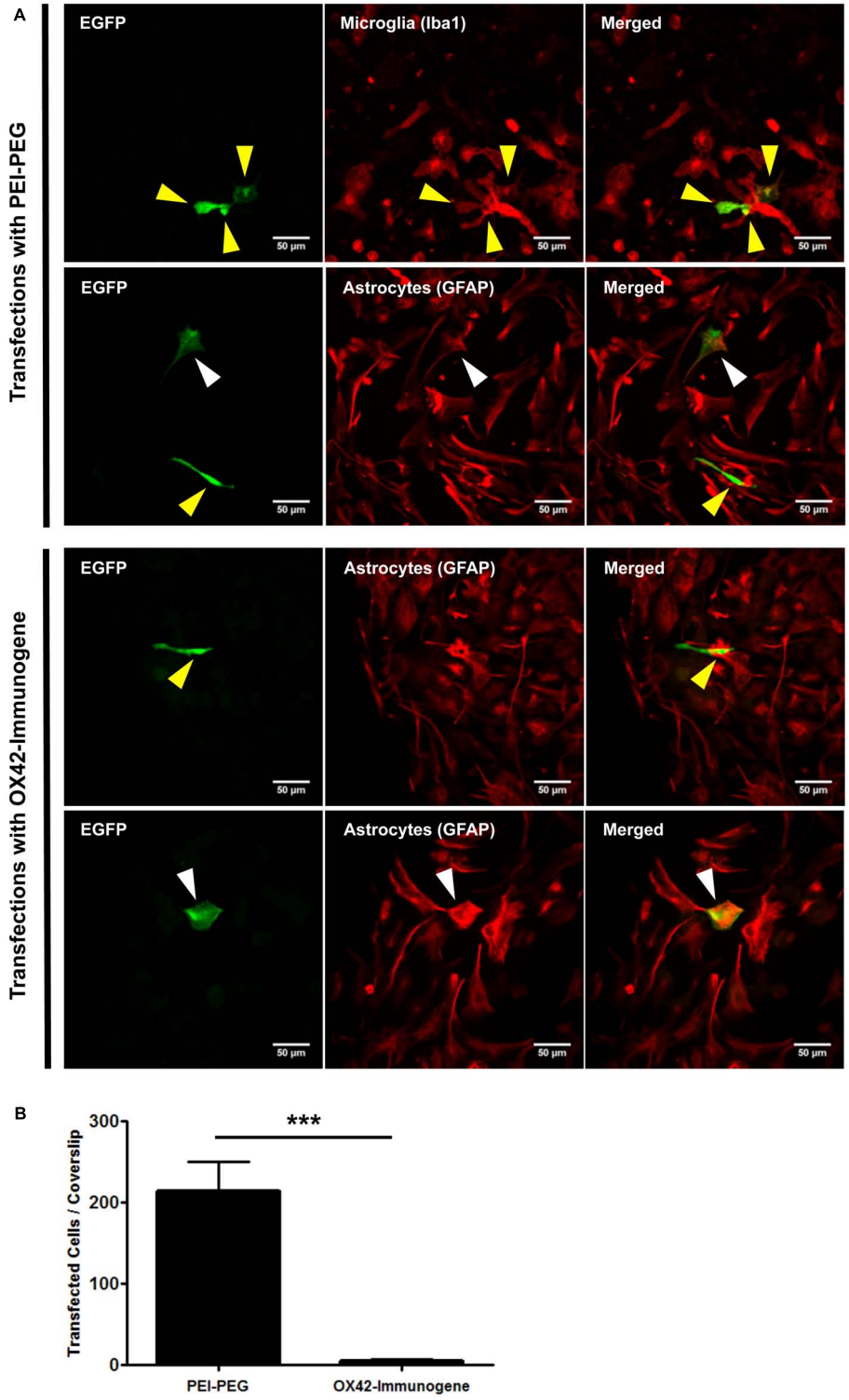

FIGURE 4 | The OX42-immunogene reduces off-target transfection of PEI–PEG *in vitro*. **(A)** Representative confocal images of transfected cells in mixed culture. Non-targeting PEI–PEG (upper panel) transfected few microglial cells (yellow arrow heads) with an EGFP reporter plasmid as judged by EGFP fluorescence (green). EGFP-transfected cells were either Iba1-immunoreactive (IR, red, microglia) or lacked GFAP expression (red). PEI–PEG also transfected GFAP-IR astrocytes (white arrow heads). The targeting OX42-immunogene (lower panel) transfected few GFAP-negative cells that potentially are microglial cells (yellow arrow heads), but it also delivered the reporter gene into few GFAP-IR astrocytes (white arrow heads). **(B)** Quantification of transfected cells per coverslip. PEI–PEG (214 ± 37 cells) transfected significantly more cells than the OX42-immunogene (5 ± 2 cells). Values are plotted as Mean ± SEM. $***P < 0.005$. $n = 6$ coverslips for PEI–PEG and $n = 4$ coverslips for OX42-immunogene. EGFP, green fluorescent protein; GFAP, glial fibrillary acidic protein.

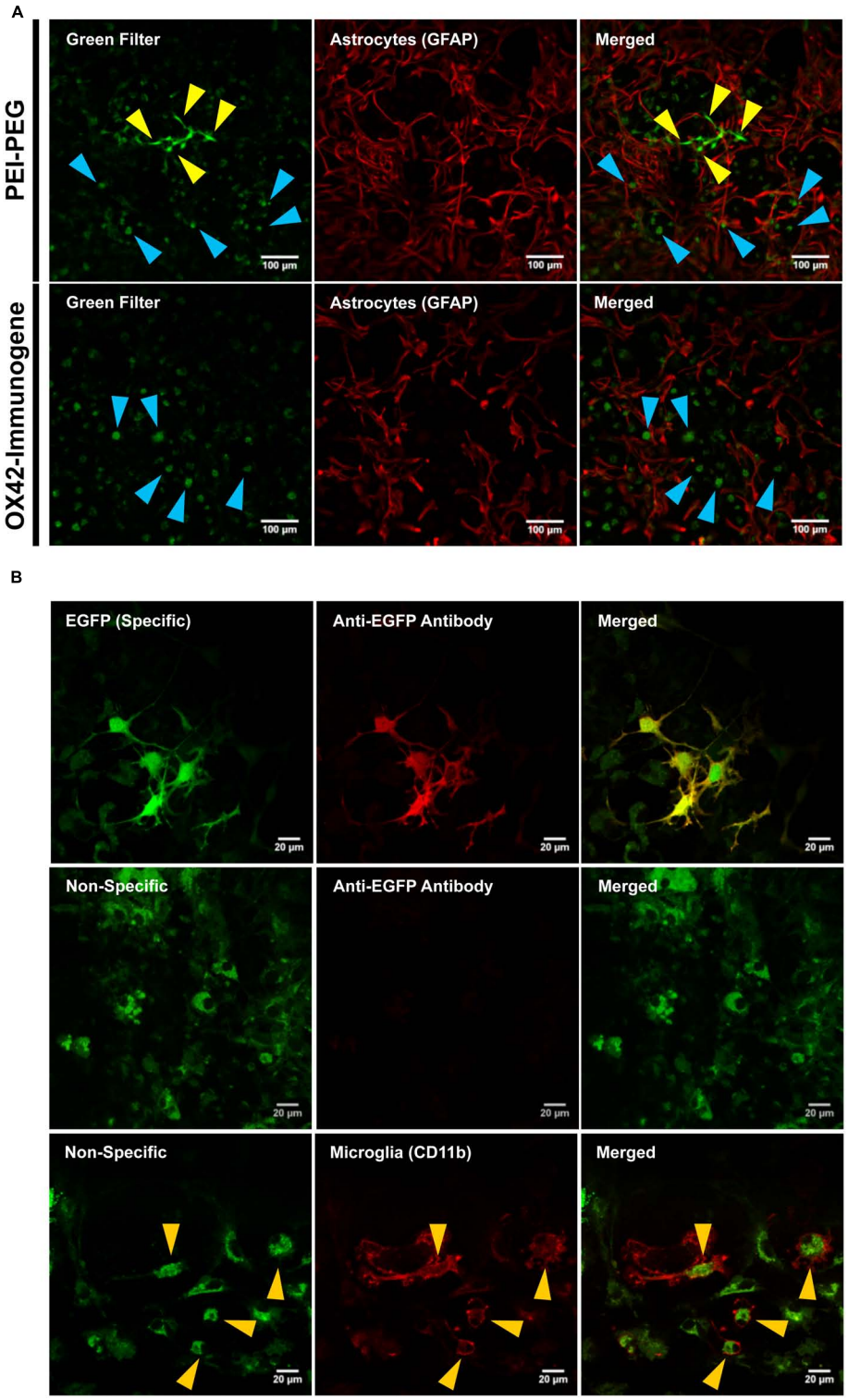

FIGURE 5 | The OX42-immunogene is taken up in microglia but does not cause gene expression *in vitro*. **(A)** PEI–PEG transfected few GFAP-negative (red) cells that potentially are microglia. Green fluorescence of high (yellow arrow heads) and low intensity (blue arrow heads) was visible for mixed cultures treated with either PEI–PEG or the OX42-immunogene. The green fluorescence of low intensity almost exclusively co-localized with GFAP-negative cells (blue arrow heads). **(B)** The green fluorescence of high intensity was EGFP-specific (green) and visible in the cytoplasm and cell nucleus. Specific fluorescence caused by EGFP-expression was confirmed with an anti-EGFP antibody (red). The green fluorescence of low intensity was unrelated to EGFP-expression (non-specific) as it did not co-localize with EGFP-IR. Non-specific fluorescence (green) was mainly localized in CD11b-IR microglia (red), appeared vesicle-like and accumulated in the perinuclear region. Note: when imaging non-specific fluorescence, laser power and gain were increased compared to imaging EGFP-specific fluorescence by confocal microscopy.

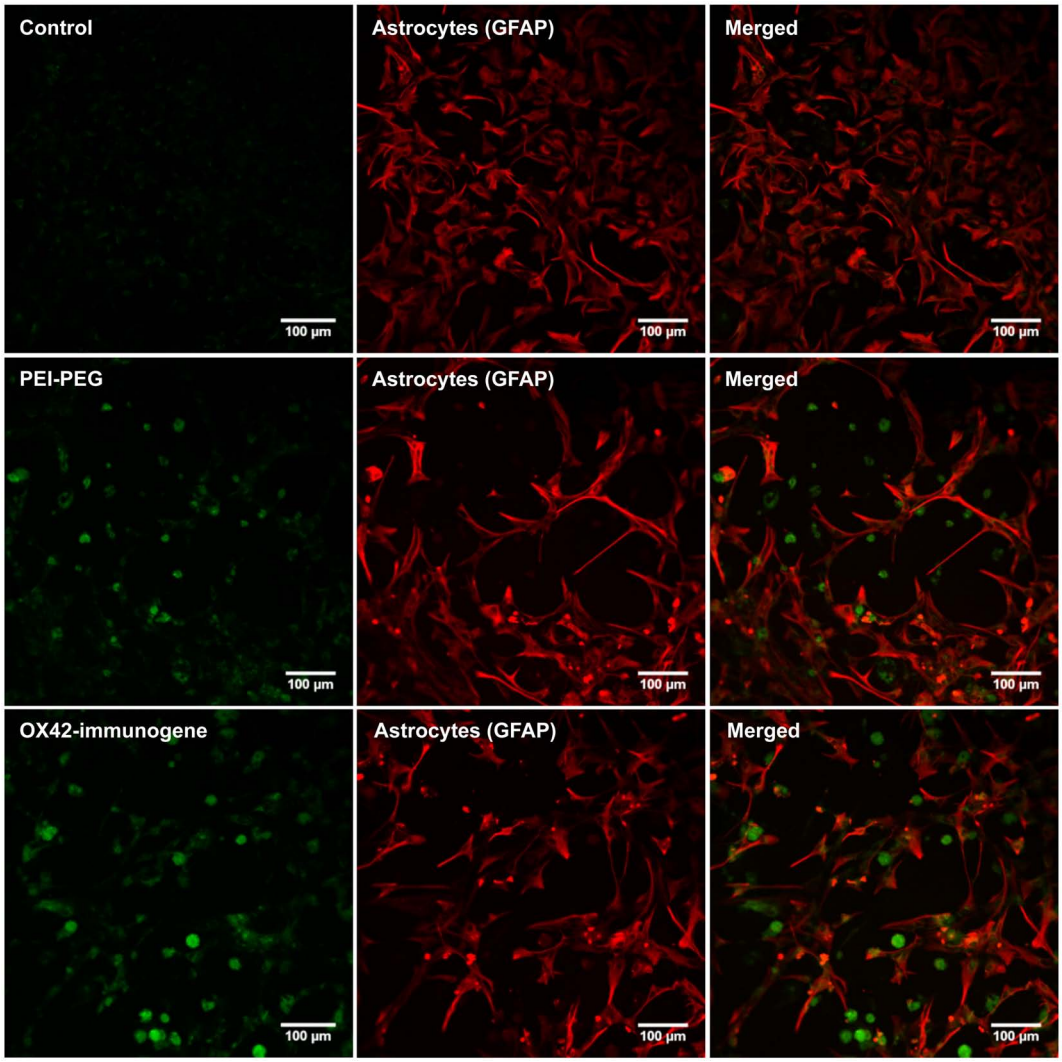

FIGURE 6 | Transfection experiments with a control vector that lacked the EGFP reporter gene caused an increase in non-specific fluorescence after treatment with PEI–PEG and the OX42-immunogene. Untreated control mixed cultures displayed very low levels of non-specific green background fluorescence.

be internalized via receptor-mediated endocytosis, but larger aggregates could trigger phagocytosis in microglia.

Further experiments were designed to understand how the aggregation behavior of the OX42-immunogene depended on sample preparation. The mode of OX42-immunogene aggregate size was found to be strongly dependent on FBS, either added as diluent after maturation of complexes in HBS or already present in the maturation buffer (**Figure 8B**). Although FBS caused a shift in the size-distribution profile to smaller aggregates, it did not markedly narrow the size-distribution (**Figure 8B**). DLS results further suggested that the absence of FBS for *in vivo* transfections would cause the formation and injection of larger aggregates as compared to *in vitro* transfections where the OX42-immunogene was formed in HBS, but FBS-containing cell culture medium was added to a final concentration of 9% FBS in the transfection medium.

The consequences of microglial phagocytosis of aggregated polyplexes were then investigated by measuring the production of ROS. There was a significant increase in the observed fluorescence of the ROS indicator in microglia treated with the OX42-immunogene (38.8 $\pm$ 3.3%, $P < 0.0001$; **Figure 8C**). DPI (1 μM), an inhibitor of the respiratory burst, abolished ROS production in microglia elicited by the aggregated OX42-immunogene (–7.02 $\pm$ 4.49%). Non-targeting PEI–PEG did not stimulate ROS production (–0.97 $\pm$ 3.74%) suggesting that the respiratory burst caused by the immunogene was mediated by specific receptors on the microglial membrane.

Further, aggregation of the OX42-immunogene as seen by DLS (**Figures 8A,B**) was crucial to trigger the respiratory burst, because OX42 antibody alone (2.57 $\pm$ 1.68%) and the non-aggregated OX42-immunoporter stimulated only low levels of ROS production (9.83 $\pm$ 2.84%). Particulate zymosan as a positive control

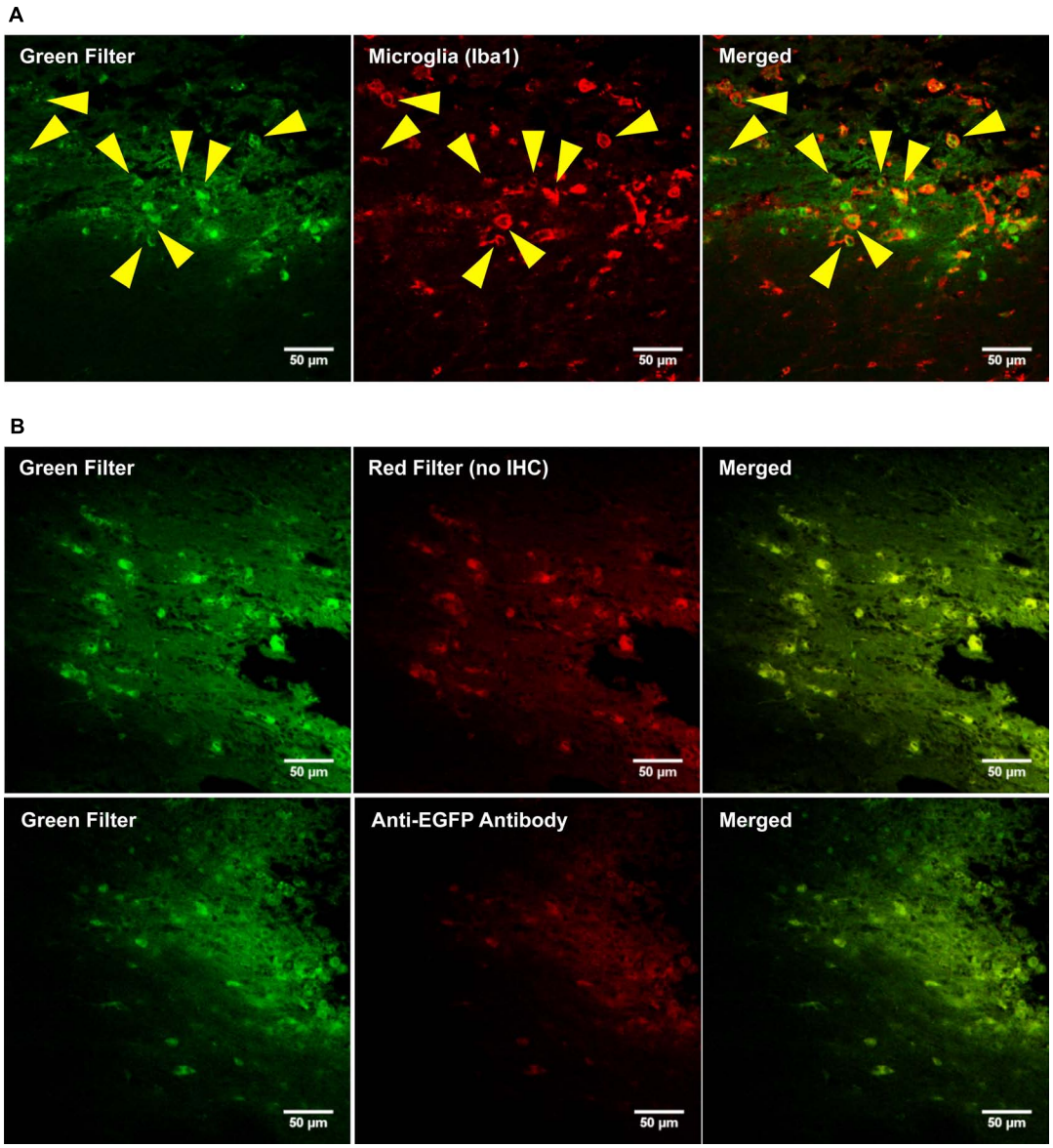

FIGURE 7 | The OX42-immunogene does not cause gene expression *in vivo*. **(A)** Representative confocal images show the OX42-immunogene injected into the right lateral ventricle caused an increase in green fluorescence that co-localized in Iba1-IR microglia which exhibited an amoeboid shape (yellow arrow heads). **(B)** Confocal imaging of brain sections (dorsal striatum) revealed that the green fluorescence observed is non-specific, because non-specific fluorescence was also seen in the red filter in absence of red fluorophore-labeled cell markers. Further, an anti-EGFP antibody did not detect EGFP-expression.

generated significant levels of ROS ($45.8 \pm 4.7\%$, $P < 0.01$) similar to the aggregated OX42-immunogene. Therefore, the aggregated OX42-immunogene triggered a strong inflammatory response in microglia as demonstrated by a phagocytosis-induced respiratory burst.

CHLOROQUINE FACILITATES ENDOSOMAL ESCAPE IN MICROGLIA

Dynamic light scattering data and the ROS assay showed that the OX42-immunogene formed large complexes with the ability to trigger phagocytosis and an unwanted immune response that potentially is linked to intracellular destruction of the immunogene. However, this data did not explain why non-targeting PEI–PEG in absence of the respiratory burst did not cause gene expression in microglia, although PEI–PEG was taken up by microglial cells (**Figures 5A,B** and **6**). Thus, we examined limited endosomal escape as an additional barrier to non-viral gene delivery into microglia.

Mixed glia cultures were transfected with PEI–PEG and the OX42-immunogene in the presence of the endosomolytic agent chloroquine. Chloroquine treatment significantly increased the total number of cells transfected with PEI–PEG (424 ± 42 vs. 74 ± 13, $P < 0.0001$) and the OX42-immunogene (71 ± 8

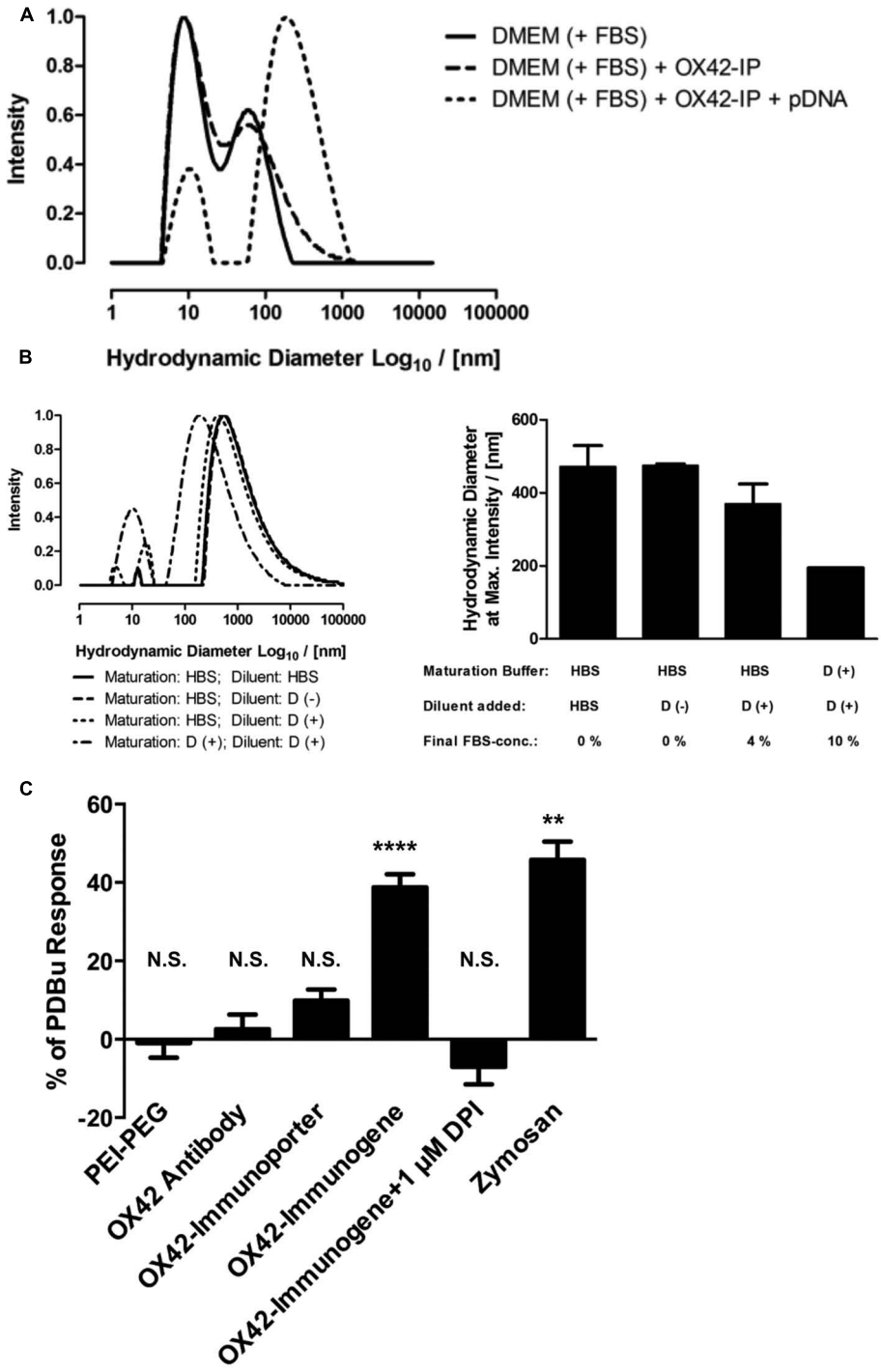

FIGURE 8 | The OX42-immunogene forms large aggregates and triggers an immune response in microglia. (A) Comparison of the size-distribution profiles between complete cell culture medium (DMEM + 10% FBS) and the OX42-immunoporter obtained by DLS shows that the non-viral vehicle did not form aggregates. After adding pDNA to form the OX42-immunogene (N/P = 4), aggregates formed over a large range (≈50–1300 nm). **(B)** Adding FBS to polyplexes after maturation in HBS and maturation of polyplexes in FBS-containing medium caused a shift in size-distribution to lower aggregate sizes, but it had no effect on the width of size-distributions. Values are plotted as Mean ± SEM (two experiments). FBS, fetal bovine serum; OX42-IP, OX42-immunoporter; HBS, HEPES-buffered saline; D (+/–), DMEM with/without 10% FBS. **(C)** ROS production in microglial cells was measured by quantifying ROS-indicator fluorescence after 60 min and reported as percentage (%) of the internal standard PDBu. The aggregated OX42-immunogene triggered the respiratory burst (38.8 ± 3.3%) which was inhibited by the respiratory burst inhibitor diphenyliodonium (–7.02 ± 4.49%). The positive control zymosan caused the release of ROS at similar levels (45.8 ± 4.7%) to the OX42-immunogene. However, PEI–PEG (–0.97 ± 3.74%), OX42 antibody (2.57 ± 1.68%) and the OX42-immunoporter (9.83 ± 2.84%) did not trigger significant ROS production. Values are plotted as Mean ± SEM. $^{**}P < 0.01$ vs. control; $^{****}P < 0.0001$ vs. control; N.S., not significant. DPI, diphenyliodonium; PDBu, phorbol 12,13-dibutyrate.

vs. 8 ± 3, $P < 0.0001$) at N/P = 4 (**Figure 9A**). Interestingly, chloroquine caused a significant increase in the percentage of transfected cells for both transfectants that were microglia (PEI–PEG: 20.3 ± 1.2% vs. 14.3 ± 1.7%, $P < 0.05$; OX42-immunogene: 32.3 ± 2.4% vs. 12.7 ± 8.0%, $P < 0.05$; **Figure 9B**) demonstrating that endosomal escape is limiting for non-viral gene transfer into microglia. However, despite this increase in presence of chloroquine the majority of the cells transfected with the OX42-immunogene were still not microglia. This showed that the OX42-immunogene is not entirely specific for microglia and the data strongly suggested the involvement of another route in internalization of the OX42-immunogene other than CD11b, for instance a receptor which is shared by microglia and other glial cells.

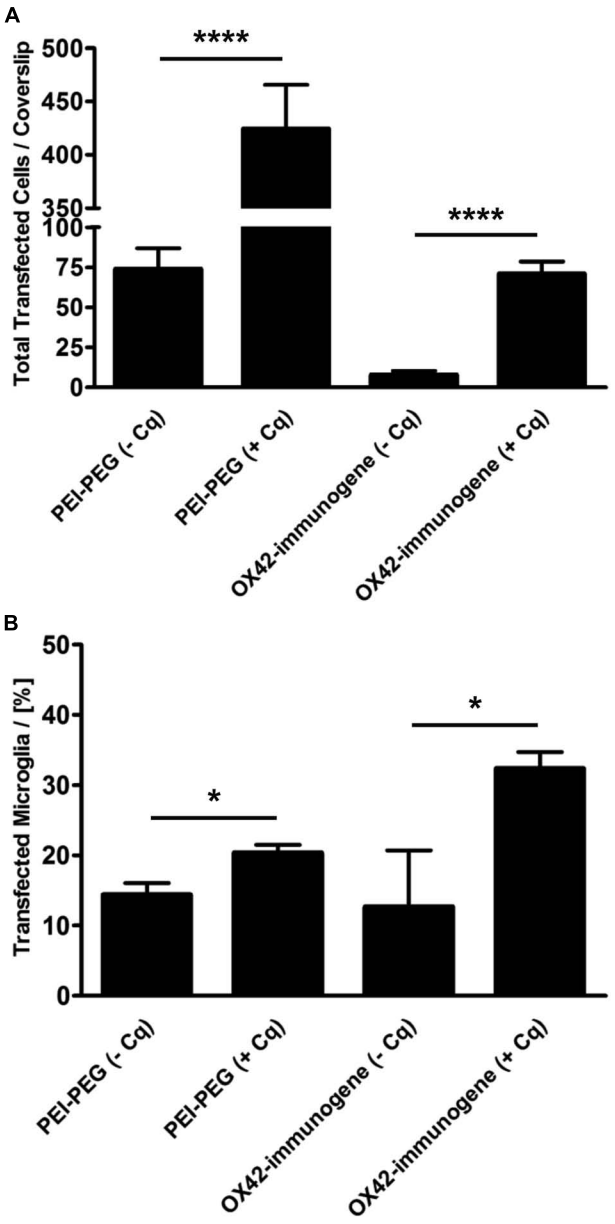

FIGURE 9 | The ability of PEI to facilitate intracellular escape in microglia is limited. (A) PEI–PEG (424 ± 42 vs. 74 ± 13) and the aggregated OX42-immunogene (71 ± 8 vs. 8 ± 3) transfected significantly more cells in the presence of chloroquine. **(B)** Chloroquine also increased specificity for microglia when transfected with PEI–PEG (20.3 ± 1.2% vs. 14.3 ± 1.7%) and the OX42-immunogene (32.3 ± 2.4% vs. 12.7 ± 8.0%). Values are plotted as Mean ± SEM. $n = 6$ coverslips (three independent experiments). $^*P < 0.05$, $^{****}P < 0.0001$. Cq, chloroquine.

DISCUSSION

This study took a systematic approach at examining the use of antibody-based non-viral vehicles for microglia-specific gene transfer. Double-labeling experiments in mixed cultures were performed with OX42 antibody and markers for the two most abundant cell types in mixed glia culture – GFAP for astrocytes and Iba1 for microglia. The experiments clearly demonstrated the specificity of CD11b for microglia. This is consistent with previous reports (Akiyama and McGeer, 1990) and accounts for the use of OX42 antibody as a selective microglial marker for immunocytochemistry and IHC. *In vivo* data confirmed the specificity of OX42 antibody for microglia and the absence of X63-binding strongly suggests attachment of OX42 to microglia via the CD11b receptor. Because microglia and other cells within the CNS express Fcγ-receptors (Ulvestad et al., 1994; Vedeler et al., 1994; Okun et al., 2010) that can bind antibodies and are also capable of ingesting extracellular material by pinocytosis (Booth and Thomas, 1991; Ward et al., 1991), the absence of these alternative internalization mechanisms is essential for specific gene transfer into microglia via CD11b.

The usefulness of the OX42 antibody was further emphasized by its property to be rapidly internalized into microglia. The negative control antibody X63 did not bind and was not taken up by microglia demonstrating that internalization of OX42 must occur via the extracellular domain of the CD11b receptor. Direct immunofluorescence studies and co-labeling with Lysotracker Red, a marker for acidic late endosomes and lysosomes, further showed that the internalized antibody was trafficked to acidic organelles in the perinuclear cytoplasm. The known perinuclear localization of lysosomes and late endosomes (Huotari and Helenius, 2011) agreed with the localization of OX42-fluorescence seen here confirming lysosomal trafficking of OX42 antibody in microglia. Lysosomal trafficking is desirable for non-viral vehicles that utilize PEI as DNA condensation agent, because the gradual acidification of endosomes facilitates the endosomal escape of the gene vehicle (Varkouhi et al., 2011). The proximity of lysosomes to the cell nucleus also improves transfection efficiency by reducing the spatial distance from endosome exit to nucleus entry (Forrest and Pack, 2002).

Since we demonstrated the usefulness of the OX42 antibody as microglia-specific ligand, a bioconjugate was developed based on the OX42 antibody and branched PEI of 25 kDa engrafted with PEG. The resulting OX42-immunoporter showed complete DNA-binding at a N/P-ratio of 5 as demonstrated in gel retardation assays. Subsequent transfection experiments were carried out at N/P = 4 to avoid an excess of PEI that can cause competing non-specific uptake mechanisms via positively charged PEI (Kircheis et al., 2001; Payne et al., 2007). Further, initial

transfection experiments with PEI–PEG at N/P = 10 reduced the number of transfected cells and appeared to have toxic effects in mixed glia culture as judged by the up-regulation of GFAP expression and morphology of astrocytes (data not shown).

The conjugation of the OX42 antibody to PEI–PEG caused significant reduction of off-target transfection of PEI–PEG *in vitro*. However, the OX42-immunogene transfected only few cells with no apparent increase in specificity for microglia. Expression of EGFP was mostly absent in microglia regardless of whether PEI–PEG or the OX42-immunogene was used for transfection *in vitro* and *in vivo*. This was demonstrated by the absence of EGFP-IR with an anti-EGFP antibody and by the observed pattern for green fluorescence of high intensity (EGFP, cytoplasmic and nuclear) and low intensity (non-specific, vesicle-like and perinuclear). Treating mixed glia cultures with PEI–PEG or the OX42-immunogene carrying a control vector that lacked the EGFP reporter gene then confirmed that the polyplexes were taken up by microglia and that the intracellular non-specific fluorescence is unrelated to EGFP expression. Thus, the non-specific fluorescence was thought to be related to an intracellular event downstream of internalization.

Previous work showed that cultured microglial cells exhibit non-specific fluorescence when treated with extracellular material destined for intracellular degradation (Stolzing et al., 2002). Importantly, microglia were shown to degrade only mildly oxidized protein efficiently while strongly oxidized proteins were accumulated intracellular and exhibited broad-spectrum auto-fluorescence (Stolzing et al., 2002). Incompletely degraded material that causes non-specific fluorescence has been termed "lipofuscin" (Sitte et al., 2000; Stolzing et al., 2002; Lei et al., 2012). The increase in non-specific, lipofuscin-like fluorescence in microglia therefore most likely originates from internalization and accumulation of incompletely degraded PEI–PEG and OX42-immunogene. The perinuclear localization of this vesicle-like, non-specific fluorescence suggests that microglia degrade the polyplexes in lysosomes. The observed amoeboid, phagocytic shape of microglia *in vivo* further indicates that microglia internalize the polyplexes by phagocytosis rather than receptor-mediated endocytosis.

Dynamic light scattering showed that the OX42-immunogene formed a heterogeneous population of aggregated polyplexes from less than 100 nm to more than 1 μm in diameter. This demonstrated that phagocytosis is one of the mechanisms by which the OX42-immunogene can be internalized. The stimulation of a respiratory burst demonstrated that the aggregated OX42-immunogene but not PEI–PEG and the OX42 antibody alone triggers a strong inflammatory response in microglia. Clearly, stimulation of an immune response is unwanted not only because this most likely trigger functions in microglia associated with their role as scavengers and cause destruction of the OX42-immunogene, but also because of potential exacerbation of neurodegeneration.

The data on ROS generation further gave evidence that the phagocytosis-induced respiratory burst not only requires aggregated large particles, but also receptors on the cell surface. Since the OX42-immunogene was developed to target CD11b on microglia and to undergo receptor-mediated endocytosis, aggregation of the OX42-immunogene most likely caused the stimulation of other receptors such as FcγR which require receptor cross-linking by antibody-coated targets (reviewed in Nimmerjahn and Ravetch, 2008). The OX42-immunogene may have mimicked antibody-coated immune complexes cleared by the phagocytic system of microglial cells. This could have occurred via phagocytosis receptors including CD11b and Fcγ-receptors as previously reported for macrophages (Thornton et al., 1996; Xia et al., 1999; Huang et al., 2011) that perform functions closely related to microglial cells.

Previous work on peripheral immune cells related to microglia revealed that CD11b and FcγRs interact to facilitate the rate of phagocytosis (Mantovani et al., 1972; Mantovani, 1975; Jongstra-Bilen et al., 2003; Huang et al., 2011). This observation becomes even more important when the binding site of OX42 on CD11b is considered. The OX42 antibody is suggested to bind to, or close to, the complement-binding site of CD11b (Robinson et al., 1986; Klegeris and McGeer, 1994; Sohn et al., 2003) which is important for phagocytosis of complement-coated apoptotic cells in absence of cytotoxic immune effector functions (Amarilyo et al., 2010; Hughes et al., 2010; Ricklin et al., 2010). The initiation of a respiratory burst therefore strongly argues for the involvement of FcγRs in uptake of the OX42-immunogene. Thus, the inability of the OX42-immunogene to cause substantial gene expression in microglia may be due to targeting receptors other than CD11b and directing the gene vehicle to a less efficient gene delivery pathway for microglial cells such as FcγR-mediated phagocytosis.

While the respiratory burst elicited by the aggregated OX42-immunogene limits its use for microglial gene transfer, non-targeting PEI–PEG at N/P = 4 did not cause substantial gene expression in microglia either albeit the absence of ROS production. Interestingly, PEI–PEG was more successful in gene transfer *in vitro*, although most of the transfected cells were astrocytes. PEI–PEG did not transfect any cells *in vivo* and was predominantly taken up by microglial cells with subsequent intracellular degradation. The unsuccessful transfection of microglia with PEI–PEG *in vivo* is consistent with a previous report that used N/P-ratios as high as 15 (Kwon et al., 2010). However, the difficulty of transfecting brain cells with non-viral vehicles *in vivo* may not be limited to PEI–PEG, because a novel cationic polymer that showed high transfection efficiency in culture was able to increase gene transfer *in vivo* only slightly as compared to naked DNA (Newland et al., 2014). The phagocytic/amoeboid morphology and expression of Iba1 on the cell membrane (Ohsawa et al., 2000) further suggested that PEI–PEG also stimulated microglial activation, although through apparent different mechanisms compared to the OX42-immunogene.

Data obtained by DLS hints at the sample preparation as decisive factor for particle size and the internalization mechanism triggered. PEI-polyplexes were prepared in physiological salt solution for *in vivo* injections. However, for *in vitro* transfections these complexes were further diluted in complete cell culture medium containing FBS. In accordance with studies performed in other cell types (Ogris et al., 1998; Petersen et al., 2002; Neu

et al., 2005), DLS data showed that sample preparation in general and the presence of FBS in particular shifts polyplex aggregates to smaller sizes that could favor endocytosis, at least for astrocytes. Therefore, larger aggregates may have been injected *in vivo* that shifted the internalization of PEI–PEG aggregates to professional phagocytes that take up large aggregates and destroy them such as microglia. While phagocytosis is a receptor-mediated internalization mechanism, non-specific internalization mechanisms such as macropinocytosis (Mayor and Pagano, 2007; Hufnagel et al., 2009; Xiang et al., 2012) may have occurred which is usually confined to immune cells such as macrophages and microglia (Kerr and Teasdale, 2009; Mandrekar et al., 2009; Mercer and Helenius, 2009).

The inability of PEI–PEG in this study to transfect a large number of microglia as compared to astrocytes point to different internalization mechanisms between these glia cells and the ineffectiveness of branched PEI (bPEI, 25 kDa) in promoting endosomal escape and gene transfer in microglia. This notion is further supported by the observation that in presence of chloroquine, a drug used previously to promote endosomal escape and enhance transfection efficiency of non-viral vehicles in other cell types (Erbacher et al., 1996; Ogris et al., 1998; Blessing et al., 2001), PEI–PEG and the OX42-immunogene transfected significantly more cells including microglia *in vitro*. Indeed, the success of gene transfer with PEI depends on polyplex type (linear or branched PEI, molecular weight) and the cell type transfected (Kircheis et al., 1997; Ogris et al., 1998; von Gersdorff et al., 2006; Intra and Salem, 2008) and may need to be optimized for microglial gene transfer. However, more than 60% of transfected cells in presence of chloroquine were not microglia even when cells were transfected with the OX42-immunogene. This supports the assumption that the aggregated OX42-immunogene not only targets the CD11b receptor but also FcγRs, because astrocytes and other brain cells express at least one FcγR subtype *in vitro* and *in vivo* (Nitta et al., 1992; Li et al., 2008; Okun et al., 2010).

CONCLUSION

This study highlighted for the first time the CD11b receptor as a potential target for non-viral gene transfer into microglia with antibodies. Data presented here show that the anti-CD11b antibody OX42 is specific for microglia, is rapidly internalized, trafficked to lysosomes and does not elicit a strong immune response. This study also demonstrates that the synthesis of a microglia-targeting non-viral vehicle can be accomplished. However, the absence of substantial reporter gene expression in microglia *in vitro* and *in vivo* demonstrates that microglia is difficult to transfect with non-viral vehicles based on branched PEI of 25 kDa. While PEI–PEG and the OX42-immunogene are both internalized into microglia, they both are subject to intracellular degradation.

Two barriers to receptor-mediated gene transfer into microglia were characterized that will help to further develop second generation immunogenes targeting microglial cells. Bypassing FcγR-mediated phagocytosis and the respiratory burst will require the use of OX42-F(ab')$_2$ antibody fragments that lack FcγR-binding sites. These antibody fragments should also increase specificity toward CD11b and microglia by avoiding cross-reaction with other cells that express FcγRs. The inability of PEI–PEG to cause substantial gene expression in microglia demonstrates that endosomal escape is another barrier for non-viral gene transfer into microglia and that alternative PEI-polymers may be required that give higher levels of gene expression in microglia. This study suggests that phagocytosis is not an efficient pathway for microglial transfection. However, it remains to be established whether phagocytosis via CD11b in absence of an immune response is able to deliver genes into microglia.

ACKNOWLEDGMENTS

We thank Prof. E. Woodcock (Baker IDI, Melbourne) for providing neonatal rat brains and acknowledge the kind donation of the OX42 hybridoma cell line by Prof. K. A. Williams (Flinders University, Adelaide). We also thank R. Nixon-Luke (RMIT University, Melbourne) for help with DLS measurements. This study was supported by an internal grant from the School of Medical Sciences and a RMIT University PhD scholarship (Markus Smolny).

REFERENCES

Aguzzi, A., Barres, B. A., and Bennett, M. L. (2013). Microglia: scapegoat, saboteur, or something else? *Science* 339, 156–161. doi: 10.1126/science.1227901

Akinc, A., Thomas, M., Klibanov, A. M., and Langer, R. (2005). Exploring polyethylenimine-mediated DNA transfection and the proton sponge hypothesis. *J. Gene Med.* 7, 657–663. doi: 10.1002/jgm.696

Akiyama, H., and McGeer, P. L. (1990). Brain microglia constitutively express β-2 integrins. *J. Neuroimmunol.* 30, 81–93. doi: 10.1016/0165-5728(90)90055-R

Amarilyo, G., Verbovetski, I., Atallah, M., Grau, A., Wiser, G., Gil, O., et al. (2010). iC3b-opsonized apoptotic cells mediate a distinct anti-inflammatory response, and transcriptional NF-κB-dependent blockade. *Eur. J. Immunol.* 40, 699–709. doi: 10.1002/eji.200838951

Aouadi, M., Tesz, G. J., Nicoloro, S. M., Wang, M., Chouinard, M., Soto, E., et al. (2009). Orally delivered siRNA targeting macrophage Map4k4 suppresses systemic inflammation. *Nature* 458, 1180–1184. doi: 10.1038/nature07774

Balcaitis, S., Weinstein, J. R., Li, S., Chamberlain, J. S., and Moeller, T. (2005). Lentiviral transduction of microglial cells. *Glia* 50, 48–55. doi: 10.1002/glia.20146

Barati, S., Hurtado, P. R., Zhang, S. H., Tinsley, R., Ferguson, I. A., and Rush, R. A. (2006). GDNF gene delivery via the p75^{NTR} receptor rescues injured motor neurons. *Exp. Neurol.* 202, 179–188. doi: 10.1016/j.expneurol.2006.05.027

Berhanu, D. A., and Rush, R. A. (2008). Targeted silencing of TrkA expression in rat forebrain neurons via the p75 receptor. *Neuroscience* 153, 1115–1125. doi: 10.1016/j.neuroscience.2008.03.025

Berton, G., and Lowell, C. A. (1999). Integrin signalling in neutrophils, and macrophages. *Cell. Signal.* 11, 621–635. doi: 10.1016/S0898-6568(99)00003-0

Blessing, T., Kursa, M., Holzhauser, R., Kircheis, R., and Wagner, E. (2001). Different strategies for formation of PEGylated EGF-conjugated PEI/DNA complexes for targeted gene delivery. *Bioconjug. Chem.* 12, 529–537. doi: 10.1021/bc0001488

Block, M. L., Zecca, L., and Hong, J. S. (2007). Microglia-mediated neurotoxicity: uncovering the molecular mechanisms. *Nat. Rev. Neurosci.* 8, 57–69. doi: 10.1038/nrn2038

Bokhoven, M., Stephen, S. L., Knight, S., Gevers, E. F., Robinson, I. C., Takeuchi, Y., et al. (2009). Insertional gene activation by lentiviral, and gammaretroviral vectors. *J. Virol.* 83, 283–294. doi: 10.1128/JVI.01865-08

Booth, P. L., and Thomas, W. E. (1991). Evidence for motility, and pinocytosis in ramified microglia in tissue culture. *Brain Res.* 548, 163–171. doi: 10.1016/0006-8993(91)91118-K

Burke, B., Sumner, S., Maitland, N., and Lewis, C. E. (2002). Macrophages in gene therapy: cellular delivery vehicles, and in vivo targets. *J. Leukoc. Biol.* 72, 417–428.

Cucchiarini, M., Ren, X. L., Perides, G., and Terwilliger, E. F. (2003). Selective gene expression in brain microglia mediated via adeno-associated virus type 2, and type 5 vectors. *Gene Ther.* 10, 657–667. doi: 10.1038/sj.gt.3301925

Davalos, D., Kyu Ryu, J., Merlini, M., Baeten, K. M., Le Moan, N., Petersen, M. A., et al. (2012). Fibrinogen-induced perivascular microglial clustering is required for the development of axonal damage in neuroinflammation. *Nat. Commun.* 3:1227. doi: 10.1038/ncomms2230

Dominguez, E., Mauborgne, A., Mallet, J., Desclaux, M., and Pohl, M. (2010). SOCS3-mediated blockade of JAK/STAT3 signaling pathway reveals its major contribution to spinal cord neuroinflammation, and mechanical allodynia after peripheral nerve injury. *J. Neurosci.* 30, 5754–5766. doi: 10.1523/JNEUROSCI.5007-09.2010

Duan, Y., Yang, C., Zhang, Z., Liu, J., Zheng, J., and Kong, D. (2010). Poly(ethylene glycol)-grafted polyethylenimine modified with G250 monoclonal antibody for tumor gene therapy. *Hum. Gene Ther.* 21, 191–198. doi: 10.1089/hum.2009.010

Erbacher, P., Bousser, M. T., Raimond, J., Monsigny, M., Midoux, P., and Roche, A. C. (1996). Gene transfer by DNA/glycosylated polylysine complexes into human blood monocyte-derived macrophages. *Hum. Gene Ther.* 7, 721–729. doi: 10.1089/hum.1996.7.6-721

Ferkol, T., Mularo, F., Hilliard, J., Lodish, S., Perales, J. C., Ziady, A., et al. (1998). Transfer of the human alpha$_1$-antitrypsin gene into pulmonary macrophages *in vivo*. *Am. J. Respir. Cell Mol. Biol.* 18, 591–601. doi: 10.1165/ajrcmb.18.5.2874

Ferkol, T., Perales, J. C., Mularo, F., and Hanson, R. W. (1996). Receptor-mediated gene transfer into macrophages. *Proc. Natl. Acad. Sci. U.S.A.* 93, 101–105. doi: 10.1073/pnas.93.1.101

Forrest, M. L., and Pack, D. W. (2002). On the kinetics of polyplex endocytic trafficking: implications for gene delivery vector design. *Mol. Ther.* 6, 57–66. doi: 10.1006/mthe.2002.0631

Germershaus, O., Merdan, T., Bakowsky, U., Behe, M., and Kissel, T. (2006). Trastuzumab-polyethylenimine-polyethylene glycol conjugates for targeting Her2-expressing tumors. *Bioconjug. Chem.* 17, 1190–1199. doi: 10.1021/bc0601119

Griffiths, M. R., Gasque, P., and Neal, J. W. (2009). The multiple roles of the innate immune system in the regulation of apoptosis, and inflammation in the brain. *J. Neuropathol. Exp. Neurol.* 68, 217–226. doi: 10.1097/NEN.0b013e3181996688

Hajishengallis, G., and Lambris, J. D. (2011). Microbial manipulation of receptor crosstalk in innate immunity. *Nat. Rev. Immunol.* 11, 187–200. doi: 10.1038/nri2918

Hu, X., Zhang, D., Pang, H., Caudle, W. M., Li, Y., Gao, H., et al. (2008). Macrophage antigen complex-1 mediates reactive microgliosis, and progressive dopaminergic neurodegeneration in the MPTP model of Parkinson's disease. *J. Immunol.* 181, 7194–7204. doi: 10.4049/jimmunol.181.10.7194

Huang, Z. Y., Hunter, S., Chien, P., Kim, M. K., Han-Kim, T. H., Indik, Z. K., et al. (2011). Interaction of two phagocytic host defense systems: Fcγ receptors, and complement receptor 3. *J. Biol. Chem.* 286, 160–168. doi: 10.1074/jbc.M110.163030

Hufnagel, H., Hakim, P., Lima, A., and Hollfelder, F. (2009). Fluid phase endocytosis contributes to transfection of DNA by PEI-25. *Mol. Ther.* 17, 1411–1417. doi: 10.1038/mt.2009.121

Hughes, M. M., Field, R. H., Perry, V. H., Murray, C. L., and Cunningham, C. (2010). Microglia in the degenerating brain are capable of phagocytosis of beads, and of apoptotic cells, but do not efficiently remove PrP^{Sc}, even upon LPS stimulation. *Glia* 58, 2017–2030. doi: 10.1002/glia.21070

Huotari, J., and Helenius, A. (2011). Endosome maturation. *EMBO J.* 30, 3481–3500. doi: 10.1038/emboj.2011.286

Intra, J., and Salem, A. K. (2008). Characterization of the transgene expression generated by branched, and linear polyethylenimine-plasmid DNA nanoparticles *in vitro*, and after intraperitoneal injection *in vivo*. *J. Control. Release* 130, 129–138. doi: 10.1016/j.jconrel.2008.04.014

Jiang, X. S., Ni, Y. Q., Liu, T. J., Zhang, M., Ren, H., Jiang, R., et al. (2012). CCR2 overexpression promotes the efficient recruitment of retinal microglia in vitro. *Mol. Vis.* 18, 2982–2992.

Jongstra-Bilen, J., Harrison, R., and Grinstein, S. (2003). Fcγ-receptors induce Mac-1 (CD11b/CD18) mobilization, and accumulation in the phagocytic cup for optimal phagocytosis. *J. Biol. Chem.* 278, 45720–45729. doi: 10.1074/jbc.M303704200

Kawakami, S., Sato, A., Nishikawa, M., Yamashita, F., and Hashida, M. (2000). Mannose receptor-mediated gene transfer into macrophages using novel mannosylated cationic liposomes. *Gene Ther.* 7, 292–299. doi: 10.1038/sj.gt.3301089

Kerr, M. C., and Teasdale, R. D. (2009). Defining macropinocytosis. *Traffic* 10, 364–371. doi: 10.1111/j.1600-0854.2009.00878.x

Kim, B., Yang, M. S., Choi, D., Kim, J. H., Kim, H. S., Seol, W., et al. (2012). Impaired inflammatory responses in murine lrrk2-knockdown brain microglia. *PLoS ONE* 7:e34693. doi: 10.1371/journal.pone.0034693

Kircheis, R., Kichler, A., Wallner, G., Kursa, M., Ogris, M., Felzmann, T., et al. (1997). Coupling of cell-binding ligands to polyethylenimine for targeted gene delivery. *Gene Ther.* 4, 409–418. doi: 10.1038/sj.gt.3300418

Kircheis, R., Wightman, L., and Wagner, E. (2001). Design, and gene delivery activity of modified polyethylenimines. *Adv. Drug Deliv. Rev.* 53, 341–358. doi: 10.1016/S0169-409X(01)00202-2

Klegeris, A., and McGeer, P. L. (1994). Inhibition of respiratory burst in macrophages by complement receptor blockade. *Eur. J. Pharmacol.* 260, 273–277. doi: 10.1016/0014-2999(94)90351-4

Kwon, E. J., Lasiene, J., Jacobson, B. E., Park, I. K., Horner, P. J., and Pun, S. H. (2010). Targeted nonviral delivery vehicles to neural progenitor cells in the mouse subventricular zone. *Biomaterials* 31, 2417–2424. doi: 10.1016/j.biomaterials.2009.11.086

Lee, J. K., Chung, J., McAlpine, F. E., and Tansey, M. G. (2011). Regulator of G-protein signaling-10 negatively regulates NF-κB in microglia, and neuroprotects dopaminergic neurons in hemiparkinsonian rats. *J. Neurosci.* 31, 11879–11888. doi: 10.1523/JNEUROSCI.1002-11.2011

Lei, L., Tzekov, R., Tang, S., and Kaushal, S. (2012). Accumulation, and autofluorescence of phagocytized rod outer segment material in macrophages, and microglial cells. *Mol. Vis.* 18, 103–113.

Li, Y. N., Qin, X. J., Kuang, F., Wu, R., Duan, X. L., Ju, G., et al. (2008). Alterations of Fc gamma receptor I, and Toll-like receptor 4 mediate the antiinflammatory actions of microglia, and astrocytes after adrenaline-induced blood-brain barrier opening in rats. *J. Neurosci. Res.* 86, 3556–3565. doi: 10.1002/jnr.21810

Liu, Y., Yang, X., Guo, C., Nie, P., and Ma, J. (2013). Essential role of MFG-E8 for phagocytic properties of microglial cells. *PLoS ONE* 8:e55754. doi: 10.1371/journal.pone.0055754

Lungwitz, U., Breunig, M., Blunk, T., and Göpferich, A. (2005). Polyethylenimine-based non-viral gene delivery systems. *Eur. J. Pharm. Biopharm.* 60, 247–266. doi: 10.1016/j.ejpb.2004.11.011

Lv, H., Zhang, S., Wang, B., Cui, S., and Yan, J. (2006). Toxicity of cationic lipids, and cationic polymers in gene delivery. *J. Control. Release* 114, 100–109. doi: 10.1016/j.jconrel.2006.04.014

Maiorino, C., Khorooshi, R., Ruffini, F., Løbner, M., Bergami, A., Garzetti, L., et al. (2013). Lentiviral-mediated administration of IL-25 in the CNS induces alternative activation of microglia. *Gene Ther.* 20, 487–496. doi: 10.1038/gt.2012.58

Mandrekar, S., Jiang, Q., Lee, C. Y. D., Koenigsknecht-Talboo, J., Holtzman, D. M., and Landreth, G. E. (2009). Microglia mediate the clearance of soluble Aβ through fluid phase macropinocytosis. *J. Neurosci.* 29, 4252–4262. doi: 10.1523/JNEUROSCI.5572-08.2009

Mantovani, B. (1975). Different roles of IgG, and complement receptors in phagocytosis by polymorphonuclear leukocytes. *J. Immunol.* 115, 15–17.

Mantovani, B., Rabinovitch, M., and Nussenzweig, V. (1972). Phagocytosis of immune complexes by macrophages. Different roles of the macrophage receptor sites for complement (C3) and for immunoglobulin (IgG). *J. Exp. Med.* 135, 780–792. doi: 10.1084/jem.135.4.780

Markovic, D. S., Vinnakota, K., Chirasani, S., Synowitz, M., Raguet, H., Stock, K., et al. (2009). Gliomas induce, and exploit microglial MT1-MMP expression for tumor expansion. *Proc. Natl. Acad. Sci. U.S.A.* 106, 12530–12535. doi: 10.1073/pnas.0804273106

Mayor, S., and Pagano, R. E. (2007). Pathways of clathrin-independent endocytosis. *Nat. Rev. Mol. Cell Biol.* 8, 603–612. doi: 10.1038/nrm2216

McCoy, M. K., Ruhn, K. A., Martinez, T. N., McAlpine, F. E., Blesch, A., and Tansey, M. G. (2008). Intranigral lentiviral delivery of dominant-negative TNF attenuates

neurodegeneration, and behavioral deficits in hemiparkinsonian rats. *Mol. Ther.* 16, 1572–1579. doi: 10.1038/mt.2008.146

Mercer, J., and Helenius, A. (2009). Virus entry by macropinocytosis. *Nat. Cell Biol.* 11, 510–520. doi: 10.1038/ncb0509-510

Meunier, A., Latremoliere, A., Dominguez, E., Mauborgne, A., Philippe, S., Hamon, M., et al. (2007). Lentiviral-mediated targeted NF-êB blockade in dorsal spinal cord glia attenuates sciatic nerve injury-induced neuropathic pain in the rat. *Mol. Ther.* 15, 687–697.

Meunier, A., Mauborgne, A., Masson, J., Mallet, J., and Pohl, M. (2008). Lentiviral-mediated targeted transgene expression in dorsal spinal cord glia: tool for the study of glial cell implication in mechanisms underlying chronic pain development. *J. Neurosci. Methods* 167, 148–159. doi: 10.1016/j.jneumeth.2007.07.022

Millili, P. G., Selekman, J. A., Blocker, K. M., Johnson, D. A., Naik, U. P., and Sullivan, M. O. (2010). Structural, and functional consequences of poly(ethylene glycol) inclusion on DNA condensation for gene delivery. *Microsc. Res. Tech.* 73, 866–877. doi: 10.1002/jemt.20839

Milner, R., and Campbell, I. L. (2002). The integrin family of cell adhesion molecules has multiple functions within the CNS. *J. Neurosci. Res.* 69, 286–291. doi: 10.1002/jnr.10321

Mishra, S., Webster, P., and Davis, M. E. (2004). PEGylation significantly affects cellular uptake, and intracellular trafficking of non-viral gene delivery particles. *Eur. J. Cell Biol.* 83, 97–111. doi: 10.1078/0171-9335-00363

Mosser, D. M., and Edelson, P. J. (1987). The third component of complement (C3) is responsible for the intracellular survival of Leishmania major. *Nature* 327, 329–331. doi: 10.1038/327329b0

Nakajima, K., Hamanoue, M., Shimojo, M., Takei, N., and Kohsaka, S. (1989). Characterization of microglia isolated from a primary culture of embryonic rat brain by a simplified method. *Biomed. Res.* 10, 411–423.

Neu, M., Fischer, D., and Kissel, T. (2005). Recent advances in rational gene transfer vector design based on poly(ethylene imine) and its derivatives. *J. Gene Med.* 7, 992–1009. doi: 10.1002/jgm.773

Newland, B., Aied, A., Pinoncely, A. V., Zheng, Y., Zhao, T., Zhang, H., et al. (2014). Untying a nanoscale knotted polymer structure to linear chains for efficient gene delivery in vitro, and to the brain. *Nanoscale* 6, 7526–7533. doi: 10.1039/c3nr06737h

Nimmerjahn, F., and Ravetch, J. V. (2008). Fcγ receptors as regulators of immune responses. *Nat. Rev. Immunol.* 8, 34–47. doi: 10.1038/nri2206

Nitta, T., Yagita, H., Sato, K., Okumura, K., and Bernstein, J. J. (1992). Expression of Fcγ receptors on astroglial cell lines, and their role in the central nervous system. *Neurosurgery* 31, 83–88. doi: 10.1227/00006123-199207000-00012

Ogris, M., Steinlein, P., Carotta, S., Brunner, S., and Wagner, E. (2001). DNA/polyethylenimine transfection particles: influence of ligands, polymer size, and PEGylation on internalization, and gene expression. *AAPS PharmSci* 3:E21. doi: 10.1208/ps030321

Ogris, M., Steinlein, P., Kursa, M., Mechtler, K., Kircheis, R., and Wagner, E. (1998). The size of DNA/transferrin-PEI complexes is an important factor for gene expression in cultured cells. *Gene Ther.* 5, 1425–1433. doi: 10.1038/sj.gt.3300745

Ohsawa, K., Imai, Y., Kanazawa, H., Sasaki, Y., and Kohsaka, S. (2000). Involvement of Iba1 in membrane ruffling, and phagocytosis of macrophages/microglia. *J. Cell Sci.* 113, 3073–3084.

Okun, E., Mattson, M. P., and Arumugam, T. V. (2010). Involvement of Fc receptors in disorders of the central nervous system. *Neuromolecular Med.* 12, 164–178. doi: 10.1007/s12017-009-8099-5

Payne, C. K., Jones, A. S., Chen, C., and Zhuang, X. (2007). Internalization, and trafficking of cell surface proteoglycans, and proteoglycan-binding ligands. *Traffic* 8, 389–401. doi: 10.1111/j.1600-0854.2007.00540.x

Pei, Z., Pang, H., Qian, L., Yang, S., Wang, T., Zhang, W., et al. (2007). MAC1 mediates LPS-induced production of superoxide by microglia: the role of pattern recognition receptors in dopaminergic neurotoxicity. *Glia* 55, 1362–1373. doi: 10.1002/glia.20545

Petersen, H., Fechner, P. M., Martin, A. L., Kunath, K., Stolnik, S., Roberts, C. J., et al. (2002). Polyethylenimine-graft-poly(ethylene glycol) copolymers: influence of copolymer block structure on DNA complexation, and biological activities as gene delivery system. *Bioconjug. Chem.* 13, 845–854. doi: 10.1021/bc025529v

Pfrieger, F. W., and Slezak, M. (2012). Genetic approaches to study glial cells in the rodent brain. *Glia* 60, 681–701. doi: 10.1002/glia.22283

Raety, J. K., Lesch, H. P., Wirth, T., and Yla-Herttuala, S. (2008). Improving safety of gene therapy. *Curr. Drug Saf.* 3, 46–53. doi: 10.2174/157488608783333925

Rana, I., Stebbing, M., Kompa, A., Kelly, D. J., Krum, H., and Badoer, E. (2010). Microglia activation in the hypothalamic PVN following myocardial infarction. *Brain Res.* 1326, 96–104. doi: 10.1016/j.brainres.2010.02.028

Ransohoff, R. M., and Cardona, A. E. (2010). The myeloid cells of the central nervous system parenchyma. *Nature* 468, 253–262. doi: 10.1038/nature09615

Ricklin, D., Hajishengallis, G., Yang, K., and Lambris, J. D. (2010). Complement: a key system for immune surveillance, and homeostasis. *Nat. Immunol.* 11, 785–797. doi: 10.1038/ni.1923

Robinson, A. P., White, T. M., and Mason, D. W. (1986). Macrophage heterogeneity in the rat as delineated by two monoclonal antibodies MRC OX-41, and MRC OX-42, the latter recognizing complement receptor type 3. *Immunology* 57, 239–247.

Ross, G. D. (2000). Regulation of the adhesion versus cytotoxic functions of the Mac-1/CR3/$^{\alpha}m^{\beta}$2-integrin glycoprotein. *Crit. Rev. Immunol.* 20, 197–222. doi: 10.1615/CritRevImmunol.v20.i3.20

Saijo, K., and Glass, C. K. (2011). Microglial cell origin, and phenotypes in health, and disease. *Nat. Rev. Immunol.* 11, 775–787. doi: 10.1038/nri3086

Schafer, D. P., Lehrman, E. K., Kautzman, A. G., Koyama, R., Mardinly, A. R., Yamasaki, R., et al. (2012). Microglia sculpt postnatal neural circuits in an activity, and complement-dependent manner. *Neuron* 74, 691–705. doi: 10.1016/j.neuron.2012.03.026

Sitte, N., Huber, M., Grune, T., Ladhoff, A., Doecke, W. D., Von Zglinicki, T., et al. (2000). Proteasome inhibition by lipofuscin/ceroid during postmitotic aging of fibroblasts. *FASEB J.* 14, 1490–1498. doi: 10.1096/fj.14.11.1490

Snyder, S. L., and Sobocinski, P. Z. (1975). An improved 2,4,6 trinitrobenzenesulfonic acid method for the determination of amines. *Anal. Biochem.* 64, 284–288. doi: 10.1016/0003-2697(75)90431-5

Sohn, J. H., Bora, P. S., Suk, H. J., Molina, H., Kaplan, H. J., and Bora, N. S. (2003). Tolerance is dependent on complement C3 fragment iC3b binding to antigen-presenting cells. *Nat. Med.* 9, 206–212. doi: 10.1038/nm814

Stolzing, A., Wengner, A., and Grune, T. (2002). Degradation of oxidized extracellular proteins by microglia. *Arch. Biochem. Biophys.* 400, 171–179. doi: 10.1016/S0003-9861(02)00003-6

Tang, G. P., Zeng, J. M., Gao, S. J., Ma, Y. X., Shi, L., Li, Y., et al. (2003). Polyethylene glycol modified polyethylenimine for improved CNS gene transfer: effects of PEGylation extent. *Biomaterials* 24, 2351–2362. doi: 10.1016/S0142-9612(03)00029-2

Thornton, B. P., Vĭtvièka, V., Pitman, M., Goldman, R. C., and Ross, G. D. (1996). Analysis of the sugar specificity, and molecular location of the β-glucan-binding lectin site of complement receptor type 3 (CD11D/CD18). *J. Immunol.* 156, 1235–1246.

Ulvestad, E., Williams, K., Vedeler, C., Antel, J., Nyland, H., Maerk, S., et al. (1994). Reactive microglia in multiple sclerosis lesions have an increased expression of receptors for the Fc part of IgG. *J. Neurol. Sci.* 121, 125–131. doi: 10.1016/0022-510X(94)90340-9

Varkouhi, A. K., Scholte, M., Storm, G., and Haisma, H. J. (2011). Endosomal escape pathways for delivery of biologicals. *J. Control. Release* 151, 220–228. doi: 10.1016/j.jconrel.2010.11.004

Vedeler, C., Ulvestad, E., Grundt, I., Conti, G., Nyland, H., Matre, R., et al. (1994). Fc receptor for IgG (FcR) on rat microglia. *J. Neuroimmunol.* 49, 19–24. doi: 10.1016/0165-5728(94)90176-7

Větvička, V., Thornton, B. P., and Ross, G. D. (1996). Soluble β-glucan polysaccharide binding to the lectin site of neutrophil or natural killer cell complement receptor type 3 (CD11b/CD18) generates a primed state of the receptor capable of mediating cytotoxicity of iC3b-opsonized target cells. *J. Clin. Invest.* 98, 50–61. doi: 10.1172/JCI118777

von Gersdorff, K., Sanders, N. N., Vandenbroucke, R., De Smedt, S. C., Wagner, E., and Ogris, M. (2006). The internalization route resulting in successful gene expression depends on both cell line, and polyethylenimine polyplex type. *Mol. Ther.* 14, 745–753. doi: 10.1016/j.ymthe.2006.07.006

Ward, S. A., Ransom, P. A., Booth, P. L., and Thomas, W. E. (1991). Characterization of ramified microglia in tissue culture: pinocytosis, and motility. *J. Neurosci. Res.* 29, 13–28. doi: 10.1002/jnr.490290103

Wrzesinski, S., Seguin, R., Liu, Y., Domville, S., Planelles, V., Massa, P., et al. (2000). HTLV type 1 tax transduction in microglial cells, and astrocytes

by lentiviral vectors. *AIDS Res. Hum. Retroviruses* 16, 1771–1776. doi: 10.1089/08892220050193290

Xia, X., Větvička, V., Yan, J., Hanikýřová, M., Mayadas, T., and Ross, G. D. (1999). The β-glucan-binding lectin site of mouse CR3 (CD11b/CD18), and its function in generating a primed state of the receptor that mediates cytotoxic activation in response to iC3b-opsonized target cells. *J. Immunol.* 162, 2281–2290.

Xiang, S., Tong, H., Shi, Q., Fernandes, J. C., Jin, T., Dai, K., et al. (2012). Uptake mechanisms of non-viral gene delivery. *J. Control. Release* 158, 371–378. doi: 10.1016/j.jconrel.2011.09.093

Yue, Y., Jin, F., Deng, R., Cai, J., Dai, Z., Lin, M. C. M., et al. (2011). Revisit complexation between DNA, and polyethylenimine – effect of length of free polycationic chains on gene transfection. *J. Control. Release* 152, 143–151. doi: 10.1016/j.jconrel.2011.03.020

Zhang, W., Dallas, S., Zhang, D., Guo, J. P., Pang, H., Wilson, B., et al. (2007). Microglial PHOX, and Mac-1 are essential to the enhanced dopaminergic neurodegeneration elicited by A30P, and A53T mutant alpha-synuclein. *Glia* 55, 1178–1188. doi: 10.1002/glia.20532

Conflict of Interest Statement: Robert A. Rush owns shares in Biosensis Pty Ltd., Adelaide, which sells the OX42 and X63 antibodies.

Received: 29 June 2014; accepted: 16 September 2014; published online: 09 October 2014.

Citation: Smolny M, Rogers M-L, Shafton A, Rush RA and Stebbing MJ (2014) Development of non-viral vehicles for targeted gene transfer into microglia via the integrin receptor CD11b. Front. Mol. Neurosci. 7:79. doi: 10.3389/fnmol.2014.00079

This article was submitted to the journal Frontiers in Molecular Neuroscience.

frontiers in Molecular Neuroscience

ORIGINAL RESEARCH
published: 28 July 2015
doi: 10.3389/fnmol.2015.00036

Systemic AAVrh10 provides higher transgene expression than AAV9 in the brain and the spinal cord of neonatal mice

*Yannick Tanguy *, Maria G. Biferi, Aurore Besse, Stephanie Astord, Mathilde Cohen-Tannoudji, Thibaut Marais and Martine Barkats **

Center of Research on Myology, FRE 3617 Centre National de la Recherche Scientifique, UMRS 974 INSERM, French Institute of Myology, Pierre and Marie Curie University, Paris, France

Systemic delivery of self-complementary (sc) adeno-associated-virus vector of serotype 9 (AAV9) was recently shown to provide robust and widespread gene transfer to the central nervous system (CNS), opening new avenues for practical, and non-invasive gene therapy of neurological diseases. More recently, AAV of serotype rh10 (AAVrh10) was also found highly efficient to mediate CNS transduction after intravenous administration in mice. However, only a few studies compared AAV9 and AAVrh10 efficiencies, particularly in the spinal cord. In this study, we compared the transduction capabilities of AAV9 and AAVrh10 in the brain, the spinal cord, and the peripheral nervous system (PNS) after intravenous delivery in neonatal mice. As reported in previous studies, AAVrh10 achieved either similar or higher transduction than AAV9 in all the examined brain regions. The superiority of AAVrh10 over AAV9 appeared statistically significant only in the medulla and the cerebellum, but a clear trend was also observed in other structures like the hippocampus or the cortex. In contrast to previous studies, we found that AAVrh10 was more efficient than AAV9 for transduction of the dorsal spinal cord and the lower motor neurons (MNs). However, differences between the two serotypes appeared mainly significant at low dose, and surprisingly, increasing the dose did not improve AAVrh10 distribution in the spinal cord, in contrary to AAV9. Similar dose-related differences between transduction efficiency of the two serotypes were also observed in the sciatic nerve. These findings suggest differences in the transduction mechanisms of these two serotypes, which both hold great promise for gene therapy of neurological diseases.

Keywords: adeno-associated virus, AAV9, AAVrh10, gene therapy, central nervous system, peripheral nervous system, motor neuron, SMA

OPEN ACCESS

Edited by:
Andrew Paul Tosolini, University of New South Wales, Australia

Reviewed by:
Alessandro Vercelli, University of Turin, Italy
Thais Buchman, Emory University, USA

****Correspondence:***
Yannick Tanguy and Martine Barkats, Center of Research on Myology, UMRS 974 INSERM, FRE 3617 Centre National de la Recherche Scientifique, Pierre and Marie Curie University, French Institute of Myology, 105 Boulevard de l'Hôpital, 75 013 Paris, France
y.tanguy@institut-myologie.org; m.barkats@institut-myologie.org

Received: *14 May 2015*
Accepted: *06 July 2015*
Published: *28 July 2015*

Citation:
Tanguy Y, Biferi MG, Besse A, Astord S, Cohen-Tannoudji M, Marais T and Barkats M (2015) Systemic AAVrh10 provides higher transgene expression than AAV9 in the brain and the spinal cord of neonatal mice. Front. Mol. Neurosci. 8:36. doi: 10.3389/fnmol.2015.00036

Introduction

Nervous system diseases, including functional and degenerative disorders, can affect all cell types in the central (CNS) and peripheral (PNS) nervous system, leading to severe disabilities and patient death in the most severe cases. Due to their devastating consequences, lack of efficient treatments, and aging of the population, these pathologies are becoming a major concern for public health. Advances in molecular technologies have allowed emergence and rapid progress of gene therapy

for high and sustained expression of therapeutic proteins in nervous cells. Particular effort has been focused on vector expression and delivery systems, those derived from the adeno-associated virus (AAV) appearing as one of the most promising for gene therapy of nervous diseases (Weinberg et al., 2013).

AAV vectors are non-pathogenic and capable of transducing non-dividing cells permanently, with no toxicity or significant immune reaction (McCown et al., 1996; Wu et al., 1998). A number of Phase I and Phase II clinical trials utilizing AAV vectors have been carried out worldwide (Grieger and Samulski, 2012), and among them, direct injection into the nervous parenchyma of patients with neurological diseases has shown its efficacy and excellent safety profile in several previous clinical trials (Mandel and Burger, 2004; Kaplitt et al., 2007; Marks et al., 2008; Christine et al., 2009; LeWitt et al., 2011; Tardieu et al., 2014). However, due to the impermeability nature of the blood-brain-barrier (BBB), systemic gene transfer to the CNS has been particularly challenging, whether with AAV or any other gene vector. A significant breakthrough has been made in 2007, with our discovery that self-complementary serotype 9 AAV vectors (scAAV9) are capable to achieve widespread gene transfer to the CNS after systemic delivery (Barkats, 2007). Although transgene expression has been firstly reported to be primarily restricted to astrocytes after intravenous (IV) injection in adult mice (Foust et al., 2009), we showed that systemic delivery of an AAV9 encoding the green-fluorescent-protein (GFP) mediated efficient transduction of a relatively large proportion of neurons in adult mice (Duqué et al., 2009). The comparison of single-stranded and self-complementary AAV of serotype 1 and 9 for transduction of the mouse CNS after IV delivery showed indeed that self-complementary AAV9 was the most efficient vector for transducing spinal cord cells including motor neurons (MNs), and that transgene expression lasted at least 5 months (the duration of the study) (Duqué et al., 2009). Importantly, this finding was successfully translated to a domestic cat strain with deletions of the LIX1 gene (Fyfe et al., 2006), a model of autosomal recessive spinal muscular atrophy (SMA) similar to human type III SMA (Duqué et al., 2009). The remarkable potential of systemic AAV9 for transducing MNs in adult animals was further confirmed in both rodents and large animals including non-human primates (NHPs) (Bevan et al., 2011; Gray et al., 2011). In addition to these IV studies, we recently reported that intramuscular (IM) delivery of AAV9 was also effective to achieve widespread gene transfer to the CNS in both neonatal and adult mice. Indeed, AAV9 delivery into the gastrocnemius muscle mediated gene transfer not only into the lumbar MNs, but also at the upper levels of the spinal cord and in discrete parts of the brain (Benkhelifa-Ziyyat et al., 2013). Importantly, either IV or IM delivery of AAV9 vectors engineered to overexpress the *Survival of Motor Neuron gene 1* (*SMN1*) gene dramatically rescued the pathological phenotype in a mouse model of spinal muscular atrophy (SMA) (Foust et al., 2010; Valori et al., 2010; Dominguez et al., 2011; Benkhelifa-Ziyyat et al., 2013). In particular, we found that a single IV delivery of an optimized *SMN1*-encoding AAV9 vector (AAV9-SMN1opti) in neonatal SMNΔ7 mice, a mouse model of human SMA (Le et al., 2005), increased life expectancy up to 355 days in mice that normally survive about 13 days (Dominguez et al., 2011). The AAV9-SMN1opti treatment also partially corrected the body weight loss phenotype, improved motor activity, and prevented MN degeneration (Dominguez et al., 2011). Systemic AAV9 delivery was further shown to be very promising for treating other neurological or lysosomal diseases, including amyotrophic lateral sclerosis (Yamashita et al., 2013), Canavan disease (Ahmed et al., 2013) or MPSIIIA (Fu et al., 2011; Ruzo et al., 2012), highlighting the outstanding potential of this approach for a large range of CNS and systemic pathologies.

Although AAV9 is usually considered as the most promising vector for achieving widespread CNS transduction, alternative AAV vectors with increased spread and transduction efficiency are currently actively investigated. In particular, the AAV of serotype rh10 (AAVrh10), which has been isolated from rhesus monkeys (Gao et al., 2002, 2003), was recently reported to be as least as efficient as AAV9 for transduction of many tissues including the CNS in neonatal mice (Hu et al., 2010; Zhang et al., 2011). In particular, using a scoring system to evaluate GFP-immunoreactivity in different CNS regions, Zhang et al. showed that AAVrh10 transduction efficiency was comparable to that of AAV9 in the spinal cord, and was globally higher than that of AAV9 in the brain (with differences according to the brain region) (Zhang et al., 2011).

In this study, we used semi-quantitative and quantitative analyses to compare the ability of AAV9 and AAVrh10 for achieving gene transfer to the CNS and the PNS following intravascular delivery in neonatal mice. We found that low dose AAVrh10 induced higher transduction than AAV9 of most regions that we examined, in particular the medulla, the cerebellum, the spinal cord and the sciatic nerve. However, differences between the two serotypes were less evident were the vector doses were increased, suggesting serotype-related differences in the transduction process.

Materials and Methods

Animals

Wild-type animals were obtained from $Smn1^{+/-}$, $Smn2^{+/+}$ breeding (FVB.Cg-Tg(SMN2)89Ahmb Tg (SMN1∗A2G)2023Ahmb Smn1 tm1Msd/J) (number 5024, Jackson Laboratories, Main Harbor, USA). Mice were housed under controlled conditions (22 ± 2°C, 50 ± 10% relative humidity, 12 h/12 h light/dark cycle, food, and water *ad libitum*). All animal experiments were carried out in accordance with European guidelines for the care and use of experimental animals and approved by the Charles Darwin N°5 Ethics Committee on Animal Experiments (agreement n°01883.02-16/9/14).

Production of AAV Vectors and Intravenous Delivery

AAV vectors of serotype 9 or rh10, carrying the GFP under the control of the cytomegalovirus immediate/early (CMV) promoter were prepared by the triple transfection method in HEK293T cells, as previously described (Duqué et al., 2009). Briefly, cells were transfected with (i) the adenovirus helper plasmid, (ii) the AAV packaging plasmid encoding the rep2

and cap9 (p5E18-VD2/9) or cap-rh10 genes, and (iii) the AAV2 plasmid expressing CMV-GFP. Seventy-two hours after transfection, cells were harvested, frozen/thawed four times, and AAV vectors were purified by ultracentrifugation through an iodixanol gradient (Sigma-Aldrich, St Quentin Fallavier, France) and concentrated with Amicon Ultra–Ultra cell 100K filter units (Millipore) in PBSMK buffer (0.1 M phosphate buffered saline solution (PBS), 1 mM $MgCl_2$ and 2.5 mM KCl). Aliquots were stored at −80°C until use. Vector titers were determined by real-time PCR and expressed as viral genomes per mL (vg/mL).

Neonatal mice (P0) received 40 µL of viral suspension containing 3×10^{10} or 1×10^{11} vg of AAV9 or AAVrh10 into the temporal vein using an Hamilton syringe with a 32-gauge needle (Hamilton).

Western Blot

Animals were lethally anesthetized and transcardially perfused with 0.1 M PBS. Tissues were immediately frozen in liquid nitrogen and stored at −80°C until use. For protein extraction, tissues were grinded in a lysis buffer (150 mM NaCl, 50 mM Tris–HCl, 0.5% sodium deoxycholate, 1% NP40, 1% SDS) supplied with protease inhibitors cocktail (Complete Mini, Roche Diagnostics). Lysates were quantified with the DC protein assay (BioRad,) and 50 µg were loaded on a 10% polyacrylamide gel (Criterion XT 10% bis-Tris, Biorad). Proteins were transferred onto a PVDF membrane (Imobilon P, Millipore). Successively, membranes were blocked with a Tris-buffered saline solution (10 mM Tris–HCl pH 7.4, 150 mM NaCl) and 0.05% Tween 20 (TBS-T) containing 5% fat-free dry milk. Membranes were incubated overnight at 4°C with a rabbit anti-GFP antibody (1:10,000; Abcam) or a mouse anti-α-tubulin antibody (1:10,000; Sigma-Aldrich) diluted in TBS-T, 5% fat-free dry milk. After washes in TBS-T buffer, membranes were incubated with horseradish peroxidase conjugated anti-mouse or anti-rabbit secondary antibodies (1:10,000, Amersham Pharmacia Biotech) for 1 h at room temperature. Western blots were developed using SuperSignal West Dura kit (Thermoscientific).

Immunofluorescence

Animals were lethally anesthetized and transcardially perfused with 0.1 M PBS followed by 4% paraformaldehyde (PFA; Sigma-Aldrich) in PBS. Tissues were harvested and successively incubated in 4% PFA (24 h at 4°C) and in a PBS-sucrose solution (30% sucrose for the spinal cord, 15% sucrose for the other organs, overnight at 4°C). Samples were imbedded with optimal cutting temperature medium (Tissue-Tek OCT; Sakura Finetek) and frozen in cold isopentane. Fourteen µm-thick sections were serially cut on a cryostat (Leica Microsystems) and stored at −80°C.

For immunofluorescence staining, sections were incubated in a blocking solution containing 4% donkey serum, 5% Bovine serum albumin in a PBS-triton X-100 buffer (0.1 M PBS, 0.4 % Triton X-100) for 1 h at room temperature. Sections were incubated with primary antibodies: anti-GFP (1:2,000, rabbit; Abcam), anti-Neurofilament (NF, mouse, 1:500; Millipore), anti-β-S100 (rabbit, 1:200; Dako) or anti-Choline Acetyltransferase (ChAT, goat, 1:100, Millipore), in the blocking solution, overnight at 4°C. After PBS washings, sections were incubated with secondary antibodies conjugated with Alexa Fluor 488 (1:500) or 594 (1:300) (Molecular Probes-Invitrogen). Nuclei were counterstained with 4′,6′-diamidino-2-phénylindole (DAPI, 0.5 µg/mL in PBS; Sigma-Aldrich) and mounted with Fluoromount (Southern Biotech). Pictures were obtained with a confocal laser scanning microscope (Leica) or a motorized fluorescence microscope (AxioImager.Z1; Zeiss).

To quantify GFP expression, representative images from each tissue were taken at identical camera and microscope settings with a fluorescence microscope. For every image, the brightness and background values were measured with ImageJ software (Rasband 1997–2006; National Institutes of Health, Bethesda, MD, http://rsb.info.nih.gov/ij/), and the results corresponded to the mean value of 6 (brain and medulla) or 12 (cerebellum, dorsal spinal cord, sciatic nerve, DRG, heart, and liver) images for each mouse.

Statistics

All data were analyzed using Prism software (version 4.0, GraphPad). A Mann-Whitney test was used for the analysis of western blot results, *t*-test and One-Way ANOVA were performed for analysis of MN counting. Fluorescence imaging data were treated with either a Mann-Whitney or a Two-Way ANOVA test, which were chosen according to the number of samples. Significant levels were noted as follows: *, $p < 0.05$; **, $p < 0.01$; ***, $p < 0.001$.

Results

Intravenous AAVrh10 Provides a Similar or Higher Brain Transduction Level than AAV9

Newborn mice were injected at P0 into the superficial temporal vein with the AAV9-GFP ($n = 4$) or AAVrh10-GFP ($n = 4$) vectors (3×10^{13} vg/kg), and transduction efficiency was first compared in the brain by immunofluorescence analysis 1 month after injection. For both vectors, a gradient of expression was observed from the brain ventricles and adjacent regions (Bregma −1.46 and −6.48 mm), to more distant brain regions (**Figure 1**). GFP immunostaining was particularly intense in the choroid plexus of the lateral, 3rd and 4th ventricles, and in neighboring structures such as the lateral habenular nucleus, the CA2 field of the hippocampus, the dorsal hippocampal commissure, the deeper layers of the cerebral cortex, the retrosplenial cortex, the vestibular nucleus and the spinal trigeminal nucleus of the medulla, and the lobule 10 of the cerebellum (**Figure 1**). In contrast, only a few GFP-expressing cells were observed in regions located far from the ventricles, such as the reticular nucleus, the thalamus or the external lobules of the cerebellum. In all the examined regions, a similar or higher level of transduction was observed with AAVrh10 compared to AAV9, AAVrh10 providing the greatest levels of expression in the cerebellar Purkinje cells, the vestibular and spinal trigeminal nuclei of the medulla, the lateral habenular nucleus, and the deep cortical layers (**Figure 1**). A quantitative analysis of the GFP signal (mean intensity/pixel) in several brain structures confirmed a strong tendency for a superior

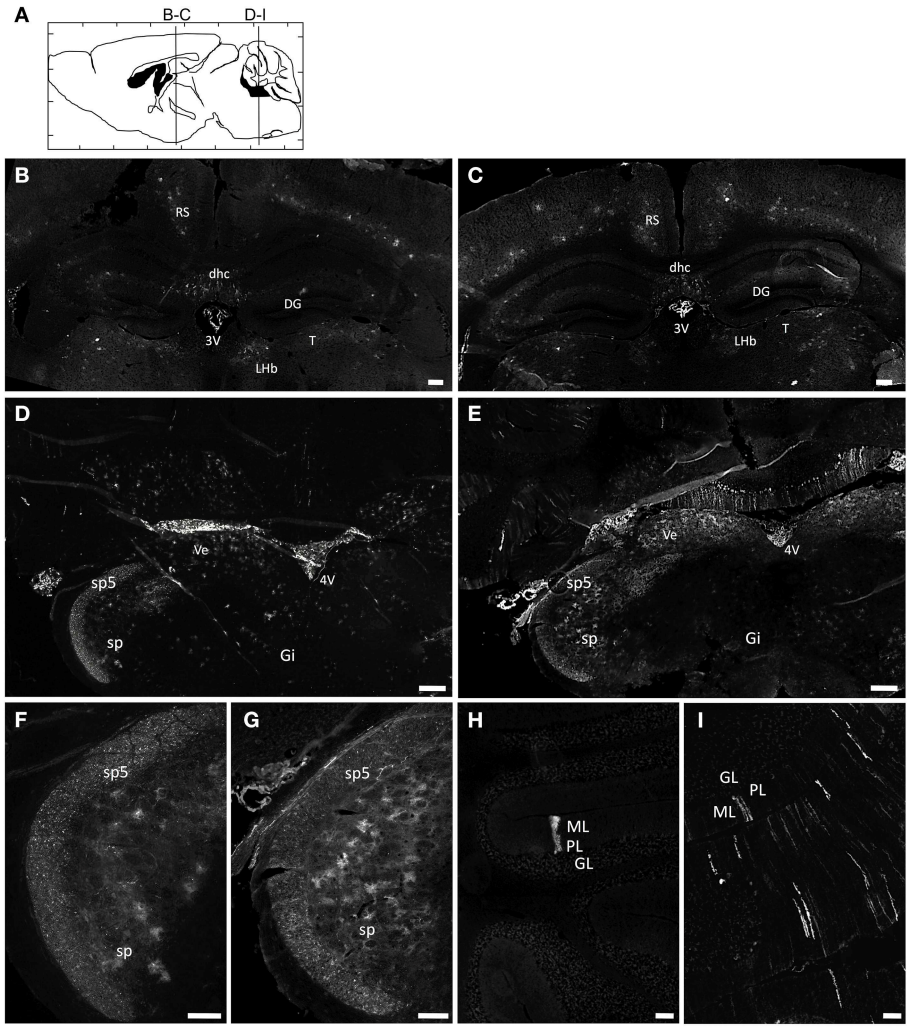

FIGURE 1 | Immunofluorescence analysis of GFP expression in the brain of AAV9 or AAVrh10 injected mice. Representative brain sections treated for GFP immunofluorescence 30 days after injection of GFP-expressing AAV9 and AAVrh10 vectors into the facial vein of neonatal mice at P0 (3×10^{13} vg/kg, $n = 4$ per group) **(A)** Schematic representation of the investigated areas (**B,C**, Bregma: −1.46 mm; **D–I**, Bregma: −6.48 mm). **(B–I)** Comparison of GFP expression in AAV9-GFP **(B,D,F,H)** or AAVrh10-GFP **(C,E,G,I)** injected mice in **(B,C)** the hippocampus **(D,E)** the medulla **(F,G)** the spinal trigeminal tractus and nucleus, and **(H,I)** the cerebellum. 3V, third Ventricle; 4V, fourth Ventricle; DG, Dentate Gyrus; dhc, dorsal hippocampal commissure; Gi, Gigantocellular reticular nucleus; GL, Granular layer; LHb, Lateral Habenular nucleus; ML, Molecular layer; PL, Purkinje layer; RS, Retrosplenial cortex; sp5, Spinal trigeminal tractus; sp, Spinal trigeminal nucleus; T, Thalamus; Ve, Vestibular nucleus. Scale bars = **(B–E)** 250 μm; **(F–I)** 125 μm.

transduction efficiency of the AAVrh10, however the difference with AAV9 only reached statistical significance for the medulla (30.9 ± 8 vs. 74.2 ± 12.9 for AAV9 and AAVrh10, respectively; $p = 0.0286$) and the cerebellum (11.7 ± 1.7 vs. 38.5 ± 6.1 for AAV9 and AAVrh10, respectively; $p = 0.0286$) (**Figure 2**).

GFP Expression in the Spinal Cord of AAV9 and AAVrh10 Injected Mice

To compare transduction levels provided by the AAV9 and AAVrh10 serotypes in the spinal cord, neonatal mice were injected at birth with the two GFP-expressing vectors. Both vectors were delivered at low (3×10^{13} vg/kg, $n = 6$ per AAV) and high dose (10^{14} vg/kg, $n = 4$ for AAV9 and $n = 3$ for AAVrh10) and GFP expression was evaluated 30 days after injection by western blot analysis on spinal cord protein extracts.

Similarly to the results in brain, GFP protein levels were found to be increased in spinal cord extracts from mice injected with AAVrh10 compared to AAV9 at 3×10^{13} vg/kg ($p = 0.011$) (**Figure 3**). At this low dose, only a weak GFP expression was observed with both vectors, which was essentially confined to the dorsal part of the spinal cord (corresponding to the sensitive nerves of the fasciculus gracilis and cuneatus) (**Figure 3Ba**). At the highest dose (10^{14} vg/kg), GFP expression levels were largely increased in the spinal cord, but no statistically significant difference was evidenced between

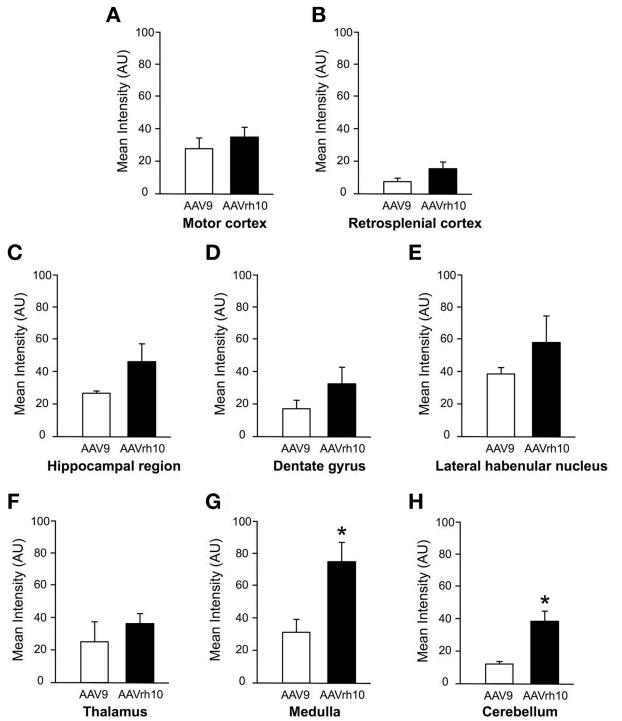

FIGURE 2 | Quantification of GFP fluorescence intensity in the brain of AAV9 or AAVrh10 injected mice. Average GFP signal intensity/pixel was measured 30 days after intravenous delivery of AAV9-GFP or AAVrh10-GFP (3×10^{13} vg/kg, $n = 4$ for each vector) in neonatal mice. **(A)** Motor cortex **(B)** retrosplenial cortex **(C)** hippocampal region **(D)** dentate gyrus **(E)** lateral habenular nucleus **(F)** thalamus **(G)** medulla **(H)** cerebellum. The data represent the mean values ± SEM of GFP fluorescence intensity/pixel (Mann-Withney test; $^*p < 0.05$).

the two vectors (**Figure 3**). Quantitative analysis of the intensity of GFP immunofluorescence in the dorsal spinal cord columns confirmed the superiority of AAVrh10 vs. AAV9 in this region at low dose ($p = 0.0157$) (**Figure 3C**).

As illustrated in **Figure 4**, GFP expression was also detected in the ventral horn of the spinal cord, from the cervical to lumbar levels (**Figure 4A**). MN transduction efficiency mediated by AAV9 and AAVrh10 was compared by co-immunofluorescence analysis using GFP and Choline Acetyltransferase (ChAT), a MN marker. Counting of GFP-positive ChAT MNs revealed that the mean percentage of transduced MNs was doubled throughout the spinal cord from mice injected with AAVrh10 compared to AAV9 at low dose (**Figures 4Ba,Bb**). Indeed, 22.1, 12.9, and 12.8% of MNs were transduced in the cervical, thoracic, and lumbar spinal cord after injection of low dose AAVrh10, vs. 11.8, 6.16, and 7.26% with AAV9 ($p = 0.0001$, 0.0403, and 0.0318) (**Figures 4Ba,Bb**). The superiority of AAVrh10 over AAV9 was less striking at the highest dose but was still significant in the whole spinal cord (**Figure 4Bc**). However, MN transduction analysis in each spinal cord segment showed a statistically significant difference only at the cervical level (25.9 vs. 20.2% for AAVrh10 and AAV9, respectively; $p = 0.0049$) (**Figure 4Bd**).

Comparison of AAV9 and AAVrh10-mediated Transduction of the Peripheral Nervous System

We further compared transgene expression provided by the two AAV serotypes in the PNS, in particular the dorsal root ganglia (DRG) and the sciatic nerve. In the DRG, no significant difference was observed between AAV9 and AAVrh10 injected animals, although a strong tendency for an increased GFP immunofluorescence intensity was noted with AAVrh10 compared to AAV9 at the low dose (**Figures 5A,C**). Similarly, a difference between the two vectors was observed for transduction of the sciatic nerve only at the low dose ($p = 0.02$) (**Figures 5B,D**). At high dose, the intensity of GFP immunofluorescence was markedly increased, in particular with AAV9, with no significant difference between the two serotypes ($p = 0.64$) (**Figures 5B,D**). This dose-related effect on the transduction efficiency provided by AAV9 and AAVrh10 was demonstrated by a statistically significant "AAV serotype by dose" interaction (Two-Way ANOVA, $p = 0.006$).

To further examine the distribution of the GFP protein in the sciatic nerve, co-immunofluorescence analyses were performed using antibodies against neurofilament (NF), a specific axonal marker, and β-S100, a marker for myelinating and non-myelinating Schwann cells. Our results showed that both AAV9 and AAVrh10 provided efficient transduction of NFs (**Figures 5Ea,Eb**) and Schwann cells (**Figures 5Ec,Ed**), with no obvious difference between the two serotypes. Of note, GFP was highly expressed in the Schwann cells that surrounded the axons, highlighting gene transfer in the myelinating subpopulation (**Figures 5Ec,Ed**).

Comparison of AAVrh10 and AAV9-mediated Heart and Liver Transduction

We finally examined two tissues, the heart and the liver, which were previously demonstrated as differentially transduced following intravascular injection of AAV9 or AAVrh10 (Hu et al., 2010; Piras et al., 2013). A global high transduction of the heart was found for both serotypes, the GFP-positive cells appearing widely distributed in the atria and ventricles (**Supplementary Figures 1Aa–d**). However, AAVrh10-mediated transduction of the cardiomyocytes was significantly higher than that provided by AAV9 at both low and high doses (Two-Way ANOVA, $p = 0.0051$) (**Supplementary Figure 1Ae**). The liver was found relatively weakly transduced, in particular at low dose (**Supplementary Figures 1Ba–d**), but similarly to results in the heart, a tendency for an increased transduction level was found with AAVrh10, although the difference between the two serotypes did not reach any statistical significance (**Supplementary Figure 1Be**).

Discussion

A number of comparative studies have reported improved CNS gene transfer after brain injection of AAV9 and AAVrh10, two newly identified AAV serotypes which have been isolated from the tissues of NHPs (rhesus or cynomolgus monkeys) (Gao et al., 2002, 2003; Mori et al., 2004). Both vectors were found to provide more efficient and widespread neuronal transduction in rodents

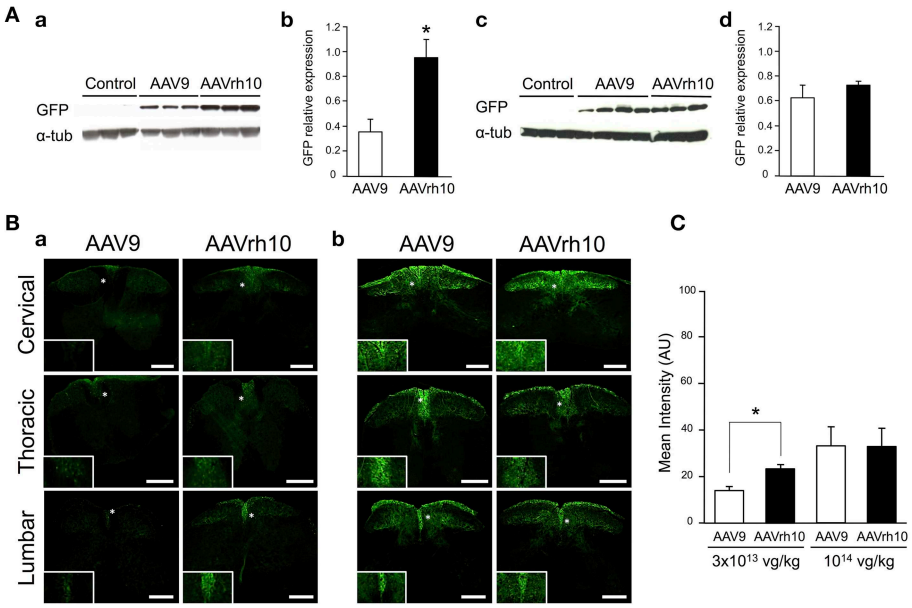

FIGURE 3 | GFP expression in the spinal cord of AAV9-GFP or AAVrh10-GFP injected mice. (A) Western blot and **(B)** immunofluorescence analyses were performed 30 days after intravenous injection of the vectors in neonatal mice. **(A)** Western-blot and corresponding densitometric analyses of GFP expression in whole spinal cord lysates injected with (a,b) low dose (3×10^{13} vg/kg) or (c,d) high dose (10^{14} vg/kg) of AAV9-GFP or AAVrh10-GFP vectors ($n = 6$ for low dose AAV9 or AAVrh10, $n = 4$ and 3 for high dose AAV9 and AAVrh10, respectively). Controls were protein extracts from non-injected mice and α-tubulin was used as internal loading control. Data in (b,d) represent the mean values ± SEM of GFP levels relative to α-tubulin levels (Mann-Withney test; $^*p < 0.05$). **(B)** Representative sections of the cervical, thoracic and lumbar spinal cord treated for GFP immunofluorescence after injection of AAV9 and AAVrh10 at (a) low dose (3×10^{13} vg/kg, $n = 4$ per vector) or (b) high dose (10^{14} vg/kg, $n = 4$ per vector). Panels at the bottom left corner showed high magnification indicated with a white asterisk. Scale bars = 250 μm. **(C)** GFP fluorescence intensity/pixel in the dorsal spinal cord of mice ($n = 4$ per vector and per dose). Results are expressed as mean of four independent experiments ± SEM (Two-Way ANOVA test, Bonferroni Post-test: $^*p < 0.05$).

as compared to the first characterized AAV2 serotype, or even to other robust serotypes such as AAV8, with some variability capabilities at spreading and transducing specific brain structures (Cearley and Wolfe, 2006; Sondhi et al., 2007; Klein et al., 2008; Miyake et al., 2011; Rafi et al., 2012; Hordeaux et al., 2015).

The unprecedented potential of self-complementary AAV9 for mediating widespread transgene expression in neuronal cells after systemic injection was recently demonstrated in both adult (Barkats, 2007; Duqué et al., 2009; Benkhelifa-Ziyyat et al., 2013) and neonatal animals (Barkats, 2007; Duqué et al., 2009; Foust et al., 2009; Benkhelifa-Ziyyat et al., 2013), including large animals such as cats (Barkats, 2007; Duqué et al., 2009) and NHPs (Bevan et al., 2011; Gray et al., 2011). This practical and non-invasive gene therapy approach has opened the way to first clinical trials in human, in particular for SMA type1 patients. Interestingly, recent studies showed that AAVrh10 also provided strong and widespread CNS transduction after intravenous administration in mice (Hu et al., 2010; Zhang et al., 2011; Mattar et al., 2013; Bucher et al., 2014; Hordeaux et al., 2015). In this study, we compared the capabilities of AAV9 and AAVrh10 at transducing different regions of the brain, the spinal cord and the PNS after intravenous injection in neonatal mice. As previously reported for AAV of serotypes 9 and rh10 by Cearley and Wolfe (2006), and with other serotypes by Davidson et al. (2000), variability was often observed between animals intravenously injected with the same serotype. However, the trends for a superiority of AAVrh10 transduction efficacy over AAV9 were evident in most CNS and PNS regions that we examined, with significant differences between the two vectors being found in the medulla, the cerebellum, the spinal cord and the sciatic nerves. Two main studies in neonatal mice have previously reported a greater transduction efficiency of AAVrh10 vs. AAV9 vectors in the brain following intravenous delivery (Hu et al., 2010; Zhang et al., 2011). As in our study, Zhang et al. showed in particular the superiority of AAVrh10 to transduce brain regions such as the hippocampus, the cerebellum or the medulla (Zhang et al., 2011). However, no difference between the two serotypes was reported in the spinal cord, in contrast to what we have demonstrated by western blot analysis of GFP protein levels in the whole spinal cord, quantification of GFP intensity levels in the dorsal spinal cord, and manual counting of the transduced MNs in the ventral spinal cord. Interestingly, our results showed that intravenous delivery of low dose AAVrh10 (3×10^{13} vg/kg) in neonatal mice led to the transduction of a number of MNs similar to that targeted with high dose AAV9 (10^{14} vg/kg). This finding suggested that using AAVrh10 could present potential for reducing the vector titer required for therapeutic translation to patients.

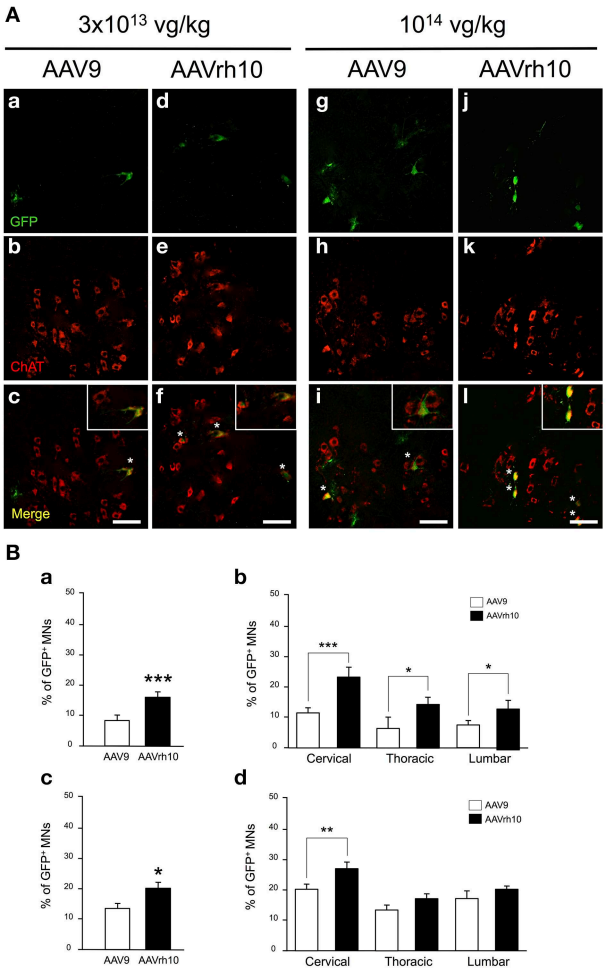

FIGURE 4 | Comparison of lower motor neuron transduction in AAV9 and AAVrh10 injected mice. (A) Representative cervical spinal cord sections treated for GFP/ChAT co-immunostaining 30 days after intravenous injection of neonatal mice with low (a–f) and high (g–l) doses of AAV9 or AAVrh10 vectors (a,d,g,j) GFP-positive cells (b,e,h,k) ChAT-positive MNs; (c,f,i,l) merge (asterisks: double-stained MNs; panels at the top right corner: high magnification). Scale bars = 50 μm. **(B)** Percentage of GFP/ChAT-positive MNs in the whole spinal cord (a,c) and in each spinal cord segment (b,d) at low (a,b) and high (c,d) dose of AAV. Data are means ± SEM ($n = 4$) and differences between groups were analyzed by Student *t*-test in (a,c) and One-Way ANOVA, Newman-Keuls *post-hoc*-test in (b,d); $^{*}p < 0.05$; $^{**}p < 0.01$; $^{***}p < 0.001$.

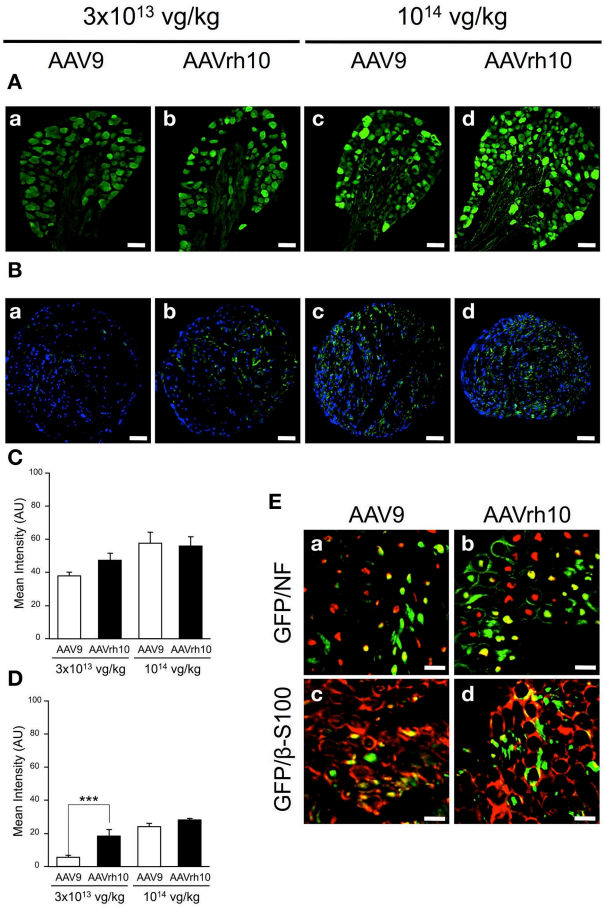

FIGURE 5 | GFP expression in the dorsal root ganglia and sciatic nerve of AAV9-GFP and AAVrh10-GFP injected mice. (A,B) Representative sections of **(A)** dorsal root ganglia and **(B)** sciatic nerve, treated for GFP immunofluorescence 30 days after neonatal delivery of AAV9 or AAVrh10 at low (a,b) and high (c,d) dose ($n = 4$ per dose and per serotype) **(C,D)** Quantification of GFP intensity/pixel in the dorsal root ganglia **(C)** and sciatic nerve **(D)** sections. Results are expressed as mean ± SEM ($n = 4$; Two-Way ANOVA analysis, Bonferroni *Post-hoc*-test: $^{***}p < 0.001$). **(E)** Representative sciatic nerve sections treated for (**a,b**) GFP/NF co-immunostaining (green: GFP; red: NF; yellow: merge) or (c,d) GFP/β-S100 co-immunostaining (green: GFP; red: β-S100; yellow: merge), 30 days after intravenous injection of neonatal mice with AAV9 (a,c) or AAVrh10 (b,d) at high dose (10^{14} vg/kg). Scale bars = **(A)** 50 μm; **(B)** 100 μm; **(C)** 20 μm.

Of note, the superiority of AAVrh10 over AAV9 for MN transduction was mainly observed at low dose, the difference between the two vectors administered at high dose being only significant in the cervical spinal cord. Indeed, the increase of the vector titer induced a rise in AAV9 transduction efficiency, without further significant augmentation of that of AAVrh10. This finding is in accordance with the assumption that more AAVrh10 than AAV9 particles could transduce a single cell, without transducing an increased number of cells, as previously suggested in the comparative study of several AAV serotypes injected into the mouse brain (Cearley and Wolfe, 2006), and more recently, after infusion of the serotypes into the striatum of rats and pigs using convection-enhanced delivery (White et al., 2011). In the latter study, no greater distribution was induced by increasing the infusion titer of AAVrh10, in contrast to AAV9 whose distribution continued to rise (White et al., 2011). Likewise, we found the sciatic nerve to be preferentially transduced by AAVrh10, but only at low dose. Increasing the vector titer induced a marked increase of GFP intensity levels in whole sciatic nerve sections from AAV9 injected mice, without further rise when mice were injected with high dose AAVrh10, corroborating the results obtained in the spinal cord. Together, these results and those of the literature suggest that the superior transduction efficacy of AAVrh10 would be related to a greatest amount of particles entering nervous cells,

rather than to a particular wide distribution of its receptors. Of note, the superiority of systemic AAVrh10 over AAV9 could also be dependent of genome conformation, since a study of Miyake et al., comparing several single-stranded AAVs (ssAAVs) intravenously delivered in neonatal mice, reported that transduction efficiencies of all vectors including ssAAVrh10 were low as compared to ssAAV9 (Miyake et al., 2011).

Differences between the serotype 9 and rh10 for CNS transduction efficiency could also be due to differential capabilities for entering nervous tissue following systemic delivery. Pathways by which AAV9 or AAVrh10 could enter the CNS could include transmigration or receptor mediated transcytosis across the endothelium of blood-brain barrier (BBB) and/or across the blood-cerebral spinal fluid barrier (blood-CSF barrier) at the choroid plexus as previously suggested (Barkats, 2007; Duqué et al., 2009) and previously assumed for HIV infection of the human brain (Falangola et al., 1995; Pereira and Nottet, 2000). As HIV viruses, AAV9 or AAVrh10 could also enter the CNS tissue at the level of the circumventricular organs (CVO), which are brain structures devoid of BBB thereby providing a possible site of infection (Johnson and Gross, 1993; Davson and Segal, 1996).

In view of the difference in the extent and intensity of transgene expression according to the brain structures, and of the gradient which was observed from the brain ventricles and adjacent regions to remote areas, our results are best in support of a preferential crossing at the choroid plexus. Indeed these structures were found to be robustly transduced in the 3rd and 4th ventricles, as well as neighboring parenchymal areas such as the hippocampus and the cerebellum. However, remote areas located far from the ventricles such as the cortex or the thalamus were also efficiently targeted, suggesting that other routes of entry into the CNS should also be taken, such as diffusion from the CVO. However, further experiments will be necessary for fully understanding the mechanism by which specific AAV serotype such as AAV9 and AAVrh10 enter into the brain and the spinal cord after systemic injection.

In addition to its high potential for CNS transduction, AAVrh10 was suggested to be an attractive alternative serotype to AAV9, particularly by the fact that it would be less prone to induce host serological immune response than AAV9 (Hordeaux et al., 2015). Indeed, humans should be less exposed to AAVrh10 since this vector is a rhesus monkey serotype, unlike the human AAV9 serotype. However, a recent study surprisingly reported a 59% IgG prevalence against AAVrh10 in humans, and 47% against AAV9 (Thwaite et al., 2015). Although most anti-AAVrh10 IgG were non-neutralizing (as anti-AAV9 IgG) their high prevalence in humans does not support the assumption of a particular immunological advantage of AAVrh10 over other serotypes. Moreover, antibody cross-recognition was also reported in humans, suggesting that a broad repertoire of preexisting antibodies would be able to react with non-human serotypes (Thwaite et al., 2015).

Although many studies have reported the high efficiency of AAVrh10 for CNS gene transfer, only a few compared AAV9 and rAAVrh10. This study suggests that, like AAV9, AAVrh10 holds promise for intravascular gene therapy of human CNS and PNS diseases affecting neurons, astrocytes, oligodendrocytes or Schwann cells. Our most significant finding was the superiority of AAVrh10 over AAV9 for MN transduction in neonatal mice, highlighting the particular potential of this serotype for SMA type1, a devastating disease affecting young children. Several brain regions were also reported to be affected in SMA type I patients, including the brainstem and the cerebellum (Harding et al., 2015), which were found highly transduced by serotype rh10. AAVrh10-mediated restoration of SMN in these brain areas could thus be important for gene therapy of SMA type 1. It should however be noted that the superiority of serotype rh10 over serotype 9 was mainly observed at low dose. The fact that AAVrh10 distribution was not improved by increasing the vector dose, whereas a dose-dependent increase of transduction efficiency was observed with AAV9, suggest differences in the transduction mechanisms of these two vectors which both present great interest for gene therapy of neurological diseases.

Acknowledgments

We are grateful to Luis Garcia (Neuromuscular disease Biotherapy laboratory, St Quentin en Yvelines University, France) and Bruno Cadot (Center of Research on Myology, UMRS 974 INSERM) for their help in microscopy image acquisitions. We thank Miss Mathilde-Alexia Pioline for her expertise in image processing. This work was supported by SMA-Europe, Association Française contre les Myopathies, the University Pierre et Marie Curie (UPMC), the Institut National de la Santé et de la Recherche Médicale (INSERM), the Centre National de la Recherche Scientifique (CNRS), and the Association Institut de Myologie (A.I.M).

Supplementary Material

The Supplementary Material for this article can be found online at: http://journal.frontiersin.org/article/10.3389/fnmol.2015.00036

Supplementary Figure 1 | Comparison of AAV9 and AAVrh10-mediated transduction of heart and liver. Representative sections of **(A)** heart and **(B)** liver, treated for GFP immunofluorescence 30 days after delivery of AAV9 or AAVrh10 at low (a,b) and high (c,d) dose in neonatal mice ($n = 4$ per dose and per serotype). Green: GFP-immunopositive cells; panels at the bottom left corner: high magnification. (e) Quantification of the average GFP signal intensity/pixel on 12 immunolabelled heart (**A,**e) and liver (**B,**e) sections per mouse. Data are presented as mean of ± SEM of GFP fluorescence intensity/pixel ($n = 4$; Two-Way ANOVA variance analysis, Bonferroni *Post-hoc*-test: $^*p < 0.05$). Scale bars = **(A)** 1 mm; **(B)** 100 μm.

References

Ahmed, S. S., Li, H., Cao, C., Sikoglu, E. M., Denninger, A. R., Su, Q., et al. (2013). A single intravenous rAAV injection as late as P20 achieves efficacious and sustained CNS Gene therapy in canavan mice. *Mol. Ther.* 21, 2136–2147. doi: 10.1038/mt.2013.138

Barkats, M. (2007). *Widespread Gene Delivery to Motor Neurons using Peripheral Injection of AAV Vectors.* PCT/EP2008/063297 GENETHON/CNRS.

Benkhelifa-Ziyyat, S., Besse, A., Roda, M., Duqué, S., Astord, S., Carcenac, R., et al. (2013). Intramuscular AAV9-SMN injection mediates widespread gene delivery to the spinal cord and decreases disease severity in SMA mice. *Mol. Ther.* 21, 282–290. doi: 10.1038/mt.2012.261

Bevan, A. K., Duque, S., Foust, K. D., Morales, P. R., Braun, L., Schmelzer, L., et al. (2011). Systemic gene delivery in large species for targeting spinal cord, brain, and peripheral tissues for pediatric disorders. *Mol. Ther.* 19, 1971–1980. doi: 10.1038/mt.2011.157

Bucher, T., Dubreil, L., Colle, M. A., Maquigneau, M., Deniaud, J., Ledevin, M., et al. (2014). Intracisternal delivery of AAV9 results in oligodendrocyte and motor neuron transduction in the whole central nervous system of cats. *Gene Ther.* 21, 522–528. doi: 10.1038/gt.2014.16

Cearley, C. N., and Wolfe, J. H. (2006). Transduction characteristics of adeno-associated virus vectors expressing cap serotypes 7, 8, 9, and Rh10 in the mouse brain. *Mol. Ther.* 13, 528–537. doi: 10.1016/j.ymthe.2005.11.015

Christine, C. W., Starr, P. A., Larson, P. S., Eberling, J. L., Jagust, W. J., Hawkins, R. A., et al. (2009). Safety and tolerability of putaminal AADC gene therapy for Parkinson disease. *Neurology* 73, 1662–1669. doi: 10.1212/WNL.0b013e3181c29356

Davidson, B. L., Stein, C. S., Heth, J. A., Martins, I., Kotin, R. M., Derksen, T. A., et al. (2000). Recombinant adeno-associated virus type 2, 4, and 5 vectors: transduction of variant cell types and regions in the mammalian central nervous system. *Proc. Natl. Acad. Sci. U.S.A.* 97, 3428–3432. doi: 10.1073/pnas.97.7.3428

Davson, H., and Segal, M. B. (1996). "Morphological aspects of the barriers," in *Physiology of the CSF and Blood-brain Barrier* (Boca Raton, FL: CRC Press), 93–192.

Dominguez, E., Marais, T., Chatauret, N., Benkhelifa-Ziyyat, S., Duque, S., Ravassard, P., et al. (2011). Intravenous AAV9 delivery of a codon-optimized SMN1 sequence rescues SMA mice. *Hum. Mol. Genet.* 20, 681–693. doi: 10.1093/hmg/ddq514

Duqué, S., Joussemet, B., Riviere, C., Marais, T., Dubreil, L., Douar, A. M., et al. (2009). Intravenous administration of self-complementary AAV9 enables transgene delivery to adult motor neurons. *Mol. Ther.* 17, 1187–1196. doi: 10.1038/mt.2009.71

Falangola, M. F., Hanly, A., Galvao-Castro, B., and Petito, C. K. (1995). HIV infection of human choroid plexus: a possible mechanism of viral entry into the CNS. *J. Neuropathol. Exp. Neurol.* 54, 497–503. doi: 10.1097/00005072-199507000-00003

Foust, K. D., Nurre, E., Montgomery, C. L., Hernandez, A., Chan, C. M., and Kaspar, B. K. (2009). Intravascular AAV9 preferentially targets neonatal neurons and adult astrocytes. *Nat. Biotechnol.* 27, 59–65. doi: 10.1038/nbt.1515

Foust, K. D., Wang, X., McGovern, V. L., Braun, L., Bevan, A. K., Haidet, A. M., et al. (2010). Rescue of the spinal muscular atrophy phenotype in a mouse model by early postnatal delivery of SMN. *Nat. Biotechnol.* 28, 271–274. doi: 10.1038/nbt.1610

Fu, H., Dirosario, J., Killedar, S., Zaraspe, K., and McCarty, D. M. (2011). Correction of neurological disease of mucopolysaccharidosis IIIB in adult mice by rAAV9 trans-blood-brain barrier gene delivery. *Mol. Ther.* 19, 1025–1033. doi: 10.1038/mt.2011.34

Fyfe, J. C., Menotti-Raymond, M., David, V. A., Brichta, L., Schäffer, A. A., Agarwala, R., et al. (2006). An approximately 140-kb deletion associated with feline spinal muscular atrophy implies an essential LIX1 function for motor neuron survival. *Genome Res.* 16, 1084–1090. doi: 10.1101/gr.5268806

Gao, G., Alvira, M. R., Somanathan, S., Lu, Y., Vandenberghe, L. H., Rux, J. J., et al. (2003). Adeno-associated viruses undergo substantial evolution in primates during natural infections. *Proc. Natl. Acad. Sci. U.S.A.* 100, 6081–6086. doi: 10.1073/pnas.0937739100

Gao, G. P., Alvira, M. R., Wang, L., Calcedo, R., Johnston, J., and Wilson, J. M. (2002). Novel adeno-associated viruses from rhesus monkeys as vectors for human gene therapy. *Proc. Natl. Acad. Sci. U.S.A.* 99, 11854–11859. doi: 10.1073/pnas.182412299

Gray, S. J., Matagne, V., Bachaboina, L., Yadav, S., Ojeda, S. R., and Samulski, R. J. (2011). Preclinical differences of intravascular AAV9 delivery to neurons and glia: a comparative study of adult mice and nonhuman primates. *Mol. Ther.* 19, 1058–1069. doi: 10.1038/mt.2011.72

Grieger, J. C., and Samulski, R. J. (2012). Adeno-associated virus vectorology, manufacturing, and clinical applications. *Meth. Enzymol.* 507, 229–254. doi: 10.1016/B978-0-12-386509-0.00012-0

Harding, B. N., Kariya, S., Monani, U. R., Chung, W. K., Benton, M., Yum, S. W., et al. (2015). Spectrum of neuropathophysiology in spinal muscular atrophy type I. *J. Neuropathol. Exp. Neurol.* 74, 15–24. doi: 10.1097/NEN.0000000000000144

Hordeaux, J., Dubreil, L., Deniaud, J., Iacobelli, F., Moreau, S., Ledevin, M., et al. (2015). Efficient central nervous system AAVrh10-mediated intrathecal gene transfer in adult and neonate rats. *Gene Ther.* 22, 316–324. doi: 10.1038/gt.2014.121

Hu, C., Busuttil, R. W., and Lipshutz, G. S. (2010). RH10 provides superior transgene expression in mice when compared with natural AAV serotypes for neonatal gene therapy. *J. Gene Med.* 12, 766–778. doi: 10.1002/jgm.1496

Johnson, A. K., and Gross, P. M. (1993). Sensory circumventricular organs and brain homeostatic pathways. *FASEB J.* 7, 678–686.

Kaplitt, M. G., Feigin, A., Tang, C., Fitzsimons, H. L., Mattis, P., Lawlor, P. A., et al. (2007). Safety and tolerability of gene therapy with an adeno-associated virus (AAV) borne *GAD* gene for Parkinson's disease: an open label, phase I trial. *Lancet* 369, 2097–2105. doi: 10.1016/S0140-6736(07)60982-9

Klein, R. L., Dayton, R. D., Tatom, J. B., Henderson, K. M., and Henning, P. P. (2008). AAV8, 9, Rh10, Rh43 vector gene transfer in the rat brain: effects of serotype, promoter and purification method. *Mol. Ther.* 16, 89–96. doi: 10.1038/sj.mt.6300331

Le, T. T., Pham, L. T., Butchbach, M. E., Zhang, H. L., Monani, U. R., Coovert, D. D., et al. (2005). SMNDelta7, the major product of the centromeric survival motor neuron (SMN2) gene, extends survival in mice with spinal muscular atrophy and associates with full-length SMN. *Hum. Mol. Genet.* 14, 845–857. doi: 10.1093/hmg/ddi078

LeWitt, P. A., Rezai, A. R., Leehey, M. A., Ojemann, S. G., Flaherty, A. W., Eskandar, E. N., et al. (2011). AAV2-GAD gene therapy for advanced Parkinson's disease: a double-blind, sham-surgery controlled, randomised trial. *Lancet Neurol.* 10, 309–319. doi: 10.1016/S1474-4422(11)70039-4

Mandel, R. J., and Burger, C. (2004). Clinical trials in neurological disorders using AAV vectors: promises and challenges. *Curr. Opin. Mol. Ther.* 6, 482–490.

Marks, W. J. Jr., Ostrem, J. L., Verhagen, L., Starr, P. A., Larson, P. S., Bakay, R. A., et al. (2008). Safety and tolerability of intraputaminal delivery of CERE-120 (adeno-associated virus serotype 2-neurturin) to patients with idiopathic Parkinson's disease: an open-label, phase I trial. *Lancet Neurol.* 7, 400–408. doi: 10.1016/S1474-4422(08)70065-6

Mattar, C. N., Waddington, S. N., Biswas, A., Johana, N., Ng, X. W., Fisk, A. S., et al. (2013). Systemic delivery of AAV9 in fetal macaques facilitates neuronal transduction of the central and peripheral nervous systems. *Gene Ther.* 20, 69–83. doi: 10.1038/gt.2011.216

McCown, T. J., Xiao, X., Li, J., Breese, G. R., and Samulski, R. J. (1996). Differential and persistent expression patterns of CNS gene transfer by an adeno-associated virus (AAV) vector. *Brain Res.* 25, 99–107. doi: 10.1016/0006-8993(95)01488-8

Miyake, N., Miyake, K., Yamamoto, M., Hirai, Y., and Shimada, T. (2011). Global gene transfer into the CNS across the BBB after neonatal systemic delivery of single-stranded AAV vectors. *Brain Res.* 1389, 19–26. doi: 10.1016/j.brainres.2011.03.014

Mori, S., Wang, L., Takeuchi, T., and Kanda, T. (2004). Two novel adeno-associated viruses from cynomolgus monkey: pseudotyping characterization of capsid protein. *Virology.* 330, 375–383. doi: 10.1016/j.virol.2004.10.012

Pereira, C. F., and Nottet, H. S. L. M. (2000). The blood-brain barrier in HIV-associated dementia. *Science* 3, 1–8

Piras, B. A., O'Connor, D. M., and French, B. A. (2013). Systemic delivery of shRNA by AAV9 provides highly efficient knockdown of ubiquitously expressed GFP in mouse heart, but not liver. *PLoS ONE* 8:e75894. doi: 10.1371/journal.pone.0075894

Rafi, M. A., Rao, H. Z., Luzi, P., Curtis, M. T., and Wenger, D. A. (2012). Extended normal life after AAVrh10-mediated gene therapy in the mouse model of Krabbe disease. *Mol. Ther.* 20, 2031–2042. doi: 10.1038/mt.2012.153

Ruzo, A., Marcó, S., García, M., Villacampa, P., Ribera, A., Ayuso, E., et al. (2012). Correction of pathological accumulation of glycosaminoglycans in central nervous system and peripheral tissues of MPSIIIA mice through systemic AAV9 gene transfer. *Hum. Gene Ther.* 23, 1237–1246. doi: 10.1089/hum.2012.029

Sondhi, D., Hackett, N. R., Peterson, D. A., Stratton, J., Baad, M., Travis, K. M., et al. (2007). Enhanced survival of the LINCL mouse following CLN2 gene transfer using the rh.10 rhesus macaque-derived adeno-associated virus vector. *Mol. Ther.* 15, 481–491. doi: 10.1038/sj.mt.6300049

Tardieu, M., Zérah, M., Husson, B., De Bournonville, S., Deiva, K., Adamsbaum, C., et al. (2014). Intracerebral administration of adeno-associated viral vector serotype rh.10 carrying human SGSH and SUMF1 cDNAs in children with mucopolysaccharidosis type IIIA disease: results of a phase I/II trial. *Hum. Gene Ther.* 5, 506–516 doi: 10.1089/hum.2013.238

Thwaite, R., Pagès, G., Chillón, M., and Bosch, A. (2015). AAVrh.10 immunogenicity in mice and humans. Relevance of antibody cross-reactivity in human gene therapy. *Gene Ther.* 22, 196–201. doi: 10.1038/gt.2014.103

Valori, C. F., Ning, K., Wyles, M., Mead, R. J., Grierson, A. J., Shaw, P. J., et al. (2010). Systemic delivery of AAV9 expressing SMN prolongs survival in a model of spinal muscular atrophy. *Sci. Transl. Med.* 2, 35–42. doi: 10.1126/scitranslmed.3000830

Weinberg, M. S., Samulski, R. J., and McCown, T. J. (2013). Adeno-associated virus (AAV) gene therapy for neurological disease. *Neuropharmacology* 69, 82–88. doi: 10.1016/j.neuropharm.2012.03.004

White, E., Bienemann, A., Megraw, L., Bunnun, C., and Gill, S. (2011). Evaluation and optimization of the administration of a selectively replicating herpes simplex viral vector to the brain by convection-enhanced delivery. *Cancer Gene Ther.* 18, 358–369. doi: 10.1038/cgt.2011.2

Wu, P., Phillips, M. I., Bui, J., and Terwilliger, E. F. (1998). Adeno-associated virus vector-mediated transgene integration into neurons and other nondividing cell targets. *J. Virol.* 72, 5919–5926.

Yamashita, T., Chai, H. L., Teramoto, S., Tsuji, S., Shimazaki, K., Muramatsu, S., et al. (2013). Rescue of amyotrophic lateral sclerosis phenotype in a mouse model by intravenous AAV9-ADAR2 delivery to motor neurons. *EMBO Mol. Med.* 5, 1710–1719. doi: 10.1002/emmm.201302935

Zhang, H., Yang, B., Mu, X., Ahmed, S. S., Su, Q., He, R., et al. (2011). Several rAAV vectors efficiently cross the blood-brain barrier and transduce neurons and astrocytes in the neonatal mouse central nervous system. *Mol. Ther.* 19, 1440–1448. doi: 10.1038/mt.2011.98

Conflict of Interest Statement: The authors declare that the research was conducted in the absence of any commercial or financial relationships that could be construed as a potential conflict of interest.

frontiers in Molecular Neuroscience

ORIGINAL RESEARCH
published: 04 November 2016
doi: 10.3389/fnmol.2016.00116

Better Targeting, Better Efficiency for Wide-Scale Neuronal Transduction with the Synapsin Promoter and AAV-PHP.B

*Kasey L. Jackson[1], Robert D. Dayton[1], Benjamin E. Deverman[2] and Ronald L. Klein[1]**

[1] Department of Pharmacology, Toxicology, and Neuroscience, Louisiana State University Health Sciences Center, Shreveport, LA, USA, [2] Division of Biology and Biological Engineering, California Institute of Technology, Pasadena, CA, USA

Widespread genetic modification of cells in the central nervous system (CNS) with a viral vector has become possible and increasingly more efficient. We previously applied an AAV9 vector with the cytomegalovirus/chicken beta-actin (CBA) hybrid promoter and achieved wide-scale CNS transduction in neonatal and adult rats. However, this method transduces a variety of tissues in addition to the CNS. Thus we studied intravenous AAV9 gene transfer with a synapsin promoter to better target the neurons. We noted in systematic comparisons that the synapsin promoter drives lower level expression than does the CBA promoter. The engineered adeno-associated virus (AAV)-PHP.B serotype was compared with AAV9, and AAV-PHP.B did enhance the efficiency of expression. Combining the synapsin promoter with AAV-PHP.B could therefore be advantageous in terms of combining two refinements of targeting and efficiency. Wide-scale expression was used to model a disease with widespread pathology. Vectors encoding the amyotrophic lateral sclerosis (ALS)-related protein transactive response DNA-binding protein, 43 kDa (TDP-43) with the synapsin promoter and AAV-PHP.B were used for efficient CNS-targeted TDP-43 expression. Intracerebroventricular injections were also explored to limit TDP-43 expression to the CNS. The neuron-selective promoter and the AAV-PHP.B enhanced gene transfer and ALS disease modeling in adult rats.

Keywords: adeno-associated virus, amyotrophic lateral sclerosis, gene therapy, gene transfer, promoter, synapsin promoter, targeting, TDP-43

OPEN ACCESS

Edited by:
Andrew Paul Tosolini, University College London, UK

Reviewed by:
Matthias Klugmann, University of New South Wales, Australia
Koichi Miyake, Nippon Medical School, Japan

****Correspondence:***
Ronald L. Klein
Klein@lsuhsc.edu

Received: *31 August 2016*
Accepted: *19 October 2016*
Published: *04 November 2016*

Citation:
Jackson KL, Dayton RD, Deverman BE and Klein RL (2016) Better Targeting, Better Efficiency for Wide-Scale Neuronal Transduction with the Synapsin Promoter and AAV-PHP.B. Front. Mol. Neurosci. 9:116. doi: 10.3389/fnmol.2016.00116

INTRODUCTION

Adeno-associated virus (AAV) is one of the most widely used systems for gene transfer to the central nervous system (CNS), for example in optogenetics, cre-lox targeting, and CRISPR gene editing. Scientists wishing to genetically modify the brain with AAV often ask: (1) which AAV serotype should I use in my gene transfer experiments; (2) which promoter/expression cassette should I be using; and (3) which route of vector administration gives me the transduction pattern with the greatest disease relevance for my gene of interest? Many of these governing parameters of AAV gene transfer have been extensively studied with focal, intraparenchymal injections. However, few of these comparative studies have been made for wide-scale CNS transduction where neurons are transduced throughout the nervous system. Wide-scale CNS

transduction is relevant for modeling and treating CNS diseases with widespread CNS pathology, so optimization of wide-scale gene transfer is important for these goals. This study attempted to improve upon previous work with AAV9 and the hybrid cytomegalovirus/chicken beta-actin (CBA, also known as the CAG promoter) promoter in terms of neuronal targeting and gene transfer efficiency. If possible, then these refinements could be applied to disease modeling and gene therapy.

If neuronal targeting is the goal, then an appropriate cell-type specific promoter is necessary. Synapsin is considered to be a neuron-specific protein (DeGennaro et al., 1983), so its neuron-specific expression pattern could potentially be harnessed to express transgenes in a neuron-specific manner. A minimal human synapsin promoter has been used in adenoviral and AAV vectors for focal injections (Kügler et al., 2003a,b; Shevtsova et al., 2005). An AAV capsid that can reach the CNS after peripheral administration, such as AAV9 (Foust et al., 2009; Wang et al., 2010; Miyake et al., 2011) or other natural AAV serotypes (Miyake et al., 2011; Snyder et al., 2011; Samaranch et al., 2013; Yang et al., 2014; Jackson et al., 2015b) is advantageous for a relatively non-invasive administration that yields wide-scale expression. Now there are several engineered capsids with increased neuronal transduction efficiency (Choudhury et al., 2016a,b; Deverman et al., 2016). Here we tested AAV-PHP.B described in Deverman et al. (2016) in rats for the first time in order to achieve greater gene transfer efficiency and potentially for improved neuronal targeting as well.

The goal of the study was to achieve more efficient CNS transduction in a more targeted manner than our previous studies using AAV9 in rats for the purpose of disease modeling. Transactive response DNA-binding protein, 43 kDa (TDP-43) is an RNA binding protein that is associated with amyotrophic lateral sclerosis (ALS): TDP-43 mutations can cause ALS (Gitcho et al., 2008), and the vast majority of ALS patients harbor TDP-43 neuropathology in post-mortem studies (Mackenzie et al., 2007). We have used the CBA promoter to express TDP-43 before, but here we attempted to better delimit the TDP-43 expression to neurons using the synapsin promoter and intracerebroventricular injections. We studied synapsin promoter-TDP-43 vectors and intracerebroventricular injections in order to address whether the motor paralysis that we see using the CBA promoter is due to TDP-43 expression in the CNS. We also studied AAV-PHP.B TDP-43 vectors since the greater efficiency could lower vector doses needed, which could decrease side effects in the animal and save costs in terms of the amount of vector production that is required. Furthermore, it is better to model an adult onset disease such as ALS in an adult onset animal model. Because adult CNS transduction requires larger amounts of vector relative to transduction of neonates, more efficient vectors will facilitate work in disease-relevant adult subjects. We hope these encouraging results with the synapsin promoter and AAV-PHP.B will help investigators in their design of wide-scale gene transfer studies.

MATERIALS AND METHODS

DNA and Viruses

cDNA for green fluorescent protein (GFP) or human wild-type TDP-43 were incorporated into an expression cassette plasmid including the AAV2 terminal repeats, the CBA promoter, (1.8 kb), the woodchuck hepatitis virus post-transcriptional regulatory element (WPRE), and the bovine growth hormone polyadenylation sequence (Klein et al., 2002). The strong CBA promoter was first incorporated into an AAV vector by Xu et al. (2001). The term CBA promoter is synonymous with the CAG promoter (Niwa et al., 1991). A plasmid for a minimal human synapsin promoter (485 bp) driving expression of yellow fluorescent protein (YFP) was provided by K. Deisseroth, Stanford University. This plasmid also contains the WPRE and human growth hormone polyadenylation sequence. Two different fluorophores were used in this study, GFP and the GFP variant, YFP. YFP should be at least as bright or a brighter fluorophore than GFP (Ormö et al., 1996; Yang et al., 1996). The difference in brightness between the two fluorophores had no bearing on the results particularly since the tissues were immuno-labeled with a GFP antibody that recognizes both proteins. cDNA for human wild-type TDP-43 (gene accession number NM_007375) was also incorporated into the synapsin promoter cassette in place of YFP.

DNAs were packaged into recombinant AAV9 or AAV-PHP.B by described methods (Klein et al., 2008b). Helper and AAV9 capsid plasmids used to generate AAV9 were from the University of Pennsylvania (Gao et al., 2004). AAV-PHP.B capsid plasmids were from the California Institute of Technology (Deverman et al., 2016). Viral stocks were sterilized using a Millipore Millex-GV syringe filter, aliquoted and stored frozen. Viral genome copies were titered using dot-blot assay, and equal titer doses were obtained by diluting stocks in lactated Ringer's solution (Baxter Healthcare).

Neonatal Studies

Litters of Sprague-Dawley rats (Envigo) were injected on post-natal day one. A total of 25 neonatal rats were used including both male and female subjects. Animals received 100 µl of virus diluted in lactated Ringer's solution administered via a 30 g needle into the facial vein, as previously described (Wang et al., 2010). The paws of the animals were tattooed (Spaulding Color, Voorheesville, NY, USA) for identification, and the pups were weaned at 3 weeks of age. The vector doses for neonates are expressed as total vector genomes (vg) injected. The neonatal rats usually weighed 6 g, so the per kg dose is 167 times higher than the total vg injected. Eleven neonatal rats were injected with AAV9 synapsin promoter-YFP at a dose of 4×10^{12} vg. Five animals were administered AAV9 CBA-GFP at a dose of 1.9×10^{12} vg, and four additional rats were administered AAV-PHP.B CBA-GFP at an equivalent dose of 1.9×10^{12} vg.

Adult Studies

Adult female Sprague-Dawley rats (approximately 6 weeks of age weighing 130 g, Envigo) were used for intravenous administrations. A total of 21 subjects were used. For tail

vein injections, animals received 200 μl of virus diluted in lactated Ringer's solution administered via a 30 g needle into the lateral tail vein. Intravenous delivery was also performed via retro-orbital injections in a subset of animals. For retro-orbital injections, animals received 100 μl of diluted virus administered via a 30 g needle into the capillary bed behind the eye. We were interested in this method to find an easier or more reliable method than tail vein injections. The retro-orbital injections yielded consistent results, but overall we did not notice any obvious, clear-cut advantage compared to the tail vein method in adult rats. Four adult rats were administered AAV9 CBA-GFP at a dose of 1×10^{13} vg/kg and one at a higher dose of 7.5×10^{13} vg/kg. Four rats were administered AAV9 synapsin promoter-YFP at a dose of 1×10^{13} vg/kg and one rat at a higher dose of 7.5×10^{13} vg/kg. Three rats were administered AAV-PHP.B synapsin promoter-YFP at a dose of 3.8×10^{13} vg/kg.

One adult female Sprague-Dawley rat (225 g) was stereotaxically administered AAV into the substantia nigra (coordinates: 5.3 mm posterior to bregma, 2.1 mm lateral, 7.6 mm ventral). One side was injected with AAV9 CBA-GFP and the other side with AAV9 synapsin promoter-YFP at matching doses (3×10^9 vg). Two adult female Sprague-Dawley rats (approximately 225 g) were stereotaxically administered AAV9 into the lateral ventricle (coordinates: 0.93 mm posterior to bregma, 1.6 mm lateral, 3.5 mm ventral).

Disease Modeling With TDP-43

To demonstrate the relevance of the GFP results for disease modeling, we administered a subset of rats with TDP-43 vectors. When AAV9 encoding TDP-43 driven by the CBA promoter is administered intravenously to either neonatal (Wang et al., 2010) or adult (Jackson et al., 2015b) rats, a progressive paresis and paralysis of the limbs develops, which may also involve mortality depending on the vector dose used (Jackson et al., 2015b). We have studied rats from 2 to 24 weeks after AAV9 TDP-43 gene transfer (Dayton et al., 2013). TDP-43 is known to induce paralysis, and at a high vector dose, mortality in rats, so we purposefully used small numbers of subjects to determine the presence of the disease state on a yes-or-no basis. Three neonatal rats were administered AAV9 synapsin promoter-TDP-43 at a dose of 4×10^{12} vg. Two neonatal rats were administered AAV-PHP.B-TDP-43 at a dose of 1.6×10^{12} vg. Three adult rats were administered AAV9 synapsin promoter-TDP-43 at a dose of 3×10^{13} vg/kg, and three rats were administered AAV-PHP.B synapsin promoter-TDP-43 at an equivalent dose of 3×10^{13} vg/kg. These rats were evaluated for motor dysfunction and mortality. All animal research conducted was approved by the Animal Care and Use Committee at Louisiana State University Health Sciences Center at Shreveport.

Analysis of Motor Function

Animals were evaluated for motor function via rotarod and escape reflex testing. Rotarod testing was performed on a Rotarod (Rota-rod/RS, Letica Scientific Instruments, Barcelona, Spain) that was accelerating from 4 to 40 rpm over 2 min. The amount of time the rat could remain walking on the rotarod before falling was measured three times and averaged. The escape reflex was evaluated by briefly lifting the rat from the tail. A normal escape reflex is the extension of forelimbs and hindlimbs. Clenching of the fore- or hindlimbs during this test is indicative of a lesion in the motor pathway. Motor deficits for the animals administered TDP-43 were noted if the averaged rotarod scores were less than 30 s or if limb clenching was demonstrated on three consecutive trials.

Immunohistochemistry

Animals were anesthetized with a cocktail of ketamine (100 mg/ml, Fort Dodge Animal Health, Fort Dodge, IA, USA), xylazine (20 mg/ml, Butler, Columbus, OH, USA), and acepromazine (10 mg/ml, Boerhinger Ingelheim, St. Joseph, MO, USA) in a 3:3:1 fluid ratio. Animals were administered 2 ml/kg of the cocktail intramuscularly before perfusion. The animals were transcardially perfused with phosphate buffered saline followed by cold 4% paraformaldehyde in phosphate-buffered saline. Tissues were removed and immersed in 4% paraformaldehyde overnight at 4°C. Tissues were cryopreserved in 30% sucrose. Fifty μm sections were cut on a sliding microtome with a freezing stage (Leica Biosystems, Buffalo Grove, IL, USA). The primary antibodies were rabbit anti-GFP (Invitrogen, 1:500), mouse anti-GFP (Invitrogen, 1:250), which efficiently label both GFP and YFP, rabbit anti-glial fibrillary acidic protein (GFAP; Chemicon, 1:1000) which labels astrocytes, mouse anti-CD11B (Chemicon, 1:500) which labels microglia, and mouse anti-NeuN (Chemicon, 1:1000) which labels neurons. The secondary antibodies were Alexa Fluor 488 and Alexa Fluor 594 (Invitrogen) at a concentration of 1:300. DAPI (Sigma, St. Louis, MO, USA) was used as a counterstain.

Analysis of Transgene Expression in The Cerebellum

After immunofluorescent staining for GFP, three evenly spaced sections of the cerebellar vermis for each animal were photomicrographed using a 2.5× lens and converted to grayscale. The fluorescent area was quantified using Scion Image as previously described (Jackson et al., 2015b), and the three sections per animal were averaged. We confirmed that non-transduced tissues had only negligible background readings by analyzing cerebellum that was not transduced with AAV but stained for GFP.

RESULTS

Promoter Studies

Transgene Expression Pattern of Synapsin Promoter-AAV9

A neonatal rat receiving AAV9 synapsin promoter-YFP intravenously at a dose of 4×10^{12} vg (6.7×10^{14} vg/kg) was evaluated at 4 weeks for CNS expression. Robust, wide-scale expression in the CNS was achieved with efficient labeling of neurons in the frontal cortex, forebrain, cerebellum and spinal

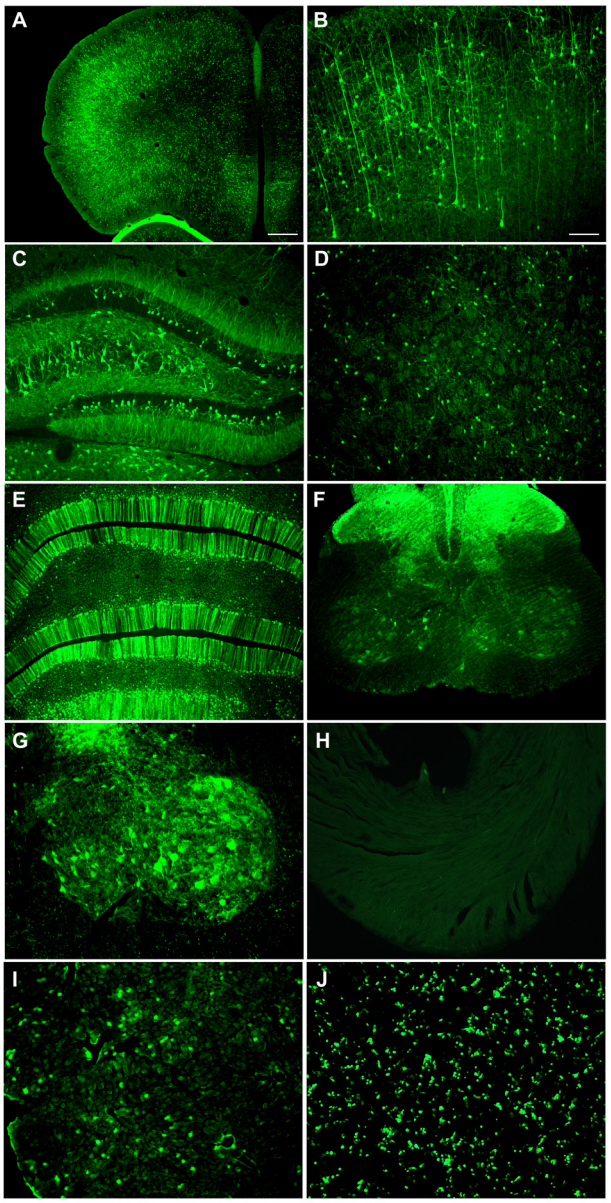

FIGURE 1 | Highly efficient wide-scale central nervous system (CNS) transgene expression in the rat using the synapsin promoter with avoidance of heart, but not liver expression. Synapsin promoter-AAV9 was administered intravenously to a neonatal rat and the tissue was analyzed 4 weeks later. **(A,B)** Expression in cortical neurons. **(C)** Hippocampus. **(D)** Striatum. **(E)** Cerebellum. **(F,G)** Spinal cord. **(H)** The heart had trace to no expression. **(I)** The synapsin promoter-AAV9 did result in expression in the liver. **(J)** This synapsin promoter DNA construct also drives expression in non-neuronal cells (HEK 293T) after transfection. Green fluorescent protein (GFP) immunostaining in **(A–I)** Native fluorescence in **(J)** Bar in **(A)** = 268 μm, same magnification in **(E,F,H–J)** Bar in **(B)** = 134 μm, same magnification in **(C,D,G–I)**.

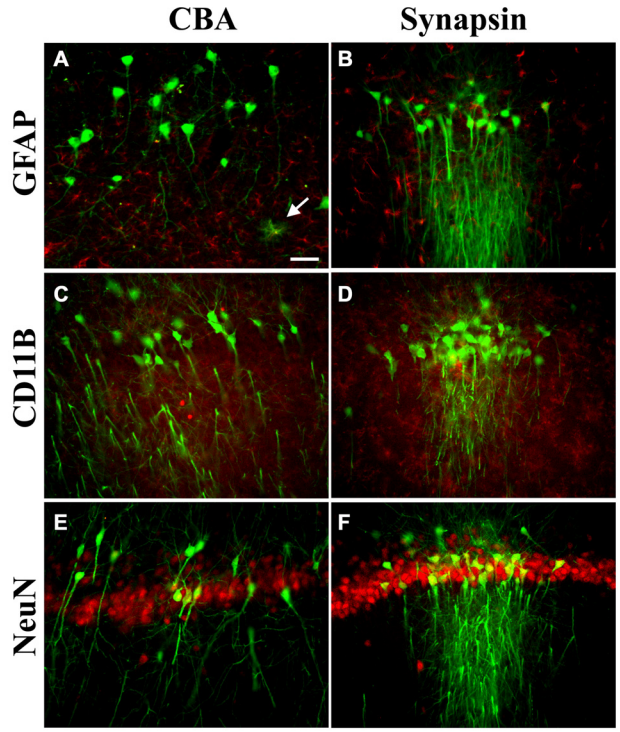

FIGURE 2 | Transgene expression profiles in astroglia, microglia, and neurons in the CNS. Pictures are mergers of GFP immunofluorescence in green and cell type specific markers in red, from the hippocampus. **(A,B)** For astroglia (glial fibrillary acidic protein, GFAP), there were occasional examples of GFP-positive cells with the cytomegalovirus/chicken beta-actin hybrid (CBA) promoter (arrow) but GFP-positive astroglia were not present using the synapsin promoter. **(C,D)** For microglia (CD11B), the adeno-associated virus (AAV) transgene did not co-localize with the microglial marker with either promoter. **(E,F)** Most of the cells expressing the transgene in the CNS were co-labeled with the neuronal marker NeuN with either the CBA or synapsin promoter. AAV-PHP.B was used for both promoters and the expression interval was 4 weeks after intravenous administration. Bar in **(A)** = 42 μm, same magnification in **(A–F)**.

cord among other regions throughout the CNS (**Figures 1A–G**). In the CNS, the transduced cells appeared exclusively neuronal and did not include cells with glial morphologies. The YFP expressed in transduced cells did not co-localize with GFAP, an astrocyte marker, or CD11B, a microglia marker (**Figure 2**). By comparison, the CBA promoter drives expression in occasional astroglia, though mostly expresses in neurons in the CNS (**Figure 2**). Outside of the CNS, with the synapsin promoter, the cardiomyocytes were largely spared from transgene expression (**Figure 1H**), a clear success of this promoter strategy as we were attempting a more restricted pattern compared to the CBA promoter, which efficiently expresses in cardiomyocytes (Wang et al., 2010). However, synapsin promoter driven YFP was observed in the liver at 4 weeks (**Figure 1I**), so the recombinant human synapsin promoter should therefore be referred to as neuron-selective, not neuron-specific in the context of a recombinant AAV9 vector. Along these lines, during the vector packaging stages, the synapsin promoter expressed in the non-neuronal HEK 293T cells (**Figure 1J**). Comparing on a qualitative basis with the heart and liver expression conferred by the CBA promoter in rats (Wang et al., 2010), expression in the heart appears to be nearly completely silenced with the synapsin promoter and partially muted in the liver.

Comparison of the Synapsin Promoter with the CBA Promoter

The two promoters, synapsin and CBA, were evaluated for CNS expression levels. One Sprague-Dawley rat was administered AAV9 CBA promoter-GFP on one side of the brain and on the other side, AAV9 synapsin promoter-YFP, each at an equal vector dose of 3×10^9 vg. After 3 weeks, the substantia nigra was analyzed for fluorescence, which clearly supported that the CBA promoter drives stronger expression than the synapsin promoter under equal conditions (**Figures 3A,B**). We then compared the CBA and synapsin promoters in adult rats on a statistical basis, using intravenous gene delivery by the retro-orbital injection method. Each of the two promoter constructs was administered at an equal dose of 1×10^{13} vg/kg. The CBA promoter group produced greater expression in the cerebellum compared to the synapsin promoter group by 5.6-fold (**Figures 3C–I**; *t*-test, $n = 3$/promoter group, $p < 0.01$, expression interval of 4 weeks).

Attenuation of Long-Term Expression with the Synapsin Promoter

The CBA promoter is known to confer high expression levels on a long-term basis, for example 1 year in rats in Klein et al. (2002) and 8 months in non-human primates in Jackson et al. (2015a). To determine if expression driven by the synapsin promoter remained stable over time, 11 neonatal rats were administered AAV9 synapsin promoter-YFP at a dose of 4×10^{12} vg (6.7×10^{14} vg/kg). Five of the rats were evaluated at 4 weeks, and the remaining six were evaluated at 22 weeks. Transduction of the cerebellum was evaluated, which clearly demonstrated attenuation of synapsin promoter driven expression at the longer interval (**Figure 4**; *t*-test, $n = 5$–6/time point, $p < 0.01$).

Studies With The AAV-PHP.B Capsid

CBA Promoter-AAV-PHP.B, Comparison with AAV9 in Neonates

AAV-PHP.B was reported to be 40-fold more efficient than AAV9 for neuronal transduction in mice by Deverman et al. (2016). Here, we made a comparison in rats using the same CBA promoter expression cassette in AAV9 or AAV-PHP.B. Four neonatal animals were administered AAV-PHP.B CBA-GFP and five neonatal animals with AAV9 CBA-GFP at an equal vector dose of 1.9×10^{12} vg (3.2×10^{14} vg/kg). Expression was evaluated 4 weeks later. The transduction of the cerebellum was increased by 2.4-fold in the AAV-PHP.B group compared to the AAV9 group (**Figure 5**; *t*-test, $n = 4$–5/capsid serotype group, $p < 0.001$). The lesser degree of fold-increase observed in rats compared to mice (Deverman et al., 2016) could be due to making this comparison closer to the vector dose saturation point in neonates. Since large doses of highly efficient, high titer AAV9 vectors are needed for wide-scale studies in adult subjects, the increased transduction efficiency of AAV-PHP.B should be able to lower this demand and save on the amount of vector production needed. Though not quantified, there was a visible trend of reduced hepatic expression using AAV-PHP.B compared to AAV9 along with the increased

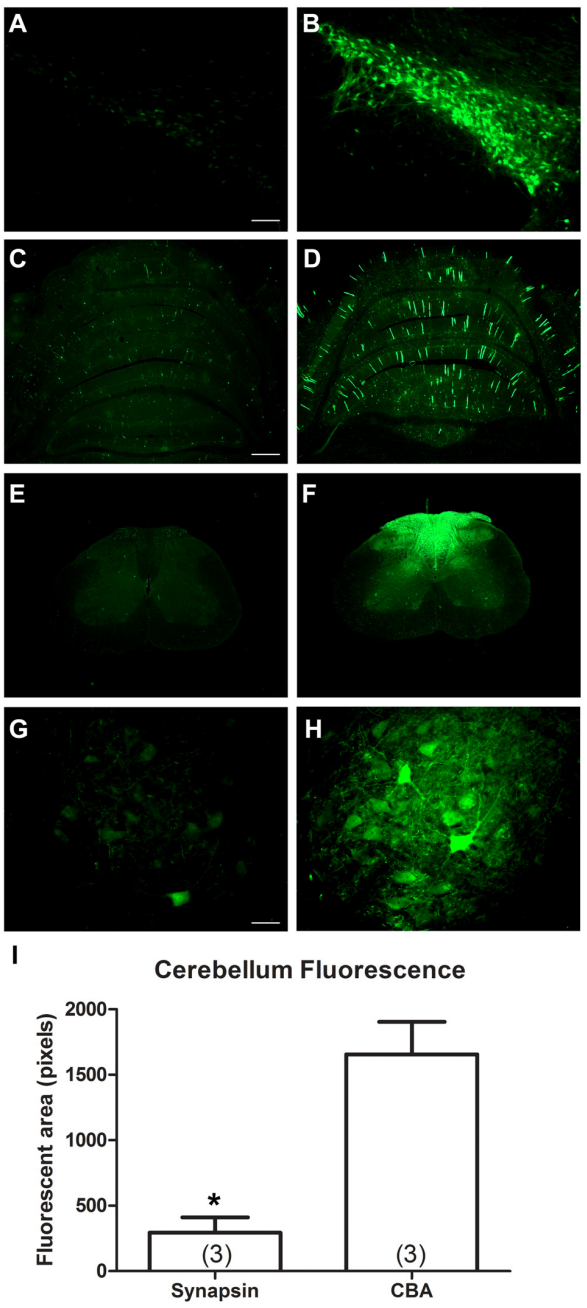

FIGURE 3 | In comparisons of the synapsin promoter and the CBA promoter, the CBA promoter clearly drives stronger expression. One rat received a bilateral stereotaxic injection into the substantia nigra. One side was injected with a synapsin promoter-AAV9 and the other with a CBA promoter-AAV9 under equal conditions. **(A,B)** The expression from the synapsin promoter-AAV9, while present, was fainter than the CBA promoter-AAV9 at equal camera exposures. **(C–H)** Similarly, after retro-orbital injections of AAV9 in adult rats under equal conditions, the expression from the synapsin promoter-AAV9 appeared fainter than the CBA promoter-AAV9, cerebellum in **(C,D)** spinal cord in **(E–H)**. **(I)** The GFP-positive area of the cerebellum was greater in the CBA promoter-AAV9 group (*t*-test, $p < 0.01$, $n = 3$/promoter group). GFP immunostaining in **(C–H).** Bar in **(A)** = 134 μm, same magnification in **(B)**. Bar in **(C)** = 536 μm, same magnification in **(D–F)**. Bar in **(G)** = 67 μm, same magnification in **(H)**. *Indicated $p < 0.01$.

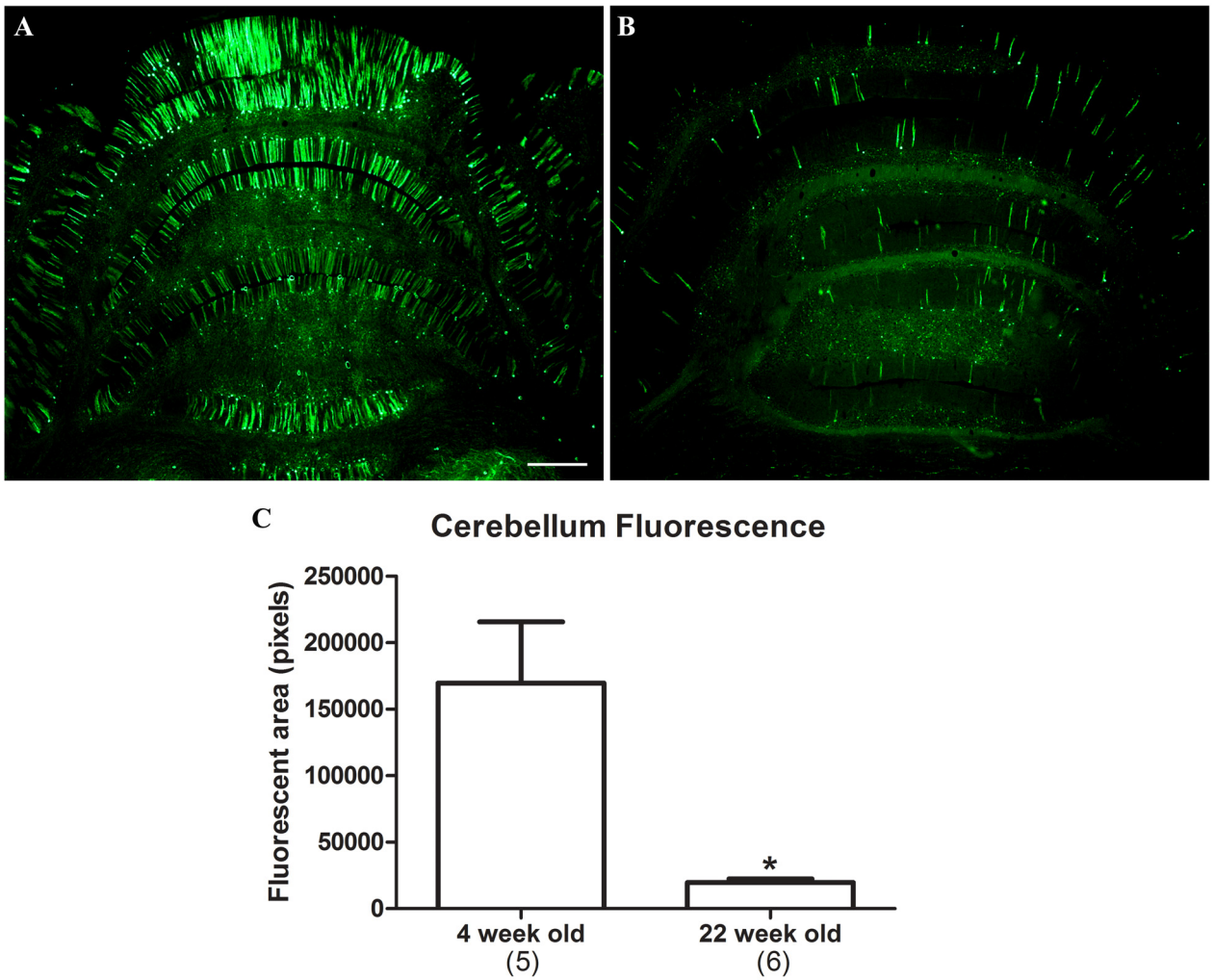

FIGURE 4 | Attenuation of synapsin promoter-driven expression at 22 weeks post gene transfer. Neonatal rats were administered synapsin promoter-AAV9 intravenously and the tissues were analyzed at time points of either 4 **(A)** or 22 **(B)** weeks. **(C)** The area of the cerebellum positive for GFP was compared. Lower level expression was found at the later time point (*t*-test, $p < 0.01$, $n = 5–6$ /per interval). GFP immunostaining in **(A,B)**. Bar in **(A)** = 536 μm, same magnification in **(B)**. *Indicates $p < 0.01$.

neuronal expression. These results are therefore consistent with the hypothesis that AAV-PHP.B is advantageous for neuronal targeting as well as greater efficiency.

Synapsin Promoter-AAV-PHP.B in Adults

Based on the increased transduction observed with AAV-PHP.B in neonates, we administered three adult animals with AAV-PHP.B synapsin promoter-YFP at a dose of 3.8×10^{13} vg/kg, and the tissues were analyzed 4 weeks later. Neuronal expression was achieved in the cerebellum and spinal cord (**Figures 6A,B**). There appeared to be no expression in the heart (**Figure 6C**) and some expression in the liver (**Figure 6D**), at a lower level than would be expected using the CBA promoter. AAV-PHP.B should therefore be advantageous to boost the expression of a weaker promoter while retaining the promoter tissue specificity.

Intracerebroventricular Route of Administration

We also conducted adult intracerebroventricular administrations to improve CNS transduction and limit peripheral transduction. Intra-ventricular AAV injections in mice have been shown to be advantageous for widespread gene transfer in the CNS and gene therapy (Lo et al., 1999; Passini and Wolfe, 2001; Li and Daly, 2002; Passini et al., 2003), whereas intraparenchymal AAV injections in the brain produce more focal expression (Klein et al., 1998, 2002, 2006, 2008a). One rat was administered AAV9 CBA promoter-GFP in the lateral ventricle at a dose of 3.8×10^{12} vg/kg, and tissues were analyzed 6 weeks later. There was a wide ranging spread of the GFP expression in the hippocampus, cerebellum and spinal cord (**Figure 7**). In the hippocampus of this sample, pyramidal neurons in CA3/CA4 were transduced, while the

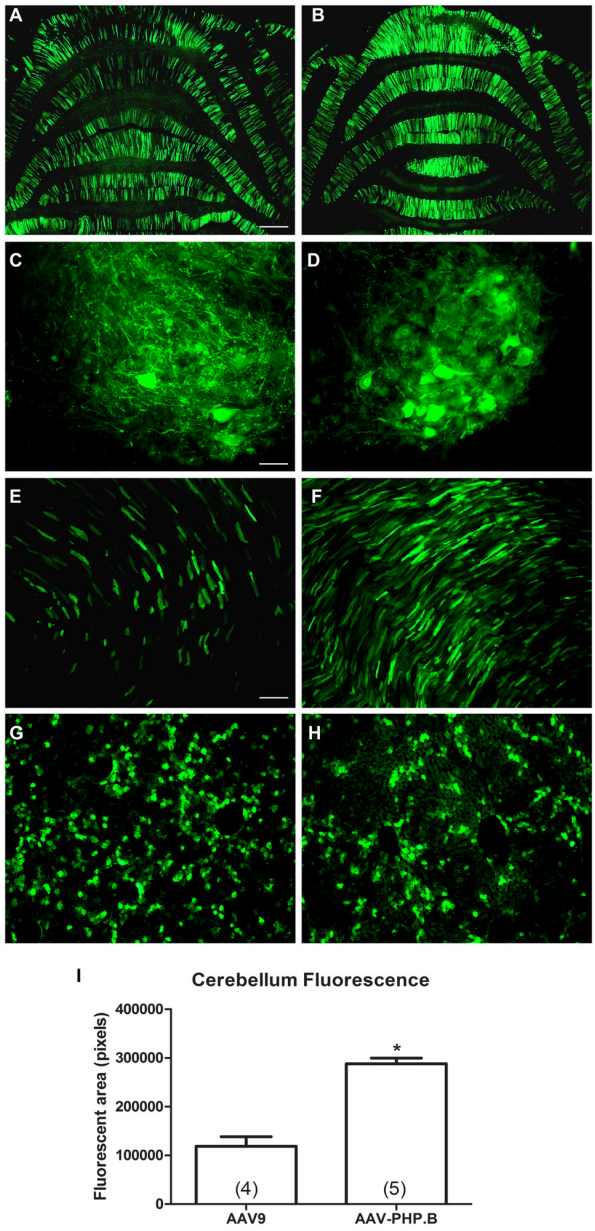

FIGURE 5 | AAV-PHP.B provides increased transduction efficiency in the CNS relative to AAV9. Neonatal rats were injected intravenously with the CBA promoter construct packaged into either AAV9 or AAV-PHP.B under equal conditions, with a 4 week expression interval. **(A,B)** There was stronger GFP expression in the cerebella of rats administered AAV-PHP.B. **(C–F)** The same pattern was found in the spinal cord **(C,D)** and the heart **(E,F)**. **(G,H)** Interestingly, AAV-PHP.B did not appear to similarly increase expression in liver, which is consistent with improved neuronal targeting. **(I)** GFP-positive area in the cerebellum (*t*-test, $p < 0.001$, $n = 4$–5/per AAV capsid serotype group). GFP immunostaining in **(A–H)**. Bar in **(A)** = 536 μm, same magnification in **(B)**. Bar in **(C)** = 67 μm, same magnification in **(D)**. Bar in **(E)** = 134 μm, same magnification in **(F–H)**. *Indicates $p < 0.001$.

CA1 region showed strong GFP expression in the neuropil though not in pyramidal neuron perikarya. However, a potential caveat of this approach was the very high degree of expression

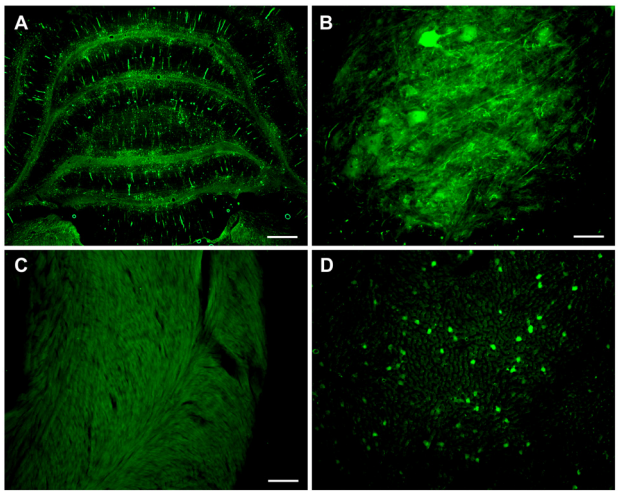

FIGURE 6 | Combining advantages for targeting and efficiency in a synapsin promoter-AAV-PHP.B vector. Neonatal rats were administered synapsin promoter-AAV-PHP.B intravenously, with an expression interval of 4 weeks. **(A)** Expression in the cerebellum. **(B)** Spinal cord. **(C)** The heart was blank for expression, as expected. **(D)** Importantly, the liver showed a relatively low level expression compared to previous CBA promoter-AAV9 vectors. GFP immunostaining in **(A–D)**. Bar in **(A)** = 536 μm. Bar in **(B)** = 67 μm. Bar in **(C)** = 134 μm, same magnification in **(D)**.

in the cortex along the injection track (**Figure 7F**), since a large vector dose was used. The cerebrospinal fluid can exit the CNS into the venous system, so peripheral organ transduction was examined. There was little transduction of cardiomyocytes (**Figure 7G**), but GFP expression in the liver was clearly evident after intracerebroventricular injections (**Figure 7H**).

TDP-43-Induced Phenotypes using the Synapsin Promoter, AAV-PHP.B and Intracerebroventricular Delivery

We know that AAV9 wide-scale gene transfer is more efficient in neonates relative to adults (Jackson et al., 2015b). When AAV9 synapsin promoter-TDP-43 was administered to a small group of three neonates, mortality resulted within 2–3 weeks. A relatively high vector dose was used (4×10^{12} vg or 6.7×10^{14} vg/kg) which would also induce mortality if the stronger CBA promoter was used (Wang et al., 2010). However, in a small group of three adult subjects, we did not observe the typical, progressive motor deficits and paralysis for up to 6 weeks after administering the AAV9 synapsin promoter-TDP-43 at a vector dose of 3×10^{13} vg/kg, a dose that is sufficient to induce the disease state using the CBA promoter in adults (Jackson et al., 2015b).

AAV-PHP.B CBA promoter-TDP-43 was noticeably stronger than the AAV9 counterpart in neonates causing severe limb dysfunction and mortality rapidly, by 10 days (1.6×10^{12} vg or 2.7×10^{14} vg/kg, $n = 2$). In adults, in contrast to AAV9, AAV-PHP.B synapsin promoter-TDP-43 did result in the characteristic paresis/paralysis of the limbs by 2 weeks

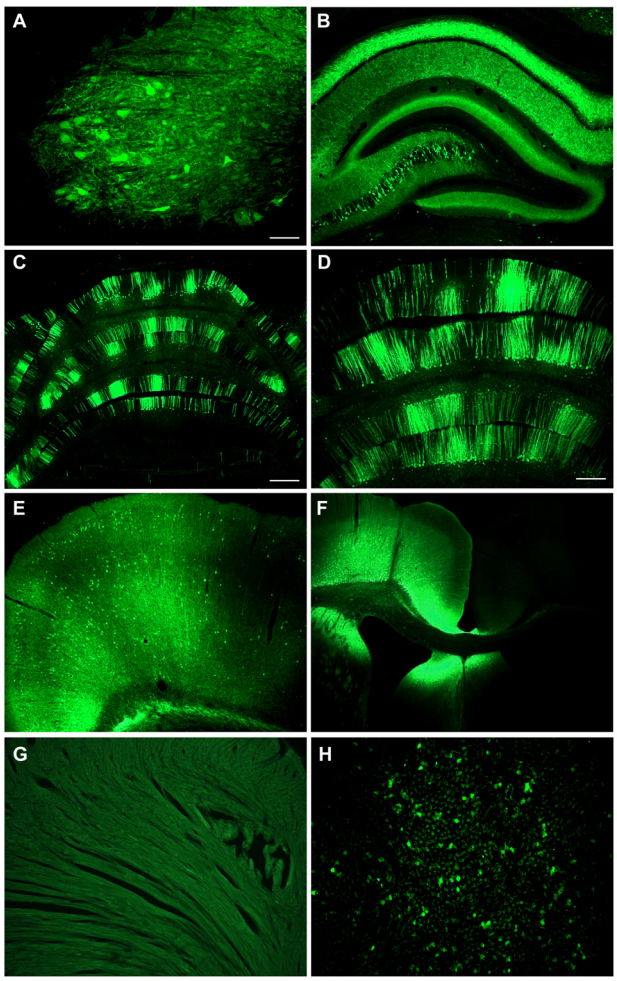

FIGURE 7 | Intracerebroventricular administration produces far reaching expression in the CNS with low level expression in liver. An adult rat was injected with CBA promoter AAV9 into the lateral ventricle. There was a widespread expression throughout the CNS including the spinal cord in the lumbar region **(A)**, the hippocampus **(B)**, the cerebellum **(C,D)**, and the cerebral cortex on the contralateral side **(E). (F)** There was extremely strong expression along the needle track into the ventricle. **(G)** No expression was seen in the heart. **(H)** There was some expression in the liver. GFP immunostaining in **(A–H)**. Bar in **(A)** = 134 μm, same magnification in **(B,H)**. Bar in **(C)** = 536 μm, same magnification in **(F)**. Bar in **(D)** = 268 μm, same magnification in **(E,G)**.

post-injection (3×10^{13} vg/kg, $n = 3$). Both the hindlimbs and the forelimbs were affected in rats in the AAV-PHP.B group during the escape reflex, but no such deficits were noticed in the AAV9 rats. In rotarod testing at 6 weeks post-injection in adults, there was a difference in fall latency between the two AAV serotype groups. The time to fall in the AAV9 synapsin promoter-TDP-43 group was 80.6 ± 10.3 s (unimpaired) and 22.6 ± 13.5 s in the AAV-PHP.B synapsin promoter-TDP-43 group ($p < 0.05$, t-test, $n = 3$/group). These results are summarized in **Table 1**. Interestingly, in one rat administered AAV9 CBA promoter-TDP-43 into the lateral ventricle at a dose of 3.8×10^{12} vg/kg, the motor deficits, limb paralysis, and overall disease state manifested within 2 weeks. Importantly, an almost 10-fold lower vector dose was used than what we would use for an intravenous vector dose to induce the disease state with this vector (Jackson et al., 2015b).

DISCUSSION

Better neuronal targeting of wide-scale gene transfer in rats was achieved using the synapsin promoter. Better efficiency was achieved using the AAV-PHP.B capsid. It will be interesting to combine these two elements since the improved capsid can make up for the low promoter strength of this tissue-specific promoter while retaining promoter specificity. This is the first example of gene transfer with AAV-PHP.B in rats. Rats are particularly advantageous compared to mice because of their larger size, because their physiological parameters are closer to human, and because there are specific behavioral, pharmacological, and toxicological assays designed for rats. Furthermore, an increasing amount transgenic rat strains are becoming available.

Within the CNS, the synapsin promoter-AAV9 appeared to avoid glial cells. The CBA promoter-AAV9 mostly expressed in neurons and in some sporadic astroglia. While the synapsin promoter was clearly not as strong as the CBA promoter, successful neuronal targeting was achieved. In contrast to the CBA promoter, the synapsin promoter avoided expression in cardiomyocytes and appeared to generate less expression in the liver. Though not absolutely neuron-specific, the synapsin promoter strategy was successful to mitigate and minimize the peripheral expression to a substantial extent. Neuron-selective, but not neuron-specific expression was also reported by Huda et al. (2014) when they applied a synapsin promoter-AAV9 vector intravenously to mice. The lack of complete neuron specificity of the synapsin promoter may be due to the short recombinant promoter sequence. On the other hand, the AAV2 inverted terminal repeats are known to possess weak promoter activity (Flotte et al., 1993; Haberman et al., 2000) which could be responsible for the non-neuronal expression. Additionally, some studies have found synapsin protein and mRNA in the liver (Bustos et al., 2001) suggesting that endogenous synapsin expression may not be neuron-specific. In any case, we were able to achieve quite robust wide-scale transgene expression with the synapsin promoter-AAV9 in rats for the first time. The efficiency of the synapsin promoter-driven expression throughout the CNS shown here is unprecedented. Critically important, and in contrast to previous results with the CBA promoter, we report reduced synapsin promoter-driven expression in the long-term (5–6 months). More work will be needed to confirm this effect and perhaps determine if the synapsin promoter is subject to silencing by DNA methylation, for example Prösch et al. (1996). The lowered expression over time with the synapsin promoter would probably not affect short-term studies on the order of 1 month, but could be critical to consider in long-term studies including neurodegenerative disease modeling. Furthermore, the widespread, diffuse expression

TABLE 1 | Outcomes of transactive response DNA-binding protein, 43 kDa (TDP-43)-induced phenotypes in small groups of rats.

Route	AAV	Promoter	Dose	*N*	Outcome
Neonatal i.v.	AAV9	CBA	2×10^{12} vg	1	Fatal by 2 weeks (Dayton et al., 2013)
Neonatal i.v.	AAV9	Synapsin	4×10^{12} vg	3	Fatal by 2–3 weeks
Neonatal i.v.	AAV-PHP.B	CBA	1.6×10^{12} vg	2	Fatal by 10 days, abnormal limb posture
Adult i.v.	AAV9	CBA	3×10^{13} vg/kg	3	Impaired motor function, fatal by 5 weeks post-injection (Jackson et al., 2015b)
Adult i.v.	AAV9	Synapsin	3×10^{13} vg/kg	3	No symptoms up to 6 weeks post-injection
Adult i.v.	AAV-PHP.B	Synapsin	3×10^{13} vg/kg	3	Impaired motor function by 2 weeks post-injection, $p < 0.05$ vs. AAV9 synapsin promoter-TDP-43 on rotarod at 6 weeks
Adult i.c.v	AAV9	CBA	3.8×10^{12} vg/kg	1	Impaired motor function by 2 weeks post-injection

pattern after intravenous injections may be more sensitive to detect reduced expression over time than in stereotaxic injections which introduce more genome copies per transduced cell. The relatively low to moderate expression conferred by the synapsin promoter may be advantageous for achieving physiologically relevant expression levels, and clearly the synapsin promoter is advantageous for neuronal targeting with the wide-scale approach.

We found that AAV-PHP.B yielded higher transduction efficiency for neurons in rats than AAV9, corroborating the results in mice in Deverman et al. (2016). We exploited this critical advantage by coupling the synapsin promoter with AAV-PHP.B which enabled a phenotype including both forelimb and hindlimb motor paralysis when expressing TDP-43. We were unable to observe a phenotype with AAV9 synapsin promoter-TDP-43 in adult rats, but this hurdle was overcome using the more efficient AAV-PHP.B, underscoring the utility of the improved engineered AAVs.

By observing the TDP-43-induced phenotype with the synapsin promoter in neonates with AAV9 and in neonates and adults with AAV-PHP.B, we are more confident that the paralysis is mediated by TDP-43 expression in neurons. We were somewhat surprised the intracerebroventricular injection resulted in such far reaching expression in the CNS, although similar findings have been reported with intra-cerebrospinal fluid injections in mice, pigs, and monkeys (Snyder et al., 2011; Federici et al., 2012; Samaranch et al., 2013; Donsante et al., 2016). We found a mosaic, sporadic labeling of clusters of Purkinje neurons in the cerebellum after intracerebroventricular administration, consistent with other studies (Hinderer et al., 2014; Donsante et al., 2016), which may reflect the flow of the cerebrospinal fluid. In contrast, the intravenous delivery produces more evenly distributed transduction in the cerebellum by comparison. As previously discussed (Gholizadeh et al., 2013; Samaranch et al., 2013; Donsante et al., 2016), the intraventricular route of administration is advantageous for wide-scale CNS transduction because it better limits the vector to the CNS and requires lower vector doses relative to intravenous delivery. We also found some degree of hepatic transduction after intracerebroventricular administration in rats as seen before in mice and monkeys (Samaranch et al., 2013; Donsante et al., 2016). We can assume that using the synapsin promoter and AAV-PHP.B would better avoid this low level expression in the liver after intracerebroventricular administration. The intracerebroventricular delivery method was advantageous for better targeting TDP-43 expression to the CNS and clearly sufficient to induce the characteristic phenotype. Thus, the paralysis should be mediated by TDP-43 expression in brain and spinal cord neurons. One caveat of this study is the low sample size used for the stereotaxic injection of CBA and synapsin promoter vectors and for the intracerebroventricular gene transfer. However, we compared the CBA and synapsin promoters on a statistical basis after i.v. administration and found a similar pattern to the focal injection, that the CBA promoter is clearly stronger. For the intracerebroventricular injections it was clear that wide-scale expression can be achieved in rats and that this method permits the characteristic TDP-43 induced paralysis. We believe that the combination of the synapsin promoter and AAV-PHP.B will be advantageous to investigators asking which configuration to use in their studies, given the improved targeting and efficiency. Though preliminary, we realized the benefits of an intracerebroventricular route of administration, while an intravenous delivery is less invasive. While not absolutely neuron-specific, the synapsin promoter did produce a highly selective expression pattern which supports that greater and greater pinpoint targeting can be achieved even after peripheral administration of vector.

We conclude that the combination of the synapsin promoter with AAV-PHP.B is advantageous for neuronal targeting and efficient expression in adults after peripheral, wide-scale intravenous delivery. We demonstrated that this combination was necessary for observing behavioral motor deficits induced by TDP-43 in adults, with neuron-selective expression. If this design worked for achieving our goal with TDP-43 here, then synapsin promoter AAV-PHP.B vectors will probably also permit new basic and clinical neuroscience approaches that were not possible before.

AUTHOR CONTRIBUTIONS

RLK and BED were involved in the conception and design of the work and the interpretation of the data. KLJ and RDD were involved in the acquisition, analysis and interpretation of the data. KLJ, RDD, BED and RLK: were involved in drafting and revision of the manuscript, approval of the final version, and agreed to be held responsible for the work.

FUNDING

This work was funded by the ALS Association and Karyopharm Therapeutics, Inc.

ACKNOWLEDGMENTS

We thank Thomas McCown and Xiao-Hong Lu for discussions.

REFERENCES

Bustos, R., Kolen, E. R., Braiterman, L., Baines, A. J., Gorelick, F. S., and Hubbard, A. L. (2001). Synapsin I is expressed in epithelial cells: localization to a unique trans-Golgi compartment. *J. Cell Sci.* 114, 3695–3704.

Choudhury, S. R., Fitzpatrick, Z., Harris, A. F., Maitland, S. A., Ferreira, J. S., Zhang, Y., et al. (2016a). *In vivo* selection yields AAV-B1 capsid for central nervous system and muscle gene therapy. *Mol. Ther.* 24, 1247–1257. doi: 10.1038/mt.2016.84

Choudhury, S. R., Harris, A. F., Cabral, D. J., Keeler, A. M., Sapp, E., Ferreira, J. S., et al. (2016b). Widespread central nervous system gene transfer and silencing after systemic delivery of novel AAV-AS vector. *Mol. Ther.* 24, 726–735. doi: 10.1038/mt.2015.231

Dayton, R. D., Gitcho, M. A., Orchard, E. A., Wilson, J. D., Wang, D. B., Cain, C. D., et al. (2013). Selective forelimb impairment in rats expressing a pathological TDP-43 25 kDa C-terminal fragment to mimic amyotrophic lateral sclerosis. *Mol. Ther.* 21, 1324–1334. doi: 10.1038/mt.2013.88

DeGennaro, L. J., Kanazir, S. D., Wallace, W. C., Lewis, R. M., and Greengard, P. (1983). Neuron-specific phosphoproteins as models for neuronal gene expression. *Cold Spring Harb. Symp. Quant. Biol.* 1, 337–345. doi: 10.1101/sqb.1983.048.01.037

Deverman, B. E., Pravdo, P. L., Simpson, B. P., Kumar, S. R., Chan, K. Y., Banerjee, A., et al. (2016). Cre-dependent selection yields AAV variants for widespread gene transfer to the adult brain. *Nat. Biotechnol.* 34, 204–209. doi: 10.1038/nbt.3440

Donsante, A., McEachin, Z., Riley, J., Leung, C. H., Kanz, L., O'Connor, D. M., et al. (2016). Intracerebroventricular delivery of self-complimentary adeno-associated virus serotype 9 to the adult rat brain. *Gene Ther.* 23, 401–407. doi: 10.1038/gt.2016.6

Federici, T., Taub, J. S., Baum, G. R., Gray, S. J., Grieger, J. C., Matthews, K. A., et al. (2012). Robust spinal motor neuron transduction following intrathecal delivery of AAV9 in pigs. *Gene Ther.* 19, 852–859. doi: 10.1038/gt.2011.130

Flotte, T. R., Afione, S. A., Solow, R., Drumm, M. L., Markakis, D., Guggino, W. B., et al. (1993). Expression of the cystic fibrosis transmembrane conductance regulator from a novel adeno-associated virus promoter. *J. Biol. Chem.* 268, 3781–3790.

Foust, K. D., Nurre, E., Montgomery, C. L., Hernandez, A., Chan, C. M., and Kaspar, B. K. (2009). Intravascular AAV9 preferentially targets neonatal neurons and adult astrocytes. *Nat. Biotechnol.* 27, 59–65. doi: 10.1038/nbt.1515

Gao, G., Vandenberghe, L. H., Alvira, M. R., Lu, Y., Calcedo, R., Zhou, X., et al. (2004). Clades of Adeno-associated viruses are widely disseminated in human tissues. *J. Virol.* 78, 6381–6388. doi: 10.1128/jvi.78.12.6381-6388.2004

Gholizadeh, S., Tharmalingam, S., Macaldaz, M. E., and Hapson, D. R. (2013). Transduction of the central nervous system after intracerebroventricular injection of adeno-associated viral vectors in neonatal and juvenile mice. *Hum. Gene Ther. Methods* 24, 205–213. doi: 10.1089/hgtb.2013.076

Gitcho, M. A., Baloh, R. H., Chakraverty, S., Mayo, K., Norton, J. B., Levitch, D., et al. (2008). TDP-43 A315T mutation in familial motor neuron disease. *Ann. Neurol.* 63, 535–538. doi: 10.1002/ana.21344

Haberman, R. P., McCown, T. J., and Samulski, R. J. (2000). Novel transcriptional regulatory signals in the adeno-associated virus terminal repeat A/D junction element. *J. Virol.* 74, 8732–8739. doi: 10.1128/jvi.74.18.8732-8739.2000

Hinderer, C., Bell, P., Vite, C. H., Louboutin, J. P., Grant, R., Bote, E., et al. (2014). Widespread gene transfer in the central nervous system of cynomolgus macaques following delivery of AAV9 into the cisterna magna. *Mol. Ther. Methods Clin. Dev.* 1:14051. doi: 10.1038/mtm.2014.51

Huda, F., Konno, A., Matsuzaki, Y., Goehawan, H., Miyake, K., Shimada, T., et al. (2014). Distinct transduction profiles in the CNS via three injection routes of AAV9 and the application to generation of a neurodegenerative mouse model. *Mol. Ther. Methods Clin. Dev.* 1:14032. doi: 10.1038/mtm.2014.32

Jackson, K. L., Dayton, R. D., Fisher-Perkins, J. M., Didier, P. J., Baker, K. C., Weimer, M., et al. (2015a). Initial gene vector dosing for studying symptomatology of amyotrophic lateral sclerosis in non-human primates. *J. Med. Primatol.* 44, 66–75. doi: 10.1111/jmp.12162

Jackson, K. L., Dayton, R. D., and Klein, R. L. (2015b). AAV9 supports wide-scale transduction of the CNS and TDP-43 disease modeling in adult rats. *Mol. Ther. Methods Clin. Dev.* 2:15036. doi: 10.1038/mtm.2015.36

Klein, R. L., Meyer, E. M., Peel, A. L., Zolotukhin, S., Meyers, C., Muzyczka, N., et al. (1998). Neuron-specific transduction in the rat septohippocampal or nigrostriatal pathway by recombinant adeno-associated virus vectors. *Exp. Neurol.* 150, 183–194. doi: 10.1006/exnr.1997.6736

Klein, R. L., Hamby, M. E., Gong, Y., Hirko, A. C., Wang, S., Hughes, J. A., et al. (2002). Dose and promoter effects of adeno-associated viral vector for green fluorescent protein expression in the rat brain. *Exp. Neurol.* 176, 66–74. doi: 10.1006/exnr.2002.7942

Klein, R. L., Dayton, R. D., Leidenheimer, N. J., Jansen, K., Golde, T. E., and Zweig, R. M. (2006). Efficient neuronal gene transfer with AAV8 leads to neurotoxic levels of tau or green fluorescent proteins. *Mol. Ther.* 13, 517–527. doi: 10.1016/j.ymthe.2005.10.008

Klein, R. L., Dayton, R. D., Tatom, J. B., Diaczynsky, C. G., and Salvatore, M. F. (2008a). Tau expression levels from various adeno-associated virus vector serotypes produce graded neurodegenerative disease states. *Eur. J. Neurosci.* 27, 1615–1625. doi: 10.1111/j.1460-9568.2008.06161.x

Klein, R. L., Dayton, R. D., Tatom, J. B., Henderson, K. M., and Henning, P. P. (2008b). AAV8, 9, Rh10, Rh43 vector gene transfer in the rat brain: effects of serotype, promoter and purification method. *Mol. Ther.* 16, 89–96. doi: 10.1038/sj.mt.6300331

Kügler, S., Kilic, E., and Bähr, M. (2003a). Human synapsin 1 gene promoter confers highly neuron-specific long-term transgene expression from an adenoviral vector in the adult rat brain depending on the transduced area. *Gene Ther.* 10, 337–347. doi: 10.1038/sj.gt.3301905

Kügler, S., Lingor, P., Schöll, U., Zolotukhin, S., and Bähr, M. (2003b). Differential transgene expression in brain cells *in vivo* and *in vitro* from AAV-2 vectors with small transcriptional control units. *Virology* 311, 89–95. doi: 10.1016/s0042-6822(03)00162-4

Li, J., and Daly, T. M. (2002). Adeno-associated virus-mediated gene transfer to the neonatal brain. *Methods* 28, 203–207. doi: 10.1016/s1046-2023(02)00224-4

Lo, W. D., Qu, G., Sferra, T. J., Clark, R., Chen, R., and Johnson, P. R. (1999). Adeno-associated virus-mediated gene transfer to the brain: duration and modulation of expression. *Hum. Gene Ther.* 10, 201–213. doi: 10.1089/10430349950018995

Mackenzie, I. R., Bigio, E. H., Ince, P. G., Geser, F., Neumann, M., Cairns, N. J., et al. (2007). Pathological TDP-43 distinguishes sporadic amyotrophic lateral sclerosis from amyotrophic lateral sclerosis with SOD1 mutations. *Ann. Neurol.* 61, 427–434. doi: 10.1002/ana.21147

Miyake, N., Miyake, K., Yamamoto, M., Hirai, Y., and Shimada, T. (2011). Global gene transfer into the CNS across the BBB after neonatal systemic delivery of single-stranded AAV vectors. *Brain Res.* 1389, 19–26. doi: 10.1016/j.brainres.2011.03.014

Niwa, H., Yamamura, K., and Miyazaki, J. (1991). Efficient selection for high-expression transfectants with a novel eukaryotic vector. *Gene* 108, 193–199. doi: 10.1016/0378-1119(91)90434-d

Ormö, M., Cubitt, A. B., Kallio, K., Gross, L. A., Tsien, R. Y., and Remington, S. J. (1996). Crystal structure of the Aequorea victoria green fluorescent protein. *Science* 273, 1392–1395. doi: 10.1126/science.273.5280.1392

Passini, M. A., Watson, D. J., Vite, C. H., Landsburg, D. J., Feigenbaum, A. L., and Wolfe, J. H. (2003). Intraventricular brain injection of adeno-associated virus type 1 (AAV1) in neonatal mice results in complementary patterns of neuronal transduction to AAV2 and total long-term correction of storage lesions in the brains of β-glucuronidase-deficient mice. *J. Virol.* 77, 7034–7040. doi: 10.1128/jvi.77.12.7034-7040.2003

Passini, M. A., and Wolfe, J. H. (2001). Widespread gene delivery and structure-specific patterns of expression in the brain after intraventricular injections of neonatal mice with an adeno-associated virus vector. *J. Virol.* 75, 12382–12392. doi: 10.1128/jvi.75.24.12382-12392.2001

Prösch, S., Stein, J., Staak, K., Liebenthal, C., Volk, H. D., and Krüger, D. H. (1996). Inactivation of the very strong HCMV immediate early promoter by DNA CpG methylation *in vitro*. *Biol. Chem. Hoppe Seyler* 377, 195–201. doi: 10.1515/bchm3.1996.377.3.195

Samaranch, L., Salegio, E. A., San Sebastian, W., Kells, A. P., Bringas, J. R., Forsayeth, J., et al. (2013). Strong cortical and spinal cord transduction after AAV7 and AAV9 delivery into the cerebrospinal fluid of nonhuman primates. *Hum. Gene Ther.* 24, 526–532. doi: 10.1089/hum.2013.005

Shevtsova, Z., Malik, J. M., Michel, U., Bähr, M., and Kügler, S. (2005). Promoters and serotypes: targeting of adeno-associated virus vectors for gene transfer in the rat central nervous system *in vitro* and *in vivo*. *Exp. Physiol.* 90, 53–59. doi: 10.1113/expphysiol.2004.028159

Snyder, B. R., Gray, S. J., Quach, E. T., Huang, J. W., Leung, C. H., Samulski, R. J., et al. (2011). Comparison of adeno-associated viral vector serotypes for spinal cord and motor neuron gene delivery. *Hum. Gene Ther.* 22, 1129–1135. doi: 10.1089/hum.2011.008

Wang, D. B., Dayton, R. D., Henning, P. P., Cain, C. D., Zhao, L. R., Schrott, L. M., et al. (2010). Expansive gene transfer to the rat CNS and amyotrophic lateral sclerosis relevant sequelae when TDP-43 is overexpressed. *Mol. Ther.* 18, 2064–2074. doi: 10.1038/mt.2010.191

Xu, L., Daly, T., Gao, C., Flotte, T. R., Song, S., Byrne, B. J., et al. (2001). CMV-beta-actin promoter directs higher expression from an adeno-associated viral vector in the liver than the cytomegalovirus or elongation factor 1 alpha promoter and results in therapeutic levels of human factor X in mice. *Hum. Gene Ther.* 12, 563–573. doi: 10.1089/104303401300042500

Yang, T. T., Cheng, L., and Kain, S. R. (1996). Optimized codon usage and chromophore mutations provide enhanced sensitivity with the green fluorescent protein. *Nucleic Acids Res.* 24, 4592–4593. doi: 10.1093/nar/24.22.4592

Yang, B., Li, S., Wang, H., Guo, Y., Gessler, D. J., Cao, C., et al. (2014). Global CNS transduction of adult mice by intravenously delivered rAAVrh.8 and rAAVrh.10 and nonhuman primates by rAAVrh.10. *Mol. Ther.* 22, 1299–1309. doi: 10.1038/mt.2014.68

Conflict of Interest Statement: BED is listed as an inventor on a patent application related to AAV-PHP.B. KLJ, RDD and RLK have no conflicts of interest to disclose.

frontiers in Molecular Neuroscience

CORRECTION
published: 22 December 2016
doi: 10.3389/fnmol.2016.00154

Corrigendum: Better Targeting, Better Efficiency for Wide-Scale Neuronal Transduction with the Synapsin Promoter and AAV-PHP.B

*Kasey L. Jackson[1], Robert D. Dayton[1], Benjamin E. Deverman[2] and Ronald L. Klein[1]**

[1] Department of Pharmacology, Toxicology, and Neuroscience, Louisiana State University Health Sciences Center, Shreveport, LA, USA, [2] Division of Biology and Biological Engineering, California Institute of Technology, Pasadena, CA, USA

Keywords: adeno-associated virus, amyotrophic lateral sclerosis, gene therapy, gene transfer, promoter, synapsin promoter, targeting, TDP-43

A corrigendum on

Better Targeting, Better Efficiency for Wide-Scale Neuronal Transduction with the Synapsin Promoter and AAV-PHP.B

by Jackson, K. L., Dayton, R. D., Deverman, B. E., Klein, R. L. (2016). Front. Mol. Neurosci. 9:116. doi: 10.3389/fnmol.2016.00116

The following acknowledgments were missing from the original article.

BD was supported by the Hereditary Disease Foundation, the Beckman Institute and the Resource Center for CLARITY, Optogenetics and Vector Engineering, which supports technology development and dissemination at the California Institute of Technology. The AAV-PHP.B plasmid was distributed from the Gradinaru Laboratory at the California Institute of Technology. The authors thank Viviana Gradinaru for her help in providing the AAV-PHP.B plasmid.

The authors apologize for this mistake. This error does not in any way change the scientific conclusions of the article.

Conflict of Interest Statement: BED is listed as an inventor on a patent application related to AAV-PHP.B. KLJ, RDD and RLK have no conflicts of interest to disclose.

OPEN ACCESS

Edited and reviewed by:
Andrew Paul Tosolini, University College London, UK

****Correspondence:***
Ronald L. Klein
klein@lsuhsc.edu

Received: *29 November 2016*
Accepted: *07 December 2016*
Published: *22 December 2016*

Citation:
Jackson KL, Dayton RD, Deverman BE and Klein RL (2016) Corrigendum: Better Targeting, Better Efficiency for Wide-Scale Neuronal Transduction with the Synapsin Promoter and AAV-PHP.B. Front. Mol. Neurosci. 9:154. doi: 10.3389/fnmol.2016.00154

frontiers in Molecular Neuroscience

ORIGINAL RESEARCH
published: 23 February 2016
doi: 10.3389/fnmol.2016.00013

Recombinant Human Myelin-Associated Glycoprotein Promoter Drives Selective AAV-Mediated Transgene Expression in Oligodendrocytes

*Georg von Jonquieres, Dominik Fröhlich, Claudia B. Klugmann, Xin Wen, Anne E. Harasta, Roshini Ramkumar, Ziggy H. T. Spencer, Gary D. Housley and Matthias Klugmann**

Translational Neuroscience Facility and Department of Physiology, School of Medical Sciences, UNSW Australia, Sydney, NSW, Australia

OPEN ACCESS

Edited by:
George Smith, Temple University School of Medicine, USA

Reviewed by:
Samaneh Maysami, The University of Manchester, UK
Shin Hyeok Kang, Temple University, USA

***Correspondence:**
Matthias Klugmann
m.klugmann@unsw.edu.au

Received: *23 December 2015*
Accepted: *05 February 2016*
Published: *23 February 2016*

Citation:
von Jonquieres G, Fröhlich D, Klugmann CB, Wen X, Harasta AE, Ramkumar R, Spencer ZHT, Housley GD and Klugmann M (2016) Recombinant Human Myelin-Associated Glycoprotein Promoter Drives Selective AAV-Mediated Transgene Expression in Oligodendrocytes. Front. Mol. Neurosci. 9:13. doi: 10.3389/fnmol.2016.00013

Leukodystrophies are hereditary central white matter disorders caused by oligodendrocyte dysfunction. Recent clinical trials for some of these devastating neurological conditions have employed an *ex vivo* gene therapy approach that showed improved endpoints because cross-correction of affected myelin-forming cells occurred following secretion of therapeutic proteins by transduced autologous grafts. However, direct gene transfer to oligodendrocytes is required for the majority of leukodystrophies with underlying mutations in genes encoding non-secreted oligodendroglial proteins. Recombinant adeno-associated viral (AAV) vectors are versatile tools for gene transfer to the central nervous system (CNS) and proof-of-concept studies in rodents have shown that the use of cellular promoters is sufficient to target AAV-mediated transgene expression to glia. The potential of this strategy has not been exploited. The major caveat of the AAV system is its limited packaging capacity of ~5 kb, providing the rationale for identifying small yet selective recombinant promoters. Here, we characterize the human myelin associated glycoprotein (*MAG*) promoter for reliable targeting of AAV-mediated transgene expression to oligodendrocytes *in vivo*. A homology screen revealed highly conserved genomic regions among mammalian species upstream of the transcription start site. Recombinant AAV expression cassettes carrying the cDNA encoding enhanced green fluorescent protein (GFP) driven by truncated versions of the recombinant *MAG* promoter (2.2, 1.5 and 0.3 kb in size) were packaged as cy5 vectors and delivered into the dorsal striatum of mice. At 3 weeks post-injection, oligodendrocytes, neurons and astrocytes expressing the reporter were quantified by immunohistochemical staining. Our results revealed that both 2.2 and 1.5 kb *MAG* promoters targeted more than 95% of transgene expression to oligodendrocytes. Even the short 0.3 kb fragment conveyed high oligodendroglial specific transgene

expression (>90%) *in vivo*. Moreover, cy5-*MAG2.2-GFP* delivery to the neonate CNS resulted in selective GFP expression in oligodendrocytes for at least 8 months. Broadly, the characterization of the extremely short yet oligodendrocyte-specific human *MAG* promoter may facilitate modeling neurological diseases caused by oligodendrocyte pathology and has translational relevance for leukodystrophy gene therapy.

Keywords: oligodendroglia, leukodystrophy, gene therapy, AAV, white matter disorders, myelin-associated glycoprotein

INTRODUCTION

Recombinant adeno-associated virus (AAV) is the preferred vector platform for gene delivery to the central nervous system (CNS) due to its minimal potential to elicit immune response, episomal localization of the vector genome and long-term transgene expression. The major restriction of the system is the small DNA packaging limit of 4.7 kb (Dong et al., 1996).

The AAV serotype-specific tropism depends on interactions between viral capsid proteins and specific receptors at the surface of host cells and transduction is determined by intracellular processing of AAV virions (Xiao et al., 2012). Finally, transgene expression is controlled by recruitment of host cell-derived transcription factors to the recombinant promoters. Direct AAV-mediated DNA transfer to neurons has proven beneficial in conditions with a primary defect in this cell population (Weinberg et al., 2013). In addition, some leukodystrophies, central white matter disorders caused by genetic deficiencies in oligodendrocyte proteins, have been trialled successfully by *ex vivo* gene therapy acting via cross-correction of dysfunctional oligodendrocytes by uptake of graft-derived, secreted transgene products (Cartier et al., 2009; Biffi et al., 2013). With the exception of Canavan Disease and its models, neurotropic AAV vectors (Klugmann et al., 2005a; Leone et al., 2012; Ahmed et al., 2013) and *ex vivo* gene therapy approaches are blunt tools for treating leukodystrophies caused by mutations in genes encoding non-secreted proteins.

The traditional view that AAV is strictly neurotropic has been based on observations of specific neuronal transgene expression driven by viral or hybrid promoters (Fitzsimons et al., 2002). Preclinical proof-of-concept studies showing successful modification of the AAV system towards selective transgene expression in oligodendrocytes used "neurotropic" serotypes but employed the promoter of the mouse myelin basic protein (*Mbp*) gene (Chen et al., 1998; Lawlor et al., 2009; von Jonquieres et al., 2013). These findings support a promoter-swapping strategy for oligodendrocyte-targeted transgene expression with AAV gene delivery.

While the *Mbp* promoter holds promise for potential clinical applications, its murine origin, relative big size and poor specificity following neonatal vector delivery, are potential caveats (von Jonquieres et al., 2013).

The aim of the present study was to characterize a human oligodendrocyte-specific promoter suitable for reliable AAV-mediated transgene expression *in vivo*. In the CNS, myelin-associated glycoprotein (MAG) is a pre-myelinating marker responsible for oligodendroglial recognition of axons and myelin maintenance (Martini and Schachner, 1997). These features provided the rationale for investigating the potential of the *MAG* gene promoter for directed AAV-mediated transgene expression in oligodendrocytes. Employing a bioinformatics approach, we identified a 2.2 kb region upstream of the putative transcription start site of the human *MAG* promoter that comprised two areas that were highly conserved across mammalian species. We then isolated the genomic DNA fragments and generated AAV plasmids expressing the enhanced green fluorescent protein (GFP) reporter under the control of either the 2.2 kb *MAG* promoter, or truncated 1.5 and 0.3 kb fragments containing both or just one conserved area, respectively. All three *MAG* promoter constructs drove GFP expression in oligodendrocytes *in vitro* as well as *in vivo* following intrastriatal infusion of the corresponding AAV vectors to adult mice. Neonatal delivery of the *MAG2.2-GFP* vector resulted in highly specific oligodendroglial expression persisting for at least 8 months. Our data suggest that the novel recombinant *MAG* promoter will be instrumental for preclinical gene function studies and clinical gene therapy alike, that require long-term and specific AAV-mediated transgene expression in oligodendrocytes.

MATERIALS AND METHODS

Animals

C57BL/6J mice were group-housed (2–4 cage mates) in a temperature-controlled room (21–22°C; 49–55% humidity) with 12 h-light-dark-cycle (lights on 7:00–19:00), where food and water were available *ad libitum*. Experiments were approved by the UNSW Animal Care and Ethics Committee (UNSW ACEC 11/130A and 14/154B).

Bioinformatics

We identified the human *MAG* gene locus using the UCSC genome browser[1]. Based on the March 2006 alignment, the genomic sequence from Chromosome 19q13.1: 40469878–40496547 (Chr. 19: 35289949–35292134 in the current GRCh38. p2 assembly) including exons, introns and a 5 kb upstream putative promoter region of the *MAG* locus was assessed for genomic conservation using the Vista browser[2]

[1]https://genome.ucsc.edu
[2]http://pipeline.lbl.gov/cgi-bin/gateway2

(Thoms et al., 2011). The putative *MAG* promoter and in particular regions of >50% interspecies conservation were screened for transcription factor binding sites known to be relevant to the oligodendroglial linage using JASPAR[3], Wilmer Bioinformatics[4] or the Patch1.0 Software[5].

Plasmid Constructs

AAV-GFP plasmids in which reporter gene expression was controlled by the 1.1 kb cytomegalovirus (CMV) enhancer/chicken β-actin hybrid (CAG) promoter (pAAV-CAG-*GFP*), the human glial fibrillary acidic protein promoter (pAAV-*GFAP-GFP*), or the mouse myelin basic protein promoter (pAAV-*Mbp-GFP*), were generated as described previously (von Jonquieres et al., 2013).

The regions 2.2 and 1.5 kb upstream of the *MAG* transcriptional start site were PCR amplified from a genomic DNA template isolated from the human oligodendroglial cell line MO3.13 using specific primers (MAG_2.2 kb_fwd: cct cagaaggaaccaacactgccag; MAG_1.5 kb_Fwd: cgactccagctccaac tagg; MAGrev: gcccccacttgccagcccctcccct). The PCR products were subcloned into the XhoI and AgeI sites of pAAV-*Mbp-GFP* to replace the *Mbp* promoter, generating pAAV-*MAG2.2-GFP* and pAAV-*MAG1.5-GFP*. For truncation of the *MAG* promoter down to 0.3 kb, pAAV-*MAG1.5-GFP* was subjected to an Acc65I/Bsu36I restriction digest. Separation of a 1.2 kb fragment corresponding to the 0.3–1.5 kb distal promoter region was confirmed by agarose gel electrophoresis. The remaining 5.4 kb fragment containing the AAV-plasmid backbone, the proximal 0.3 kb *MAG* promoter and the GFP cDNA was gel-extracted, blunted by Klenow fill-in and re-ligated to obtain pAAV-*MAG0.3-GFP*. The integrity of the recombinant clones was confirmed by analytical digests and DNA sequencing.

AAV Vector Production

AAV vector packaging was performed as described previously (Harasta et al., 2015). Briefly, human embryonic kidney 293 (HEK 293) cells were triple-transfected with the AAV-GFP plasmid, the serotype-specific AAV helper plasmid and the adenovirus helper plasmid (pFΔ6) by standard calcium phosphate transfection. Chimeric AAV1/2 vectors carrying VP1, VP2 and VP3 capsid proteins from AAV1 and AAV2 at roughly equal ratios, were produced as described following quadruple plasmid transfection (Klugmann et al., 2005b; McClure et al., 2011). All vectors were harvested 60 h after transfection, purified using iodixanol (OptiPrep™, Sigma-Aldrich) gradient ultracentrifugation and concentrated 3× by refilling with phosphate-buffered saline containing 1 mM $MgCl_2$ and 2.5 mM KCl using Microsep™ Advanced Centrifugal Device 100 K MWCO concentrators (Pall, Surry Hills, NSW, Australia). Genomic titres were determined with primers designed to WPRE (During et al., 2003).

[3]http://jaspar.genereg.net
[4]http://bioinfo.wilmer.jhu.edu/PDI/index.html
[5]http://www.gene-regulation.com/pub/databases.html

AAV Vector Delivery *In Vivo*

Intraparenchymal delivery of AAV vectors into the striatum of neonatal or adult mice was performed as described (von Jonquieres et al., 2013). Briefly, 1 μl of AAV-GFP vector, adjusted to 2×10^{12} vector genomes (vg)/ml, was injected into the dorsal striatum. Vector delivery was performed using a microprocessor-controlled mini-pump (World Precision Instruments (WPI), Sarasota, FA, USA) with a 34G bevelled needle (WPI).

Adult mice (2–4 months; both sexes) were anesthetized with isoflurane (4% induction, then 1% maintenance with O_2). Animals were placed into a stereotaxic frame (Kopf instruments, Tujunga, CA, USA). One microlitre of AAV-GFP vector was injected into the striatum (+1.1 mm AP, −1.7 mm ML, −3.5 mm DV from bregma). Vector delivery was performed at a rate of 150 nl/min and the needle was left in place for 5 min prior to slowly retracting it from the brain.

For neonatal vector delivery (P0), pups (8–24 h after birth) were cryo-anesthetized and AAV administered as described (Pilpel et al., 2009). Briefly, pups were immobilized by wrapping in a paper towel covered with wet-ice for 3–5 min and then positioned in a custom-made styrofoam mold for vector delivery (100 nl/s) into the striatum (+2.0 mm AP, −1.5 mm ML, −2.0 mm DV from lambda) using a hand-held needle (WPI). The needle was left in place for additional 10 s at the end of the injection to prevent backflow of virus containing solution. The pups were then re-warmed on a heating matt and rolled in the bedding of their pre-warmed home cage before being returned to the dam.

Cell Culture

HEK 293 cells were cultured in Dulbecco's Modified Eagle Medium with 10% fetal calf serum and 1 mM sodium pyruvate and transfected using the calcium phosphate precipitation method. The mouse oligodendroglial cell line Oli-neu was cultured in Sato with 1% horse serum and transfected by electroporation as described (Krämer et al., 1997; Frühbeis et al., 2013). Differentiation was induced by daily application of 1 mM dibutyryl cyclic adenosine monophosphate (dbcAMP). Cells were seeded at a density of 5×10^4 per 11 mm glass coverslip and then kept for additional 4 days before fixation or lysis.

Immunoblotting

Detection of the GFP antigen in HEK 293 and Oli-neu protein lysates following sodium dodecyl sulfate polyacrylamide gel electrophoresis and electroblotting was performed as described (Harasta et al., 2015). Forty eight hours (HEK 293) and 96 h (Oli-neu) post transfection, protein lysates were extracted and 10 μg of total protein was size separated and immobilized on a polyvinyl fluoride membrane. Equal loading was confirmed by staining the membrane with Ponceau S. After washing and blocking using 5% milk powder, the membranes were incubated with a rabbit anti-GFP antibody, produced in-house (von Jonquieres et al., 2013). This was followed by application of an anti-rabbit horseradish peroxidase-conjugated

secondary antibody (Dianova, Hamburg, Germany), detection of the immunoreactivity by the enhanced chemiluminescence system (BioRad, Gladesville, NSW, Australia) and signal capture (GelDoc, BioRad, Gladesville, NSW, Australia).

Immunohistochemistry

Mice were fixed by transcardial perfusion with 10% buffered neutral formalin (Sigma) and 40 μm coronal cryosections spanning the subcortical striatal nuclei (including globus pallidus and caudate putamen) were collected after cryoprotection in 30% sucrose. Tissue treatment by antigen retrieval followed by immunodetection of antigens has been described elsewhere (von Jonquieres et al., 2014). Sections were treated with a combination of primary antibodies including rabbit-anti GFP or mouse anti-GFP (Roche, Switzerland) with either mouse anti-NeuN (Millipore, MA, USA), mouse anti-glial fibrillary acidic protein (GFAP; Sigma-Aldrich, MO, USA), or rabbit anti-aspartoacylase (ASPA; Mersmann et al., 2011). ASPA is a marker of mature oligodendrocytes. In this population, ASPA positive cells have been reported to overlap 100 and 93% with the widely used oligodendrocyte soma markers glutathione S-transferase π isoform and CC1, respectively (Kawai et al., 2009). Following incubation with the appropriate Alexa-conjugated secondary antibodies (Invitrogen, Carlsbad, CA, USA), sections were mounted on slides and coverslipped with Mowiol (Calbiochem, Darmstadt, Germany). Fluorescence was visualized using a Zeiss Z1 AxioExaminer NLO710 confocal microscope (Carl Zeiss MicroImaging, Germany).

Quantification of Cell-Type Specific Transgene Expression

Specificity of AAV-mediated transgene expression was assessed following our previous work (von Jonquieres et al., 2013). Neonates (P0), or adult mice (n = 3) injected with AAV were humanely killed by transcardial perfusion 3 weeks later. Some neonatally injected mice were examined at 8 months for a long-term study. The identity of GFP-expressing cells in the striatum was examined by double-immunofluorescence with antibodies against GFP and ASPA (oligodendrocytes), NeuN (neurons), or GFAP (astrocytes) in confocal images at 20× and 40× magnification. The percentage of GFP-expressing cells per cell-type was determined by counting at least 50 cells from each of three non-adjacent sections for a total of at least 150 GFP^+ cells using the "cell counter" plugin for ImageJ version 1.45 k (NIH). GFAP is a marker, generally regarded as pan-astrocytic. However, recent evidence has shown that GFAP is heterogeneously expressed in the astroglial compartment with a bias towards white matter and reactive astrocytes (Cahoy et al., 2008). Therefore, transduced astrocytes were identified based on the presence of GFAP and morphological criteria. The latter was possible as the soluble GFP reporter filled the processes of the host cells.

Statistics

All graphs and statistical analyses were done with GraphPad Prism 6 Software (La Jolla, CA, USA). Quantitative measures were analyzed by one-way or two-way analysis of variance (ANOVA) as appropriate, followed by Tukey's *post hoc* test. Values are presented as the mean ± SEM.

RESULTS

Mbp Promoter-Driven Transgene Expression in Oligodendrocytes Following Intracranial Injection of AAV1/2, rh39, rh20 and cy5

We reported previously on the efficacy of chimeric AAV1/2 for the transfer of an *Mbp* promoter driven GFP expression cassette to the developing, or adult mouse brain (von Jonquieres et al., 2013). To expand this gene delivery system towards a potential clinical setting, we screened the transduction specificity of non-chimeric AAV vector variants rh20, rh39 and cy5, derived from non-human primates (Gao et al., 2004). These vectors, expressing GFP under the control of the *Mbp* promoter, were injected into the striatum of adult mice. Chimeric AAV1/2-*Mbp-GFP* served as a control (**Figure 1**). Three weeks later, we determined the relative numbers of GFP^+ cells among oligodendrocytes, neurons or astrocytes by immunohistochemistry. We found that AAV1/2 and rh20 resulted in highly preferential oligodendroglial GFP expression, exceeded by rh39 and cy5. For all other experiments we focused on cy5 as it is a variant of AAV7 that, based on its extremely weak immunogenicity, has been proposed to have a strong potential to be developed as a clinical gene therapy vector (Gao et al., 2002).

Characterization of the Human *MAG* Promoter *In Silico*

Our *in silico* search of AAV-compatible promoter regions of oligodendrocyte-specific genes identified a human *MAG* promoter region entailing the sequence from position −2184 to the transcription start site. We located a number of known transcription factor binding sites of the oligodendrocyte lineage (**Figure 2**). The distal segment of this fragment contained binding sites for both positive and negative transcriptional regulators such as Yin Yang 1 (YY1) and Inhibitor of DNA Binding 4 (Id4; Marin-Husstege et al., 2006; He et al., 2007; Zolova and Wight, 2011). We therefore decided to also investigate the proximal 1.5 kb of the long fragment since this fragment was devoid of these motifs but contained binding sites for myelin cell lineage factors Oligodendrocyte Transcription Factor 1 (Olig1) and SRY-Box 10 (Sox10) and an evolutionary highly conserved sequence (Wang et al., 2014). Finally, we also selected the proximal 300 bp fragment for further characterization as it contains evolutionary conserved binding sites for myelin gene regulatory factor (MRF) and Ring Finger Protein 10 (RNF10), critical activators of myelination in oligodendrocytes or Schwann cells, respectively (Hoshikawa et al., 2008; Emery et al., 2009; Bujalka et al., 2013). Another conserved DNA stretch was located between −1315 to −1176. A comprehensive list of transcription factor binding motifs in the 2.2 kb upstream sequence of the *MAG* transcription start site is summarized in **Table 1**.

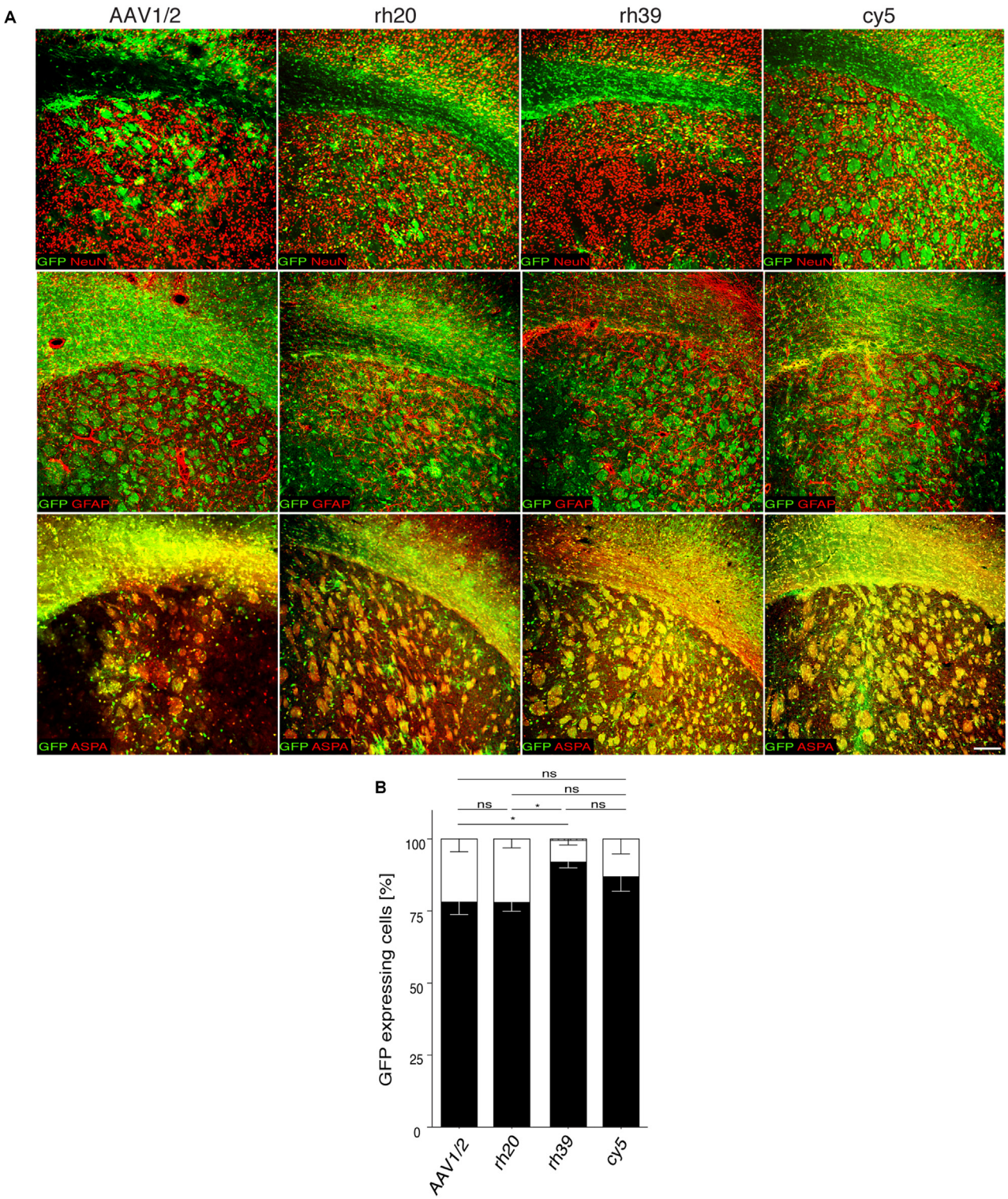

FIGURE 1 | *Mbp* promoter selectivity targets transgene expression to oligodendrocytes in the adult brain. (A) The indicated adeno-associated viral (AAV) vectors (2×10^9 vg) were injected into the striatum of adult mice ($n = 3$). Representative images showing immunohistochemistry for green fluorescent protein (GFP; green) and cell type specific markers (red) including ASPA (oligodendrocytes), NeuN (neurons) and GFAP (astrocytes). **(B)** Quantification of relative GFP reporter expressing in ASPA$^+$ oligodendrocytes, NeuN$^+$ neurons and GFAP$^+$ astrocytes. Two-way analysis of variance (ANOVA) with Tukey's *post hoc* test revealed differences in oligodendroglial GFP expression between AAV1/2 (78.2 ± 4.4%) and rh39 (91.0 ± 1.5%; $p < 0.05$) as well as rh20 (78.0 ± 1.7%) and rh39 ($p < 0.05$). There was no significant difference between rh39 and cy5 (87.0 ± 5.1%); one-way ANOVA with Tukey's *post hoc* test. *$p < 0.05$. Bar: 200 μm.

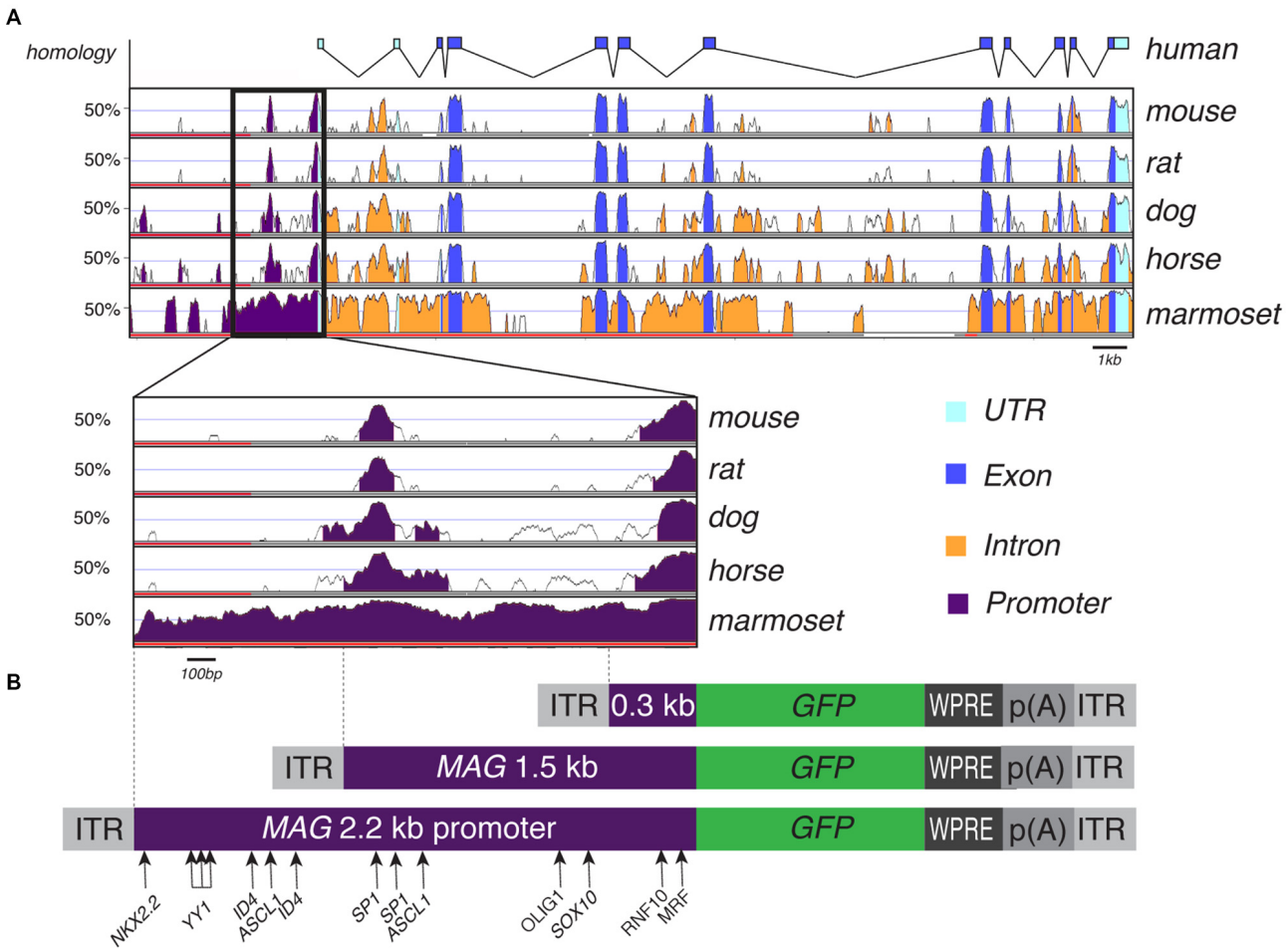

FIGURE 2 | Myelin Associated Glycoprotein (*MAG*) promoter inter-species alignment and AAV expression cassettes. (A) VISTA plot of human sequence across the *MAG* locus and its genomic conservation in mouse, rat, dog, horse and marmoset. A close-up of the 2.2 kb upstream promoter region shows two regions of high conservation, suggestive of functional importance, from −118 to −1 bp and from −1315 to −1176 bp upstream the putative transcription start site. **(B)** AAV expression cassettes for GFP reporter expression controlled by the 0.3 kb, 1.5 and 2.2 kb human *MAG* promoter. Transcription factor binding sites with relevance to oligodendroglial gene expression are indicated.

TABLE 1 | Position of putative transcription factor binding sites in the recombinant human *MAG* promoter.

Transcription factor	Binding motif	Site 1	Site 2	Site 3
*MRF	ctggcac	−40 to −33	–	–
*RNF10	acaagggccccttttgtgccc	−108 to −92	–	–
*SOX10	acaatg	−293 to −287	–	–
OLIG1	tcagatg	−388 to −381	–	–
NKX2.2	acttga	−2158 to −2152	–	–
SP1	ccccctcccca	−91 to −79	−1114 to −1103	−1219 to −1208
YY1	gccatg	−1894 to −1888	−1949 to −1943	−2000 to −1994
ASCL1	cagctg	−1014 to −1008	−1715 to −1709	–
FOXD3	ttttgtttgttt	−2111 to −2099	–	–
ID4	cacctg	−1656 to −1650	−1737 to −1731	–
Zfp191	ggagggg	−735 to −728	–	–

*Notes: *Transcription factor binding sites that have been experimentally validated in the rodent MAG promoter. See text for references.*

Recombinant *MAG* Promoter Shows Oligodendroglial Selectivity *In Vitro*

We isolated three overlapping *MAG* promoter fragments stretching from position −2.2, −1.5, or −0.3 kb to the transcription start site. These fragments were inserted in an AAV2 expression cassette containing the cDNA encoding GFP (**Figure 2**). The recombinant AAV plasmids were then used for transient transfection of HEK 293 cells and subsequent immunocytochemistry (not shown) or immunoblot detection of the GFP reporter (**Figure 3A**). Low level GFP expression was detectable following transfection with the *MAG* promoter-driven constructs. In contrast, the control plasmids in which reporter gene transcription was driven by the CAG or *Mbp* promoter produced robust GFP expression. The difference between *Mbp* and *MAG* promoter activity in HEK 293 cells suggested better selectivity of the latter.

In order to substantiate this notion by positive data, we electroporated Oli-neu cells, an *in vitro* model of oligodendrocytes, with the GFP reporters controlled by either one of the three *MAG* promoter fragments, the *GFAP*, *Mbp*,

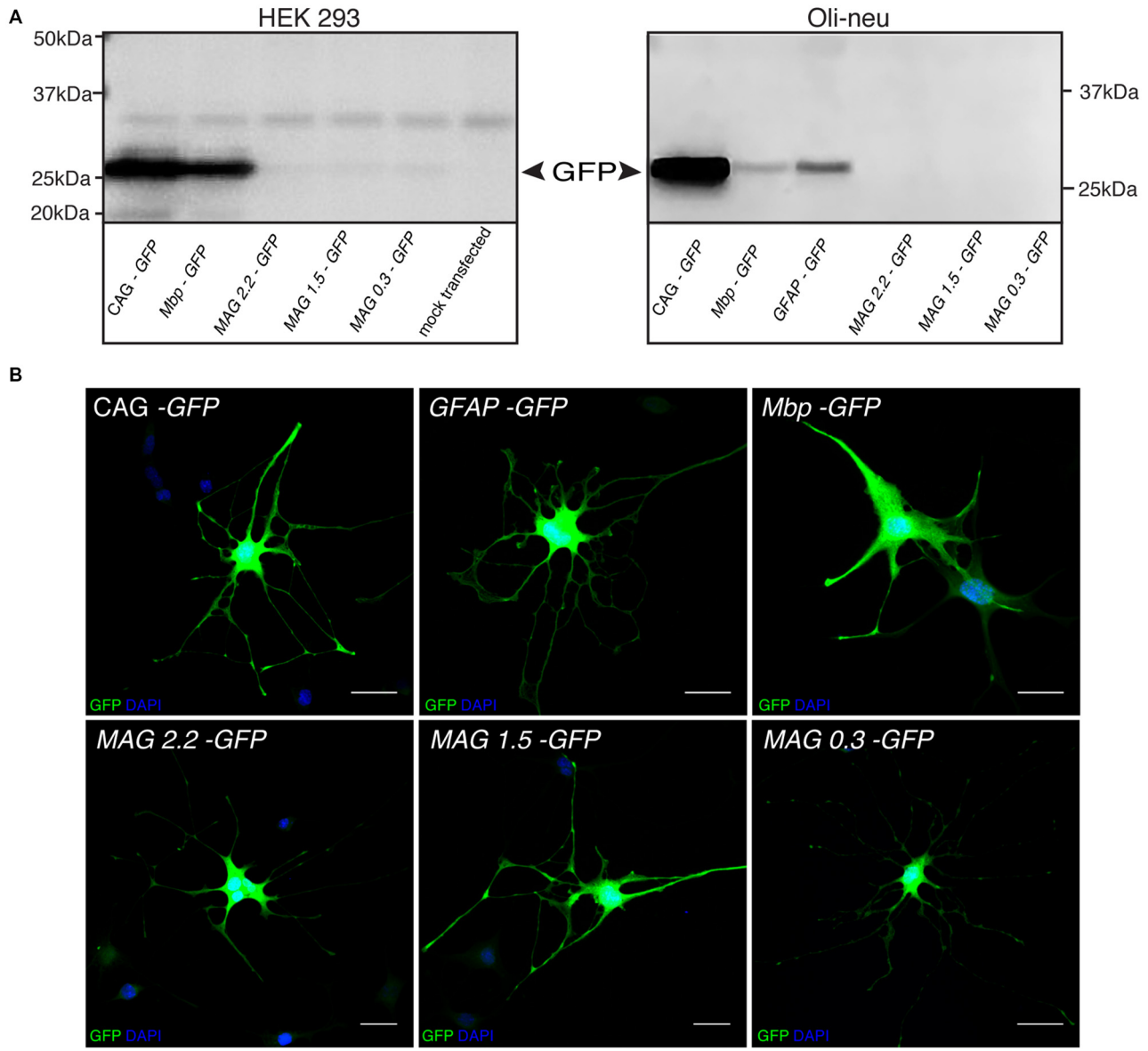

FIGURE 3 | *MAG* promoter selectivity *in vitro*. (A) GFP Immunoblots of HEK 293 and Oli-neu cells transiently transfected with the indicated plasmids. **(B)** Immunofluorescence detection of GFP expression following dbcAMP-induced differentiation of Oli-neu cells transfected with the indicated plasmids. Activity of the GFAP promoter was restricted to cells with astroglial morphology while the other promoters drove transgene expression in cells exhibiting oligodendrocyte morphology. Representative results of three independent experiments are shown. Bars: 30 μm.

or CAG promoter. The cultures were then differentiated to adopt a mature oligodendrocyte-like phenotype, and finally assessed by immunoblot or GFP-immunocytochemistry. Unexpectedly, GFP-expression was below the detection limits of the immunoblot following transfection with any of the three *MAG* promoter-GFP constructs (**Figure 3A**). As the transfection efficiency was generally >70% judged by CAG-GFP transfectants (not shown) this result suggested that our recombinant *MAG* promoters were hardly active in the Oli-neu model. However, at the single cell level *MAG*-GFP transfection resulted in GFP-immunoreactivity in Oli-neu with oligodendrocyte morphology (**Figure 3B**).

Specificity of *MAG* Promoter Driven cy5 Vectors in the CNS of Adult Mice

We then investigated the potential of the *MAG* promoter for AAV-mediated transgene expression *in vivo*. All three AAV-*MAG-GFP* constructs were packaged into cy5 vectors and delivered to the dorsal striatum of adult mice. At 3 weeks following vector injection, when AAV-mediated transgene expression has peaked to stable levels (Klugmann et al., 2005a), animals were killed and the brains assessed by immunohistochemistry to detect GFP in immuno-identified neurons, oligodendrocytes, and astrocytes. Quantitative analyses of cy5-*MAG2.2-GFP* specificity judged by relative numbers of GFP^+ cells revealed a definitive oligodendroglial selectivity of the long *MAG* promoter fragment *in vivo* (**Figures 4A,B**). Neurons and astrocytes were almost entirely excluded from GFP-expression. Most oligodendrocytes in the target area, identified by ASPA immunoreactivity, expressed the GFP reporter (**Figure 4C**). Only a negligible number of neurons were GFP-positive. Similar results were obtained using cy5-*MAG1.5-GFP* (**Figure 5**) and cy5-*MAG0.3-GFP* (**Figure 6**). The use of the GFAP antibody precluded this sort of analysis for astroglia

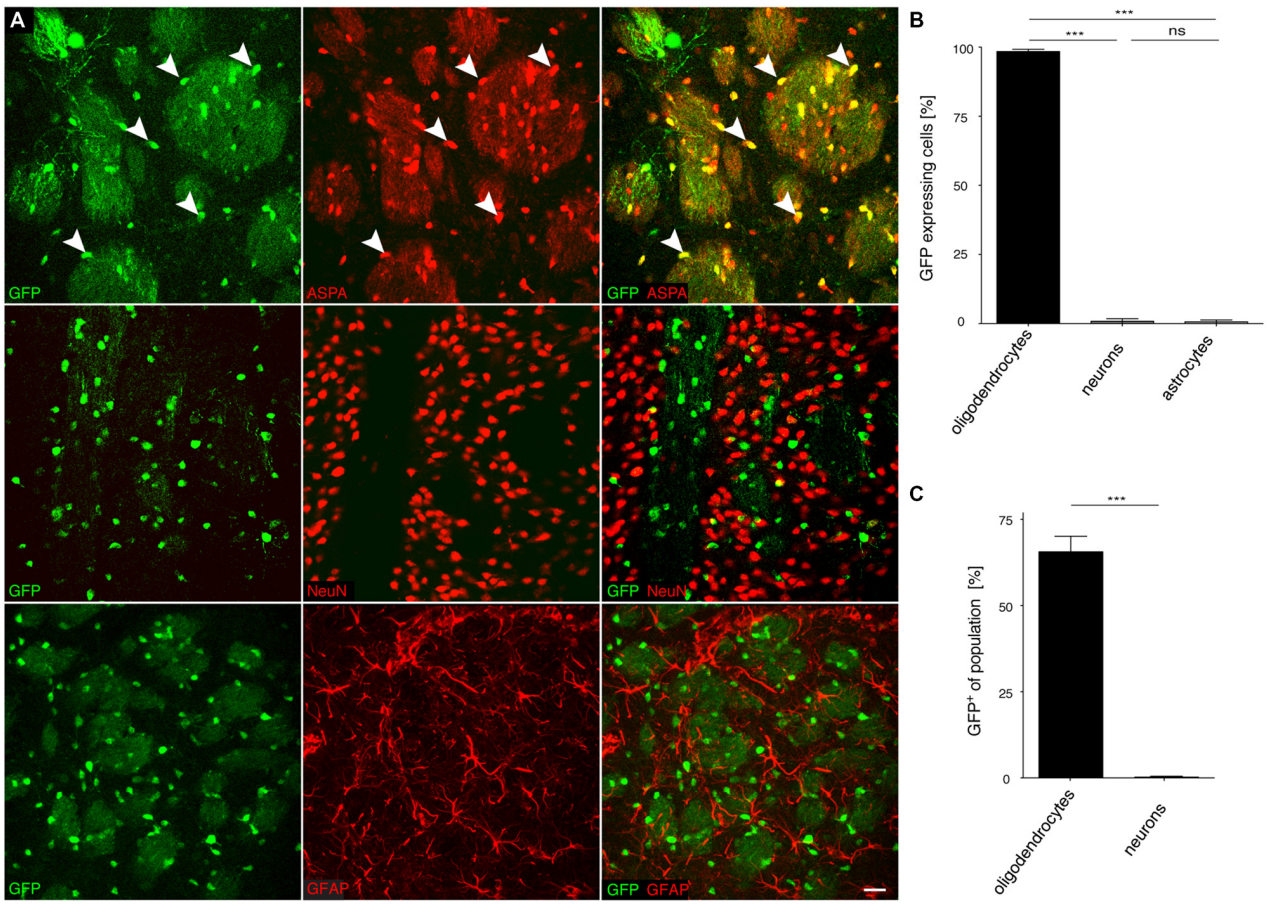

FIGURE 4 | The recombinant *MAG* 2.2 promoter drives oligodendrocyte-specific transgene expression in the central nervous system (CNS). **(A)** cy5-*MAG2.2-GFP* (2×10^9 vg) was injected into the dorsal striatum of adult mice 3 weeks prior to analysis ($n = 3$). Immunohistochemical staining was performed for GFP (green) and cell type specific markers (red) including ASPA (oligodendrocytes), NeuN (neurons) and GFAP (astrocytes). Arrowheads indicate representative cells showing colocalization. **(B)** Quantification of the results in **(A)** showed that GFP reporter gene expression was almost completely restricted to oligodendrocytes (98.4 ± 0.8%). Expression in neurons (0.9 ± 0.9%) and astrocytes (0.7 ± 0.67%) was negligible. **(C)** Relative quantification of the percentage of GFP expressing cells in each population revealed that 65.1 ± 4.0% of all oligodendrocytes expressed the GFP transgene while the ratio of GFP expressing neurons was extremely low (0.3 ± 0.27%); One-way ANOVA with Tukey's *post hoc* test. ***$p < 0.001$. Bar: 20 μm.

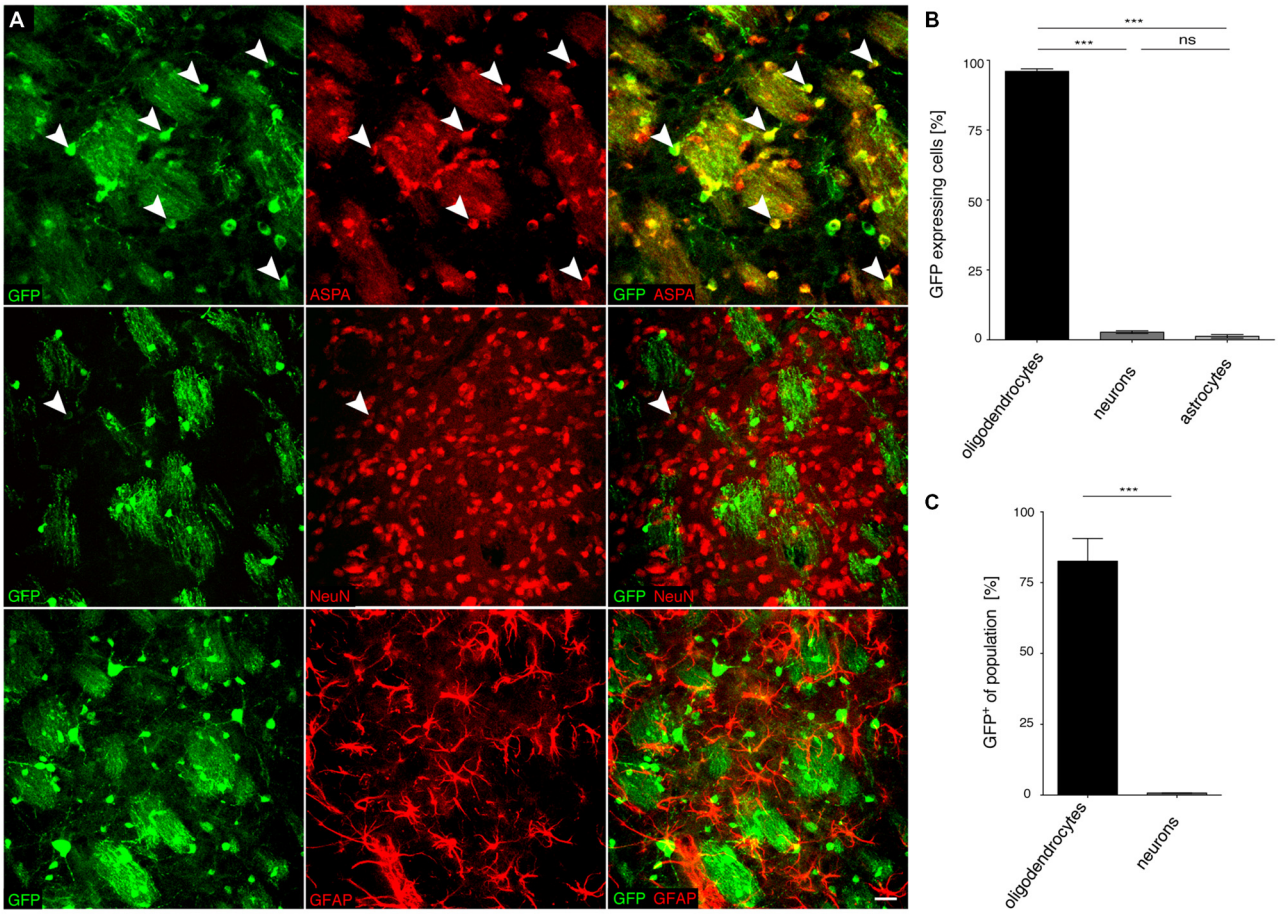

FIGURE 5 | The *MAG* 1.5 promoter restricts GFP transgene expression to oligodendrocytes. (A) cy5-*MAG1.5-GFP* (2×10^9 vg) was injected into the dorsal striatum of adult mice 3 weeks prior to analysis ($n = 3$). Immunohistochemical staining was performed for GFP (green) and cell type specific markers (red) including ASPA (oligodendrocytes), NeuN (neurons) and GFAP (astrocytes). Arrowheads indicate representative cells showing colocalization. **(B)** Quantification of the results in **(A)** showed that GFP reporter gene expression was almost completely restricted to oligodendrocytes (96.0 ± 0.9%). Expression in neurons (2.8 ± 0.5%) and astrocytes (1.3 ± 0.6%) was significantly less. **(C)** Relative quantification of the percentage of GFP expressing cells in each population revealed that 82.6 ± 7.7% of all oligodendrocytes expressed the GFP transgene while the ratio of GFP expressing neurons was extremely low (0.8 ± 0.1%); One-way ANOVA with Tukey's *post hoc* test. ***$p < 0.001$. Bar: 20 μm.

as it labels heterogeneous astrocyte populations (Cahoy et al., 2008).

Selectivity of cy5-*MAG2.2-GFP* in the CNS of Neonatal Mice

Somatic transgenesis in the mouse, achieved by neonatal vector administration and transduction of target oligodendrocytes, holds potential for disease modeling and gene function studies. In the rodent forebrain, MAG expression starts at P5 (Mingorance et al., 2005) and AAV-mediated gene activation in the CNS takes several days as it requires uncoating, nuclear translocation and second-strand synthesis of the ssAAV genome. Moreover, we have previously reported a largely superior vector spread following neonatal compared with adult AAV delivery to the CNS (von Jonquieres et al., 2013). We therefore investigated the long-term effects of the *MAG* promoter in brain sections obtained 8 months after intracranial AAV-injection to neonates (**Figure 7A**). We selected cy5-*MAG2.2-GFP* for this experiment based on the strict oligodendroglial selectivity evident from the adult 3 week expression pattern. GFP in the striatum of animals injected neonatally was predominantly found in oligodendrocytes, but also in some neurons and astrocytes (**Figure 7B**). The number of GFP^+ cells within the oligodendroglial compartments was limited (**Figure 7C**). A similar trend was observed in neonatally infused animals that were analyzed after 3 weeks (not shown).

Broadly, the performance of the three different MAG promoter fragments following AAV vector delivery to the CNS, summarized in **Figure 8**, was excellent. In the adult mouse, we observed a remarkably moderate trade-off between

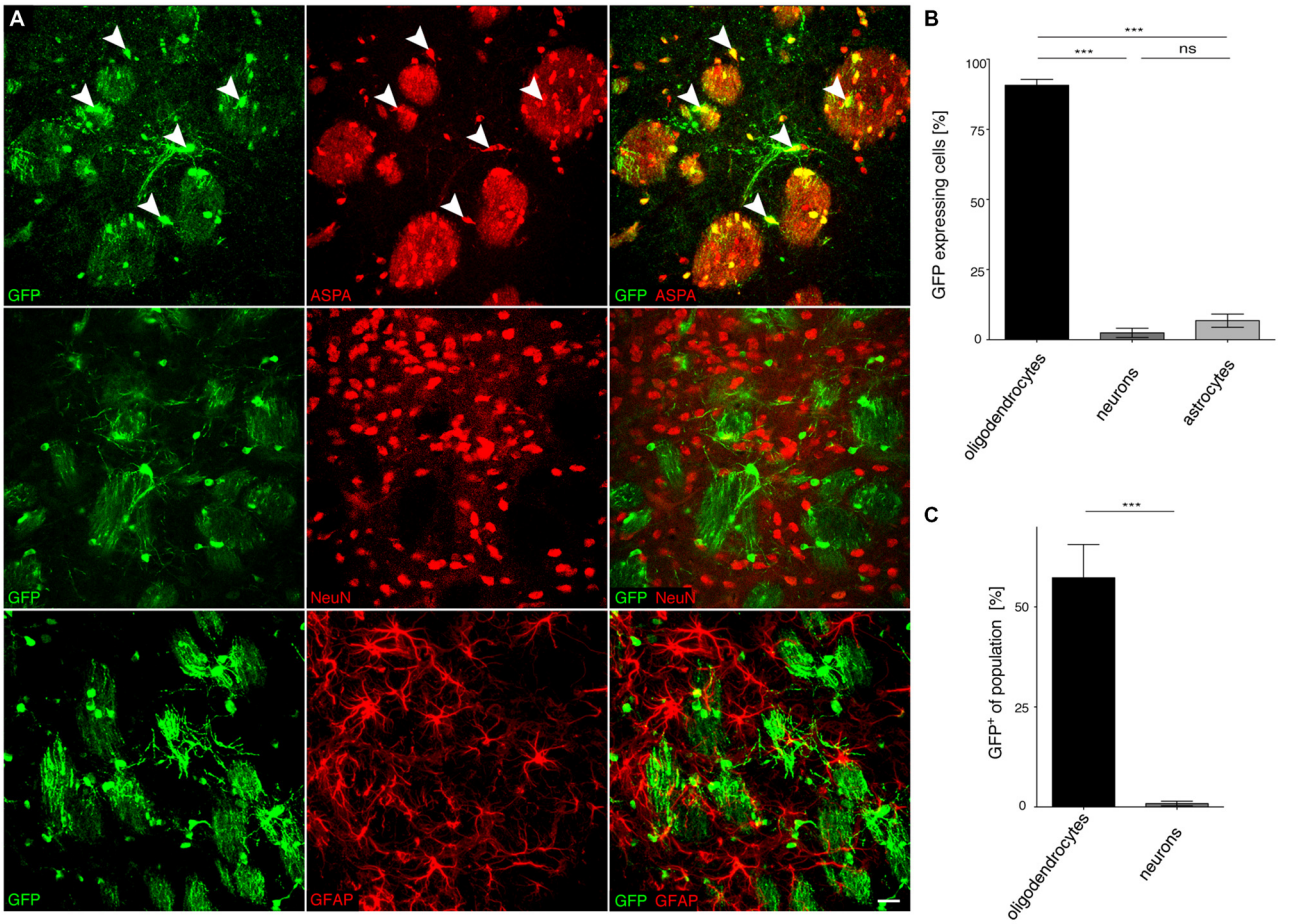

FIGURE 6 | The truncated *MAG0.3* promoter is sufficient to restrict AAV-mediated transgene expression to oligodendrocytes. (A) cy5-*MAG0.3-GFP* (2×10^9 vg) was injected into the dorsal striatum of adult mice 3 weeks prior to analysis ($n = 3$). Immunohistochemical staining was performed for GFP (green) and cell type specific markers (red) including ASPA (oligodendrocytes), NeuN (neurons) and GFAP (astrocytes). Arrowheads indicate representative cells showing colocalization. **(B)** Quantification of the results in **(A)** showed that GFP reporter gene expression was almost completely restricted to oligodendrocytes (90.7 ± 2.1%). Expression in neurons (2.5 ± 1.7%) and astrocytes (6.8 ± 2.4%) was significantly less. **(C)** Relative quantification of the percentage of GFP expressing cells in each population revealed that 57.3 ± 8.4% of all oligodendrocytes expressed the GFP transgene while the ratio of GFP expressing neurons was extremely low (0.9 ± 0.6%); One-way ANOVA with Tukey's *post hoc* test. ***$p < 0.001$. Bar: 20 μm.

MAG promoter length and oligodendroglial selectivity. Even the short 0.3 kb fragment greatly limited transgene expression to oligodendrocytes (**Figure 8A**). Moreover, the 0.3 kb fragment also showed activity in the majority of oligodendrocytes in the target area comparable to the 2.2 kb fragment (**Figure 8B**).

DISCUSSION

Conventional transgenic mouse lines utilizing myelin gene-specific promoters have informed on selective cis-acting elements that were shown to restrict the expression of transgenes to myelinating glia. There is virtually no size limitation for myelin gene promoters used in transgenic mouse lines. In contrast, the somatic gene delivery system represented by AAV depends on efficient incorporation of an expression cassette of less than 4.7 kb into the confined space of the viral capsid (Warrington and Herzog, 2006).

Only a few small cellular promoters have been described to reliably drive transgene expression in oligodendrocytes in genetically modified animals. Therefore, the number of candidates to be adopted for use in viral gene transfer has been limited. Recently, the 2,3-cyclic nucleotide 3-phosphodiesterase promoter, first described in transgenic mice (Gravel et al., 1998), has been reported to convey oligodendroglial-specific GFP reporter gene expression following lentiviral delivery to the neonatal mouse brain (Kagiava et al., 2014). Although this 4 kb promoter fragment is useful in the lentiviral setting harboring vector genomes up to 8.5 kb, it does not match the AAV size criteria.

To date, the only cellular promoter used for AAV-mediated transgene expression in oligodendrocytes is the murine 1.9 kb *Mbp* cis-regulating element and a truncated version spanning the proximal 1.3 kb upstream region including parts of *Mbp* exon 1 (Chen et al., 1998; Lawlor et al., 2009;

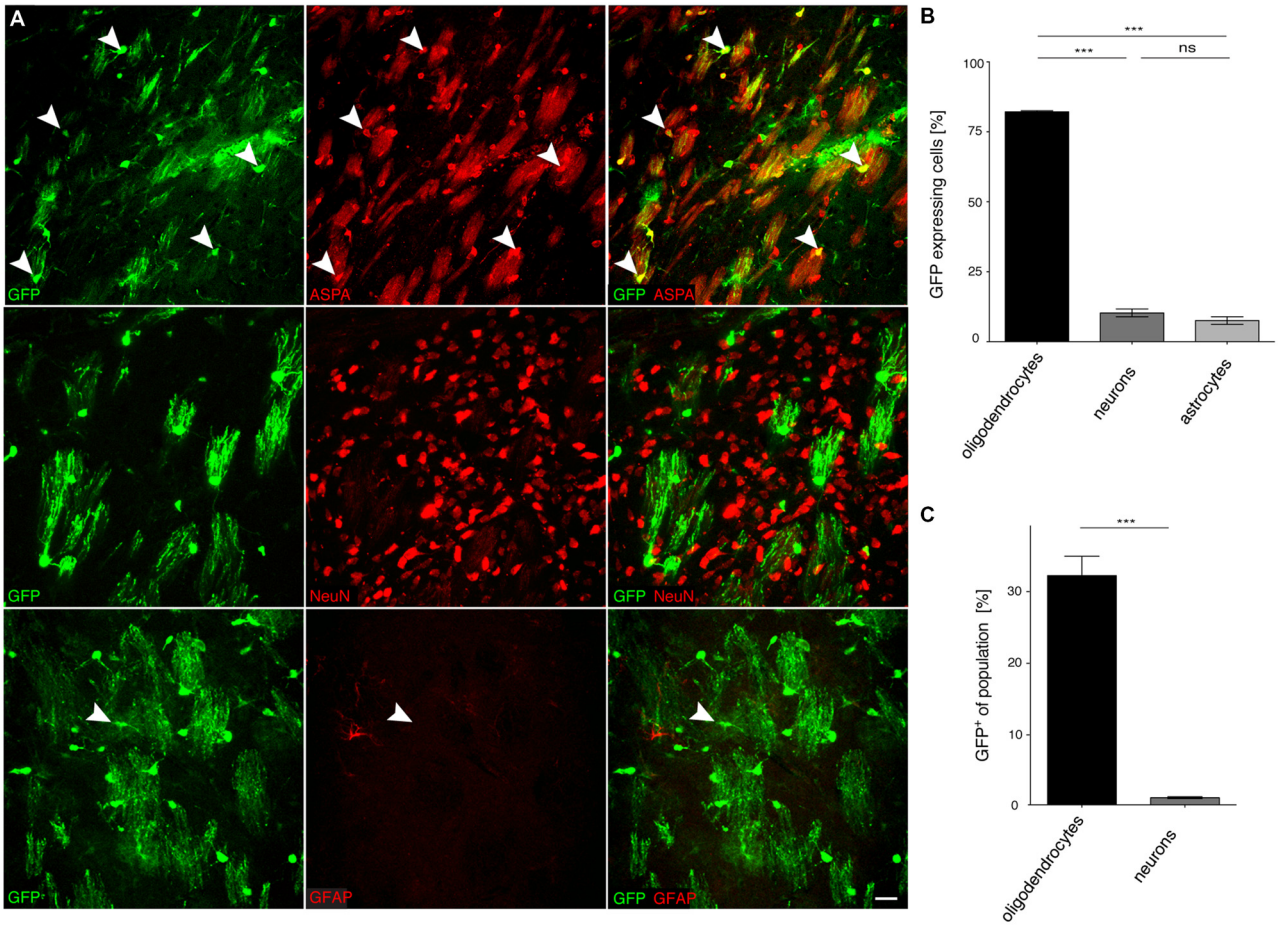

FIGURE 7 | Long-term expression in oligodendrocytes following neonatal cy5-*MAG2.2-GFP* delivery. (A) cy5-*MAG2.2-GFP* (2×10^9 vg) was injected into the dorsal striatum of neonatal mice ($n = 4$). At 8 months, immunohistochemical staining was performed for GFP (green) and cell type specific markers (red) including ASPA (oligodendrocytes), NeuN (neurons) and GFAP (astrocytes). Arrowheads indicate representative cells showing colocalization. **(B)** Quantification of the results in **(A)** showed that GFP reporter gene expression was enriched in the oligodendroglial compartment (82.2 ± 0.4%). Expression in neurons (10.3 ± 1.4%) and astrocytes (7.6 ± 1.4%) was significantly less. **(C)** Relative quantification of the percentage of GFP expressing cells in each population revealed that 32.8 ± 2.8% of all oligodendrocytes expressed the GFP transgene while the ratio of GFP expressing neurons was extremely low (1.0 ± 0.1%). ***$p < 0.001$. Bar: 20 μm.

von Jonquieres et al., 2013). The *Mbp* promoters have been used independently to achieve reporter gene expression in the adult rodent CNS using AAV2, AAV8, rh39, rh20 and cy5 (Chen et al., 1998; Lawlor et al., 2009). Like the 2,3-cyclic nucleotide 3-phosphodiesterase promoter both *Mbp* promoters were selected as they had been shown to drive transgenes in the oligodendrocyte lineage in transgenic mouse lines generated by pronucleus injections (Gow et al., 1992; Orian et al., 1994).

To date there is no oligodendrocyte-specific alternative to the 1.3 and 1.9 kb *Mbp* promoter variants appropriate for AAV viral gene delivery. The goal of this investigation was to delineate a novel recombinant promoter suited for clinical gene therapy of white matter disorders. To that end, we have selected a 2.2 kb region upstream of the transcription start site in the human *MAG* gene and two truncated variants, that harbor an abundance of binding motifs for transcription factors known to regulate gene activity and myelination in oligodendrocytes or Schwann cells (Emery, 2010).

All three recombinant *MAG* promoters showed very little activity in HEK 293 cells despite good transfection efficacy confirmed to be greater than 80% in CAG-*GFP* samples. Compared with the CAG promoter, the 1.9 kb *Mbp* promoter showed weaker yet robust GFP expression in HEK 293 cells. We have, however, identified Oli-neu cells as a suitable model for qualitative observations on glial promoter selectivity given that differentiated cultures contain cells with either oligodendrocyte or astroglial morphology that were permissive for *MAG* or *GFAP* promoter driven GFP expression, respectively.

Our previous data using the *Mbp* promoter were obtained using a chimeric AAV vector system that inherently lacks translational relevance due to the heterogeneity of viral particles consisting of a wide range of ratios between AAV1 and AAV2 capsid proteins (von Jonquieres et al., 2013). Therefore, the

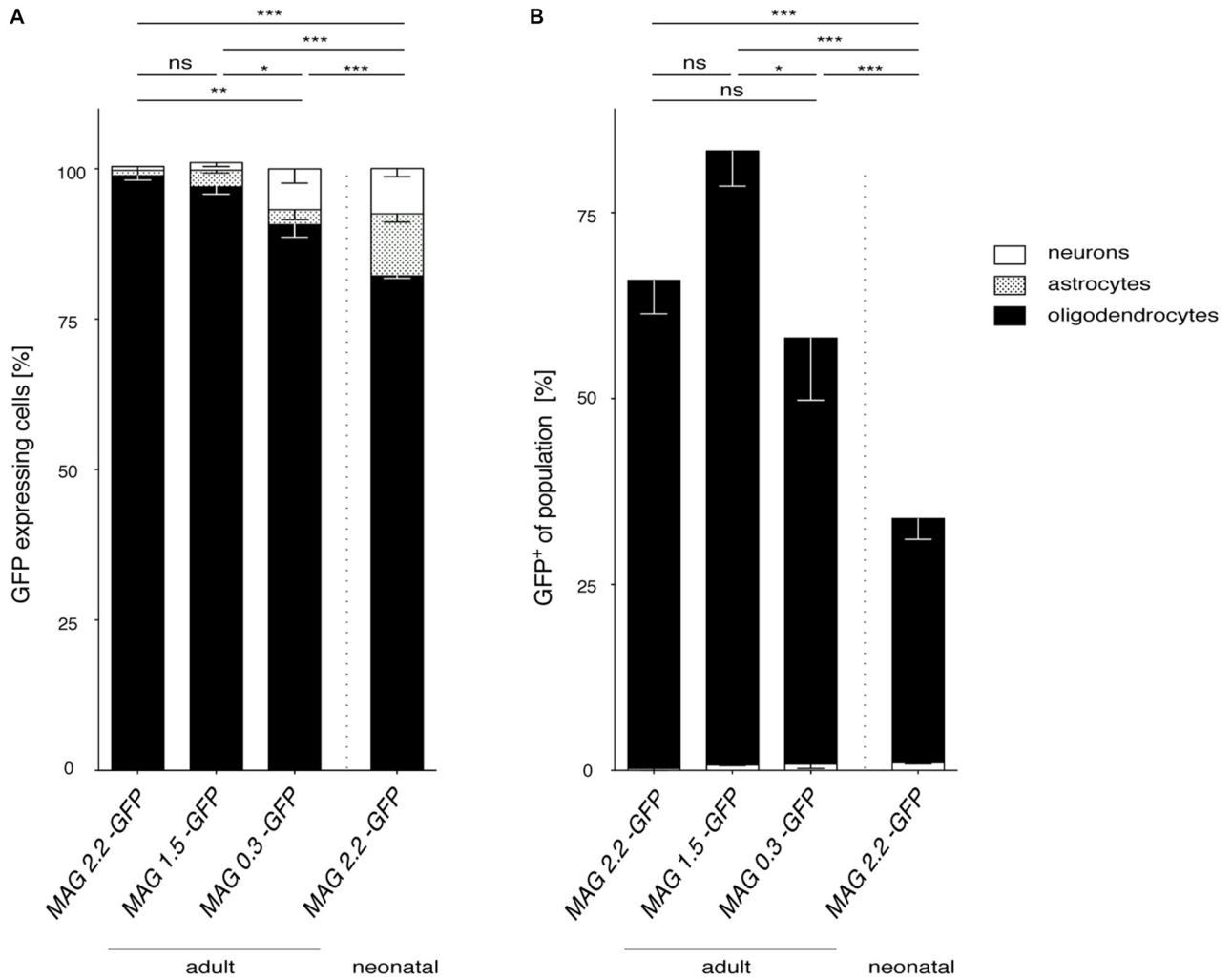

FIGURE 8 | Comparison of *MAG* promoter-controlled selectivity of AAV-mediated transgene expression. (A) The proportion of oligodendrocytes, neurons and astrocytes was calculated for each *MAG* promoter variant in adult AAV injected mice and for cy5-*Mag2.2-GFP* delivered to neonates. Statistically significant differences in AAV-mediated oligodendrocyte-specific GFP reporter gene expression were detected between the *MAG2.2* and the *MAG0.3* promoter following AAV delivery to adult mice ($P < 0.05$). In all cases AAV mediated delivery of any of the three *MAG*-GFP expression constructs resulted in slight but significantly better restriction of transgene expression to oligodendrocytes than neonatal delivery of *MAG*2.2-*GFP* ($p < 0.01$). **(B)** Summery of the percentage of GFP^+ cells relative to the population of oligodendrocytes and neurons in the target area. Irrespective of the time point of AAV-delivery the *MAG* promoter robustly targeted the oligodendrocyte population. Adult cy5 mediated delivery of any of the three *MAG*-GFP expression constructs targeted the oligodendrocyte population significantly more efficiently than cy5-*MAG2.2-GFP* following neonatal delivery. Two-way ANOVA with Tukey's *post hoc* test. $^*p < 0.05$; $^{**}p < 0.01$; $^{***}p < 0.001$.

current study employed the AAV7-derived variant cy5 as a candidate for clinical gene therapy applications since neutralizing antibodies to AAV7 are rare in human serum (Gao et al., 2002). While a recent pioneering study has confirmed very good vector spread following cy5-CAG-*GFP* delivery to the adult rodent brain the effects of cellular promoters were not examined (Lawlor et al., 2009).

We have shown previously that the vector spread depends on the developmental stage of the target tissue at the time of infusion but not on the cellular promoter used in the expression cassette (von Jonquieres et al., 2013). Thus, our current investigations focused on promoter selectivity rather than vector spread. We have previously reported that the *Mbp* promoter exhibits mostly astroglial activity following injection at P0. As this developmental stage in the mouse CNS corresponds to the second prenatal trimester in humans (Clancy et al., 2001), it is of limited clinical relevance. However, somatic transgenesis in the mouse, achieved by vector delivery at P0, is instrumental for disease modeling (Dayton et al., 2012). Therefore, we selected cy5-*MAG2.2-GFP* for intracranial injection at P0 and noticed GFP expression mostly in oligodendrocytes for at least 8 months.

Although a comparison between the transduction profiles of the vectors carrying the *MAG* promoter (this study) and the

Mbp promoter (von Jonquieres et al., 2013) is not feasible, it appears that in neonates the *MAG* promoter might be better suited for transgene expression targeted to oligodendrocytes (90%) than the *Mbp* promoter (25%). We hypothesized that the potential gene delivery to oligodendrocyte precursor cells (OPCs) available at P0, a time point preceding MAG expression, would prime the transduced cells for MAG promoter-driven transgene expression at later stages as the recombinant AAV-genome stably remains in the host cell nucleus. However, we observed only a moderate total number of GFP-expressing oligodendrocytes following neonatal injections which might reflect a poor initial transduction efficiency of OPCs and limited available AAV particles when oligodendrocytes are born.

To our best knowledge, this is the first report on a *MAG* cis-acting element to drive transgene expression *in vivo*. The identification of the potential of the 0.3 kb *MAG* promoter fragment might be the most important result of the present study. The significance of this result is outstanding as this promoter fragment allows incorporation in the genome of self-complementary (sc) AAV vectors that inherently possess only half the packaging capacity yet have a superior transduction profile compared with single-stranded vectors (McCarty, 2008). Although not investigated here, the presence of a RNF10 site within all three MAG promoter fragments might enable transgene expression in Schwann cells. This would be an improvement over the *Mbp* promoter that lacks the Schwann cell-specific enhancers required for activity in the peripheral nervous system (Mathis et al., 2000).

In conclusion, the *MAG* promoter has superior features considering its human origin, small size and oligodendroglial selectivity in adults and neonates. Combined with its potential to sustain long-term transgene expression, the recombinant *MAG* promoter represents a valuable addition to the AAV toolbox.

AUTHOR CONTRIBUTIONS

Conceived and designed the experiments: MK and GvJ. Performed the experiments: GvJ, XW, RR, DF, CBK, AEH, ZHTS and MK. Analyzed the data: GvJ, DF and GDH. Wrote the article: MK and GvJ.

ACKNOWLEDGMENTS

We thank Keith Chua for help with cell counting. The AAV packaging plasmids for rh20, rh39 and cy5 were kindly provided by the Penn Vector Core, University of Pennsylvania. MK was an Australian Research Council Future Fellow. DF was a German Research Foundation Fellow. This work was supported by the NHMRC (Project Grant APP1050277) to MK.

REFERENCES

Ahmed, S. S., Li, H., Cao, C., Sikoglu, E. M., Denninger, A. R., Su, Q., et al. (2013). A single intravenous rAAV injection as late as P20 achieves efficacious and sustained CNS gene therapy in Canavan mice. *Mol. Ther.* 21, 2136–2147. doi: 10.1038/mt.2013.138

Biffi, A., Montini, E., Lorioli, L., Cesani, M., Fumagalli, F., Plati, T., et al. (2013). Lentiviral hematopoietic stem cell gene therapy benefits metachromatic leukodystrophy. *Science* 341:1233158. doi: 10.1126/science.1233158

Bujalka, H., Koenning, M., Jackson, S., Perreau, V. M., Pope, B., Hay, C. M., et al. (2013). MYRF is a membrane-associated transcription factor that autoproteolytically cleaves to directly activate myelin genes. *PLoS Biol.* 11:e1001625. doi: 10.1371/journal.pbio.1001625

Cahoy, J. D., Emery, B., Kaushal, A., Foo, L. C., Zamanian, J. L., Christopherson, K. S., et al. (2008). A transcriptome database for astrocytes, neurons and oligodendrocytes: a new resource for understanding brain development and function. *J. Neurosci.* 28, 264–278. doi: 10.1523/JNEUROSCI.4178-07.2008

Cartier, N., Hacein-Bey-Abina, S., Bartholomae, C. C., Veres, G., Schmidt, M., Kutschera, I., et al. (2009). Hematopoietic stem cell gene therapy with a lentiviral vector in X-linked adrenoleukodystrophy. *Science* 326, 818–823. doi: 10.1126/science.1171242

Chen, H., McCarty, D. M., Bruce, A. T., and Suzuki, K. (1998). Gene transfer and expression in oligodendrocytes under the control of myelin basic protein transcriptional control region mediated by adeno-associated virus. *Gene Ther.* 5, 50–58. doi: 10.1038/sj.gt.3300547

Clancy, B., Darlington, R. B., and Finlay, B. L. (2001). Translating developmental time across mammalian species. *Neuroscience* 105, 7–17. doi: 10.1016/s0306-4522(01)00171-3

Dayton, R. D., Wang, D. B., and Klein, R. L. (2012). The advent of AAV9 expands applications for brain and spinal cord gene delivery. *Expert Opin. Biol. Ther.* 12, 757–766. doi: 10.1517/14712598.2012.681463

Dong, J. Y., Fan, P. D., and Frizzell, R. A. (1996). Quantitative analysis of the packaging capacity of recombinant adeno-associated virus. *Hum. Gene. Ther.* 7, 2101–2112. doi: 10.1089/hum.1996.7.17-2101

During, M. J., Young, D., Baer, K., Lawlor, P., and Klugmann, M. (2003). Development and optimization of adeno-associated virus vector transfer into the central nervous system. *Methods Mol. Med.* 76, 221–236. doi: 10.1385/1-59259-304-6:221

Emery, B. (2010). Regulation of oligodendrocyte differentiation and myelination. *Science* 330, 779–782. doi: 10.1126/science.1190927

Emery, B., Agalliu, D., Cahoy, J. D., Watkins, T. A., Dugas, J. C., Mulinyawe, S. B., et al. (2009). Myelin gene regulatory factor is a critical transcriptional regulator required for CNS myelination. *Cell* 138, 172–185. doi: 10.1016/j.cell.2009.04.031

Fitzsimons, H. L., Bland, R. J., and During, M. J. (2002). Promoters and regulatory elements that improve adeno-associated virus transgene expression in the brain. *Methods* 28, 227–236. doi: 10.1016/s1046-2023(02)00227-x

Frühbeis, C., Frohlich, D., Kuo, W. P., Amphornrat, J., Thilemann, S., Saab, A. S., et al. (2013). Neurotransmitter-triggered transfer of exosomes mediates oligodendrocyte-neuron communication. *PLoS Biol.* 11:e1001604. doi: 10.1371/journal.pbio.1001604

Gao, G. P., Alvira, M. R., Wang, L., Calcedo, R., Johnston, J., and Wilson, J. M. (2002). Novel adeno-associated viruses from rhesus monkeys as vectors for human gene therapy. *Proc. Natl. Acad. Sci. U S A* 99, 11854–11859. doi: 10.1073/pnas.182412299

Gao, G., Vandenberghe, L. H., Alvira, M. R., Lu, Y., Calcedo, R., Zhou, X., et al. (2004). Clades of Adeno-associated viruses are widely disseminated in human tissues. *J. Virol.* 78, 6381–6388. doi: 10.1128/jvi.78.12.6381-6388.2004

Gow, A., Friedrich, V. L., Jr., and Lazzarini, R. A. (1992). Myelin basic protein gene contains separate enhancers for oligodendrocyte and Schwann cell expression. *J. Cell Biol.* 119, 605–616. doi: 10.1083/jcb.119.3.605

Gravel, M., Di Polo, A., Valera, P. B., and Braun, P. E. (1998). Four-kilobase sequence of the mouse CNP gene directs spatial and temporal expression of

lacZ in transgenic mice. *J. Neurosci. Res.* 53, 393–404. doi: 10.1002/(sici)1097-4547(19980815)53:4<393::aid-jnr1>3.3.co;2-y

Harasta, A. E., Power, J. M., von Jonquieres, G., Karl, T., Drucker, D. J., Housley, G. D., et al. (2015). Septal Glucagon-like peptide 1 receptor expression determines suppression of cocaine-induced behavior. *Neuropsychopharmacology* 40, 1969–1978. doi: 10.1038/npp.2015.47

He, Y., Dupree, J., Wang, J., Sandoval, J., Li, J., Liu, H., et al. (2007). The transcription factor Yin Yang 1 is essential for oligodendrocyte progenitor differentiation. *Neuron* 55, 217–230. doi: 10.1016/j.neuron.2007.06.029

Hoshikawa, S., Ogata, T., Fujiwara, S., Nakamura, K., and Tanaka, S. (2008). A novel function of RING finger protein 10 in transcriptional regulation of the myelin-associated glycoprotein gene and myelin formation in Schwann cells. *PLoS One* 3:e3464. doi: 10.1371/journal.pone.0003464

Kagiava, A., Sargiannidou, I., Bashiardes, S., Richter, J., Schiza, N., Christodoulou, C., et al. (2014). Gene delivery targeted to oligodendrocytes using a lentiviral vector. *J. Gene Med.* 16, 364–373. doi: 10.1002/jgm.2813

Kawai, K., Itoh, T., Itoh, A., Horiuchi, M., Wakayama, K., Bannerman, P., et al. (2009). Maintenance of the relative proportion of oligodendrocytes to axons even in the absence of BAX and BAK. *Eur. J. Neurosci.* 30, 2030–2041. doi: 10.1111/j.1460-9568.2009.06988.x

Klugmann, M., Leichtlein, C. B., Symes, C. W., Serikawa, T., Young, D., and During, M. J. (2005a). Restoration of aspartoacylase activity in CNS neurons does not ameliorate motor deficits and demyelination in a model of Canavan disease. *Mol. Ther.* 11, 745–753. doi: 10.1016/j.ymthe.2005.01.006

Klugmann, M., Symes, C. W., Leichtlein, C. B., Klaussner, B. K., Dunning, J., Fong, D., et al. (2005b). AAV-mediated hippocampal expression of short and long Homer 1 proteins differentially affect cognition and seizure activity in adult rats. *Mol. Cell. Neurosci.* 28, 343–360. doi: 10.1016/j.mcn.2004.10.002

Krämer, E. M., Koch, T., Niehaus, A., and Trotter, J. (1997). Oligodendrocytes direct glycosyl phosphatidylinositol-anchored proteins to the myelin sheath in glycosphingolipid-rich complexes. *J. Biol. Chem.* 272, 8937–8945. doi: 10.1074/jbc.272.14.8937

Lawlor, P. A., Bland, R. J., Mouravlev, A., Young, D., and During, M. J. (2009). Efficient gene delivery and selective transduction of glial cells in the mammalian brain by AAV serotypes isolated from nonhuman primates. *Mol. Ther.* 17, 1692–1702. doi: 10.1038/mt.2009.170

Leone, P., Shera, D., McPhee, S. W., Francis, J. S., Kolodny, E. H., Bilaniuk, L. T., et al. (2012). Long-term follow-up after gene therapy for canavan disease. *Sci. Transl. Med.* 4:165ra163. doi: 10.1126/scitranslmed.3003454

Marin-Husstege, M., He, Y., Li, J., Kondo, T., Sablitzky, F., and Casaccia-Bonnefil, P. (2006). Multiple roles of Id4 in developmental myelination: predicted outcomes and unexpected findings. *Glia* 54, 285–296. doi: 10.1002/glia.20385

Martini, R., and Schachner, M. (1997). Molecular bases of myelin formation as revealed by investigations on mice deficient in glial cell surface molecules. *Glia* 19, 298–310. doi: 10.1002/(sici)1098-1136(199704)19:4<298::aid-glia3>3.3.co;2-l

Mathis, C., Hindelang, C., LeMeur, M., and Borrelli, E. (2000). A transgenic mouse model for inducible and reversible dysmyelination. *J. Neurosci.* 20, 7698–7705.

McCarty, D. M. (2008). Self-complementary AAV vectors; advances and applications. *Mol. Ther.* 16, 1648–1656. doi: 10.1038/mt.2008.171

McClure, C., Cole, K. L., Wulff, P., Klugmann, M., and Murray, A. J. (2011). Production and titering of recombinant adeno-associated viral vectors. *J. Vis. Exp.* 57:e3348. doi: 10.3791/3348

Mersmann, N., Tkachev, D., Jelinek, R., Roth, P. T., Mobius, W., Ruhwedel, T., et al. (2011). Aspartoacylase-LacZ Knockin mice: an engineered model of canavan disease. *PLoS One* 6:e20336. doi: 10.1371/journal.pone.0020336

Mingorance, A., Fontana, X., Soriano, E., and Del Rio, J. A. (2005). Overexpression of myelin-associated glycoprotein after axotomy of the perforant pathway. *Mol. Cell. Neurosci.* 29, 471–483. doi: 10.1016/j.mcn.2005.03.016

Orian, J. M., Mitchell, A. W., Marshman, W. E., Webb, G. C., Ayers, M. M., Grail, D., et al. (1994). Insertional mutagenesis inducing hypomyelination in transgenic mice. *J. Neurosci. Res.* 39, 604–612. doi: 10.1002/jnr.490390512

Pilpel, N., Landeck, N., Klugmann, M., Seeburg, P. H., and Schwarz, M. K. (2009). Rapid, reproducible transduction of select forebrain regions by targeted recombinant virus injection into the neonatal mouse brain. *J. Neurosci. Methods* 182, 55–63. doi: 10.1016/j.jneumeth.2009.05.020

Thoms, J. A., Birger, Y., Foster, S., Knezevic, K., Kirschenbaum, Y., Chandrakanthan, V., et al. (2011). ERG promotes T-acute lymphoblastic leukemia and is transcriptionally regulated in leukemic cells by a stem cell enhancer. *Blood* 117, 7079–7089. doi: 10.1182/blood-2010-12-317990

von Jonquieres, G., Froud, K. E., Klugmann, C. B., Wong, A. C., Housley, G. D., and Klugmann, M. (2014). Loss of central auditory processing in a mouse model of Canavan disease. *PLoS One* 9:e97374. doi: 10.1371/journal.pone.0097374

von Jonquieres, G., Mersmann, N., Klugmann, C. B., Harasta, A. E., Lutz, B., Teahan, O., et al. (2013). Glial promoter selectivity following AAV-delivery to the immature brain. *PLoS One* 8:e65646. doi: 10.1371/journal.pone.0065646

Wang, J., Pol, S. U., Haberman, A. K., Wang, C., O'Bara, M. A., and Sim, F. J. (2014). Transcription factor induction of human oligodendrocyte progenitor fate and differentiation. *Proc. Natl. Acad. Sci. U S A* 111, E2885–E2894. doi: 10.1073/pnas.1408295111

Warrington, K. H. Jr., and Herzog, R. W. (2006). Treatment of human disease by adeno-associated viral gene transfer. *Hum. Genet.* 119, 571–603. doi: 10.1007/s00439-006-0165-6

Weinberg, M. S., Samulski, R. J., and McCown, T. J. (2013). Adeno-associated virus (AAV) gene therapy for neurological disease. *Neuropharmacology* 69, 82–88. doi: 10.1016/j.neuropharm.2012.03.004

Xiao, P. J., Li, C., Neumann, A., and Samulski, R. J. (2012). Quantitative 3D tracing of gene-delivery viral vectors in human cells and animal tissues. *Mol. Ther.* 20, 317–328. doi: 10.1038/mt.2011.250

Zolova, O. E., and Wight, P. A. (2011). YY1 negatively regulates mouse myelin proteolipid protein (Plp1) gene expression in oligodendroglial cells. *ASN Neuro* 3:e00067. doi: 10.1042/AN20110021

Conflict of Interest Statement: The authors declare that the research was conducted in the absence of any commercial or financial relationships that could be construed as a potential conflict of interest.

frontiers in Molecular Neuroscience

ORIGINAL RESEARCH
published: 24 August 2016
doi: 10.3389/fnmol.2016.00076

Neuroprotective Effect of Non-viral Gene Therapy Treatment Based on Tetanus Toxin C-fragment in a Severe Mouse Model of Spinal Muscular Atrophy

*Sara Oliván[1,2], Ana C. Calvo[1], Amaya Rando[1], Mireia Herrando-Grabulosa[3], Raquel Manzano[4], Pilar Zaragoza[1], Eduardo F. Tizzano[5], Jose Aquilera[3] and Rosario Osta[1]**

[1] Laboratorio de Genética Bioquímica, Facultad de Veterinaria, Instituto Agroalimentario de Aragón (IA2), Centro de Investigación y Tecnología Agroalimentaria de Aragón, Instituto de Investigación Sanitaria Aragón, Universidad de Zaragoza, Zaragoza, Spain, [2] Centro de Investigación Biomédica en Red en Bioingeniería, Biomateriales y Nanomedicina, Grupo AMB, Instituto de Investigación en Ingeniería de Aragón (I3A), Universidad de Zaragoza, Zaragoza, Spain, [3] Centro de Investigación Biomédica en Red sobre Enfermedades Neurodegenerativas, Spain Institut de Neurociències and Departament de Bioquímica i de Biologia Molecular, Facultat de Medicina, Universitat Autònoma de Barcelona, Cerdanyola del Vallès, Spain, [4] Department of Physiology, Anatomy and Genetics, University of Oxford, Oxford, UK, [5] Área de Genética Clínica y Molecular, Hospital Vall d'Hebron, Centros de Investigación Biomédica en Red, Barcelona, Spain

Spinal muscular atrophy (SMA) is a hereditary childhood disease that causes paralysis and progressive degeneration of skeletal muscles and spinal motor neurons. SMA is associated with reduced levels of full-length Survival of Motor Neuron (SMN) protein, due to mutations in the Survival of Motor Neuron 1 gene. Nowadays there are no effective therapies available to treat patients with SMA, so our aim was to test whether the non-toxic carboxy-terminal fragment of tetanus toxin heavy chain (TTC), which exhibits neurotrophic properties, might have a therapeutic role or benefit in SMA. In this manuscript, we have demonstrated that TTC enhance the SMN expression in motor neurons "*in vitro*" and evaluated the effect of intramuscular injection of TTC-encoding plasmid in the spinal cord and the skeletal muscle of SMNdelta7 mice. For this purpose, we studied the weight and the survival time, as well as, the survival and cell death pathways and muscular atrophy. Our results showed that TTC treatment reduced the expression of autophagy markers (*Becn1*, *Atg5*, *Lc3,* and *p62*) and pro-apoptotic genes such as *Bax* and *Casp3* in spinal cord. In skeletal muscle, TTC was able to downregulate the expression of the main marker of autophagy, *Lc3*, to wild-type levels and the expression of the apoptosis effector protein, *Casp3*. Regarding the genes related to muscular atrophy (*Ankrd1, Calm1, Col19a1, Fbox32, Mt2, Myod1, NogoA, Pax7, Rrad,* and *Sln*), TTC suggest a compensatory effect for muscle damage response, diminished oxidative stress and modulated calcium homeostasis. These preliminary findings suggest the need for further experiments to depth study the effect of TTC in SMA disease.

Keywords: spinal muscular atrophy, *c*-terminal fragment of the tetanus toxin, muscle, spinal cord, autophagy, apoptosis, muscular atrophy

Abbreviations: SEM: standard error of the mean; SMA: spinal muscular atrophy; SMN: survival motor neuron; TTC: C-terminal fragment of the tetanus toxin; WT: wild type.

OPEN ACCESS

Edited by:
George Smith,
Temple University School of Medicine, USA

Reviewed by:
Tatsuro Mutoh,
Fujita Health University, Japan
Yanyong Kang,
Van Andel Institute, USA

****Correspondence:***
Rosario Osta
osta@unizar.es

Received: *29 January 2016*
Accepted: *10 August 2016*
Published: *24 August 2016*

Citation:
Oliván S, Calvo AC, Rando A, Herrando-Grabulosa M, Manzano R, Zaragoza P, Tizzano EF, Aquilera J and Osta R (2016) Neuroprotective Effect of Non-viral Gene Therapy Treatment Based on Tetanus Toxin C-fragment in a Severe Mouse Model of Spinal Muscular Atrophy. Front. Mol. Neurosci. 9:76. doi: 10.3389/fnmol.2016.00076

INTRODUCTION

Motor neuron diseases, a group of heterogeneous neurological disorders such as Amyotrophic Lateral Sclerosis (ALS) and Spinal Muscular Atrophy (SMA), are characterized by varying degrees of motor neuron degeneration. In particular, SMA is an autosomal recessive motor neuron disease and the first genetic cause of infant mortality, characterized by the degeneration of motor neurons in the anterior horn of the spinal cord, resulting in muscular atrophy and weakness. SMA patients have a homozygous loss of the survival motor neuron 1 (*SMN1*) gene, but retain one or more copies of a nearly identical homolog, *SMN2*. Therefore this disease is the result of insufficient amounts of SMN protein and its levels are generally inversely correlated with the severity of the disease, hence making *SMN2* copy number the predominant modifier of the neuromuscular phenotype (Monani and De Vivo, 2014). In SMA pathology, the most striking component is the loss of alpha motor neurons in the ventral horn of the spinal cord, resulting in progressive paralysis and eventually premature death. Despite the time that has elapsed since the SMA genes were identified, the currently available treatments for patients affected by the disease are palliative, based on symptomatic treatments and supportive care (Monani and De Vivo, 2014). Nowadays, the most interesting therapeutic strategies are represented by molecular, gene and stem cell-mediated approaches which are focused on activating *SMN2* expression, modulating splicing of *SMN2* or replacing *SMN1* (Zanetta et al., 2014; d'Ydewalle and Sumner, 2015).

A promising therapeutic approach could be the non-viral gene therapy based on the use of atoxic *C*-terminal fragment of the tetanus toxin (TTC). Tetanus neurotoxin is a protein produced by *Clostridium tetani* that cause tetanus, a fatal condition characterized by painful and uncontrolled muscle contractions (Farrar et al., 2000). The toxin is synthesized as a single polypeptide and is posts-translationally modified to produce light and heavy chains linked by disulfide bonds (Turton et al., 2002). The catalytic domain of the toxin resides in the light chain, while the translocation and receptor-binding domains are present in the heavy chain (Montal, 2010). Moreover, the heavy chain consists of two non-toxic fragments, the *N*-terminal or translocation domain and the *C*-terminal or receptor-binding domain (Chen et al., 2012). The atoxic TTC heavy chain (hereafter called TTC) can be retrogradely transported to the central nervous system and may be linked to different molecules without apparent loss of biological activity. The ganglioside-binding properties of fragment C have demonstrated that the presence of polysialic acids within the gangliosides, such as GD1b (disialic acid residues attached to the internal galactose residue) and GT1b (disialic acid residues attached to the terminal galactose residue) in cell membranes are neccesary to enable the tetanus-toxin internalization and therefore the TTC internalization in neurons. Additionally, the neurotrophin receptor p75NTR and TrkB is also essential in the retrograde pathway of TTC, sharing with NGF and BDNF the same retrograde transport organelles (Calvo et al., 2012b). These features allow the use of TTC as a valuable biological carrier of therapeutic molecules such as reporter genes or neurotrophic factors to ameliorate the disease advances of neurodegenerative disorders (Toivonen et al., 2010). In ALS, the delivery of glial cell-derived neurotrophic factor (GDNF) or brain derived neurotrophic factor (BDNF) to the spinal cord is improved by conjugation with TTC after intramuscular administration (Ciriza et al., 2008; Calvo et al., 2011). In SMA, one therapeutic strategy could be based on increasing the levels of neuronal SMN, for this reason, the genetic fusion of SMN and TTC was applied to deliver exogenous SMN to the cytosolic compartment of motor neurons (Francis et al., 2004). Interestingly, *in vitro* and *in vivo* studies have also shown that TTC itself may well harbor neuroprotective properties (Toivonen et al., 2010; Calvo et al., 2012b). In this way, in the mouse model SOD1G93A of ALS, the intramuscular injection of naked DNA encoding for TTC ameliorated the decline of hind limb muscle innervation, significantly delayed the onset of symptoms and functional deficits, improved spinal motor neuron survival and prolonged lifespan (Moreno-Igoa et al., 2010).

In the light of these preliminary results, the aim of the present study was to evaluate the possible therapeutic effect of intramuscular delivery of a TTC-encoding plasmid in the spinal cord and the skeletal muscle tissues of an intermediate mouse model of SMA, the SMNdelta7 mouse. In order to evaluate the neuroprotective effects under TTC treatment, we firstly registered the weight and the survival time, and the survival rate to further analyze the expression of several genes related to neurodegenerative process, in particular, autophagy, apoptosis and muscle atrophy.

MATERIALS AND METHODS

The care and use of animals were performed accordingly with the Spanish Policy for Animal Protection RD53/2013, which meets the European Union Directive 2010/63/UE on the protection of animals used for experimental and other scientific purposes. The in-house Ethic Committees for Animal Experiments of the Universidad de Zaragoza and Universitat Autònoma de Barcelona approved all of the experimental procedures.

Spinal Cord Organotypic Culture and TTC Supplementation

Spinal cord organotypic cultures were obtained from lumbar spinal cords of 8-day-old Sprague-Dawley rat pups as previously described (Herrando-Grabulosa et al., 2013). Cultures were let to stabilize for 1 week, and after this point the medium was changed twice per week until 15 days *in vitro* (DIV).

TTC protein used in spinal cord organotypic culture treatments were purificated as previously described (Herrando-Grabulosa et al., 2013). TTC protein was added to the warm-fresh culture medium at a concentration of 10 nM.

Immunoblotting

Spinal cord slices were collected in lysis buffer, homogenated, and quantified by BCA assay. Equal amounts of protein (20 μg/well) were resolved in SDS-PAGE and transferred to nitrocellulose membrane. Membranes were blocked with 6% non-fat dry milk

in phosphate buffered saline (PBS) for 1 h at room temperature (RT) and incubated overnight with the corresponding primary antibody diluted in blocking buffer (SMN, 1:500, BD Biosciences and anti-β-tubulin, Becton-Dickinson). After several washes, membranes were incubated for 1 h with an appropriate secondary antibody. Blots were developed using a chemoluminiscent mix and exposed to enzymatic chemoluminiscence (ECL) films (Amersham Pharmacia Biotech). Densitometry was carried out using ImageJ software.

Immunofluorescence

For organotypic cultures, spinal cord slices were fixed with 4% paraformaldehyde (PFA) at RT for 1 h. Slices were then washed twice with PBS for 15 min, blocked with 5% normal horse serum and 0.2% Triton-X-100 in PBS, and incubated overnight at 4°C with antibody against mouse anti-neurofilament heavy-chain (NF-H) (SMI-32; 1:1000, Sternberger Monoclonals Inc.) and rabbit anti-survival motor neuron (SMN; 1:50, Santa Cruz). Slices were then thoroughly washed in PBS with 0.2% Tween-20 and incubated with appropriate secondary antibody Alexa Fluor®555 goat anti-rabbit IgG (1:500) and Alexa Fluor®488 goat anti-mouse IgG (1: 1000) diluted in blocking buffer for 1 h at RT. Then, slices were incubated for 20 min with 4′-6-Diamidino-2-phenylindole (DAPI). Finally, slices were mounted in Superfrost®Plus slides (Thermo Fisher Scientific) with Fluoromount-G mounting medium (SouthernBiotech) and fluorescence was visualized under epifluorescence microscope (Nikon Eclipse 90i; Nikon Instruments Inc.) or Olympus FluoViewTM FV1000). Motor neurons in the organotypic spinal cord slices were identified by SMI-32 immunostaining on the basis of their morphology and size (>20 μm) and their localization in the ventral horn. A minimum of 15 sections were used for MN counting for each experimental condition.

In case of SMA mice, animals were perfused transcardially with cold 4% PFA in PBS. Spinal cords were dissected, post-fixed in PFA for 24 h, and transferred to 30% sucrose in PBS for at least 48 h at 4°C. Sample tissues were embedded in OCT (Tissue-Tek, Sakura Finetek) and frozen in liquid nitrogen-cooled 2-methylbutane. Transverse sections of spinal cord (10 μm) were cut with using a cryostat (CM1510S Leica Microsystems). Tissue sections were re-fixed on ice with formalin solution 10% (HT5014, Sigma) for 10 min, permeabilized with 0.1% Triton X-100 and 0.1% sodium citrate in PBS for 10 min at RT, and blocked with 10% goat serum and 1% BSA in PBS for 30 min at RT. After washes, sections were incubated with LC3 primary antibody (1:200; PD014, MBL) over night at 4°C, and subsequently incubated with Alexa Fluor 546 goat anti-rabbit IgG (Invitrogen) for 1 h at RT. Nuclear staining (in blue) was performed using a mounting medium with DAPI (Vectashield, H-1200, Vector Laboratories) and visualized on an Olympus IX81 fluorescence microscope.

SMA Mice

Moderate Type II SMA mice FVB.Cg-Tg(SMN2*delta7) 4299Ahmb Tg(SMN2)89Ahmb *Smn1*^{tm1Msd}/J were kindly provided by Dra. Lucía Tabares (Universidad de Sevilla). Transgenic Smn$^{+/-}$;SMN2;SMNΔ7 mice were maintained as heterozygous breeding pairs in the Servicio General de Apoyo a la Investigación-SAI of the Universidad de Zaragoza.

This mouse model at birth is noticeably smaller than normal littermates. Signs of muscle weakness appear progressively after day 5 and the mouse displays an abnormal gait, shakiness in the hind limbs and a tendency to fall over with a lifespan of 13 days (Le et al., 2005). Body weight and survival measures were taken daily in the morning. To evaluate these parameters, we produced 9 l with 71 pups, 5 lwere injected with pCMV–TTC plasmid (TTC treatment) and 4 with pCMV plasmid (untreated). In relation of the 71 pups, 21 were SMA mice (10 treated with TTC and 11 untreated), 35 were heterozygous mice (25 treated with TTC and 10 untreated) and 15 were WT (7 treated with TTC and 8 untreated).

To study the gene expression by real-time PCR, we produced 9 l with 81 pups, 5 lwere injected with pCMV-TTC plasmid and 4 with pCMV plasmid. In relation of the 81 pups, 10 were SMA mice (5 treated with TTC and 5 untreated), 48 were heterozygous mice (25 treated with TTC and 23 untreated) and 23 were WT (14 treated with TTC and 9 untreated).

Finally, in relation to immunofluorescence assay, we produced 7 l with 43 pups, 5 l were injected with pCMV-TTC plasmid and 2 with pCMV plasmid. In relation of the 43 pups, 6 were SMA mice (3 treated with TTC and 3 untreated), 21 were heterozygous mice (12 treated with TTC and 9 untreated), and 23 were WT (10 treated with TTC and 6 untreated).

Plasmid Purification and Intramuscular Injection

The TTC gene used in mice treatments was constructed in the pcDNA3.1 eukaryotic expression plasmid under the control of the cytomegalovirus (CMV) immediate-early promoter. pCMV:TTC was obtained by cloning a BamHI/NotI TTC fragment from the pGex:TTC vector (Coen et al., 1997) into pcDNA3.1 as previously described (Moreno-Igoa et al., 2010).

For the transformation assay, competent cells (*Escherichia coli* DH5α bacteria) were used, and the constructed plasmids were purified with QIAprep Spin Miniprep kit (QIAGEN). The sequence of the purified plasmids (BigDye Terminator v3.1 Cycle Sequencing kit, Applied Biosystems) was checked to confirm that the cloned DNA fragments were correctly inserted in the vectors. The recombinant plasmids were finally expanded in DH5α bacteria and purified using the EndoFree Plasmid Mega Kit (Qiagen). The recombinant plasmids were subjected to 1% agarose gel in 1X Tris-boric-EDTA (TBE) to yield fragments of the expected molecular weight. The quantity of the obtained recombinant plasmids was measured using a NanoDrop® Spectrophotometer (ND-1000 V3.3.0).

At post-natal day 1 (P1) mice were immobilized via cryoanesthesia and injected intramuscularly with 100 μg of naked DNA encoding for pCMV-TTC or non-coding pCMV plasmids into the *quadriceps femoris* muscles (one injection with 50 μg per muscle).

At P7 (early-symptomatic), the pups were lightly anesthetized with isoflurane and were euthanized by rapid decapitation. The

skeletal muscle and spinal cord tissues were harvested, snap-frozen in liquid nitrogen, and then stored at −80°C for RNA extraction.

Quantitative PCR

Spinal cord and muscle tissue were pulverized in liquid nitrogen with a cell crusher. For RNA extraction, powdered samples were resuspended with Trizol Reagent (Invitrogen). RNA extracted was treated to eliminate genomic DNA using the Turbo DNA-freeTM kit (Ambion) and the reverse transcription was carried out according to the SuperScript^{TM} First-Strand Synthesis System kit (Invitrogen). Gene expression was assayed by real-time PCR in a StepOne^{TM} Real-Time PCR System (Applied Biosystems). Primer and probe mixtures for each gene of interest were supplied by Applied Biosystems (**Table 1**). Two endogenous genes (*Gapdh* and β-*actin*) were used for normalization of the data. All reactions were performed in triplicate and all reaction efficiencies of the primer/probe sets were close to 100%. Target gene expression was normalized using the geometric mean of these two housekeeping genes and relative gene expression was determined using the $2^{-\Delta\Delta CT}$ method.

Statistical Analysis

Statistical significance was determined by one-way ANOVA followed by Bonferroni's *post-hoc* test. Survival data was analyzed using the Kaplan-Meir test. All of the values were expressed as means and error bars represent standard error of the mean (mean ± SEM). The statistical significance threshold was set at $p < 0.05$.

RESULTS

TTC Treatment Increase SMN Expression in Motor Neurons

Prior to the *in vivo* assays, the effects of TTC on SMN expression and motor neuron survival were studied *in vitro*. In spinal cord organotypic cultures, TTC protein enhanced levels of SMN and also significantly increased the number of motor neurons (**Figures 1A,B**). This effect was more evident than the observed in the case of NGF supplementation. These results suggested that TTC achieve a neuroprotective effect in motor neurons. Moreover, immunoblotting quantification of SMN showed that its expression was increased along the days of culture and reached the highest level at 15DIV (**Figure 1C**).

The next step and prior to performing the assay in our severe mice model of SMA, the non-viral gene therapy with pCMV-TTC was assessed *in vivo* in a mouse model of motor neuron disease (Supplementary Material S1). The results obtained showed that, 10 days after inoculation, TTC treatment significantly increased the levels of the SMN gene in muscle and spinal cord tissues in this animal model.

Improvement of the Autophagy and Apoptosis Markers Under TTC Treatment

mRNA expression levels of the well-known markers of autophagy (*Becn1*, *Lc3,* and *p62*) and apoptosis (*Bax* and *Casp3*) were quantified by real-time PCR in spinal cord and skeletal muscle samples of WT and SMA mice to evaluate the possible effect of TTC treatment (**Figure 2**).

TABLE 1 | Taqman® probe and primer mixtures used in gene expression assays.

Name	Gen symbol	Part number
Autophagy related 5	*Atg5*	Mm00504340_m1
Beclin 1, autophagy related	*Becn1*	Mm00517174_m1
E2F transcription factor 1	*E2f1*	Mm00432939_m1
Microtubule-associated protein 1 light chain 3 alpha	*Map1lc3a (Lc3)*	Mm00458724_m1
Sequestosome 1	*Sqstm1 (p62)*	Mm00448091_m1
BCL2-associated X protein	*Bax*	Mm00432050_m1
B cell leukemia/lymphoma 2	*Bcl2*	Mm00477631_m1
Caspase 1	*Casp1*	Mm00438023_m1
Caspase 3	*Casp3*	Mm01195085_m1
Ankyrin repeat domain 1	*Ankrd1*	Mm00496512_m1
Calmodulin 1	*Calm*	Mm00486655_m1
Collagen type XIX alpha 1	*Col19a1*	Mm00483576_m1
F-box only protein 32	*Fbxo32*	Mm01207878_m1
Metallothionein 2	*Mt2*	Mm00809556_s1
Myogenic differentiation 1	*Myod1*	Mm00440387_m1
Paired box gene 7	*Pax7*	Mm00834079_m1
Ras-related associated with diabetes	*Rrad*	Mm00451053_m1
Sarcolipin	*Sln*	Mm00481536_m1
Survival motor neuron 1 (SMN 1)	*Smn1*	Hs00165806_m1
Glyceraldehyde-3-phospate dehydrogenase	*Gapdh*	4352932E
Actin, beta, cytoplasmic	*Actb (β-actin)*	4352933E

Gapdh and Actb (β-actin) were used as housekeeping genes.

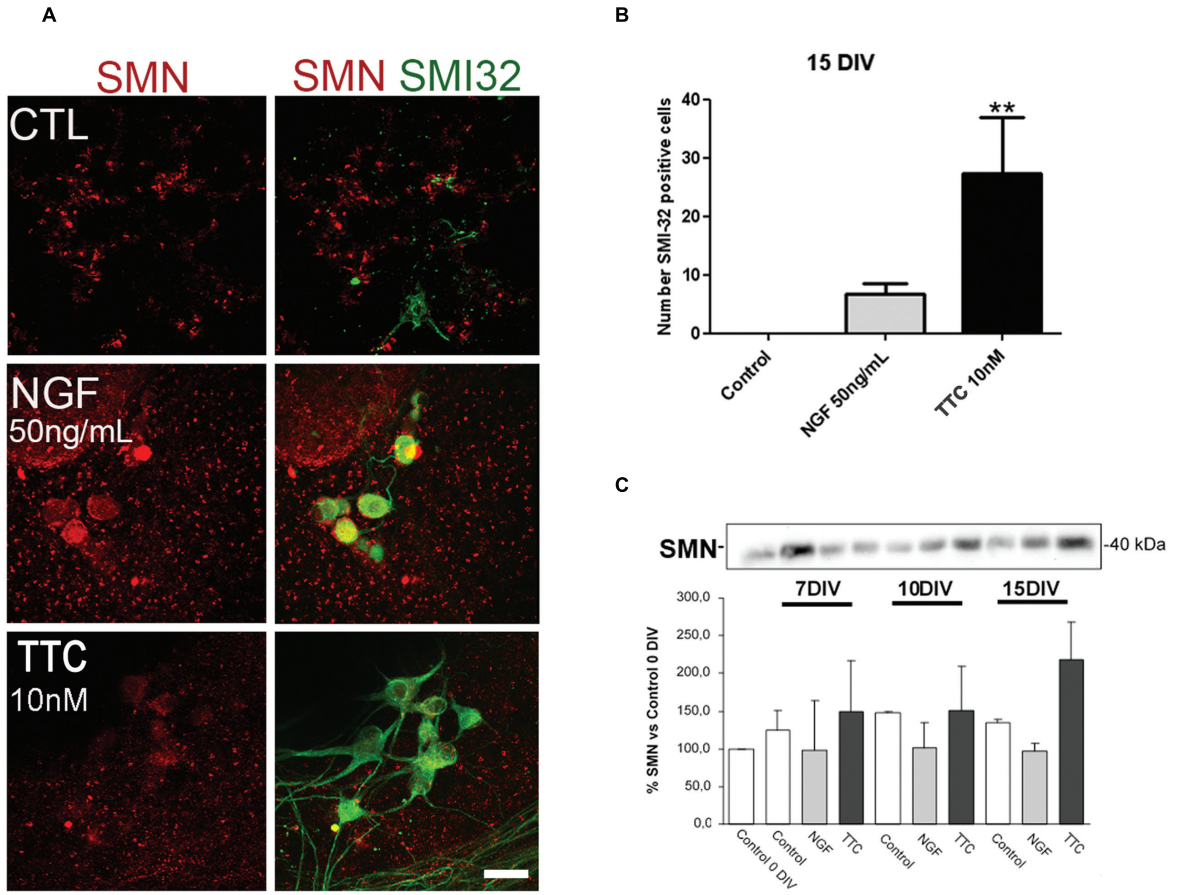

FIGURE 1 | Enhanced levels of SMN protein after TTC treatment. (A) Representative images of the ventral horn hemisections immunolabeled against SMN protein (red) and motor neuron marker SMI32 (green). Scale bar: 50 μm. **(B)** Bar graph showing the number of SMI-32 positive cells at the ventral horns with a diameter >25 μm at 15DIV alone or under the treatment of NGF (50 ng/mL) or TTC (10 nM). Values are the mean ± SEM of at least 15 sections per treatment. $^{**}p < 0.01$. **(C)** Evaluation by western blot analysis the levels of SMN protein under the treatment of NGF 50 ng/mL and TTC 10 nM along the progression of the spinal cord organotypic culture (0, 7, 10, and 15DIV). All results were from at least two independent experiments. Equal amount of protein was added to each well.

In spinal cord tissue (**Figure 2A**), autophagy markers were significantly upregulated in untreated SMA mice, suggesting a potential autophagy activation due to the neurodegenerative progression of the disease. Under TTC treatment, the mRNA expression levels were significantly downregulated with respect to untreated SMA mice, pointing out to an improvement of autophagy markers, which tend to reach WT levels. Furthermore, inmunofluorescence against LC3 demonstrated that the over-expression of the LC3 transcripts was accompanied to an activation of the expression of LC3 protein, suggesting an activation of the autophagy process as a compensatory mechanism (**Figure 3**). On the contrary, LC3 protein expression was not observed in wild-type animals resembling what was observed in the case of the mRNA transcript levels (**Figure 3**).

The expression levels of pro-apoptotic genes *Bax* and *Casp3* were significantly upregulated with respect to WT mice suggesting an apoptosis enhancement in this tissue due to the neurodegeneration. However, TTC treatment significantly decreased the levels of both genes in relation to untreated SMA mice, favoring an amelioration of apoptosis (**Figure 2A**).

In relation to the skeletal muscle tissue (**Figure 2B**), the significant upregulated levels of *Becn1, Lc3,* and *p62*, in untreated SMA mice were indicative of an autophagy activation, as it was observed in spinal cord tissue. TTC treatment especially improved *Lc3* levels that reached the ones observed in WT mice, suggesting a significant amelioration of autophagy process. Furthermore, in SMA mice the levels of the pro-apoptotic gene *Bax* were found significantly upregulated, while *Casp3* levels showed a tendency to be upregulated. Under TTC treatment, only the *Casp3* showed a significantly downregulation with respect to untreated SMA mice, which could indicate a lack of apoptosis activation.

Compensatory Response of TTC Treatment for Muscular Atrophy in SMA Mice

Spinal muscular atrophy and ALS, two lethal motor neuron diseases, share affected target tissues such as the skeletal muscle. In addition, muscle weakness and atrophy have been described in

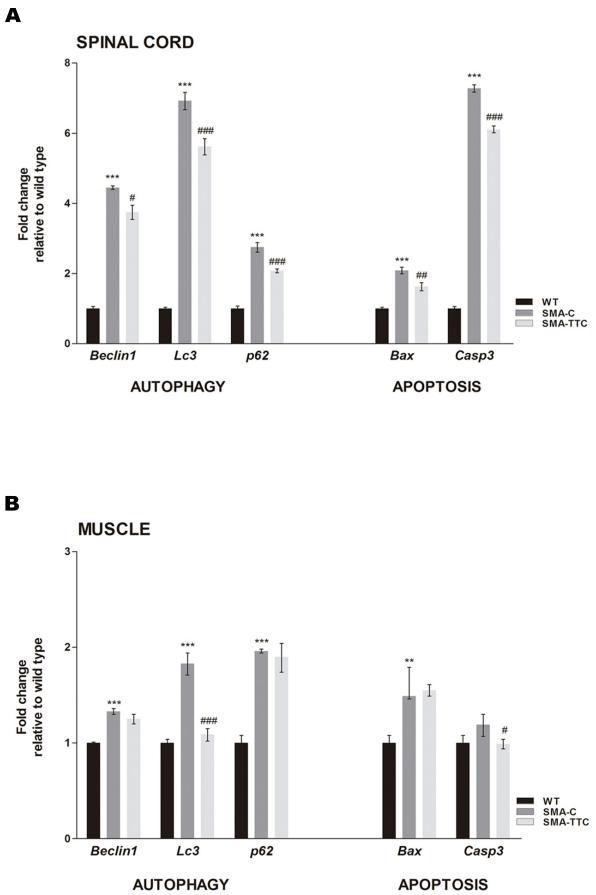

FIGURE 2 | Effect of TTC-encoding plasmid in autophagy and apoptotic markers. Relative expression values of autophagy (*Becn1, Lc3,* and *p62)* and apoptotic (*Bax* and *Casp3*) genes in WT mice (WT, black bars), untreated SMA mice (SMA-C, dark gray bars) and SMA mice treated with TTC (SMA-TTC, light gray bars) in spinal cord **(A)** and skeletal muscle **(B)**. Each data point represented the mean ± SEM, $n = 5$ animals per group. WT *versus* SMA-C: $^{**}p < 0.01$ and $^{***}p < 0.001$. SMA-C *versus* SMA-TTC: $^{\#}p < 0.05$, $^{\#\#}p < 0.01$ and $^{\#\#\#\#}p < 0.001$.

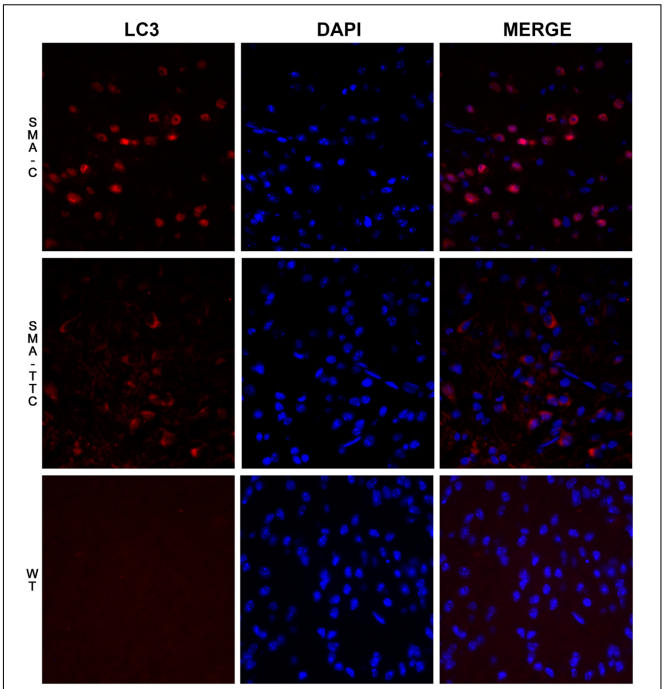

FIGURE 3 | Immunofluorescence staining for LC3 on spinal cord tissue under TTC treatment. LC3 staining (red) was performed in WT mice and SMA mice untreated and treated with TTC in spinal cord slices. DAPI staining was also performed (blue). A merged image of the double staining is presented. A representative image presents of three independent animals for genotype and disease stages (40X).

SMA mouse models. Previous work from our group has described a list of genetic biomarkers for ALS disease, some of which were in close relation to muscle atrophy (Calvo et al., 2012a). Consequently, transcriptional expression levels of seven genes related to muscle atrophy (*Ankrd1, Calm1, Col19a1, Mt2, Myod1, NogoA,* and *Sln*) (Calvo et al., 2012a) were tested in skeletal muscle tissue from SMA mice (**Figure 4**).

Our results showed a significant upregulation of these genes in untreated SMA mice, except for *Myod1* that was significantly downregulated. TTC treatment reduced significantly *Ankrd1*, *Calm1*, *Col19a1*, *Mt2,* and *NogoA* levels, levels, and increased *Myod1* levels tending to reach WT ones, which could suggest an improvement of the muscle atrophy under TTC treatment. The significant upregulation of *Sln1* levels under TTC treatment could also indicate an improvement of the relaxation-contraction cycles, favoring an amelioration of muscle atrophy (Casas et al., 2013).

Body Weight and Survival Rates Under TTC Treatment

To evaluate the possible effect of TTC treatment in the SMA mice phenotype, the body weight was registered daily along disease progression. The results showed that the intramuscular injection of TTC-encoding plasmid at P1 did not significantly affect the body weight of WT or SMA mice during the first ten days of life (**Figure 5A**). Nevertheless, the body weight of WT mice significantly reached low levels from P12 until P16, while in treated SMA mice, a significant decrement was only detected at P11 and then a modest but no significant improvement in the body weight was observed from P12 until P16, with respect to untreated SMA mice.

Regarding the survival time, the data showed no significant differences between WT or SMA mice after TTC injection (**Figure 5B**). Albeit, it should be pointed out the high mortality rate and the variable life expectancy of the SMA pups, and therefore less severe animal model of the disease may allow a long-lasting monitoring of TTC effects.

DISCUSSION

In recent years the neuroprotective effects of TTC have been described in relation to the antiapoptotic and survival pathways, suggesting a similar way of action as in the case of neurotrophins

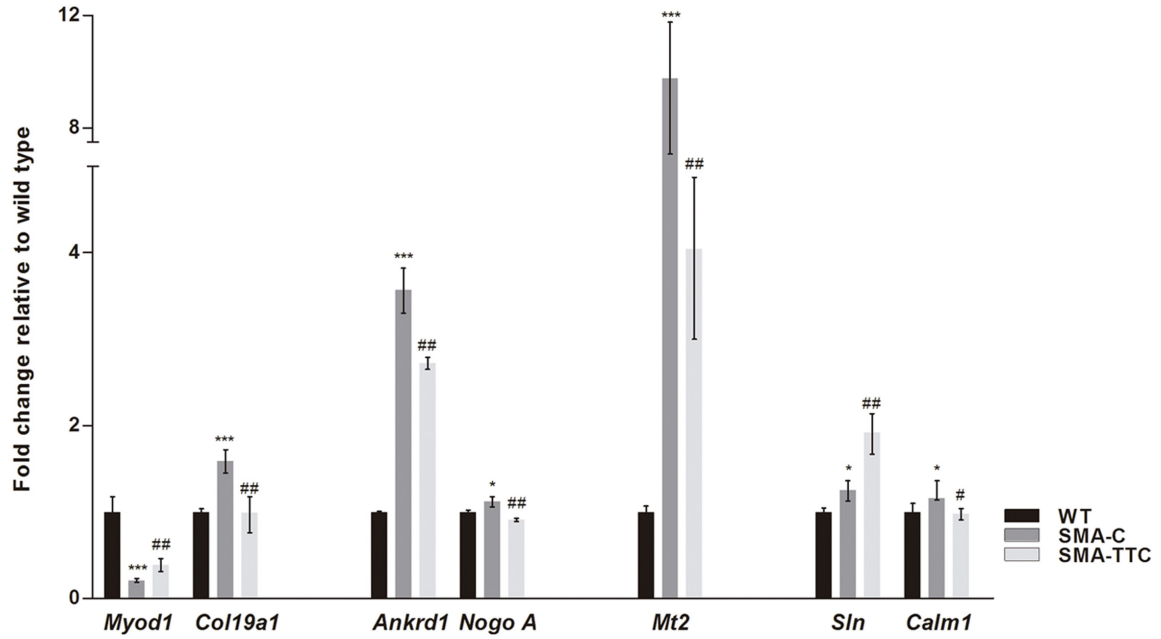

FIGURE 4 | Amelioration of genes related to muscular atrophy in SMA mice. Relative expression values of *Myod1, Col19a1, Ankrd1, NogoA, Mt2, Sln,* and *Calm1* in WT mice (WT, black bars), untreated SMA mice (SMA-C, dark gray bars) and SMA mice treated with TTC (SMA-TTC, light gray bars) in skeletal muscle tissue. Each data point represented the mean ± SEM, $n = 5$ animals per group. WT *versus* SMA-C: $^{*}p < 0.05$ and $^{***}p < 0.001$. SMA-C *versus* SMA-TTC: $^{\#}p < 0.05$ and $^{\#\#}p < 0.01$.

in animal models of several neurodegenerative diseases (Chaib-Oukadour et al., 2004). In this sense, it has been demonstrated in neurons of mSOD1 mouse model of ALS that the neuroprotective role of TTC was possibly due to its pro-survival and anti-apoptotic properties (Moreno-Igoa et al., 2010; Herrando-Grabulosa et al., 2013). A recent work in a mouse model intermediate of SMA showed that this disease in skeletal muscle emerges before pathology in spinal cord, including loss of motor neurons. (Fayzullina and Martin, 2014). This cellular loss may be mediated by apoptosis or autophagy, therefore therapeutic strategies based on modulating these molecular mechanisms may have potential beneficial effects in the SMA pathology or disease progression. Moreover, the increment of SMN observed after non-viral gene therapy treatment with pCMV-TTC could be improved the beneficial effects related to TTC.

Autophagy has come to the forefront in motor neuron diseases as a common molecular pathway altered in degenerating motor neurons. The loss of critical genes involved in the execution of the autophagy pathway in the central nervous system results in profound severe neurodegenerative diseases (Komatsu et al., 2006). Moreover, induction of autophagy has been reported in numerous models of neurodegenerative diseases, and may be a component of the cellular response to depleted SMN levels (Custer and Androphy, 2014). At P7, the SMA pups were still active and significantly smaller than their phenotypically normal siblings (2.17 ± 0.28 vs. 4.18 ± 0.11), but signs of muscle weakness were observed compared to their normal littermates. Moreover, their relative mobility insured that they were still gaining access to milk. The presence of milk in the stomach was also visible through the skin, preventing any potential autophagy induction due to poor nursing following the onset of major motor coordination losses. In a severe model of SMA, *in vitro* experiments showed a deregulated autophagy in spinal cord motor neurons (Garcera et al., 2013). Moreover, LC3-II and p62 protein levels were increased in lysates of spinal cord from a severe mouse model of SMA indicating that autophagy is dysregulated (Custer and Androphy, 2014). In accordance with these results, our data revealed a significant increase in the expression levels of all autophagy markers in spinal cord and skeletal muscle tissues and therefore an activation of this process. Although autophagy remained activated under TTC treatment in SMA mice, the gene expression profile observed in treated SMA mice tended to reach WT levels. In case of muscle, TTC treatment decreased *Lc3* expression to WT ones. This reduction of *Lc3* levels suggested that TTC was able to reduce the pathological autophagy until a constitutive autophagy, since Lc3 is considered the main marker of autophagosomes.

In relation to apoptosis, the anti-apoptotic properties of TTC were evidenced by *in vitro* studies in cultured neurons in which TTC preserve mitochondrial function decreased nuclear fragmentation and reduced activation of pro-Casp3 (Chaib-Oukadour et al., 2004). Similarly, *in vivo* experiments in a model of Parkinson's (Mendieta et al., 2009) or ALS's (Moreno-Igoa et al., 2010) diseases, showed an anti-apoptotic effect of TTC. In regard to apoptosis and neurodegenerative disorders, a deregulation of this process is associated with a long list of pathologies (Marino et al., 2014). In SMA disease, genetic studies in mice (Kerr et al., 2000; Anderton et al., 2013) support a role

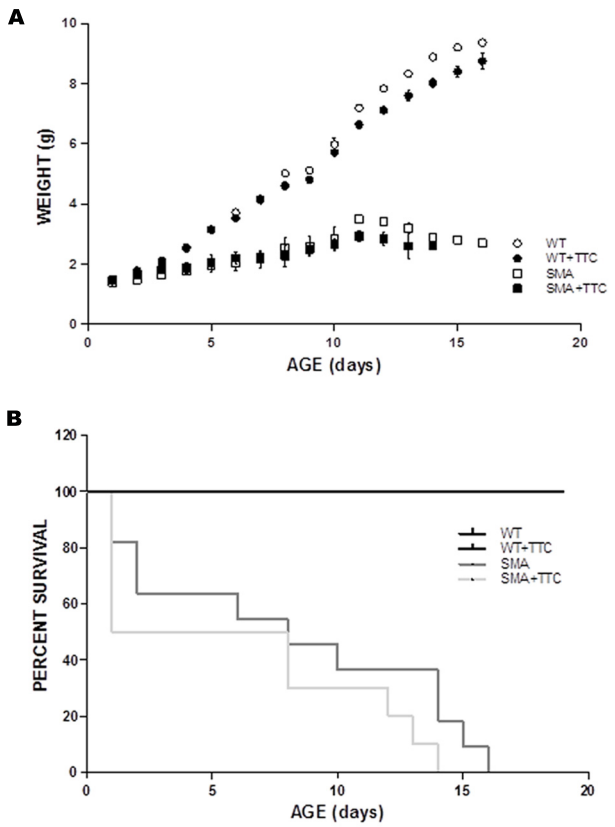

FIGURE 5 | Phenotype and survival time of treated and untreated SMA mice. (A) Weight curves of WT (circles) and SMA mice (squares) treat (closed forms) and untreat (open forms) with TTC. All plots are shown as means of weight at each day with error bars representing standard deviation. $*p < 0.05$. **(B)** Kaplan–Meier survival analysis of WT and SMA mice with and without TTC treatment.

for programmed neuronal death. Thus, in the central nervous system of SMA mouse models, elevated levels of pro-apoptotic genes and an enhancement of apoptosis have been observed (Tsai et al., 2006). Moreover, a significant loss of large motor neurons was observed in the spinal cord from SMNdelta7 mouse at P7 (Baumer et al., 2009), and 2 days later this loss was over 50% (Edens et al., 2014). Furthermore, in the skeletal muscle of severe SMA model mice, the presence of apoptotic cell death signs was detected (Dachs et al., 2011). In connection with these results, we observed that the pro-apoptotic gen *Bax* was upregulated as well as the gen *Casp3*. Both genes encode for the "executioner" proteins in apoptosis, suggesting that apoptosis was activated. In relation to the skeletal muscle, a recent work using the "Taiwanese" SMA mouse model, detected at birth DNA damage that was getting worse until P6 when the muscle exhibited cell death (Fayzullina and Martin, 2014). However, in our SMA mice, the upregulation of *Bax* together with the lack of upregulation of *Casp3* suggested an absence of apoptotic cell death in untreated SMA mice, which is in accordance with the results obtained by Hayhurst and co-workers that revealed normal proportion of apoptotic cells. After TTC treatment, the expression levels of *Bax* and *Casp3* in spinal cord and *Casp3* in skeletal muscle were downregulated untreated SMA mice, suggesting that TTC favored the normalization of the expression levels of both genes and therefore played a relevant role in the modulation of apoptosis in this animal model.

Although the importance of motor neuron pathology is well-established in SMA, a cumulative body of work supports the involvement of other cell types, including myocytes (Hamilton and Gillingwater, 2013; Martinez-Hernandez et al., 2013; Iascone et al., 2015). In SMA disease, muscle weakness and atrophy are also principal pathological hallmarks. In this way, in mouse models of the disease, several works reported an abnormal skeletal muscle development (Boyer et al., 2013).

Consequently, our next step was the evaluation of the expression of several genetic biomarkers related to muscular atrophy, previously characterized by our group (Calvo et al., 2012a). TTC administration significantly reduced the transcriptional level of *Myod1,* an early marker of myogenesis (Manzano et al., 2011), and *Col19a1* which increasing levels are related to the regenerative response to muscle damage (Sumiyoshi et al., 2001), shifting their expression toward the wild-type levels. Additionally, after TTC treatment the expression levels of *Ankrd1,* a marker of muscle damage (Laure et al., 2009), and *Nogo A* that accelerates the progressive failure of motor neuron innervation (Pradat et al., 2007) decreased to reach WT ones, suggesting that TTC could ameliorate muscle atrophy. Finally, TTC treatment modified the expression of *Mt2*, *Calm1* and *Sln* genes which are also associated to muscle atrophy (Hyldahl et al., 2010; Casas et al., 2013).

In summary, non-viral gene therapy based on TTC improved the expression levels of main genes related to autophagy and apoptosis in SMA mice. In particular, in response to the neurodegenerative progression in SMA mice, TTC treatment modifies the expression of autophagy and apoptotic genes. Additionally, TTC reduced the expression of autophagy markers and pro-apoptotic genes in spinal cord while in skeletal muscle TTC was able to downregulate the expression of the main marker of autophagy (*Lc3*) to WT levels, as well as the expression of the apoptosis effector, *Casp3.* Furthermore, in the skeletal muscle tissue of treated SMA mice, TTC showed a compensatory effect in the expression of genes involved in muscle damage response, oxidative stress and calcium homeostasis. These preliminary findings provide new insights into the effect of TTC in the spinal cord and the skeletal muscle tissues in SMA disease and suggest the need for further experiments to accurate study the effect of TTC in this disorder.

AUTHOR CONTRIBUTIONS

Conceived and designed the experiments: SO, ACC, RO, and JA. Performed the experiments: SO, AR, MH-G, and RM. Analyzed data: SO, ACC, and AR. Contributed reagents/materials/analysis tools: JA, PZ, and RO. Wrote the manuscript: SO, ACC, EFT, and RO.

FUNDING

This work was supported by Grant PI14/00947 from Instituto de Salud Carlos III Fondos FEDER (to RO), SMA Europe and FMM (to EFT) and GENAME Project.

ACKNOWLEDGMENTS

The authors would like to thank Miriam de la Torre, Silvia Garcés, Pilar Lierta, Susana Murillo, and Eduardo Romanos for their expert technical assistance and to Dra. Lucía Tabares (Universidad de Sevilla), for kindly providing the animal model.

SUPPLEMENTARY MATERIAL

The Supplementary Material for this article can be found online at: http://journal.frontiersin.org/article/10.3389/fnmol.2016.00076

REFERENCES

Anderton, R. S., Meloni, B. P., Mastaglia, F. L., and Boulos, S. (2013). Spinal muscular atrophy and the antiapoptotic role of survival of motor neuron (SMN) protein. *Mol. Neurobiol.* 47, 821–832. doi: 10.1007/s12035-013-8399-5

Baumer, D., Lee, S., Nicholson, G., Davies, J. L., Parkinson, N. J., Murray, L. M., et al. (2009). Alternative splicing events are a late feature of pathology in a mouse model of spinal muscular atrophy. *PLoS Genet.* 5:e1000773. doi: 10.1371/journal.pgen.1000773

Boyer, J. G., Ferrier, A., and Kothary, R. (2013). More than a bystander: the contributions of intrinsic skeletal muscle defects in motor neuron diseases. *Front. Physiol.* 4:356. doi: 10.3389/fphys.2013.00356

Calvo, A. C., Manzano, R., Atencia-Cibreiro, G., Olivan, S., Munoz, M. J., Zaragoza, P., et al. (2012a). Genetic biomarkers for ALS disease in transgenic SOD1(G93A) mice. *PLoS ONE* 7:e32632. doi: 10.1371/journal.pone.0032632

Calvo, A. C., Olivan, S., Manzano, R., Zaragoza, P., Aguilera, J., and Osta, R. (2012b). Fragment C of tetanus toxin: new insights into its neuronal signaling pathway. *Int. J. Mol. Sci.* 13, 6883–6901. doi: 10.3390/ijms13066883

Calvo, A. C., Moreno-Igoa, M., Mancuso, R., Manzano, R., Olivan, S., Munoz, M. J., et al. (2011). Lack of a synergistic effect of a non-viral ALS gene therapy based on BDNF and a TTC fusion molecule. *Orphanet J. Rare Dis.* 6:10. doi: 10.1186/1750-1172-6-10

Casas, C., Herrando-Grabulosa, M., Manzano, R., Mancuso, R., Osta, R., and Navarro, X. (2013). Early presymptomatic cholinergic dysfunction in a murine model of amyotrophic lateral sclerosis. *Brain Behav.* 3, 145–158. doi: 10.1002/brb3.104

Chaib-Oukadour, I., Gil, C., and Aguilera, J. (2004). The C-terminal domain of the heavy chain of tetanus toxin rescues cerebellar granule neurones from apoptotic death: involvement of phosphatidylinositol 3-kinase and mitogen-activated protein kinase pathways. *J. Neurochem.* 90, 1227–1236. doi: 10.1111/j.1471-4159.2004.02586.x

Chen, S., Karalewitz, A. P., and Barbieri, J. T. (2012). Insights into the different catalytic activities of *Clostridium* neurotoxins. *Biochemistry* 51, 3941–3947. doi: 10.1021/bi3000098

Ciriza, J., Moreno-Igoa, M., Calvo, A. C., Yague, G., Palacio, J., Miana-Mena, F. J., et al. (2008). A genetic fusion GDNF-C fragment of tetanus toxin prolongs survival in a symptomatic mouse ALS model. *Restor. Neurol. Neurosci.* 26, 459–465.

Coen, L., Osta, R., Maury, M., and Brulet, P. (1997). Construction of hybrid proteins that migrate retrogradely and transynaptically into the central nervous system. *Proc. Natl. Acad. Sci. U.S.A.* 94, 9400–9405. doi: 10.1073/pnas.94.17.9400

Custer, S. K., and Androphy, E. J. (2014). Autophagy dysregulation in cell culture and animals models of spinal muscular atrophy. *Mol. Cell. Neurosci.* 61, 133–140. doi: 10.1016/j.mcn.2014.06.006

Dachs, E., Hereu, M., Piedrafita, L., Casanovas, A., Caldero, J., and Esquerda, J. E. (2011). Defective neuromuscular junction organization and postnatal myogenesis in mice with severe spinal muscular atrophy. *J. Neuropathol. Exp. Neurol.* 70, 444–461. doi: 10.1097/NEN.0b013e31821cbd8b

d'Ydewalle, C., and Sumner, C. J. (2015). Spinal muscular atrophy therapeutics: where do we stand? *Neurotherapeutics* 12, 303–316. doi: 10.1007/s13311-015-0337-y

Edens, B. M., Ajroud-Driss, S., Ma, L., and Ma, Y. C. (2014). Molecular mechanisms and animal models of spinal muscular atrophy. *Biochim. Biophys. Acta* 1852, 685–692. doi: 10.1016/j.bbadis.2014.07.024

Farrar, J. J., Yen, L. M., Cook, T., Fairweather, N., Binh, N., Parry, J., et al. (2000). Tetanus. *J. Neurol. Neurosurg. Psychiatry* 69, 292–301. doi: 10.1136/jnnp.69.3.292

Fayzullina, S., and Martin, L. J. (2014). Skeletal muscle DNA damage precedes spinal motor neuron DNA damage in a mouse model of Spinal Muscular Atrophy (SMA). *PLoS ONE* 9:e93329. doi: 10.1371/journal.pone.0093329

Francis, J. W., Figueiredo, D., vanderSpek, J. C., Ayala, L. M., Kim, Y. S., Remington, M. P., et al. (2004). A survival motor neuron:tetanus toxin fragment C fusion protein for the targeted delivery of SMN protein to neurons. *Brain Res.* 995, 84–96. doi: 10.1016/j.brainres.2003.09.063

Garcera, A., Bahi, N., Periyakaruppiah, A., Arumugam, S., and Soler, R. M. (2013). Survival motor neuron protein reduction deregulates autophagy in spinal cord motoneurons in vitro. *Cell Death Dis.* 4:e686. doi: 10.1038/cddis.2013.209

Hamilton, G., and Gillingwater, T. H. (2013). Spinal muscular atrophy: going beyond the motor neuron. *Trends Mol. Med.* 19, 40–50. doi: 10.1016/j.molmed.2012.11.002

Herrando-Grabulosa, M., Casas, C., and Aguilera, J. (2013). The C-terminal domain of tetanus toxin protects motoneurons against acute excitotoxic damage on spinal cord organotypic cultures. *J. Neurochem.* 124, 36–44. doi: 10.1111/jnc.12062

Hyldahl, R. D., O'Fallon, K. S., Schwartz, L. M., and Clarkson, P. M. (2010). Knockdown of metallothionein 1 and 2 does not affect atrophy or oxidant activity in a novel in vitro model. *J. Appl. Physiol. (1985)* 109, 1515–1523. doi: 10.1152/japplphysiol.00588.2010

Iascone, D. M., Henderson, C. E., and Lee, J. C. (2015). Spinal muscular atrophy: from tissue specificity to therapeutic strategies. *F1000Prime Rep.* 7:04. doi: 10.12703/P7-04

Kerr, D. A., Nery, J. P., Traystman, R. J., Chau, B. N., and Hardwick, J. M. (2000). Survival motor neuron protein modulates neuron-specific apoptosis. *Proc. Natl. Acad. Sci. U.S.A.* 97, 13312–13317. doi: 10.1073/pnas.230364197

Komatsu, M., Waguri, S., Chiba, T., Murata, S., Iwata, J., Tanida, I., et al. (2006). Loss of autophagy in the central nervous system causes neurodegeneration in mice. *Nature* 441, 880–884. doi: 10.1038/nature04723

Laure, L., Suel, L., Roudaut, C., Bourg, N., Ouali, A., Bartoli, M., et al. (2009). Cardiac ankyrin repeat protein is a marker of skeletal muscle pathological remodelling. *FEBS J.* 276, 669–684. doi: 10.1111/j.1742-4658.2008.06814.x

Le, T. T., Pham, L. T., Butchbach, M. E., Zhang, H. L., Monani, U. R., Coovert, D. D., et al. (2005). SMNDelta7, the major product of the centromeric survival motor neuron (SMN2) gene, extends survival in mice with spinal muscular atrophy and associates with full-length SMN. *Hum. Mol. Genet.* 14, 845–857. doi: 10.1093/hmg/ddi078

Manzano, R., Toivonen, J. M., Olivan, S., Calvo, A. C., Moreno-Igoa, M., Munoz, M. J., et al. (2011). Altered expression of myogenic regulatory factors in the mouse model of amyotrophic lateral sclerosis. *Neurodegener. Dis.* 8, 386–396. doi: 10.1159/000324159

Marino, G., Niso-Santano, M., Baehrecke, E. H., and Kroemer, G. (2014). Self-consumption: the interplay of autophagy and apoptosis. *Nat. Rev. Mol. Cell Biol.* 15, 81–94. doi: 10.1038/nrm3735

Martinez-Hernandez, R., Bernal, S., Also-Rallo, E., Alias, L., Barcelo, M. J., Hereu, M., et al. (2013). Synaptic defects in type I spinal muscular

atrophy in human development. *J. Pathol.* 229, 49–61. doi: 10.1002/path.4080

Mendieta, L., Venegas, B., Moreno, N., Patricio, A., Martinez, I., Aguilera, J., et al. (2009). The carboxyl-terminal domain of the heavy chain of tetanus toxin prevents dopaminergic degeneration and improves motor behavior in rats with striatal MPP(+)-lesions. *Neurosci. Res.* 65, 98–106. doi: 10.1016/j.neures.2009.06.001

Monani, U. R., and De Vivo, D. C. (2014). Neurodegeneration in spinal muscular atrophy: from disease phenotype and animal models to therapeutic strategies and beyond. *Future Neurol.* 9, 49–65. doi: 10.2217/fnl.13.58

Montal, M. (2010). Botulinum neurotoxin: a marvel of protein design. *Annu. Rev. Biochem.* 79, 591–617. doi: 10.1146/annurev.biochem.051908.125345

Moreno-Igoa, M., Calvo, A. C., Penas, C., Manzano, R., Olivan, S., Munoz, M. J., et al. (2010). Fragment C of tetanus toxin, more than a carrier. Novel perspectives in non-viral ALS gene therapy. *J. Mol. Med. (Berl)* 88, 297–308. doi: 10.1007/s00109-009-0556-y

Pradat, P. F., Bruneteau, G., Gonzalez de Aguilar, J. L., Dupuis, L., Jokic, N., Salachas, F., et al. (2007). Muscle Nogo-A expression is a prognostic marker in lower motor neuron syndromes. *Ann. Neurol.* 62, 15–20. doi: 10.1002/ana.21122

Sumiyoshi, H., Laub, F., Yoshioka, H., and Ramirez, F. (2001). Embryonic expression of type XIX collagen is transient and confined to muscle cells. *Dev. Dyn.* 220, 155–162. doi: 10.1002/1097-0177(2000)9999:9999<::AID-DVDY1099>3.3.CO;2-N

Toivonen, J. M., Olivan, S., and Osta, R. (2010). Tetanus toxin C-fragment: the courier and the cure? *Toxins (Basel)* 2, 2622–2644. doi: 10.3390/toxins2112622

Tsai, M. S., Chiu, Y. T., Wang, S. H., Hsieh-Li, H. M., Lian, W. C., and Li, H. (2006). Abolishing Bax-dependent apoptosis shows beneficial effects on spinal muscular atrophy model mice. *Mol. Ther.* 13, 1149–1155. doi: 10.1016/j.ymthe.2006.02.008

Turton, K., Chaddock, J. A., and Acharya, K. R. (2002). Botulinum and tetanus neurotoxins: structure, function and therapeutic utility. *Trends Biochem. Sci.* 27, 552–558. doi: 10.1016/S0968-0004(02)02177-1

Zanetta, C., Riboldi, G., Nizzardo, M., Simone, C., Faravelli, I., Bresolin, N., et al. (2014). Molecular, genetic and stem cell-mediated therapeutic strategies for spinal muscular atrophy (SMA). *J. Cell Mol. Med.* 18, 187–196. doi: 10.1111/jcmm.12224

Conflict of Interest Statement: The authors declare that the research was conducted in the absence of any commercial or financial relationships that could be construed as a potential conflict of interest.

frontiers in Molecular Neuroscience

ORIGINAL RESEARCH
published: 05 July 2016
doi: 10.3389/fnmol.2016.00049

Expressing Constitutively Active Rheb in Adult Dorsal Root Ganglion Neurons Enhances the Integration of Sensory Axons that Regenerate Across a Chondroitinase-Treated Dorsal Root Entry Zone Following Dorsal Root Crush

*Di Wu[1], Michelle C. Klaw[1], Nikolai Kholodilov[2], Robert E. Burke[2,3], Megan R. Detloff[1], Marie-Pascale Côté[1] and Veronica J. Tom[1]**

[1] Department of Neurobiology and Anatomy, Drexel University College of Medicine, Philadelphia, PA, USA, [2] Department of Neurology, Columbia University in the City of New York, New York, NY, USA, [3] Department of Pathology and Cell Biology, Columbia University in the City of New York, New York, NY, USA

While the peripheral branch of dorsal root ganglion neurons (DRG) can successfully regenerate after injury, lesioned central branch axons fail to regrow across the dorsal root entry zone (DREZ), the interface between the dorsal root and the spinal cord. This lack of regeneration is due to the limited regenerative capacity of adult sensory axons and the growth-inhibitory environment at the DREZ, which is similar to that found in the glial scar after a central nervous system (CNS) injury. We hypothesized that transduction of adult DRG neurons using adeno-associated virus (AAV) to express a constitutively-active form of the GTPase Rheb (caRheb) will increase their intrinsic growth potential after a dorsal root crush. Additionally, we posited that if we combined that approach with digestion of upregulated chondroitin sulfate proteoglycans (CSPG) at the DREZ with chondroitinase ABC (ChABC), we would promote regeneration of sensory axons across the DREZ into the spinal cord. We first assessed if this strategy promotes neuritic growth in an *in vitro* model of the glial scar containing CSPG. ChABC allowed for some regeneration across the once potently inhibitory substrate. Combining ChABC treatment with expression of caRheb in DRG significantly improved this growth. We then determined if this combination strategy also enhanced regeneration through the DREZ after dorsal root crush in adult rats *in vivo*. After unilaterally crushing C4-T1 dorsal roots, we injected AAV5-caRheb or AAV5-GFP into the ipsilateral C5-C8 DRGs. ChABC or PBS was injected into the ipsilateral dorsal horn at C5-C8 to digest CSPG, for a total of four animal groups (caRheb + ChABC, caRheb + PBS, GFP + ChABC, GFP + PBS). Regeneration was rarely observed in PBS-treated animals, whereas short-distance regrowth across the DREZ was observed in ChABC-treated animals. No difference in axon number or length between the ChABC groups was observed, which may be related to

OPEN ACCESS

Edited by:
Andrew Paul Tosolini, University College of London, UK

Reviewed by:
Kevin Kyung Park, University of Miami, USA
Murray Blackmore, Marquette University, USA

***Correspondence:**
Veronica J. Tom
veronica.tom@drexelmed.edu

Received: *28 April 2016*
Accepted: *07 June 2016*
Published: *05 July 2016*

Citation:
Wu D, Klaw MC, Kholodilov N, Burke RE, Detloff MR, Côté M-P and Tom VJ (2016) Expressing Constitutively Active Rheb in Adult Dorsal Root Ganglion Neurons Enhances the Integration of Sensory Axons that Regenerate Across a Chondroitinase-Treated Dorsal Root Entry Zone Following Dorsal Root Crush. Front. Mol. Neurosci. 9:49. doi: 10.3389/fnmol.2016.00049

intraganglionic inflammation induced by the injection. ChABC-mediated regeneration is functional, as stimulation of ipsilateral median and ulnar nerves induced neuronal c-Fos expression in deafferented dorsal horn in both ChABC groups. Interestingly, caRheb + ChABC animals had significantly more c-Fos$^+$ nuclei indicating that caRheb expression in DRGs promoted functional synaptogenesis of their axons that regenerated beyond a ChABC-treated DREZ.

Keywords: dorsal root crush, axon regeneration, Rheb, chondroitinase, c-fos, inflammation

INTRODUCTION

Dorsal root ganglia (DRG) neurons have long been exploited to study axon regeneration because they feature both peripheral and central axon branches (Devor, 1999; Mar et al., 2015). While the peripheral axon can successfully regenerate after injury, lesion of the central branch, such as after trauma to the dorsal columns tract within the spinal cord or a dorsal root, often results in permanent sensory deficits (Qiu et al., 2005; Wang et al., 2008). Interestingly, after a dorsal root injury, the centrally projecting axons attempt to regenerate as long as the root is contiguous, allowing for the alignment of Schwann cells upon which these axons extend. However, this advancement ceases when the growing axon tip reaches the dorsal root entry zone (DREZ), the interface between the peripheral nervous system (PNS) and the central nervous system (CNS). The failure of sensory axon regeneration after dorsal root injury is partly attributed to a CNS environment that is not favorable for growth (Zhang et al., 2001; Mar et al., 2015). After injury, the CNS is rich in growth inhibitory proteins including Nogo, myelin-associated glycoprotein and chondroitin sulfate proteoglycans (CSPG) and lacks trophic support (Fraher, 2000; Zhang et al., 2001; Silver and Miller, 2004). Thus, at the DREZ, the transition from a permissive PNS environment to a hostile CNS one results in growth cone collapse and stalling (Fraher, 2000; Woolf and Bloechlinger, 2002; Di Maio et al., 2011). Additionally, limited intrinsic regenerative capacity of adult sensory axons also contributes to the failure of axon regeneration (Verma et al., 2005; Mar et al., 2014). Peripheral injury triggers the expression of regeneration-associated genes, such as activating transcription factor 3 (ATF-3) and growth associated protein 43 (GAP-43) whereas dorsal root injury fails to elicit a similar response (Schreyer and Skene, 1993; Seijffers et al., 2006).

While strategies aimed at overcoming either intrinsic or extrinsic obstacles of axon regeneration have shown some success in boosting axonal regrowth (Wang et al., 2008; Peng et al., 2010; Carmel et al., 2015), stimulation of the intrinsic capacity for axonal extension coupled with decreasing extrinsic barriers generates even more regeneration. For instance, activating macrophages in the eye switches mature retinal ganglion cells (RGCs) into an active growth state in an optic nerve crush injury model. When macrophage activation is combined with RhoA inactivation or Nogo receptor suppression, further axon regeneration across the lesion site was observed (Fischer et al., 2004a,b). Moreover, when zymosan-triggered inflammation to enhance the intrinsic growth capacity was combined with use of the bacterial enzyme chondrotinase ABC (ChABC) to digest inhibitory CSPG, substantially more axon regeneration across the harsh environment of DREZ was observed (Steinmetz et al., 2005).

Previously, we showed that adeno-associated virus (AAV) transduction of adult neurons with constitutively active Rheb (caRheb; Ras homolog enriched in brain) enhances regeneration of descending axons across a ChABC-treated glial scar after spinal cord injury (Wu et al., 2015). Rheb is directly upstream of mTOR (Durán and Hall, 2012). It is active when bound to GTP and is inactive when bound to GDP. caRheb is a mutated form of Rheb that is persistently bound to GTP, resulting in continual activation of mTOR (Kim et al., 2011, 2012). Increasing mTOR activity in adult neurons is sufficient to augment axonal growth from different neuron populations, including RGCs (Park et al., 2008), propriospinal neurons (Wu et al., 2015), cortical neurons (Liu et al., 2010; Du et al., 2015) and DRGs (Abe et al., 2010; Christie et al., 2010; Zhou et al., 2012). Here we assessed if a similar strategy aimed at concurrently tackling both intrinsic and extrinsic obstacles has an additive effect and promotes more adult sensory axon regeneration across the DREZ into spinal cord after a dorsal root crush than either approach alone. We transduced adult DRG neurons with caRheb to increase their intrinsic growth capacity after dorsal root injury. Additionally, we injected ChABC into spinal cord dorsal horn to digest upregulated CSPGs at the DREZ. We found this combination did not improve the ability of axons to grow back into spinal cord (though this result may be clouded by intraganglionic inflammation that was induced by the viral injections), but did enhance integration of those axons that did regenerate to form synapses.

MATERIALS AND METHODS

Adeno-Associated Virus (AAV)

AAV5 vectors were obtained and prepared as described before (Wu et al., 2015). All single-stranded AAV5 vectors were obtained from the University of North Carolina's Gene Therapy Center (Chapel Hill, NC, USA). The expression of GFP and caRheb-FLAG were under the control of a chicken ß-actin promoter driven by a chicken ß-actin promoter.

In vitro Analysis of DRG Neurite Regeneration

Culture plates and coverslips were prepared prior to cell harvesting. Six well plates were coated with poly-L-lysine

(0.1 mg/mL; Sigma-Aldrich, Saint Louis, MO, USA). Coverslips with aggrecan-laminin spot gradients were prepared according to a previous protocol (Tom et al., 2004). Briefly, glass coverslips were coated with poly-L-Lysine (0.1 mg/ml) and nitrocellulose. Then four drops of 2 μl aggrecan (0.4 mg/ml aggrecan, Sigma-Aldrich, Saint Louis, MO, USA) were spotted on each coverslip and allowed to air dry. Coverslips were incubated with laminin (10 μg/ml, Sigma-Aldrich, Saint Louis, MO, USA) at 37°C for 6–8 h before cell plating.

Single cell suspensions of DRG neurons were prepared as described previously (Tom et al., 2004). DRGs were harvested from adult Wistar rats (225–250 g, Charles River). After trimming the roots, the DRGs were incubated with collagenase (2000 Units/mL) and neutral protease (25 Units/mL; Worthington Biochemical Corporation, Lakewood, NJ, USA) in HBSS (Gibco, Grand Island, NY, USA), at 37°C for 30 min. The DRGs were rinsed several times with HBSS and then gently triturated in culture media that consisted of Neurobasal-A, B-27, GlutaMax and penicillin/streptomycin (Gibco, Grand Island, NY, USA). After two rounds of low-speed spins (2000 rpm × 2 min), the pellet containing the dissociated DRG neurons was resuspended into culture media at a density of 8000 neurons per milliliter. The cells were plated onto poly-L-lysine coated 6-well plates and incubated with AAV5-caRheb or -GFP (1×10^9 GC/mL). Three days later, the DRG neurons were detached from plates using 0.25% trypsin (Sigma-Aldrich, Saint Louis, MO, USA), rinsed three times with fresh culture media, and re-plated on aggrecan–laminin spot gradient coverslips at a density of 4000 cells per coverslip. Half of the coverslips were also incubated with ChABC (Amsbio; 0.5 U/ml) to digest the aggrecan. Cells detached from six well plates were replated on spot assay coverslips and incubated for 5 days.

After 5 days, the cultures were fixed with 4% PFA in 0.1 M PBS and then processed for immunocytochemistry. The coverslips were rinsed in fresh PBS, incubated in blocking solution (5% normal goat serum, 0.1% BSA, 0.1% Triton X-100 in PBS) for 1 h at room temperature and then in primary antibody diluted in blocking solution overnight at 4°C. The primary antibodies used were anti β tubulin type III (Sigma-Aldrich, 1:1000), anti-FLAG (Sigma-Aldrich 1:500), and anti-GFP (Millipore, 1:500). The next day, the coverslips were rinsed in PBS and then incubated in the appropriate AlexaFluor-conjugated secondary antibody (Invitrogen) for 2 h at room temperature. The coverslips were rinsed in PBS, mounted onto glass slides using FluorSave (EMD Biosciences), and examined using an Olympus BX51 fluorescence microscope.

To quantify the number of neurites crossing the rim, neurites that completely crossed the rim region were counted per spot and normalized to the number of neurons present in the center region of the aggrecan spot. The average number of crossing neurites per spot was calculated per group and normalized to the value of the AAV-GFP + ChABC group. Three independent experiments were conducted. The data were analyzed for statistical relevance using analysis of variance (ANOVA) followed by a *post hoc* Tukey's test (GraphPad Prism). A p-value < 0.05 was considered significant.

Animals

Adult female Wistar rats from Charles River weighing 150–175 g were used in all experiments. Animals were housed, given unlimited access to food and water, and used in accordance with Drexel University Institutional Animal Care and Use Committee and National Institutes of Health guidelines for experimentation with laboratory animals. Animals were allowed to acclimate for a least 1 week after arrival before any procedure was done.

Surgical Procedures

Dorsal Root Crush Injury

We chose to crush C4-T1 dorsal roots because these roots correspond to the the dermatomes of the majority of the forelimb (Takahashi and Nakajima, 1996) and because this is an established model to assess axon regeneration across a DREZ (Ramer et al., 2001). Animals were anesthetized with isoflurane and kept on a heating pad to prevent hypothermia. Under aseptic technique, the right C4 to T1 DRGs and associated dorsal roots were fully exposed. A small slit was made in the dura immediately caudal to each dorsal root and the tines of a #5 forceps were inserted above and below the root, halfway between the distal end of the dorsal root and the DRG. The forceps were squeezed for 10 s to crush the root. This process was repeated three times to ensure injury completeness.

Virus Injection

Similar to what we saw previously (Wu et al., 2015), the expression of the reporter GFP was identified in the soma and axons of transduced neurons, but the expression of the FLAG tag was restricted to the soma. Therefore, we mixed AAV5-GFP with AAV5-caRheb before injection so that we could use GFP to identify the axons of caRheb-expressing neurons. For caRheb-treated animals, 2 μl of AAV5-GFP (8×10^9 GC/μL) and 8 μL of AAV5-caRheb (2×10^9 GC/μL) were mixed (final titer of 1.6×10^9 GC/μL for each vector). For GFP treated animals, 2 μL of AAV5-GFP (8×10^9 GC/μl) was mixed with 8 μL of PBS for a final titer of 1.6×10^9 GC/μl. Immediately after dorsal root crush, a glass micropipette attached to a 5 μL Hamilton syringe was carefully inserted into fully exposed ipsilateral C5–C8 DRGs. One microliter of the mixture of AAV5-GFP and AAV5-caRheb or AAV5-GFP alone was slowly injected into each DRG (0.1 μl AAV5 per min). The glass needle was left in place an additional 1–2 min before removal to prevent reflux.

ChABC Injection

Immediately after AAV injections were completed, 1 μl ChABC (50 U/ml) or PBS was slowly injected (0.1 μl per min) into the ipsilateral dorsal horn from C5 to C8 for each rat.

After all surgical procedures, a piece of silastic membrane (BioBrane; UDL Laboratories, Rockford, IL, USA) was placed over the cord and DRGs that has been exposed. The overlying musculature was closed using 5–0 sutures, and the skin was closed using wound clips. Animals were given Lactated Ringer's, cefazolin (20 mg/kg), and slow-release buprenorphine (0.1 mg/kg; ZooPharm, Windsor, CO, USA) peri-operatively.

They were returned to their home cages once they became alert and responsive.

Overall, five groups of animals (GFP + PBS, caRheb + PBS, GFP + ChABC, caRheb + ChABC, an additional control group which only received dorsal root crush) were used in the *in vivo* study. Each experimental group has six animals and the control group has three animals.

Behavioral Analyses

All animals were habituated to the testing apparatus at least once prior to obtaining baseline scores. Behavioral testing was conducted pre-operatively to establish the baseline responses and then weekly after dorsal root crush injuries on both left (contralateral) and right (ipsilateral) front paws. Paw testing order was determined randomly to minimize an order effect.

Hargraeves Test

Changes in thermal sensation after injuries were measured by the Ugo Basile Plantar Heat test (Comerio VA, Italy) as first described by Hargreaves et al. (1988). Briefly, on each testing day, animals were placed in a clear Plexiglass box and allowed to acclimate for at least 10 min. Afterwards, a noxious infrared light beam was applied to the plantar surface of the paw by placing the infrared heat source directly beneath the center of the plantar surface of the paw to be tested. The infrared stimulus application and timer were activated simultaneously. When animals withdrew their paws, the light source turned off and the paw withdrawal latency was recorded in seconds. The infrared stimulus automatically shuts off at 30 s to avoid tissue damage to the paw of any aresponsive animals. Observations of any responses occurred during application of the thermal stimulus, including licking the paw, turning the head to look at the stimulus, or vocalization during stimulation were also recorded. Five trials were performed for each paw with at least 1 min intervals between each trial. The recorded paw withdrawal latencies for each paw were averaged and analyzed for significant differences between groups using a two-way ANOVA and Bonferroni post tests for each time point (GraphPad Prism5). A p-value of <0.05 was considered significant.

Von Frey Filament Test

The up-down method described by Chaplan et al. (1994) for Von Frey filaments testing was used to measure the degree of tactile sensory changes after dorsal root crush injuries. On each testing day, animals were placed in a metal chamber with a wire mesh bottom and acclimated to the testing environment for at least 10 min. Each trial session began using filament size 4.93 (8 g). If a positive response to a particular filament was observed, the next lower value filament was to be used in the subsequent trial. A negative response resulted in the next higher value filament being used in the subsequent trial. A total of 10 trials were conducted for each paw. The response threshold was the lowest force that produced a positive response, which included paw withdrawal, vocalizing, licking, or guarding in at least 50% of the applications. Similar to the Hargraeves test, the response thresholds of animals in different groups were compared using a two-way ANOVA and Bonferroni post tests for each time point (GraphPad Prism5). A p-value of <0.05 was considered significant.

Electrical Stimulation to Induce c-Fos Expression

One month after dorsal root crush, animals were anesthetized with ketamine and xylazine. The ulnar and median nerves were isolated, dissected free and placed on a bipolar hook electrode for stimulation. The nerves were bathed in a pool of mineral oil to prevent dessication of the nerves throughout the recording period. The nerve was stimulated for 30 min using 1 mA amplitude, 100 μs pulse duration and 50 Hz frequency, similar to what we did previously (Tom et al., 2009, 2013). Animals were perfused 1 h later with 4% PFA and immunofluorescent staining for c-Fos and NeuN were performed on C5–C8 spinal cord sections. The number of c-Fos expression nuclei in spinal cord dorsal horn were counted and compared between groups using a one-way ANOVA and Bonferroni *post hoc* tests.

Histology

One month after dorsal root crush injury, animals were euthanized with Euthasol and perfused with ice cold 0.9% saline followed by ice cold 4% PFA. Under magnification, the spinal cords from C4 to T1 with roots attached and DRGs from C5 to C8 were dissected out, postfixed in the same fixative overnight at 4°C, and cryoprotected in 30% sucrose for at least 48 h. Tissues were embedded in OCT prior to sectioning using a cryostat. Twenty five micrometer coronal sections of spinal cord tissue were cut and collected serially. DRGs were cryosectioned at a thickness of 20 μm and mounted onto gelatin-coated slides. Sections were blocked in 5% normal goat serum and 10% BSA with 0.1% Triton X-100 in PBS for 1 h. After blocking, sections were incubated with primary antibodies at 4°C overnight. The primary antibodies used were anti-GFP (1:500; Millipore), anti-FLAG (1:1000; Sigma-Aldrich), anti-phosphorylated ribosomal protein S6 (p-S6; 1:800; Cell Signaling), anti-C-4S (1:400, Millipore), anti-calcitonin gene related peptide (CGRP; 1:1000, Peninsula Laboratories International), anti-IB4 (1:1000, Sigma), anti-NF-200 (1:500, Sigma), anti-Iba1 (1:2000, Wako), anti-ED1 (1:200 Millipore), anti-p75 (1:1000 Millipore), and anti-c-Fos (1:1000, Abcam). The next day, sections were washed, incubated with appropriate AlexaFluor-conjugated secondary antibodies (Invitrogen) for 2 h, washed in PBS, mounted onto slides, and coverslipped with FluorSave (EMD Chemical). Stained sections were analyzed on Olympus BX51 and Leica DM5500B epifluorescent microscopes and a Leica TCS SP2 confocal microscope equipped with a Leica DMRE microscope.

Quantification of p-S6 Expression in AAV Transduced Neurons

To assess numbers of transduced DRG neurons expressing p-S6, DRG sections from DRGs injected with AAV5-GFP ($n = 3$) or the mixture of AAV5-caRheb/AAV5-GFP ($n = 3$) were processed for immunohistochemistry. An additional group of DRG sections from animals that received dorsal root crush but

not virus injections were included as an additional control. Every sixth section (120 μm apart) from DRG was immunostained for p-S6 and GFP. All sections were processed at the same time and images for all sections were acquired with the same digital camera and exposure times. Images of naïve DRGs were used to set the threshold to eliminate background noise. Using ImageJ, GFP^+ and $p\text{-}S6^+$ neurons whose signal intensities were above the threshold were identified and counted. The percentage of GFP^+ neurons that also expressed p-S6 was calculated and compared amongst groups using a Chi-square test (GraphPad, Prism5).

Quantitation of Axons Regenerating Across the DREZ

A subset of coronal spinal cords sections at 750 μm intervals were immunostained for GFP to visualize axons of transduced DRG neurons. We also stained these sections for p75 to visualize Schwann cells within the dorsal root to allow us to definitively determine the boundary of the DREZ. While blinded to treatment group, GFP^+ axons beyond the $p75^+$ labeled CNS/PNS boundary were counted using an Olympus BX51 microscope that had an ocular micrometer. Based on the distance they traveled across the DREZ, axons were binned into 50 μm intervals. The numbers of axons per distance in each section were averaged for each rat subset. The numbers of axons at each length for each treatment group were compared for statistical significance using a one-way ANOVA followed by a Bonferroni correction ($p < 0.05$ criterion for significance; GraphPad Prism5).

RESULTS

Expression of caRheb in Adult DRG Neurons Promotes Axon Growth *in vitro*

We first sought to determine if activation of mTOR could enhance axonal regeneration on an inhibitory substrate *in vitro* that mimics the environment of the DREZ after injury (Steinmetz et al., 2005). To do so, we plated dissociated, adult DRG neurons on an established *in vitro* model of the glial scar containing the CSPG aggrecan and laminin (Tom et al., 2004). While neurons were able to attach in the center of the CSPG spot, where the concentration of CSPG is low, the rim of the spot has a high concentration of CSPG and a low concentration of laminin, making for an area of marked inhibition for growth (area between dashed lines in **Figure 1A**). Without any manipulation of the DRG cultures, neurites appeared trapped in the aggrecan spot when they encountered the potently inhibitory rim. Indeed, β-tubulin III labeled neurites from DRGs transduced with AAV-GFP did not cross this rim (**Figures 1A,E**), similar to the inability of axons to regrow across an untreated DREZ following dorsal root crush. Expressing caRheb alone in the DRGs did not improve neurites' ability to cross the rim (**Figures 1B,E**). When the CSPGs in the substrate were digested with ChABC, ∼30% of neurites axons were able to cross (arrowhead in **Figure 1C**), suggesting improved regeneration of a small percentage of sensory axons after cleavage of the inhibitory moieties from the CSPGs. This also suggests that some inhibitory molecules remain within the rim after ChABC, like the CSPG protein core (Imagama et al., 2011). Interestingly, when ChABC is combined with expressing caRheb in DRGs, twice as many axons were able to overcome this lingering inhibition and traverse the rim (arrows in **Figures 1D,E**; $p < 0.05$). These data suggest that expressing caRheb in adult DRG neurons allows more axons to overcome inhibition that remains after ChABC digestion, resulting in even more regeneration.

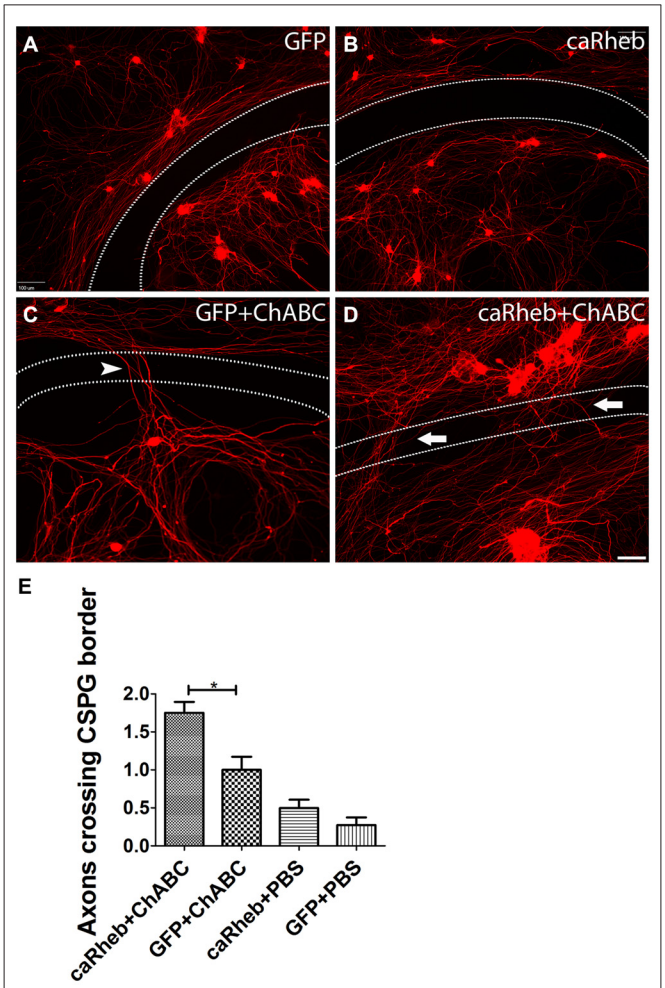

FIGURE 1 | Combining caRheb expression and chondroitinase ABC (ChABC) promoted neurite crossing of an inhibitory proteoglycan barrier. (A–D) Representative images of dorsal root ganglion (DRG) cultures are shown. DRG neurons and their neurites were visualized with β-tubulin III staining (red). Neurons transduced with adeno-associated virus (AAV)-GFP **(A)** and AAV-caRheb **(B)** failed to traverse the inhibitory rim (the region between the two dashed lines). ChABC treatment of the aggrecan-containing substrate enabled neurites to cross the inhibitory rim (**C**, arrowhead). Combining ChABC with expression of caRheb in DRG neurons resulted in significantly more robust axon crossing of the rim (**D**, arrows). **(E)** The number of axons crossing the inhibitory rim was counted and averaged in each of the four groups of DRG cultures ($n = 6$ per group). The most crossing was observed in ChABC-treated cultures transduced with AAV-caRheb. $^*P < 0.05$ (one-way ANOVA and *post hoc* Tukey's tests). Scale bar: 100 μm.

Characterization of DRG Transduction

To determine if the improved axon growth we observed in the *in vitro* experiments translates to an *in vivo* injury setting, we shifted to a cervical dorsal root crush model. Animals received unilateral intraganglionic injections at C5–C8 of either AAV5-GFP or a mixture of AAV5-GFP/AAV5-caRheb after dorsal root crush. The caRheb vector also contains a FLAG tag. Thus, cells transduced with AAV5-GFP were GFP^+ and cells transduced with AAV-caRheb were both GFP^+ and $FLAG^+$. We first sought to characterize how efficient our transduction was and which DRG neurons were transduced. We stained DRGs 1 month after injection. We found that injections of AAV-GFP (**Figures 2D–F**) or -caRheb (**Figures 2G–I**) into DRGs transduced many DRG neurons, as over 50% β-tubulin III^+ DRG neurons (**Figures 2E,H**) co-expressed GFP (**Figures 2D,G**). Transduction appeared to be neuron specific, as all GFP^+ cells were also β-tubulin III^+. Additionally, we found that AAV5-GFP and AAV5-caRheb targeted the same cell population when viruses were mixed and injected together. Neuronal cell bodies expressing GFP (**Figures 2A,C**) were also labeled with FLAG (**Figures 2B,C**). Unlike GFP, FLAG was not robustly expressed in axons. Therefore we used GFP to visualize neurons expressing caRheb and their axons in other analyses described below.

DRGs contain several subtypes of sensory neurons that can be generally classified as large diameter, small diameter, peptidergic, or small diameter, nonpeptidergic neurons. We wanted to determine if AAV5 has the same transfection

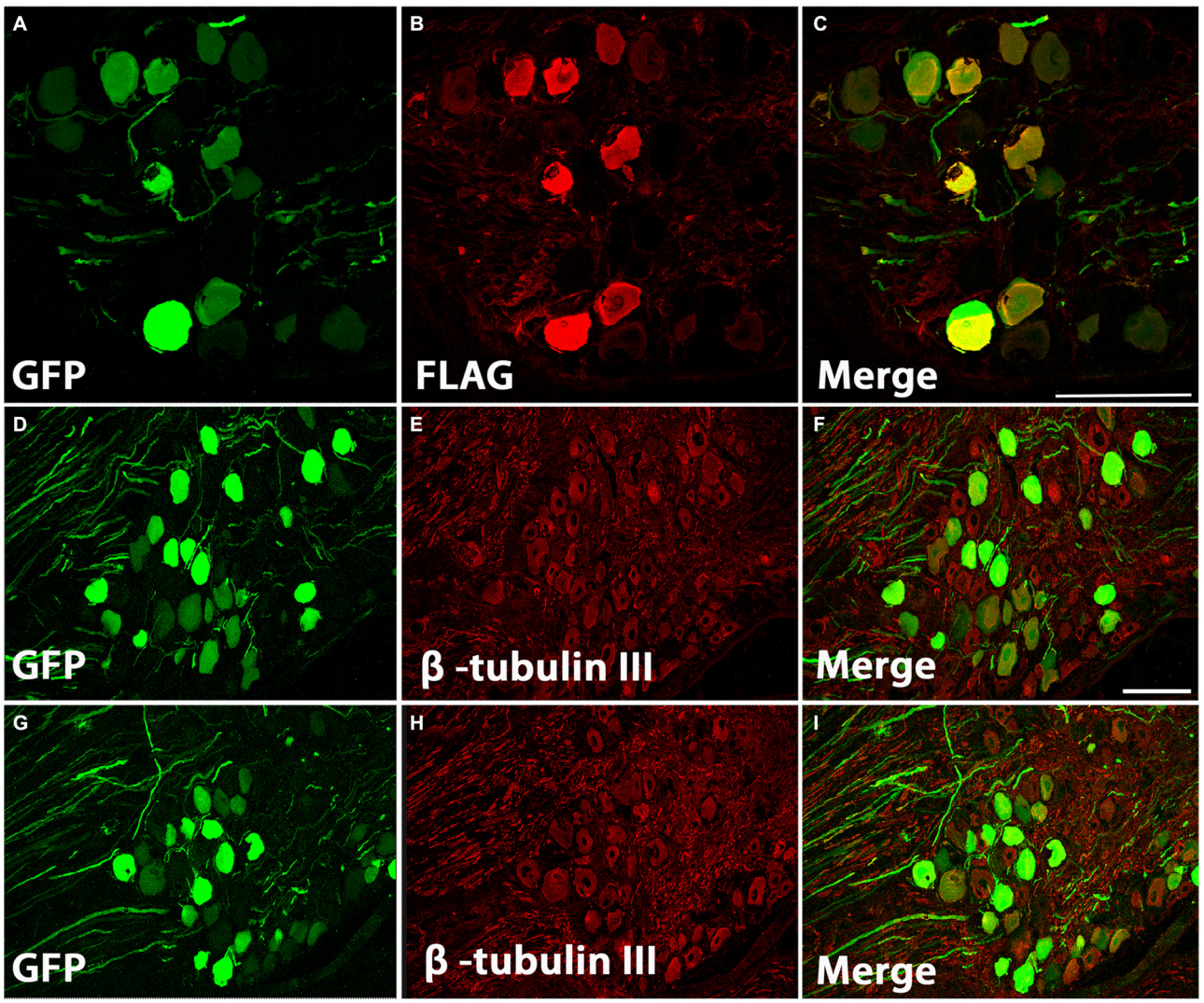

FIGURE 2 | AAV5 effectively transduced DRG neurons. (A–C) DRG neurons were transduced with a mixture of AAV-GFP and AAV-caRheb, the latter of which also contained a FLAG tag. One month later, DRGs were stained for GFP **(A)** or FLAG **(B)**. GFP^+ neurons coexpress FLAG **(C)**, indicating both viruses transduced the same neuron population. **(D–I)** DRGs injected with AAV-GFP **(D–F)** or AAV-GFP/-caRheb **(G–I)** were sectioned and processed for GFP (green) and β -tubulin III (red) staining. In both groups of DRG sections, over 50% of β-tubulin III labeled neuronal cells were also GFP^+. Scale bar: 100 μm.

efficiency for all DRG neurons. One month after AAV5-GFP injections, sections from injected DRGs were incubated with antibodies against GFP and NF-200, CGRP or IB4. The vast majority of GFP$^+$ neurons (**Figures 3A,C**) co-stained with NF-200 (**Figures 3B,C**), a marker for large-diameter neurons. Significantly fewer GFP$^+$ neurons were co-stained with

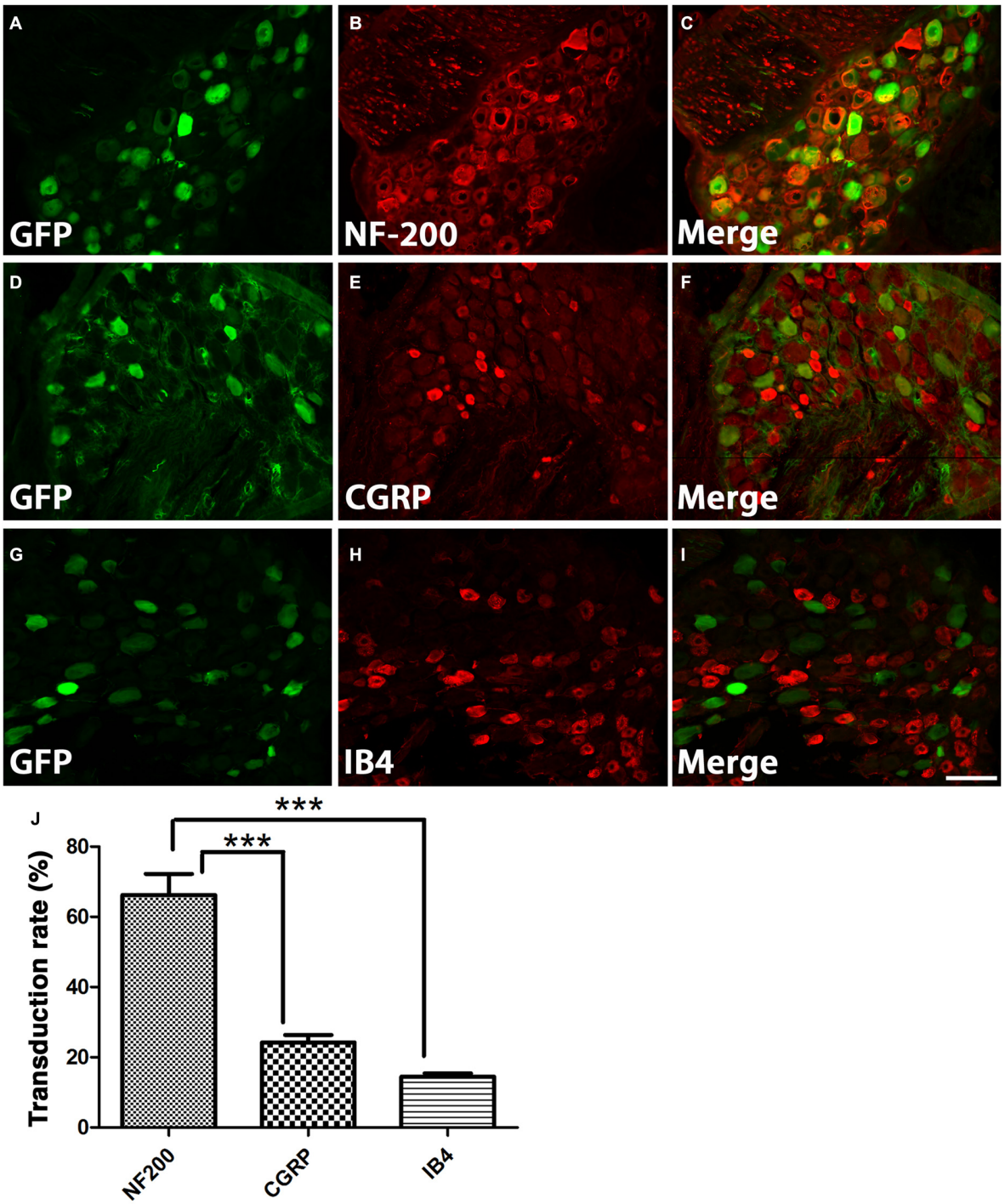

FIGURE 3 | Characterization of what DRGs subtypes were transduced. (A–I) DRGs were immunostained for GFP (green) and NF-200 (**B**, red), calcitonin gene related peptide (CGRP; **E**, red), or IB4 (**H**, red) 1 month after AAV injections. GFP expression **(A,D,G)** was mostly observed in NF-200$^+$ neurons **(C)**, rather than CGRP$^+$ **(F)** or IB4$^+$ neurons **(I). (J)** Quantification of transduction efficiencies of AAV5 in NF-200$^+$, CGRP$^+$ and IB4$^+$ DRG neurons revealed that AAV5 has a significantly higher transduction rate for NF-200$^+$ neurons, which are large diameter DRG neurons. Sections 120 μm apart from three animals were analyzed. ***$P < 0.005$ (one-way ANOVA followed by *post hoc* Bonferroni tests). Scale bar: 100 μm.

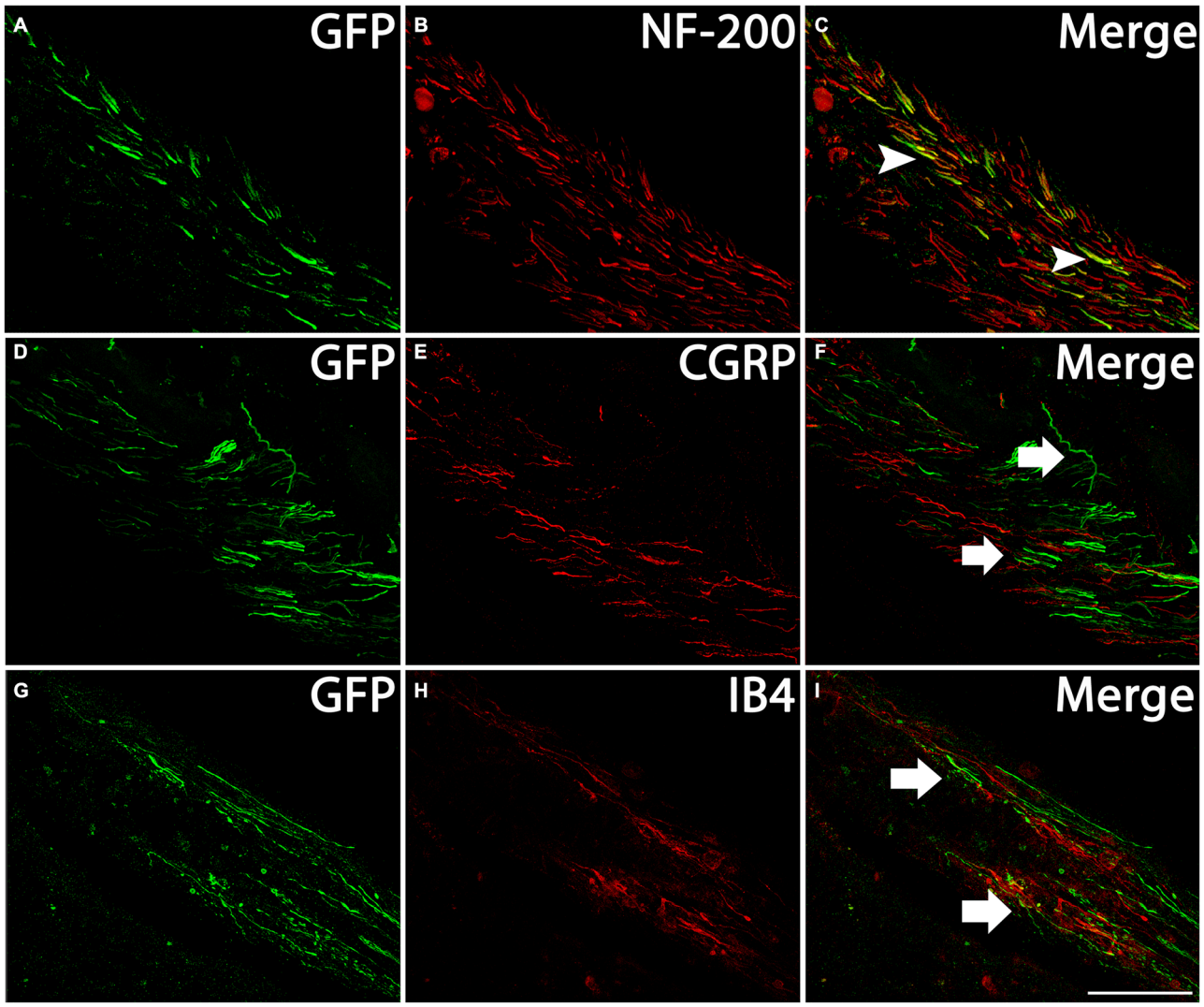

FIGURE 4 | Profile of axons of transduced neurons in the dorsal root. Transverse sections of spinal cord at cervical level with the dorsal roots attached were immunostained for GFP (green) and NF-200 (**B**, red), CGRP (**E**, red), or IB4 (**H**, red) 1 month after AAV injections. Many GFP$^+$ axons **(A,D,G)** were present in the dorsal root, including near the dorsal root entry zone (DREZ). Merged images indicate GFP-expressing axons coexpressed NF-200 (**C**, arrowheads), but not CGRP (**F**, arrows) or IB4 (**I**, arrows). Scale bar: 100 μm.

CGRP (**Figures 3D–F**), a marker for the small, peptidergic neurons, or IB4, a marker for small, nonpeptidergic neurons (**Figures 3G–I**). Quantification of transduction efficiencies of AAV5 in NF-200$^+$, CGRP$^+$ and IB4$^+$ DRG neurons are shown in **Figure 3J**. Consistent with what we observed in DRG, we detected abundant GFP$^+$ axons in the dorsal root 1 month after AAV5 injections. When transverse spinal cord sections containing the dorsal roots were co-stained with antibodies against GFP and NF-200, CGRP or IB4 (**Figure 4**), GFP$^+$ axons were mostly colocalized with NF-200$^+$ axons (**Figure 4C**, arrowheads) rather than CGRP$^+$ axons (**Figure 4F**, arrows) or IB4$^+$ axons (**Figure 4I**, arrows) in the root. These data indicate that mainly large caliber neurons were transduced to express caRheb and/or GFP.

Expressing caRheb in DRG Neurons Activates Phosphorylation of S6

Rheb-mediated activation of mTOR causes phosphorylation, and thus activation of, S6 ribosomal protein. To provide evidence that the caRheb enhanced activation of S6 in DRGs, we determined the level of phosphorylation of S6 in DRGs from animals 1 month after dorsal root crush and injecting AAV5-GFP (**Figures 5A–C**) or AAV5-caRheb (**Figures 5D–F**) via immunohistochemistry for p-S6. DRG sections from animals that received dorsal root crush only without virus injection were also immunostained for p-S6 (**Figure 5G**). Dorsal root crush alone did not appear to significantly activate S6, as indicated by a virtual absence of any p-S6 immunoreactivity (**Figure 5G**). We noticed that in the animals that received virus injections, regardless of which vector

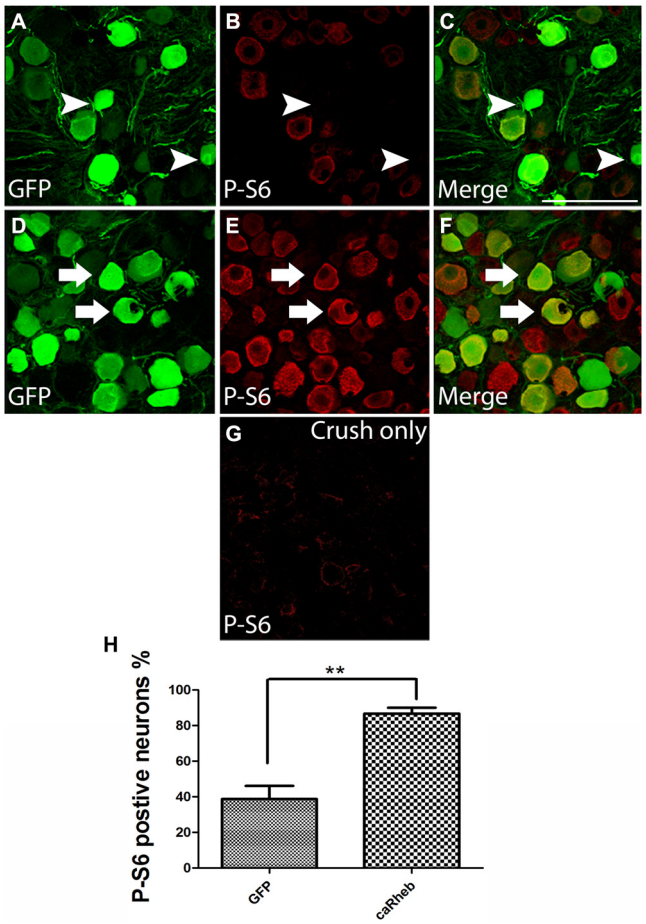

FIGURE 5 | Expressing caRheb in DRG neurons induced p-S6. (A–F) DRG sections from rats 1 month after intraganglionic AAV-GFP or AAV-GFP/-caRheb injections were stained for GFP (green) and p-S6 (red). GFP^+ neurons **(A)** showed low immunoreactivity for p-S6 **(B)**. The merged image confirmed that some GFP^+ control neurons did not express p-S6 (**C**, arrowheads). $CaRheb^+$ neurons **(D)** had significantly higher levels of p-S6 expression (**E,F**, arrows). **(G)** In DRGs from animals that received a dorsal root crush but no virus injection, there was virtually no detectable p-S6. **(H)** Quantification of the AAV-transduced neurons that were also p-$S6^+$. AAV-GFP injection induced p-S6 expression in about 40% transduced neurons. Injecting AAV-caRheb increased the number of p-S6 expressing neurons to over 80%. Sections 120 μm apart per animal were analyzed and there were three animals per group, $^{**}P < 0.05$ (Chi-squared tests). Scale bar: 100 μm.

was used, some neurons (both those that were transduced and those that were not) expressed p-S6 (**Figures 5B,E**), suggesting that the injection of virus activated S6 to a certain degree. Moreover, we found that expressing caRheb increased this. Around 40% of the GFP-expressing neurons (**Figures 5A,C**) had some p-S6 immunoreactivity (**Figures 5B,C**), though most did not (arrowheads in **Figures 5A–C,H**). On the other hand, strong p-S6 immunoreactivity was detected in more than 80% of caRheb-expressing neurons (arrows in **Figures 5D–F,H**). These data suggest that virus injection alone activates mTOR but that expressing caRheb in DRG neurons further activates the mTOR pathway.

ChABC Digests CSPGs at the DREZ

It was shown that the bacterial enzyme ChABC delivered via a single *in vivo* microinjection can maintain activity for at least 10 days (Lin et al., 2008). However, we wanted to confirm that a single ChABC injection digested upregulated CSPGs at the DREZ after dorsal root crush. One month after we injected ChABC or PBS into the dorsal horn immediately after dorsal root crush, we incubated sections of spinal cord with the dorsal root attached with the C-4-S antibody to detect the 4-sugar "stub" that remains following ChABC-digestion. PBS treatment failed to produce any digestion of CSPGs in spinal cord and DREZ, as there was virtually no C-4-S staining in these animals (**Figure 6A**). On the other hand, ChABC injection resulted in widespread C-4-S immunoreactivity (**Figure 6B**), indicating that one injection of ChABC was effective and resulted in wide-spread digestion of CSPGs, including in the dorsal columns, dorsal horn, and the DREZ (asterisk in **Figure 6B**).

Axonal Regeneration at DREZ

It has been demonstrated that ChABC-mediated digestion of glycosaminoglycan chains on CSPGs can promote axonal regeneration, including at the DREZ (Cafferty et al., 2007, 2008; Tom et al., 2009; Cheng et al., 2015). Here we assesssed whether expressing caRheb in DRG would allow more axons to extend beyond a ChABC-treated DREZ. One month after dorsal root injury, very few GFP^+ axons were found to have extended beyond a PBS-treated DREZ boundary in AAV5-GFP + PBS treated animals (**Figure 7A**). Similar to what we observed with descending CNS axons (Wu et al., 2015), expressing caRheb in neurons while leaving the glial scar intact did not improve sensory axons' ability to extend across the inhibitory environment of the DREZ (**Figure 7B**). Almost all axons failed to regenerate past the DREZ. Modification of the scar with ChABC did improve regeneration (**Figures 7C,D**), as shown previously. ChABC treatment significantly increased the number of axons that grew beyond the DREZ (**Figure 7E**). While axons were observed to penetrate the DREZ, the majority traveled only small distances across the DREZ. When we combined AAV-caRheb microinjection into the DRG along with ChABC microinjection into the spinal cord dorsal horn, a similar number of GFP^+ regenerating axons were found across the DREZ. These data indicate that ChABC increased the number of axons regenerating through DREZ and expressing caRheb in DRGs did not further enhance this growth response.

Behavioral Analysis

To determine if treatment with ChABC or ChABC and AAV5-caRheb promoted any functional improvement after dorsal root crush, sensory function of the animals was assessed using the Hargreaves test to examine thermal sensation and the Von Frey filament test to examine fine touch sensation. Because the animals did not place their injured paws down during the first week after surgery, the earliest time point for both behavioral tests was 1 week post injury. Interestingly, all animals that received AAV injections were responsive to both mechanical (**Figure 8A**) and thermal stimuli (**Figure 8B**). Furthermore, all

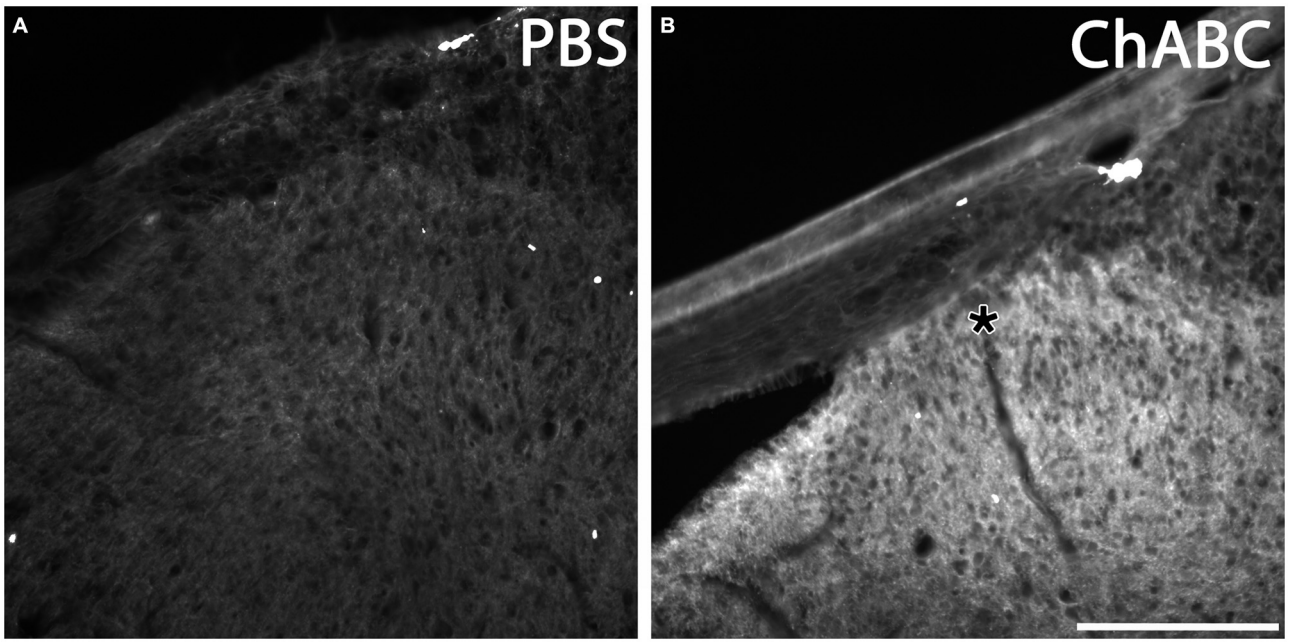

FIGURE 6 | ChABC digested chondroitin sulfate proteoglycans (CSPG) in spinal cord dorsal horn and DREZ. Transverse sections of spinal cord with dorsal root from animals 1 month after PBS or ChABC injection into dorsal horn were sectioned and stained with C-4-S, enabling visualization of the sugar stub that remained following ChABC-digestion. After PBS treatment, there was no detectable C-4-S immunoreactivity throughout the spinal cord tissue, including the dorsal root and DREZ **(A)**. In contrast, tissue treated with ChABC **(B)** exhibited high immunoreactivity for C-4-S near the ChABC injection site, including in the dorsal columns, dorsal horn, and the DREZ (asterisk). Scale bar: 200 μm.

AAV animals, even the PBS-treated animals that did not have any afferent regeneration (**Figure 7**), responded similarly—there was no significant difference between any of the treatment groups at any time point. In comparison, animals that received dorsal root crush only (and no intraganglionic injections of AAV) did not respond in either sensory test at any testing point, suggesting that our surgical technique resulted in complete lesions that interrupted afferent input. Thus, intraganglionic injections after a complete dorsal root crush somehow resulted in a sensory "response" that was independent of any regeneration.

Intraganglionic Injections Activate Macrophages/Microglia

There is compelling evidence indicating that the activity of macrophages/microglia play an important role in initiating neuropathic pain (Detloff et al., 2008; Richter et al., 2012; Segond von Banchet et al., 2013; McDonald et al., 2014; Kobayashi et al., 2015). Moreover, some pro-inflammatory cytokines have been shown to augment neurite outgrowth from injured sensory neurons (Bastien and Lacroix, 2014;Osório et al., 2014; Habash et al., 2015). Thus, we examined whether macrophages invaded the DRGs in animals that were injected with AAV. We noticed that 1 month after AAV injection, an influx of ED-1-positive macrophages can be identified in the DRG (arrows in **Figure 9A**). No detectable ED-1 was observed in DRGs from animals that received dorsal root crush only and no AAV injections (**Figure 9B**), indicating that this invasion of macrophages into the DRG was triggered by virus injections. We also wanted to identify whether dorsal root injury and virus injections trigger an inflammatory response in the cervical spinal cord. Iba-1 was used to identify activated microglia in spinal cord sections collected from dorsal root crush only animals (**Figure 10B**) and animals that received dorsal root crush and AAV5 injections into the DRGs (**Figure 10A**). Strong Iba-1 immunoreactivity was detected in the spinal cord, especially near the DREZ and dorsal horn, from animals that received dorsal root crush and virus injections (**Figure 10A**). Immunoreactivity for Iba-1 in animals that only received dorsal root crush was markedly lower (**Figure 10B**). Moreover, the contralateral side of the spinal cord, showed minimum immunoreactivity for Iba-1 (**Figure 10C**). The striking differences in levels of Iba-1 between groups indicate dorsal root injury induced the activation of microglia in dorsal horn ipsilateral to the injury and that this inflammatory response was further augmented by injury to the DRG caused by virus injections.

caRheb Enhances Integration of Regenerated Axons

We previously showed that when we combine caRheb expression with ChABC treatment, CNS axons can regrow beyond a distal peripheral nerve graft interface to extend into gray matter of host spinal cord tissue and form putative synapses upon host neurons (Wu et al., 2015). Here, we determined whether the afferents that regenerated back into spinal cord formed functional synapses.

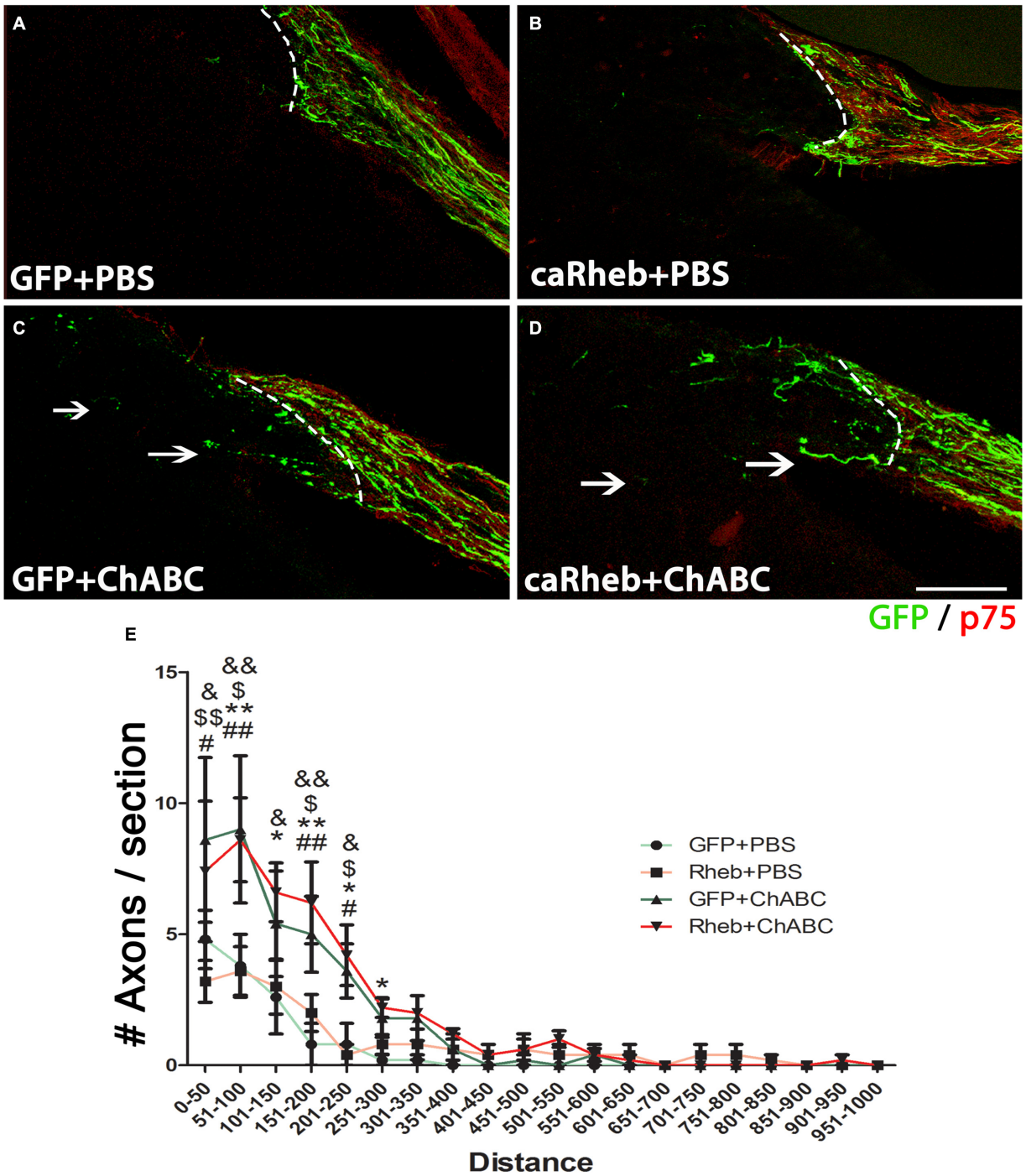

FIGURE 7 | ChABC treatment enhanced axon regeneration across the DREZ. (A–D) Transverse spinal cord tissue sections containing the dorsal root and the DREZ (indicated by the dashed line) were immunostained for GFP (green; to visualize axons from transduced DRG neurons) and p75 (red; to visualize Schwann cells within the dorsal root to best determine the boundary between the peripheral nervous system (PNS) and the CNS). Confocal images of the dorsal root and spinal cord of representative sections 1 month after dorsal root crush are shown. Regardless of whether DRGs were transduced with GFP **(A)** or caRheb **(B)**, there was very little to no axon regeneration across a PBS-treated DREZ. CSPG digestion with ChABC improved the ability of axons to traverse the PNS/CNS interface. When ChABC digestion of CSPG at DREZ was combined with AAV-GFP **(C)** or AAV-caRheb **(D)** injection into the DRGs, many more axons were able to extend across the DREZ (arrows). **(E)** Regenerating GFP^+ axons beyond the DREZ were counted in a subset of sections and binned into four groups based on the distance distal to the DREZ boundary. Significantly more axons grew short distances (0–300 μm) across the DREZ in both ChABC-treated groups than in both PBS-treated groups. Expressing caRheb did not enhance this ChABC-facilitated regeneration. There were six animals per group and five sections per animal were analyzed. $^{\#}P < 0.05$, $^{\#\#}P < 0.01$ GFP + PBS vs. GFP + ChABC; $^{*}P < 0.05$, $^{**}P < 0.01$ GFP + PBS vs. caRheb + ChABC; $^{\$}P < 0.05$, $^{\$\$}P < 0.01$, caRheb + PBS vs. GFP + ChABC; $^{\&}P < 0.05$, $^{\&\&}P < 0.01$, caRheb + PBS vs. caRheb + ChABC (one-way ANOVA followed by *post hoc* Bonferroni tests). Scale bar: 200 μm.

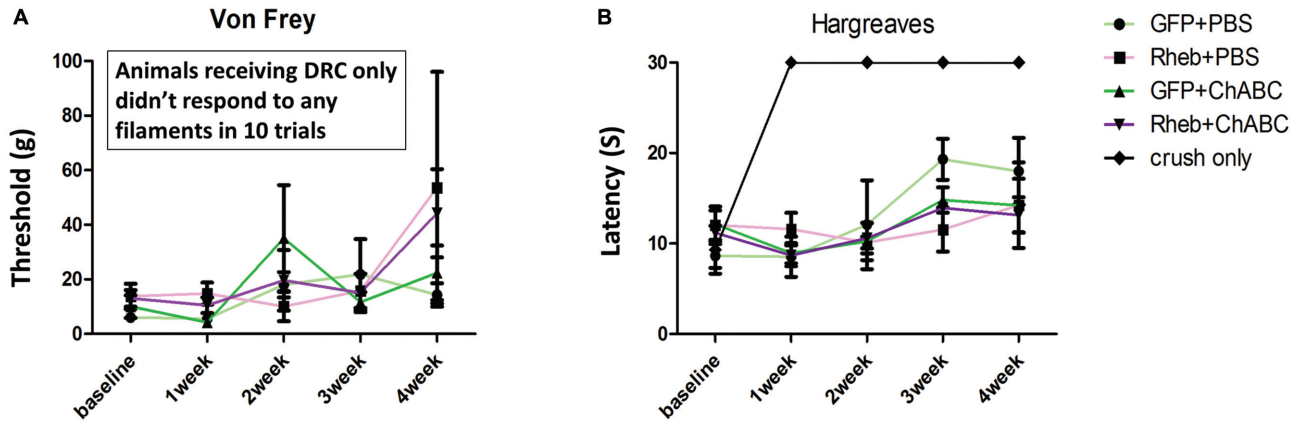

FIGURE 8 | All AAV-injected animals "responded" to sensory stimuli. Five groups of animals (GFP + PBS, caRheb + PBS, GFP + ChABC, caRheb + ChABC, an additional control group which only received dorsal root crush) were tested using the Von Frey filament and Hargreaves tests before surgery and weekly after surgery. As expected, dorsal root crush only animals were aresponsive to mechanical **(A)** or thermal **(B)** stimuli. Interestingly, all animals with AAV injections responded to both forms of sensory stimuli. No differences between the AAV groups were observed in either test at any time point ($N = 6$, two-way ANOVA).

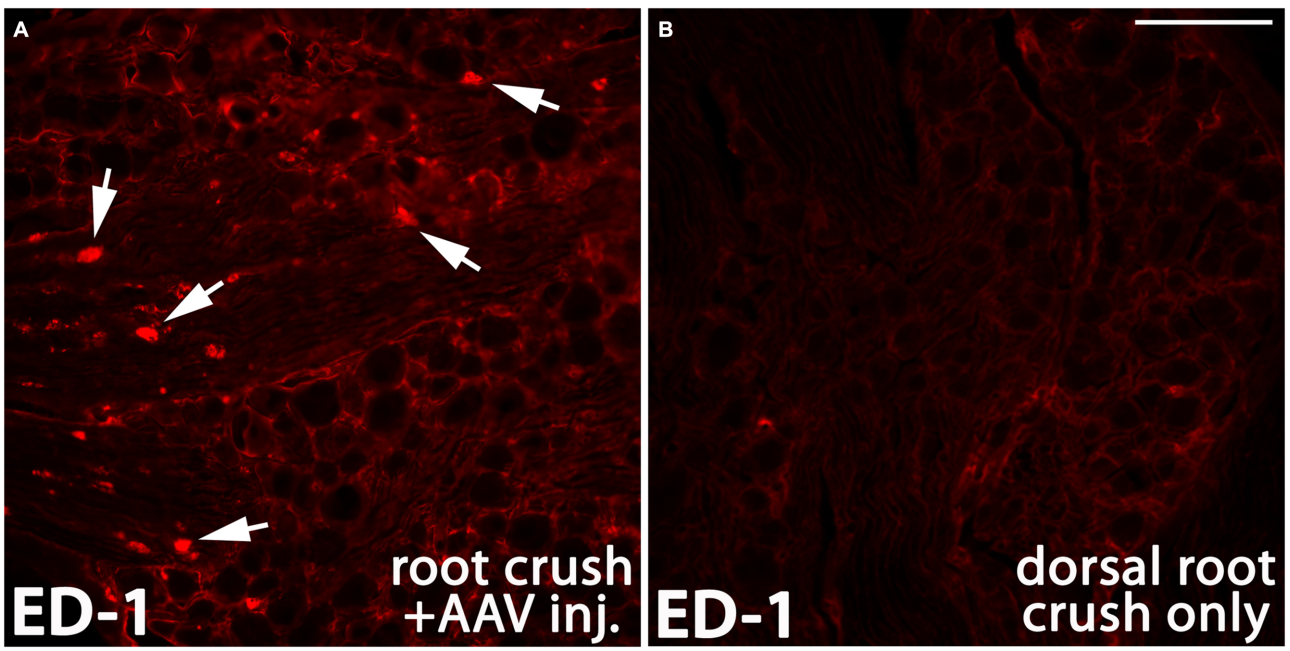

FIGURE 9 | AAV injection induced invasion of macrophages into the DRG. One month after AAV injection, ED-1 positive macrophages (arrows in **A**, red) were identified in the DRG. In the control DRGs that did not receive AAV injections, there was very little immunoreactivity for ED-1 **(B)**. Scale bar: 100 μm.

One month after injury, we electrically stimulated the ulnar and median nerves ipsilateral to the injury side prior to perfusion and performed histological analysis for c-Fos induction in neurons located in the dorsal horn. In both groups of animals that were treated with PBS [AAV-GFP (**Figure 11A**); AAV-caRheb (**Figure 11B**)], we saw very few c-Fos$^+$ neurons in ipsilateral gray matter. The c-Fos$^+$ immunoreactivity was observed mainly in the root, proximal to the DREZ, where the axons stopped elongation. On the other hand, in animals treated with ChABC, significantly more c-Fos$^+$ neurons were identified in ipsilateral dorsal horn (**Figures 11C,D**; arrows). Interestingly, despite there being similar numbers of axon extending across the DREZ in both groups of ChABC-treated animals (**Figure 7**), stimulation of the median and ulnar nerves in animals treated with ChABC and AAV-caRheb (**Figures 11D,D',E**) induced c-Fos in significantly more neurons than in animals treated with ChABC and AAV-GFP (**Figures 11C,C',E**). Thus, caRheb expression appears to enhance synaptic formation and/or function of axons that regenerated back into spinal cord gray matter.

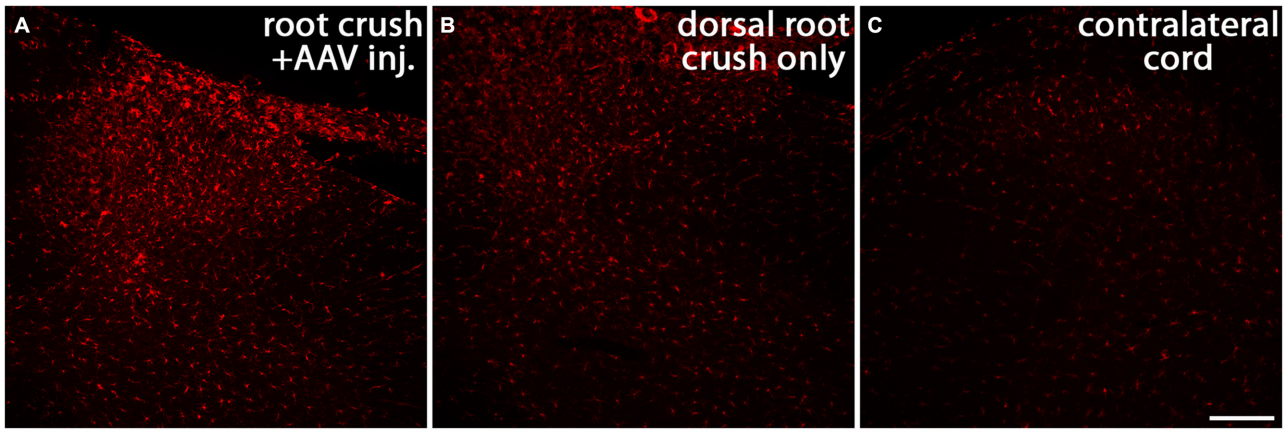

FIGURE 10 | Both dorsal root crush and intraganglionic AAV injections activate microglia in spinal cord. Cervical spinal cords were collected 1 month after animals received dorsal root crush only **(B)** or dorsal root crush and virus injection into the DRG **(A)**. Microglia in spinal cord sections were labeled with Iba-1 (red). Strong Iba-1 immunoreactivity was detected in reactive microglia near the DREZ and in the ipsilateral dorsal horn in animals that received both dorsal root crush and AAV injection **(A)**. The immunoreactivity for Iba-1 was significantly lower in animals that only received dorsal root crush **(B)**. There was very little Iba-1 staining in the contralateral dorsal horn **(C)**. Scale bar: 100 μm.

DISCUSSION

Axon regeneration of the peripherally-projecting DRG axon branch after injury to peripheral nerves can be successful. After a dorsal root crush that results in injury to the centrally-projecting branch, almost all axons can grow across the lesion site, extend along the root, and arrive at the DREZ. However, their regeneration ceases at the DREZ and axons remain in the PNS/CNS transitional zone (Di Maio et al., 2011), demonstrating that the DREZ is a potent barrier for axonal regeneration. Both oligodendrocyte-associated inhibitors and astrocyte-associated inhibitors present there cause growth cone collapse and axon retraction, repelling axons from entering the CNS (Golding et al., 1997, 1999). Moreover, Schwann cells in the dorsal root that provide a highly growth-promoting ensheathment do not intermingle with astrocytes in the spinal cord, constraining the extension of axons into CNS territory (Grimpe et al., 2005; Afshari et al., 2010a,b). Neutralization of the inhibitory molecules such as CSPG (Cafferty et al., 2007) or Nogo (Harvey et al., 2009) at the DREZ or increasing levels of neurotrophic factors, such as NGF (Ramer et al., 2000; Romero et al., 2000, 2001), GDNF (Ramer et al., 2000; Harvey et al., 2010) or NT-3 (Ramer et al., 2000, 2002), in the dorsal horn have been partially effective in luring the injured sensory axons back into the spinal cord.

Limited intrinsic growth capacity also contributes to the regeneration failure at the DREZ. Whereas peripheral nerve injury triggers high expression of regeneration associated genes, fostering regeneration of injured peripherally-projecting DRG axons, injury to the dorsal root fails to elicit a similar pro-regenerative gene expression profile (Mason et al., 2002; Seijffers et al., 2006). Peripheral conditioning lesions have been used to enhance the intrinsic regeneration capacity of the centrally-projecting axon after a spinal cord injury (Neumann and Woolf, 1999) or dorsal root injury (Zhang et al., 2007; Di Maio et al., 2011) with some degree of success. Thus, it appears that it is possible to manipulate the intrinsic potential for growth of the central branch. However, even with a conditioning lesion, the growth response of the central branch is still less than that of the peripheral branch. This difference has been attributed to decreased levels of local protein synthesis in central axons vs. PN axons. PNS axons have a high growth capacity with a high content of locally generated proteins that contribute to regenerative growth whereas CNS axons in the adult animals have very low level of translational machinery and low intra-axonal protein synthesis (Verma et al., 2005; Kalinski et al., 2015).

In the current study, we tested the efficacy of a strategy aimed at both activation of intrinsic axon growth capacity (i.e., caRheb-mediated) and digestion of upregulated inhibitory molecules with ChABC to promote sensory axon regrowth across the DREZ. mTOR is a serine/threonine protein kinase expressed in the mammalian nervous system that plays a critical role in protein synthesis (Liang et al., 2013). Importantly, mTOR and its downstream effectors, such as p-S6K, pS6 and p-4EBP1 are found in DRG somas and axons (Verma et al., 2005; Jiménez-Díaz et al., 2008; Liang et al., 2013). The activation of mTOR and its downstream effectors are implicated in the control of growth cone dynamics and guidance during development and axon regeneration after injury (Campbell and Holt, 2001; Nie et al., 2010). Activation of mTOR also promotes compensatory axonal sprouting after CNS injuries (Lee et al., 2014). Furthermore, its activation enhances axon growth capacity in different neuron types (Verma et al., 2005; Park et al., 2008; Liu et al., 2010). Interestingly, it has also been reported that although mTOR is expressed in adult DRGs, its phosphorylated form, which activates its downstream effectors, is expressed at a very low level under normal conditions (Xu et al., 2010). Injuries to

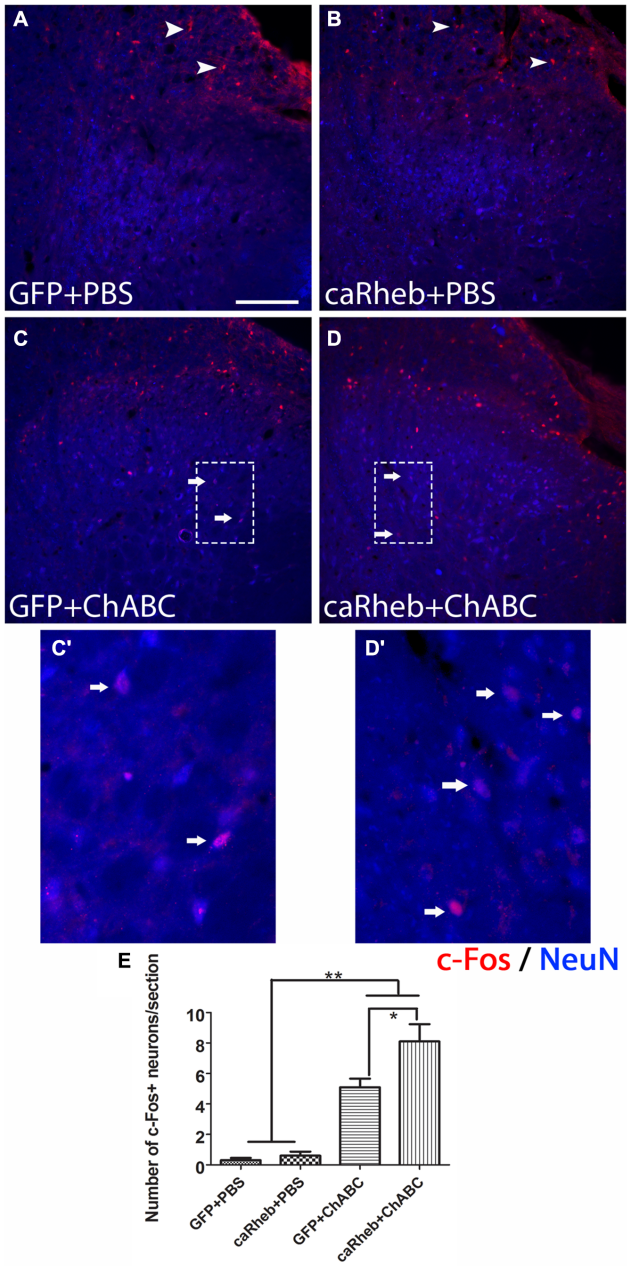

FIGURE 11 | Expressing caRheb increased the integration of axons that regenerate across the DREZ. One month after injury, median and ulnar nerves were electrically stimulated for 30 min and animals were sacrificed 1 h later. **(A–D)** Transverse sections of cervical spinal cords were sectioned and processed for c-Fos (red) and NeuN (blue) immunohistochemistry (Lavdas et al., 1997). Animals that were treated with GFP + PBS **(A)** or caRheb + PBS **(B)** had very few c-Fos$^+$ nuclei in spinal cord gray matter. Almost all neuronal c-Fos staining was detected in the dorsal root (**A,B**, arrowheads). On the contrary, in both groups of animals treated with ChABC, significantly more c-Fos$^+$ neuronal nuclei were detected in gray matter (**C,D**, arrows). High magnification images of the boxed regions in **(C,D)** are depicted in **(C',D')**, respectively. **(E)** c-Fos$^+$ neuronal nuclei in spinal gray matter were counted and compared. We found that electrical stimulation in caRheb + ChABC animals induced *c-Fos* in the most neurons. Scale bar: 100 μm. $N = 6$. $^*P < 0.05$, $^{**}P < 0.01$ (one-way ANOVA followed by *post hoc* Bonferroni tests).

peripheral nerve transiently activate mTOR. This activation appears to be important for regeneration as blocking mTOR activity pharmacologically with rapamycin reduces axon growth ability following peripheral injury (Abe et al., 2010; Melemedjian et al., 2011). These observations indicate that protein synthesis mediated by mTOR signaling regulation plays a critical role in promoting sensory axon regeneration. However, what was still unclear is if directly activating mTOR in DRG neurons without injuring the PNS will affect the central branch's ability to regenerate into the CNS.

In recent years, activation of mTOR has been achieved by genetically silencing its negative regulators, such as tuberous sclerosis complex (TSC) or PTEN (Park et al., 2008; Abe et al., 2010; Liu et al., 2010). In our study, we expressed caRheb, a mutant form of Rheb in DRG, which can directly and constitutively activate mTOR (Kim et al., 2011, 2012). We found that stimulation of the intrinsic growth capacity by caRheb increased mTOR activation was not robust enough to foster regeneration of DRG axons across inhibitory environments, either in an *in vitro* model of glial scar (Tom et al., 2004) or *in vivo* across the DREZ following a dorsal root crush. Manipulation of the inhibitory environment with ChABC *in vitro* augments this growth such that the combination of caRheb with ChABC resulted in more neuritic growth than either treatment alone. However, this was not observed *in vivo*. Combining AAV-caRheb injection in DRG with ChABC treatment of the dorsal horn did not have an additive effect on inducing more axons to grow beyond the DREZ.

The discrepancy between the effects of caRheb + ChABC *in vitro* and *in vivo* might be explained by the more complex, inhospitable environment that the regenerating axons encounter *in vivo*. At the DREZ, both CSPGs and oligodendrocyte-derived inhibitors constrain regeneration (Ramer et al., 2001). In our *in vivo* study, these inhibitors existed and remained intact. The difference in *in vitro* and *in vivo* DRG neuron transduction rates with AAV-caRheb may also contribute to the disparity in the regeneration capacity. In DRG cultures, over 80% DRG neurons were transduced by AAV-caRheb and AAV-GFP. There was no apparent variance in the transduction rate between different DRG neuron subtypes. On the other hand, in animals with AAV injections into DRGs, the overall transduction rate was around 50% and AAV mostly transduced large diameter DRG neurons rather than small diameter neurons. This observation conflicts with findings from a previous study that found that AAV5 transduces small diameter DRG neurons (Mason et al., 2010). The inconsistency between that study and the present one may be explained by differences in the promoter. In that study, GFP expression was under the control of CMV while here, transgene expression was driven by CBA. It is possible that the capacity for regrowth varies greatly among different population of DRG neurons. Indeed, large caliber, myelinated axons are thought to regenerate more poorly than those of small, non-myelinated axons projecting from small DRG neurons (Guseva and Chelyshev, 2006; Di Maio et al., 2011). Therefore, in our *in vivo* study, we examined the regeneration of a subpopulation of axons whose propensity for regeneration is particularly weak.

Another possible explanation between the disparity between the *in vitro* and the *in vivo* data is that injecting AAV intraganglionically appeared to induce p-S6 expression and inflammation in the DRGs. Though p-S6 levels in the caRheb-treated animals was significantly stronger than in the GFP-treated ones, even injecting just AAV-GFP increased the level of the activated form of the mTOR downstream effector p-S6 compared to DRGs from animals that received dorsal root crush only and no virus injections (**Figure 5**). We speculate that the activation of mTOR in AAV-GFP animals resulted from injection-induced inflammation, as we see an influx of ED-1^{+}, activated macrophages into these DRGs. Inflammation, including the recruitment of macrophages into the DRG (Lu and Richardson, 1991; Steinmetz et al., 2005; Kwon et al., 2013) has long been associated with promoting a growth state (Gensel and Zhang, 2015). Interestingly, it has been reported that complete Freund's adjuvant (Wieseler et al., 2010) induced inflammation significantly increases the activity of mTOR and S6k1 in DRGs and spinal cord dorsal horn (Liang et al., 2013). Thus, it is possible that mTOR plays a role in inflammation-enhanced regeneration.

This potential mechanism has been more extensively studied in RGCs injury models. An inflammatory stimulus induced by injury or by application of mediators of inflammatory stimulation, such as astrocyte-derived ciliary neurotrophic factor (CNTF), leukemia inhibitory factor (LIF) and interleukin-6 (IL-6), or the yeast cell wall component zymosan produce neuroprotective and axon growth stimulating effects (Leon et al., 2000; Yin et al., 2003, 2006; Müller et al., 2007; Leibinger et al., 2012, 2013). The activation of JAK/STAT3 and PI3K/AKT/mTOR signaling cascades were shown to contribute to how an inflammatory stimulus pushes RGCs into a regenerative state (Leibinger et al., 2012). It is possible that inflammation can have a similar effect on DRG neurons and may help to explain the similar extent of anatomical regeneration we observed in the GFP + ChABC and caRheb + ChABC animals. Virus injection inevitably caused some trauma and triggered the infiltration of macrophages into the ganglia. For reasons discussed above, this inflammation may have activated mTOR to levels sufficient to enhance the regenerative capacity.

Whether ChABC digestion alone promotes sensory regeneration is unclear. While some reported that CSPG digestion by ChABC promotes regeneration of the dorsal columns (Bradbury et al., 2002; Grimpe et al., 2005) and transgenic expression of ChABC under the GFAP promoter in mice promotes rhizotomized axons to grow back into spinal cord (Cafferty et al., 2007), there are also reports showing that ChABC treatment alone only allows for a negligible amount of regeneration of sensory axons across DREZ after dorsal root crush in rats (Steinmetz et al., 2005; Cafferty et al., 2008). Our study does not contradict these previous studies. Similar to what was demonstrated previously with zymosan (Steinmetz et al., 2005), inflammation induced by injecting AAV-GFP or AAV-caRheb intraganglionically in our study may have enhanced the effect of ChABC treatment, increasing the number of axons extending across the DREZ.

The injection-induced inflammatory response may also help to explain the inconclusive behavioral data we obtained in the Hargraves and Von Frey behavioral tests. We do not believe that the behavior we observed was mediated by regeneration, as even the PBS-treated animals that did not display any regeneration had "responses" to the sensory stimuli. Rather, we posit that the "responses" were indicative of some form of neuropathic pain. In support of this, the animals with root crushes and AAV injections had considerably more activated microglia within the dorsal horn than the crush-only animals (**Figure 10**). Furthermore, the extent of activated microglia within the dorsal horn has been shown to be predictive of the development and the extent of neuropathic pain (Detloff et al., 2008). Thus, we may have failed to observe any differences in the responses to thermal and mechanical stimuli between groups because intraspinal inflammation was triggered in all treatment groups.

Although we did not observe any behavioral differences between groups, we did find that regenerated axons in the caRheb + ChABC animals formed significantly more functional synapses on dorsal horn neurons than in GFP + ChABC animals (as indicated by the induction of c-Fos expression in dorsal horn neurons upon the stimulation of ipsilateral median and ulnar nerves). This indicates mTOR activation enhances the integration of sensory axons that regenerate back into spinal cord. Interestingly, mTOR activity is associated with various aspects of excitatory and inhibitory synaptic function, including increasing synaptic strength and affecting synapse number and synaptic vesicle number. Studies have demonstrated that activation of mTOR by PTEN knockdown *in vivo* results in excitatory synapse formation with granule cells (Luikart et al., 2011). Likewise, inhibition of mTOR with rampamycin blocks excitatory synaptic output of cultured dentate neurons (Weston et al., 2012) and reactive excitatory synaptogenesis in the brain after epilepsy-induced synaptic reorganization (Yamawaki et al., 2015). Thus, it has been suggested that mTOR-mediated protein synthesis may participate in synaptogenesis, maintaining synaptic homeostasis, and synaptic output (Lyu et al., 2013). The specific molecular mechanisms underlying mTOR's role in these activities remain unclear.

In conclusion, we confirmed that caRheb expression effectively activates the mTOR signaling pathway in DRGs and this mTOR activation can promote sensory axon regeneration when combined with CSPG digestion by ChABC *in vitro*. Combining caRheb expression with ChABC digestion of CSPG did not promote more axonal regeneration across the DREZ compared to what was observed with ChABC treatment alone *in vivo*, though this may be attributed to intraganglionic inflammation. However, expressing caRheb did enhance the integration of these regenerated axons with spinal neurons. Even though the underlying mechanisms of mTOR mediated axonal regeneration and synaptogenesis remain to be determined, our data suggest that increasing

mTOR level has the potential to facilitate regenerating axons to form synapses with the appropriately-located target neurons. Therefore, this combined treatment has the potential to promote functional recovery after dorsal root injury.

AUTHOR CONTRIBUTIONS

DW and VJT designed the experiments. DW, MCK and M-PC performed the experiments. NK and REB provided constructs for transduction. MRD provided technical expertise and assisted with data interpretation. DW and MCK analyzed the data. DW and VJT prepared the manuscript.

ACKNOWLEDGMENTS

This work was funded by National Institutes of Health (NIH) R01 NS085426 (VJT), the Craig H. Neilsen Foundation (280557 to DW and 221439 to VJT) and NIH P50 NS038370 (REB). The authors gratefully acknowledge the use of core facilities within the Drexel University Spinal Cord Research Center. We thank Dr. Michael A. Lane for generously providing the c-Fos antibody.

REFERENCES

Abe, N., Borson, S. H., Gambello, M. J., Wang, F., and Cavalli, V. (2010). Mammalian target of rapamycin (mTOR) activation increases axonal growth capacity of injured peripheral nerves. *J. Biol. Chem.* 285, 28034–28043. doi: 10.1074/jbc.M110.125336

Afshari, F. T., Kwok, J. C., and Fawcett, J. W. (2010a). Astrocyte-produced ephrins inhibit schwann cell migration via VAV2 signaling. *J. Neurosci.* 30, 4246–4255. doi: 10.1523/JNEUROSCI.3351-09.2010

Afshari, F. T., Kwok, J. C., White, L., and Fawcett, J. W. (2010b). Schwann cell migration is integrin-dependent and inhibited by astrocyte-produced aggrecan. *Glia* 58, 857–869. doi: 10.1002/glia.20970

Bastien, D., and Lacroix, S. (2014). Cytokine pathways regulating glial and leukocyte function after spinal cord and peripheral nerve injury. *Exp. Neurol.* 258, 62–77. doi: 10.1016/j.expneurol.2014.04.006

Bradbury, E. J., Moon, L. D., Popat, R. J., King, V. R., Bennett, G. S., Patel, P. N., et al. (2002). Chondroitinase ABC promotes functional recovery after spinal cord injury. *Nature* 416, 636–640. doi: 10.1038/416636a

Cafferty, W. B., Bradbury, E. J., Lidierth, M., Jones, M., Duffy, P. J., Pezet, S., et al. (2008). Chondroitinase ABC-mediated plasticity of spinal sensory function. *J. Neurosci.* 28, 11998–12009. doi: 10.1523/JNEUROSCI.3877-08.2008

Cafferty, W. B., Yang, S. H., Duffy, P. J., Li, S., and Strittmatter, S. M. (2007). Functional axonal regeneration through astrocytic scar genetically modified to digest chondroitin sulfate proteoglycans. *J. Neurosci.* 27, 2176–2185. doi: 10.1523/jneurosci.5176-06.2007

Campbell, D. S., and Holt, C. E. (2001). Chemotropic responses of retinal growth cones mediated by rapid local protein synthesis and degradation. *Neuron* 32, 1013–1026. doi: 10.1016/s0896-6273(01)00551-7

Carmel, J. B., Young, W., and Hart, R. P. (2015). Flipping the transcriptional switch from myelin inhibition to axon growth in the CNS. *Front. Mol. Neurosci.* 8:34. doi: 10.3389/fnmol.2015.00034

Chaplan, S. R., Bach, F. W., Pogrel, J. W., Chung, J. M., and Yaksh, T. L. (1994). Quantitative assessment of tactile allodynia in the rat paw. *J. Neurosci. Methods* 53, 55–63. doi: 10.1016/0165-0270(94)90144-9

Cheng, C. H., Lin, C. T., Lee, M. J., Tsai, M. J., Huang, W. H., Huang, M. C., et al. (2015). Local delivery of high-dose chondroitinase ABC in the sub-acute stage promotes axonal outgrowth and functional recovery after complete spinal cord transection. *PLoS One* 10:e0138705. doi: 10.1371/journal.pone.0138705

Christie, K. J., Webber, C. A., Martinez, J. A., Singh, B., and Zochodne, D. W. (2010). PTEN inhibition to facilitate intrinsic regenerative outgrowth of adult peripheral axons. *J. Neurosci.* 30, 9306–9315. doi: 10.1523/JNEUROSCI.6271-09.2010

Detloff, M. R., Fisher, L. C., McGaughy, V., Longbrake, E. E., Popovich, P. G., and Basso, D. M. (2008). Remote activation of microglia and pro-inflammatory cytokines predict the onset and severity of below-level neuropathic pain after spinal cord injury in rats. *Exp. Neurol.* 212, 337–347. doi: 10.1016/j.expneurol.2008.04.009

Devor, M. (1999). Unexplained peculiarities of the dorsal root ganglion. *Pain* 6, S27–S35. doi: 10.1016/s0304-3959(99)00135-9

Di Maio, A., Skuba, A., Himes, B. T., Bhagat, S. L., Hyun, J. K., Tessler, A., et al. (2011). *In vivo* imaging of dorsal root regeneration: rapid immobilization and presynaptic differentiation at the CNS/PNS border. *J. Neurosci.* 31, 4569–4582. doi: 10.1523/JNEUROSCI.4638-10.2011

Du, K., Zheng, S., Zhang, Q., Li, S., Gao, X., Wang, J., et al. (2015). Pten deletion promotes regrowth of corticospinal tract axons 1 year after spinal cord injury. *J. Neurosci.* 35, 9754–9763. doi: 10.1523/JNEUROSCI.3637-14.2015

Durán, R. V., and Hall, M. N. (2012). Regulation of TOR by small GTPases. *EMBO Rep.* 13, 121–128. doi: 10.1038/embor.2011.257

Fischer, D., He, Z., and Benowitz, L. I. (2004a). Counteracting the Nogo receptor enhances optic nerve regeneration if retinal ganglion cells are in an active growth state. *J. Neurosci.* 24, 1646–1651. doi: 10.1523/jneurosci.5119-03.2004

Fischer, D., Petkova, V., Thanos, S., and Benowitz, L. I. (2004b). Switching mature retinal ganglion cells to a robust growth state *in vivo*: gene expression and synergy with RhoA inactivation. *J. Neurosci.* 24, 8726–8740. doi: 10.1523/jneurosci.2774-04.2004

Fraher, J. P. (2000). The transitional zone and CNS regeneration. *J. Anat.* 196, 137–158.

Gensel, J. C., and Zhang, B. (2015). Macrophage activation and its role in repair and pathology after spinal cord injury. *Brain Res.* 1619, 1–11. doi: 10.1016/j.brainres.2014.12.045

Golding, J. P., Bird, C., McMahon, S., and Cohen, J. (1999). Behaviour of DRG sensory neurites at the intact and injured adult rat dorsal root entry zone: postnatal neurites become paralysed, whilst injury improves the growth of embryonic neurites. *Glia* 26, 309–323. doi: 10.1002/(sici)1098-1136(199906)26:4<309::aid-glia5 >3.0.co;2-0

Golding, J., Shewan, D., and Cohen, J. (1997). Maturation of the mammalian dorsal root entry zone-from entry to no entry. *Trends Neurosci.* 20, 303–308. doi: 10.1016/s0166-2236(96)01044-2

Grimpe, B., Pressman, Y., Lupa, M. D., Horn, K. P., Bunge, M. B., and Silver, J. (2005). The role of proteoglycans in Schwann cell/astrocyte interactions and in regeneration failure at PNS/CNS interfaces. *Mol. Cell. Neurosci.* 28, 18–29. doi: 10.1016/j.mcn.2004.06.010

Guseva, D., and Chelyshev, Y. (2006). The plasticity of the DRG neurons belonging to different subpopulations after dorsal rhizotomy. *Cell. Mol. Neurobiol.* 26, 1225–1234. doi: 10.1007/s10571-006-9005-4

Habash, T., Saleh, A., Roy Chowdhury, S. K., Smith, D. R., and Fernyhough, P. (2015). The proinflammatory cytokine, interleukin-17A, augments mitochondrial function and neurite outgrowth of cultured adult sensory neurons derived from normal and diabetic rats. *Exp. Neurol.* 273, 177–189. doi: 10.1016/j.expneurol.2015.08.016

Hargreaves, K., Dubner, R., Brown, F., Flores, C., and Joris, J. (1988). A new and sensitive method for measuring thermal nociception in cutaneous hyperalgesia. *Pain* 32, 77–88. doi: 10.1016/0304-3959(88)90026-7

Harvey, P., Gong, B., Rossomando, A. J., and Frank, E. (2010). Topographically specific regeneration of sensory axons in the spinal cord. *Proc. Natl. Acad. Sci. U S A* 107, 11585–11590. doi: 10.1073/pnas.1003287107

Harvey, P. A., Lee, D. H., Qian, F., Weinreb, P. H., and Frank, E. (2009). Blockade of Nogo receptor ligands promotes functional regeneration of sensory axons after dorsal root crush. *J. Neurosci.* 29, 6285–6295. doi: 10.1523/JNEUROSCI.5885-08.2009

Imagama, S., Sakamoto, K., Tauchi, R., Shinjo, R., Ohgomori, T., Ito, Z., et al. (2011). Keratan sulfate restricts neural plasticity after spinal cord injury. *J. Neurosci.* 31, 17091–17102. doi: 10.1523/JNEUROSCI.5120-10.2011

Jiménez-Díaz, L., Geranton, S. M., Passmore, G. M., Leith, J. L., Fisher, A. S., Berliocchi, L., et al. (2008). Local translation in primary afferent fibers regulates nociception. *PLoS One* 3:e1961. doi: 10.1371/journal.pone.0001961

Kalinski, A. L., Sachdeva, R., Gomes, C., Lee, S. J., Shah, Z., Houle, J. D., et al. (2015). mRNAs and protein synthetic machinery localize into regenerating spinal cord axons when they are provided a substrate that supports growth. *J. Neurosci.* 35, 10357–10370. doi: 10.1523/JNEUROSCI.1249-15.2015

Kim, S. R., Chen, X., Oo, T. F., Kareva, T., Yarygina, O., Wang, C., et al. (2011). Dopaminergic pathway reconstruction by Akt/Rheb-induced axon regeneration. *Ann. Neurol.* 70, 110–120. doi: 10.1002/ana.22383

Kim, S. R., Kareva, T., Yarygina, O., Kholodilov, N., and Burke, R. E. (2012). AAV transduction of dopamine neurons with constitutively active Rheb protects from neurodegeneration and mediates axon regrowth. *Mol. Ther.* 20, 275–286. doi: 10.1038/mt.2011.213

Kobayashi, Y., Kiguchi, N., Fukazawa, Y., Saika, F., Maeda, T., and Kishioka, S. (2015). Macrophage-T cell interactions mediate neuropathic pain through the glucocorticoid-induced tumor necrosis factor ligand system. *J. Biol. Chem.* 290, 12603–12613. doi: 10.1074/jbc.M115.636506

Kwon, M. J., Kim, J., Shin, H., Jeong, S. R., Kang, Y. M., Choi, J. Y., et al. (2013). Contribution of macrophages to enhanced regenerative capacity of dorsal root Ganglia sensory neurons by conditioning injury. *J. Neurosci.* 33, 15095–15108. doi: 10.1523/JNEUROSCI.0278-13.2013

Lavdas, A. A., Blue, M. E., Lincoln, J., and Parnavelas, J. G. (1997). Serotonin promotes the differentiation of glutamate neurons in organotypic slice cultures of the developing cerebral cortex. *J. Neurosci.* 17, 7872–7880.

Lee, D. H., Luo, X., Yungher, B. J., Bray, E., Lee, J. K., and Park, K. K. (2014). Mammalian target of rapamycin's distinct roles and effectiveness in promoting compensatory axonal sprouting in the injured CNS. *J. Neurosci.* 34, 15347–15355. doi: 10.1523/JNEUROSCI.1935-14.2014

Leibinger, M., Andreadaki, A., and Fischer, D. (2012). Role of mTOR in neuroprotection and axon regeneration after inflammatory stimulation. *Neurobiol. Dis.* 46, 314–324. doi: 10.1016/j.nbd.2012.01.004

Leibinger, M., Müller, A., Gobrecht, P., Diekmann, H., Andreadaki, A., and Fischer, D. (2013). Interleukin-6 contributes to CNS axon regeneration upon inflammatory stimulation. *Cell Death Dis.* 4:e609. doi: 10.1038/cddis.2013.126

Leon, S., Yin, Y., Nguyen, J., Irwin, N., and Benowitz, L. I. (2000). Lens injury stimulates axon regeneration in the mature rat optic nerve. *J. Neurosci.* 20, 4615–4626.

Liang, L., Tao, B., Fan, L., Yaster, M., Zhang, Y., and Tao, Y. X. (2013). mTOR and its downstream pathway are activated in the dorsal root ganglion and spinal cord after peripheral inflammation, but not after nerve injury. *Brain Res.* 1513, 17–25. doi: 10.1016/j.brainres.2013.04.003

Lin, R., Kwok, J. C., Crespo, D., and Fawcett, J. W. (2008). Chondroitinase ABC has a long-lasting effect on chondroitin sulphate glycosaminoglycan content in the injured rat brain. *J. Neurochem.* 104, 400–408.

Liu, K., Lu, Y., Lee, J. K., Samara, R., Willenberg, R., Sears-Kraxberger, I., et al. (2010). PTEN deletion enhances the regenerative ability of adult corticospinal neurons. *Nat. Neurosci.* 13, 1075–1081. doi: 10.1038/nn.2603

Lu, X., and Richardson, P. M. (1991). Inflammation near the nerve cell body enhances axonal regeneration. *J. Neurosci.* 11, 972–978.

Luikart, B. W., Schnell, E., Washburn, E. K., Bensen, A. L., Tovar, K. R., and Westbrook, G. L. (2011). Pten knockdown *in vivo* increases excitatory drive onto dentate granule cells. *J. Neurosci.* 31, 4345–4354. doi: 10.1523/JNEUROSCI.0061-11.2011

Lyu, D., Yu, W., Tang, N., Wang, R., Zhao, Z., Xie, F., et al. (2013). The mTOR signaling pathway regulates pain-related synaptic plasticity in rat entorhinal-hippocampal pathways. *Mol. Pain* 9:64. doi: 10.1186/1744-8069-9-64

Mar, F. M., Bonni, A., and Sousa, M. M. (2014). Cell intrinsic control of axon regeneration. *EMBO Rep.* 15, 254–263. doi: 10.1002/embr.201337723

Mar, F. M., Simões, A. R., Rodrigo, I. S., and Sousa, M. M. (2015). Inhibitory injury signaling represses axon regeneration after dorsal root injury. *Mol. Neurobiol.* doi: 10.1007/s12035-015-9397-6 [Epub ahead of print].

Mason, M. R., Ehlert, E. M., Eggers, R., Pool, C. W., Hermening, S., Huseinovic, A., et al. (2010). Comparison of AAV serotypes for gene delivery to dorsal root ganglion neurons. *Mol. Ther.* 18, 715–724. doi: 10.1038/mt.2010.19

Mason, M. R., Lieberman, A. R., Grenningloh, G., and Anderson, P. N. (2002). Transcriptional upregulation of SCG10 and CAP-23 is correlated with regeneration of the axons of peripheral and central neurons *in vivo*. *Mol. Cell. Neurosci.* 20, 595–615. doi: 10.1006/mcne.2002.1140

McDonald, M. K., Tian, Y., Qureshi, R. A., Gormley, M., Ertel, A., Gao, R., et al. (2014). Functional significance of macrophage-derived exosomes in inflammation and pain. *Pain* 155, 1527–1539. doi: 10.1016/j.pain.2014.04.029

Melemedjian, O. K., Asiedu, M. N., Tillu, D. V., Sanoja, R., Yan, J., Lark, A., et al. (2011). Targeting adenosine monophosphate-activated protein kinase (AMPK) in preclinical models reveals a potential mechanism for the treatment of neuropathic pain. *Mol. Pain* 7:70. doi: 10.1186/1744-8069-7-70

Müller, A., Hauk, T. G., and Fischer, D. (2007). Astrocyte-derived CNTF switches mature RGCs to a regenerative state following inflammatory stimulation. *Brain* 130, 3308–3320. doi: 10.1093/brain/awm257

Neumann, S., and Woolf, C. J. (1999). Regeneration of dorsal column fibers into and beyond the lesion site following adult spinal cord injury. *Neuron* 23, 83–91. doi: 10.1016/s0896-6273(00)80755-2

Nie, D., Di Nardo, A., Han, J. M., Baharanyi, H., Kramvis, I., Huynh, T., et al. (2010). Tsc2-Rheb signaling regulates EphA-mediated axon guidance. *Nat. Neurosci.* 13, 163–172. doi: 10.1038/nn.2477

Osório, C., Chacon, P. J., White, M., Kisiswa, L., Wyatt, S., Rodriguez-Tebar, A., et al. (2014). Selective regulation of axonal growth from developing hippocampal neurons by tumor necrosis factor superfamily member APRIL. *Mol. Cell. Neurosci.* 59, 24–36. doi: 10.1016/j.mcn.2014.01.002

Park, K. K., Liu, K., Hu, Y., Smith, P. D., Wang, C., Cai, B., et al. (2008). Promoting axon regeneration in the adult CNS by modulation of the PTEN/mTOR pathway. *Science* 322, 963–966. doi: 10.1126/science.1161566

Peng, X., Zhou, Z., Hu, J., Fink, D. J., and Mata, M. (2010). Soluble Nogo receptor down-regulates expression of neuronal Nogo-A to enhance axonal regeneration. *J. Biol. Chem.* 285, 2783–2795. doi: 10.1074/jbc.M109.046425

Qiu, J., Cafferty, W. B., McMahon, S. B., and Thompson, S. W. (2005). Conditioning injury-induced spinal axon regeneration requires signal transducer and activator of transcription 3 activation. *J. Neurosci.* 25, 1645–1653. doi: 10.1523/jneurosci.3269-04.2005

Ramer, M. S., Bishop, T., Dockery, P., Mobarak, M. S., O'Leary, D., Fraher, J. P., et al. (2002). Neurotrophin-3-mediated regeneration and recovery of proprioception following dorsal rhizotomy. *Mol. Cell. Neurosci.* 19, 239–249. doi: 10.1006/mcne.2001.1067

Ramer, M. S., Duraisingam, I., Priestley, J. V., and McMahon, S. B. (2001). Two-tiered inhibition of axon regeneration at the dorsal root entry zone. *J. Neurosci.* 21, 2651–2660.

Ramer, M. S., Priestley, J. V., and McMahon, S. B. (2000). Functional regeneration of sensory axons into the adult spinal cord. *Nature* 403, 312–316. doi: 10.1038/35002084

Richter, F., Natura, G., Ebbinghaus, M., von Banchet, G. S., Hensellek, S., Konig, C., et al. (2012). Interleukin-17 sensitizes joint nociceptors to mechanical stimuli and contributes to arthritic pain through neuronal interleukin-17 receptors in rodents. *Arthritis Rheum.* 64, 4125–4134. doi: 10.1002/art.37695

Romero, M. I., Rangappa, N., Garry, M. G., and Smith, G. M. (2001). Functional regeneration of chronically injured sensory afferents into adult spinal cord after neurotrophin gene therapy. *J. Neurosci.* 21, 8408–8416.

Romero, M. I., Rangappa, N., Li, L., Lightfoot, E., Garry, M. G., and Smith, G. M. (2000). Extensive sprouting of sensory afferents and hyperalgesia induced by conditional expression of nerve growth factor in the adult spinal cord. *J. Neurosci.* 20, 4435–4445.

Schreyer, D. J., and Skene, J. H. (1993). Injury-associated induction of GAP-43 expression displays axon branch specificity in rat dorsal root ganglion neurons. *J. Neurobiol.* 24, 959–970. doi: 10.1002/neu.480240709

Segond von Banchet, G., Boettger, M. K., Konig, C., Iwakura, Y., Brauer, R., and Schaible, H. G. (2013). Neuronal IL-17 receptor upregulates TRPV4 but not TRPV1 receptors in DRG neurons and mediates mechanical but not thermal hyperalgesia. *Mol. Cell. Neurosci.* 52, 152–160. doi: 10.1016/j.mcn.2012.11.006

Seijffers, R., Allchorne, A. J., and Woolf, C. J. (2006). The transcription factor ATF-3 promotes neurite outgrowth. *Mol. Cell. Neurosci.* 32, 143–154. doi: 10.1016/j.mcn.2006.03.005

Silver, J., and Miller, J. H. (2004). Regeneration beyond the glial scar. *Nat. Rev. Neurosci.* 5, 146–156. doi: 10.1038/nrn1326

Steinmetz, M. P., Horn, K. P., Tom, V. J., Miller, J. H., Busch, S. A., Nair, D., et al. (2005). Chronic enhancement of the intrinsic growth capacity of sensory neurons combined with the degradation of inhibitory proteoglycans allows functional regeneration of sensory axons through the dorsal root entry zone in the mammalian spinal cord. *J. Neurosci.* 25, 8066–8076. doi: 10.1523/jneurosci.2111-05.2005

Takahashi, Y., and Nakajima, Y. (1996). Dermatomes in the rat limbs as determined by antidromic stimulation of sensory C-fibers in spinal nerves. *Pain* 67, 197–202. doi: 10.1016/0304-3959(96)03116-8

Tom, V. J., Sandrow-Feinberg, H. R., Miller, K., Domitrovich, C., Bouyer, J., Zhukareva, V., et al. (2013). Exogenous BDNF enhances the integration of chronically injured axons that regenerate through a peripheral nerve grafted into a chondroitinase-treated spinal cord injury site. *Exp. Neurol.* 239, 91–100. doi: 10.1016/j.expneurol.2012.09.011

Tom, V. J., Sandrow-Feinberg, H. R., Miller, K., Santi, L., Connors, T., Lemay, M. A., et al. (2009). Combining peripheral nerve grafts and chondroitinase promotes functional axonal regeneration in the chronically injured spinal cord. *J. Neurosci.* 29, 14881–14890. doi: 10.1523/JNEUROSCI.3641-09.2009

Tom, V. J., Steinmetz, M. P., Miller, J. H., Doller, C. M., and Silver, J. (2004). Studies on the development and behavior of the dystrophic growth cone, the hallmark of regeneration failure, in an *in vitro* model of the glial scar and after spinal cord injury. *J. Neurosci.* 24, 6531–6539. doi: 10.1523/jneurosci.0994-04.2004

Verma, P., Chierzi, S., Codd, A. M., Campbell, D. S., Meyer, R. L., Holt, C. E., et al. (2005). Axonal protein synthesis and degradation are necessary for efficient growth cone regeneration. *J. Neurosci.* 25, 331–342. doi: 10.1523/jneurosci.3073-04.2005

Wang, R., King, T., Ossipov, M. H., Rossomando, A. J., Vanderah, T. W., Harvey, P., et al. (2008). Persistent restoration of sensory function by immediate or delayed systemic artemin after dorsal root injury. *Nat. Neurosci.* 11, 488–496. doi: 10.1038/nn2069

Weston, M. C., Chen, H., and Swann, J. W. (2012). Multiple roles for mammalian target of rapamycin signaling in both glutamatergic and GABAergic synaptic transmission. *J. Neurosci.* 32, 11441–11452. doi: 10.1523/JNEUROSCI.1283-12.2012

Wieseler, J., Ellis, A. L., McFadden, A., Brown, K., Starnes, C., Maier, S. F., et al. (2010). Below level central pain induced by discrete dorsal spinal cord injury. *J. Neurotrauma* 27, 1697–1707. doi: 10.1089/neu.2010.1311

Woolf, C. J., and Bloechlinger, S. (2002). Neuroscience. *Science* 297, 1132–1134. doi: 10.1126/science.1076247

Wu, D., Klaw, M. C., Connors, T., Kholodilov, N., Burke, R. E., and Tom, V. J. (2015). Expressing constitutively active Rheb in adult neurons after a complete spinal cord injury enhances axonal regeneration beyond a chondroitinase-treated glial scar. *J. Neurosci.* 35, 11068–11080. doi: 10.1523/JNEUROSCI.0719-15.2015

Xu, J. T., Zhao, X., Yaster, M., and Tao, Y. X. (2010). Expression and distribution of mTOR, p70S6K, 4E-BP1 and their phosphorylated counterparts in rat dorsal root ganglion and spinal cord dorsal horn. *Brain Res.* 1336, 46–57. doi: 10.1016/j.brainres.2010.04.010

Yamawaki, R., Thind, K., and Buckmaster, P. S. (2015). Blockade of excitatory synaptogenesis with proximal dendrites of dentate granule cells following rapamycin treatment in a mouse model of temporal lobe epilepsy. *J. Comp. Neurol.* 523, 281–297. doi: 10.1002/cne.23681

Yin, Y., Cui, Q., Li, Y., Irwin, N., Fischer, D., Harvey, A. R., et al. (2003). Macrophage-derived factors stimulate optic nerve regeneration. *J. Neurosci.* 23, 2284–2293.

Yin, Y., Henzl, M. T., Lorber, B., Nakazawa, T., Thomas, T. T., Jiang, F., et al. (2006). Oncomodulin is a macrophage-derived signal for axon regeneration in retinal ganglion cells. *Nat. Neurosci.* 9, 843–852. doi: 10.1038/nn1701

Zhang, Y., Tohyama, K., Winterbottom, J. K., Haque, N. S., Schachner, M., Lieberman, A. R., et al. (2001). Correlation between putative inhibitory molecules at the dorsal root entry zone and failure of dorsal root axonal regeneration. *Mol. Cell. Neurosci.* 17, 444–459. doi: 10.1006/mcne.2000.0952

Zhang, Y., Zhang, X., Wu, D., Verhaagen, J., Richardson, P. M., Yeh, J., et al. (2007). Lentiviral-mediated expression of polysialic acid in spinal cord and conditioning lesion promote regeneration of sensory axons into spinal cord. *Mol. Ther.* 15, 1796–1804. doi: 10.1038/sj.mt.6300220

Zhou, S., Shen, D., Wang, Y., Gong, L., Tang, X., Yu, B., et al. (2012). microRNA-222 targeting PTEN promotes neurite outgrowth from adult dorsal root ganglion neurons following sciatic nerve transection. *PLoS One* 7:e44768. doi: 10.1371/journal.pone.0044768

Conflict of Interest Statement: The authors declare that the research was conducted in the absence of any commercial or financial relationships that could be construed as a potential conflict of interest.

frontiers in Molecular Neuroscience

ORIGINAL RESEARCH
published: 05 May 2017
doi: 10.3389/fnmol.2017.00126

MiR-30b Attenuates Neuropathic Pain by Regulating Voltage-Gated Sodium Channel Nav1.3 in Rats

Songxue Su[1†], Jinping Shao[1†], Qingzan Zhao[1], Xiuhua Ren[1], Weihua Cai[1], Lei Li[1], Qian Bai[2], Xuemei Chen[1], Bo Xu[3], Jian Wang[4], Jing Cao[1] and Weidong Zang[1]**

[1] Department of Anatomy, Basic Medical Sciences College, Zhengzhou University, Zhengzhou, China, [2] Department of Anesthesiology, The Second Affiliated Hospital of Zhengzhou University, Zhengzhou, China, [3] Department of Anesthesiology, General Hospital of Guangzhou Military Command of People's Liberation Army, Guangzhou, China, [4] Department of Anesthesiology and Critical Care Medicine, Johns Hopkins University School of Medicine, Baltimore, MD, USA

Nav1.3 is a tetrodotoxin-sensitive isoform among voltage-gated sodium channels that are closely associated with neuropathic pain. It can be up-regulated following nerve injury, but its biological function remains uncertain. MicroRNAs (miRNAs) are endogenous non-coding RNAs that can regulate post-transcriptional gene expression by binding with their target mRNAs. Using Target Scan software, we discovered that SCN3A is the major target of miR-30b, and we then determined whether miR-30b regulated the expression of Nav1.3 by transfecting miR-30b agomir through the stimulation of TNF-α or by transfecting miR-30b antagomir in primary dorsal root ganglion (DRG) neurons. The spinal nerve ligation (SNL) model was used to determine the contribution of miR-30b to neuropathic pain, to evaluate changes in Nav1.3 mRNA and protein expression, and to understand the sensitivity of rats to mechanical and thermal stimuli. Our results showed that miR-30b agomir transfection down-regulated Nav1.3 mRNA stimulated with TNF-α in primary DRG neurons. Moreover, miR-30b overexpression significantly attenuated neuropathic pain induced by SNL, with decreases in the expression of Nav1.3 mRNA and protein both in DRG neurons and spinal cord. Activation of Nav1.3 caused by miR-30b antagomir was identified. These data suggest that miR-30b is involved in the development of neuropathic pain, probably by regulating the expression of Nav1.3, and might be a novel therapeutic target for neuropathic pain.

Perspective: This study is the first to explore the important role of miR-30b and Nav1.3 in spinal nerve ligation-induced neuropathic pain, and our evidence may provide new insight for improving therapeutic approaches to pain.

Keywords: Nav1.3, miR-30b, neuropathy pain, dorsal root ganglion, spinal cord

OPEN ACCESS

Edited by:
Robert J. Harvey,
UCL School of Pharmacy, UK

Reviewed by:
Pascal Darbon,
University of Strasbourg, France
Sung Jun Jung,
Hanyang University, South Korea

****Correspondence:***
Weidong Zang
zwd@zzu.edu.cn
Jing Cao
caojing@126.com

† These authors have contributed equally to this work and should be considered co-first authors.

Received: *30 November 2016*
Accepted: *18 April 2017*
Published: *05 May 2017*

Citation:
Su S, Shao J, Zhao Q, Ren X, Cai W, Li L, Bai Q, Chen X, Xu B, Wang J, Cao J and Zang W (2017) MiR-30b Attenuates Neuropathic Pain by Regulating Voltage-Gated Sodium Channel Nav1.3 in Rats. Front. Mol. Neurosci. 10:126. doi: 10.3389/fnmol.2017.00126

INTRODUCTION

The IASP (International Association for the Study of Pain) defines pain as an unpleasant sensory and emotional experience associated with actual or potential tissue damage, or described in terms of such damage (Merskey, 1979). The approximate prevalence of neuropathic pain in the gross population is 7–10% (Bouhassira et al., 2008; de Moraes Vieira et al., 2012) and remains extremely

difficult to cure, mainly due to barely understood pathogenesis and a lack of well-defined molecular targets.

The voltage-gated sodium channels (VGSCs, Nav1.1–Nav1.9 and Nax) containing tetrodotoxin-sensitive (TTXS) channels and tetrodotoxin-resistant channels (TTX-R) are involved in the generation and propagation of action-potential (Casals-Díaz et al., 2015). Moreover, TTX-S Nav1.3 and Nav1.7, as well as the TTX-R Nav1.8 and Nav1.9 have been shown to implicate chronic neuropathic pain (Dib-Hajj et al., 2009). Nav1.3 is a subunit among the VGSCs, encoded by the SCN3A gene, and located on chromosome 2 (Estacion et al., 2010). SCN3A has a high expression in the central nervous system of embryos and newborns but is poorly expressed in adult rats (Estacion et al., 2010). Epilepsy (Guo et al., 2008; Vanoye et al., 2014), mental retardation (Bartnik et al., 2011), autism (Celle et al., 2013), and neuropathic pain (Chen et al., 2014) are perhaps caused by the aberrant expression of SCN3A. Nav1.3 is re-expressed in DRG neurons after peripheral nerve injury (Kim et al., 2001; Huang et al., 2014). Similarly, the level of Nav1.3 increases in lumbar dorsal horn neurons following SCI surgery (Hains et al., 2003; Lindia et al., 2005). In a previous study, the repression of Nav1.3 using Nav1.3-specific antisense (AS) oligodeoxynucleotide (ODN) blocked mechanical and thermal allodynia (Hains et al., 2005). However, the mechanism of altered Nav1.3 expression continues to perplex. It was reported that inhibition of the expression of NF-K B could prevent neuropathic pain by suppressing Nav1.3 re-expression in an L5-VRT model (Hains et al., 2004). Several studies focused on intrathecal lidocaine delivery to attenuate neuropathic pain through modulating Nav1.3 expression and reducing the activation of the spinal microglial (Zang et al., 2010).

Although studies have partly elucidated the mechanism of altered Nav1.3 expression, the entire, specific mechanism has not yet been made explicit. Non-coding RNA (ncRNA) regulating the expression of proteins has emerged as a target. In our study, we concerned on the relevant ncRNA that regulated the pain-related proteins. MicroRNAs (miRNAs) are endogenous ncRNAs from a single RNA precursor of 70–90 bases processed by a dicer enzyme to produce 19–25 mature nucleotides. They are responsible for the regulation of gene expression through the targeting of the gene 3′UTR (Monroig Pdel et al., 2014; Khan et al., 2015). MiRNAs are highly deregulated in diseases and might be a critical molecule for treatment, as they can be directly transfected into cells both *in vitro* and *in vivo* (Rajendiran et al., 2014; Yang et al., 2016), owing to the short nucleotide sequence (Griffiths-Jones et al., 2008).

Using Target Scan software, miR-30b, miR-96, mir-183, and miR-132 were predicted to highly relate to SCN3A. Furthermore, bioinformatics software showed that there are eight nucleotides that match miR-30b and SCN3A 3′UTR. In the present study, we focused on miR-30b, and we intended to verify whether miR-30b could regulate the expression of Nav1.3, as well as to explore the possibility that miR-30b could potentially alleviate neuropathic pain by changing the expression of Nav1.3 in DRG and the spinal cord

MATERIALS AND METHODS

Animals

Male Sprague–Dawley rats (200–250 g), with food and water ad libitum, were housed in separate cages in a clean and open room with a stable and controlled temperature and a 12 h light–dark cycle. The rats were kept for at least 7 days before the operation. The procedures for the care and use of animals followed the recommendations and guidelines of the National Institutes of Health and were approved by Zhengzhou University Animal Care and Use Committee.

Surgical Procedures and Drug Infusion

The rats underwent unilateral L5 SNL modification, as previously described (Fan et al., 2014). After the animals were anesthetized, the transverse process of the left L6 was removed to expose the L4 and L5 spinal nerves. After isolating the left L5 spinal nerve, a tight ligature was made with 3–0 silk, and the nerve was transected distal to this ligature. In the sham-operated group, the left L5 spinal nerve was separated but remained complete and unscathed with no ligature or transection.

Rats underwent intrathecal catheter implantation for drug delivery in the same manner as previously described (Liang et al., 2013). Briefly, under 2% isoflurane-induced anesthesia, a lumber laminectomy of the L5 vertebra was carried out and the dura was cut. At the location of the L4/5 spinal cord, we inserted a polyethylene-10 catheter into the subarachnoid space. An intrathecal catheter was implanted in the lumbar enlargement (close to the L4–5 segments) according to the method of Wu et al. (2004). A sudden movement of the tail or the hind limb indicated dura penetration. Following catheter implantation, the animals underwent 7 days of recovery prior to SNL or sham surgery. The rats were divided into six groups: naïve + scramble (miR-30b inhibitor N.C; 20 μM, 10 μl, GenePharma), naïve + miR-30b antagomir (a selective inhibitor of miR-30b), naïve + scramble (miR-30b agomir N.C), naïve + miR-30b agomir (a selective mimic of miR-30b), SNL + scramble (miR-30b agomir N.C) and SNL + miR-30b agomir. Beginning 1 day after naïve or 10 days after SNL surgery, continuous intrathecal infusion was delivered once a day for 4 days, from day 1 to 3 for naïve rats and from day 10 to 13 for SNL rats. Rats with neurological deficits were excluded from the experiment. The location of the intrathecal catheter was validated after the experiments (Guan et al., 2008; Xu et al., 2015).

Behavioral Tests

Mechanical Paw Withdrawal Threshold

The latency of paw withdrawal response to mechanical stimulus was determined using the up–down method, following a previously described procedure (Malmquist et al., 2012). Mechanical paw withdrawal thresholds (PWTs) were measured on days 0, 3, 7, 14, and 21 for the evaluation of SNL model or on days 0, 3, 7, 10, 11, 12, 13, and 14 during continuous miR-30b agomir injection following SNL surgery. They were measured on days 0, 1, 2, 3, and 4 during continuous miR-30b antagomir injection in naïve rats, always between 8 and 10 AM

in the morning. We placed each animal in a separate Plexiglas chamber on a raised wire screen, then we used Von Frey hairs (North Coast Medical Inc., Gilroy, CA, USA) in log increments of force (0.407, 0.692, 1.202, 2.041, 3.63, 5.495, 8.511, 15.14, and 26.0 g) to stimulate the plantar surface of the bilateral hind paws, beginning with the 2.041 g Von Frey hair. If the animal exhibited a positive reaction, the nearest smaller von Frey hair was applied; if a negative reaction was observed, the nearest larger von Frey hair was applied. The test was considered finished if one of two conditions were met: a negative reaction was acquired for the largest force (26.0 g) or three stimuli were performed after the first positive response. A formula provided by Dixon (Zang et al., 2010) was applied to convert the patterns of positive and negative reactions into a 50% threshold value (Coggeshall et al., 1997).

Thermal Paw Withdrawal Latency

The sample sizes and time points for the thermal tests were the same as those for the mechanical tests. The thermal paw withdrawal latency (PWL) was measured in the same manner as described by Kim and Chung (Coggeshall et al., 1997; Hargreaves et al., 1988; Malmquist et al., 2012). In Plexiglas chambers on a glass plate that could be heated through a hole in the light box by aiming a light beam, radiant heat was delivered to each hind paw through the glass plate, stimulating the middle of the plantar surface (UGO BASILE S.R.L., ITALY). When the rat lifted its foot, the beam of light was turned off. The time between the start of the beam of light and the lifting of the foot was considered as the PWL. Each test was repeated three times at 5 min intervals for each hind paw. A shut-off time of 15 s was applied to avoid any tissue injury.

Luciferase Assay

A dual luciferase reporter assay was performed as outlined for a previous procedure (Huang et al., 2016). The pmirGLO dual-luciferase vector (pmirGLO vector), which contained both the firefly luciferase gene and the renilla luciferase gene, was purchased from Promega (Madison, WI, USA). SCN3A 3′UTR, including the predicted binding sites of miR-30b, was inserted into the 3′UTR region downstream of the firefly luciferase gene of the pmirGLO vector (pmir-GLO-UTR). A site-directed gene mutagenesis kit (GenePharma, Shanghai, China) was used to construct the mutant type of the miR-30b binding site vector (pmirGLO-mUTR) according to the protocol provided by the manufacturer. PC12 cells were cultivated in high glucose Dulbecco's modified Eagle's medium (Solarbio, Hyclone), which contained 5% fetal bovine serum (FBS, Gibco), 5% horse serum (Gibco), and 1% antibiotics (Gibco). The cells were incubated in a humidified incubator with 5% CO_2 at 37°C. When the PC12 cells had a confluency of 70–80%, the reporter plasmids were determined to be fit to be transfected. After cultivation for 24 h, co-transfection of miRNA mimics (miR-30b agomir; GenePharma, Shanghai, China) at different doses of 10, 50, and 100 pM (50 nmol/L) with wild-type reporter vectors (0.5 μg/mL) was performed with Invitrogen lipofectamine 2000 (Invitrogen, Carlsbad, CA, USA). Then, co-transfection of other miRNAs with wild-type and mutant-type reporter vectors was conducted without serum medium or antibody as per the manufacturer's instructions. After 6 h, we replaced the medium with a high glucose medium containing 1% antibiotics and 5% FBS. After another 48 h of culture, we used 1 × passive lysis buffer to lyse the transfected cells, and 20 μL supernatant was achieved for luciferase activity using the Dual-Luciferase Reporter Assay System (Promega). The ratio of firefly activity to renilla activity was recognized as relative reporter activity. Experiments were performed in triplicate and repeated three times.

Cell Culture and Transfection

Culture and transfection of primary DRG neurons were carried out as described elsewhere (Zhao et al., 2013). Three-week-old rats were euthanized with isoflurane. All DRG neurons were collected in cold Neurobasal Medium (Gibco/ThermoFisher Scientific) with 10% FBS (JRScientific, Woodland, CA, USA), 100 μg/mL streptomycin, and 100 units/mL penicillin (Quality Biological, Gaithersburg, MD, USA). They were then treated with enzyme solution (1 mg/mL collagenase type I, 5 mg/mL dispase, in Hank's balanced salt solution, excluding Mg^{2+} and Ca^{2+} [Gibco/Thermo Fisher Scientific]). The isolated cells were resuspended in mixed Neurobasal Medium and plated in a six-well plate coated with 50 μg/mL poly-D-lysine purchased from Sigma (St. Louis, MO, USA) with a seeding density of 10^5 DRG neurons/mL. The cells were incubated at 37°C, 95% O_2, and 5% CO_2. One day later, 2 μL TNF-α (100 ng/mL, Peprotech) was added to each 2 mL well 30 min before the small miRNAs (GenePharma, Shanghai, China) were added. 100 μL Neurobasal Medium was used to dilute 5 μL (20 μM) miR-30b agomir/antagomir or 5 μL negative control (20 μM) for 5 min. One hundred microlitres Neurobasal Medium was simultaneously used to dilute 2 μL Lipofectamine 2000 (Invitrogen, Carlsbad, CA) for 5 min, then the two solutions were mixed. After 25 min, the mixture was placed into each 2 mL well and 800 Neurobasal Medium was added. The cells were collected 48 h later for PCR and western-blot examinations.

Quantitative Reverse Transcription Polymerase Chain Reaction

For the quantitative real-time reverse transcription polymerase chain reaction (RT-PCR), two unilateral DRG neurons or 100 mg spinal cord (from the left side of one animal) were pooled to obtain sufficient RNA. Total RNA was extracted using Trizol reagent (Invitrogen), treated using DNase I (New England Biolabs, Ipswich, MA, USA), and reverse transcribed with the RevertAid First Strand cDNA Synthesis Kit (Thermo). The miRNA was reverse transcribed with an miRcute miRNA First Strand cDNA Synthesis Kit (TIANGEN). A template (2 μL) was used for amplification by real-time PCR with random hexamers, oligo (dT) primers, or specific RT primers, as shown in **Table 1**. GAPDH and u6 were taken as internal controls for normalization. Each sample was run in triplicate in a 20 μL volume for reaction with 250 nM forward and reverse primers, 10 μL Thermo Scientific Maxima SYBR Green qPCR Master Mix (2×; Thermo Scientific Maxima SYBR Green qPCR Master Mix, Rox solution provided), and 20 ng total cDNA. For miRNA quantitative real-time RT-PCR, a miRcute miRNA

qPCR Detection Kit (SYBR Green, TIANGEN, Beijing, China) was used. Reactions were implemented in a 7500 Fast Real-Time PCR Detection System (Applied Biosystems, USA). The ratios of the SNL-operated mRNA level to the sham-operated mRNA level were calculated using the ÄCt method ($2^{-\ddot{A}\ddot{A}Ct}$). All SCN3A data were normalized to GAPDH, and all miR-30b data were normalized to u6, which was confirmed to be stable (Zhao et al., 2013; Huang et al., 2016).

Western Blot

To ensure a sufficient amount of protein, two unilateral rat DRG neurons were pooled together and a section of ipsilateral Lumbar enlargement was prepared. Based on established protocol (Zhao et al., 2015), tissues were homogenized in a chilled lysis buffer (10 mM Tris, 1 mM phenylmethylsulfonyl fluoride, 5 mM $MgCl_2$, 5 mM EGTA, 1 mM EDTA, 1 mM DTT, 40 μM leupeptin, 250 mM sucrose). After centrifugation at 4°C for 15 min at 1,000 × *g*, the supernatant was collected to analyze cytosolic proteins and the pellet was collected to analyze nuclear proteins. The contents of the proteins in the samples were measured using the Bio-Rad protein assay (Bio-Rad) and were then heated at 99°C for 5 min. Samples of 30 μg total protein were separated by 6% SDS-polyacrylamide gel electrophoresis and electrophoretically transferred onto a polyvinylidene difluoride membrane. After the membranes were blocked with 3% BSA (Solarbio, Beijing, China) in Tris-buffered saline containing 0.1% Tween-20 for 3 h, rabbit anti-Nav1.3 (1:300, Borson) and rabbit anti-β-actin (1:1000, Zhongshan Jinqiao, China) primary antibodies would be used. The proteins were detected using horseradish peroxidase-conjugated anti-rabbit secondary antibody (1:1000, Jackson) and visualized using Western peroxide reagent and luminol/enhancer reagent (Clarity Western ECL Substrate, Bio-Rad); the intensity exposure using t using FluorChem E (Alphalmager proteinsimple, San Jose, CA, USA). The intensity of the blots was quantified via densitometry using Image Lab software (Bio-Rad). All cytosol protein bands were normalized to β-actin.

Immunofluorescence

Rats were perfused with 4% paraformaldehyde after they were anesthetized with isoflurane for the preparation of double-labeled immunohistochemistry, as described previously (Xu et al., 2013; Wang et al., 2013). L4 and L5 DRG neurons were removed, post-fixed, and dehydrated before frozen sectioning at 16 μm. After the sections were blocked for 1–2 h in 0.01 M PBS containing 10% goat serum and 0.3% Triton X-100 at room temperature, they were incubated with the following primary antibodies over one or two nights at 4°C. The antibodies and reagents included rabbit anti-Nav1.3 (1:800, Abcam), mouse anti-NF200 (1:200, Abcam), biotinylated IB4 (1:100, Sigma), mouse anti-CGRP (1:50, Abcam), mouse anti-Gelsolin (GS; 1:200, R&D), rabbit anti-NF200 (1:200, Abcam), rabbit anti-CGRP (1:50, Abcam), and rabbit anti-Gelsolin (GS; 1:200, R&D). The sections were then incubated with either goat anti-rabbit antibody conjugated to Cy3 (1:200, Jackson Immunity Research, West Grove, PA, USA) or goat anti-mouse antibody conjugated to Cy2 (1:200, Jackson Immunity Research) for 2 h in the incubator at 37°C. All immunofluorescence-stained images were examined using a Leica DMI4000 fluorescence microscope and captured with a DFC365FX camera (Leica, Germany). Double-stained neurons were quantified manually or by using NIH Image J Software.

TABLE 1 | Primer sets used for qRT-PCR for rat samples.

Gene name	Primer sequence
SCN3A	5′-TATCCGTGTCAACTGGAC-3′ 5′-ACTTGTGGACTTAGCAAC-3′
GAPDH	5′-TCG GTG TGA ACG GAT TTG GC-3′ 5′-CCT TCA GGT GAG CCC CAG C-3′
U6	5′-GCT TCG GCA GCA CAT ATA CTA A-3′ 5′-CGA ATT TGC GTG TCA TCC TT-3′
miR-30b	5′-CCAGCAACTGTAAACATCCTACAC-3′ 5′-TATGGTTTTGACGACTGTGTGAT-3′

In Situ Hybridization

The L5 DRGs of animals were prepared for measurements and perfused intracardially with 0.01 M PBS followed by 4% cold buffered paraformaldehyde. They were sectioned at 16 μm and frozen after they were post-fixed in 4% paraformaldehyde for 30 min and dehydrated overnight in 30% sucrose at 4°C.

The rat miR-30b *in situ* hybridization Assay kit we used in this experiment was purchased from Boster Bio-Tech (Wuhan, China). The special probe sequence for miR-30b was as follows: 5′—AGCTG AGTGT AGGAT GTTTA CA—3′. We performed the experiment as per the protocol provided by the manufacturer. In brief, we first mixed 30% H_2O_2 with pure methanol in a 1:50 ratio before dropping it to each section at room temperature for 30 min, then washed three times with distilled water. 3% citric acid was added to sections to expose the mRNA (two drops pepsase in 1 mL 3% citric acid) for 2 min at room temperature. We then washed the section with PBS three times at intervals of 5 min, using distilled water during the third wash. Later, we post-fixed it with 1% paraformaldehyde 0.1 M PBS at room temperature for 10 min and washed again. We added 20 μL preliminary hybrid liquid to each section and incubated them for 2–4 h at 37°C with one humidified box of 20 mL 20% glycerin for pre-hybridization. Afterward, 20 μL hybrid liquid would be applied to them overnight in the incubator for hybridization. We then washed each section with 2 × SSC two times at an interval of 5 min and with 0.5 × SSC and 0.2 × SSC, one time each, for 15 min post-hybridization. After they were blocked for 30 min at 37°C, we incubated them with anti-rat biotin digoxin at 37°C for 60 min or at room temperature for 120 min. Finally, SABC-FITC/CY3 was used for fluorescent coloring, and the mRNA cell cytoplasm was colored green/red for visibility under a fluorescence microscope.

Statistical Analysis

The data are presented as means ± SEM. For comparisons between two groups, the *P* value was evaluated and calculated using a two-tailed paired *t*-test. When there were multiple factors involved, a two-way analysis of variance (ANOVA) was

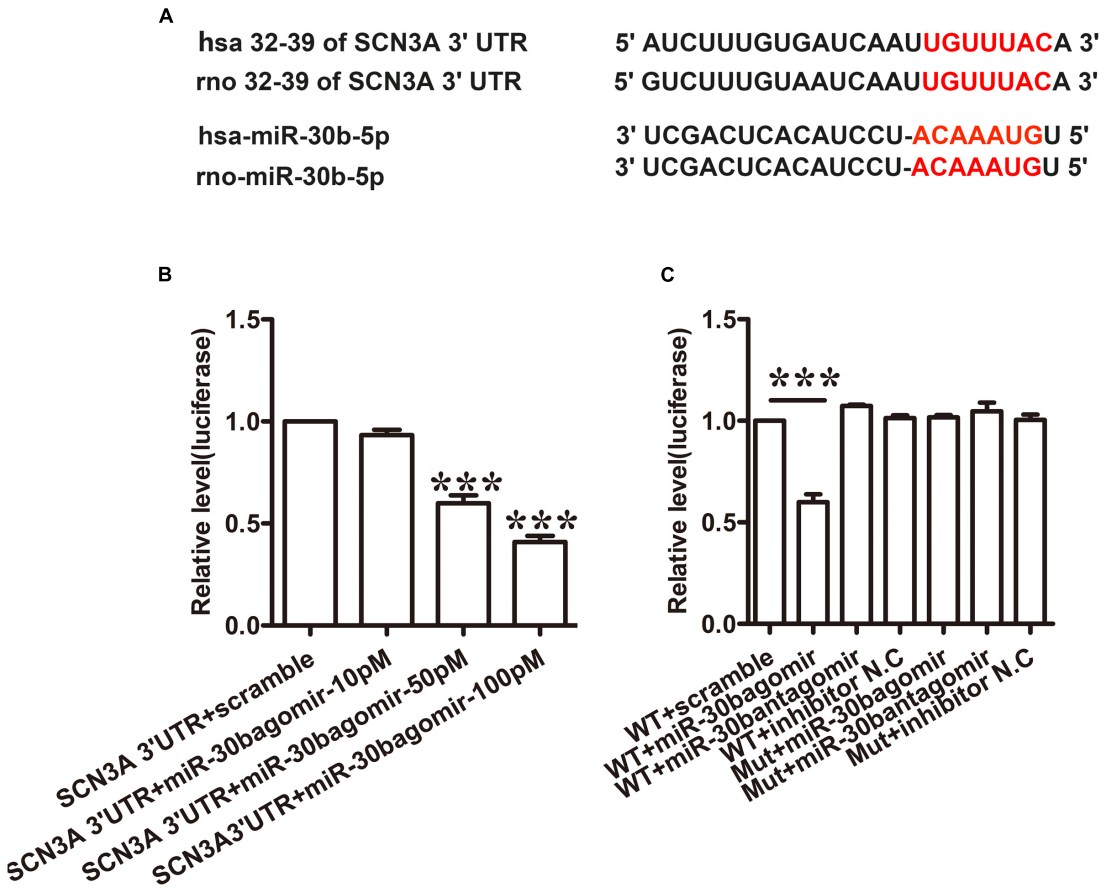

FIGURE 1 | miR-30b directly targets SCN3A 3′UTR. (A) The matched seed region between miR-30b and SCN 3′UTR predicted by Target Scan is in red. **(B)** MiR-30b agomir decreased relative luciferase activity in a dose-dependent manner with wild-type (WT) SCN3A 3′UTR plasmid vector in PC12 cells, $^{***}P < 0.0001$ vs. scramble. One-way ANOVA, $n = 3$. **(C)** Transfection of miR-30b agomir with WT SCN3A 3′UTR reduced relative luciferase activity, but no change in luciferase activity was detected in the scramble or mutant SCN3A 3′UTR group, $^{***}P < 0.0001$ vs. WT+ scramble, $n = 3$. Data are shown as means ± SEM.

used; multiple groups were compared using a one-way or two-way ANOVA. Values of $P < 0.05$ were considered statistically significant.

RESULTS

MiR-30b Directly Targets SCN3A by Binding with the 3′UTR of SCN3A in PC12 Cells

Tetrodotoxin-sensitive VGSC Nav1.3 was encoded by SCN3A. We discovered that SCN3A was the primary target of miR-30b using Target Scan software. The matched seed sequences between miR-30b-5p and SCN3A 3′UTR were highly conserved between human and rats as shown in **Figure 1A**. The Target Scan software demonstrated that the seed sequence of the miR-30b position (2–8) was paired with SCN3A 3′UTR from 32–39 bps in both humans and rats.

To verify whether miR-30b targets SCN3A 3′UTR, a dual luciferase reporter vector containing the sequence of SCN3A 3′UTR was designed (pmirGLO SCN3A 3′UTR). Transfecting the wild-type plasmid vector with three different doses of miR-30b agomir (10, 50, and 100 pM) into PC12 cells with Lipofectamine 2000, miR-30b agomir reduced relative luciferase activity in a dose-dependent manner (**Figure 1B**, $^{***}P < 0.0001$). However, the luciferase activities of miR-30b antagomir and scrambled miRNAs were unchanged (**Figure 1C**, $P > 0.05$), indicating that the inhibition of miR-30b agomir was sequence specific. To further prove the specificity of SCN3A 3′UTR, we transfected mutant 3′UTR plasmid with miR-30b agomir into PC12 cells. As expected, miR-30b had no effect on luciferase activity (**Figure 1C**).

MiR-30bagomir Transfection Is Essential to Inhibit the Expression of Nav1.3 mRNA in Primary DRG Neurons

To determine whether miR-30b may regulate the expression of Nav1.3, we used TNF-α (2 μL, 100 ng/mL) to stimulate the primary DRG neurons. 30 min later, we transfected miR-30b agomir. The levels of miR-30b and SCN3A mRNA were measured by qRT-PCR and the changes in Nav1.3 protein expression

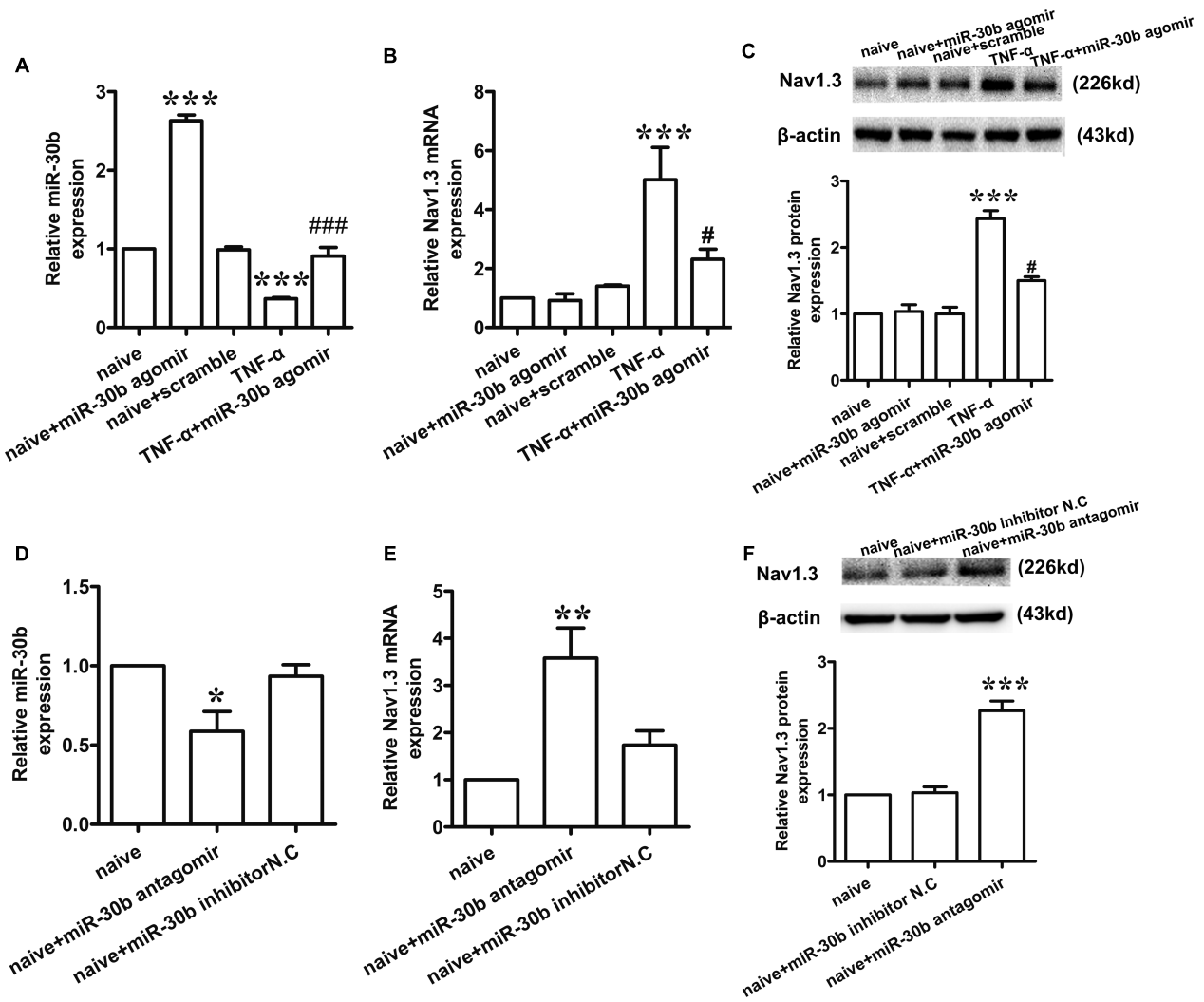

FIGURE 2 | miR-30b regulated the expression of Nav1.3 in primary cultured DRG neurons. (A–C) The relative expression of miR-30b **(A)** and Nav1.3 mRNA **(B)** and protein **(C)** treated with TNF-α and miR-30b agomir/scramble in primary cultured DRG neurons, $^{***}P = 0.0007$, $^{***}P = 0.0010$ vs. naïve, $^{\#\#\#}P < 0.0001$ vs. TNF-α; $^{***}P = 0.0003$ vs. naïve, $^{\#}P = 0.042$ vs. TNF-α; $^{***}P < 0.0001$ vs. naïve, $^{\#}P = 0.0162$ vs. TNF-α. One-way ANOVA, $n = 3$ rats. **(D–F)** The relative expression of miR-30b **(D)** and Nav1.3 mRNA **(E)** and protein **(F)** treated with miR-30b antagomir in primary cultured DRG neurons, $^{*}P = 0.0140$, $^{**}P = 0.0043$, $^{***}P = 0.0001$ vs. naïve, one-way ANOVA, $n = 3$ rats. Data are shown as means ± SEM.

were determined by western-blot. Compared to the naïve non-transfected group, TNF-α stimulation induced a significant increase in Nav1.3 at mRNA (**Figure 2B**, $^{***}P = 0.0003$) and protein level (**Figure 2C**, $^{***}P < 0.0001$), while a reduction of miR-30b was observed (**Figure 2A**, $^{***}P = 0.0007$). However, miR-30b overexpression, by transfecting miR-30b agomir, reversed the up-regulation of SCN3A (**Figure 2B**, $^{\#}P = 0.042$) and Nav1.3 (**Figure 2C**, $^{\#}P = 0.0162$) and attenuated the down-regulation of miR-30b (**Figure 2A**, $^{\#\#\#}P < 0.0001$). Moreover, miR-30b agomir transfection increased the expression of miR-30b (**Figure 2A**, $^{***}P = 0.0010$) but did not influence SCN3A (**Figure 2B**, $P = 0.73$) or Nav1.3 (**Figure 2C**, $P = 0.75$) in untreated DRG cells. In addition, we found that miR-30b antagomir transfection up-regulated Nav1.3 (**Figures 2E,F**), while it down-regulated miR-30b (**Figure 2D**, $^{*}P = 0.014$). On the other hand, the role of endogenous miR-30b in regulating Nav1.3 expression was identified in primary DRG neurons. Taken together, we demonstrated that miR-30b suppressed the expression of Nav1.3 mRNA by binding with SCN3A 3′UTR.

Up-Regulation of Nav1.3 Is Inversely Correlated with Down-Regulation of miR-30b in SNL Rats

Compared to baseline pre-injury values observed at day 0 (50% PWTs and (10–15) g PWLs and (10–15) s), L5 SNL induced a conspicuous reduction in PWTs (**Figure 3A**, $^{***}P < 0.0001$) and PWLs (**Figure 3C**, $^{***}P < 0.0001$) of the ipsilateral hindpaw of the injured side from day 3 to 21 post-SNL, but did not change the basal contralateral PWTs (**Figure 3B**, $P = 0.96$)

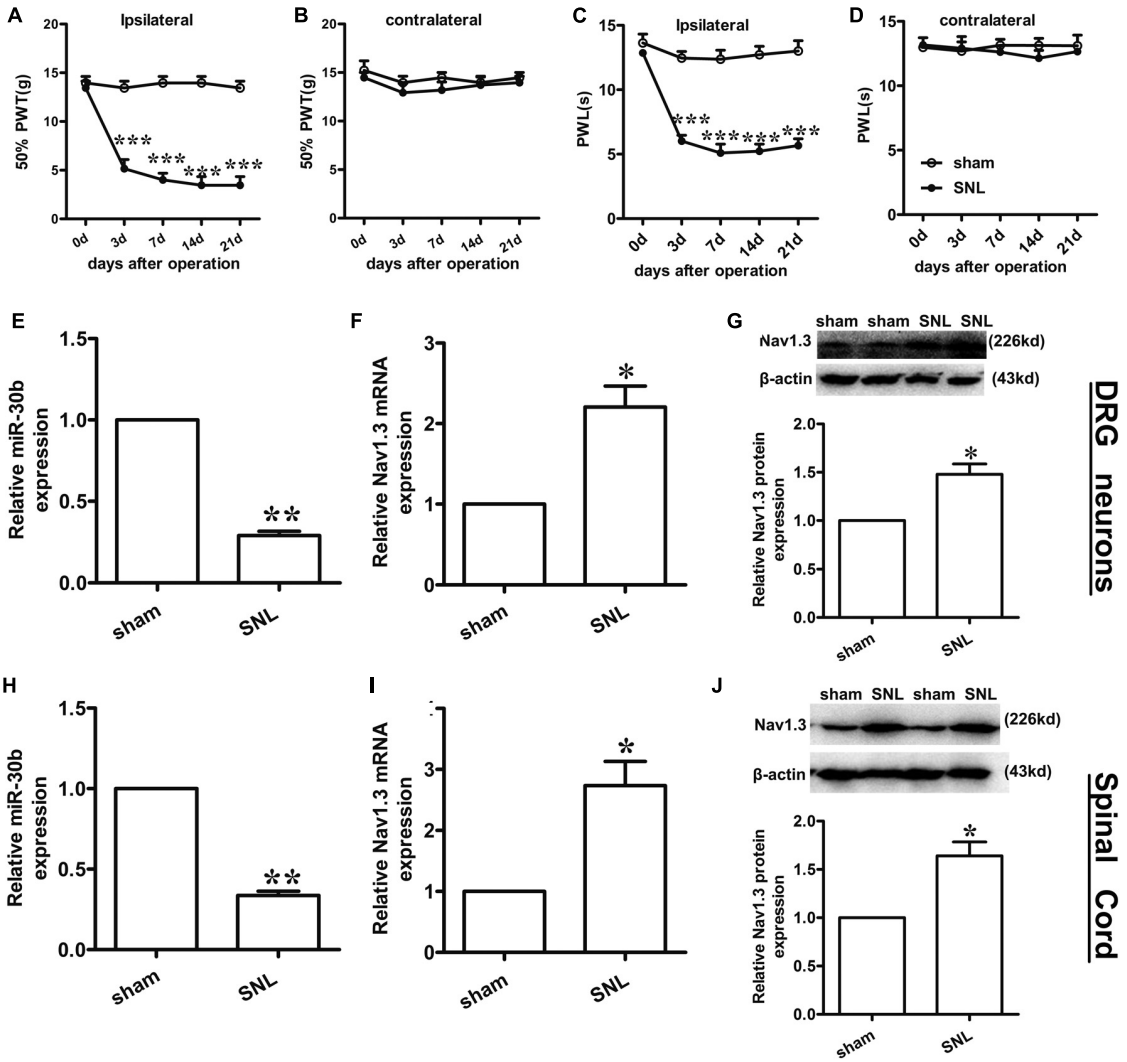

FIGURE 3 | Spinal nerve ligation-induced mechanical and thermal allodynia and the change in expression of Nav1.3 and miR-30b. (A,C) Responses of the ipsilateral paw to mechanical and thermal stimuli, $^{***}P < 0.001$ vs. sham, two-way ANOVA, $n = 6$ rats; **(B,D)** Responses of the contralateral paw to mechanical and thermal stimuli, $P > 0.05$ vs. sham, two-way ANOVA, $n = 6$ rats. **(E–G)** The decreased expression of miR-30b **(E)** and increased expression of Nav1.3 mRNA **(F)** and protein **(G)** in DRG neurons of SNL rats, $^{**}P = 0.0013$, $^{*}P = 0.043$, $^{*}P = 0.045$ vs. sham, two-tailed paired t-test, $n = 3$ rats. **(H–J)** The decreased expression of miR-30b **(H)** and increased expression of Nav1.3 mRNA **(I)** and protein **(J)** in spinal cord of SNL rats, $^{**}P = 0.0015$, $^{*}P = 0.0488$, $^{*}P = 0.0471$ vs. sham, two-tailed paired t-test, $n = 3$ rats. Data are shown as means ± SEM.

and PWLs (**Figure 3D**, $P = 0.82$) during the observation period. By comparison, no changes in the mechanical and thermal thresholds for paw withdrawal were observed in the sham-operated group.

To determine the expression of miR-30b and Nav1.3 in DRG neurons and the spinal cord of SNL rats, we performed qRT-PCR and western blot analysis (tissues were acquired at day 14 post-SNL surgery). Compared to sham-operated rats, SNL caused an obvious down regulation of miR-30b expression (**Figure 3E**, $^{**}P = 0.0013$) and up-regulation of Nav1.3 mRNA expression in DRG neurons (**Figure 3F**, $^{*}P = 0.043$) as well as in the spinal cord (**Figures 3H,I**). Western blot results showed that Nav1.3 protein strongly increased after nerve injury (**Figures 3G,J**), consistent with the data from the behavioral test. As a consequence, the increased expression of Nav1.3 mRNA and protein and the decreased expression of miR-30b in the DRG and spinal cord of SNL rats confirmed the potential ability of miR-30b to alleviate SNL-induced neuropathic pain.

MiR-30b Is Co-Localized with Nav1.3 in DRG Neurons

To define the localization of Nav1.3 and miR-30b, double-labeled immunofluorescence and *in situ* hybridization were performed in DRG neurons. As shown in **Figure 4**, we stained Nav1.3 with NF-200 (a–c), a marker of large myelinated non-nociceptive neurons, CGRP (g–i), a marker for small nociceptive peptidergic neurons, IB4 (d–f), a marker for a fraction of small, non-myelinated

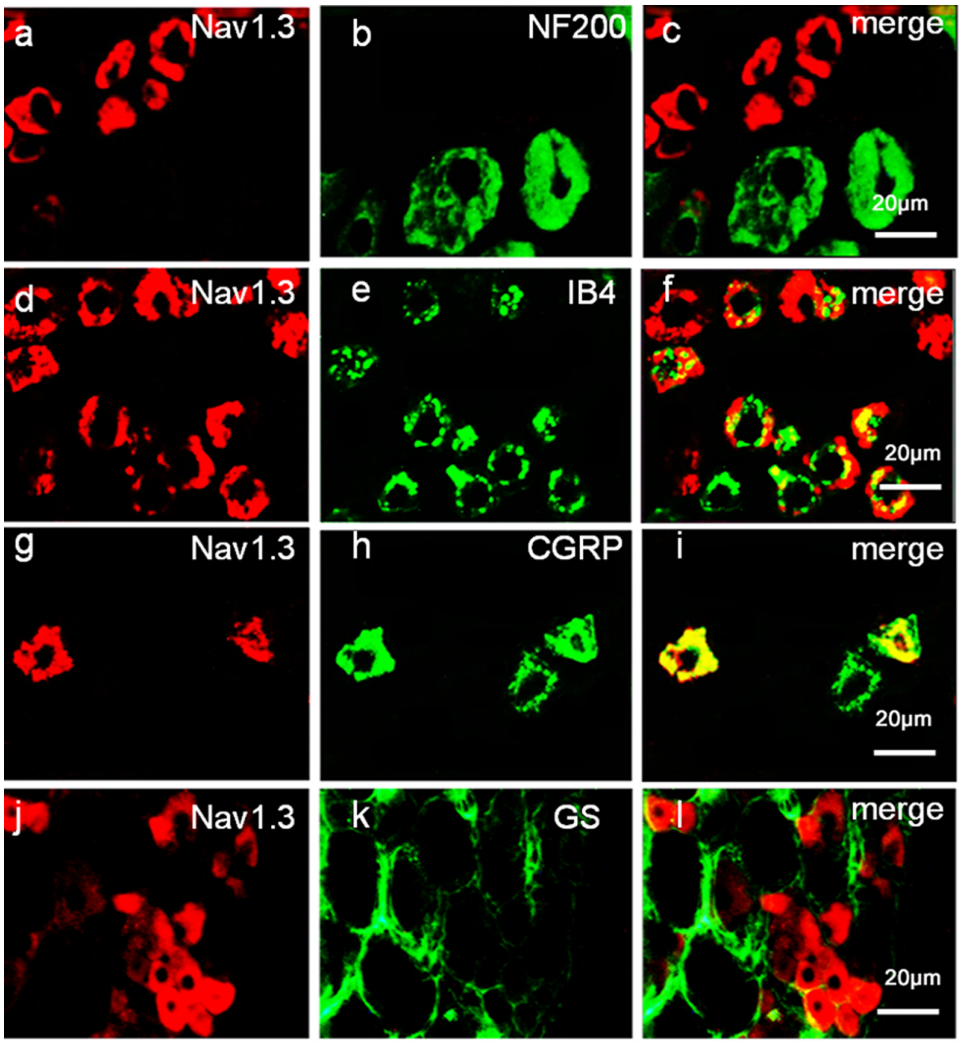

FIGURE 4 | Expression distribution of Nav1.3 protein in DRG neurons of SNL rats. Nav1.3 was double-stained with IB4 **(d–f)** and CGRP **(g–i)**; but Nav1.3 was not found to stain with NF200 **(a–c)** and GS **(j–l)**. Immunofluorescence staining of IB4 **(d–f)** and CGRP **(g–i)** show that Nav1.3 was mainly co-localized with nociceptive neuronal marker, $n = 3$ rats. Scale bar: 20 μm.

nociceptive neurons and GS (j–l), a marker for glial cells. Results showed that the Nav1.3 signal was mainly double-labeled with IB4 and CGRP (f, i) while it was not found to localize with NF-200 and GS (c, l). In **Figure 5**, *in situ* hybridization results expressed that miR-30b was double-labeled with NF200, IB4, and CGRP (f, i, l). Importantly, the cells containing miR-30b express Nav1.3 in DRG neurons (a–c), indicating a potential interaction between miR-30b and Nav1.3.

Intrathecal miR-30b Agomir Inhibits the Expression of Nav1.3 in DRG and Spinal Cord and Attenuates Neuropathic Pain in SNL Rats

To assess the exact impact of miR-30b on neuropathic pain, we delivered miR-30b agomir to SNL rats for 4 days following day 10 with intrathecal injection, and 50% PWTs and PWLs were tested. At day 10 after SNL, neuropathic pain was established ($^{***}P < 0.0001$). From day 2 following drug administration, the mechanical allodynia (**Figure 6A**) and thermal hyperalgesia (**Figure 6C**) caused by SNL were attenuated by intrathecal injection with miR-30b agomir, not scrambled miRNA, but the thresholds of the contralateral hind paw were unchanged (**Figures 6B,D**, $P > 0.05$). MiR-30b agomir did not affect the baseline of PWTs (**Figure 6A**) and PWLs (**Figure 6C**) in naïve rats.

To test whether miR-30b agomir could repress the expression of Nav1.3, we measured the expression of miR-30b and Nav1.3 by qPCR and western blot (tissues were acquired at day 14 post-SNL surgeon). MiR-30b agomir reversed the upregulation of SCN3A (**Figures 6F,I**) and downregulation of miR-30b (**Figures 6E,H**) in SNL rats. Meanwhile, in naïve rats, it increased miR-30b levels (**Figures 6E,H**) but had no influence on the expression of SCN3A ($P > 0.05$). In western-blot data, the upregulation

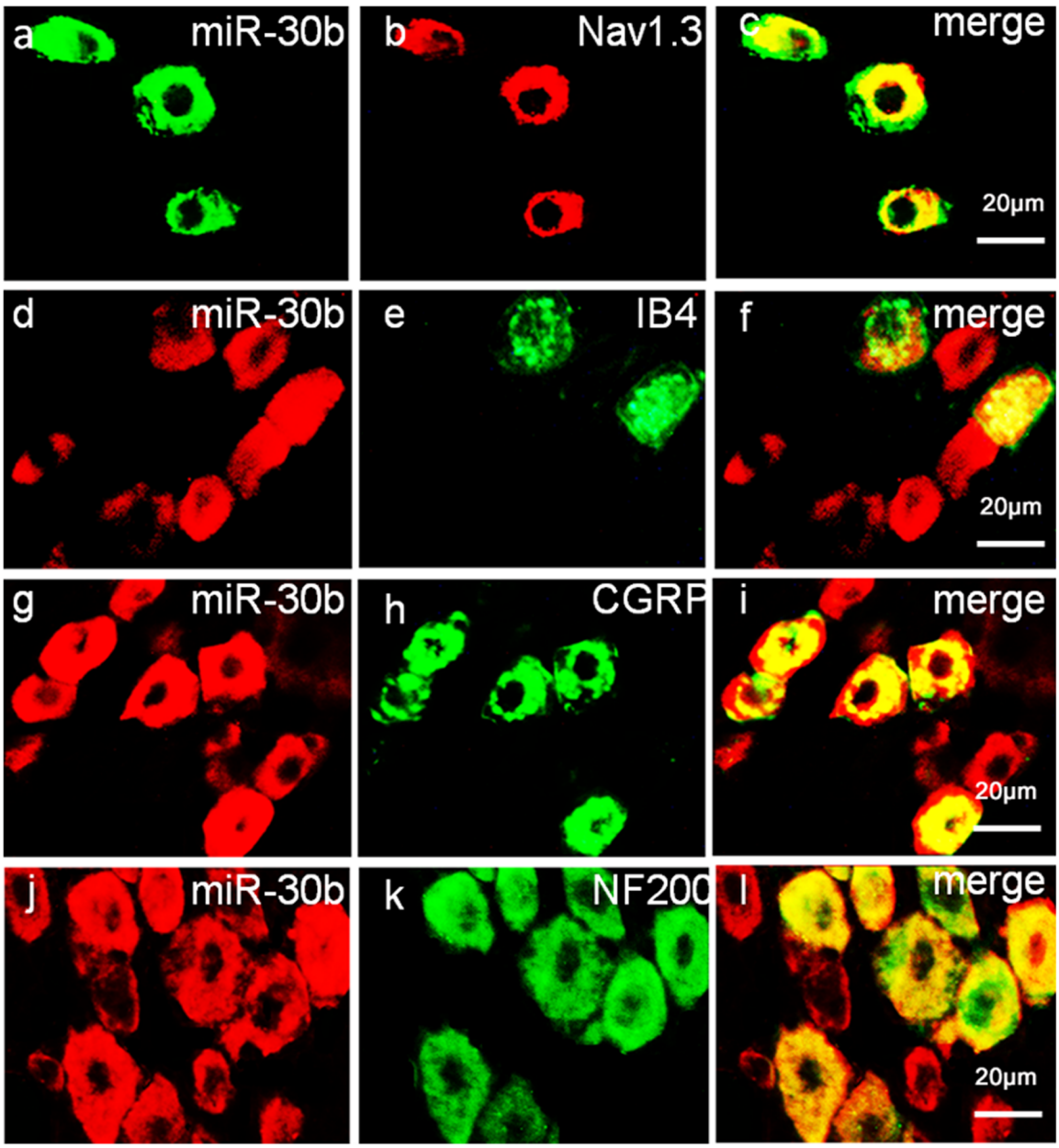

FIGURE 5 | Expression distribution of miR-30b and co-localization with Nav1.3 in DRG neurons of naïve rats. *In situ* hybridization of miR-30b and immunofluorescence staining of NF200 **(a–c)**, IB4 **(d–f)**, CGRP **(g–i)**, and NF200 **(j–l)** showed that miR-30b was co-localized with nociceptive neuronal and non-nociceptive neurons marker and miR-30b was co-localized with Nav1.3 **(a–c)**, $n = 3$ rats. Scale bars: 20 μm.

of Nav1.3 protein was effectively inhibited by miR-30b agomir in DRG neurons (**Figure 6G**, $^{*}P = 0.0303$) and spinal cord (**Figure 6J**, $^{*}P = 0.0110$) in SNL rats. In accordance with the mRNA level of Nav1.3 in naïve rats, the protein expression of Nav1.3 had no significant change between scramble and miR-30b agomir injected in spinal cord (**Figure 7C**, $P = 0.6914$). These results confirm that miR-30b overexpression reverses the upward tendency of Nav1.3 in SNL rats at the level of mRNA and protein, leading to a partial easement of pain.

Intrathecal miR-30b Antagomir Increases the Expression of Nav1.3 in Naïve Rats

To further explore the regulation of Nav1.3 by miR-30b, we down regulated miR-30b by intrathecal injection with miR-30b antagomir in naïve rats. We applied miR-30b antagomir to naïve rats for 4 days and determined their sensitivity to mechanical and thermal stimulus. We found that the threshold values for mechanical and thermal stimulus were significantly lower during miR-30b antagomir delivery than those of naïve rats injected with

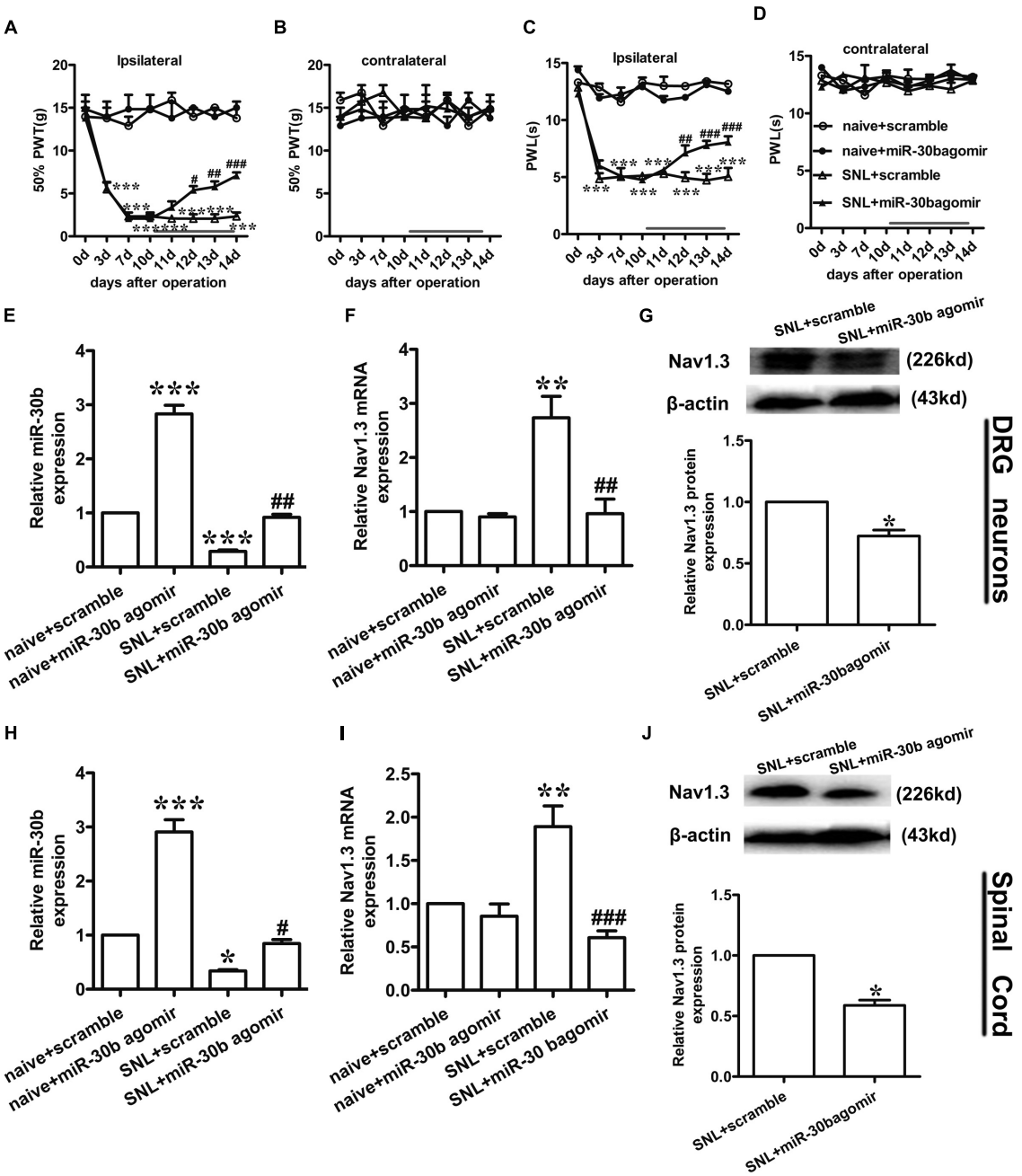

FIGURE 6 | miR-30b agomir down regulated Nav1.3 and alleviated neuropathic pain. (A,C) Ipsilateral paw withdrawal to mechanical and thermal thresholds, $^{***}P < 0.001$ vs. naïve + scramble; $^{\#}P = 0.025$, $^{\#\#}P = 0.0062$, $^{\#\#\#}P = 0.00048$; $^{\#}P = 0.032$, $^{\#\#\#}P = 0.00053$, $^{\#\#\#}P = 0.00025$ vs. SNL + scramble, two-way ANOVA, $n = 6$ rats. **(B,D)** Contralateral paw withdrawal to mechanical and thermal thresholds, $P > 0.05$ vs. naïve + scramble; $P > 0.05$ vs. SNL + scramble, two-way ANOVA, $n = 6$ rats. **(E,F)** The relative expression of miR-30b **(E)** and SCN3A **(F)** with intrathecal miR-30b agomir in DRG neurons of SNL rats was determined by qRT-PCR, $^{**}P < 0.01$, $^{***}P < 0.001$ vs. naïve + scramble; $^{\#\#}P = 0.0034$, $^{\#\#}P = 0.0018$ vs. SNL + scramble, one-way ANOVA, $n = 3$ rats. **(G)** Nav1.3 protein expression in DRG neurons of SNL rats at 14 days injected with intrathecal miR-30b agomir, $^{*}P = 0.0303$ vs. SNL + scramble, two-tailed paired t-test, $n = 3$ rats. **(H,I)** The relative expression of miR-30b **(H)** and SCN3A **(I)** with intrathecal miR-30b agomir in spinal cord of SNL rats, $^{*}P < 0.05$, $^{**}P < 0.01$ $^{***}P < 0.001$ vs. naïve + scramble; $^{\#}P = 0.0366$, $^{\#\#\#}P = 0.00087$ vs. SNL + scramble, one-way ANOVA, $n = 3$ rats. **(J)** Nav1.3 protein expression in spinal cord of SNL rats at 14 days injected with intrathecal miR-30b agomir, $^{*}P = 0.0110$ vs. SNL + scramble, two-tailed paired t-test, $n = 3$ rats. Data are shown as means ± SEM.

scrambled miRNAs (**Figures 7A,B**), demonstrating that miR-30b antagomir produced pain behaviors in naïve rats. Furthermore, ipsilateral L4-L5 DRGs and spinal cord were acquired at day 4 in order to assess expression of Nav1.3 at the mRNA and protein levels. Down regulation of miR-30b (**Figures 7D,G**) induced increases in Nav1.3 mRNA in DRG neurons (**Figure 7E**,

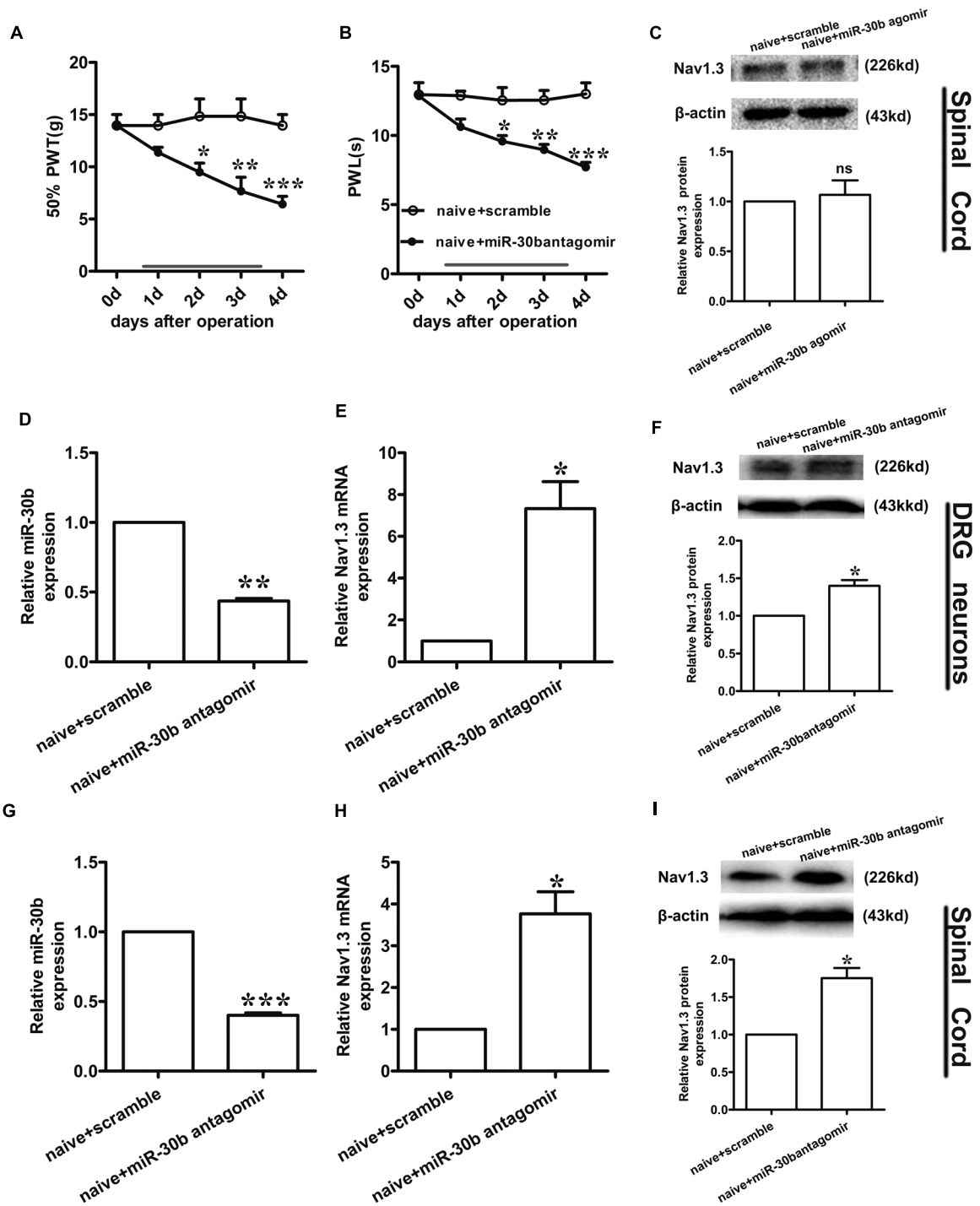

FIGURE 7 | Nav1.3 was upregulated by miR-30b antagomir with pain behaviors. (A,B) Responses to mechanical and thermal stimulus, $^{*}P < 0.05$, $^{**}P < 0.01$, $^{***}P < 0.001$ vs. naïve + scramble, two-way ANOVA, $n = 6$ rats. **(C)** Nav1.3 protein expression in spinal cord of rats injected with miR-30b agomir, $P = 0.6914$ vs. naïve + scramble, two-tailed paired t-test, $n = 3$ rats. **(D,E)** The relative mRNA expression of miR-30b **(D)** and SCN3A **(E)** with intrathecal miR-30b antagomir in DRG neurons of naïve rats, $^{*}P = 0.0394$, $^{**}P = 0.0011$ vs. naïve + scramble, one-way ANOVA, $n = 3$ rats. **(F)** Nav1.3 protein expression in DRG neurons of naïve rats at 4 days injected with intrathecal miR-30b antagomir, $^{*}P = 0.0341$ vs. naïve + scramble, two-tailed paired t-test, $n = 3$ rats. **(G,H)** The relative mRNA expression of miR-30b **(G)** and SCN3A **(H)** with intrathecal miR-30b antagomir in spinal cord of naïve rats, $^{*}P = 0.0344$, $^{***}P = 0.0009$ vs. naïve + scramble, one-way ANOVA, $n = 3$ rats. **(I)** Nav1.3 protein expression in spinal cord of naïve rats at 4 days injected with intrathecal miR-30b antagomir, $^{*}P = 0.0309$ vs. naïve + scramble, two-tailed paired t-test, $n = 3$ rats. Data are shown as means ± SEM.

$^{**}P = 0.0011$) and in spinal cord (**Figure 7H**, $^{*}P = 0.0344$), as well as in protein expression (**Figures 7F,I**).

DISCUSSION

Nav1.3, an isform of the tetrodotoxin-sensitive (TTX-S) VGSC, was capable of producing sodium ion currents with rapid repriming dynamics that can facilitate neuronal hyperexcitability, enhanced repetitive firing characteristics and ectopic discharge in injured neurons (Waxman and Hains, 2006). Nav1.3 has been reported to be upregulated in different pain states, such as STZ-induced pain (Tan et al., 2015), nerve transection and chronic constriction injury models (CCI) of neuropathic pain with pain behaviors (Hains et al., 2005; Samad et al., 2013; Chen et al., 2014). Downregulation of Nav1.3 mRNA and protein through intrathecal administration of AS ODNs can decrease neuronal hyperexcitability and alleviate mechanical allodynia and thermal hyperalgesia following Spinal Cord Injury (SCI) (Hains et al., 2003). Samad et al. (2013) showed that knockdown of Nav1.3 was able to relieve neuropathic pain. Accordingly, in the present study, the expression of Nav1.3 mRNA and protein increased in SNL rats, not only in DRG neurons (**Figures 3F,G**; Hains et al., 2005; Samad et al., 2013; Chen et al., 2014) but also in the spinal cord (**Figures 3I,J**). In comparison to Hains et al. (2003), which stated that Nav1.3 expression was increased in the spinal cord following SCI, the increased Nav1.3 expression we observed in the spinal cord in SNL rats was likely a consequence of the increased expression in DRG neurons that end up in superficial layers of the spinal cord. But we preferred another explanation, as it appeared that peripheral nerve injury induced central hyperalgesia through some signaling pathways or inflammatory cytokines, leading to the up-regulation of Nav1.3 in spinal dorsal horn neurons. However, the underlying mechanism was still unknown, which would require further experiments to prove. Additionally, Nav1.3 was mostly double-labeled with IB4 and CGRP (**Figures 4F,I**), which are markers of C fibers that are essentially involved in nociceptive information transfer. These findings, together with our results, strongly suggested that Nav1.3 played a crucial role in neuropathic pain. Despite recent advances, understanding the transcriptional or translational regulatory mechanisms underlying the changes in expression and function of Nav1.3 remained a major challenge.

In recent years, non-coding RNAs have been extensively researched. NcRNAs participate in the regulation of numerous cellular processes, which might modulate disease onset, progression and prognosis. MiRNAs have widely existed *in vivo*, and were implicated in the post-transcription regulation of gene expression by repressing mRNA translation or inhibiting mRNA and protein degradation (Bartel, 2004; Lutz et al., 2014). There has been a focus on studies that have associated miRNAs with chronic neuropathic pain states. MiR-132 was upregulated in SNI rats (Leinders et al., 2016), while miR-182, miR-183, miR-96 decreased in SNL rats (Aldrich et al., 2009). In particular, miR-96 was also involved in CCI model (Chen et al., 2014). These findings provide us with information that we can use to identify major players in neuropathic pain mechanisms.

Using Target Scan software, miR-30b, miR-96, miR-183, and miR-132 were found to target SCN3A. In a recent study, miR-183 and miR-96 were observed a significant down-regulation with the increase of Nav1.3 expression in L5 DRG after SNL, which were abundant in DRG neurons (Aldrich et al., 2009; Lin et al., 2014), overexpression of miR-183 and miR-96 were capable to attenuate neuropathic pain by repressing Nav1.3. During the study, we focused on miR-30b and attempted to explore the potential role of miR-30b and SCN3A in SNL rats. Through Luciferase assay we verified that miR-30b negatively regulated SCN3A by combining with SCN3A 3′UTR (**Figure 1B**). As expected, the transfection of scrambled miRNA or mutant SCN3A 3′UTR was not able to change the Firefly/Rellia ratio significantly (**Figures 1B,C**, $P > 0.05$), indicating that miR-30b and the 3′UTR of SCN3A were specific. Moreover, immunofluorescence and *in situ* hybridization determined that miR-30b was co-localized with Nav1.3 in rat DRGs (**Figure 5**), providing evidence for the interaction between miR-30b and Nav1.3.

TNF-α that could increase VGSC mRNA quantity and the number of available channels in the plasma membrane was used to stimulate the primary DRG neurons. In accordance with Chen et al. (2015), Nav1.3 was increased at both the mRNA and protein levels at the stimulation of TNF-α. The increased expression of Nav1.3 (**Figures 2B,C**) proved that the enhanced excitability of neurons induced by TNF-α was mediated by the up-regulation of Nav1.3. Consistently (Zang et al., 2011), administration of rrTNF to primary DRG neurons induced Nav1.3 re-expression. Furthermore, increased Nav1.3 levels were inhibited by the transfection of miR-30b agomir (**Figure 2B**, $^{\#}P = 0.042$; **Figure 2C**, $^{\#}P = 0.0162$). Hence, miR-30b was validated to regulate Nav1.3 at transcription level. Meanwhile, transfecting miR-30b agomir did not alter the level of SCN3A in naïve DRG neurons (**Figure 2C**, $P = 0.75$; **Figure 7C**, $P = 0.6914$), which seemed to be ambivalent with the results we acquired from TNF-α treated group or from SNL rats, however, it did match with the characteristics of SCN3A, which was almost undetectable in adult neurons (Estacion et al., 2010), consequently, miR-30b agomir failed to induce changes in the expression of SCN3A in naïve rats.

Similar to our previous study (Shao et al., 2016), miR-30b was proved to ease neuropathic pain by regulating SCN9A after SNI. In the present study, we demonstrated that miR-30b alleviated pain by inhibiting SCN3A through the evaluation of behaviors and changes in molecular levels in SNL rats. The observed pain-related behaviors were consistently recovered (**Figures 3A,C**), meanwhile, the increased expression of Nav1.3 was found to reverse (**Figures 3F,G,I,J**) with intrathecal administration miR-30b agomir in SNL rats, which just verified that a single miRNA was able to act on multiple target genes. The finding that Nav1.3 and Nav1.7 were both regulated by miR-30b in neuropathic pain emphasized the importance role of miR-30b in different models of neuropathic pain, implying that miR-30b might be a practicable drug target for the treatment of

neuropathic pain. Likewise, one gene was likely to be targeted by multiple miRNAs. SCN3A was not only targeted by miR-30b, but also controlled by miR-183 and miR-96 in SNL rat DRGs (Aldrich et al., 2009). These accumulated evidence revealed that miR-30b and SCN3A were crucial players in neuropathic pain, thus, illustrating the potential mechanism would provide a new direction and serviceable theoretical foundation for the clinical intervention of neuropathic pain.

Moreover, we found that intrathecal administration of miR-30b antagomir contributed to pain behaviors (**Figures 7A,B**) and the up-regulation of Nav1.3 (**Figures 7E,F**, DRG neurons; H,I, spinal cord) in naïve rats. In conformity to previous report (Leinders et al., 2016), intrathecal injection of miR-132-3p mimetic dose-dependently produced pain behavior in naïve rats, miR-132-3p was reported to up-regulated in neuropathic pain, which was in contrast to miR-30b. Even so, the effect of miR-30b antagomir was not unsustainable given the momentariness, along with miR-30b agomir, which have to be settled urgently.

There are some limitations in our study. Firstly, the upstream molecules of miR-30b remain uncertain. Secondly, miR-30b was involved in neuropathic pain by targeting several proteins, and we did not evaluate all of the possible targets of miR-30b. Thirdly, Nav1.3 was reported to take part in STZ-induced pain (Tan et al., 2015) and Nav1.7 was changed in inflammatory pain (Yeomans et al., 2005), but whether miR-30b participated in STZ-induced pain or inflammatory pain by targeting SCN3A or SCN9A confused us. Prominently, it is essential to supplement patch clamp recording in our follow-up work because of the contribution of VGSCs to physiological and pathophysiological electrical signaling (McCormack et al., 2013). However, it did address the fact that miR-30b directly regulated SCN3A and further demonstrated that miR-30b had a potential use for the therapy invention for the treatment of neuropathic pain.

CONCLUSION

We found that miR-30b directly targeted SCN3A 3′UTR both *in vitro* and *in vivo*, and that miR-30b alleviated neuropathic pain by suppressing the expression of Nav1.3 in DRG neurons and spinal cord following SNL. These findings indicate that miR-30b is involved in the regulation of neuropathic pain by targeting Nav1.3, which might be a potential therapeutic target for neuropathic pain.

AUTHOR CONTRIBUTIONS

WZ and JC conceived the project, supervised all experiments, and wrote manuscript. SS and JS designed the project, researched data, and wrote manuscript. QZ, XR, and WC researched data and reviewed/edited manuscript. LL, QB, XC, BX, and JW reviewed/edited manuscript. All authors read and approved the final manuscript. SS and JS contributed equally to this study.

FUNDING

This work was supported by the National Natural Science Foundation of China (grant number 81671071 and 81471144), the Outstanding Young Talent Research Fund of Zhengzhou University (No.1421328058), the Youth Development Foundation of Zhengzhou University (No. JCYXY2016-YQ-10), and the National Institutes of Health (R01 NS078026 and R01 AT007317).

ACKNOWLEDGMENT

We thank Jiarui Wang for assistance with this manuscript.

REFERENCES

Aldrich, B. T., Frakes, E. P., Kasuya, J., Hammond, D. L., and Kitamoto, T. (2009). Changes in expression of sensory organ-specific microRNAs in rat dorsal root ganglia in association with mechanical hypersensitivity induced by spinal nerve ligation. *Neuroscience* 164, 711–723. doi: 10.1016/j.neuroscience.2009.08.033

Bartel, D. P. (2004). MicroRNAs: genomics, biogenesis, mechanism, and function. *Cell* 116, 281–297. doi: 10.1016/S0092-8674(04)00045-5

Bartnik, M., Chun-Hui Tsai, A., Xia, Z., Cheung, S. W., and Stankiewicz, P. (2011). Disruption of the SCN2A and SCN3A genes in a patient with mental retardation, neurobehavioral and psychiatric abnormalities, and a history of infantile seizures. *Clin. Genet.* 80, 191–195. doi: 10.1111/j.1399-0004.2010.01526.x

Bouhassira, D., Lanteri-Minet, M., Attal, N., Laurent, B., and Touboul, C. (2008). Prevalence of chronic pain with neuropathic characteristics in the general population. *Pain* 136, 380–387. doi: 10.1016/j.pain.2007.08.013

Casals-Díaz, L., Casas, C., and Navarro, X. (2015). Changes of voltage-gated sodium channels in sensory nerve regeneration and neuropathic pain models. *Restor. Neurol. Neurosci.* 33, 321–334. doi: 10.3233/RNN-140444

Celle, M. E., Cuoco, C., Porta, S., Gimelli, G., and Tassano, E. (2013). Interstitial 2q24.3 deletion including SCN2A and SCN3A genes in a patient with autistic features, psychomotor delay, microcephaly and no history of seizures. *Gene* 532, 294–296. doi: 10.1016/j.gene.2013.09.073

Chen, H. P., Zhou, W., Kang, L. M., Yan, H., Zhang, L., Xu, B. H., et al. (2014). Intrathecal miR-96 inhibits Nav1.3 expression and alleviates neuropathic pain in rat following chronic construction injury. *Neurochem. Res.* 39, 76–83. doi: 10.1007/s11064-013-1192-z

Chen, W., Sheng, J., Guo, J., Gao, F., Zhao, X., Dai, J., et al. (2015). Tumor necrosis factor-α enhances voltage-gated Na^+ currents in primary culture of mouse cortical neurons. *J. Neuroinflammation* 12:126. doi: 10.1186/s12974-015-0349-x

Coggeshall, R. E., Zhou, S., and Carlton, S. M. (1997). Opioid receptors on peripheral sensory axons. *Brain Res.* 764, 126–132. doi: 10.1016/S0006-8993(97)00446-0

de Moraes Vieira, E. B., Garcia, J. B., da Silva, A. A., Mualem Araujo, R. L., and Jansen, R. C. (2012). Prevalence, characteristics, and factors associated with chronic pain with and without neuropathic characteristics in Sao Luis, Brazil. *J. Pain Symptom Manage.* 44, 239–251. doi: 10.1016/j.jpainsymman.2011.08.014

Dib-Hajj, S. D., Black, J. A., and Waxman, S. G. (2009). Voltage-gated sodium channels: therapeutic targets for pain. *Pain Med.* 10, 1260–1269. doi: 10.1111/j.1526-4637.2009.00719.x

Estacion, M., Gasser, A., Dib-Hajj, S. D., and Waxman, S. G. (2010). A sodium channel mutation linked to epilepsy increases ramp and persistent current of

Nav1.3 and induces hyperexcitability in hippocampal neurons. *Exp. Neurol.* 224, 362–368. doi: 10.1016/j.expneurol.2010.04.012

Fan, L., Guan, X., Wang, W., Zhao, J. Y., Zhang, H., Tiwari, V., et al. (2014). Impaired neuropathic pain and preserved acute pain in rats overexpressing voltage-gated potassium channel subunit Kv1.2 in primary afferent neurons. *Mol. Pain* 10:8. doi: 10.1186/1744-8069-10-8

Griffiths-Jones, S., Saini, H. K., van Dongen, S., and Enright, A. J. (2008). MiRBase: tools for microRNA genomics. *Nucleic Acids Res.* 36, D154–D158. doi: 10.1093/nar/gkm952

Guan, Y., Johanek, L. M., Hartke, T. V., Shim, B., Tao, Y.-X., Ringkamp, M., et al. (2008). Peripherally acting mu-opioid receptor agonist attenuates neuropathic pain in rats after L5 spinal nerve injury. *Pain* 138, 318–329. doi: 10.1016/j.pain.2008.01.004

Guo, F., Yu, N., Cai, J. Q., Quinn, T., Zong, Z. H., Zeng, Y. J., et al. (2008). Voltage-gated sodium channel Nav1.1, Nav1.3 and beta1 subunit were up-regulated in the hippocampus of spontaneously epileptic rat. *Brain Res. Bull.* 75, 179–187. doi: 10.1016/j.brainresbull.2007.10.005

Hains, B. C., Klein, J. P., Saab, C. Y., Craner, M. J., Black, J. A., and Waxman, S. G. (2003). Upregulation of sodium channel Nav1.3 and functional involvement in neuronal hyperexcitability associated with central neuropathic pain after spinal cord injury. *J. Neurosci.* 23, 8881–8892.

Hains, B. C., Saab, C. Y., Klein, J. P., Craner, M. J., and Waxman, S. G. (2004). Altered sodium channel expression in second-order spinal sensory neurons contributes to pain after peripheral nerve injury. *J. Neurosci.* 24, 4832–4839. doi: 10.1523/JNEUROSCI.0300-04.2004

Hains, B. C., Saab, C. Y., and Waxman, S. G. (2005). Changes in electrophysiological properties and sodium channel Nav1.3 expression in thalamic neurons after spinal cord injury. *Brain* 128(Pt 10), 2359–2371. doi: 10.1093/brain/awh623

Hargreaves, K., Dubner, R., Brown, F., Flores, C., and Joris, J. (1988). A new and sensitive method for measuring thermal nociception in cutaneous hyperalgesia. *Pain* 32, 77–88. doi: 10.1016/0304-3959(88)90026-7

Huang, X. J., Li, W. P., Lin, Y., Feng, J. F., Jia, F., Mao, Q., et al. (2014). Blockage of the upregulation of voltage-gated sodium channel nav1.3 improves outcomes after experimental traumatic brain injury. *J. Neurotrauma* 31, 346–357. doi: 10.1089/neu.2013.2899

Huang, Y., Li, Y., Wang, F. F., Lv, W., Xie, X., and Cheng, X. (2016). Over-expressed miR-224 promotes the progression of cervical cancer via targeting RASSF8. *PLoS ONE* 11:e0162378. doi: 10.1371/journal.pone.0162378

Khan, H. A., Zhao, Y., Wang, L., Li, Q., Du, Y. A., Dan, Y., et al. (2015). Identification of miRNAs during mouse postnatal ovarian development and superovulation. *J. Ovarian Res.* 8, 44. doi: 10.1186/s13048-015-0170-2

Kim, C. H., Oh, Y., Chung, J. M., and Chung, K. (2001). The changes in expression of three subtypes of TTX sensitive sodium channels in sensory neurons after spinal nerve ligation. *Brain Res. Mol.* 95, 153–161. doi: 10.1016/S0169-328X(01)00226-1

Leinders, M., Üçeyler, N., Pritchard, R. A., Sommer, C., and Sorkin, L. S. (2016). Increased miR-132-3p expression is associated with chronic neuropathic pain. *Exp. Neurol.* 283, 276–286. doi: 10.1016/j.expneurol.2016.06.025

Liang, L., Tao, B., Fan, L., Yaster, M., Zhang, Y., and Tao, Y. X. (2013). mTOR and its downstream pathway are activated in the dorsal root ganglion and spinal cord after peripheral inflammation, but not after nerve injury. *Brain Res.* 1513, 17–25. doi: 10.1016/j.brainres.2013.04.003

Lin, C.-R., Chen, K.-H., Yang, C.-H., Huang, H.-W., and Sheen-Chen, S.-M. (2014). Intrathecal miR-183 delivery suppresses mechanical allodynia in mononeuropathic rats. *Eur. J. Neurosci.* 39, 1682–1689. doi: 10.1111/ejn.12522

Lindia, J. A., Kohler, M. G., Martin, W. J., and Abbadie, C. (2005). Relationship between sodium channel nav1.3 expression and neuropathic pain behavior in rats. *Pain* 117, 145–153. doi: 10.1016/j.pain.2005.05.027

Lutz, B. M., Bekker, A., and Tao, Y. X. (2014). Noncoding RNAs: new players in chronic pain. *Anesthesiology* 121, 409–417. doi: 10.1097/ALN.0000000000000265

Malmquist, N. A., Moss, T. A., Mecheri, S., Scherf, A., and Fuchter, M. J. (2012). Small-molecule histone methyltransferase inhibitors display rapid antimalarial activity against all blood stage forms in *Plasmodium falciparum*. *Proc. Natl. Acad. Sci. U.S.A.* 109, 16708–16713. doi: 10.1073/pnas.1205414109

McCormack, K., Santos, S., Chapman, M. L., Krafte, D. S., Marron, B. E., West, C. W., et al. (2013). Voltage sensor interaction site for selective small molecule inhibitors of voltage-gated sodium channels. *Proc. Natl. Acad. Sci. U.S.A.* 110, E2724–E2732. doi: 10.1073/pnas.1220844110

Merskey, H. (1979). Pain terms a list with definitions and notes on usage recommended by the IASP subcommittee on taxonomy. *Pain* 6, 249–252.

Monroig Pdel, C., Pasculli, B., and Calin, G. A. (2014). MicroRNAome genome: a treasure for cancer diagnosis and therapy. *CA Cancer J. Clin.* 64, 311–336. doi: 10.3322/caac.21244

Rajendiran, S., Parwani, A. V., Hare, R. J., Dasgupta, S., Roby, R. K., and Vishwanatha, J. K. (2014). MicroRNA-940 suppresses prostate cancer migration and invasion by regulating MIEN1. *Mol. Cancer* 13:250. doi: 10.1186/1476-4598-13-250

Samad, O. A., Tan, A. M., Cheng, X., Foster, E., Dib-Hajj, S. D., and Waxman, S. G. (2013). Virus-mediated shRNA knockdown of nav1.3 in rat dorsal root ganglion attenuates nerve injury-induced neuropathic pain. *Mol. Ther.* 21, 49–56. doi: 10.1038/mt.2012.169

Shao, J., Cao, J., Wang, J., Ren, X., Su, S., Li, M., et al. (2016). MicroRNA-30b regulates expression of the sodium channel nav1.7 in nerve injury-induced neuropathic pain in the rat. *Mol. Pain* 12:1744806916671523. doi: 10.1177/1744806916671523

Tan, A. M., Samad, O. A., Dib-Hajj, S. D., and Waxman, S. G. (2015). Virus-mediated knockdown of nav1.3 in dorsal root ganglia of STZ-induced diabetic rats alleviates tactile allodynia. *Mol. Med.* 21, 544–552. doi: 10.2119/molmed.2015.00063

Vanoye, C. G., Gurnett, C. A., Holland, K. D., George, A. L. Jr., and Kearney, J. A. (2014). Novel SCN3A variants associated with focal epilepsy in children. *Neurobiol. Dis.* 62, 313–322. doi: 10.1016/j.nbd.2013.10.015

Wang, J., Yu, L., Jiang, C., Chen, M., Ou, C., and Wang, J. (2013). Bone marrow mononuclear cells exert long-term neuroprotection in a rat model of ischemic stroke by promoting arteriogenesis and angiogenesis. *Brain Behav. Immun.* 34, 56–66. doi: 10.1016/j.bbi.2013.07.010

Waxman, S. G., and Hains, B. C. (2006). Fire and phantoms after spinal cord injury: Na^+ channels and central pain. *Trends Neurosci.* 29, 207–215. doi: 10.1016/j.tins.2006.02.003

Wu, W. P., Xu, X. J., and Hao, J. X. (2004). Chronic lumbar catheterization of the spinal subarachnoid space in mice. *J. Neurosci. Methods* 133, 65–69. doi: 10.1016/j.jneumeth.2003.09.015

Xu, J., Wang, H., Ding, K., Lu, X., Li, T., Wang, J., et al. (2013). Inhibition of cathepsin S produces neuroprotective effects after traumatic brain injury in mice. *Mediat. Inflamm.* 2013:187873. doi: 10.1155/2013/187873

Xu, J.-T., Sun, L., Marie Lutz, B., Bekker, A., and Tao, Y.-X. (2015). Intrathecal rapamycin attenuates morphine-induced analgesic tolerance and hyperalgesia in rats with neuropathic pain. *Transl. Perioper. Pain Med.* 2, 27–34.

Yang, C. H., Wang, Y., Sims, M., Cai, C., He, P., Yue, J., et al. (2016). MiRNA203 suppresses the expression of protumorigenic STAT1 in glioblastoma to inhibit tumorigenesis. *Oncotarget* 7, 84017–84029. doi: 10.18632/oncotarget.12401

Yeomans, D. C., Levinson, S. R., Peters, M. C., Koszowski, A. G., Tzabazis, A. Z., Gilly, W. F., et al. (2005). Decrease in inflammatory hyperalgesia by herpes vector-mediated knockdown of nav1.7 sodium channels in primary afferents. *Hum. Gene Ther.* 16, 271–277. doi: 10.1089/hum.2005.16.271

Zang, Y., He, X. H., Xin, W. J., Pang, R. P., Wei, X. H., Zhou, L. J., et al. (2010). Inhibition of NF-kappaB prevents mechanical allodynia induced by spinal ventral root transection and suppresses the re-expression of nav1.3 in DRG neurons in vivo and in vitro. *Brain Res.* 1363, 151–158. doi: 10.1016/j.brainres.2010.09.048

Zang, Y., Xin, W. J., Pang, R. P., Li, Y. Y., and Liu, X. G. (2011). Upregulation of nav1.3 channel induced by rrTNF in cultured adult rat DRG neurons via p38 MAPK and JNK pathways. *Chin. J. Physiol.* 54, 241–246. doi: 10.4077/CJP.2011.AMM075

Zhao, X., Tang, Z., Zhang, H., Atianjoh, F. E., Zhao, J. Y., Liang, L., et al. (2013). A long noncoding RNA contributes to neuropathic pain by silencing Kcna2 in primary afferent neurons. *Nat. Neurosci.* 16, 1024–1031. doi: 10.1038/nn.3438

Zhao, X., Wu, T., Chang, C. F., Wu, H., Han, X., Li, Q., et al. (2015). Toxic role of prostaglandin E2 receptor EP1 after intracerebral hemorrhage in mice. *Brain Behav. Immun.* 46, 293–310. doi: 10.1016/j.bbi.2015.02.011

Conflict of Interest Statement: The authors declare that the research was conducted in the absence of any commercial or financial relationships that could be construed as a potential conflict of interest.

frontiers in
MOLECULAR NEUROSCIENCE

REVIEW ARTICLE
published: 19 September 2014
doi: 10.3389/fnmol.2014.00076

Biology of adeno-associated viral vectors in the central nervous system

Giridhar Murlidharan[1,2], Richard J. Samulski[2,3]* and Aravind Asokan[2,4]*

[1] *Curriculum in Genetics and Molecular Biology, School of Medicine, University of North Carolina at Chapel Hill, Chapel Hill, NC, USA*
[2] *Gene Therapy Center, School of Medicine, University of North Carolina at Chapel Hill, Chapel Hill, NC, USA*
[3] *Department of Pharmacology, School of Medicine, University of North Carolina at Chapel Hill, Chapel Hill, NC, USA*
[4] *Department of Genetics and Department of Biochemistry and Biophysics, School of Medicine, University of North Carolina at Chapel Hill, Chapel Hill, NC, USA*

Edited by:
George Smith, Temple University School of Medicine, USA

Reviewed by:
Eldi Schonfeld-Dado, Stanford University, USA
Armin Blesch, University Hospital Heidelberg, Germany

****Correspondence:***
Richard J. Samulski and Aravind Asokan, Gene Therapy Center, School of Medicine, University of North Carolina at Chapel Hill, Chapel Hill, NC 27599-7352, USA
e-mail: rjs@med.unc.edu; aravind@med.unc.edu

Gene therapy is a promising approach for treating a spectrum of neurological and neurodegenerative disorders by delivering corrective genes to the central nervous system (CNS). In particular, adeno-associated viruses (AAVs) have emerged as promising tools for clinical gene transfer in a broad range of genetic disorders with neurological manifestations. In the current review, we have attempted to bridge our understanding of the biology of different AAV strains with their transduction profiles, cellular tropisms, and transport mechanisms within the CNS. Continued efforts to dissect AAV-host interactions within the brain are likely to aid in the development of improved vectors for CNS-directed gene transfer applications in the clinic.

Keywords: adeno-associated virus (AAV), viral vectors, gene therapy, neurological disorders, neurodegenerative diseases

INTRODUCTION

Numerous congenital disorders exhibit distinct manifestations in the central nervous system (CNS). Loss of functionality in affected cell types within the brain can often be attributed to defects in single genes. For instance, a range of neurological disorders arise from the inability of cells in the CNS to break down metabolic end products [e.g., lysosomal storage disorders (LSDs)]. One such example of LSDs with fatal manifestations includes globoid-cell leukodystrophy (GLD) or Krabbe disease in which mutations in galactosylceramidase leads to accumulation of the toxin "psychosine" in the CNS (Wenger et al., 2002). This disease shows early onset of symptoms like demyelination, astrocyte gliosis etc., and progresses to the death of patients within 2 years of age (Lin et al., 2005). Other examples of LSDs include Fabry disease, Gaucher disease, GM1/GM2 gangliosidosis, mucopolysaccharidoses disorders, Pompe disease, and neuronal ceroid lipofuscinosis amongst others (Boustany, 2013; Simonato et al., 2013).

Another broad category is neurodegenerative disorders, where functionally distinct neuronal subpopulations are lost due to genetic predispositions or environmental toxins. Commonly known examples of this category include dopaminergic (DA) neuronal loss in Parkinson's disease and GABAergic neuronal loss in Huntington's disease (Orr and Zoghbi, 2007; Irwin et al., 2013). A common feature for most of these diseases is severe impairment of combinations of cognitive, motor and sensory functions, leading to loss of quality of life and ultimately death of the patients. Gene therapy holds promise for treating these severely debilitating disorders by delivering healthy cargo of genetic information to specific cell types in the CNS. In particular, adeno-associated viruses (AAVs) have emerged as promising tools for clinical gene transfer in a broad range of genetic disorders with neurological manifestations (Gray, 2013). In this review, we have attempted to bridge our understanding of the capsid biology of different AAVs with their properties such as transduction efficiencies, cellular tropism and transport within the CNS.

RECOMBINANT ADENO-ASSOCIATED VIRAL VECTORS

Adeno-associated viruses are non-enveloped, helper-dependent parvoviruses with an icosahedral capsid architecture ~25 nm in diameter. AAVs package ~4.7 kb genome flanked by ~145 bp inverted terminal repeats (ITRs) on the 5′ and 3′ ends (Bowles et al., 2006). The wildtype AAV (wtAAV) genome is a linear single stranded DNA consisting of two open reading frames (ORFs). AAV ORFs encode four replication proteins (Rep) and three capsid proteins (Cap/VP) and an assembly activating protein (AAP; Agbandje-McKenna and Kleinschmidt, 2011). In addition, wtAAV requires co-infection by adenoviruses or herpes simplex viruses (HSVs) for successful replication and production of viable AAV particles (Bowles et al., 2006). Three advancements have been instrumental in enabling the use of AAV as a recombinant vector for gene transfer applications: (a) the ability to pseudotype AAV vectors by employing AAV capsids of natural or synthetic origin (Gao et al., 2002, 2004; Rabinowitz et al., 2002; Vandenberghe et al., 2009); (b) cloning and characterization of adenoviral helper genes that are minimally required for generation of infectious AAV particles (Xiao et al., 1998); and (c) understanding that ITRs are the only *cis*-acting molecular signature for successful packaging of a transgene within an AAV capsid (Xiao et al., 1997). These streamlined components are now used to manufacture recombinant AAV (rAAV) vectors packaging a broad spectrum of promoter elements and transgene cassettes for different gene

transfer applications (Grieger et al., 2006). It is noteworthy that due to the aforementioned discoveries, we are now able to manufacture AAV vectors with minimal contamination of the wildtype virions.

Different AAV serotypes exhibit a range of properties pertaining to antigenicity, *in vivo* tropism and receptor interactions based on their capsid structures (Agbandje-McKenna and Kleinschmidt, 2011). Capsids of different AAV strains bind a spectrum of cell surface glycan receptors and utilize co-receptors for infection (Huang et al., 2014). These differences in capsid-receptor interactions play a major role in determining the regional and cellular transduction efficiencies of AAV strains across different mammalian organs. Continued progress in understanding the biology of AAV infection over the past two decades has provided the scientific and clinical community with an arsenal of AAV strains that offer desirable features for CNS gene transfer (Lentz et al., 2012). In addition to natural isolates, several laboratory-derived AAV strains have been engineered or evolved for specific CNS gene transfer applications. These efforts have yielded novel AAV vectors for targeting (a) glioblastoma cells (Maguire et al., 2010); (b) rat, mouse and human neural stem cells (Jang et al., 2011); and (c) specific regions (piriform cortex and ventral hippocampus) of blood–brain barrier (BBB) compromised rats (Gray et al., 2010). We discuss the existing inventory of AAV vectors and their characterization within the CNS below.

BIOLOGY OF AAV CELL ENTRY AND IMPLICATIONS FOR CNS GENE TRANSFER

Successful transduction by AAV vectors is contingent on many key steps like cell surface receptor binding, endocytic uptake, endosomal escape, subsequent nuclear entry, capsid uncoating, genome release, second strand synthesis, and subsequent transcription. Surface exposed regions on the AAV capsids dictate the interactions with the host cell surface (Huang et al., 2014). Cell surface glycans have been identified as the preferred primary receptors for many natural AAVs (Asokan et al., 2012). Accordingly, differences in glycan architecture have been attributed to variations in the efficiency of gene transfer by AAV capsids in different organs. AAV serotypes 1, 5, and 6 bind *N*-linked sialic acid (SA), whereas AAV4 is the only natural AAV isolate that binds *O*-linked SA moieties on mammalian cell surfaces (Kaludov et al., 2001; Walters et al., 2001; Wu et al., 2006b). AAV2, three and six bind heparan sulfate (HS) proteoglycans, whereas AAV9 requires N-terminal galactose residues to perform successful gene transfer (Summerford and Samulski, 1998; Handa et al., 2000; Bell et al., 2011; Shen et al., 2011). Direct injection of HS binding AAV2 in the CNS leads to a largely neuronal transduction profile, whereas SA binding vectors like AAV1 and AAV5 perform efficient neuronal and some glial transduction (Bartlett et al., 1998; Davidson et al., 2000; Mandel and Burger, 2004). The preferential neuronal tropism of AAV2 was later identified to correlate with the comparatively larger availability of heparan sulfate proteoglycans (HSPGs) on the surface of neurons than glia (Hsueh et al., 1998; Hsueh and Sheng, 1999). Interestingly, in addition to enabling the neurotropic bias of AAV2, HS binding has also been associated with restriction of the CNS volume that is effectively targeted by AAV vectors.

It is now known that the lysine residue at position 531 on AAV6 capsid plays an indispensable role in HS binding (Kawamoto et al., 2005; Wu et al., 2006a). By creating HS binding and non-binding variants of AAV1 (AAV1E531K) and AAV6 (AAV6K531E) respectively, Arnett et al. (2013) demonstrated antagonistic effect of HS binding on CNS transduction of intracranially injected AAVs. Supporting these point mutation studies, co-injection of safe doses of soluble heparin also led to substantial increase in CNS transduction by AAV2 (Nguyen et al., 2001; Mastakov et al., 2002). On the other hand, N-terminal galactose binding AAV9 is one of the most efficient vectors for CNS gene transfer. AAV9 has been shown to perform extensive neuronal and glial transduction from different routes of injection in small and large animal models (Cearley and Wolfe, 2007; Foust et al., 2009; Bevan et al., 2011; Dayton et al., 2012; Ahmed et al., 2013; Benkhelifa-Ziyyat et al., 2013; Iwata et al., 2013; Yamashita et al., 2013). In addition to important features on the capsid surfaces, efficiency of AAV vector mediated gene transfer can be affected by several post-entry, trafficking and genome-related events within the CNS. Studies pertaining to some of these aspects of AAV biology have been performed within the context of the CNS and discussed later. First we discuss how different AAV strains are influenced by the route of CNS administration below.

DIRECT AAV ADMINISTRATION INTO THE CNS

Direct injections of AAV into the CNS have been used to achieve high levels of transgene expression across different animal models (McCown et al., 1996; Chamberlin et al., 1998; Tenenbaum et al., 2004; Bockstael et al., 2012). This strategy of AAV vector administration can be broadly classified into intra-cerebrospinal fluid (CSF) administration and intra-parenchymal administration. The CSF plays a multi-functional role by providing nutrients; molecular and physical cues for important processes like stem cell migration; and removal of interstitial solutes from the brain parenchyma (Sawamoto et al., 2006; Iliff et al., 2012). The CSF is housed within the subarachnoid space, cerebral ventricles, cisterna magna and openings under the cerebellum (foramena), and is in close contact with the spinal cord and brain tissue in the rostrocaudal axis (Koh et al., 2005; Lehtinen et al., 2013). Understandably, efficient delivery of reporter/therapeutic transgenes to large areas of the CNS has been achieved using AAV injections into cerebral ventricles, cisterna magna, or intravertebral lumbar puncture (Davidson et al., 2000; Passini and Wolfe, 2001; Fu et al., 2003, 2007; Liu et al., 2005b; Cabrera-Salazar et al., 2010; Glascock et al., 2012; Rafi et al., 2012; Samaranch et al., 2012, 2013; Chakrabarty et al., 2013). Serotypes such as AAV9 and rh.10 exhibit inherently superior ability to spread within the brain parenchyma. These vectors have been used to achieve widespread and long term expression of corrective transgenes from intra-CSF injections toward disease models of spinal muscular atrophy and Krabbe disease (Glascock et al., 2012; Rafi et al., 2012). On the other hand, some AAV vectors exhibit highly cell-specific transduction profiles from intra-CSF injections. For instance, intracerebroventricular (ICV) administration of AAV4 leads to selective targeting of astrocytes in the k zone surrounding the cerebral ventricles (Davidson et al., 2000; Liu et al., 2005a,b). The ependyma consists of adult neural stem cells that have the

ability to perform lifelong migration, differentiation and repopulation of functionally defined regions in the brain (Alvarez-Buylla and Lim, 2004). Indeed, targeted delivery of neurogenic cargo, e.g., noggin and brain derived neurotrophic factor (BDNF) packaged in AAV4 has shown long-term rescue of mouse models of severely debilitating CNS disorders like Huntington's disease (Liu et al., 2005b; Benraiss et al., 2012). In addition to these *in vivo* studies, biophysical analysis of the AAV4 capsid has revealed distinct structural features and low capsid homology among other natural AAV isolates (Padron et al., 2005; Govindasamy et al., 2006).

Due to the advantages offered by the CSF connectivity of the brain and the spinal cord, AAV vector administration has also been extensively characterized through intrathecal injections (ITs). Traditionally, these injections have been performed by exposing the subarachnoid space at the suboccipital cisterna magna region or the intravertebral space at lumbar region. In general, applications requiring enhanced transduction at the motor, sensory and nociceptive neuronal subpopulations [e.g., within dorsal root ganglia (DRG)] utilize lumbar punctures. AAV serotypes 1, 5, 8, and 9 have shown extensive transduction in the spinal cord and DRG neurons from IT injections at the intravertebral lumbar region (Vulchanova et al., 2010; Hirai et al., 2012; Jacques et al., 2012). In an independent study, Snyder et al. (2011) compared IT injections of AAV vectors 1, 6, 8, and 9 for transduction of motor neurons in the spinal cord and brain stem, and reported superior transduction properties of AAV6 and 9. From studies conducted in large animals like pigs and non-human primates (NHPs), a single IT injection of AAV9 has emerged as the candidate procedure for clinical correction of motor neuron disorders affecting the different regions of the spinal cord (Federici et al., 2012; Gray et al., 2013). As with all these studies, it remains to be seen how vectors pseudotyped with these different capsids respond in a human setting and more importantly, in manifestations of human brain disease.

Direct parenchymal injections of AAV vectors in rodents and NHPs have been traditionally used to achieve transduction within, focused, spatio-functionally distinct regions of the brain (Burger et al., 2004; Lin et al., 2005; Cearley and Wolfe, 2006). AAV2 shows minimal ability to spread from the parenchymal site of injection and performs preferential gene transfer in the neurons (Davidson et al., 2000). Unlike other capsid-receptor interactions, the high affinity for HSPGs has been shown to be detrimental to the spread of AAV2 in the brain parenchyma (Mastakov et al., 2002). As discussed earlier, another vector that lacks the ability to spread from the site of intracerebral injection is the NHP isolate AAV4 (Davidson et al., 2000). In another study performed in adult rats, Burger et al. (2004) demonstrated that *N*-linked SA binding AAV1 and AAV5 are superior to AAV2 in terms of spread of transduction from a single parenchymal microinjection into the hippocampus, substantia nigra, globus pallidus, striatum, and spinal cord. Widespread transgene expression was also achieved by parenchymal injections of AAV7, 8 and 9 in rodents (Broekman et al., 2006; Cearley and Wolfe, 2006). On a cellular level, these vectors preferentially transduced neurons in the adult rodents from clinically relevant stereotaxic injections into the hippocampus, thalamus, cortex and striatum (Cearley and Wolfe, 2006). Interestingly, in addition to capsid serotype, other parameters like age of the animal also seem to affect cellular tropism of AAV vectors from direct brain injections. Using ICV injections of AAVs 1, 8, and 9, Chakrabarty et al. (2013) demonstrated, that injections performed on postnatal day 0 (P0) leads to preferential neuronal tropism. On the other hand the same vectors showed neuronal and astrocytic transduction profiles from injections performed on P1 or later. Against this backdrop of AAV isolates and serotypes that have been extensively characterized for their receptor interactions, novel AAV serotypes isolated from human beings – AAVhu32, 37, 11, 48R3; and NHPs – AAVrh.8 and 10 have been evaluated in neonatal and adult rodents (Cearley and Wolfe, 2007; Cearley et al., 2008). Preliminary studies have confirmed the ability of these vectors to perform transduction comparable to AAV9 in rodents, expanding the AAV vector toolkit for CNS gene transfer. For instance, a recent study conducted head to head comparison of AAV 2, 5, 8, and rh.10 for therapeutic delivery of functional "CLN2" transgene in a late infantile neuronal ceroid lipofuscinosis (LINCL) mouse model. Among different serotypes, AAVrh.10 demonstrated comparatively larger spread of transgene expression and restoration of functional levels of the enzyme tripeptidyl-peptidase I, originally lost as a result of mutations in the CLN2 gene. Improvement in motor activities like gait, balance and grip; and amelioration of seizures led to enhanced survival of the treated mice from a single direct brain parenchymal injection (Sondhi et al., 2007). More recent studies evaluating AAVrh.10 administered through different routes in primates have been reviewed in detail in the context of AAV transport within the CNS below.

INTRAVENOUS ADMINISTRATION OF AAV VECTORS FOR CNS GENE TRANSFER

Systemic administration of vectors has the potential to achieve ubiquitous gene transfer of the CNS from a single injection. Additionally, the minimally invasive nature of intravenous (IV) injections adds value to clinical administration of AAV vectors via the bloodstream. Two major roadblocks currently impede our ability to utilize this technique for therapeutic gene transfer of the CNS. The first major concern is the broad biodistribution of AAV vector particles into off-target tissues such as the liver, spleen and kidneys during IV administration of AAVs. For instance, IV injections of AAV9 achieves exceptional transduction of neurons and glia in rodents and NHPs, but also leads to enrichment of viral genomes (∼10 fold or more) in the liver and spleen as compared to the brain (Gray et al., 2011). Careful optimization and use of safe dosages of AAV vectors can lead to reduced systemic leakage and associated viral clearance due to neutralizing antibodies (Gray et al., 2011). Another approach to reduce peripheral organ toxicity is the occlusion of blood flow into organs like liver and spleen during IV injections of AAVs (Bevan et al., 2011). Clearly, the use of such techniques requires meticulous optimization of complicated surgical procedures during vector administration before being approved for the clinic. However, it should also be noted that several of these techniques are already approved for use with other drugs/treatments in the clinical setting. Another important problem is the inability of the majority of well-characterized AAV vectors to efficiently cross

the BBB and transduce cells within the CNS. In order to successfully transduce cells in the CNS, systemically injected virions are thought to undergo receptor mediated transport to cross the brain microvasculature. However, the exact mechanism(s), paracellular or transcellular remain to be determined. Tight junctions in the endothelial cells, astrocytic endfeet and pericytes are known to collectively constitute the BBB (Zhang et al., 2011; Yang et al., 2014). Intra-arterial infusion of mannitol leads to transient opening of the BBB without eliciting any permanent damage (Fu et al., 2003). Short-term disruption of these checkpoints by administration of mannitol led to effective CNS transduction by IV injections of AAV2 which is unable to cross the BBB (Fu et al., 2003; McCarty et al., 2009).

A recent study compared CNS transduction from injections of AAVs 1, 2, 5, 6, 7, 9, Rh.10, Rh.39, and Rh.43 into the superficial temporal vein of neonatal mice (P1). Successful, but differential levels of CNS transduction were reported from all tested vectors (except AAVs 2 and 5; Zhang et al., 2011). Additionally, some leading examples of AAV vectors that have been tested in adult rodents and NHPs include AAVs 8, 9, Rh.8, and Rh.10 (Shen et al., 2013; Yang et al., 2014). These results clearly indicate that many AAV serotypes have been associated with a range of cellular and regional CNS gene transfer properties from systemic injections. In this regard, a better understanding of capsid structural motifs that allow certain AAV strains to traverse the BBB is critical. For instance, using directed evolution, Gray et al. (2010) have engineered two AAV capsids capable of crossing seizure compromised-BBB in rats. The original library of AAVs from which the candidate capsid was isolated included AAVs 1–6, 8, and 9. Careful assessment of the parental and evolved capsid sequences might provide further insights into capsid domains possibly involved in CNS transduction after IV administration (Gray et al., 2010). Along similar lines, peptide motifs have been identified that impart AAV capsids with the ability to cross the brain microvasculature. IV injection of a peptide modified version of the AAV2 packaging β-glucuronidase was used to achieve significant clearance of lysosomal storage burden, leading to cognitive benefits and prolonged survival in a mucopolysacharidoses VII mouse model (Chen et al., 2012). It is noteworthy that IV administration of the corrective transgene packaged in AAV9 capsid was unable to confer therapeutic benefits. It was later identified using fluorescein labeled *Sambucus nigra* lectin that enhanced SA depositions in the MPS VII affected mouse CNS might be detrimental for AAV9-mediated CNS transduction (Chen et al., 2012). Such results demonstrate that the biology of different AAV strains can be affected by specific disease phenotypes that alter the molecular composition(s) of different cell types within the brain.

AAV TRANSPORT WITHIN THE CNS

Subsequent to vector administration and engagement of cell surface attachment factors such as glycans, AAV vectors appear to undergo interstitial as well as intracellular transport within the CNS. For instance, recent studies in the primate brain have demonstrated that AAVrh.10 displays distinct transduction patterns following different routes of administration (Rosenberg et al., 2014). Of the five routes tested, delivery to parenchyma resulted in more efficient gene transfer than intraventricular or intraarticular routes of administration. Another study in marmosets demonstrated that IV administration of AAVrh.10 is capable of efficient CNS transduction (Yang et al., 2014). These results highlight the potential diversity in AAV vector transport mechanisms not only in the context of brain physiology, but also possibly due to vector serotype, receptor usage and animal models. Although not completely understood, two mechanisms, namely paravascular CSF transport and axonal transport appear to play a role in controlling the spread of AAV vectors within the CNS. It has been established that the paravascular transport of CSF plays a major role in the spread of interstitial fluid (ISF) within the CNS. One of the earliest studies demonstrated that proteins accumulate along highly vascularized regions of forebrain and brainstem within minutes of ICV injections (Rennels et al., 1985). Further, medically induced blood pressure fluctuations have been directly shown to control the spread of nanoparticles including AAVs in the brain (Hadaczek et al., 2006). The brain is distinct from other organs in that it lacks lymphatic circulation (Cserr et al., 1992; Abbott, 2004). To understand compensatory mechanisms, Iliff et al. (2012) performed CNS-injections of differently sized (between 750 da and 2000 kda) molecular tracers. Using compelling visual evidence provided by 2-photon microscopy, the authors concluded that paravascular movement of CSF clears solutes from the CNS (Iliff et al., 2012). Specifically, the para-arterial influx and the paravenous efflux of subarachnoid CSF drain accumulations of metabolic end products and other solutes within the brain parenchyma. These results suggest that mechanisms like the CSF transport can possibly play a role in determining the extent of spread of viruses within the CNS. Clearly, understanding the structure-function correlates of AAV capsids and host factors that might dictate their ability to spread in the brain against the backdrop of CNS physiology will be valuable.

Another known pathway that viruses utilize to spread within the CNS is axonal transport post-entry into host neurons. Viruses can travel long distances by getting transported across synaptic connections in various sectors of mammalian central and peripheral nervous system (Beier et al., 2011; Taylor et al., 2012). Over the years, HSV and pseudorabies virus (PRV) have been used to visualize axonal transport and the resulting patterns of viral infections in the CNS milieu (Granstedt et al., 2013). Although accurate neuronal tracing has been achieved using these viruses, a major disadvantage is the loss of gene expression and neuronal death observed in the labeled cells between 5 days and 2 weeks post-infection (Wickersham et al., 2007; Osakada et al., 2011; Rothermel et al., 2013). In case of AAVs, both unidirectional and bidirectional axonal transport has been observed depending on the viral strain (Hollis et al., 2008; Salegio et al., 2013). During retrograde transport, intact virions are taken up at the axonal projections and are transported to the neuronal cell body (soma), where the virus enters the nucleus to perform transduction. Conversely, a successful anterograde transport requires virions to enter the neuronal soma and travel along the length of the axon to finally get released at the projections. The released virions are then free to transduce new cellular subpopulations in the region.

Understandably, directional axonal transport of AAV can be utilized to achieve safe and targeted gene delivery in spatially and functionally distinct neuronal subpopulations. For instance, AAV2 specifically undergoes anterograde transport (Kells et al., 2009; Ciesielska et al., 2011). On the other hand, AAV6 exhibits exclusive retrograde transport in both rat and primate brain (San Sebastian et al., 2013). In addition, AAV9 has been shown to efficiently travel in both anterograde and retrograde directions (Masamizu et al., 2011; Low et al., 2013; Castle et al., 2014b). Specifically, Castle et al. (2014b) visualized dye-conjugated AAV9 vectors during their anterograde and retrograde movements within cultured rat cortical neurons. These studies showed that axonal transport of AAV9 occurs in Rab7 positive late endosomal/lysosomal compartments. Further, cytoplasmic dynein and kinesin-2 were identified as being critical for successful retrograde and anterograde transport, respectively (Castle et al., 2014a,b).

SAFETY ASPECTS

Recombinant AAV vector genomes display inefficient integration into the host chromosome and predominantly persist in episomal form (McCarty et al., 2004). This reduces the risk of insertional mutagenesis, often associated with other viral vectors like retroviruses (Bokhoven et al., 2009). The vector genomes subsequently require the host cellular machinery to carry out second strand synthesis, transcription and translation (Duan et al., 1998; Nash et al., 2008). Safety aspects pertaining to persistence of AAV vector genomes in the CNS are forthcoming and have been reviewed in general elsewhere (McCarty et al., 2004; Lentz et al., 2012; Dismuke et al., 2013). Another important safety consideration is the observation that rAAV mediated overexpression of non-self transgenes can elicit immune responses due to antigen presentation of the expressed transgene product. For instance, direct primate brain infusion of AAV1 packaging a humanized *Renilla* GFP transgene triggered an immune response against the translated reporter product (Hadaczek et al., 2009). Similarly, a cell mediated immune response and neuronal loss was observed in rats injected with AAV9 vectors packaging the GFP reporter transgene or a human L-amino acid decarboxylase transgene (Ciesielska et al., 2013). More recently, certain AAV serotypes have been shown to undergo systemic leakage resulting in off-target biodistribution in organs like liver and spleen (Gray et al., 2011; Rosenberg et al., 2014; Yang et al., 2014). These preliminary observations in animal models highlight the need to better understand the parameters that determine potential toxicity/biodistribution profiles and immune response in AAV-mediated CNS gene transfer. It is also important to acknowledge that aspects related to manufacturing, downstream processing and purity of AAV vector preparations are critical toward ensuring the safety of AAV vectors. A comprehensive comparison of different viral gene transfer vectors for parameters such as packaging capacity, host chromosomal integration and other biosafety aspects can be found elsewhere (Lentz et al., 2012; Dismuke et al., 2013).

SUMMARY

As of early 2014, 5.3% of world-wide clinical trials involving gene therapy have utilized AAV vectors (109 ongoing trials; Journal of Gene Medicine). Only a few of these trials are aimed at treating diseases with CNS manifestations. In the current review, we have attempted to provide an overview of various parameters that might play a role in determining the success of AAV mediated therapeutic gene transfer to the CNS. Interactions of AAV vectors with different primary receptors, directional transport and cellular tropisms following different routes of administration are summarized in **Table 1**. Although we were unable to cover every contribution to the field of CNS gene therapy, we hope that the information

Table 1 | Capsid-receptor interactions, transduction profiles, and axonal transport properties of some of the well-characterized adeno-associated viral serotypes in the mammalian CNS.

Serotype	Primary receptor	Intra-CSF or intra-parenchymal administration		Intravascular administration		Axonal transport
		Neuronal transduction	Glial transduction	Neuronal transduction	Glial transduction	
AAV1	α2,3/α2,6 *N*-linked SA	++	+	+	+	A–,R+
AAV2	Heparan sulfate	+	–	–	–	A+,R–
AAV4	α2,3 *O*-linked SA	–	+	–	–	?
AAV5	α2,3 *N*-linked SA	++	+	–	–	?
AAV6	α2,3/α2,6 *N*-linked SA/heparan sulfate	++	–	+	+	A–,R+
AAV8	?	++	++	++	++	A+, R+
AAV9	Galactose	+++	++	+++	+++	A+,R+
AAVRh.8	?	++	++	+++	+++	?
AAVRh.10	?	+++	+	+++	+++	?

? Receptor usage/axonal transport has not been characterized; + low levels of transduction; ++ moderate levels of transduction; +++ high levels of transduction; – no transduction; ? A+ or R+ (AAV vector undergoes axonal transport in the anterograde (A) or retrograde (R) direction during in vivo characterization).

provided in this review not only highlights potential gaps in our understanding of AAV-host interactions within the CNS, but will assist with continued vector development for CNS-directed gene transfer applications in the clinic.

ACKNOWLEDGMENTS

We would like to acknowledge NIH grant support awarded to Aravind Asokan (R01HL089221, P01HL112761) and Richard J. Samulski (R01DK084033, P01HL112761, R01AI072176, and R01AR064369).

REFERENCES

Abbott, N. J. (2004). Evidence for bulk flow of brain interstitial fluid: significance for physiology and pathology. *Neurochem. Int.* 45, 545–552. doi: 10.1016/j.neuint.2003.11.006

Agbandje-McKenna, M., and Kleinschmidt, J. (2011). AAV capsid structure and cell interactions. *Methods Mol. Biol.* 807, 47–92. doi: 10.1007/978-1-61779-370-7_3

Ahmed, S. S., Li, H., Cao, C., Sikoglu, E. M., Denninger, A. R., Su, Q., et al. (2013). A single intravenous rAAV injection as late as P20 achieves efficacious and sustained CNS gene therapy in canavan mice. *Mol. Ther.* 21, 2136–2147. doi: 10.1038/mt.2013.138

Alvarez-Buylla, A., and Lim, D. A. (2004). For the long run: maintaining germinal niches in the adult brain. *Neuron* 41, 683–686. doi: 10.1016/S0896-6273(04)00111-4

Arnett, A. L., Beutler, L. R., Quintana, A., Allen, J., Finn, E., Palmiter, R. D., et al. (2013). Heparin-binding correlates with increased efficiency of AAV1- and AAV6-mediated transduction of striated muscle, but negatively impacts CNS transduction. *Gene Ther.* 20, 497–503. doi: 10.1038/gt.2012.60

Asokan, A., Schaffer, D. V., and Jude Samulski, R. (2012). The AAV vector toolkit: poised at the clinical crossroads. *Mol. Ther.* 20, 699–708. doi: 10.1038/mt.2011.287

Bartlett, J. S., Samulski, R. J., and McCown, T. J. (1998). Selective and rapid uptake of adeno-associated virus type 2 in brain. *Hum. Gene Ther.* 9, 1181–1186. doi: 10.1089/hum.1998.9.8-1181

Beier, K. T., Saunders, A., Oldenburg, I. A., Miyamichi, K., Akhtar, N., Luo, L., et al. (2011). Anterograde or retrograde transsynaptic labeling of CNS neurons with vesicular stomatitis virus vectors. *Proc. Natl. Acad. Sci. U.S.A.* 108, 15414–15419. doi: 10.1073/pnas.1110854108

Bell, C. L., Vandenberghe, L. H., Bell, P., Limberis, M. P., Gao, G. P., Van Vliet, K., et al. (2011). The AAV9 receptor and its modification to improve in vivo lung gene transfer in mice. *J. Clin. Invest.* 121, 2427–2435. doi: 10.1172/JCI57367

Benkhelifa-Ziyyat, S., Besse, A., Roda, M., Duque, S., Astord, S., Carcenac, R., et al. (2013). Intramuscular scAAV9-SMN injection mediates widespread gene delivery to the spinal cord and decreases disease severity in SMA mice. *Mol. Ther.* 21, 282–290. doi: 10.1038/mt.2012.261

Benraiss, A., Bruel-Jungerman, E., Lu, G., Economides, A. N., Davidson, B., and Goldman, S. A. (2012). Sustained induction of neuronal addition to the adult rat neostriatum by AAV4-delivered noggin and BDNF. *Gene Ther.* 19, 483–493. doi: 10.1038/gt.2011.114

Bevan, A. K., Duque, S., Foust, K. D., Morales, P. R., Braun, L., Schmelzer, L., et al. (2011). Systemic gene delivery in large species for targeting spinal cord, brain, and peripheral tissues for pediatric disorders. *Mol. Ther.* 19, 1971–1980. doi: 10.1038/mt.2011.157

Bockstael, O., Melas, C., Pythoud, C., Levivier, M., McCarty, D., Samulski, R. J., et al. (2012). Rapid transgene expression in multiple precursor cell types of adult rat subventricular zone mediated by adeno-associated type 1 vectors. *Hum. Gene Ther.* 23, 742–753. doi: 10.1089/hum.2011.216

Bokhoven, M., Stephen, S. L., Knight, S., Gevers, E. F., Robinson, I. C., Takeuchi, Y., et al. (2009). Insertional gene activation by lentiviral and gammaretroviral vectors. *J. Virol.* 83, 283–294. doi: 10.1128/JVI.01865-08

Boustany, R. M. (2013). Lysosomal storage diseases – the horizon expands. *Nat. Rev. Neurol.* 9, 583–598. doi: 10.1038/nrneurol.2013.163

Bowles, D. E., Rabinowitz, J. E., and Samulski, R. J. (2006). "The genus dependovirus," in *Parvoviruses* eds J. R. Kerr, S. F. Cotmore, M. E. Bloom, R. M. Linden, and C. R. Parrish (New York: Edward Arnold Ltd.), 15–24.

Broekman, M. L., Comer, L. A., Hyman, B. T., and Sena-Esteves, M. (2006). Adeno-associated virus vectors serotyped with AAV8 capsid are more efficient than AAV-1 or -2 serotypes for widespread gene delivery to the neonatal mouse brain. *Neuroscience* 138, 501–510. doi: 10.1016/j.neuroscience.2005.11.057

Burger, C., Gorbatyuk, O. S., Velardo, M. J., Peden, C. S., Williams, P., Zolotukhin, S., et al. (2004). Recombinant AAV viral vectors pseudotyped with viral capsids from serotypes 1, 2, and 5 display differential efficiency and cell tropism after delivery to different regions of the central nervous system. *Mol. Ther.* 10, 302–317. doi: 10.1016/j.ymthe.2004.05.024

Cabrera-Salazar, M. A., Bercury, S. D., Ziegler, R. J., Marshall, J., Hodges, B. L., Chuang, W. L., et al. (2010). Intracerebroventricular delivery of glucocerebrosidase reduces substrates and increases lifespan in a mouse model of neuronopathic gaucher disease. *Exp. Neurol.* 225, 436–444. doi: 10.1016/j.expneurol.2010.07.023

Castle, M. J., Gershenson, Z. T., Giles, A. R., Holzbaur, E. L., and Wolfe, J. H. (2014a). Adeno-associated virus serotypes 1, 8, and 9 share conserved mechanisms for anterograde and retrograde axonal transport. *Hum. Gene Ther.* 25, 705–720. doi: 10.1089/hum.2013.189

Castle, M. J., Perlson, E., Holzbaur, E. L., and Wolfe, J. H. (2014b). Long-distance axonal transport of AAV9 is driven by dynein and kinesin-2 and is trafficked in a highly motile Rab7-positive compartment. *Mol. Ther.* 22, 554–566. doi: 10.1038/mt.2013.237

Cearley, C. N., Vandenberghe, L. H., Parente, M. K., Carnish, E. R., Wilson, J. M., and Wolfe, J. H. (2008). Expanded repertoire of AAV vector serotypes mediate unique patterns of transduction in mouse brain. *Mol. Ther.* 16, 1710–1718. doi: 10.1038/mt.2008.166

Cearley, C. N., and Wolfe, J. H. (2006). Transduction characteristics of adeno-associated virus vectors expressing cap serotypes 7, 8, 9, and Rh10 in the mouse brain. *Mol. Ther.* 13, 528–537. doi: 10.1016/j.ymthe.2005.11.015

Cearley, C. N., and Wolfe, J. H. (2007). A single injection of an adeno-associated virus vector into nuclei with divergent connections results in widespread vector distribution in the brain and global correction of a neurogenetic disease. *J. Neurosci.* 27, 9928–9940. doi: 10.1523/JNEUROSCI.2185-07.2007

Chakrabarty, P., Rosario, A., Cruz, P., Siemienski, Z., Ceballos-Diaz, C., Crosby, K., et al. (2013). Capsid serotype and timing of injection determines AAV transduction in the neonatal mice brain. *PLoS ONE* 8:e67680. doi: 10.1371/journal.pone.0067680

Chamberlin, N. L., Du, B., de Lacalle, S., and Saper, C. B. (1998). Recombinant adeno-associated virus vector: use for transgene expression and anterograde tract tracing in the CNS. *Brain Res.* 793, 169–175. doi: 10.1016/S0006-8993(98)00169-3

Chen, Y. H., Claflin, K., Geoghegan, J. C., and Davidson, B. L. (2012). Sialic acid deposition impairs the utility of AAV9, but not peptide-modified AAVs for brain gene therapy in a mouse model of lysosomal storage disease. *Mol. Ther.* 20, 1393–1399. doi: 10.1038/mt.2012.100

Ciesielska, A., Hadaczek, P., Mittermeyer, G., Zhou, S., Wright, J. F., Bankiewicz, K. S., et al. (2013). Cerebral infusion of AAV9 vector-encoding non-self proteins can elicit cell-mediated immune responses. *Mol. Ther.* 21, 158–166. doi: 10.1038/mt.2012.167

Ciesielska, A., Mittermeyer, G., Hadaczek, P., Kells, A. P., Forsayeth, J., and Bankiewicz, K. S. (2011). Anterograde axonal transport of AAV2-GDNF in rat basal ganglia. *Mol. Ther.* 19, 922–927. doi: 10.1038/mt.2010.248

Cserr, H. F., Harling-Berg, C. J., and Knopf, P. M. (1992). Drainage of brain extracellular fluid into blood and deep cervical lymph and its immunological significance. *Brain Pathol.* 2, 269–276. doi: 10.1111/j.1750-3639.1992.tb00703.x

Davidson, B. L., Stein, C. S., Heth, J. A., Martins, I., Kotin, R. M., Derksen, T. A., et al. (2000). Recombinant adeno-associated virus type 2, 4, and 5 vectors: transduction of variant cell types and regions in the mammalian central nervous system. *Proc. Natl. Acad. Sci. U.S.A.* 97, 3428–3432. doi: 10.1073/pnas.97.7.3428

Dayton, R. D., Wang, D. B., and Klein, R. L. (2012). The advent of AAV9 expands applications for brain and spinal cord gene delivery. *Expert Opin. Biol. Ther.* 12, 757–766. doi: 10.1517/14712598.2012.681463

Dismuke, D. J., Tenenbaum, L., and Samulski, R. J. (2013). Biosafety of recombinant adeno-associated virus vectors. *Curr. Gene Ther.* 13, 434–452. doi: 10.2174/15665232113136660007

Duan, D., Sharma, P., Yang, J., Yue, Y., Dudus, L., Zhang, Y., et al. (1998). Circular intermediates of recombinant adeno-associated virus have defined structural

characteristics responsible for long-term episomal persistence in muscle tissue. *J. Virol.* 72, 8568–8577.

Federici, T., Taub, J. S., Baum, G. R., Gray, S. J., Grieger, J. C., Matthews, K. A., et al. (2012). Robust spinal motor neuron transduction following intrathecal delivery of AAV9 in pigs. *Gene Ther.* 19, 852–859. doi: 10.1038/gt.2011.130

Foust, K. D., Nurre, E., Montgomery, C. L., Hernandez, A., Chan, C. M., and Kaspar, B. K. (2009). Intravascular AAV9 preferentially targets neonatal neurons and adult astrocytes. *Nat. Biotechnol.* 27, 59–65. doi: 10.1038/nbt.1515

Fu, H., Kang, L., Jennings, J. S., Moy, S. S., Perez, A., Dirosario, J., et al. (2007). Significantly increased lifespan and improved behavioral performances by rAAV gene delivery in adult mucopolysaccharidosis IIIB mice. *Gene Ther.* 14, 1065–1077. doi: 10.1038/sj.gt.3302961

Fu, H., Muenzer, J., Samulski, R. J., Breese, G., Sifford, J., Zeng, X., et al. (2003). Self-complementary adeno-associated virus serotype 2 vector: global distribution and broad dispersion of AAV-mediated transgene expression in mouse brain. *Mol. Ther.* 8, 911–917. doi: 10.1016/j.ymthe.2003.08.021

Gao, G. P., Alvira, M. R., Wang, L., Calcedo, R., Johnston, J., and Wilson, J. M. (2002). Novel adeno-associated viruses from rhesus monkeys as vectors for human gene therapy. *Proc. Natl. Acad. Sci. U.S.A.* 99, 11854–11859. doi: 10.1073/pnas.182412299

Gao, G., Vandenberghe, L. H., Alvira, M. R., Lu, Y., Calcedo, R., Zhou, X., et al. (2004). Clades of adeno-associated viruses are widely disseminated in human tissues. *J. Virol.* 78, 6381–6388. doi: 10.1128/JVI.78.12.6381-6388.2004

Glascock, J. J., Osman, E. Y., Wetz, M. J., Krogman, M. M., Shababi, M., and Lorson, C. L. (2012). Decreasing disease severity in symptomatic, smn(–/–);SMN2(+/+), spinal muscular atrophy mice following scAAV9-SMN delivery. *Hum. Gene Ther.* 23, 330–335. doi: 10.1089/hum.2011.166

Govindasamy, L., Padron, E., McKenna, R., Muzyczka, N., Kaludov, N., Chiorini, J. A., et al. (2006). Structurally mapping the diverse phenotype of adeno-associated virus serotype 4. *J. Virol.* 80, 11556–11570. doi: 10.1128/JVI.01536-06

Granstedt, A. E., Brunton, B. W., and Enquist, L. W. (2013). Imaging the transport dynamics of single alphaherpesvirus particles in intact peripheral nervous system explants from infected mice. *MBio* 4:e00358–e00313. doi: 10.1128/mBio.00358-13

Gray, S. J. (2013). Gene therapy and neurodevelopmental disorders. *Neuropharmacology* 68, 136–142. doi: 10.1016/j.neuropharm.2012.06.024

Gray, S. J., Blake, B. L., Criswell, H. E., Nicolson, S. C., Samulski, R. J., McCown, T. J., et al. (2010). Directed evolution of a novel adeno-associated virus (AAV) vector that crosses the seizure-compromised blood-brain barrier (BBB). *Mol. Ther.* 18, 570–578. doi: 10.1038/mt.2009.292

Gray, S. J., Matagne, V., Bachaboina, L., Yadav, S., Ojeda, S. R., and Samulski, R. J. (2011). Preclinical differences of intravascular AAV9 delivery to neurons and glia: a comparative study of adult mice and nonhuman primates. *Mol. Ther.* 19, 1058–1069. doi: 10.1038/mt.2011.72

Gray, S. J., Nagabhushan Kalburgi, S., McCown, T. J., and Jude Samulski, R. (2013). Global CNS gene delivery and evasion of anti-AAV-neutralizing antibodies by intrathecal AAV administration in non-human primates. *Gene Ther.* 20, 450–459. doi: 10.1038/gt.2012.101

Grieger, J. C., Choi, V. W., and Samulski, R. J. (2006). Production and characterization of adeno-associated viral vectors. *Nat. Protoc.* 1, 1412–1428. doi: 10.1038/nprot.2006.207

Hadaczek, P., Forsayeth, J., Mirek, H., Munson, K., Bringas, J., Pivirotto, P., et al. (2009). Transduction of nonhuman primate brain with adeno-associated virus serotype 1: vector trafficking and immune response. *Hum. Gene Ther.* 20, 225–237. doi: 10.1089/hum.2008.151

Hadaczek, P., Yamashita, Y., Mirek, H., Tamas, L., Bohn, M. C., Noble, C., et al. (2006). The "perivascular pump" driven by arterial pulsation is a powerful mechanism for the distribution of therapeutic molecules within the brain. *Mol. Ther.* 14, 69–78. doi: 10.1016/j.ymthe.2006.02.018

Handa, A., Muramatsu, S., Qiu, J., Mizukami, H., and Brown, K. E. (2000). Adeno-associated virus (AAV)-3-based vectors transduce haematopoietic cells not susceptible to transduction with AAV-2-based vectors. *J. Gen. Virol.* 81(Pt 8), 2077–2084.

Hirai, T., Enomoto, M., Machida, A., Yamamoto, M., Kuwahara, H., Tajiri, M., et al. (2012). Intrathecal shRNA-AAV9 inhibits target protein expression in the spinal cord and dorsal root ganglia of adult mice. *Hum. Gene Ther. Methods* 23, 119–127. doi: 10.1089/hgtb.2012.035

Hollis, E. R. II, Kadoya, K., Hirsch, M., Samulski, R. J., and Tuszynski, M. H. (2008). Efficient retrograde neuronal transduction utilizing self-complementary AAV1. *Mol. Ther.* 16, 296–301. doi: 10.1038/sj.mt.6300367

Hsueh, Y. P., and Sheng, M. (1999). Regulated expression and subcellular localization of syndecan heparan sulfate proteoglycans and the syndecan-binding protein CASK/LIN-2 during rat brain development. *J. Neurosci.* 19, 7415–7425.

Hsueh, Y. P., Yang, F. C., Kharazia, V., Naisbitt, S., Cohen, A. R., Weinberg, R. J., et al. (1998). Direct interaction of CASK/LIN-2 and syndecan heparan sulfate proteoglycan and their overlapping distribution in neuronal synapses. *J. Cell Biol.* 142, 139–151. doi: 10.1083/jcb.142.1.139

Huang, L. Y., Halder, S., and Agbandje-McKenna, M. (2014). *Parvovirus* glycan interactions. *Curr. Opin. Virol.* 7C, 108–118. doi: 10.1016/j.coviro.2014.05.007

Iliff, J. J, Wang, M., Liao, Y., Plogg, B. A., Peng, W., Gundersen, G. A., et al. (2012). A paravascular pathway facilitates CSF flow through the brain parenchyma and the clearance of interstitial solutes, including amyloid beta. *Sci. Transl. Med.* 4:147ra111. doi: 10.1126/scitranslmed.3003748

Irwin, D. J., Lee, V. M., and Trojanowski, J. Q. (2013). Parkinson's disease dementia: convergence of alpha-synuclein, tau and amyloid-beta pathologies. *Nat. Rev. Neurosci.* 14, 626–636. doi: 10.1038/nrn3549

Iwata, N., Sekiguchi, M., Hattori, Y., Takahashi, A., Asai, M., Ji, B., et al. (2013). Global brain delivery of neprilysin gene by intravascular administration of AAV vector in mice. *Sci. Rep.* 3:1472. doi: 10.1038/srep01472

Jacques, S. J., Ahmed, Z., Forbes, A., Douglas, M. R., Vigenswara, V., Berry, M., et al. (2012). AAV8(gfp) preferentially targets large diameter dorsal root ganglion neurones after both intra-dorsal root ganglion and intrathecal injection. *Mol. Cell. Neurosci.* 49, 464–474. doi: 10.1016/j.mcn.2012.03.002

Jang, J. H., Koerber, J. T., Kim, J. S., Asuri, P., Vazin, T., Bartel, M., et al. (2011). An evolved adeno-associated viral variant enhances gene delivery and gene targeting in neural stem cells. *Mol. Ther.* 19, 667–675. doi: 10.1038/mt.2010.287

Kaludov, N., Brown, K. E., Walters, R. W., Zabner, J., and Chiorini, J. A. (2001). Adeno-associated virus serotype 4 (AAV4) and AAV5 both require sialic acid binding for hemagglutination and efficient transduction but differ in sialic acid linkage specificity. *J. Virol.* 75, 6884–6893. doi: 10.1128/JVI.75.15.6884-6893.2001

Kawamoto, S., Shi, Q., Nitta, Y., Miyazaki, J., and Allen, M. D. (2005). Widespread and early myocardial gene expression by adeno-associated virus vector type 6 with a beta-actin hybrid promoter. *Mol. Ther.* 11, 980–985. doi: 10.1016/j.ymthe.2005.02.009

Kells, A. P., Hadaczek, P., Yin, D., Bringas, J., Varenika, V., Forsayeth, J., et al. (2009). Efficient gene therapy-based method for the delivery of therapeutics to primate cortex. *Proc. Natl. Acad. Sci. U.S.A.* 106, 2407–2411. doi: 10.1073/pnas.0810682106

Koh, L., Zakharov, A., and Johnston, M. (2005). Integration of the subarachnoid space and lymphatics: is it time to embrace a new concept of cerebrospinal fluid absorption? *Cerebrospinal Fluid Res.* 2:6. doi: 10.1186/1743-8454-2-6

Lehtinen, M. K., Bjornsson, C. S., Dymecki, S. M., Gilbertson, R. J., Holtzman, D. M., and Monuki, E. S. (2013). The choroid plexus and cerebrospinal fluid: emerging roles in development, disease, and therapy. *J. Neurosci.* 33, 17553–17559. doi: 10.1523/JNEUROSCI.3258-13.2013

Lentz, T. B., Gray, S. J., and Samulski, R. J. (2012). Viral vectors for gene delivery to the central nervous system. *Neurobiol. Dis.* 48, 179–188. doi: 10.1016/j.nbd.2011.09.014

Lin, D., Fantz, C. R., Levy, B., Rafi, M. A., Vogler, C., Wenger, D. A., et al. (2005). AAV2/5 vector expressing galactocerebrosidase ameliorates CNS disease in the murine model of globoid-cell leukodystrophy more efficiently than AAV2. *Mol. Ther.* 12, 422–430. doi: 10.1016/j.ymthe.2005.04.019

Liu, G., Martins, I. H., Chiorini, J. A., and Davidson, B. L. (2005a). Adeno-associated virus type 4 (AAV4) targets ependyma and astrocytes in the subventricular zone and RMS. *Gene Ther.* 12, 1503–1508. doi: 10.1038/sj.gt.3302554

Liu, G., Martins, I., Wemmie, J. A., Chiorini, J. A., and Davidson, B. L. (2005b). Functional correction of CNS phenotypes in a lysosomal storage disease model using adeno-associated virus type 4 vectors. *J. Neurosci.* 25, 9321–9327. doi: 10.1523/JNEUROSCI.2936-05.2005

Low, K., Aebischer, P., and Schneider, B. L. (2013). Direct and retrograde transduction of nigral neurons with AAV6, 8, and 9 and intraneuronal persistence of viral particles. *Hum. Gene Ther.* 24, 613–629. doi: 10.1089/hum.2012.174

Maguire, C. A., Gianni, D., Meijer, D. H., Shaket, L. A., Wakimoto, H., Rabkin, S. D., et al. (2010). Directed evolution of adeno-associated virus for glioma cell transduction. *J. Neurooncol.* 96, 337–347. doi: 10.1007/s11060-009-9972-7

Mandel, R. J., and Burger, C. (2004). Clinical trials in neurological disorders using AAV vectors: promises and challenges. *Curr. Opin. Mol. Ther.* 6, 482–490.

Masamizu, Y., Okada, T., Kawasaki, K., Ishibashi, H., Yuasa, S., Takeda, S., et al. (2011). Local and retrograde gene transfer into primate neuronal pathways via adeno-associated virus serotype 8 and 9. *Neuroscience* 193, 249–258. doi: 10.1016/j.neuroscience.2011.06.080

Mastakov, M. Y., Baer, K., Kotin, R. M., and During, M. J. (2002). Recombinant adeno-associated virus serotypes 2- and 5-mediated gene transfer in the mammalian brain: quantitative analysis of heparin co-infusion. *Mol. Ther.* 5, 371–380. doi: 10.1006/mthe.2002.0564

McCarty, D. M., DiRosario, J., Gulaid, K., Muenzer, J., and Fu, H. (2009). Mannitol-facilitated CNS entry of rAAV2 vector significantly delayed the neurological disease progression in MPS IIIB mice. *Gene Ther.* 16, 1340–1352. doi: 10.1038/gt.2009.85

McCarty, D. M., Young, S. M. Jr., and Samulski, R. J. (2004). Integration of adeno-associated virus (AAV) and recombinant AAV vectors. *Annu. Rev. Genet.* 38, 819–845. doi: 10.1146/annurev.genet.37.110801.143717

McCown, T. J., Xiao, X., Li, J., Breese, G. R., and Samulski, R. J. (1996). Differential and persistent expression patterns of CNS gene transfer by an adeno-associated virus (AAV) vector. *Brain Res.* 713, 99–107. doi: 10.1016/0006-8993(95)01488-8

Nash, K., Chen, W., and Muzyczka, N. (2008). Complete in vitro reconstitution of adeno-associated virus DNA replication requires the minichromosome maintenance complex proteins. *J. Virol.* 82, 1458–1464. doi: 10.1128/JVI.01968-07

Nguyen, J. B., Sanchez-Pernaute, R., Cunningham, J., and Bankiewicz, K. S. (2001). Convection-enhanced delivery of AAV-2 combined with heparin increases TK gene transfer in the rat brain. *Neuroreport* 12, 1961–1964. doi: 10.1097/00001756-200107030-00037

Orr, H. T., and Zoghbi, H. Y. (2007). Trinucleotide repeat disorders. *Annu. Rev. Neurosci.* 30, 575–621. doi: 10.1146/annurev.neuro.29.051605.113042

Osakada, F., Mori, T., Cetin, A. H., Marshel, J. H., Virgen, B., and Callaway, E. M. (2011). New rabies virus variants for monitoring and manipulating activity and gene expression in defined neural circuits. *Neuron* 71, 617–631. doi: 10.1016/j.neuron.2011.07.005

Padron, E., Bowman, V., Kaludov, N., Govindasamy, L., Levy, H., Nick, P., et al. (2005). Structure of adeno-associated virus type 4. *J. Virol.* 79, 5047–5058. doi: 10.1128/JVI.79.8.5047-5058.2005

Passini, M. A., and Wolfe, J. H. (2001). Widespread gene delivery and structure-specific patterns of expression in the brain after intraventricular injections of neonatal mice with an adeno-associated virus vector. *J. Virol.* 75, 12382–12392. doi: 10.1128/JVI.75.24.12382-12392.2001

Rabinowitz, J. E., Rolling, F., Li, C., Conrath, H., Xiao, W., Xiao, X., et al. (2002). Cross-packaging of a single adeno-associated virus (AAV) type 2 vector genome into multiple AAV serotypes enables transduction with broad specificity. *J. Virol.* 76, 791–801. doi: 10.1128/JVI.76.2.791-801.2002

Rafi, M. A., Rao, H. Z., Luzi, P., Curtis, M. T., and Wenger, D. A. (2012). Extended normal life after AAVrh10-mediated gene therapy in the mouse model of krabbe disease. *Mol. Ther.* 20, 2031–2042. doi: 10.1038/mt.2012.153

Rennels, M. L., Gregory, T. F., Blaumanis, O. R., Fujimoto, K., and Grady, P. A. (1985). Evidence for a "paravascular" fluid circulation in the mammalian central nervous system, provided by the rapid distribution of tracer protein throughout the brain from the subarachnoid space. *Brain Res.* 326, 47–63. doi: 10.1016/0006-8993(85)91383-6

Rosenberg, J. B., Sondhi, D., Rubin, D. G., Monette, S., Chen, A., Cram, S., et al. (2014). Comparative efficacy and safety of multiple routes of direct CNS administration of adeno-associated virus gene transfer vector serotype rh.10 expressing the human arylsulfatase A cDNA to nonhuman primates. *Hum. Gene Ther. Clin. Dev.* doi: 10.1089/humc.2013.239 [Epub ahead of print].

Rothermel, M., Brunert, D., Zabawa, C., Diaz-Quesada, M., and Wachowiak, M. (2013). Transgene expression in target-defined neuron populations mediated by retrograde infection with adeno-associated viral vectors. *J. Neurosci.* 33, 15195–15206. doi: 10.1523/JNEUROSCI.1618-13.2013

Salegio, E. A., Samaranch, L., Kells, A. P., Mittermeyer, G., San Sebastian, W., Zhou, S., et al. (2013). Axonal transport of adeno-associated viral vectors is serotype-dependent. *Gene Ther.* 20, 348–352. doi: 10.1038/gt.2012.27

Samaranch, L., Salegio, E. A., San Sebastian, W., Kells, A. P., Bringas, J. R., Forsayeth, J., et al. (2013). Strong cortical and spinal cord transduction after AAV7 and AAV9 delivery into the cerebrospinal fluid of nonhuman primates. *Hum. Gene Ther.* 24, 526–532. doi: 10.1089/hum.2013.005

Samaranch, L., Salegio, E. A., San Sebastian, W., Kells, A. P., Foust, K. D., Bringas, J. R., et al. (2012). Adeno-associated virus serotype 9 transduction in the central nervous system of nonhuman primates. *Hum. Gene Ther.* 23, 382–389. doi: 10.1089/hum.2011.200

San Sebastian, W., Samaranch, L., Heller, G., Kells, A. P., Bringas, J., Pivirotto, P., et al. (2013). Adeno-associated virus type 6 is retrogradely transported in the non-human primate brain. *Gene Ther.* 20, 1178–1183. doi: 10.1038/gt.2013.48

Sawamoto, K., Wichterle, H., Gonzalez-Perez, O., Cholfin, J. A., Yamada, M., Spassky, N., et al. (2006). New neurons follow the flow of cerebrospinal fluid in the adult brain. *Science* 311, 629–632. doi: 10.1126/science.1119133

Shen, F., Kuo, R., Milon-Camus, M., Han, Z., Jiang, L., Young, W. L., et al. (2013). Intravenous delivery of adeno-associated viral vector serotype 9 mediates effective gene expression in ischemic stroke lesion and brain angiogenic foci. *Stroke* 44, 252–254. doi: 10.1161/STROKEAHA.112.662965

Shen, S., Bryant, K. D., Brown, S. M., Randell, S. H., and Asokan, A. (2011). Terminal N-linked galactose is the primary receptor for adeno-associated virus 9. *J. Biol. Chem.* 286, 13532–13540. doi: 10.1074/jbc.M110.210922

Simonato, M., Bennett, J., Boulis, N. M., Castro, M. G., Fink, D. J., Goins, W. F., et al. (2013). Progress in gene therapy for neurological disorders. *Nat. Rev. Neurol.* 9, 277–291. doi: 10.1038/nrneurol.2013.56

Snyder, B. R., Gray, S. J., Quach, E. T., Huang, J. W., Leung, C. H., Samulski, R. J., et al. (2011). Comparison of adeno-associated viral vector serotypes for spinal cord and motor neuron gene delivery. *Hum. Gene Ther.* 22, 1129–1135. doi: 10.1089/hum.2011.008

Sondhi, D., Hackett, N. R., Peterson, D. A., Stratton, J., Baad, M., Travis, K. M., et al. (2007). Enhanced survival of the LINCL mouse following CLN2 gene transfer using the rh.10 rhesus macaque-derived adeno-associated virus vector. *Mol. Ther.* 15, 481–491. doi: 10.1038/sj.mt.6300049

Summerford, C., and Samulski, R. J. (1998). Membrane-associated heparan sulfate proteoglycan is a receptor for adeno-associated virus type 2 virions. *J. Virol.* 72, 1438–1445.

Taylor, M. P., Kobiler, O., and Enquist, L. W. (2012). Alphaherpesvirus axon-to-cell spread involves limited virion transmission. *Proc. Natl. Acad. Sci. U.S.A.* 109, 17046–17051. doi: 10.1073/pnas.1212926109

Tenenbaum, L., Chtarto, A., Lehtonen, E., Velu, T., Brotchi, J., and Levivier, M. (2004). Recombinant AAV-mediated gene delivery to the central nervous system. *J. Gene Med.* 6(Suppl. 1), S212–S222. doi: 10.1002/jgm.506

Vandenberghe, L. H., Wilson, J. M., and Gao, G. (2009). Tailoring the AAV vector capsid for gene therapy. *Gene Ther.* 16, 311–319. doi: 10.1038/gt.2008.170

Vulchanova, L., Schuster, D. J., Belur, L. R., Riedl, M. S., Podetz-Pedersen, K. M., Kitto, K. F., et al. (2010). Differential adeno-associated virus mediated gene transfer to sensory neurons following intrathecal delivery by direct lumbar puncture. *Mol. Pain* 6:31. doi: 10.1186/1744-8069-6-31

Walters, R. W., Yi, S. M., Keshavjee, S., Brown, K. E., Welsh, M. J., Chiorini, J. A., et al. (2001). Binding of adeno-associated virus type 5 to 2,3-linked sialic acid is required for gene transfer. *J. Biol. Chem.* 276, 20610–20616. doi: 10.1074/jbc.M101559200

Wenger, D. A., Coppola, S., and Liu, S. L. (2002). Lysosomal storage disorders: diagnostic dilemmas and prospects for therapy. *Genet. Med.* 4, 412–419. doi: 10.1097/00125817-200211000-00003

Wickersham, I. R., Finke, S., Conzelmann, K. K., and Callaway, E. M. (2007). Retrograde neuronal tracing with a deletion-mutant rabies virus. *Nat. Methods* 4, 47–49. doi: 10.1038/nmeth999

Wu, Z., Asokan, A., Grieger, J. C., Govindasamy, L., Agbandje-McKenna, M., and Samulski, R. J. (2006a). Single amino acid changes can influence titer, heparin binding, and tissue tropism in different adeno-associated virus serotypes. *J. Virol.* 80, 11393–11397. doi: 10.1128/JVI.01288-06

Wu, Z., Miller, E., Agbandje-McKenna, M., and Samulski, R. J. (2006b). Alpha2,3 and alpha2,6 *N*-linked sialic acids facilitate efficient binding and transduction by adeno-associated virus types 1 and 6. *J. Virol.* 80, 9093–9103. doi: 10.1128/JVI.00895-06

Xiao, X., Li, J., and Samulski, R. J. (1998). Production of high-titer recombinant adeno-associated virus vectors in the absence of helper adenovirus. *J. Virol.* 72, 2224–2232.

Xiao, X., Xiao, W., Li, J., and Samulski, R. J. (1997). A novel 165-base-pair terminal repeat sequence is the sole cis requirement for the adeno-associated virus life cycle. *J. Virol.* 71, 941–948.

Yamashita, T., Chai, H. L., Teramoto, S., Tsuji, S., Shimazaki, K., Muramatsu, S., et al. (2013). Rescue of amyotrophic lateral sclerosis phenotype in a mouse model by intravenous AAV9-ADAR2 delivery to motor neurons. *EMBO Mol. Med.* 5, 1710–1719. doi: 10.1002/emmm.201302935

Yang, B., Li, S., Wang, H., Guo, Y., Gessler, D. J., Cao, C., et al. (2014). Global CNS transduction of adult mice by intravenously delivered rAAVrh.8 and rAAVrh.10 and nonhuman primates by rAAVrh.10. *Mol. Ther.* 22, 1299–1309. doi: 10.1038/mt.2014.68

Zhang, H., Yang, B., Mu, X., Ahmed, S. S., Su, Q., He, R., et al. (2011). Several rAAV vectors efficiently cross the blood-brain barrier and transduce neurons and astrocytes in the neonatal mouse central nervous system. *Mol. Ther.* 19, 1440–1448. doi: 10.1038/mt.2011.98

Conflict of Interest Statement: The authors declare that the research was conducted in the absence of any commercial or financial relationships that could be construed as a potential conflict of interest.

Received: 04 August 2014; paper pending published: 18 August 2014; accepted: 04 September 2014; published online: 19 September 2014.

*Citation: Murlidharan G, Samulski RJ and Asokan A (2014) Biology of adeno-associated viral vectors in the central nervous system. Front. Mol. Neurosci. **7**:76. doi: 10.3389/fnmol.2014.00076*

This article was submitted to the journal Frontiers in Molecular Neuroscience.

frontiers in Molecular Neuroscience

REVIEW
published: 18 May 2015
doi: 10.3389/fnmol.2015.00014

Lentiviral vectors as tools to understand central nervous system biology in mammalian model organisms

*Louise C. Parr-Brownlie[1,2], Clémentine Bosch-Bouju[3†], Lucia Schoderboeck[2,4,5†], Rachel J. Sizemore[1,2], Wickliffe C. Abraham[2,5] and Stephanie M. Hughes[2,4]**

[1] Department of Anatomy, Brain Health Research Centre, University of Otago, Dunedin, New Zealand, [2] Brain Research New Zealand Centre of Research Excellence, Dunedin, New Zealand, [3] NutriNeuro, UMR 1286 INRA, University of Bordeaux, Bordeaux, France, [4] Department of Biochemistry, Brain Health Research Centre, University of Otago, Dunedin, New Zealand, [5] Department of Psychology, Brain Health Research Centre, University of Otago, Dunedin, New Zealand

Lentiviruses have been extensively used as gene delivery vectors since the mid-1990s. Usually derived from the human immunodeficiency virus genome, they mediate efficient gene transfer to non-dividing cells, including neurons and glia in the adult mammalian brain. In addition, integration of the recombinant lentiviral construct into the host genome provides permanent expression, including the progeny of dividing neural precursors. In this review, we describe targeted vectors with modified envelope glycoproteins and expression of transgenes under the regulation of cell-selective and inducible promoters. This technology has broad utility to address fundamental questions in neuroscience and we outline how this has been used in rodents and primates. Combining viral tract tracing with immunohistochemistry and confocal or electron microscopy, lentiviral vectors provide a tool to selectively label and trace specific neuronal populations at gross or ultrastructural levels. Additionally, new generation optogenetic technologies can be readily utilized to analyze neuronal circuit and gene functions in the mature mammalian brain. Examples of these applications, limitations of current systems and prospects for future developments to enhance neuroscience knowledge will be reviewed. Finally, we will discuss how these vectors may be translated from gene therapy trials into the clinical setting.

Keywords: lentivirus, temporal and spatial specificity, neuron phenotype, optogenetics, confocal and electron microscopy

OPEN ACCESS

Edited by:
George Smith, Temple University School of Medicine, USA

Reviewed by:
Nicole Déglon, Lausanne University Hospital – Centre Hospitalier Universitaire Vaudois, Switzerland
Amy Lasek, University of Illinois at Chicago, USA

****Correspondence:***
Stephanie M. Hughes, Department of Biochemistry, Brain Health Research Centre, University of Otago, P.O. BOX 56, Dunedin 9054, New Zealand
stephanie.hughes@otago.ac.nz

† These authors have contributed equally to this work.

Received: *23 February 2015*
Accepted: *30 April 2015*
Published: *18 May 2015*

Citation:
Parr-Brownlie LC, Bosch-Bouju C, Schoderboeck L, Sizemore RJ, Abraham WC and Hughes SM (2015) Lentiviral vectors as tools to understand central nervous system biology in mammalian model organisms. Front. Mol. Neurosci. 8:14. doi: 10.3389/fnmol.2015.00014

Recombinant Lentiviruses in Neuroscience

Lentiviral biology has been extensively studied since the early 1980s following evidence that human immunodeficiency virus (HIV) was the causative agent of AIDS. Harnessing aspects of this knowledge, gene therapy researchers developed recombinant viral vectors based on HIV (Verma and Somia, 1997; Naldini, 1998), feline, and equine equivalents. Lentivirus is a member of the *Retroviridae* family of viruses, named because reverse transcription of viral RNA genomes to DNA is required before integration into the host genome. Unlike other retroviral genra, such as gamma-retroviruses that are also used in gene therapy, lentiviruses are able to infect both dividing and non-dividing cells by virtue of the entry mechanism through the intact host nuclear envelope

(Naldini, 1998; Vodicka, 2001). This characteristic makes it an ideal viral vector for neuroscience, where the majority of cells in the postnatal brain do not divide.

Lentiviral genomes are single-stranded RNA with *gag*, *pol* and *env* genes encoding polyprotein components of the capsid, the enzymes reverse transcriptase, protease and integrase, and envelope glycoproteins, respectively. The viral genome is flanked by long terminal repeats (LTRs), required for genome replication and integration (Naldini, 1998). Lentiviruses have additional accessory genes, but these are dispensable in recombinant vectors. Instead, a recombinant lentiviral vector genome contains LTRs flanking a packaging signal, plus an exogenous promoter used to express a transgene that enables identification of subpopulations of cells, overexpression or knockdown of genes or to target cells with a drug- or light-inducible protein to analyze cell function (Dull et al., 1998). The genome capacity is 8–10 kb for maximal packaging efficiency and viral particles are packaged in human cell lines (usually HEK293 derivatives) by co-transfection of helper plasmids encoding *gag*, *pol,* and *env* (Dull et al., 1998). In post-mitotic cells, lentiviral vectors integrate at random, whereas integration preferentially occurs into active genes in mitotically active cells (Bartholomae et al., 2011). An alternative and additional safety aspect for post-mitotic cell transduction is the development of integrase deficient lentiviral vectors (Liu et al., 2014). Removal of the integrase from the packaging construct prevents integration, resulting in episomal maintenance of the transgene vector in post-mitotic cells. Recombinant lentiviral vectors appear to offer greater safety over gamma retroviral vectors in which activation of oncogenes has been reported (Hacein-Bey-Abina et al., 2003; Zhou et al., 2010). Although lentiviral vectors have some limitations, mainly in respect to limited spread within the brain parenchyma, this provides an additional advantage in some cases. Permanent integration of lentiviral delivered transgenes into mitotic or post-mitotic cells, similar to episomal maintenance of integrase-deficient lentivirus or AAV in post-mitotic cells, should allow stable transgene expression for the life of the organism or cell, preventing the need for repeated vector administration (Linterman et al., 2011). An important advantage of lentiviral vectors over other vector systems, including adeno-associated virus (AAV), is that inflammatory, and immune responses associated with the vector itself are limited (Abordo-Adesida et al., 2005; Annoni et al., 2007).

This review highlights how lentiviral vectors have been used in neuroscience research. We focus on targeting gene expression to selected neuronal phenotypes, both spatially and temporally, to answer specific biological questions surrounding gene function and the anatomy and physiology of neural circuits in the mature brain.

Targeting Gene Expression to Structures and Cells

The design of lentiviral vectors has increased in complexity over the last 20 years. As lentiviral vectors have been used as a tool to address more refined neuroscience questions, expectations for increased spatial and temporal accuracy of gene expression have resulted, making it more challenging to design new lentiviral vectors for cutting edge experiments.

Transgene expression can be restricted (i) to certain structures or cell types for refined spatial resolution, (ii) in a constitutive or inducible manner for temporal resolution, and (iii) by activation of the gene product by additional stimuli like light or drugs (post-translational regulation). Below we outline how these restrictions are routinely used to improve knowledge of brain circuitry.

Spatial Restriction of Gene Expression

In its simplest form, spatial restriction of gene expression is achieved by injecting low volumes and/or titres of the lentiviral vector in the target brain region where its spread will be restricted depending on its tropism and diffusion through the target tissue. Lentiviral tropism is defined by the glycoproteins on the surface of the viral particles that determine which cell surface receptor the virus binds to and thereby the cells or subcellular compartments the virus can enter. Tropism can be modified by pseudotyping, which is the expression of glycoproteins originating from a different virus (Indraccolo et al., 1998; Cronin et al., 2005; Trabalza et al., 2013). The most common pseudotyping method uses the vesicular stomatitis virus glycoprotein (VSVg). VSVg pseudotyped particles have wide tropism as they use low-density lipoprotein receptors to enter cells (Finkelshtein et al., 2013), which are almost ubiquitously expressed on cell membranes (Willnow, 1999), including by both glia and neurons (Jakobsson et al., 2003). By differential pseudotyping, specific populations of neurons within a brain region can be targeted (**Figure 1A**). An example of differential tropism is in the hippocampus, where VSVg pseudotyped vectors mainly transduce cells in the subgranular zone and dentate granule cell layer, while murine leukemia virus glycoprotein (MuLV) pseudotyped vectors more specifically transduce mature granule cells (Watson et al., 2002).

Unlike AAVs, which have a diameter of approximately 20 nm, the larger particle size of lentiviruses (100 nm) limits spread through the extracellular space (Cetin et al., 2006; Lerchner et al., 2014; **Figure 1**), and methods to increase AAV spread, like convection-enhanced delivery or mannitol, are therefore not promising for lentiviral particles. The spread of one microliter of VSVg pseudotyped vector in the brain is restricted to 1–2 mm from the injection site (Desmaris et al., 2001; Linterman et al., 2011), with no retrograde transport. By exchanging the VSVg for a rabies glycoprotein (Rbg; Mazarakis et al., 2001), or a chimera of these two (Kato et al., 2011a,b, 2014; Carpentier et al., 2012; Schoderboeck et al., 2015) retrograde transport is enabled so that after transduction of axonal terminals, viral contents (minus envelope) are transported to the cell body (**Figure 1**).

Cell-Specific Gene Expression Using Promoters

The promoter controlling gene expression in the lentiviral construct provides a further level of restriction. In addition to ubiquitous promoters, a range of brain cell-type specific promoters are available and well characterized. A list of promoters that are frequently used in neuroscience research is detailed in **Table 1**. Ubiquitous promoters that cause expression of non-native

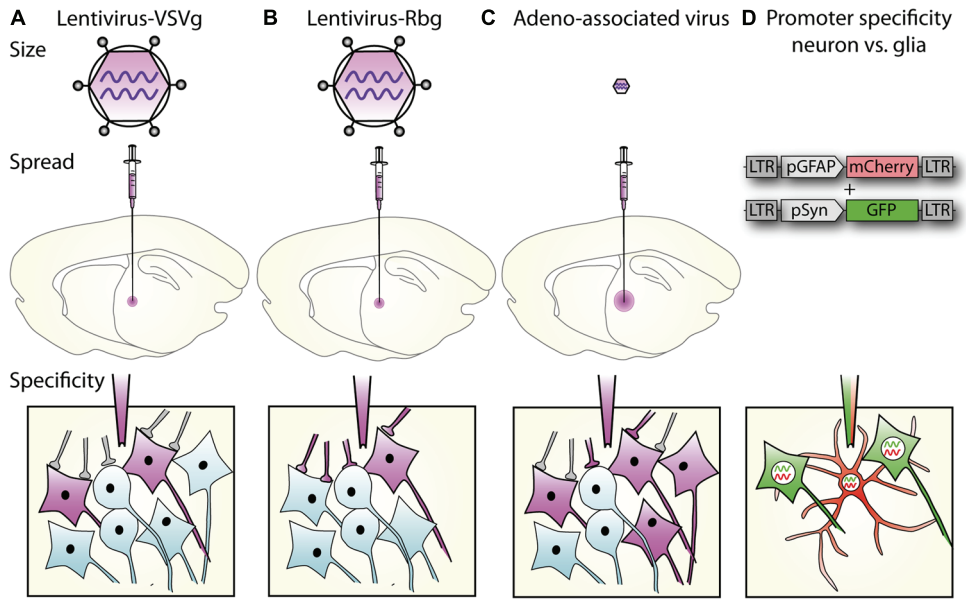

FIGURE 1 | Lentiviral vector spread, transduction, and expression is mediated by particle size, envelope properties and promoter usage. **(A)** Lentiviral vectors pseudotyped with vesicular stomatitis virus glycoprotein (VSVg) mediate local transduction with no retrograde or trans-synaptic viral transport. **(B)** In contrast, lentiviral vectors pseudotyped with a rabies glycoprotein (Rbg) transduce both the soma of local neurons and also afferents to the area. **(C)** AAV, depending on serotype, mediates larger physical spread, and can transduce either local neurons or afferent terminals. **(A–C)** Schematics of relative virus particle size represented in upper panels indicate that lentiviral vectors are approximately 5 × larger than AAVs. **(D)** Transgene expression can be restricted to specific cell types using specific promoters. Using the glial fibrillary acidic protein (GFAP) promoter driving mCherry and synapsin promoter to drive GFP, lentiviral constructs differentially label astrocytes, and neurons, respectively.

proteins in virtually all transduced cells include elongation factor 1 alpha (EF1α), cytomegalovirus enhancer/promoter element (CMV), β-actin, β-globin chimeric promoter (CAG), and phosphoglycerate kinase promoter (PGK; for a comparison see (Qin et al., 2010) and (Yaguchi et al., 2013). Promoters providing specific expression in all neurons include synapsin 1 (syn; Hioki et al., 2007; Nathanson et al., 2009; van Hooijdonk et al., 2009; Yaguchi et al., 2013) and neuron specific enolase (NSE;

TABLE 1 | Commonly used promoters in lentiviruses.

Common abbreviation	Promoter origin	Expressed in	Comments
EF1α	Mammalian elongation factor 1 alpha promoter	Ubiquitous	Endogenous mammalian promoter (Jakobsson et al., 2003).
CMV	Human cytomegalovirus immediate-early enhancer/promoter	Ubiquitous	Methylation-dependent silencing of transgene expression (Brooks et al., 2004)
CAG	CMV coupled with chicken β-actin promoter and first exon and rabbit β-globin splice acceptor.	Ubiquitous	Stable long term expression (Jakobsson et al. (2003), Delzor et al. (2012)).
PGK	Mammalian phosphoglycerate kinase 1 promoter	Ubiquitous	Endogenous mammalian gene Delzor et al. (2012)
MND	Myeloproliferative sarcoma virus enhancer, Negative control region deleted, dl587rev primer-binding site substituted	Ubiquitous	Li et al. (2010), Linterman et al. (2011)
Syn	Mammalian synapsin 1 promoter	Neurons	Dittgen et al. (2004)
GAD67	Mammalian glutamate decarboxylase 67	Inhibitory neurons	Nathanson et al. (2009), Delzor et al. (2012)
CaMKIIα	Mammalian calcium/calmodulin-dependent protein kinase II alpha promoter	Excitatory glutamatergic neurons	Postnatal expression – later in development then synapsin (Dittgen et al., 2004; van Hooijdonk et al., 2009).
NSE	Mammalian neuron-specific enolase promoter	Neurons	Relatively weak expression (Delzor et al., 2012)
MBP	Mammalian myelin basic protein promoter	Oligodendrocytes	McIver et al. (2005, 2010)
GFAP	Mammalian glial fibrilliary acidic protein promoter	Astrocytes	Higher expression in activated astrocytes (Chow et al., 2008).
Nes	Mammalian nestin promoter	Neural progenitor cells	Can also be expressed in activated astrocytes. (Beech et al., 2004; Cheng et al., 2004; Sun et al., 2014).

Delzor et al., 2012). Neuronal type specific promoters, that have a size compatible with lentiviral vectors are still limited, but include calcium/calmodulin-dependent protein kinase II alpha (CaMKIIα; Dittgen et al., 2004; van Hooijdonk et al., 2009; Seeger-Armbruster et al., 2015), which restricts expression to excitatory glutamatergic neurons and glutamate decarboxylase 67 (GAD67; Delzor et al., 2012) that should restrict expression to inhibitory GABAergic neurons. The parvalbumin promoter targets a subset of GABAergic neurons (Sohal et al., 2009) and ppHcrt targets hypocretin neurons (Zhang et al., 2010). However, because LV-VSVg has strong tropism for excitatory neurons, transgene expression from the GAD67 promoter has also been found in excitatory neurons (Nathanson et al., 2009). The glial fibrillary acid protein (GFAP) promoter is most commonly used to restrict gene expression to astrocytes (Jakobsson et al., 2003), myelin basic protein (MBP) to target oligodendrocytes (McIver et al., 2005), and the nestin (nes) promoter for neural progenitor cells (Beech et al., 2004). The specificity of these promoters is not absolute and can be impaired by viral preparation properties (titre) and promoter properties in certain subregions of the brain. Promoters used in lentiviral vectors typically only comprise minimal promoter sequences, while their endogenous counterparts are often significantly longer and more complex including enhancer and insulator elements. Using a minimal promoter sequence simplifies cloning and helps keep the vector size small, but this also compromises the specificity as parts of the promoter or enhancer and insulator elements will be missing. Integration of vectors close to enhancer or repressor sequences can also impact vector promoter fidelity.

Tighter cell-type specificity can be achieved by combining lentiviruses with the cre-lox system in transgenic animals. The system involves two components: cre recombinase and a transgene flanked by lox sites ("floxed"), the recognition sites for cre recombinase. The bacterial cre protein uses the lox sites for site-specific recombination in mammalian cells (Sauer and Henderson, 1988). Both components can be supplied by viral vectors or a transgenic animal used to express either cre recombinase, or a floxed transgene; either of which can be controlled by a cell-type specific promoter (**Figure 2**). The lentiviral vector supplies the other component (cre or floxed transgene), which might include a protein under posttranslational regulation (See Posttranslational Control of Gene Expression).

Conditional knockdown of gene expression is another powerful method to analyze protein function in the adult brain. microRNA (miRNA)-based short hairpin knockdown can be combined with cell specific promoters (Nielsen et al., 2009), or used in combination with cre-lox or drug-inducible cre-lox systems for spatial and temporal control of gene knockdown (Stern et al., 2008; Heitz et al., 2014). For example, Heitz et al. (2014) use a lentiviral vector expressing a floxed GFP miRNA to transduce mice expressing GFAP or CaMKII regulated tamoxifen-inducible cre (creERT2).

Further restriction of gene expression can be achieved by miRNA de-targeting. In this system, incorporating miR binding sites into the 3′ UTR of transgene constructs within a viral vector limits expression to those cells that do not express that miR.

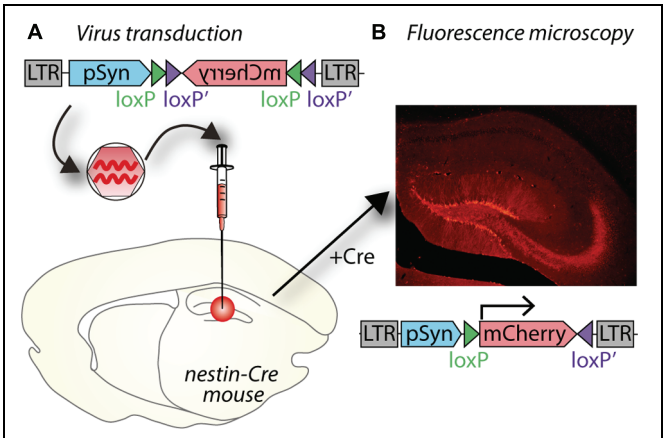

FIGURE 2 | A potential use of Cre–lox and cell specific promoters to target gene expression both spatially and temporally. (A) A lentiviral vector (LV- synapsin-double-floxed mCherry) injected in the hippocampal dentate gyrus (DG) of a nestin-cre mouse. **(B)** Cre expressed in nestin-positive neural progenitor cells reverses mCherry and allows expression in new neurons as they differentiate in granule neurons. mCherry expression is therefore restricted to granule neurons born after virus injection.

For example, miR-9 is expressed in all cells in the brain with the exception of microglia. By incorporating miR-9 binding sites into the transgene construct, miR-9 will bind to, and degrade transgene RNAs in all cells except microglia, resulting in selective expression of the transgene in microglia (Akerblom et al., 2013). Similarly, preventing transgene expression in neurons, and enhancing astrocyte expression can be aided by incorporation of the miR-124 binding sequences into the vector (Colin et al., 2009). As further advances in understanding miR biology and cell type specificity emerge, these constructs can be further refined for selective gene expression.

Temporal Control of Gene Expression

Temporal control of gene expression is achieved using inducible promoters. These promoters are activated by an additional factor that is added to or removed from the system. They are widely used in bacterial expression systems and include promoters controlled by drugs, metal ions, heat shock, or hormones – only some of which are useable in mammalian cells, and even fewer in the CNS where drugs need to cross the blood brain barrier. Most commonly, drug-inducible promoters are used in neuroscience, where the transgene is expressed under the control of a minimal promoter sequence that is only active if bound by a transactivator. The ability of this transactivator to bind the promoter is regulated by co-factors. The most famous and widely used inducible promoter system is the Tet-On/Off system and derivatives thereof. In this system, the transgene is downstream of a minimal promoter under the control of a Tet response element (TRE) based on an *Escherichia coli* operon conferring resistance to the antibiotic tetracycline. For use in mammalian cells, the Tet repressor (Tet-On) is fused to the activating domain of virion protein 16 of herpes simplex virus (VP16) that constitutes the tetracycline-controlled transactivator (tTA). When tTA binds to the TRE, transcription from the minimal promoter is

stimulated by tetracycline or its derivative doxycycline (DOX) in a concentration-dependent manner, thus providing a reversible on and off switch (Gossen and Bujard, 1995; Gossen et al., 1995; Pluta et al., 2005). In the Tet-Off system, the tTA binds to the TRE in the absence of tetracycline and activates gene expression; when tetracycline or DOX is administered, gene expression is repressed (Gossen and Bujard, 1992). The Tet-On system was derived by mutation of the tTA leading to the opposite phenotype, where administration of tetracycline induces gene expression (Gossen et al., 1995).

Light-inducible promoters have recently expanded the potential of inducible promoters (Wang et al., 2012). In a system similar to the Tet concept, a photoactivatable transactivator dimerises upon exposure to light of a certain wavelength, permitting it to bind to its response element and thereby induce gene expression. The advantages of this optogenetic system over drug-inducible promoters are the higher spatial and temporal accuracy of induction and reversibility (ms to s resolution), whereas tetracycline (and DOX) is usually delivered systemically and its effects can last from hours to days (Agwuh and MacGowan, 2006).

Some specific research questions require tight spatial and temporal control of gene expression and aim to express the transgene in only a specific subset of very similar cells, which can be optimally addressed by combining several techniques. Studying neurogenesis in the adult mammalian brain requires several techniques to be combined to obtain the necessary specificity. In order to only target newborn granule cells, which are very similar to their developmentally born neighboring granule cells, a cre transgenic mouse can be combined with cell-type specific promoter (**Figure 2**). The transgenic mouse expresses cre recombinase under a nestin promoter only present in neural progenitor cells, which reside in the subgranular and subventricular zones in the hippocampus. To only target newly born cells in the hippocampus, a VSVg-pseudotyped lentivirus with the transgene is injected into the dentate gyrus; in **Figure 2**, the transgene encodes the fluorescent protein mCherry. The transgene is inverted and flanked by two sets of loxP sites to prevent leaky expression in cells without cre recombinase. By placing the transgene under a syn promoter, it will only be expressed in mature neurons born after the injection of the lentivirus. Including a Tet system to induce cre expression only at very specific time points could further enhance temporal resolution (Chen et al., 2009).

Posttranslational Control of Gene Expression

Posttranslational regulation of transgene expression can be used to control neural activity by using reversibly activatable ion channels or G-protein coupled receptors (GPCR; reviewed in Rogan and Roth, 2011). The expressed channels and GPCRs are responsive to either light or drugs. Below we focus on the utility of light (optogenetic stimulation) to alter cell function or structure because it has the most accurate (shortest) time resolution (ms) and can mimic the time course of real neural activity. However, sophisticated, highly specific and activatable changes in gene expression can occur over longer time frames using drugs (min-days), so are ideally suited for examining biological states such as circadian rhythm, sleep-wake cycle, stress, and the control of feeding. One of the most recent advances is to completely isolate the introduced transgene from the endogenous ligand–GPCR combinations by developing designer receptors exclusively activated by designer drugs (DREADDs; Armbruster et al., 2007). One advantage of DREADDs is that both receptors and ligands are specifically designed to have high affinity to each other, but not with other targets *in vivo*.

Light Inducible Control of Neuronal Function – Optogenetics

In the field of neuroscience, a major new application of lentiviral vectors has been the development of optogenetic technology. Optogenetic stimulation (optogenetics) is the result of 30 years of intense research in both gene therapy and light-activated proteins. Since the first article in 2005 describing the use of optogenetics in neuroscience (Boyden et al., 2005), optogenetics has genuinely revolutionized neuroscience research and the number of publications using optogenetics has increased exponentially (Aston-Jones and Deisseroth, 2013). Optogenetics was chosen as the method of the year by the prestigious Nature Methods journal in 2010.

The principle of optogenetics is to express a light-activated protein in brain cells via a viral vector, such as a lentivirus, and then activate this particular population of brain cells with light of a specific wavelength (**Figure 3A**). The power of optogenetics resides in its spatial, temporal, and neuronal phenotype specificity to control brain cells (Fenno et al., 2011), which was previously lacking despite many attempts to solve it using other neuroscience methods. Precise timing of optogenetic stimulation is achieved by light pulses [using a laser or light emitting diode (LED) as a light source and to deliver the light at a target area of the brain using an optical fiber], at millisecond resolution, which is in accordance with rapid generation and transmission of action potentials at the initial segment or along the axon. Spatial specificity is achieved by locally injecting the viral vector into a specific part of the brain and restricting its spread to only the target nucleus by optimizing the number of injections and volume injected at each site to match the three dimensional shape of the target. In cases when a target site has a neuronal phenotype that differs from surrounding nuclei, spatial specificity is also achieved by using a promoter for that neuronal phenotype. Spatial specificity can be further enhanced by careful positioning of the fiber optic probe for controlled application of light within the target nucleus. Transduction of a specific population of neurons is achieved by pseudotyping viral vectors and promoters as described in Section "Spatial Restriction of Gene Expression" and "Cell-Specific Gene Expression Using Promoters," respectively. Temporal control of channel activity is dependent on activation of the laser. At first, optogenetics was used to replace electrical stimulation because it achieves the goal of activating specific neuronal circuits to understand how they work with significantly improved accuracy. In contrast, electrical stimulation has the major drawback of activating all excitable tissues in the area, including passing fibers (Bosch et al., 2011). Since 2005, the tools for optogenetics (types and properties of light-activated

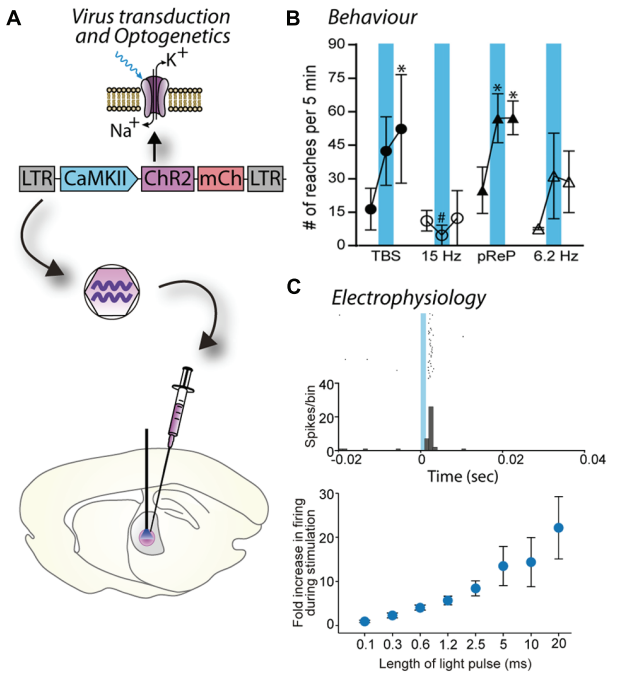

FIGURE 3 | Blue light stimulation of neurons expressing a channelrhodopsin alters cell activity and behavior. (A) A lentiviral vector (LV-CaMKII-ChR2-mCherry) was injected into the motor thalamus of rats to transduce glutamatergic neurons. Blue light stimulation of motor thalamus opened channelrhodopsin2 cation channels in the membrane of transduced neurons. **(B)** Effect of blue light stimulation of motor thalamus on movement performance in an acute model of parkinsonism. For each pattern, the number of reaches executed by rats is represented for 5 min before, during and after blue light (473 nm) stimulation. Theta burst stimulation (TBS) and the physiological reaching pattern (pReP) are irregular patterns and significantly increased reaching performance. Conversely, the equivalent tonic patterns (15 and 6.2 Hz, respectively) did not improve reaching. $*p < 0.05$, versus prestimulation (Tukey's test). $\#p < 0.05$ versus pREP pattern (Tukey's test). Reproduced with permission from Seeger-Armbruster et al. (2015). **(C)** A similar experiment performed with injection of LV-EF1α-hChR2(H134R)-eYFP into ventrolateral motor thalamus of a rhesus monkey. Upper panel, data show the firing rate (spikes/bin) of one neuron before (−20–0 ms), during (0–1.2 ms), and after (1.2–40 ms) blue light stimulation (1.2 ms pulse). The cell responded with a brief increase of spiking activity just after the pulse of blue light. Bottom panel, the duration of blue light stimulation affected the responses of motor thalamus neurons; longer pulses caused larger increases in firing rate. Reproduced with permission from Galvan et al. (2012).

proteins, promoters, viral vectors, light sources, stimulation, and recording devices) have been rapidly developing enabling scientists to create new paradigms and innovative approaches to address complex scientific questions. In particular, optogenetics can be used to dissect the anatomy and function of neuronal circuits (Atasoy et al., 2012) and induce or restore behaviors (Fanselow and Connors, 2005; Chaudhury et al., 2013; Seeger-Armbruster et al., 2015; **Figures 3B,C**). Moreover, while electrical stimulation has been focused on controlling neuronal activity, optogenetics also allows manipulation of glial cells (astrocytes, microglia), which constitutes an incomparable way to understand the role of glia in the brain (Figueiredo et al., 2011; Li et al., 2013).

More recently, optogenetics has evolved beyond controlling cell excitability (ion channels). Light-activated proteins are able to activate downstream signaling pathways, for example OptoXR, a category of light-activated proteins that are able to activate signaling pathways from G_q, G_s, or G_i proteins when they are activated by 500 nm-light (Fenno et al., 2011). A photoactivatable version of adenylyl cyclase is also available, which has notably been used to increase levels of glucocorticoids to study stress responses in zebrafish (De Marco et al., 2013). Optogenetics can also work by dimerization or interactions of the light-activated proteins upon light stimulation, which can control an almost infinite variety of signaling pathways and have been used notably to trigger cell migration (Pathak et al., 2013).

Lentiviruses were chosen as the viral vector for the first article describing optogenetics (Boyden et al., 2005). Currently, most studies use either lentiviruses or AAVs as the vector of choice in rodents or monkeys. Despite differences in their transduction, specificity, and spread in the brain (**Figure 1**), the selection of one or other vector is rarely explained in research articles. The main difference between lentivirus and AAV is their ability to diffuse in the brain (Packer et al., 2013). Indeed, AAV transduces a much larger area around the injection site compared to lentivirus, which is usually restricted to the site of injection (**Figure 1**). As a consequence, AAVs are preferred when high expression levels of light-activated proteins are needed in a large area of the brain. AAV also seems to cause higher expression at the cell level by inserting a larger number of copies into each cell (Diester et al., 2011); however, this may not be advantageous. Recent studies suggest that high level of gene transfer with AAV increases the probability of developing aggregates of non-native expressed proteins in cells (Diester et al., 2011) and/or axonal malformation (Miyashita et al., 2013). This is less likely to occur with lentivirus, due to the lower level of transduction. Moreover, high levels of light-activated proteins lead to higher stimulation rates, which can lead to artificial effects and thus bias the conclusions (Hausser, 2014). In contrast, lentiviruses are preferred when spatial specificity is needed, despite lower levels of expression, and when the genetic code for expression of the required protein is large. In mice where transgenic technologies are well established, optogenetics is commonly performed with transgenic mice in combination with AAV, using the cre-lox system. In this configuration, spatial specificity is achieved by the injection of a floxed transgene construct and high level of expression is achieved by using AAV. Overall, the choice of viral vector is complex and depends on the experimental design required to answer the research question and it is particularly important because many optogenetic studies are performed on freely moving animals, addressing complex behavioral questions over weeks or months.

In the few studies performing optogenetics in monkey, lentivirus and AAV have both been used successfully (Han et al., 2009; Diester et al., 2011; Galvan et al., 2012; Lerchner et al., 2014) with the difference that lentivirus leads to a smaller proportion of aggregates and may thus be a better option for long term studies, as is usually the case with monkeys.

In the future, optogenetics may evolve towards more specific stimulation of neuronal populations with fewer side effects, and

lentiviral tools may play a key role in this. For basic neuroscience research, one of the ultimate goals of optogenetic stimulation techniques is to mimic activity in a normally functioning neuronal network to understand the neuronal coding responsible for brain function (Seeger-Armbruster et al., 2015). Another perspective is to use optogenetics with very specific patterns of light stimulation (such as theta burst stimulation in the cortex) to promote plasticity and restore normal behavior in a brain with a neurological disorder (Seeger-Armbruster et al., 2015). A potential future extension of optogenetics will be its use in humans. Although lentivirus has a limited transduction capacity compared to AAV, this is less important when combined with optogenetic stimulation because that the area of brain transduced by the vector and stimulated by the fiber-optic probe are of similar size. From this perspective, lentivirus may be preferred for optogenetic stimulation to treat or cure neurological diseases in humans in the future because of its specificity and limited long-term toxicity on brain tissue.

Exploring Neuronal Circuitry in the Brain

Another field being redefined by lentiviral vectors is neural tracing. Lentivirus provides several advantages with spatially defined expression and combinations of tracers with optogenetic and other functional constructs allowing examination of questions not previously possible using traditional tracing techniques.

Analysis of neuronal circuitry has traditionally relied on neuronal tracers such as biotinylated dextran amine (BDA), phaseolus vulgaris leucoagglutinin (PHAL), wheat-germ agglutinin (WGA), horseradish peroxidase (HRP), cholera toxin, and more recently pseudorabies virus to label neuronal pathways (Callaway, 2008; Huh et al., 2010). Some of these tracers label neurons in a predominantly anterograde [high molecular weight (Mr) BDA, PHAL] or retrograde (low Mr BDA, pseudorabies, cholera toxin, HRP), or bidirectional (WGA) way. While these tracers confer spatial specificity that is dependent on the volume injected, all neurons in the injected region are labeled regardless of the phenotype.

More recently, lentiviral vectors have been combined with microscopy and other biological techniques to investigate the anatomy of neural circuits in many brain areas, including the cerebral cortex, thalamus, basal ganglia, hippocampus, and brainstem (Trono, 2000; Vigna and Naldini, 2000; Duale et al., 2005; Grinevich et al., 2005; Benzekhroufa et al., 2009; Huh et al., 2010; Takada et al., 2013; **Figure 4**). Depending on the lentivirus type and the promoter used in the construct, viral vectors can transduce dendrites, the somata, and terminals of neurons and express proteins at a particular subcellular component, such as in the cell membrane or nucleus (Klein et al., 1998; Gradinaru et al., 2010; Lobbestael et al., 2010; Konermann et al., 2013; Dautan et al., 2014). With careful experimental design, viral vectors can accurately label a particular neuronal phenotype, which affords the possibility of labeling just one distinct pathway in the brain (Tye and Deisseroth, 2012; Dautan et al., 2014; Hasegawa et al., 2014). In addition to spatial specificity, viral vectors allow temporal specificity in neuroanatomy studies, determined by the time of injection and harvesting of tissue (Dull et al., 1998; Takada et al., 2013). In contrast, immunohistochemistry labels all neurons of a phenotype irrespective of the pathways that they belong to and only selected brain slices are stained and analyzed, which means that neurons of interest are only partially visualized (e.g., axon and terminals, but not somata and dendrites, or the converse), unless large numbers of serial sections are analyzed. Viral vectors permit neurons to be transduced in a controlled area of the brain (Huh et al., 2010) because they diffuse smaller distances than traditional neuronal tracers, however, transduction of large populations of neurons can be achieved by injecting a larger volume, injecting multiple times or using a higher titre

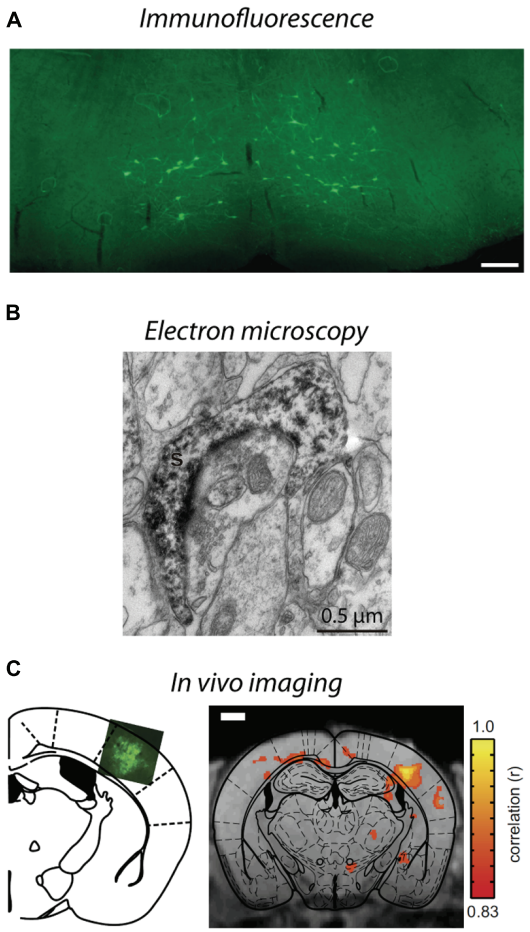

FIGURE 4 | Visualization of lentivirus transduced neurons in *post-mortem* tissue and *in situ* imaging. (A) Injection of B19/VSVg-LV-GFP into the lumbar spinal cord resulted in prominent transduction of neurons in the brainstem. Scale bar = 50 µm. Reproduced with permission from Schoderboeck et al. (2015). **(B)** An electron micrograph of a lentivirus transduced spine in the monkey striatum expressing eYFP. eYFP-tagged neuronal elements were made electron dense by using immunoperoxidase labeling with DAB as the chromogen, prior to general processing for electron microscopy. Reproduced with permission from Galvan et al. (2012). **(C)** *In situ* BOLD signals from opto-functional MRI in mice (Desai et al., 2011). Channelrhodopsin-GFP expression following injection of LV-FCK-ChR2- GFP into the somatosensory cortex (left). Voxels with significant increases in BOLD signal (color scale) are shown 1 mm posterior to bregma (right). Reproduced with permission from Desai et al. (2011).

(Miyoshi et al., 1997; Cai et al., 2013). Furthermore, it is possible to combine viral vectors with conditional systems so that neurons are labeled during a specific period of development (Dull et al., 1998; Wiznerowicz and Trono, 2003). Helper-viruses have also been used in short-term anatomical experiments to specifically label excitatory and inhibitory pathways to better understand whole circuits and to improve cloning capacity (Kumar-Singh, 2008; Liu et al., 2013). For all of these reasons, viral vectors permit unprecedented precise descriptions of pathways and connections for subpopulations of neurons.

As described in Section "Spatial Restriction of Gene Expression," lentiviral vectors can be pseudotyped with envelopes that modify vector uptake, allowing neuronal tracing studies to be conducted. VSVg-pseudotyped vectors transduce neurons and astrocytes only within the local injection site. Delivery of a cytoplasmic-localized transgene via a VSVg-lentivirus will result in labeling of cell soma within the injection site and fills their projections, allowing tracing of neural target zones. In contrast, Rbg-pseudotyped lentiviral vectors deliver transgenes both locally and via retrograde transport to distal somata with axonal projections localized in the injection zone (Mazarakis et al., 2001; **Figure 1**). The transgene-encoded protein is expressed by transduced neurons – the precise site of expression (e.g., axon, nucleus, cell membrane, histone residues of DNA, etc.) is dependent on where the targeted protein is usually located in the cell. This labeling specificity can be critical because of the complexity of the brain. Here, lentiviral vectors offer improved specificity because most AAV serotypes would label both afferent and efferent neurons in the region (Klaw et al., 2013; **Figure 1**). In addition, the flexibility to have the vectors endocytosed at the terminals or somata of target neurons means that the investigator can select the vector so that injection and uptake is in an area that will not be visualized (Schoderboeck et al., 2015; **Figure 4A**). The advantage for experiments with an anatomical focus is that the physical damage or artifact caused by the injection does not interfere with the interpretation or analysis of images taken at high-resolution, such as electron microscopy. For example, if the somata of neurons will be visualized, injection damage will be minimized by targeting uptake at the terminals of the neurons of interest by using a vector containing a Rbg envelope. Conversely, if the terminals will be visualized, the injection should be targeted at the somata of the neurons of interest by using a VSVg envelope.

Neuroanatomy studies using lentiviral vectors can also be enhanced by combining with other techniques. Generally, the reporter fluorophores expressed by transduced neurons are imaged *post-mortem* using fluorescence or confocal microscopy, and often immunohistochemical staining is conducted to confirm that a subpopulation of neurons has been transduced. However, these techniques can be further exploited to determine which cellular compartments express the proteins (Pastrana, 2011; Konermann et al., 2013), for example using epitope tags (Lobbestael et al., 2010), or to detect structural elements, such as synapses, that cannot be definitively determined using light microscopy (Shu et al., 2011; Galvan et al., 2012). Improved tissue clearing techniques (Hama et al., 2011; Chung et al., 2013; Ke et al., 2013) and microscope optics have enabled visualization of transduced neurons in whole brains, and although this has been done using AAVs so far (Deisseroth and Schnitzer, 2013; Tomer et al., 2014; Yang et al., 2014), lentiviral vectors could be used to provide greater spatial specificity. Electron microscopy is another option that permits visualization of small structural elements and subcellular compartments to investigate circuitry at the ultrastructural level. This can be achieved by immunohistochemically tagging the fluorophore expressed by the viral vector and labeling it with an electron dense chromogen such as intensified diaminobenzidine (DAB, **Figure 4B**), using a genetic tag (miniSOG) that polymerizes DAB when exposed to blue light, or application of immunogold particles during postmortem tissue processing (Grinevich et al., 2005; Sosinsky et al., 2007; Scotto-Lomassese et al., 2011; Shu et al., 2011; Galvan et al., 2012; Dautan et al., 2014; Pollock et al., 2014). By combining lentiviral vectors, optogenetic stimulation, and cutting edge processing techniques for electron microscopy, such as high pressure freezing, the impact of changes in physiology on anatomical circuits can be investigated (Watanabe et al., 2014). Furthermore, because lentiviral vectors produce little to no immune or inflammatory response compared to many other vectors (Blomer et al., 1997), they maintain normal morphology and cellular composition in the area to be investigated, which is critical for studies at the ultrastructural level. This technology could be extended to examine the consequence of activating a G-protein by optogenetic stimulation and imaging how that changes the location of proteins in neurons, thus providing a greater understanding of the function and interactions of proteins at the subcellular level (Pastrana, 2011; Konermann et al., 2013). Thus, viral vectors and lentiviruses in particular, have broad utility to investigate neural circuits at synapse, neuronal, and complete circuit levels.

Importantly, the anatomy of brain circuitry can also be explored *in vivo* by imaging neurons transduced by a viral vector *in situ* using functional magnetic resonance imaging (fMRI) or bioluminescence. Bioluminescence imaging *in vivo* requires a reporter gene to encode a bioluminescent enzyme that generates light, usually in yellow-infrared spectral wavelengths, which are detected by the biosensor without using invasive procedures (Massoud et al., 2008; Shah et al., 2008). Generally, imaging of structures deep within an animal or tissue block is facilitated by having a longer wavelength (Contag and Bachmann, 2002; Zhang et al., 2007). Bioluminescence imaging is limited by its low resolution because light is scattered in body tissues; however, this imaging does provide valuable structural information within an animal (Contag and Bachmann, 2002). Bioluminescence imaging has been used to investigate therapeutic applications of gene expression using AAV, (Contag and Bachmann, 2002), adenovirus (Cho et al., 2005; Massoud et al., 2008), and lentiviral vectors (Deroose et al., 2006). Combining optogenetic stimulation of transduced neurons with fMRI offers a greater understanding of how neural activity alters blood oxygen level dependent (BOLD) signals at stimulated and downstream sites (Adriani et al., 2010; Lee et al., 2010; Desai et al., 2011; **Figure 4C**). In addition, positron emission tomography (PET) has been used to image changes in brain glucose metabolism following optogenetic stimulation to examine functionally connected brain

structures (Thanos et al., 2013). Neurons transduced with lentiviral vectors express non-native proteins for at least 6 months (Blomer et al., 1997), enabling changes in structure to be assessed over long periods of time, thus may provide insights to disease processes, for example, changes in structure associated with animal models of neurodegenerative diseases such as Alzheimer's. An alternative method to trace transduced neurons in more superficial areas of the brain *in situ* is to create a window for imaging transduced neurons via multiphoton microscopy. This usually involves live cell imaging to explore when and how large populations of neurons interact as a network (Shah et al., 2008; Mittmann et al., 2011; Knöpfel, 2012), but could be extended to investigate anatomical studies over time.

In the future, there are many ways that lentiviral vectors could be combined with imaging techniques and exploring these possibilities will greatly improve knowledge of the anatomy of neural circuits. Some applications may include optogenetic stimulation and clearing post-mortem tissue to examine a circuit within large blocks of brain for imaging using confocal microscope. Alternatively optogenetic stimulation combined with high pressure freezing of the tissue and electron microscopy would permit activity-dependent changes in ultrastructural circuitry to be investigated. Enhancing the resolution of *in situ* imaging by fMRI or bioluminescence would greatly improve knowledge of how circuitry changes over time in animal models of neurodegenerative diseases. Future improvements might include development of brain bow-like technology (Weber, 2012) using lentiviral vectors so that multiple pathways and neuronal phenotypes can be investigated in whole brains. The exciting prospect is to explore new combinations of lentiviral gene therapy with optogenetic stimulation, tissue processing, and imaging to address previously unprecedented neuroscience questions about health and disease.

Current Limitations and Future Prospects

Our understanding of the brain is rapidly expanding. Sophisticated technologies allow us to answer complex questions, understand gene function, and visualize the anatomy of neural circuits. The use of viral vectors is enhancing much of this work. Viral vectors have developed substantially from basic gene addition or knockdown with constitutive promoters to drug and light regulation of gene and protein expression. Further refinements of vectors, promoter regulation and transgenes continue. One recent example illustrating the potential of vectors in neuroscience involves mind-controlled gene regulation (Folcher et al., 2014). Combining EEG recorded brain waves and a computer interface, gene expression and/or optogenetic channel activity can be remotely regulated and changes in behavior can be measured. While this is currently in the proof-of concept phase, such technology has huge implications for the treatment of many brain disorders including epilepsy and Parkinson's disease.

Clinically, lentiviral vectors have predominantly been used to transduce cells *ex vivo*, which have then been later transplanted as a reservoir for production of useful gene products. To date AAV and lentivirus have been used to treat Parkinson's disease using standard gene therapy technology and although AAV has been preferred for injection into humans because it does not cause any known pathology, both AAV and lentivirus appear to be safe and well-tolerated by these patients (LeWitt et al., 2011; Palfi et al., 2014). The translatability of lentivirus use is currently limited by its restricted spread in large brains; however, further modification of envelope glycoproteins or injection strategies will alleviate this clinical dilemma in the future.

The frontiers of modern biological science will be expanded by developing new biological tools and refining new technologies by collaborative research teams with skills ranging from molecular biology and viral development to functional neuroanatomy and physiology. Involvement by clinical teams will ensure that these technologies address health-related questions and are readily translated to the clinical setting to improve the health and wellbeing of patients.

Acknowledgments

Research funded by Neurological Foundation of New Zealand (LP-B, SH), Health Research Council of New Zealand (LP-B, WA, SH), Cure Kids (SH), and the Royal Society of New Zealand Marsden Fund (WA, SH).

References

Abordo-Adesida, E., Follenzi, A., Barcia, C., Sciascia, S., Castro, M. G., Naldini, L., et al. (2005). Stability of lentiviral vector-mediated transgene expression in the brain in the presence of systemic antivector immune responses. *Hum. Gene Ther.* 16, 741–751. doi: 10.1089/hum.2005.16.741

Adriani, W., Boyer, F., Leo, D., Canese, R., Podo, F., Perrone-Capano, C., et al. (2010). Social withdrawal and gambling-like profile after lentiviral manipulation of DAT expression in the rat accumbens. *Int. J. Neuropsychopharmacol.* 13, 1329–1342. doi: 10.1017/S1461145709991210

Agwuh, K. N., and MacGowan, A. (2006). Pharmacokinetics and pharmacodynamics of the tetracyclines including glycylcyclines. *J. Antimicrob. Chemother.* 58, 256–265. doi: 10.1093/jac/dkl224

Akerblom, M., Sachdeva, R., Quintino, L., Wettergren, E. E., Chapman, K. Z., Manfre, G., et al. (2013). Visualization and genetic modification of resident brain microglia using lentiviral vectors regulated by microRNA-9. *Nat. Commun.* 4, 1770. doi: 10.1038/ncomms2801

Annoni, A., Battaglia, M., Follenzi, A., Lombardo, A., Sergi-Sergi, L., Naldini, L., et al. (2007). The immune response to lentiviral-delivered transgene is modulated in vivo by transgene-expressing antigen-presenting cells but not by CD4+CD25+ regulatory T cells. *Blood* 110, 1788–1796. doi: 10.1182/blood-2006-11-059873

Armbruster, B. N., Li, X., Pausch, M. H., Herlitze, S., and Roth, B. L. (2007). Evolving the lock to fit the key to create a family of G protein-coupled receptors potently activated by an inert ligand. *Proc. Natl. Acad. Sci. U.S.A.* 104, 5163–5168. doi: 10.1073/pnas.0700293104

Aston-Jones, G., and Deisseroth, K. (2013). Recent advances in optogenetics and pharmacogenetics. *Brain Res.* 1511, 1–5. doi: 10.1016/j.brainres.2013.01.026

Atasoy, D., Betley, J. N., Su, H. H., and Sternson, S. M. (2012). Deconstruction of a neural circuit for hunger. *Nature* 488, 172–177. doi: 10.1038/nature11270

Bartholomae, C. C., Arens, A., Balaggan, K. S., Yáñez-Muñoz, R. J., Montini, E., Howe, S. J., et al. (2011). Lentiviral vector integration profiles differ in rodent postmitotic tissues. *Mol. Ther.* 19, 703–710. doi: 10.1038/mt.2011.19

Beech, R. D., Cleary, M. A., Treloar, H. B., Eisch, A. J., Harrist, A. V., Zhong, W., et al. (2004). Nestin promoter/enhancer directs transgene expression to precursors of adult generated periglomerular neurons. *J. Comp. Neurol.* 475, 128–141. doi: 10.1002/cne.20179

Benzekhroufa, K., Liu, B. H., Teschemacher, A. G., and Kasparov, S. (2009). Targeting central serotonergic neurons with lentiviral vectors based on a transcriptional amplification strategy. *Gene Ther.* 16, 681–688. doi: 10.1038/gt.2009.7

Blomer, U., Naldini, L., Kafri, T., Trono, D., Verma, I. M., and Gage, F. H. (1997). Highly efficient and sustained gene transfer in adult neurons with a lentivirus vector. *J. Virol.* 71, 6641–6649.

Bosch, C., Degos, B., Deniau, J. M., and Venance, L. (2011). Subthalamic nucleus high-frequency stimulation generates a concomitant synaptic excitation-inhibition in substantia nigra pars reticulata. *J. Physiol.* 589(Pt 17), 4189–4207. doi: 10.1113/jphysiol.2011.211367

Boyden, E. S., Zhang, F., Bamberg, E., Nagel, G., and Deisseroth, K. (2005). Millisecond-timescale, genetically targeted optical control of neural activity. *Nat. Neurosci.* 8, 1263–1268. doi: 10.1038/nn1525

Brooks, A. R., Harkins, R. N., Wang, P., Qian, H. S., Liu, P., and Rubanyi, G. M. (2004). Transcriptional silencing is associated with extensive methylation of the CMV promoter following adenoviral gene delivery to muscle. *J. Gene Med.* 6, 395–404. doi: 10.1002/jgm.516

Cai, D., Cohen, K. B., Luo, T., Lichtman, J. W., and Sanes, J. R. (2013). Improved tools for the Brainbow toolbox. *Nat. Methods* 10, 540–547. doi: 10.1038/nmeth.2450

Callaway, E. M. (2008). Transneuronal circuit tracing with neurotropic viruses. *Curr. Opin. Neurobiol.* 18, 617–623. doi: 10.1016/j.conb.2009.03.007

Carpentier, D. C., Vevis, K., Trabalza, A., Georgiadis, C., Ellison, S. M., Asfahani, R. I., et al. (2012). Enhanced pseudotyping efficiency of HIV-1 lentiviral vectors by a rabies/vesicular stomatitis virus chimeric envelope glycoprotein. *Gene Ther.* 19, 761–774. doi: 10.1038/gt.2011.124

Cetin, A., Komai, S., Eliava, M., Seeburg, P. H., and Osten, P. (2006). Stereotaxic gene delivery in the rodent brain. *Nat. Protoc.* 1, 3166–3173. doi: 10.1038/nprot.2006.450

Chaudhury, D., Walsh, J. J., Friedman, A. K., Juarez, B., Ku, S. M., and Koo, J. W. (2013). Rapid regulation of depression-related behaviours by control of midbrain dopamine neurons. *Nature* 493, 532–536. doi: 10.1038/nature11713

Chen, J., Kwon, C. H., Lin, L., Li, Y., and Parada. L. F. (2009). Inducible site-specific recombination in neural stem/progenitor cells. *Genesis* 47, 122–131. doi: 10.1002/dvg.20465

Cheng, L., Jin, Z., Liu, L., Yan, Y., Li, T., Zhu, X., et al. (2004). Characterization and promoter analysis of the mouse nestin gene. *FEBS Lett.* 565, 195–202. doi: 10.1016/j.febslet.2004.03.097

Cho, S. Y., Ravasi, L., Szajek, L. P., Seidel, J., Green, M. V., Fine, H. A., et al. (2005). Evaluation of ^{76}Br-FBAU as a PET reporter probe for HSV1-tk gene expression imaging using mouse models of human glioma. *J. Nucl. Med.* 46, 1923–1930.

Chow, L. M., Zhang, J., and Baker, S. J. (2008). Inducible Cre recombinase activity in mouse mature astrocytes and adult neural precursor cells. *Transgenic Res.* 17, 919–928. doi: 10.1007/s11248-008-9185-4

Chung, K., Wallace, J., Kim, S.-Y., Kalyanasundaram, S., Andalman, A. S., Davidson, T. J., et al. (2013). Structural and molecular interrogation of intact biological systems. *Nature* 497, 332–337. doi: 10.1038/nature12107

Colin, A., Faideau, M., Dufour, N., Auregan, G., Hassig, R., Andrieu, T., et al. (2009). Engineered lentiviral vector targeting astrocytes in vivo. *Glia* 57, 667–679. doi: 10.1002/glia.20795

Contag, C. H., and Bachmann, M. H. (2002). Advances in in vivo bioluminescence imaging of gene expression. *Annu. Rev. Biomed. Eng.* 4, 235–260. doi: 10.1146/annurev.bioeng.4.111901.093336

Cronin, J., Zhang, X. Y., and Reiser, J. (2005). Altering the tropism of lentiviral vectors through pseudotyping. *Curr. Gene Ther.* 5, 387–398. doi: 10.2174/1566523054546224

Dautan, D., Huerta-Ocampo, I., Witten, I. B., Deisseroth, K., Bolam, J. P., Gerdjikov, T., et al. (2014). A major external source of cholinergic innervation of the striatum and nucleus accumbens originates in the brainstem. *J. Neurosci.* 34, 4509–4518. doi: 10.1523/JNEUROSCI.5071-13.2014

Deisseroth, K., and Schnitzer, M. J. (2013). Engineering approaches to illuminating brain structure and dynamics. *Neuron* 80, 568–577. doi: 10.1016/j.neuron.2013.10.032

Delzor, A., Dufour, N., Petit, F., Guillermier, M., Houitte, D., Auregan, G., et al. (2012). Restricted transgene expression in the brain with cell-type specific neuronal promoters. *Hum. Gene Ther. Methods* 23, 242–254. doi: 10.1089/hgtb.2012.073

De Marco, R. J., Groneberg, A. H., Yeh, C. M., Castillo Ramírez, L. A., and Ryu, S. (2013). Optogenetic elevation of endogenous glucocorticoid level in larval zebrafish. *Front. Neural Circuits* 7:82. doi: 10.3389/fncir.2013.00082

Deroose, C. M., Reumers, V., Gijsbers, R., Bormans, G., Debyser, Z., Mortelmans, L., et al. (2006). Noninvasive monitoring of long-term lentiviral vector-mediated gene expression in rodent brain with bioluminescence imaging. *Mol. Ther.* 14, 423–431. doi: 10.1016/j.ymthe.2006.05.007

Desai, M., Kahn, I., Knoblich, U., Bernstein, J., Atallah, H., Yang, A., et al. (2011). Mapping brain networks in awake mice using combined optical neural control and fMRI. *J. Neurophysiol.* 105, 1393–1405. doi: 10.1152/jn.00828.2010

Desmaris, N., Bosch, A., Salaün, C., Petit, C., Prévost, M. C., Tordo, N., et al. (2001). Production and neurotropism of lentivirus vectors pseudotyped with lyssavirus envelope glycoproteins. *Mol. Ther.* 4, 149–156. doi: 10.1006/mthe.2001.0431

Diester, I., Kaufman, M. T., Mogri, M., Pashaie, R., Goo, W., Yizhar, O., et al. (2011). An optogenetic toolbox designed for primates. *Nat. Neurosci.* 14, 387–397. doi: 10.1038/nn.2749

Dittgen, T., Nimmerjahn, A., Komai, S., Licznerski, P., Waters, J., Margrie, T. W., et al. (2004). Lentivirus-based genetic manipulations of cortical neurons and their optical and electrophysiological monitoring in vivo. *Proc. Natl. Acad. Sci. U.S.A.* 101, 18206–18211. doi: 10.1073/pnas.0407976101

Duale, H., Kasparov, S., Paton, J. F., and Teschemacher, A. G. (2005). Differences in transductional tropism of adenoviral and lentiviral vectors in the rat brainstem. *Exp. Physiol.* 90, 71–78. doi: 10.1113/expphysiol.2004.029173

Dull, T., Zufferey, R., Kelly, M., Mandel, R. J., Nguyen, M., Trono, D., et al. (1998). A third-generation lentivirus vector with a conditional packaging system. *J. Virol.* 72, 8463–8471.

Fanselow, E. E., and Connors, B. W. (2005). Navigating a sensorimotor loop. *Neuron* 45, 329–330. doi: 10.1016/j.neuron.2005.01.022

Fenno, L., Yizhar, O., and Deisseroth, K. (2011). The development and application of optogenetics. *Annu. Rev. Neurosci.* 34, 389–412. doi: 10.1146/annurev-neuro-061010-113817

Figueiredo, M., Lane, S., Tang, F., Liu, B. H., Hewinson, J., Marina, N., et al. (2011). Optogenetic experimentation on astrocytes. *Exp. Physiol.* 96, 40–50. doi: 10.1113/expphysiol.2010.052597

Finkelshtein, D., Werman, A., Novick, D., Barak, S., and Rubinstein, M. (2013). LDL receptor and its family members serve as the cellular receptors for vesicular stomatitis virus. *Proc. Natl. Acad. Sci. U.S.A.* 110, 7306–7311. doi: 10.1073/pnas.1214441110

Folcher, M., Oesterle, S., Zwicky, K., Thekkottil, T., Heymoz, J., Hohmann, M., et al. (2014). Mind-controlled transgene expression by a wireless-powered optogenetic designer cell implant. *Nat. Commun.* 5, 5392. doi: 10.1038/ncomms6392

Galvan, A., Hu, X., Smith, Y., and Wichmann, T. (2012). In vivo optogenetic control of striatal and thalamic neurons in non-human primates. *PLoS ONE* 7:e50808. doi: 10.1371/journal.pone.0050808

Gossen, M., and Bujard, H. (1992). Tight control of gene expression in mammalian cells by tetracycline-responsive promoters. *Proc. Natl. Acad. Sci. U.S.A.* 89, 5547–5551. doi: 10.1073/pnas.89.12.5547

Gossen, M., and Bujard, H. (1995). Efficacy of tetracycline-controlled gene expression is influenced by cell type: commentary. *BioTechniques* 19, 213–216.

Gossen, M., Freundlieb, S., Bender, G., Müller, G., Hillen, W., Bujard, H., et al. (1995). Transcriptional activation by tetracyclines in mammalian cells. *Science* 268, 1766–1769. doi: 10.1126/science.7792603

Gradinaru, V., Zhang, F., Ramakrishnan, C., Mattis, J., Prakash, R., Diester, I., et al. (2010). Molecular and cellular approaches for diversifying and extending optogenetics. *Cell* 141, 154–165. doi: 10.1016/j.cell.2010.02.037

Grinevich, V., Brecht, M., and Osten, P. (2005). Monosynaptic pathway from rat vibrissa motor cortex to facial motor neurons revealed by lentivirus-based axonal tracing. *J. Neurosci.* 25, 8250–8258. doi: 10.1523/JNEUROSCI.2235-05.2005

Hacein-Bey-Abina, S., Von Kalle, C., Schmidt, M., McCormack, M. P., Wulffraat, N., Leboulch, P., et al. (2003). LMO2-associated clonal T cell proliferation in two patients after gene therapy for SCID-X1. *Science* 302, 415–419. doi: 10.1126/science.1088547

Hama, H., Kurokawa, H., Schmidt, M., McCormack, M. P., Wulffraat, N., Leboulch, P., et al. (2011). Scale: a chemical approach for fluorescence imaging

and reconstruction of transparent mouse brain. *Nat. Neurosci.* 14, 1481–1488. doi: 10.1038/nn.2928

Han, X., Qian, X., Bernstein, J. G., Zhou, H. H., Franzesi, G. T., Stern, P., et al. (2009). Millisecond-timescale optical control of neural dynamics in the nonhuman primate brain. *Neuron* 62, 191–198. doi: 10.1016/j.neuron.2009.03.011

Hasegawa, E., Yanagisawa, M., Sakurai, T., and Mieda, M. (2014). Orexin neurons suppress narcolepsy via 2 distinct efferent pathways. *J. Clin. Invest.* 124, 604–616. doi: 10.1172/JCI71017

Hausser, M. (2014). Optogenetics: the age of light. *Nat. Methods* 11, 1012–1014. doi: 10.1038/nmeth.3111

Heitz, F., Johansson, T., Baumgärtel, K., Gecaj, R., Pelczar, P., and Mansuy, I. M. (2014). Heritable and inducible gene knockdown in astrocytes or neurons in vivo by a combined lentiviral and RNAi approach. *Front. Cell Neurosci.* 8:62. doi: 10.3389/fncel.2014.00062

Hioki, H., Kameda, H., Nakamura, H., Okunomiya, T., Ohira, K., Nakamura, K., et al. (2007). Efficient gene transduction of neurons by lentivirus with enhanced neuron-specific promoters. *Gene Ther.* 14, 872–882. doi: 10.1038/sj.gt.3302924

Huh, Y., Oh, M. S., Leblanc, P., and Kim, K. S. (2010). Gene transfer in the nervous system and implications for transsynaptic neuronal tracing. *Expert Opin. Biol. Ther.* 10, 763–772. doi: 10.1517/14712591003796538

Indraccolo, S., Minuzzo, S., Feroli, F., Mammano, F., Calderazzo, F., Chieco-Bianchi, L., et al. (1998). Pseudotyping of Moloney leukemia virus-based retroviral vectors with simian immunodeficiency virus envelope leads to targeted infection of human CD4+ lymphoid cells. *Gene Ther.* 5, 209–217. doi: 10.1038/sj.gt.3300603

Jakobsson, J., Ericson, C., Jansson, M., Björk, E., and Lundberg, C. (2003). Targeted transgene expression in rat brain using lentiviral vectors. *J. Neurosci. Res.* 73, 876–885. doi: 10.1002/jnr.10719

Kato, S., Kobayashi, K., Inoue, K., Kuramochi, M., Okada, T., Yaginuma, H., et al. (2011a). A lentiviral strategy for highly efficient retrograde gene transfer by pseudotyping with fusion envelope glycoprotein. *Hum. Gene Ther.* 22, 197–206. doi: 10.1089/hum.2009.179

Kato, S., Kuramochi, M., Takasumi, K., Kobayashi, K., Inoue, K., Takahara, D., et al. (2011b). Neuron-specific gene transfer through retrograde transport of lentiviral vector pseudotyped with a novel type of fusion envelope glycoprotein. *Hum. Gene Ther.* 22, 1511–1523. doi: 10.1089/hum.2011.111

Kato, S., Kobayashi, K., and Kobayashi, K. (2014). Improved transduction efficiency of a lentiviral vector for neuron-specific retrograde gene transfer by optimizing the junction of fusion envelope glycoprotein. *J. Neurosci. Methods* 227, 151–158. doi: 10.1016/j.jneumeth.2014.02.015

Ke, M. T., Fujimoto, S., and Imai, T. (2013). SeeDB: a simple and morphology-preserving optical clearing agent for neuronal circuit reconstruction. *Nat. Neurosci.* 16, 1154–1161. doi: 10.1038/nn.3447

Klaw, M. C., Xu, C., and Tom, V. J. (2013). Intraspinal AAV injections immediately rostral to a thoracic spinal cord injury site efficiently transduces neurons in spinal cord and brain. *Mol. Ther. Nucleic Acids* 2:e108. doi: 10.1038/mtna.2013.34

Klein, R. L., Meyer, E. M., Peel, A. L., Zolotukhin, S., Meyers, C., Muzyczka, N., et al. (1998). Neuron-specific transduction in the rat septohippocampal or nigrostriatal pathway by recombinant adeno-associated virus vectors. *Exp. Neurol.* 150, 183–194. doi: 10.1006/exnr.1997.6736

Knöpfel, T. (2012). Genetically encoded optical indicators for the analysis of neuronal circuits. *Nat. Rev. Neurosci.* 13, 687–700. doi: 10.1038/nrn3293

Konermann, S., Brigham, M. D., Trevino, A. E., Hsu, P. D., Heidenreich, M., Cong, L., et al. (2013). Optical control of mammalian endogenous transcription and epigenetic states. *Nature* 500, 472–476. doi: 10.1038/nature12466

Kumar-Singh, R. (2008). Barriers for retinal gene therapy: separating fact from fiction. *Vision Res.* 48, 1671–1680. doi: 10.1016/j.visres.2008.05.005

Lee, J. H., Durand, R., Gradinaru, V., Zhang, F., Goshen, I., Kim, D.-S., et al. (2010). Global and local fMRI signals driven by neurons defined optogenetically by type and wiring. *Nature* 465, 788–792. doi: 10.1038/nature09108

Lerchner, W., Corgiat, B., Der Minassian, V., Saunders, R. C., and Richmond, B. J. (2014). Injection parameters and virus dependent choice of promoters to improve neuron targeting in the nonhuman primate brain. *Gene Ther.* 21, 233–241. doi: 10.1038/gt.2013.75

LeWitt, P. A., Rezai, A. R., Leehey, M. A., Ojemann, S. G., Flaherty, A. W., Eskandar, E. N., et al. (2011). AAV2-GAD gene therapy for advanced Parkinson's disease: a double-blind, sham-surgery controlled, randomised trial. *Lancet Neurol.* 10, 309–319. doi: 10.1016/S1474-4422(11)70039-4

Li, M., Husic, N., Lin, Y., Christensen, H., Malik, I., McIver, S., et al. (2010). Optimal promoter usage for lentiviral vector-mediated transduction of cultured central nervous system cells. *J. Neurosci. Methods* 189, 56–64. doi: 10.1016/j.jneumeth.2010.03.019

Li, Y., Du, X. F., and Du, J. L. (2013). Resting microglia respond to and regulate neuronal activity in vivo. *Commun. Integr. Biol.* 6:e24493. doi: 10.4161/cib.24493

Linterman, K. S., Palmer, D. N., Kay, G. W., Barry, L. A., Mitchell, N. L., McFarlane, R. G., et al. (2011). Lentiviral-mediated gene transfer to the sheep brain: implications for gene therapy in Batten disease. *Hum. Gene Ther.* 22, 1011–1020. doi: 10.1089/hum.2011.026

Liu, K. C., Lin, B. S., Gao, A. D., Ma, H. Y., Zhao, M., Zhang, R., et al. (2014). Integrase-deficient lentivirus: opportunities and challenges for human gene therapy. *Curr. Gene Ther.* 14, 352–364. doi: 10.2174/1566523214666140825124311

Liu, Y. J., Ehrengruber, M. U., Negwer, M., Shao, H. J., Cetin, A. H., and Lyon, D. C. (2013). Tracing inputs to inhibitory or excitatory neurons of mouse and cat visual cortex with a targeted rabies virus. *Curr. Biol.* 23, 1746–1755. doi: 10.1016/j.cub.2013.07.033

Lobbestael, E., Reumers, V., Ibrahimi, A., Paesen, K., Thiry, I., Gijsbers, R., et al. (2010). Immunohistochemical detection of transgene expression in the brain using small epitope tags. *BMC Biotechnol.* 10:16. doi: 10.1186/1472-6750-10-16

Massoud, T. F., Singh, A., and Gambhir, S. S. (2008). Noninvasive molecular neuroimaging using reporter genes: part I, principles revisited. *AJNR Am. J. Neuroradiol.* 29, 229–234. doi: 10.3174/ajnr.A0864

Mazarakis, N. D., Azzouz, M., Rohll, J. B., Ellard, F. M., Wilkes, F. J., Olsen, A. L., et al. (2001). Rabies virus glycoprotein pseudotyping of lentiviral vectors enables retrograde axonal transport and access to the nervous system after peripheral delivery. *Hum. Mol. Genet.* 10, 2109–2121. doi: 10.1093/hmg/10.19.2109

McIver, S. R., Lee, C. S., Lee, J. M., Green, S. H., Sands, M. S., Snider, B. J., et al. (2005). Lentiviral transduction of murine oligodendrocytes in vivo. *J. Neurosci. Res.* 82, 397–403. doi: 10.1002/jnr.20626

McIver, S. R., Muccigrosso, M., Gonzales, E. R., Lee, J. M., Roberts, M. S., Sands, M. S., et al. (2010). Oligodendrocyte degeneration and recovery after focal cerebral ischemia. *Neuroscience* 169, 1364–1375. doi: 10.1016/j.neuroscience.2010.04.070

Mittmann, W., Wallace, D. J., Czubayko, U., Herb, J. T., Schaefer, A. T., Looger, L. L., et al. (2011). Two-photon calcium imaging of evoked activity from L5 somatosensory neurons in vivo. *Nat. Neurosci.* 14, 1089–1093. doi: 10.1038/nn.2879

Miyashita, T., Shao, Y. R., Chung, J., Pourzia, O., and Feldman, D. E. (2013). Long-term channelrhodopsin-2 (ChR2) expression can induce abnormal axonal morphology and targeting in cerebral cortex. *Front. Neural Circuits* 7:8. doi: 10.3389/fncir.2013.00008

Miyoshi, H., Takahashi, M., Gage, F. H., and Verma, I. M. (1997). Stable and efficient gene transfer into the retina using an HIV-based lentiviral vector. *Proc. Natl. Acad. Sci. U.S.A.* 94, 10319–10323. doi: 10.1073/pnas.94.19.10319

Naldini, L. (1998). Lentiviruses as gene transfer agents for delivery to non-dividing cells. *Curr. Opin. Biotechnol.* 9, 457–463. doi: 10.1016/S0958-1669(98)80029-3

Nathanson, J. L., Yanagawa, Y., Obata, K., and Callaway, E. M. (2009). Preferential labeling of inhibitory and excitatory cortical neurons by endogenous tropism of adeno-associated virus and lentivirus vectors. *Neuroscience* 161, 441–450. doi: 10.1016/j.neuroscience.2009.03.032

Nielsen, T. T., Marion, I., Hasholt, L., and Lundberg, C. (2009). Neuron-specific RNA interference using lentiviral vectors. *J. Gene Med.* 11, 559–569. doi: 10.1002/jgm.1333

Packer, A. M., Roska, B., and Häusser, M. (2013). Targeting neurons and photons for optogenetics. *Nat. Neurosci.* 16, 805–815. doi: 10.1038/nn.3427

Palfi, S., Gurruchaga, J. M., Ralph, G. S., Lepetit, H., Lavisse, S., Buttery, P. C., et al. (2014). Long-term safety and tolerability of ProSavin, a lentiviral vector-based gene therapy for Parkinson's disease: a dose escalation, open-label, phase 1/2 trial. *Lancet* 383, 1138–1146. doi: 10.1016/S0140-6736(13)61939-X

Pastrana, E. (2011). Perfecting ChR2. *Nat. Methods* 8, 447. doi: 10.1038/nmeth0611-447

Pathak, G. P., Vrana, J. D., and Tucker, C. L. (2013). Optogenetic control of cell function using engineered photoreceptors. *Biol. Cell* 105, 59–72. doi: 10.1111/boc.201200056

Pluta, K., Luce, M. J., Bao, L., Agha-Mohammadi, S., and Reiser, J. (2005). Tight control of transgene expression by lentivirus vectors containing second-generation tetracycline-responsive promoters. *J. Gene Med.* 7, 803–817. doi: 10.1002/jgm.712

Pollock, J. D., Wu, D. Y., and Satterlee, J. S. (2014). Molecular neuroanatomy: a generation of progress. *Trends Neurosci.* 37, 106–123. doi: 10.1016/j.tins.2013.11.001

Qin, J. Y., Zhang, L., Clift, K. L., Hulur, I., Xiang, A. P., Ren, B.-Z., et al. (2010). Systematic comparison of constitutive promoters and the doxycycline-inducible promoter. *PLoS ONE* 5:e10611. doi: 10.1371/journal.pone.0010611

Rogan, S. C., and Roth, B. L. (2011). Remote control of neuronal signaling. *Pharmacol. Rev.* 63, 291–315. doi: 10.1124/pr.110.003020

Sauer, B., and Henderson. N. (1988). Site-specific DNA recombination in mammalian cells by the Cre recombinase of bacteriophage P1. *Proc. Natl. Acad. Sci. U.S.A.* 85, 5166–5170. doi: 10.1073/pnas.85.14.5166

Schoderboeck, L., Riad, S., Bokor, A. M., Wicky, H. E., Strauss, M., Bostina, M., et al. (2015). Chimeric rabies SADB19-VSVg pseudotyped lentiviral vectors mediate long-range retrograde transduction from the mouse spinal cord. *Gene Ther*. doi: 10.1038/gt.2015.3 [Epub ahead of print].

Scotto-Lomassese, S., Nissant, A., Mota, T., Néant-Féry, M., Oostra, B. A., Greer, C. A., et al. (2011). Fragile X mental retardation protein regulates new neuron differentiation in the adult olfactory bulb. *J. Neurosci.* 31, 2205–2215. doi: 10.1523/JNEUROSCI.5514-10.2011

Seeger-Armbruster, S., Bosch-Bouju, C., Little, S. T., Smither, R. A., Hughes, S. M., Hyland, B. I., et al. (2015). Patterned, but not tonic, optogenetic stimulation in motor thalamus improves reaching in acute drug-induced parkinsonian rats. *J. Neurosci.* 35, 1211–1216. doi: 10.1523/JNEUROSCI.3277-14.2015

Shah, K., Hingtgen, S., Kasmieh, R., Figueiredo, J. L., Garcia-Garcia, E., Martinez-Serrano, A., et al. (2008). Bimodal viral vectors and in vivo imaging reveal the fate of human neural stem cells in experimental glioma model. *J. Neurosci.* 28, 4406–4413. doi: 10.1523/JNEUROSCI.0296-08.2008

Shu, X., Lev-Ram, V., Deerinck, T. J., Qi, Y., Ramko, E. B., Davidson, M. W., et al. (2011). A genetically encoded tag for correlated light and electron microscopy of intact cells, tissues, and organisms. *PLoS Biol.* 9:e1001041. doi: 10.1371/journal.pbio.1001041

Sohal, V. S., Zhang, F., Yizhar, O., and Deisseroth, K. (2009). Parvalbumin neurons and gamma rhythms enhance cortical circuit performance. *Nature* 459, 698–702. doi: 10.1038/nature07991

Sosinsky, G. E., Giepmans, B. N., Deerinck, T. J., Gaietta, G. M., and Ellisman, M. H. (2007). Markers for correlated light and electron microscopy. *Methods Cell Biol.* 79, 575–591. doi: 10.1016/S0091-679X(06)79023-9

Stern, P., Astrof, S., Erkeland, S. J., Schustak, J., Sharp, P. A., and Hynes, R. O. (2008). A system for Cre-regulated RNA interference in vivo. *Proc. Natl. Acad. Sci. U.S.A.* 105, 13895–13900. doi: 10.1073/pnas.0806907105

Sun, M. Y., Yetman, M. J., Lee, T.-C., Chen, Y., and Jankowsky, J. L. (2014). Specificity and efficiency of reporter expression in adult neural progenitors vary substantially among nestin-CreER(T2) lines. *J. Comp. Neurol.* 522, 1191–1208. doi: 10.1002/cne.23497

Takada, M., Inoue, K., Koketsu, D., Kato, S., Kobayashi, K., and Nambu, A. (2013). Elucidating information processing in primate basal ganglia circuitry: a novel technique for pathway-selective ablation mediated by immunotoxin. *Front. Neural Circuits* 7:140. doi: 10.3389/fncir.2013.00140

Thanos, P. K., Robison, L., Nestler, E. J., Kim, R., Michaelides, M., Lobo, M. K., et al. (2013). Mapping brain metabolic connectivity in awake rats with muPET and optogenetic stimulation. *J. Neurosci.* 33, 6343–6349. doi: 10.1523/JNEUROSCI.4997-12.2013

Tomer, R., Ye, L., Hsueh, B., and Deisseroth, K. (2014). Advanced CLARITY for rapid and high-resolution imaging of intact tissues. *Nat. Protoc.* 9, 1682–1697. doi: 10.1038/nprot.2014.123

Trabalza, A., Georgiadis, C., Eleftheriadou, I., Hislop, J. N., Ellison, S. M., Karavassilis, M. E., et al. (2013). Venezuelan equine encephalitis virus glycoprotein pseudotyping confers neurotropism to lentiviral vectors. *Gene Ther.* 20, 723–732. doi: 10.1038/gt.2012.85

Trono, D. (2000). Lentiviral vectors: turning a deadly foe into a therapeutic agent. *Gene Ther.* 7, 20–23. doi: 10.1038/sj.gt.3301105

Tye, K. M., and Deisseroth, K. (2012). Optogenetic investigation of neural circuits underlying brain disease in animal models. *Nat. Rev. Neurosci.* 13, 251–266. doi: 10.1038/nrn3171

van Hooijdonk, L. W., Ichwan, M., Dijkmans, T. F., Schouten, T. G., de Backer, M. W. A., Adan, R. A. H., et al. (2009). Lentivirus-mediated transgene delivery to the hippocampus reveals sub-field specific differences in expression. *BMC Neurosci.* 10:2. doi: 10.1186/1471-2202-10-2

Verma, I. M., and Somia, N. (1997). Gene therapy – promises, problems and prospects. *Nature* 389, 239–242. doi: 10.1038/38410

Vigna, E., and Naldini, L. (2000). Lentiviral vectors: excellent tools for experimental gene transfer and promising candidates for gene therapy. *J. Gene Med.* 2, 308–316. doi: 10.1002/1521-2254(200009/10)2:5<308::AID-JGM131>3.0.CO;2-3

Vodicka, M. A. (2001). Determinants for lentiviral infection of non-dividing cells. *Somat. Cell Mol. Genet.* 26, 35–49. doi: 10.1023/A:10210226 29126

Wang, X., Chen, X., and Yang, Y. (2012). Spatiotemporal control of gene expression by a light-switchable transgene system. *Nat. Methods* 9, 266–269. doi: 10.1038/nmeth.1892

Watanabe, S., Davis, M. W., and Jorgenson, E. M. (2014). Flash-and-freeze electron microscopy: coupling optogenetics with high-pressure freezing. *Nanoscale Imag. Synap.* 84, 43–57. doi: 10.1007/978-1-4614-9179-8_3

Watson, D. J., Kobinger, G. P., Passini, M. A., Wilson, J. M., and Wolfe. J. H. (2002). Targeted transduction patterns in the mouse brain by lentivirus vectors pseudotyped with VSV, Ebola, Mokola, LCMV, or MuLV envelope proteins. *Mol. Ther.* 5(Pt 1), 528–537. doi: 10.1006/mthe.2002.0584

Weber, B. (2012). Neuroscience: the case for brain imaging technology. *Nature* 483, 541. doi: 10.1038/483541d

Willnow, T. E. (1999). The low-density lipoprotein receptor gene family: multiple roles in lipid metabolism. *J. Mol. Med. (Berl.)* 77, 306–315. doi: 10.1007/s001090050356

Wiznerowicz, M., and Trono, D. (2003). Conditional suppression of cellular genes: lentivirus vector-mediated drug-inducible RNA interference. *J. Virol.* 77, 8957–8961. doi: 10.1128/JVI.77.16.8957-8951.2003

Yaguchi, M., Ohashi, Y., Tsubota, T., Sato, A., Koyano, K. W., Wang, N., et al. (2013). Characterization of the properties of seven promoters in the motor cortex of rats and monkeys after lentiviral vector-mediated gene transfer. *Hum. Gene Ther. Methods* 24, 333–344. doi: 10.1089/hgtb.20 12.238

Yang, B., Treweek, J. B., Kulkarni, R. P., Deverman, B. E., Chen, C.-K., Lubeck, E., et al. (2014). Single-cell phenotyping within transparent intact tissue through whole-body clearing. *Cell* 158, 945–958. doi: 10.1016/j.cell.2014. 07.017

Zhang, F., Aravanis, A. M., Adamantidis, A., de Lecea, L., and Deisseroth, K. (2007). Circuit-breakers: optical technologies for probing neural signals and systems. *Nat. Rev. Neurosci.* 8, 577–581. doi: 10.1038/nrn2192

Zhang, F., Gradinaru, V., Adamantidis, A. R., Durand, R., Airan, R. D., de Lecea, L., et al. (2010). Optogenetic interrogation of neural circuits: technology for probing mammalian brain structures. *Nat. Protoc.* 5, 439–456. doi: 10.1038/nprot.2009.226

Zhou, S., Mody, D., DeRavin, S. S., Hauer, J., Lu, T., Ma, Z., et al. (2010). A self-inactivating lentiviral vector for SCID-X1 gene therapy that does not activate LMO2 expression in human T cells. *Blood* 116, 900–908. doi: 10.1182/blood-2009-10-250209

Conflict of Interest Statement: The authors declare that the research was conducted in the absence of any commercial or financial relationships that could be construed as a potential conflict of interest.

frontiers in Molecular Neuroscience

REVIEW
published: 01 November 2016
doi: 10.3389/fnmol.2016.00108

Non-Viral Nucleic Acid Delivery Strategies to the Central Nervous System

*James-Kevin Y. Tan[1], Drew L. Sellers[1], Binhan Pham[1], Suzie H. Pun[1] and Philip J. Horner[2]**

[1] Department of Bioengineering and Molecular Engineering & Sciences Institute, University of Washington, Seattle, WA, USA,
[2] Center for Neuroregenerative Medicine, Houston Methodist Research Institute, Houston, TX, USA

With an increased prevalence and understanding of central nervous system (CNS) injuries and neurological disorders, nucleic acid therapies are gaining promise as a way to regenerate lost neurons or halt disease progression. While more viral vectors have been used clinically as tools for gene delivery, non-viral vectors are gaining interest due to lower safety concerns and the ability to deliver all types of nucleic acids. Nevertheless, there are still a number of barriers to nucleic acid delivery. In this focused review, we explore the *in vivo* challenges hindering non-viral nucleic acid delivery to the CNS and the strategies and vehicles used to overcome them. Advantages and disadvantages of different routes of administration including: systemic injection, cerebrospinal fluid injection, intraparenchymal injection and peripheral administration are discussed. Non-viral vehicles and treatment strategies that have overcome delivery barriers and demonstrated *in vivo* gene transfer to the CNS are presented. These approaches can be used as guidelines in developing synthetic gene delivery vectors for CNS applications and will ultimately bring non-viral vectors closer to clinical application.

Keywords: central nervous system, delivery, *in vivo*, non-viral, nucleic acid

OPEN ACCESS

Edited by:
George Smith, Temple University School of Medicine, USA

Reviewed by:
Eduardo Fernandez, Universidad Miguel Hernández de Elche, Spain
Marianna Foldvari, University of Waterloo, Canada

****Correspondence:***
Philip J. Horner
pjhorner@houstonmethodist.org

Received: *13 July 2016*
Accepted: *11 October 2016*
Published: *01 November 2016*

Citation:
Tan J-KY, Sellers DL, Pham B, Pun SH and Horner PJ (2016) Non-Viral Nucleic Acid Delivery Strategies to the Central Nervous System. Front. Mol. Neurosci. 9:108. doi: 10.3389/fnmol.2016.00108

INTRODUCTION

The incidence of neurological diseases and injuries is increasing with the rising life expectancy (Mattson and Magnus, 2006). Nucleic acid therapeutics, such as genes and small interfering RNA (siRNA) oligonucleotides have emerged as a promising treatment strategy to preserve neuron function, enhance neurogenesis and prevent the progression of neurological diseases. The delivery of nucleic acids encoding brain-derived neurotrophic factor (Huang et al., 2012a), epidermal growth factor (Sugiura et al., 2005), fibroblast growth factor-2 (Matsuoka et al., 2003), Huntingtin (Burgess et al., 2012), neurogenin-2 (Zhang et al., 2013; Masserdotti et al., 2015), insulin growth factor-1 (Kaspar et al., 2003), and vascular endothelial growth factor (Dodge et al., 2010) have been shown to increase neuron regeneration or delay the progression of neurological diseases in mice, rats and gerbils. Targeting gene delivery vehicles to the appropriate cells and proper protein regulation remain the primary challenges to making these pathways feasible. While viral vectors such as the adeno-associated virus have typically been used clinically, interest in non-viral nucleic acid delivery remains high due to lower safety concerns, greater customizability and an ease in manufacturing (Pack et al., 2005; Burke et al., 2013). In fact, the number of synthetic vectors used in gene therapy clinical trials has been steadily increasing over the last 10 years (Gene Therapy Clinical Trials Worldwide, Wiley).

With neurological diseases specifically affecting different parts of the brain and even sub-phenotypes of neural cells, the route of administration is a crucial aspect of nucleic acid delivery. Intraventricular injection places therapeutics closer to the subventricular zone, one of the stem cell niches of the brain, whereas localized intraparenchymal injections may be used to target a specific part of the brain where neurodegeneration is occurring or at the location of disease (e.g., brain tumor). In this focused review, we explore the barriers facing *in vivo* nucleic acid delivery and highlight the recent synthetic vehicles and different strategies that have overcome these challenges to deliver nucleic acids to the central nervous system (CNS). First, we briefly discuss nucleic acid protection and targeting the CNS since these strategies apply to any route of administration. In later sections, we discuss the common routes of administration and the specific barriers and vehicular solutions accompanying each method. While a wide variety of delivery vehicles have been applied to nucleic acid CNS delivery, we primarily focused on lipidic and polymeric vehicles with a few selected examples of inorganic delivery vehicles.

Nucleic Acid Protection

With any route of administration, nucleic acids are susceptible to chemical degradation and clearance from the body due to the presence of extracellular nucleases and the immune system (Abdelhady et al., 2003). While naked nucleic acid delivery is feasible, carrier-mediated delivery has the potential to be more efficient by protecting nucleic acids and chaperoning nucleic acids through the extracellular and cellular barriers to gene delivery (**Figure 1**). Thus, this focused review focused on carrier-mediated delivery of nucleic acids. Typically, negatively charged nucleic acids are complexed and condensed with cationic, synthetic materials which allows for nucleic acids to remain hidden and avoid degradation (Pack et al., 2005). Common complexation agents used for *in vitro* gene transfer include cationic polymers such as polyethylenimine (PEI), which electrostatically bind to nucleic acids to form "polyplexes," or polymer-nucleic acid complexes. Similarly, cationic lipids can also be used to complex nucleic acids to form "lipoplexes". Another method of enhancing stability is by modifying the nucleic acid itself so that it avoids recognition and degradation. For example, altering the ribose moiety and introducing 2′-fluoro and phosphorothioate near the terminal region of siRNA duplexes enhanced stability and prolonged siRNA half-life *in vivo* (Wang et al., 2008).

Despite the protection afforded to nucleic acids by electrostatic complexation, these cationic complexes are still subject to challenges such as aggregation, toxicity, premature sequestration by phagocytic cells, and non-specific interaction with cell membranes and serum proteins (Morille et al., 2008). When intravenously administered, PEI, one of the most effective transfection agents *in vitro*, causes severe toxic side effects due to polyplex aggregation and strong electrostatic interactions with cell membranes, proteins and the extracellular matrix (Al-Dosari and Gao, 2009). To overcome these challenges, shielding strategies have been developed to hide nucleic acid delivery vehicle by moieties like poly(ethylene glycol) (PEG) and albumin (Lu et al., 2006; Laga et al., 2012).

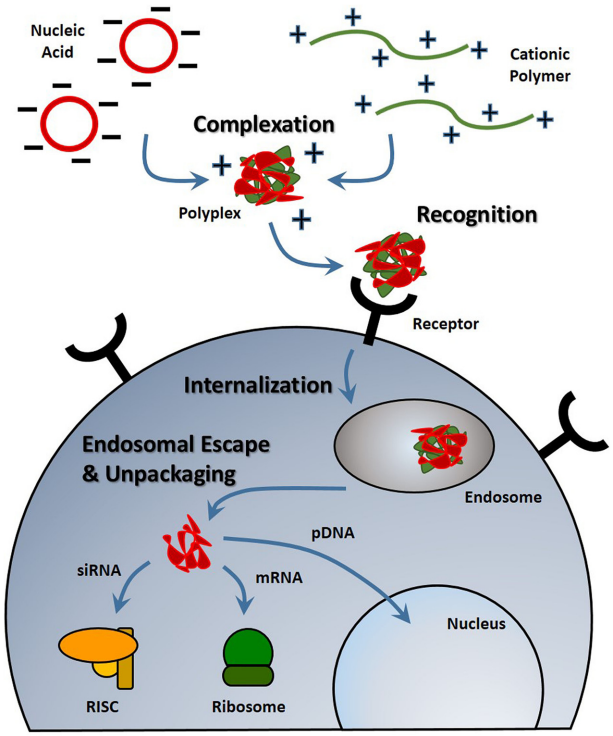

FIGURE 1 | Stages of nucleic acid delivery into a cell. Nucleic acids are typically condensed and complexed with a cationic material. This complex must be recognized by a cell, be internalized and escape the endosomal-lysosomal degradation pathway. Once in the cell cytoplasm, the nucleic acid can separate from its vehicle and traffic to its intended target based on its type.

PEG, a biocompatible, hydrophilic polymer, is commonly used as a shielding agent for nanoparticles (Immordino et al., 2006). By creating a barrier around the complex, it was previously believed that PEG prevents the adsorption of proteins (Pombo García et al., 2014). However, recent studies suggest that PEGylation of nanoparticles results in preferential binding of clusterin, a chaperone protein that binds to hydrophobic domains of unfolded proteins and prevents non-specific binding (Schöttler et al., 2016). When conjugated to delivery vehicles, PEG has been shown to improve the stability and increase the circulation half-life of polyplexes, liposomes and other types of vectors. For example, when conjugated to PEI, PEG prevented the aggregation of PEI-plasmid DNA complexes in fetal bovine serum-enhanced media, resulting in complexes that could circulate long enough for observed localization in the brain (Son et al., 2011). With encapsulation in PEGylated liposomes, PEI-oligonucleotide complexes were able to circulate substantially longer and had plasma concentrations significantly higher than naked complexes after 60 min (Ko et al., 2009). By any route of

administration, protecting delivery vehicles with a shielding agent minimizes aggregation and premature sequestration and can increase the distribution of the nucleic acids to desired cells.

Targeting the CNS and Neuronal Cells

Nevertheless, prolonged stability and circulation is not sufficient for substantial nucleic acid delivery to the brain and spinal cord because the nervous system is protected by barriers that grossly prevent the access of therapeutics (Barchet and Amiji, 2009). Cells of the CNS can potentially be accessed through several contact points including: (1) the blood system; (2) the cerebral spinal fluid (CSF) in the ventricles or lumbar space; (3) intraparenchymal fluid in the extracellular space; or (4) nerve endings that extend outside of the nervous system (Cipolla, 2009). The nervous system is sequestered behind a barrier system composed of vascular tight junctions and glial elements that ensheath the blood supply producing a blood-brain and blood-spinal cord barrier (BBB and BSCB, respectively; Banks, 2016). Each of these compartments represent a potential entry point as well as unique challenges for neuronal targeting. Vehicles for systemic delivery must utilize a mechanism that will facilitate penetration and uptake across the BBB or BSCB (Spencer and Verma, 2007; Tobinick, 2016). Within the brain, paracellular flow of neuro-active cytokines is controlled by pulsation of the blood vessels that mechanically drives a peristaltic movement of extracellular fluid (Johanson et al., 2011; Iliff et al., 2013). Meanwhile, gene delivery vehicles directly administered into the ventricles need to bind to cells of interest before being washed out of the CNS (Syková and Nicholson, 2008). At the periphery, a vehicle that promotes uptake at nerve termini and retrograde transport must be able to target a neuron for transfection and promote travel along the neuronal cytoskeleleton into the CNS (Hanz and Fainzilber, 2004; von Bartheld, 2004; Medina-Kauwe, 2007; Tarragó-Trani and Storrie, 2007). Consequently, the advent and development of targeting ligands has greatly enhanced the capacity of non-viral vectors to deliver nucleic acids into the CNS.

Drug delivery vehicles have been modified with targeting agents such as peptides, antibodies, proteins and sugars to specifically home therapeutics to desired tissues and cell types. For systemic administration, active targeting is important in directing the accumulation of vehicles at the brain endothelium. One commonly used brain-targeting molecule is transferrin, a glycoprotein that binds to iron. Transferrin receptor is expressed on the brain endothelium and the binding of transferrin-decorated nucleic acid delivery vehicles to these receptors allows for accumulation right outside the brain (Huang et al., 2007).

Vehicles administered directly into brain by intraventricular or intraparenchymal methods can also benefit from active targeting by directing the delivery of nucleic acids to pertinent cells. For example, to more specifically transfect neural progenitor cells, Tet 1, a peptide that specifically binds to neuronal cells, was conjugated to PEI complexes (Kwon et al., 2010). This Tet1-PEI polymer led to a significantly improved transfection of neural progenitors by targeted complexes over untargeted complexes. Thus, targeting moieties can help deliver nucleic acids to cells and tissues of interest while minimizing non-specific delivery. In addition, targeting ligands can improve the intracellular delivery of nucleic acids since many targeting ligands are endocytosed by cells after binding to its receptor. Decorated macromolecules such as polyplexes and liposomes show enhanced uptake in cells compared to their non-targeted counterparts.

SYSTEMIC DELIVERY

Intravenous administration is one of the most common routes of administration for macromolecule therapeutics such as nucleic acids and has the advantage of rapid distribution and high bioavailability. However, systemic circulation presents a major challenge for nucleic acid delivery. Naked DNA has poor stability and is rapidly broken down by nucleases, sequestered by the liver, and cleared from circulation with a plasma half-life of mere minutes (Emlen and Mannik, 1984; Kawabata et al., 1995). To prevent premature degradation and prolong circulation, nucleic acids have been complexed with PEGylated cationic materials, such as polymers and liposomes, which act to shield the polyplex and facilitate compact packaging and protection. Targeting ligands conjugated to the synthetic vectors can facilitate recognition of brain endothelium. However, transport into the brain requires crossing the BBB, a tight network of endothelial cells that restricts entry into the brain parenchyma (Gabathuler, 2010). The brain endothelium has a high expression of efflux pumps and transporter proteins that exclude nearly 100% of large-molecule therapeutics and more than 98% of all small-molecule drugs (Begley, 2003; Pardridge, 2005). Recent *in vivo* investigations have focused on transportation across the BBB and temporarily disrupting the BBB after systemic administration.

Transport Across the Blood-Brain Barrier

Strategic selection of brain targeting ligands can result in both recognition of the brain endothelium and facilitated transcytosis across the BBB. This process, called receptor-mediated transcytosis, has been demonstrated with cationic proteins and is believed to be carried out by clathrin-coated pits or caveolae (Hervé et al., 2008; **Table 1**). After these materials bind to the luminal surface of the brain endothelial cells, vesicular transcytosis is mediated by different proteins and the high concentration of mitochondria in endothelial cells to cause exocytosis at the abluminal surface.

The transferrin receptor is frequently targeted for BBB transcytosis. After binding the transferrin receptor carrier protein, the transferrin-iron complex is internalized at the apical side of the brain endothelium and is eventually exocytosed at the opposite basal surface. Since transferrin receptor is expressed on the BBB and transcytoses transferrin, it can be utilized as an uptake pathway into the brain by nucleic acid vehicles functionalized with transferrin. In one example, polyamidoamine (PAMAM) dendrimers were decorated with transferrin by a PEG linker and showed a ∼2-fold higher brain

TABLE 1 | Properties of effective nucleic acid delivery vehicles.

Property	Function	Material examples	Schematic
Nucleic acid packaging	Condense, package, and protect DNA, RNA, or siRNA	PEI, PLL, PAMAM, liposomes	
Stability	Prevent premature unpackaging and avoid sequestration and clearance	PEG, albumin	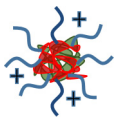
Targeting	CNS localization and cell-specific uptake	Peptides, antibodies, proteins	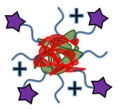
Endosomal escape	Facilitate release from the endosome to avoid lysosomal degradation	Melittin, pH sensitive materials, amines for proton sponge effect	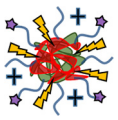
Cargo release	Triggered release or detachment from nucleic acid	Disulfide linkages	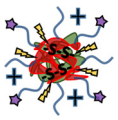

uptake and gene transfer compared to PEGylated dendrimers alone (Huang et al., 2007). In another example, transferrin antibodies were used to decorate liposomes that hid plasmid DNA. This system was able to show a 10-fold greater β-glucuronidase enzyme activity in murine brains deficient of the protein (Zhang et al., 2008).

Another BBB transcytosis moiety is the rabies viral glycoprotein (RVG) peptide, a 29-amino acid peptide which binds to nicotinic acetylcholine receptors. Modifying the peptide sequence to include nine arginines on the C-terminus allows for complexation with nucleic acids (Kumar et al., 2007). Upon systemic intravenous administration, these complexes were able to transvascularly deliver siRNA to the brain through clathrin- and caveolae-mediated endocytosis by endothelial cells, which lead to extended lives of encephalitic mice. The RVG peptide can also modulate the accumulation of larger vehicles and has delivered macro-structures such as PAMAM dendrimers (Liu et al., 2009), liposomes (Pulford et al., 2010), chitosan nanoparticles (Gao et al., 2014), poly(mannitol-*co*-PEI) complexes (Park et al., 2015) and exosomes (Alvarez-Erviti et al., 2011) across the BBB and into the brain parenchyma. Other targeting agents have included: angiopep, a peptide that binds to low-density lipoprotein receptor-related protein-1 (Ke et al., 2009); lactoferrin, an iron-binding protein of the transferrin family (Huang et al., 2008, 2010); leptin, a peptide that binds to leptin receptor in different parts of the brain (Liu et al., 2010); chlorotoxin, a scorpion-derived venom that is a specific marker for gliomas (Costa et al., 2013); TGN peptide, a BBB targeting peptide isolated by phage display (Qian et al., 2013); and LIMK2 NoLs peptide, a nucleolar translocation signal sequence derived from the LIM Kinase 2 protein (Yao et al., 2015). Collectively, these targeting agents have shown to facilitate the accumulation of PEGylated PAMAM dendrimers, lysine dendrimers, liposomes, and polymeric polyplexes in the brain.

Blood-Brain Barrier Disruption

Other methods of systemic nucleic acid delivery focus on temporarily disrupting the BBB to enhance the diffusion of vehicles into the brain. These strategies can be combined with delivery vehicles to further augment gene transfection. Small molecules, such as mannitol, have been shown to temporarily open the BBB and allow the penetration of larger molecules into the brain parenchyma. Hypertonic solutions of these molecules is believed to widen tight junctions by shrinking vascular endothelial cells (Rapoport, 2001). Consequently, the co-administration of mannitol with RVG-decorated PEI was able to significantly enhance the distribution of complexes throughout the brain when compared to carriers alone (Hwang et al., 2011).

More recently microbubbles, or gas-filled microspheres, have been coupled with ultrasound as a method to temporarily disrupt the BBB (Meairs and Alonso, 2007; Panje et al., 2013; Rychak and Klibanov, 2014; **Figure 2**). This process, called sonoporation, creates micropores, permeabilizes cell membranes and breaks up tight junctions as microbubbles act as local enhancers of the ultrasound acoustic energy and cavitate causing local shear flow, microstreams and microjets (Greenleaf et al., 1998; Zhou et al., 2012; Panje et al., 2013). These BBB openings are large enough to allow for the permeation of macromolecules into

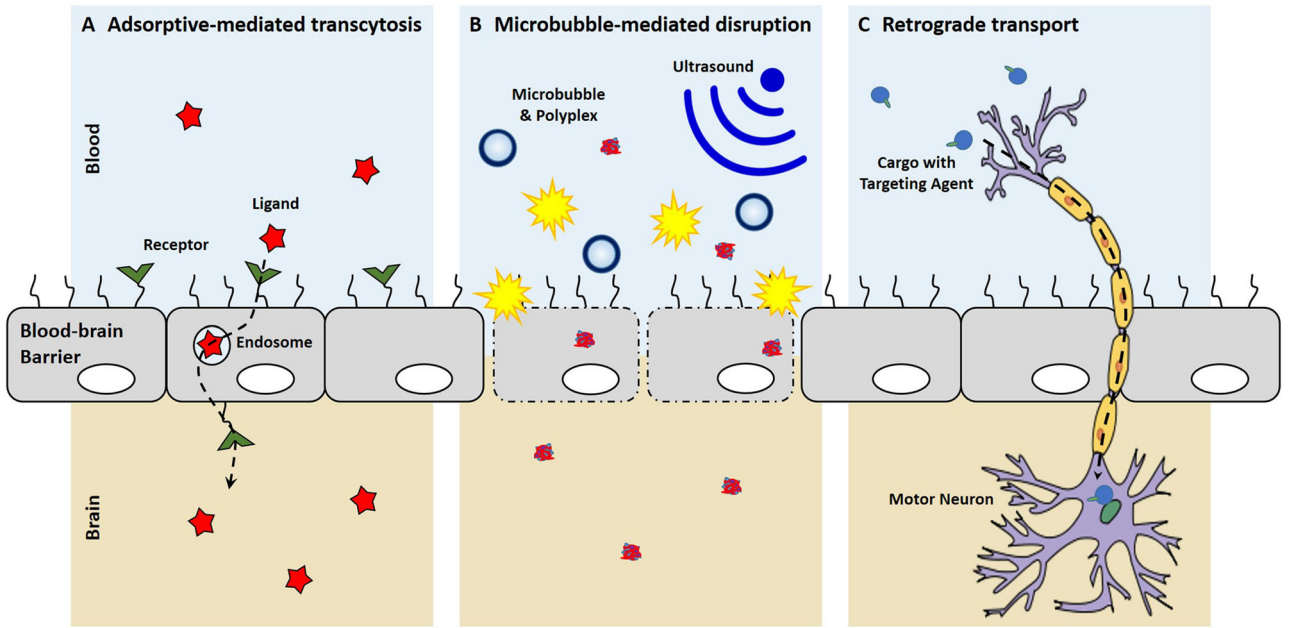

FIGURE 2 | Mechanisms of entering the central nervous system (CNS). (A) With receptor-mediated endocytosis, the binding of a ligand to its receptor on the brain endothelium facilitates cellular endocytosis, vesicular trafficking and eventually exocytosis on the contralateral side into the brain. **(B)** Microbubble-mediated disruption of the choroid plexus epithelium breaks tight junctions and creates micropores, allowing for the enhanced penetration of polyplexes into the brain. **(C)** New targeting ligands allow for uptake by peripheral neurons and the retrograde transport of cargo along axons to cell bodies in the CNS.

the brain such as immunoglobulin G and 70 kDa dextran (Sheikov et al., 2004; Choi et al., 2007, 2010, 2011; Xie et al., 2008). The safety of microbubble-mediated BBB disruption has been evaluated in rats and macaque monkeys with no or limited damage to brain tissue and no behavioral or visual deficits (McDannold et al., 2012; Kobus et al., 2015). Microbubble-mediated disruption of the BBB has been used to increase anti-Huntingtin siRNA delivery into the murine brain to reduce Huntingtin protein levels in animal disease models (Burgess et al., 2012). In another example, DNA can be complexed with cationic polymer-decorated microbubbles to prevent premature degradation. In this manner, microbubble and DNA complexes were used to markedly enhance the expression of brain-derived neurotrophic factor and enhanced green fluorescence protein in murine brains (Huang et al., 2012a,b). Microbubbles can also be co-administered with liposomal gene carriers to specifically open a region of the BBB by focused US, which uses an acoustic lens to center the US at a specific point (Lin et al., 2015). Co-administration of microbubbles with dense PEG-coated nanoparticles was able to open the BBB and transfect a variety of brain cells for at least 28 days with systemic administration (Nance et al., 2014; Mead et al., 2016).

In some cases, such as brain gliomas and traumatic brain injury, there is a natural disruption of the BBB. In small rat brain tumors, there is no BBB permeability; however, as the tumor grows and neovascularization occurs, ultrastructural defects in the capillary vessels arise causing a stark disruption in the tumor (Yamada et al., 1982). This leaky BBB vasculature can be exploited by gene delivery vehicles as a facile method of CNS entry and can greatly complement receptor-mediated transcytosis. PEGylated nanoparticles and liposomes decorated with receptor-mediated transcytosis ligands were able to accumulate in gliomas after systemic administration and delay tumor growth (Lu et al., 2006; Yue et al., 2014).

CEREBROSPINAL FLUID INJECTION

The CSF is produced by the choroid plexus deep in the ventricles and drains along paravenous circulation (Cipolla, 2009). The CNS is unique in that it does not have a traditional lymph system and waste material and metabolites drain from the extracellular space to the CSF (Iliff et al., 2012). While non-viral gene delivery into CSF-filled spaces is not as facile as intravenous administration, it does have the advantages of avoiding systemic circulation and placing therapeutics in close proximity to the brain parenchyma (Johanson et al., 2011). For example, lateral intraventricular injections allow for close proximity to the subventricular zone, a region of the brain containing neural progenitor cells, and may be an appropriate injection site for neurogenesis applications. In addition, there are excellent access points that are used routinely in the clinic including a lumbar puncture or intraventricular cannulas (Belverud et al., 2008; Tobinick, 2016). Substances directly injected into the CSF circumvent the BBB and distribute in the brain depending on size and charge. The ependymal barriers in ventricles are comprised of the choroid plexus cells and in

the sub-arachnoid space, the arachnoid barrier cells of glia and pial vessels (Abbott et al., 2006). For intraventricular delivery, large molecular weight proteins are not free to diffuse into the brain parenchyma due to the choroid plexus epithelium, which lines the cavities of the ventricles and the cranial and spinal sub-arachnoid space and secretes cerebrospinal fluid (Dohrmann, 1970; Mortazavi et al., 2014). While the ependymal barrier is not as stringent as the BBB, access and penetration into the brain parenchyma are still difficult due to the low diffusion and the constant movement of CSF fluid through the CNS and back into the bloodstream (Pardridge, 2011). While ventricular access of therapeutics to the brain is restricted, delivery to the sub-arachnoid space often results in widespread brain delivery of small molecular weight proteins (Iliff et al., 2012).

Designing Vehicles to Overcome Delivery Barriers

While the choroid plexus ependymal cell layer acts as a barrier, nucleic acid therapeutics intraventricularly injected are still able to have some efficacy likely due to the direct sampling of neural stem cells into the CSF and some penetration into the parenchyma. Certain formulations of linear PEI were able to diffuse throughout the ventricular space and transfect neurons and glia near the edge (Goula et al., 1998). After intraventricular injection, PEI and DNA complexes have been shown to transfect neural progenitor cells (Lemkine et al., 2002); while PEI complexes decorated with Tet1, a peptide that specifically binds to neuronal cells, bound better to neural progenitor cells and showed an improved transfection of neural progenitors over untargeted complexes (Kwon et al., 2010). Other carrier structures such as liposomes and silica nanoparticles have also been used as nucleic acid delivery vehicles for intraventricular administration. Cationic liposomes and organically modified silica nanoparticles were used to successfully deliver siRNA and plasmid DNA to neuronal cells *in vivo*, respectively (Bharali et al., 2005; Zou et al., 2010). All of these carriers can help protect nucleic acids as lipoplexes protected mRNA from premature degradation in CSF for up to 4 h while mRNA alone degraded within 5 min (Anderson et al., 2004). Peptide-decorated micelles filled with dexamethasone, a glucocorticoid that facilitates transport to the nucleus, were able to significantly reduce infarct size after middle cerebral artery occlusion by gene delivery.

Recently, multifunctional gene delivery vehicles have been synthesized with the aim of overcoming many of the barriers to gene delivery such as premature unpackaging, endosomal escape, and DNA release (**Table 1**). A statistical copolymer of *N*-(2-hydroxypropyl)methacrylate (HPMA), oligo-*L*-lysine, and melittin was developed for gene delivery after intraventricular injection (Schellinger et al., 2013). The HPMA monomers were for stability, the lysines were developed for DNA condensation and packaging, and the melittin, a membrane-lytic peptide developed from honey bee venom, was included to enhance endosomal escape after vesicular uptake. This polymer efficiently condensed DNA into stable particles to form polyplexes and increased brain transfection about 35-fold compared to melittin-free analogs. Another polymer designed for *in vivo* gene delivery utilized a double-headed reversible addition-fragmentation chain transfer agent and a ring-opening polymerization initiator to create two different polymer segments that contribute to different aspects of gene delivery (Wei et al., 2013). This copolymer, PCL-SS-p[(GMA-TEPA)-*s*-OEGMA], consisted of a block of poly(ε-caprolactone) (PCL) connected by a reducible disulfide to a statistical copolymer of tetraethylenepentamine (TEPA)-decorated poly(glycidyl methacrylate) (GMA) and oligo(ethylene glycol) monomethyl ether methacrylate (OEGMA). The TEPA amine groups bind to and condense nucleic acids to form polyplexes while the hydrophobic PCL and hydrophilic OEGMA provide extracellular stability. After polyplex internalization, the amine groups contribute to endosomal escape by pH buffering and the internal disulfide bond can be reduced by cytosolic glutathione facilitating polyplex destabilization and nucleic acid release. These polyplexes were shown to have diameters less than 200 nm, transfected HeLa cells more efficiently than PEI *in vitro*, and delivered luciferase genes to the brain more efficiently than its individual components. To improve transfection further, the amines of this polymer were guanidinylated and investigated *in vivo*. The delocalized charge of guanidinium groups is attributed to stronger interaction with DNA than amines and greater cell internalization by interacting with cell surface phosphates and sulfates (Wehling et al., 1975; Cheng et al., 2013). While guanidinium groups show improved transfection *in vitro*, they did not translate to augmented transfection *in vivo* likely due to premature unpackaging as guanidinium groups have a predilection for sulfates of heparan sulfate proteoglycans over nucleic acid phosphate groups (Choi et al., 2015). Recently, we developed a new endosomal-escaping, polymeric vehicle that has a triggered exposure of a membrane lytic peptide when in the acidic pH of endosomes (Cheng et al., 2016). This polymer, called Virus-Inspired Polymer for Endosomal Release (VIPER), is composed of a cationic block, poly(OEGMA)-*co*-poly(2-(dimethylamino)ethyl methacrylate) (p(OEGMA-DMAEMA)), for nucleic acid condensation and a pH-sensitive block, poly(2-diisopropylaminoethyl methacrylate)-*co*-poly(pyridyl disulfide ethyl methacrylate) (p(DIPAMA-PDSEMA)), for triggered display of a membrane lytic peptide, melittin, in acidic conditions. VIPER polyplexes, or polymer-DNA complexes, showed membrane-lytic activity only in the acidic conditions of the cell endosome and efficient gene transfer to a variety of cell types and therefore may be useful for CNS gene transfer.

Cerebrospinal fluid injections into other areas of the CNS have also been employed for the administration of nucleic acid carriers. After injection into the cisterna magma of rats, liposomes delivered luciferase plasmid throughout the brain that was still detectable 7–10 days later (Hauck et al., 2008). Interestingly, when the same system was directly injected into the parenchyma, luciferase expression was not as distributed. A micelle system of PEG-aspartic acid polymer was able to provide sustained protein expression with minimal immunogenicity

(Uchida et al., 2013). Nucleic acid administration into the lumbar subarachnoid space has also been accomplished with a variety of delivery vehicles. Poly(lactic-co-glycolic acid) microparticles containing plasmid DNA that encodes IL-10 were able to relieve neuropathic pain in rats for greater than 74 days (Soderquist et al., 2010). PEI complexes decorated with a peptide from nerve growth factor were able to more specifically transfect dorsal root ganglia (Zeng et al., 2007). By creating Tat decorated-PEI complexes with magnetic iron beads, researchers were able to use magnetic fields to direct the movement of DNA complexes into remote areas away from the injection site in rat spinal cords (Song et al., 2010). While sufficient levels of gene transfection are achieved after CSF injection, the choroid plexus epithelium still prevents most of the vehicles from entering the parenchyma which results in a significant loss of transfection potential.

Choroid Plexus Epithelium Disruption

In a similar fashion to BBB disruption, the choroid plexus epithelium may be transiently disrupted by microbubbles and ultrasound to allow for the enhanced penetration of materials into the brain parenchyma from the CSF fluid. Custom microbubbles were prepared and did not aggregate with aforementioned PCL-SS-p[(GMA-TEPA)-*s*-OEGMA] polyplexes (Tan et al., 2016). In *in vitro* transwell assays, these microbubbles were able to sonoporate immortalized choroid plexus monolayers to allow for the enhanced flow through of 5 kDa PEG and 70 kDa dextran. Upon *in vivo* administration into murine ventricles, the microbubbles and ultrasound were able to significantly increase polyplex transfection of cells with luciferase compared to polyplexes alone or polyplexes and microbubbles without ultrasound. Temporary microbubble-mediated disruption of the choroid plexus epithelium seems like a viable strategy to enhance the penetration of polyplexes and may garner more research in the future.

INTRAPARENCHYMAL INJECTION

Intraparenchymal injection is the most direct access to discrete anatomy and cells of the brain and spinal cord. However, there are several critical challenges notwithstanding the inherent risk of an invasive CNS injection. Injection or probe placement alone can create a reactive gliosis that may limit the transport of a therapeutic or exacerbate the disease (Polikov et al., 2005; Potts et al., 2013). Methods for convection enhanced delivery and the use of small caliber pipettes can mitigate some of these concerns and allow targeted delivery of relatively large volumes without harm (Mano et al., 2016). Once in the parenchyma, therapeutics have variable degrees of diffusion and entrapment that can be modeled based on protein or drug size and composition (Patlak et al., 1983; Ghersi-Egea et al., 2002; Hrabe et al., 2004; Nicholson et al., 2011). After parenchymal diffusion, clearance is regulated by the lymphatic system which is comprised of the glia cells that ensheath the venous system of the brain which is localized primarily near the dural surfaces (Iliff et al., 2012; Louveau et al., 2015). In general, small molecular weight substances are able to diffuse readily and are cleared in minutes. Larger molecular weight substances may either lack significant diffusion or be cleared over a course of hours (Syková and Nicholson, 2008).

Bolus Injection

While the location of intraparenchymal injections into the brain can vary, the same type of nucleic acid delivery vehicles is still utilized. PEI decorated with 2 kDa PEG chains resulted in improved gene delivery after intrathecal administration into the lumber spinal cord subarachnoid space compared to PEI (Tang et al., 2003). Reducible arginine-PAMAM dendrimers were able to knockdown genes after injection into the cortex (Kim et al., 2010). Biodegradable poly(β-amino esters) that were lyophilized and stored for over 2 years effectively transfected brain glioblastomas, demonstrating long-term storage and efficacy for clinical translation (Guerrero-Cázares et al., 2014). Reversibly conjugated siRNA to liposomes was able to efficiently silence genes in oligodendrocytes after administration into the corpus callosum (Chen et al., 2010). Liposomes encapsulating siRNA have also shown effective gene knockdown of the GluN1 subunit of NMDA receptors in neurons (Rungta et al., 2013). Targeting agents have also been used to enhance the nucleic acid delivery vehicles. PEGylated PEI was targeted with folate, which binds to folate receptor often overexpressed on cancer cells, and liposomes were targeted with transferrin to improve the delivery of plasmids and siRNA after injection into the right striatum (Cardoso et al., 2008; Liang et al., 2009).

Sustained Delivery

The compact and tortuous morphology of the brain parenchyma severely limits the diffusion of nucleic acid delivery vehicles away from the administration site. To overcome this, sustained delivery is utilized to constantly introduce more vehicles and increase the diffusion throughout the brain. In one example, an osmotic pump was able to continually inject siRNA and liposome complexes into the frontal lobe to knockdown the resistance of gliomas to therapy (Kato et al., 2010). This treatment significantly sensitized tumors to the chemotherapeutic agents and extended the survival of mice. In other cases, a cannula is implanted in the brain for acute direct injections or chronic administration. Repeated dosing of siRNA against toxic Huntingtin protein in β-cyclodextin carriers was able to alleviate motor deficits in a Huntington's disease mouse model (Godinho et al., 2013).

Like the osmotic pump, convection-enhanced delivery is administered intraparenchymally and used to continually introduce therapeutics. A cannula is typically inserted stereotaxically into a designated spot in the brain and a therapeutic fluid is continuously injected under positive pressure (Allard et al., 2009). The administration of siRNA by convection-enhanced delivery was able to silence genes in oligodendrocytes (Querbes et al., 2009) and silence Huntingtin gene in a widespread manner across the brain (Stiles et al.,

2012). When a cell-penetrating peptide, TAT, was attached to liposomes, gene transfection increased *in vivo*; however, expression was restricted to the vicinity of the infusion catheter (MacKay et al., 2008). When comparing positively and negatively charged liposomes, anionic liposomes were better able to spread throughout the brain parenchyma with similar transfection levels (Kenny et al., 2013).

RETROGRADE TRANSPORT

While there have been substantial advances in brain-targeted delivery to treat diseases that affect specific parts of the brain like Alzheimer's Disease (Kumar et al., 2007; Spencer and Verma, 2007; Yu et al., 2011), few therapeutic options are available for degenerative diseases that affect motor neurons because many of the potential genes and siRNA drugs show limited diffusion and penetration to motor neurons deep in the CNS parenchyma (Monani, 2005; Mitchell and Borasio, 2007). For decades, classes of viruses have been known to infect neuronal projections in the periphery and undergo retrograde axonal transport into the brain and spinal cord (LaVail and LaVail, 1972; Salinas et al., 2010). Thus, several lab have begun to systematically mutate adeno-associated vectors in order to expand their clinical application and increase delivery into the CNS (Maheshri et al., 2006; Kotterman and Schaffer, 2014), innovative strategies have been adopted to utilize retrograde axonal transport to deliver biologics into the spinal cord (Xu et al., 2005; Hollis et al., 2008; Snyder et al., 2011). As a result, these viruses have been engineered and shown to be effective for remote gene transfer into the CNS after intramuscular injection to induce neurotrophic factor expression in animal models of neurodegenerative disease (Kaspar et al., 2003; Azzouz et al., 2004; Petruska et al., 2010; Benkhelifa-Ziyyat et al., 2013; Hirano et al., 2013).

Recently, small targeting agents have been used to direct the trafficking of cargo into the CNS after peripheral administration (**Figure 2**). Tetanus toxin subunit-C (TTC), an atoxic fragment of tetanus toxin that contains the ganglioside-binding site, is able to mediate uptake at both pre- and post-synaptic at nerve termini to allow retrograde transport passage of TTC within neurons (Price et al., 1975; Schwab et al., 1979). Consequently, these trans-synaptic properties of TTC have been exploited as a fusion protein to enable delivery into the spinal cord after TTC uptake at peripheral nerve termini (Francis et al., 2004; Chian et al., 2009; Li et al., 2009). While the TTC fusion-proteins were shown to increase delivery into the spinal cord, these studies were not able to discern a therapeutic benefit, which may suggest that that TTC-fusions do not escape the endosome after uptake and remain sequestered in the vescicle that mediated uptake. More recently, a targeted axonal import peptide (TAxI) was identified by *in vivo* phage display. The TAxI peptide was able to mediate uptake and delivery of an active Cre recombinase into the nucleus of spinal cord motor neurons after hind limb intramuscular injection (Sellers et al., 2016). These data suggest that small peptides are not only able to mediate synaptic uptake at nerve termini and retrograde transport within neurons, but they allow for functional protein cargo delivery via the neuron. While there have yet to be any reports of synthetic, retrograde nucleic acid delivery into the CNS, the discovery of targeting ligands that mediate uptake by neurons in the periphery, transport within neurons to the CNS, and release of active cargo into the cytoplasm has the potential of opening a whole new delivery route for non-viral technologies to target motor neurons for gene delivery.

Another route of administration that takes advantage of retrograde transport through neurons is intranasal administration. After introduction into the nasal cavity, molecules are believed to travel along olfactory nerve pathways and end up in the brain parenchyma and CSF by bypassing the BBB (Patel et al., 2009). Peptides, proteins, and small molecules have shown to be able to be delivered into the CNS after intranasal administration. While this route is non-invasive, the nasal cavity has many barriers including enzymes and mucous; furthermore, compounds similar to those that have shown CNS delivery have reportedly not entered the CNS after intranasal administration (Dhuria et al., 2010). The formulation and method of delivery may affect retrograde transport as well as other experimental factors such as head position, volume, pH and osmolarity (Dhuria et al., 2010). Plasmid DNA ranging from 3.5 kb to 14.2 kb were able to show absorption and brain distribution after intranasal administration (Han et al., 2007). Intranasal delivery of an telomerase-inhibiting oligonucleotide was able to prolong the survival of human tumor-bearing rats by over 30 days (Hashizume et al., 2008). Carriers for intranasal gene delivery follow the same principles as other vehicles administered by other routes. Polymeric vehicles comprised of methoxy PEG, poly(ε-caprolactone) and TAT peptide demonstrated better delivery of siRNA to the brain than naked siRNA or carrier-mediated intravenous delivery (Kanazawa et al., 2013).

CONCLUSION

While viral vectors are still the main type of vehicles used in clinical trials, non-viral vectors are gaining traction due to their potential safety advantages, greater customization, ease of manufacturing and ability to deliver all nucleic acid varieties (Niidome and Huang, 2002; Thomas et al., 2003). The ability of viral vectors to permanently alter the genome and activate the immune system make non-viral vectors more compelling for clinical trials. However, the lower efficacy and transfection levels by synthetic vectors hinder their wide clinical use. For any application, nucleic acid delivery vehicles face cellular obstacles such as recognition by pertinent cells, internalization into cells, escaping the lysosomal degradation pathway and unpackaging the nucleic acids in the cell cytosol. Delivery into the CNS presents an even greater challenge due to the supracellular BBB and BSCB. An apropos administration route must be chosen to maximize therapeutics at the treatment site (i.e., direct injections); however, caution must be heeded in avoiding unnecessary damage to healthy tissues by direct administration into the CNS (i.e., intravenous and peripheral administration). Each

route of administration has its advantages and disadvantages, as well as local barriers, as previously discussed. Fortunately, the advances in vehicular design, materials and synthesis described above have allowed for specific engineering of gene delivery vehicles to overcome these challenges and step closer to the transfection efficiency of viruses. Improvements such as nucleic acid shielding and targeting have lessened premature degradation and increased the localization of cargo in the CNS. Advances in crossing the BBB and sustained delivery directly into the brain allow for improved gene transfection and a step closer to clinical application. Meanwhile, new techniques such as microbubble-mediated sonoporation and small molecule-mediated retrograde transport allow the permeation of otherwise excluded vehicles into the brain and spinal cord. All of these examples can serve as guidelines and inspiration for the next generation of synthetic gene delivery vectors. With these improvements, we anticipate that synthetic delivery systems will be applied more successfully for nucleic acid therapies in animal models of CNS disease and will make significant progress toward clinical evaluation in the upcoming years.

AUTHOR CONTRIBUTIONS

J-KYT: led conception, writing of review, drafting and editing figures. SHP and PJH: conceived, assisted in writing and editing topic. BP and DLS: assisted in writing and editing topic.

ACKNOWLEDGMENTS

This work was supported by NIH 2R01NS064404 (SHP & PJH), Congressionally Directed Medical Research Programs DOD W81XWH-14-1-0586 (PJH & SHP). J-KYT was supported by National Science Foundation (NSF) GRFP (2011128558); Binhan Pham was supported by Mary Gates Undergraduate Research Fellowship.

REFERENCES

Abbott, N. J., Rönnbäck, L., and Hansson, E. (2006). Astrocyte-endothelial interactions at the blood-brain barrier. *Nat. Rev. Neurosci.* 7, 41–53. doi: 10.1038/nrn1824

Abdelhady, H. G., Allen, S., Davies, M. C., Roberts, C. J., Tendler, S. J. B., and Williams, P. M. (2003). Direct real-time molecular scale visualisation of the degradation of condensed DNA complexes exposed to DNase 1. *Nucleic Acids Res.* 31, 4001–4005. doi: 10.1093/nar/gkg462

Al-Dosari, M. S., and Gao, X. (2009). Nonviral gene delivery: principle, limitations and recent progress. *AAPS J.* 11, 671–681. doi: 10.1208/s12248-009-9143-y

Allard, E., Passirani, C., and Benoit, J.-P. (2009). Convection-enhanced delivery of nanocarriers for the treatment of brain tumors. *Biomaterials* 30, 2302–2318. doi: 10.1016/j.biomaterials.2009.01.003

Alvarez-Erviti, L., Seow, Y., Yin, H., Betts, C., Lakhal, S., and Wood, M. J. A. (2011). Delivery of siRNA to the mouse brain by systemic injection of targeted exosomes. *Nat. Biotechnol.* 29, 341–345. doi: 10.1038/nbt.1807

Anderson, D. M., Hall, L. L., Ayyalapu, A. R., Irion, V. R., Nantz, M. H., and Hecker, J. G. (2004). Stability of mRNA/cationic lipid lipoplexes in human and rat cerebrospinal fluid: methods and evidence for nonviral mRNA gene delivery to the central nervous system. *Hum. Gene Ther.* 14, 191–202. doi: 10.1089/10430340360535751

Azzouz, M., Ralph, G. S., Storkebaum, E., Walmsley, L. E., Mitrophanous, K. A., Kingsman, S. M., et al. (2004). VEGF delivery with retrogradely transported lentivector prolongs survival in a mouse ALS model. *Nature* 429, 413–417. doi: 10.1038/nature02544

Banks, W. A. (2016). From blood—brain barrier to blood—brain interface: new opportunities for CNS drug delivery. *Nat. Rev. Drug Discov.* 15, 275–292. doi: 10.1038/nrd.2015.21

Barchet, T. M., and Amiji, M. M. (2009). Challenges and opportunities in CNS delivery of therapeutics for neurodegenerative diseases. *Expert Opin. Drug Deliv.* 6, 211–225. doi: 10.1517/17425240902758188

Begley, D. (2003). Understanding and circumventing the blood–brain barrier. *Acta Paediatr. Suppl.* 443, 83–91. doi: 10.1111/j.1651-2227.2003.tb00226.x

Belverud, S., Mogilner, A., and Schulder, M. (2008). Intrathecal pumps. *Neurotherapeutics* 5, 114–122. doi: 10.1016/j.nurt.2007.10.070

Benkhelifa-Ziyyat, S., Besse, A., Roda, M., Duque, S., Astord, S., Carcenac, R., et al. (2013). Intramuscular scAAV9-SMN injection mediates widespread gene delivery to the spinal cord and decreases disease severity in SMA mice. *Mol. Ther.* 21, 282–290. doi: 10.1038/mt.2012.261

Bharali, D. J., Klejbor, I., Stachowiak, E. K., Dutta, P., Roy, I., Kaur, N., et al. (2005). Organically modified silica nanoparticles: a nonviral vector for *in vivo* gene delivery and expression in the brain. *Proc. Natl. Acad. Sci. U S A* 102, 11539–11544. doi: 10.1073/pnas.0504926102

Burgess, A., Huang, Y., Querbes, W., Sah, D. W., and Hynynen, K. (2012). Focused ultrasound for targeted delivery of siRNA and efficient knockdown of Htt expression. *J. Control. Release* 163, 125–129. doi: 10.1016/j.jconrel.2012.08.012

Burke, P. A., Pun, S. H., and Reineke, T. M. (2013). Advancing polymeric delivery systems amidst a nucleic acid therapy renaissance. *ACS Macro Lett.* 2, 928–934. doi: 10.1021/mz400418j

Cardoso, A. L. C., Simões, S., de Almeida, L. P., Plesnila, N., Pedroso de Lima, M. C., Wagner, E., et al. (2008). Tf-lipoplexes for neuronal siRNA delivery: a promising system to mediate gene silencing in the CNS. *J. Control. Release* 132, 113–123. doi: 10.1016/j.jconrel.2008.08.014

Chen, Q., Butler, D., Querbes, W., Pandey, R. K., Ge, P., Maier, M. A., et al. (2010). Lipophilic siRNAs mediate efficient gene silencing in oligodendrocytes with direct CNS delivery. *J. Control. Release* 144, 227–232. doi: 10.1016/j.jconrel.2010.02.011

Cheng, Q., Huang, Y., Zheng, H., Wei, T., Zheng, S., Huo, S., et al. (2013). The effect of guanidinylation of PEGylated poly(2-aminoethyl methacrylate) on the systemic delivery of siRNA. *Biomaterials* 34, 3120–3131. doi: 10.1016/j.biomaterials.2013.01.043

Cheng, Y., Yumul, R. C., and Pun, S. H. (2016). Virus-inspired polymer for efficient *in vitro* and *in vivo* gene delivery. *Angew. Chem. Int. Ed Engl.* 55, 12013–12017. doi: 10.1002/anie.201605958

Chian, R.-J. J., Li, J., Ay, I., Celia, S. A., Kashi, B. B., Tamrazian, E., et al. (2009). IGF-1: tetanus toxin fragment C fusion protein improves delivery of IGF-1 to spinal cord but fails to prolong survival of ALS mice. *Brain Res.* 1287, 1–19. doi: 10.1016/j.brainres.2009.06.066

Choi, J. J., Pernot, M., Small, S. A., and Konofagou, E. E. (2007). Noninvasive, transcranial and localized opening of the blood-brain barrier using focused ultrasound in mice. *Ultrasound Med. Biol.* 33, 95–104. doi: 10.1016/j.ultrasmedbio.2006.07.018

Choi, J. J., Selert, K., Gao, Z., Samiotaki, G., Baseri, B., and Konofagou, E. E. (2011). Noninvasive and localized blood-brain barrier disruption using focused ultrasound can be achieved at short pulse lengths and low pulse repetition frequencies. *J. Cereb. Blood Flow Metab.* 31, 725–737. doi: 10.1038/jcbfm.2010.155

Choi, J. L., Tan, J. Y., Sellers, D. L., Wei, H., Horner, P. J., and Pun, S. H. (2015). Guanidinylated block copolymers for gene transfer: a comparison with amine-based materials for *in vitro* and *in vivo* gene transfer efficiency. *Biomaterials* 54, 87–96. doi: 10.1016/j.biomaterials.2015.03.008

Choi, J. J., Wang, S., Tung, Y.-S., Morrison, B. III., and Konofagou, E. E. (2010). Molecules of various pharmacologically-relevant sizes can cross the ultrasound-induced blood-brain barrier opening *in vivo*. *Ultrasound Med. Biol.* 36, 58–67. doi: 10.1016/j.ultrasmedbio.2009.08.006

Cipolla, M. J. (2009). "Colloquium series on integrated systems physiology: from molecule to function," in *The Cerebral Circulation*, eds D. N. Granger and J. Granger (Williston, VT: Morgan & Claypool life Sciences), 1–69.

Costa, P. M., Cardoso, A. L., Mendonça, L. S., Serani, A., Custódia, C., Conceição, M., et al. (2013). Tumor-targeted chlorotoxin-coupled nanoparticles for nucleic acid delivery to glioblastoma cells: a promising system for glioblastoma treatment. *Mol. Ther. Nucleic Acids* 2:e100. doi: 10.1038/mtna.2013.30

Dhuria, S. V., Hanson, L. R., and Frey, W. H. I. II. (2010). Intranasal delivery to the central nervous system: mechanisms and experimental considerations. *J. Pharm. Sci.* 99, 1654–1673. doi: 10.1002/jps.21924

Dodge, J. C., Treleaven, C. M., Fidler, J. A., Hester, M., Haidet, A., Handy, C., et al. (2010). AAV4-mediated expression of IGF-1 and VEGF within cellular components of the ventricular system improves survival outcome in familial ALS mice. *Mol. Ther.* 18, 2075–2084. doi: 10.1038/mt.2010.206

Dohrmann, G. J. (1970). The choroid plexus: a historical review. *Brain Res.* 18, 197–218. doi: 10.1016/0006-8993(70)90324-0

Emlen, W., and Mannik, M. (1984). Effect of DNA size and strandedness on the *in vivo* clearance and organ localization of DNA. *Clin. Exp. Immunol.* 56, 185–192.

Francis, J. W., Figueiredo, D., vanderSpek, J. C., Ayala, L. M., Kim, Y. S., Remington, M. P., et al. (2004). A survival motor neuron:tetanus toxin fragment C fusion protein for the targeted delivery of SMN protein to neurons. *Brain Res.* 995, 84–96. doi: 10.1016/j.brainres.2003.09.063

Gabathuler, R. (2010). Development of new peptide vectors for the transport of therapeutic across the blood-brain barrier. *Ther. Deliv.* 1, 571–586. doi: 10.4155/tde.10.35

Gao, Y., Wang, Z.-Y., Zhang, J., Zhang, Y., Huo, H., Wang, T., et al. (2014). RVG-peptide-linked trimethylated chitosan for delivery of siRNA to the brain. *Biomacromolecules* 15, 1010–1018. doi: 10.1021/bm401906p

Ghersi-Egea, J.-F., Gorevic, P. D., Ghiso, J., Frangione, B., Patlak, C. S., and Fenstermacher, J. D. (2002). Fate of cerebrospinal fluid-borne amyloid β-peptide: rapid clearance into blood and appreciable accumulation by cerebral arteries. *J. Neurochem.* 67, 880–883. doi: 10.1046/j.1471-4159.1996.67020880.x

Godinho, B. M. D. C., Ogier, J. R., Darcy, R., O'Driscoll, C. M., and Cryan, J. F. (2013). Self-assembling modified β–cyclodextrin nanoparticles as neuronal siRNA delivery vectors: focus on Huntington's disease. *Mol. Pharm.* 10, 640–649. doi: 10.1021/mp3003946

Goula, D., Remy, J. S., Erbacher, P., Wasowicz, M., Levi, G., Abdallah, B., et al. (1998). Size, diffusibility and transfection performance of linear PEI/DNA complexes in the mouse central nervous system. *Gene Ther.* 5, 712–717. doi: 10.1038/sj.gt.3300635

Greenleaf, W. J., Bolander, M. E., Sarkar, G., Goldring, M. B., and Greenleaf, J. F. (1998). Artificial cavitation nuclei significantly enhance acoustically induced cell transfection. *Ultrasound Med. Biol.* 24, 587–595. doi: 10.1016/s0301-5629(98)00003-9

Guerrero-Cázares, H., Tzeng, S. Y., Young, N. P., Abutaleb, A. O., Quiñones-Hinojosa, A., and Green, J. J. (2014). Biodegradable polymeric nanoparticles show high efficacy and specificity at DNA delivery to human glioblastoma *in vitro* and *in vivo*. *ACS Nano* 8, 5141–5153. doi: 10.1021/nn501197v

Han, I. K., Kim, M. Y., Byun, H. M., Hwang, T. S., Kim, J. M., Hwang, K. W., et al. (2007). Enhanced brain targeting efficiency of intranasally administered plasmid DNA: an alternative route for brain gene therapy. *J. Mol. Med. (Berl.)* 85, 75–83. doi: 10.1007/s00109-006-0114-9

Hanz, S., and Fainzilber, M. (2004). Integration of retrograde axonal and nuclear transport mechanisms in neurons: implications for therapeutics. *Neuroscientist* 10, 404–408. doi: 10.1177/1073858404267884

Hashizume, R., Ozawa, T., Gryaznov, S. M., Bollen, A. W., Lamborn, K. R., Frey, W. H., et al. (2008). New therapeutic approach for brain tumors: intranasal delivery of telomerase inhibitor GRN163. *Neuro. Oncol.* 10, 112–120. doi: 10.1215/15228517-2007-052

Hauck, E. S., Zou, S., Scarfo, K., Nantz, M. H., and Hecker, J. G. (2008). Whole animal *in vivo* imaging after transient, nonviral gene delivery to the rat central nervous system. *Mol. Ther.* 16, 1857–1864. doi: 10.1038/mt.2008.183

Hervé, F., Ghinea, N., and Scherrmann, J.-M. (2008). CNS delivery *via* adsorptive transcytosis. *AAPS J.* 10, 455–472. doi: 10.1208/s12248-008-9055-2

Hirano, M., Kato, S., Kobayashi, K., Okada, T., Yaginuma, H., and Kobayashi, K. (2013). Highly efficient retrograde gene transfer into motor neurons by a lentiviral vector pseudotyped with fusion glycoprotein. *PLoS One* 8:e75896. doi: 10.1371/journal.pone.0075896

Hollis, E. R. II., Kadoya, K., Hirsch, M., Samulski, R. J., and Tuszynski, M. H. (2008). Efficient retrograde neuronal transduction utilizing self-complementary AAV1. *Mol. Ther.* 16, 296–301. doi: 10.1038/sj.mt.6300367

Hrabe, J., Hrabětová, S., and Segeth, K. (2004). A model of effective diffusion and tortuosity in the extracellular space of the brain. *Biophys. J.* 87, 1606–1617. doi: 10.1529/biophysj.103.039495

Huang, Q., Deng, J., Wang, F., Chen, S., Liu, Y., Wang, Z., et al. (2012a). Targeted gene delivery to the mouse brain by MRI-guided focused ultrasound-induced blood—brain barrier disruption. *Exp. Neurol.* 233, 350–356. doi: 10.1016/j.expneurol.2011.10.027

Huang, Q., Deng, J., Xie, Z., Wang, F., Chen, S., Lei, B., et al. (2012b). Effective gene transfer into central nervous system following ultrasound-microbubbles-induced opening of the blood-brain barrier. *Ultrasound Med. Biol.* 38, 1234–1243. doi: 10.1016/j.ultrasmedbio.2012.02.019

Huang, R., Ke, W., Han, L., Liu, Y., Shao, K., Jiang, C., et al. (2010). Lactoferrin-modified nanoparticles could mediate efficient gene delivery to the brain *in vivo*. *Brain Res. Bull.* 81, 600–604. doi: 10.1016/j.brainresbull.2009.12.008

Huang, R., Ke, W., Liu, Y., Jiang, C., and Pei, Y. (2008). The use of lactoferrin as a ligand for targeting the polyamidoamine-based gene delivery system to the brain. *Biomaterials* 29, 238–246. doi: 10.1016/j.biomaterials.2007.09.024

Huang, R.-Q., Qu, Y.-H., Ke, W.-L., Zhu, J.-H., Pei, Y.-Y., and Jiang, C. (2007). Efficient gene delivery targeted to the brain using a transferrin-conjugated polyethyleneglycol-modified polyamidoamine dendrimer. *FASEB J.* 21, 1117–1125. doi: 10.1096/fj.06-7380com

Hwang, D. W., Son, S., Jang, J., Youn, H., Lee, S., Lee, D., et al. (2011). A brain-targeted rabies virus glycoprotein-disulfide linked PEI nanocarrier for delivery of neurogenic microRNA. *Biomaterials* 32, 4968–4975. doi: 10.1016/j.biomaterials.2011.03.047

Iliff, J. J., Wang, M., Liao, Y., Plogg, B. A., Peng, W., Gundersen, G. A., et al. (2012). A paravascular pathway facilitates CSF flow through the brain parenchyma and the clearance of interstitial solutes, including amyloid β. *Sci. Transl. Med.* 4:147ra111. doi: 10.3410/f.717953972.793459499

Iliff, J. J., Wang, M., Zeppenfeld, D. M., Venkataraman, A., Plog, B. A., Liao, Y., et al. (2013). Cerebral arterial pulsation drives paravascular CSF-interstitial fluid exchange in the murine brain. *J. Neurosci.* 33, 18190–18199. doi: 10.1523/JNEUROSCI.1592-13.2013

Immordino, L., Dosio, F., and Cattel, L. (2006). Stealth liposomes: review of the basic science, rationale and clinical applications. *Int. J. Nanomedicine* 1, 297–315.

Johanson, C. E., Stopa, E. G., and McMillan, P. N. (2011). The blood—cerebrospinal fluid barrier: structure and functional significance. *Methods Mol. Biol.* 686, 101–131. doi: 10.1007/978-1-60761-938-3_4

Kanazawa, T., Akiyama, F., Kakizaki, S., Takashima, Y., and Seta, Y. (2013). Delivery of siRNA to the brain using a combination of nose-to-brain delivery and cell-penetrating peptide-modified nano-micelles. *Biomaterials* 34, 9220–9226. doi: 10.1016/j.biomaterials.2013.08.036

Kaspar, B. K., Lladó, J., Sherkat, N., Rothstein, J. D., and Gage, F. H. (2003). Retrograde viral delivery of IGF-1 prolongs survival in a mouse ALS model. *Science* 301, 839–842. doi: 10.1126/science.1086137

Kato, T., Natsume, A., Toda, H., Iwamizu, H., Sugita, T., Hachisu, R., et al. (2010). Efficient delivery of liposome-mediated MGMT-siRNA reinforces the cytotoxity of temozolomide in GBM-initiating cells. *Gene Ther.* 17, 1363–1371. doi: 10.1038/gt.2010.88

Kawabata, K., Takakura, Y., and Hashida, M. (1995). The fate of plasmid DNA after intravenous injection in mice: involvement of scavenger receptors in its hepatic uptake. *Pharm. Res.* 12, 825–830. doi: 10.1023/A:1016248701505

Ke, W., Shao, K., Huang, R., Han, L., Liu, Y., Li, J., et al. (2009). Gene delivery targeted to the brain using an Angiopep-conjugated polyethyleneglycol-modified polyamidoamine dendrimer. *Biomaterials* 30, 6976–6985. doi: 10.1016/j.biomaterials.2009.08.049

Kenny, G. D., Bienemann, A. S., Tagalakis, A. D., Pugh, J. A., Welser, K., Campbell, F., et al. (2013). Multifunctional receptor-targeted nanocomplexes for the delivery of therapeutic nucleic acids to the brain. *Biomaterials* 34, 9190–9200. doi: 10.1016/j.biomaterials.2013.07.081

Kim, I. D., Lim, C. M., Kim, J. B., Nam, H. Y., Nam, K., Kim, S. W., et al. (2010). Neuroprotection by biodegradable PAMAM ester (e-PAM-R)-mediated HMGB1 siRNA delivery in primary cortical cultures and in the

postischemic brain. *J. Control. Release* 142, 422–430. doi: 10.1016/j.jconrel.2009.11.011

Ko, Y. T., Bhattacharya, R., and Bickel, U. (2009). Liposome encapsulated polyethylenimine/ODN polyplexes for brain targeting. *J. Control. Release* 133, 230–237. doi: 10.1016/j.jconrel.2008.10.013

Kobus, T., Vykhodtseva, N., Pilatou, M., Zhang, Y., and McDannold, N. (2015). Safety validation of repeated blood-brain barrier disruption using focused ultrasound. *Ultrasound Med. Biol.* 42, 481–492. doi: 10.1016/j.ultrasmedbio.2015.10.009

Kotterman, M. A., and Schaffer, D. V. (2014). Engineering adeno-associated viruses for clinical gene therapy. *Nat. Rev. Genet.* 15, 445–451. doi: 10.1038/nrg3742

Kumar, P., Wu, H., McBride, J. L., Jung, K.-E., Kim, M. H., Davidson, B. L., et al. (2007). Transvascular delivery of small interfering RNA to the central nervous system. *Nature* 448, 39–43. doi: 10.1038/nature05901

Kwon, E. J., Lasiene, J., Jacobson, B. E., Park, I.-K., Horner, P. J., and Pun, S. H. (2010). Targeted nonviral delivery vehicles to neural progenitor cells in the mouse subventricular zone. *Biomaterials* 31, 2417–2424. doi: 10.1016/j.biomaterials.2009.11.086

Laga, R., Carlisle, R., Tangney, M., Ulbrich, K., and Seymour, L. W. (2012). Polymer coatings for delivery of nucleic acid therapeutics. *J. Control. Release* 161, 537–553. doi: 10.1016/j.jconrel.2012.02.013

LaVail, J. H., and LaVail, M. M. (1972). Retrograde axonal transport in the central nervous system. *Science* 176, 1416–1417. doi: 10.1126/science.176.4042.1416

Lemkine, G. F., Mantero, S., Migné, C., Raji, A., Goula, D., Normandie, P., et al. (2002). Preferential transfection of adult mouse neural stem cells and their immediate progeny *in vivo* with polyethylenimine. *Mol. Cell. Neurosci.* 19, 165–174. doi: 10.1006/mcne.2001.1084

Li, J., Chian, R. J., Ay, I., Kashi, B. B., Celia, S. A., Tamrazian, E., et al. (2009). Insect GDNF:TTC fusion protein improves delivery of GDNF to mouse CNS. *Biochem. Biophys. Res. Commun.* 390, 947–951. doi: 10.1016/j.bbrc.2009.10.083

Liang, B., He, M.-L., Chan, C.-Y., Chen, Y.-C., Li, X.-P., Li, Y., et al. (2009). The use of folate-PEG-grafted-hybranched-PEI nonviral vector for the inhibition of glioma growth in the rat. *Biomaterials* 30, 4014–4020. doi: 10.1016/j.biomaterials.2009.04.011

Lin, C. Y., Hsieh, H. Y., Pitt, W. G., Huang, C. Y., Tseng, I. C., Yeh, C. K., et al. (2015). Focused ultrasound-induced blood-brain barrier opening for non-viral, non-invasive and targeted gene delivery. *J. Control. Release* 212, 1–9. doi: 10.1016/j.jconrel.2015.06.010

Liu, Y., Huang, R., Han, L., Ke, W., Shao, K., Ye, L., et al. (2009). Brain-targeting gene delivery and cellular internalization mechanisms for modified rabies virus glycoprotein RVG29 nanoparticles. *Biomaterials* 30, 4195–4202. doi: 10.1016/j.biomaterials.2009.02.051

Liu, Y., Li, J., Shao, K., Huang, R., Ye, L., Lou, J., et al. (2010). A leptin derived 30-amino-acid peptide modified pegylated poly-l-lysine dendrigraft for brain targeted gene delivery. *Biomaterials* 31, 5246–5257. doi: 10.1016/j.biomaterials.2010.03.011

Louveau, A., Smirnov, I., Keyes, T. J., Eccles, J. D., Rouhani, S. J., Peske, J. D., et al. (2015). Structural and functional features of central nervous system lymphatic vessels. *Nature* 523, 337–341. doi: 10.1038/nature14432

Lu, W., Sun, Q., Wan, J., She, Z., and Jiang, X. G. (2006). Cationic albumin—conjugated pegylated nanoparticles allow gene delivery into brain tumors via intravenous administration. *Cancer Res.* 66, 11878–11887. doi: 10.1158/0008-5472.can-06-2354

MacKay, J. A., Li, W., Huang, Z., Dy, E. E., Huynh, G., Tihan, T., et al. (2008). HIV TAT peptide modifies the distribution of DNA nanolipoparticles following convection-enhanced delivery. *Mol. Ther.* 16, 893–900. doi: 10.1038/mt.2008.36

Maheshri, N., Koerber, J. T., Kaspar, B. K., and Schaffer, D. V. (2006). Directed evolution of adeno-associated virus yields enhanced gene delivery vectors. *Nat. Biotechnol.* 24, 198–204. doi: 10.1038/nbt1182

Mano, Y., Saito, R., Haga, Y., Matsunaga, T., Zhang, R., Chonan, M., et al. (2016). Intraparenchymal ultrasound application and improved distribution of infusate with convection-enhanced delivery in rodent and nonhuman primate brain. *J. Neurosurg.* 124, 1490–1500. doi: 10.3171/2015.3.jns142152

Masserdotti, G., Gillotin, S., Sutor, B., Drechsel, D., Irmler, M., Jørgensen, H. F., et al. (2015). Transcriptional mechanisms of proneural factors and REST in regulating neuronal reprogramming of astrocytes. *Cell Stem Cell* 17, 74–88. doi: 10.1016/j.stem.2015.05.014

Matsuoka, N., Nozaki, K., Takagi, Y., Nishimura, M., Hayashi, J., Miyatake, S.-I., et al. (2003). Adenovirus-mediated gene transfer of fibroblast growth factor-2 increases BrdU-positive cells after forebrain ischemia in gerbils. *Stroke* 34, 1519–1525. doi: 10.1161/01.str.0000070840.56414.3b

Mattson, M. P., and Magnus, T. (2006). Ageing and neuronal vulnerability. *Nat. Rev. Neurosci.* 7, 278–294. doi: 10.1038/nrn1886

McDannold, N., Arvanitis, C. D., Vykhodtseva, N., and Livingstone, M. S. (2012). Temporary disruption of the blood-brain barrier by use of ultrasound and microbubbles: safety and efficacy evaluation in rhesus macaques. *Cancer Res.* 72, 3652–3663. doi: 10.1158/0008-5472.can-12-0128

Mead, B. P., Mastorakos, P., Suk, J. S., Klibanov, A. L., Hanes, J., and Price, R. J. (2016). Targeted gene transfer to the brain via the delivery of brain-penetrating DNA nanoparticles with focused ultrasound. *J. Control. Release* 223, 109–117. doi: 10.1016/j.jconrel.2015.12.034

Meairs, S., and Alonso, A. (2007). Ultrasound, microbubbles and the blood-brain barrier. *Prog. Biophys. Mol. Biol.* 93, 354–362. doi: 10.1016/j.pbiomolbio.2006.07.019

Medina-Kauwe, L. K. (2007). "Alternative" endocytic mechanisms exploited by pathogens: new avenues for therapeutic delivery? *Adv. Drug Deliv. Rev.* 59, 798–809. doi: 10.1016/j.addr.2007.06.009

Mitchell, J. D., and Borasio, G. D. (2007). Amyotrophic lateral sclerosis. *Lancet* 369, 2031–2041. doi: 10.1016/S0140-6736(07)60944-1

Monani, U. R. (2005). Spinal muscular atrophy: a deficiency in a ubiquitous protein; a motor neuron-specific disease. *Neuron* 48, 885–896. doi: 10.1016/j.neuron.2005.12.001

Morille, M., Passirani, C., Vonarbourg, A., Clavreul, A., and Benoit, J. P. (2008). Progress in developing cationic vectors for non-viral systemic gene therapy against cancer. *Biomaterials* 29, 3477–3496. doi: 10.1016/j.biomaterials.2008.04.036

Mortazavi, M. M., Griessenauer, C. J., Adeeb, N., Deep, A., Shahripour, R. B., Loukas, M., et al. (2014). The choroid plexus: a comprehensive review of its history, anatomy, function, histology, embryology and surgical considerations. *Childs Nerv. Syst.* 30, 205–214. doi: 10.1007/s00381-013-2326-y

Nance, E., Timbie, K., Miller, G. W., Song, J., Louttit, C., Klibanov, A. L., et al. (2014). Non-invasive delivery of stealth, brain-penetrating nanoparticles across the blood–Brain barrier using MRI-guided focused ultrasound. *J. Control. Release* 189, 123–132. doi: 10.1016/j.jconrel.2014.06.031

Nicholson, C., Kamali-Zare, P., and Tao, L. (2011). Brain extracellular space as a diffusion barrier. *Comput. Vis. Sci.* 14, 309–325. doi: 10.1007/s00791-012-0185-9

Niidome, T., and Huang, L. (2002). Gene therapy progress and prospects: nonviral vectors. *Gene Ther.* 9, 1647–1652. doi: 10.1038/sj.gt.3301923

Pack, D. W., Hoffman, A. S., Pun, S., and Stayton, P. S. (2005). Design and development of polymers for gene delivery. *Nat. Rev. Drug Discov.* 4, 581–593. doi: 10.1038/nrd1775

Panje, C. M., Wang, D. S., and Willmann, J. K. (2013). Ultrasound and microbubble-mediated gene delivery in cancer: progress and perspectives. *Invest. Radiol.* 48, 755–769. doi: 10.1097/RLI.0b013e3182982cc1

Pardridge, W. M. (2005). The blood-brain barrier: bottleneck in brain drug development. *NeuroRx* 2, 3–14. doi: 10.1007/bf03206638

Pardridge, W. M. (2011). Drug transport in brain via the cerebrospinal fluid. *Fluids Barriers CNS* 8:7. doi: 10.1186/2045-8118-8-7

Park, T. E., Singh, B., Li, H., Lee, J. Y., Kang, S. K., Choi, Y. J., et al. (2015). Enhanced BBB permeability of osmotically active poly(mannitol-co-PEI) modified with rabies virus glycoprotein via selective stimulation of caveolar endocytosis for RNAi therapeutics in Alzheimer's disease. *Biomaterials* 38, 61–71. doi: 10.1016/j.biomaterials.2014.10.068

Patel, M., Goyal, B., Bhadada, S., Bhatt, J., and Amin, A. (2009). Getting into the brain. *CNS Drugs* 23, 35–58. doi: 10.2165/0023210-200923010-00003

Patlak, C. S., Blasberg, R. G., and Fenstermacher, J. D. (1983). Graphical evaluation of blood-to-brain transfer constants from multiple-time uptake data. *J. Cereb. Blood Flow Metab.* 3, 1–7. doi: 10.1038/jcbfm.1983.1

Petruska, J. C., Kitay, B., Boyce, V. S., Kaspar, B. K., Pearse, D. D., Gage, F. H., et al. (2010). Intramuscular AAV delivery of NT-3 alters synaptic transmission to motoneurons in adult rats. *Eur. J. Neurosci.* 32, 997–1005. doi: 10.1111/j.1460-9568.2010.07392.x

Polikov, V. S., Tresco, P. A., and Reichert, W. M. (2005). Response of brain tissue to chronically implanted neural electrodes. *J. Neurosci. Methods* 148, 1–18. doi: 10.1016/j.jneumeth.2005.08.015

Pombo García, K., Zarschler, K., Barbaro, L., Barreto, J. A., O'Malley, W., Spiccia, L., et al. (2014). Zwitterionic-coated "stealth" nanoparticles for biomedical applications: recent advances in countering biomolecular corona formation and uptake by the mononuclear phagocyte system. *Small* 10, 2516–2529. doi: 10.1002/smll.201303540

Potts, M. B., Silvestrini, M. T., and Lim, D. A. (2013). Devices for cell transplantation into the central nervous system: design considerations and emerging technologies. *Surg. Neurol. Int.* 4, S22–S30. doi: 10.4103/2152-7806.109190

Price, D., Griffin, J., Young, A., Peck, K., and Stocks, A. (1975). Tetanus toxin: direct evidence for retrograde intraaxonal transport. *Science* 188, 945–947. doi: 10.1126/science.49080

Pulford, B., Reim, N., Bell, A., Veatch, J., Forster, G., Bender, H., et al. (2010). Liposome-siRNA-peptide complexes cross the blood-brain barrier and significantly decrease PrPC on neuronal cells and PrPRES in infected cell cultures. *PLoS One* 5:e11085. doi: 10.1371/journal.pone.0011085

Qian, Y., Zha, Y., Feng, B., Pang, Z., Zhang, B., Sun, X., et al. (2013). PEGylated poly(2-(dimethylamino) ethyl methacrylate)/DNA polyplex micelles decorated with phage-displayed TGN peptide for brain-targeted gene delivery. *Biomaterials* 34, 2117–2129. doi: 10.1016/j.biomaterials.2012.11.050

Querbes, W., Ge, P., Zhang, W., Fan, Y., Costigan, J., Charisse, K., et al. (2009). Direct CNS delivery of siRNA mediates robust silencing in oligodendrocytes. *Oligonucleotides* 19, 23–30. doi: 10.1089/oli.2008.0165

Rapoport, S. I. (2001). Advances in osmotic opening of the blood-brain barrier to enhance CNS chemotherapy. *Expert Opin. Investig. Drugs* 10, 1809–1818. doi: 10.1517/13543784.10.10.1809

Rungta, R. L., Choi, H. B., Lin, P. J., Ko, R. W., Ashby, D., Nair, J., et al. (2013). Lipid nanoparticle delivery of siRNA to silence neuronal gene expression in the brain. *Mol. Ther. Nucleic Acids* 2:e136. doi: 10.1038/mtna.2013.65

Rychak, J. J., and Klibanov, A. L. (2014). Nucleic acid delivery with microbubbles and ultrasound. *Adv. Drug Deliv. Rev.* 72, 82–93. doi: 10.1016/j.addr.2014.01.009

Salinas, S., Schiavo, G., and Kremer, E. J. (2010). A hitchhiker's guide to the nervous system: the complex journey of viruses and toxins. *Nat. Rev. Microbiol.* 8, 645–655. doi: 10.1038/nrmicro2395

Schellinger, J. G., Pahang, J. A., Johnson, R. N., Chu, D. S. H., Sellers, D. L., Maris, D. O., et al. (2013). Melittin-grafted HPMA-oligolysine based copolymers for gene delivery. *Biomaterials* 34, 2318–2326. doi: 10.1016/j.biomaterials.2012.09.072

Schöttler, S., Becker, G., Winzen, S., Steinbach, T., Mohr, K., Landfester, K., et al. (2016). Protein adsorption is required for stealth effect of poly(ethylene glycol)- and poly(phosphoester)-coated nanocarriers. *Nat. Nanotechnol.* 11, 372–377. doi: 10.1038/nnano.2015.330

Schwab, M. E., Suda, K., and Thoenen, H. (1979). Selective retrograde synaptic transer of a protein, tetanus toxin, subsequent to its retrotransport. *J. Cell Biol.* 82, 798–810. doi: 10.1083/jcb.82.3.798

Sellers, D. L., Bergen, J. M., Johnson, R. N., Back, H., Ravits, J. M., and Horner, P. J. (2016). Targeted axonal import (TAxI) peptide delivers functional proteins into the spinal cord motor neurons after peripheral administration. *Proc. Natl. Acad. Sci. U S A* 113, 2514–2519. doi: 10.1073/pnas.1515526113

Sheikov, N., McDannold, N., Vykhodtseva, N., Jolesz, F., and Hynynen, K. (2004). Cellular mechanisms of the blood-brain barrier opening induced by ultrasound in presence of microbubbles. *Ultrasound Med. Biol.* 30, 979–989. doi: 10.1016/j.ultrasmedbio.2004.04.010

Snyder, B. R., Gray, S. J., Quach, E. T., Huang, J. W., Leung, C. H., Samulski, R. J., et al. (2011). Comparison of adeno-associated viral vector serotypes for spinal cord and motor neuron gene delivery. *Hum. Gene Ther.* 22, 1129–1135. doi: 10.1089/hum.2011.008

Soderquist, R., Sloane, E., Loram, L., Harrison, J., Dengler, E., Johnson, S., et al. (2010). Release of Plasmid DNA-encoding IL-10 from PLGA microparticles facilitates long-term reversal of neuropathic pain following a single intrathecal administration. *Pharm. Res.* 27, 841–854. doi: 10.1007/s11095-010-0077-y

Song, H. P., Yang, J. Y., Lo, S. L., Wang, Y., Fan, W. M., Tang, X. S., et al. (2010). Gene transfer using self-assembled ternary complexes of cationic magnetic nanoparticles, plasmid DNA and cell-penetrating tat peptide. *Biomaterials* 31, 769–778. doi: 10.1016/j.biomaterials.2009.09.085

Son, S., Hwang, D. W., Singha, K., Jeong, J. H., Park, T. G., Lee, D. S., et al. (2011). RVG peptide tethered bioreducible polyethylenimine for gene delivery to brain. *J. Control. Release* 155, 18–25. doi: 10.1016/j.jconrel.2010.08.011

Spencer, B. J., and Verma, I. M. (2007). Targeted delivery of proteins across the blood-brain barrier. *Proc. Natl. Acad. Sci. U S A* 104, 7594–7599. doi: 10.1073/pnas.0702170104

Stiles, D. K., Zhang, Z., Ge, P., Nelson, B., Grondin, R., Ai, Y., et al. (2012). Widespread suppression of huntingtin with convection-enhanced delivery of siRNA. *Exp. Neurol.* 233, 463–471. doi: 10.1016/j.expneurol.2011.11.020

Sugiura, S., Kitagawa, K., Tanaka, S., Todo, K., Omura-Matsuoka, E., Sasaki, T., et al. (2005). Adenovirus-mediated gene transfer of heparin-binding epidermal growth factor-like growth factor enhances neurogenesis and angiogenesis after focal cerebral ischemia in rats. *Stroke* 36, 859–864. doi: 10.1161/01.str.0000158905.22871.95

Syková, E., and Nicholson, C. (2008). Diffusion in brain extracellular space. *Physiol. Rev.* 88, 1277–1340. doi: 10.1152/physrev.00027.2007

Tan, J.-K. Y., Pham, B., Zong, Y., Perez, C., Maris, D. O., Hemphill, A., et al. (2016). Microbubbles and ultrasound increase intraventricular polyplex gene transfer to the brain. *J. Control. Release* 231, 86–93. doi: 10.1016/j.jconrel.2016.02.003

Tang, G. P., Zeng, J. M., Gao, S. J., Ma, Y. X., Shi, L., Li, Y., et al. (2003). Polyethylene glycol modified polyethylenimine for improved CNS gene transfer: effects of PEGylation extent. *Biomaterials* 24, 2351–2362. doi: 10.1016/s0142-9612(03)00029-2

Tarragó-Trani, M. T., and Storrie, B. (2007). Alternate routes for drug delivery to the cell interior: pathways to the Golgi apparatus and endoplasmic reticulum. *Adv. Drug Deliv. Rev.* 59, 782–797. doi: 10.1016/j.addr.2007.06.006

Thomas, C. E., Ehrhardt, A., and Kay, M. A. (2003). Progress and problems with the use of viral vectors for gene therapy. *Nat. Rev. Genet.* 4, 346–358. doi: 10.1038/nrg1066

Tobinick, E. L. (2016). Perispinal delivery of CNS drugs. *CNS Drugs* 30, 469–480. doi: 10.1007/s40263-016-0339-2

Uchida, S., Itaka, K., Uchida, H., Hayakawa, K., Ogata, T., Ishii, T., et al. (2013). *in vivo* messenger RNA introduction into the central nervous system using polyplex nanomicelle. *PLoS One* 8:e56220. doi: 10.1371/journal.pone.0056220

von Bartheld, C. S. (2004). Axonal transport and neuronal transcytosis of trophic factors, tracers and pathogens. *J. Neurobiol.* 58, 295–314. doi: 10.1002/neu.10315

Wang, H., Ghosh, A., Baigude, H., Yang, C. S., Qiu, L., Xia, X., et al. (2008). Therapeutic gene silencing delivered by a chemically modified small interfering RNA against mutant SOD1 slows amyotrophic lateral sclerosis progression. *J. Biol. Chem.* 283, 15845–15852. doi: 10.1074/jbc.m800834200

Wehling, K., Arfmann, H.-A., Standke, K.-H. C., and Wagner, K. G. (1975). Specfificity of DNA-basic polypeptide interactions. Influence of neutral residues incorporated into polylysine and polyarginine. *Nucleic Acids Res.* 2, 799–807. doi: 10.1093/nar/2.6.799

Wei, H., Volpatti, L. R., Sellers, D. L., Maris, D. O., Andrews, I. W., Hemphill, A. S., et al. (2013). Dual responsive, stabilized nanoparticles for efficient *in vivo* plasmid delivery. *Angew. Chem. Int. Ed Engl.* 52, 5377–5381. doi: 10.1002/anie.201301896

Xie, F., Boska, M. D., Lof, J., Uberti, M. G., Tsutsui, J. M., and Porter, T. R. (2008). Effects of transcranial ultrasound and intravenous microbubbles on blood brain barrier permeability in a large animal model. *Ultrasound Med. Biol.* 34, 2028–2034. doi: 10.1016/j.ultrasmedbio.2008.05.004

Xu, J., Ma, C., Bass, C., and Terwilliger, E. F. (2005). A combination of mutations enhances the neurotropism of AAV-2. *Virology* 341, 203–214. doi: 10.1016/j.virol.2005.06.051

Yamada, K., Ushio, Y., Hayakawa, T., Kato, A., Yamada, N., and Mogami, H. (1982). Quantitative autoradiographic measurements of blood-brain barrier permeability in the rat glioma model. *J. Neurosurg.* 57, 394–398. doi: 10.3171/jns.1982.57.3.0394

Yao, H., Wang, K., Wang, Y., Wang, S., Li, J., Lou, J., et al. (2015). Enhanced blood-brain barrier penetration and glioma therapy mediated by a new peptide modified gene delivery system. *Biomaterials* 37, 345–352. doi: 10.1016/j.biomaterials.2014.10.034

Yue, P., He, L., Qiu, S., Li, Y., Liao, Y., Li, X., et al. (2014). OX26/CTX-conjugated PEGylated liposome as a dual-targeting gene delivery system for brain glioma. *Mol. Cancer* 13:191. doi: 10.1186/1476-4598-13-191

Yu, Y. J., Zhang, Y., Kenrick, M., Hoyte, K., Luk, W., Lu, Y., et al. (2011). Boosting brain uptake of a therapeutic antibody by reducing its affinity for a transcytosis target. *Sci. Transl. Med.* 3:84ra44. doi: 10.1126/scitranslmed.3002230

Zeng, J., Wang, X., and Wang, S. (2007). Self-assembled ternary complexes of plasmid DNA, low molecular weight polyethylenimine and targeting peptide for nonviral gene delivery into neurons. *Biomaterials* 28, 1443–1451. doi: 10.1016/j.biomaterials.2006.11.015

Zhang, Y., Pak, C., Han, Y., Ahlenius, H., Zhang, Z., Chanda, S., et al. (2013). Rapid single-step induction of functional neurons from human pluripotent stem cells. *Neuron* 78, 785–798. doi: 10.1016/j.neuron.2013.05.029

Zhang, Y., Wang, Y., Boado, R. J., and Pardridge, W. M. (2008). Lysosomal enzyme replacement of the brain with intravenous non-viral gene transfer. *Pharm. Res.* 25, 400–406. doi: 10.1007/s11095-007-9357-6

Zhou, Y., Yang, K., Cui, J., Ye, J., and Deng, C. (2012). Controlled permeation of cell membrane by single bubble acoustic cavitation. *J. Control. Release* 157, 103–111. doi: 10.1016/j.jconrel.2011.09.068

Zou, S., Scarfo, K., Nantz, M. H., and Hecker, J. G. (2010). Lipid-mediated delivery of RNA is more efficient than delivery of DNA in non-dividing cells. *Int. J. Pharm.* 389, 232–243. doi: 10.1016/j.ijpharm.2010.01.019

Conflict of Interest Statement: Authors have a US patent (61/532,982) regarding TAxI peptide.

frontiers in Molecular Neuroscience

REVIEW
published: 12 August 2016
doi: 10.3389/fnmol.2016.00067

Gene, Stem Cell, and Alternative Therapies for SCA 1

*Jacob L. Wagner, Deirdre M. O'Connor, Anthony Donsante and Nicholas M. Boulis**

Boulis Laboratory, Department of Neurosurgery, Emory School of Medicine, Atlanta, GA, USA

Spinocerebellar ataxia 1 is an autosomal dominant disease characterized by neurodegeneration and motor dysfunction. In disease pathogenesis, polyglutamine expansion within Ataxin-1, a gene involved in transcriptional repression, causes protein nuclear inclusions to form. Most notably, neuronal dysfunction presents in Purkinje cells. However, the effect of mutant Ataxin-1 is not entirely understood. Two mouse models are employed to represent spinocerebellar ataxia 1, a B05 transgenic model that specifically expresses mutant Ataxin-1 in Purkinje cells, and a *Sca1 154Q/2Q* model that inserts the polyglutamine expansion into the mouse Ataxin-1 locus so that the mutant Ataxin-1 is expressed in all cells that express Ataxin-1. This review aims to summarize and evaluate the wide variety of therapies proposed for spinocerebellar ataxia 1, specifically gene and stem cell therapies.

Keywords: SCA 1, gene therapy, stem cell therapy, mouse model, Ataxin-1, RNAi

OPEN ACCESS

Edited by:
George Smith,
Temple University School of Medicine, USA

Reviewed by:
Christian Gonzalez-Billault,
University of Chile, Chile
Michele Papa,
Seconda Università degli Studi di Napoli, Italy

****Correspondence:***
Nicholas M. Boulis
nboulis@emory.edu

Received: *12 May 2016*
Accepted: *26 July 2016*
Published: *12 August 2016*

Citation:
Wagner JL, O'Connor DM, Donsante A and Boulis NM (2016) Gene, Stem Cell, and Alternative Therapies for SCA 1. Front. Mol. Neurosci. 9:67. doi: 10.3389/fnmol.2016.00067

INTRODUCTION

Spinocerebellar ataxia (SCA) is a group of autosomal dominant neurodegenerative diseases characterized by progressive degeneration in the spinal cord, brain stem, and cerebellum. SCA types 1–36 have been identified, each attributable to a different gene. SCA genetic abnormalities are most commonly caused by cytosine-adenosine-guanine (CAG) repeat expansion leading to a polyglutamine expanded protein product presumed to be toxic to neurons (Whaley et al., 2011; **Table 1**).

In spinocerebellar ataxia 1 (SCA 1), the accumulation of the mutant ataxin-1 protein (ATXN1) causes loss of cerebellar Purkinje cells (PC) and dysfunction and degeneration in the cerebellum, brain stem, and spinal cord. To date, treatment consists of managing the symptoms with pharmacologic agents. No fundamental therapies for SCA 1 have been identified yet (Whaley et al., 2011), although several experimental studies have shown promising results.

This review will provide background information on SCA 1 and the mouse models used as well as inform the reader about promising gene and stem cell therapy approaches. Challenges regarding these novel approaches will be discussed and other alternative therapies will be briefly reviewed.

FACTS AND DEMOGRAPHICS

According to the National Ataxia Foundation, approximately 1–2 in 100,000 people will develop SCA 1, but the frequency varies depending on ethnic background and location (National Ataxia Foundation, https://www.ataxia.org/).

The onset of the disease begins around the 3rd–4th decade but can develop between the ages of 4 and 74 (Schols et al., 2004). From onset, patient survival ranges from 10 to 28 years (average = 15 years; Jayadev and Bird, 2013). In cases of early onset (before 13 years old), disease progression

TABLE 1 | Autosomal dominant hereditary ataxias.

Disease Name[a]	Gene	Average onset (range in years)	Average duration (range in years)	Distinguishing features[b]
SCA1	*ATXN1*	3rd–4th decade (<10 to >60)	15 years (10–28)	Pyramidal signs, peripheral neuropathy
SCA2	*ATXN2*	3rd–4th decade (<10 to >60)	10 years (1–30)	Slow saccadic eye movements, peripheral neuropathy, decreased DTRs, dementia
SCA3	*ATXN3*	4th decade (10–70)	10 years (1–20)	Pyramidal and extrapyramidal signs; lid retraction, nystagmus, decreased saccade velocity; amyotrophy fasciculations, sensory loss
SCA4	16q22.1	4th–7th decade (19–72)	Decades	Sensory axonal neuropathy, deafness; may be allelic with 16q22-linked SCA
SCA5	*SPTBN2*	3rd–4th decade (10–68)	>25 years	Early onset, slow course; first reported in descendants of Abraham Lincoln
SCA6	*CACNA1A*	5th–6th decade (19–71)	>25 years	Sometimes episodic ataxia, very slow progression
SCA7	*ATXN7*	3rd–4th decade (0.5–60)	20 years (1–45; early onset correlates with shorter duration)	Visual loss with retinopathy
SCA8	*ATXN8I*	4th decade (1–65)	Normal life span	Slowly progressive, sometimes brisk DTRs, decreased vibration sense; rarely, cognitive impairment
	ATXN80S			
SCA10	*ATXN10*	4th decade (12–48)	9 years	Occasional seizures; most families are of Native American background
SCA11	*TTBK2*	Age 30 years (15–70)	Normal life span	Mild, remain ambulatory
SCA12	*PPP2R2B*	4th decade (8–62)		Slowly progressive ataxia; action tremor in the 30s; hyperreflexia; subtle Parkinsomism possible; cognitive/psychiatric disorders including dementia
SCA13	*KCNC3*	Childhood or adulthood	Unknown	Mild intellectual disability, short stature
SCA14	*PRKCG*	3rd–4th decade (3–70)	Decades (1–30)	Early axial myoclonus
SCA15	ITPR1	4th decade (7–66)	Decades	Pure ataxia, very slow progression
SCA16	*SCA16*	Age 39 years (20–66)	1–40 years	Head tremor; one Japanese family
SCA17	*TBP*	4th decade (3–55)	>8 years	Mental deterioration; occasional chorea, dystonia, myoclonus
SCA18	7q22-q32	Adolescence (12–25)	Decades	Ataxia with early sensory/motor neuropathy, nystagmus, dysarthria, decreased tendon reflexes, muscle weakness, atrophy, fasiculations, Babinski responses
SCA 19/22	*KCND3*	4th decade (10–51)	Decades	Slowly progressive, rare cognitive impairment, myoclonus, hyperreflexia
SCA20	11q12.2	5th decade (19–64)	Decades	Early dysarthria, spasmodic dysphonia, hyperreflexia, bradykinesia; calcification of the dentate nucleus
	11q12.3			
SCA21	*SCA21*	6–30	Decades	Mild cognitive impairment
SCA23	*PDYN*	5th–6th decade	>10 years	Dysarthria, abnormal eye movements, reduced vibration and position sense; one Dutch family; neuropathology
SCA25	*SCA25*	(1.5–39)	Unknown	Sensory neuropathy; one French family
SCA26	*EEF2*	(26–60)	Unknown	Dysarthria, irregular visual pursuits; one Norwegian-American family; MRI: cerebellar atrophy
SCA27	*FGF14*	Age 11 years (7–20)	Decades	Early-onset tremor; dyskinesia, cognitive deficits; one Dutch family
SCA28	*AFG3L2*	Age 19.5 years (12–36)	Decades	Nystagmus, opthalmoparesis, ptosis, increased tendon reflexes; two Italian families
SCA29	3p26	Early childhood	Lifelong	Learning deficits
SCA30	4q34.3–q35.1	(45–76)	Lifelong	Hyperreflexia
SCA31	*BEAN1*	5th–6th decade	Lifelong	Normal sensation
SCA35	*TGM6*	43.7 ± 2.9 (40–48) years	15.9 ± 8.8 (5–31) years	Hyperreflexia, Babinski respsonses; spasmodic torticollis
SCA36	*NOP56*	52.8 ± 4.3 years	Decades	Muscle fasiculations, tongue atrophy, hyperreflexia

DTR, deep tendon reflex.

[a] *SCA9 has not been assigned.*

[b] *All have gait ataxia.*

Reprinted by permission from Macmillan Publishers Ltd: Genetics in Medicine (Jayadev and Bird, 2013), copyright (2013).

is more rapid and severe, with patients usually dying before the age of 16 (Zoghbi et al., 1988).

Clinically, SCA 1 symptoms include limb ataxia, gait disturbance, slurred speech, balance difficulty, brisk tendon reflexes, hypermetric saccades, nystagmus, mild dysphagia, and cognitive impairment. SCA 1 symptoms can be distinguished from other hereditary ataxias by the predominance of pyramidal symptoms. Amyotrophy and sensory loss can also be present in affected individuals. Olivopontocerebellar atrophy is the major finding on MRI/CT (Schols et al., 2004). Eventually, affected individuals develop respiratory failure, the main cause of death for SCA 1 (Subramony and Ashizawa, 1993).

MOLECULAR PATHOGENESIS

SCA 1 is caused by a CAG repeat expansion in the *ATXN1* gene (OMIM: 601556) that encodes ATXN1. In normal *ATXN1*, the triplet CAG is repeated 6 to 36 times while in mutant forms (polyQ-ATXN1) the number of repeats can exceed 100. Similar to other polyglutamine (polyQ) diseases such as Huntington's, as the polyQ expansion becomes longer, disease onset occurs earlier, and the symptoms are more severe (Kang and Hong, 2009). The polyQ expansion is thought to be due to errors in the DNA replication machinery (Kang et al., 1995). The number of repeats can increase from generation to generation, particularly in the paternal germline (Matilla et al., 1993).

ATXN1 is mainly localized to the nucleus of neuronal cells; however, in Purkinje cells, it is found in both the cytoplasm and the nucleus (Servadio et al., 1995). It associates with a collection of high molecular weight protein complexes that also contain Capicua (CIC), a transcriptional repressor containing a high mobility group (HMG) box. The presence of human polyQ-ATXN1 alters the size distribution of these complexes and inhibits the repressor activity of CIC. Overexpression of CIC in a fly model suppresses the morphologic changed induced by polyQ-ATXN1 (Lam et al., 2006). Additionally, Yue et al. found that ATXN1 binds RNA and that, as size of its polyQ tract increases, its ability to bind RNA decreases. Thus, expansion of the ATXN1 polyQ tract may alter its role in RNA metabolism (Yue et al., 2001). polyQ-ATXN1 aggregates and forms inclusions in the nucleus and cytoplasm of neurons, especially in PCs (Kang and Hong, 2009). PolyQ-ATXN1 alters several cellular pathways, including transcription (Cvetanovic et al., 2007; Lee S. et al., 2008), RNA processing (Hong et al., 2003), and signal transduction (Goold et al., 2007; Gatchel et al., 2008), disrupting normal cell function and leading to cell death (Kang and Hong, 2009).

Phosphorylation contributes to the regulation of ATXN1 folding and distribution. Emamian et al. found that serine 776 (S776) was phosphorylated in transgenic mice carrying ATXN1. Mutating S776 to alanine altered the intracellular deposition of polyQ-ATXN1, preventing nuclear inclusions from forming. When the S776 and A776 forms of polyQ-ATXN1 (polyQ-ATXN1-S776 and polyQ-ATXN1-A776, respectively) were expressed in Purkinje cells in mice, polyQ-ATXN1-A776 was substantially less toxic than polyQ-ATXN1-S776, demonstrating that phosphorylation of this serine residue contributes significantly to the harmful effects of the mutant protein (Emamian et al., 2003). The protective effect of A776 appears to be due to the fact that polyQ-ATXN1-A776 does not produce the abnormal, high molecular weight complexes that are observed in mice carrying polyQ-ATXN1-S776, even though both forms associated strongly with CIC. Interestingly, it appears that toxicity arises, not due to novel interactions between polyQ-ATXN1 and other proteins, but from polyQ-ATXN1 adversely affecting the function of proteins it normally interacts with (Lam et al., 2006). Protein Kinase A (PKA) is the cAMP-dependent kinase responsible for S776 of ATXN1 (Chen et al., 2003; Jorgensen et al., 2009). In addition to S776, Vierra-Green et al. found through matrix-assisted laser description ionization time-of-flight mass spectrometry (MALDI TOF) and mutational analysis that S239 is also a phosphorylation site of ATXN1 (Vierra-Green et al., 2005), although further research is required to determine if S239 is linked to SCA 1 pathogenesis. Understanding the phosphorylation of ATXN1 allows for a better understanding of the role ATXN1 has within neurons, specifically with post-translational modifications, which is vital for future therapeutic strategies.

Relevant to polyQ-ATXN1 cytotoxicity, Lee et al. found that ATXN1 levels might be post-transcriptionally regulated by miRNA, specifically miR-19, miR-101, and miR-130. When miR-19, miR101, and miR130 were transfected into HEK293T, HeLa and MCF7 cells, a marked decrease in ATXN1 levels was observed. When 2′-O-methyl inhibitors against the miRNA were added to HEK293T cells, ATXN1 levels increased. These findings present the possibility that miRNA-binding site mutations or miRNA genes might lead to the SCA 1 neurodegenerative phenotypes (Lee Y. et al., 2008).

MOUSE MODELS

Mouse models have been generated to study the cerebellar degeneration associated with SCA 1. In the B05 transgenic mouse model (B05) the human SCA 1 cDNA was modified to contain 82 CAG repeats and expressed under the control of the Purkinje cell protein 2 (pcp2) promoter to form a pcp2/SCA1 transgene. The 5′ regulatory sequences of *pcp2* are sufficient to restrict transgene expression to PCs (Oberdick et al., 1990; Vandaele et al., 1991). B05 transgenic mice overexpress polyQ-ATXN1, which leads to the loss of PCs from the cerebellum and thus present the neurological phenotype of ataxia. Abnormalities include reduced activity, head swaying and incoordination. Ataxia onset begins at 12 weeks of life. However, because the mutant cDNA is only expressed in Purkinje cells, this model only displays symptoms of degenerating PCs and these mice have a normal life span (Burright et al., 1995). Patients, in contrast, experience dysfunction in a variety of neurons in addition to PCs (Bürk et al., 2001). These other neurons produce cognitive dysfunction that is not represented in the B05 mouse model (**Table 2**), which makes comparisons to SCA 1 patients difficult.

To better model SCA 1, Watase et al. generated a SCA 1 knock-in model by introducing a 154-CAG expansion into exon 8 of the endogenous ATXN 1 locus. The knock-in mouse model, called *Sca1 154Q/2Q* (154Q/2Q), expresses polyQ-ATXN1 in neurons in the cortex, thalamus, hypocampus, caudate nucleus,

putamen, brain stem, cerebellum, and spinal cord. With polyQ-ATXN1 allele present throughout the central nervous system, the 154Q/2Q model displays more of the human disease features, such as motor incoordination, muscle wasting, cognitive impairment, and premature death, making it a more relevant physiological model of the disease. Disease onset begins at 7–8 weeks and mice die prematurely at 35–45 weeks of age (Watase et al., 2002; **Table 2**).

No non-rodent animal model exists for SCA 1. A transgenic model of Huntington's disease, another polyQ disease involving an expanded polyglutamine repeat in *HTT,* exists in rhesus macaque (Yang et al., 2008), suggesting that a SCA 1 model could be made as well.

GENE THERAPY

SCA 1 is a monogenic disease; thus, gene therapy is an obvious treatment approach. Gene therapeutic intervention involves either reducing expression of the mutant *ATXN1* through gene silencing or overexpressing a paralog of ATXN1, ataxin-1-like (ATXN1L), to competitively inhibit the formation of toxic complexes by polyQ-ATXN1 (Keiser et al., 2013).

The RNAi approach regulates gene expression through small RNAs, including artificial microRNA (miRNA), small interfering RNA (siRNA), and short hairpin RNA (shRNA). Short hairpin RNA, siRNA, and miRNA are all non-coding RNA that post-transcriptionally regulate mRNA transcript levels. siRNA acts on a particular sequence for degradation while miRNA is more likely to target mRNA for transcriptional silencing (Lam et al., 2015). Unlike siRNA which requires two independent RNA strands, a sense and antisense strand that guides the RNA-induced silencing complex (RISC), shRNA is a single strand that folds back on itself to produce a double-stranded molecule (Davidson and Paulson, 2004). The Davidson research group showed that RNAi platforms (Keiser et al., 2013) expressed using viral vectors could potentially have therapeutic effects on polyglutamine diseases. Xia et al. investigated the possibility that virally expressed siRNA could decrease levels of polyglutamine expanded proteins in neural PC12 clonal cells. The lines were developed to express tetracycline-repressible eGFP-polyglutamine fusion proteins, which the siRNA targeted. Decrease in protein aggregate levels was shown by western blot analysis and cellular fluorescence (Xia et al., 2002; **Table 3**).

RNA interference (RNAi) has already been proven to be effective in a number of diseases caused by CAG repeat expansion. Harper et al. injected AAV2/1 targeting huntingtin (HTT) intracranially and found reduced HTT mRNA levels and protein expression in HTT transgenic mice. Mice showed improved behavioral outcomes and reduced neuropathic HTT abnormalities (Harper et al., 2005). Additionally, Monteys et al. found preferential silencing of the mutant HTT allele *in vitro* by miRNA. Preferential knockdown of the mutant allele was achieved *in vivo* when one of the miRNAs tested was delivered through AAV2 by striatal bilateral injection into HTT double transgenic mice, However, knockdown of the wild-type allele was also detected (Monteys et al., 2015). Miller et al. generated siRNA that silences the SCA 3-associated allele, ataxin-3 (ATXN3), targeting an adjacent single nucleotide polymorphism (SNP). *In vitro,* the RNAi approach successfully silenced both plasmid and viral expression of ATXN3 (Miller et al., 2003). *In vivo*, AAV2 vector was delivered via intracerebellar injection into SCA 3 mice. Rodriguez-Lebron et al. found that anti-ATXN3 miRNA suppressed ATXN3 expression and cleared nuclear accumulation of mutant ATXN3 (Rodriguez-Lebron et al., 2013). Lastly, for SCA 7, Ramachandran et al. found more than 50% reduction of mutant human and wildtype mouse ATXN7 allele after AAV2/1 subretinal space injection of miRNA into SCA 7 transgenic mice. Mice preserved normal retinal function after injection (Ramachandran et al., 2014). Keiser et al. found that ATXN1 levels can be reduced 30% by miS1 knockdown through AAV1 deep cerebellar nuclei injection in an adult rhesus. The intervention was well tolerated and there were no clinical complications. The biodistribution and tolerability of the miS1 treatment supports its use as a clinical therapeutic (Keiser et al., 2015; **Table 3**).

Xia et al. tested shRNA to target the *Sca 1* locus. They generated AAV serotype 2/1 (AAV 2/1) that expressed shRNA which was delivered via intracerebellar injection. This treatment resolved ATXN1 nuclear inclusions and PC morphology as well as improving motor coordination in transgenic B05 mice

TABLE 2 | Overview of mouse models for SCA 1.

	B05 transgenic mice (B05)	***Sca1 154Q/2Q* mice (154Q/2Q)**
Phenotype	Motor incoordination, ataxia (12 weeks), no cognitive impairment	motor incoordination, muscle wasting, cognitive impairment, memory deficits
Physical Onset	5 weeks	7–8 weeks
Course of the disease	Normal life span	Premature, 35–45 weeks
Neuropathology	PC loss, Bergmann glial proliferation, shrinkage and gliosis of molecular layer	Reduced dendritic arborization of PCs (early stage)
		Neuronal intranuclear inclusions and PC loss (advanced disease)
	Purkinje neuron dendritic and somatic atrophy	Hypocampal synaptic dysfunction but no significant loss
Mechanism	Overexpression of polyQ-ATXN1 (82 CAG repeats) under the control of Purkinje Cell pcp2 promoter	Expanded repeat of 154 CAGs was inserted into the mouse Sca 1 locus (knock-in)
References	Burright et al., 1995; Clark et al., 1997	Watase et al., 2002

TABLE 3 | Overview of gene therapies for SCA 1.

	Treatment/vector	Animal model	Route	Outcome
Keiser et al., 2013	(1) miRNA/AAV serotype 2/1 (2) Atxn1 Like/AAV serotype 2/1	B05 mice	DCN injection	Widespread PC transduction Improved histology and behavioral profiles
Xia et al., 2004	siRNA/AAV2	B05 mice	Direct injection into the cerebellar lobules	Cerebellar morphology restoration, PC inclusions resolution, improved motor coordination
Keiser et al., 2014	RNAi/AAV serotype 2/5	SCA1 154Q/2Q knock-in mice	Deep cerebellar nuclei (DCN)	Preserved neurohistology and rotarod performance
Venkatraman et al., 2014	HDAC 3 depletion	(1) PC-specific HDAC3 null knock-in mice (2) SCA1 154Q/2Q mice (heterozygous HDAC3+/− mice)	N/A	(1) No improvement in cognitive and cerebellar function (2) Deleterious effects both behaviorally and histologically

(Xia et al., 2004). Keiser et al. tested the therapeutic utility of SCA 1-targeted AAV 2/1 miRNA to suppress ATXN1 expression. The construct was delivered via deep cerebellar nuclei injection and resulted in PC transduction and improved gait and balance in transgenic B05 mice (Keiser et al., 2013). To our knowledge, siRNA or shRNA targeting ATXN1 has not been evaluated in 154Q/2Q mice. Keiser et al. found that miRNA therapy in 154Q/2Q mice was sufficient to reduce SCA 1 symptoms. They tested the efficacy of miRNA delivered via AAV 2/5 to the deep cerebellar nuclei. The RNAi inhibited SCA 1-related transcriptional changes, preserved the cerebellar lobule, and improved motor coordination (Keiser et al., 2014; **Table 3**).

The potential toxicity of small RNA should be noted. Grimm et al. studied the long-term effect of high shRNA expression in the livers of mice through AAV8 intravenous infusion. Of the 49 AAV/shRNA vectors tested, 36 caused does-dependent liver injury, with 23 of those leading to death. Grimm et al. found the morbidity to be associated with downregulation of miRNAs derived from the liver, possibly indicating competition with the shRNAs (Grimm et al., 2006). The study demonstrates the risk of oversaturating small RNA pathways with RNAi therapy.

As an alternate approach to RNAi, overexpression of the ATXN1L protein also represents a feasible therapy for SCA 1. ATXN1 and ATXN1L interact with a similar set of proteins, including CIC, through their ATXN1 and HMG-box protein 1 domain (AXH domain). Overexpression of ATXN1L could outcompete polyQ-ATXN1 for binding to CIC, reducing the amount of toxic complexes and disease severity (de Chiara et al., 2003; Lam et al., 2006; Bowman et al., 2007; Lim et al., 2008). Keiser et al. showed that overexpression of ATXN1L from an AAV2/1 vector has protective effects in B05 mice. In their study, human ATXN1L was expressed using AAV 2/1 and was delivered into the deep cerebellar nuclei. Mice receiving the injection exhibited improved gait, agility, and hind limb musculature and also decreased nuclear inclusions and PC loss, similar to that observed with the miRNA. Keiser et al. concludes that both overexpression of ATXN1L and RNAi are potentially viable treatment options for SCA 1 patients (Keiser et al., 2013; **Table 3**).

Alternatives to targeting the gene directly through RNAi and ATXN1L include histone deacetylase transcriptional repression. ATXN1 binds HDAC3, a class 1 histone deacetylase (HDAC) required for ATXN1 induced transcriptional repression (Karagianni and Wong, 2007). Venkatraman et al. tested the effect of PC-specific HDAC3 depletion in 154Q/2Q mice by siRNA knock down. However, mice did not show improvement in cerebellar or cognitive function. Additionally, Venkatraman et al. crossed a floxed HDAC3 mouse line with a mouse driving *Cre* expression from a *pcp-2* promoter. The *pcp-2* promoter turns on 6 days after birth in PC cells and reaches a maximum by 2–3 weeks after birth, which is about the time that transcriptional problems manifest (Lin et al., 2000; Gatchel et al., 2008). The offspring line has a conditional complete loss of HDAC3 in PCs and demonstrated dramatic PC degeneration and early onset ataxia. These results warn of the risk of neurotoxic side effects that can be caused by altering HDAC3 expression to treat SCA 1 (Venkatraman et al., 2014; **Table 3**).

In our opinion of the gene therapies, RNAi knockdown treats the cause of the disease while ATXN1L might not, as the polyQ-ATXN1 aggregates are still present. On the other hand, this cannot be definitive known until a side by side comparison between ATXN1L and RNAi with stringent control of the conditions is performed. Additionally, the issue of small RNA oversaturation arises. As with most gene therapies, the question also remains, is there adequate transduction of the therapeutic into the affected cells?

STEM CELL THERAPY

Stem-cell-based therapies represent a new strategy for spinocerebellar ataxias. Neurotransplantation has been performed in various cerebellar mutant mice using different types of cells and delivery techniques to stop PC degeneration and restore normal cerebellar architecture. Currently, a few studies have tried stem cell transplantation in SCA 1 mouse models and showed positive results both functionally and histologically.

An interesting approach by Chen et al. combines stem cell and gene therapy for gene delivery in SCA 1 mice. Bone marrow-derived cells (BMDCs) can fuse *in vivo* with somatic

cells, including Purkinje neurons (Alvarez-Dolado et al., 2003; Weimann et al., 2003). Bone marrow derived cells (BMDC) were genetically modified using AAV7 to carry two SCA 1 modifier genes, DnaJB4 and Pcbp3. The genes were determined by Fernandez-Funez et al. to have attenuating effects on SCA 1 onset by assisting chaperone activity and transcription stabilization, respectively (Fernandez-Funez et al., 2000). Chen et al. delivered BMDC by a retroorbital sinus injection into 154Q/2Q mice. PC and BMDC fused to produce heterokaryons with PC properties. In the treated 154Q/2Q mice, there was some improvement in pathology. Mice showed a diminished number of nuclear inclusions and an increased number of surviving PC, highlighting the potential neuroprotective effects of this combined strategy (Chen et al., 2011; **Table 4**).

Chintawar et al. transplanted neural precursor cells (NPCs) from the subventricular zone of adult mice to cerebellar white matter of B05 mice. Mice received injections into three separate sites of the cerebellar white matter at 5-, 13-, or 24-weeks-old time points where cerebellar pathology is not yet observed, PC loss begins, and PC are mostly abnormal, respectively. Grafted NPCs only migrated to the cerebellar cortex in 24-week-old mice. Additionally, motor skills only improved in mice treated at 24 weeks when compared to shams. When grafted NPCs did migrate to the cerebellar cortex, grafts did not adopt PC characteristics, but NPC-grafted B05 mice did exhibit thicker molecular layer and diminished PC loss (Chintawar et al., 2009; **Table 4**).

Matsuura et al. found that intrathecal injection of mesenchymal stem cells (MSCs) into the meningeal covering of the cerebellum improved PC organization in B05 mice injected at 5 weeks of age. At 24 weeks of age, untreated B05 mice displayed multilayered PC as a result of ectopically located PC bodies, but mice of the same age injected with MSCs had monolayered PCs. Additionally, MSC treatment reduced PC dendrite atrophy and normalized behavior and motor deficits (Matsuura et al., 2014; **Table 4**).

Stem cell therapies on non-SCA 1 mouse models are relevant to mention. In Lercher mutant mice, a mouse model characterized by the selective early post-natal death of PCs in the cerebellum, Jones et al. found that bone marrow-derived mesenchymal stem cells injected into the cerebellum migrated throughout the cerebellum. Their results showed an increase in the number of surviving PCs due to the neurotrophic factors released by adjacent grafted cells as well as an improvement in motor function (Jones et al., 2010).

Stem cell therapy in SCA 2 mice has also proven successful. Human MSC were delivered intravenously at 12, 23, 33, and 42 weeks of age (disease onset for untreated mice was 33–40 weeks of age). The injections resulted in a delay in the onset of motor function deterioration. In the same study, human MSC were injected into the cerebellum through the foramen magnum both before and after motor function loss but, unlike the intravenous route, there was no improvement (Chang et al., 2011).

Two clinical trials have looked at the safety and efficacy of stem cell transplantation in SCA. In a phase I/II trial, Jin et al. intrathecally and intravenously infused human umbilical cord mesenchymal stem cells (UC-MSC) into 16 patients with genetically diagnosed SCA 1, 2, or 3. Results showed that no serious transplantation side effects occurred during the 12 month follow-up period. Berg Balance Scale (BBS) and International Cooperative Ataxia Rating Scale (ICARS) scores improved for at least 6 months following the transplantation. Results were scored by a blinded neurologist (Jin et al., 2013) (NCT01360164).

Dongmei et al. also studied the effect of intrathecal injection of umbilical cord mesenchymal stem cells (UC-MSC) in 14 patients with SCA. The types of SCA were not specified. Serial weekly injection, with four injections total, significantly improved Activity of Daily Living Scale (ADL), and ICARS scores. ICARS and ADL scores decreased significantly 1 month after treatment. For follow-up, 8 patients remained stable for an average period of 9 month and 6 progressed after treatment with average stabilization of 4 months (Dongmei et al., 2011).

These studies may represent a proof of principle of the therapeutic potential of stem cells in SCA. However, both trials were open label, and substantial placebo effects cannot be discounted. Further clinical studies including more patients need to be performed in order to better assess safety and efficacy.

ALTERNATIVE THERAPIES

While gene and stem cell therapies are currently most prominent, many alternative therapies, including protein delivery, are also potentially relevant treatments for SCA 1. Main approaches

TABLE 4 | Overview of stem cell therapies for SCA 1.

	Mouse model	Type of stem cells	Route	Histology results	Functional results
Chen et al., 2011	SCA1 154Q/2Q mice	BMDC (genetically modified using AAV7 to carry SCA 1 modifier genes)	Right retro-orbital sinus injection	Diminished nuclear inclusions, increased number of surviving PC	Not assessed
Chintawar et al., 2009	B05 transgenic mice	Subventricular zone derived NPCs	Stereotactic cerebellar white matter microinjection	Thicker molecular layer.	Improved motor skills
				Diminished PC loss	Normalized behavior
Matsuura et al., 2014	B05 transgenic mice	Bone marrow derived MSC	Intrathecal injections	Suppression of PC dendrites atrophy	Improved motor coordination
				Thicker molecular layer	

include vascular endothelial growth factor (VEGF), cAMP-dependent protein kinase A (PKA) inhibitory polypeptide, and 3,4-diaminopyridine.

Cvetanovic et al. found that vascular endothelial growth factor (VEGF) improves the SCA 1 phenotype in 154Q/2Q mice. VEGF is an angiogenic and neurotrophic factor, and it is down-regulated in SCA 1 mice. Cvetanovic et al. crossed 154Q/2Q mice with transgenic mice that overexpress VEGF. These mice exhibited thicker molecular layers and improved motor performance. This study went further to show the positive effect that recombinant VEGF has on 154Q/2Q mice. As it cannot cross the blood brain barrier (BBB), an intracerebroventricular osmotic pump was inserted subcutaneously into 11-week-old mice to deliver VEGF via a catheter into the right lateral ventricle over 2 weeks. Mice with the pump exhibited thicker molecular layers and improved motor performance. The authors proposed that VEGF could be a biomarker for human disease progression (Cvetanovic et al., 2011; **Table 5**).

PC degeneration in SCA 1 is enhanced by the phosphorylation of S776 of polyQ-ATXN1 by PKA (Chen et al., 2003; Emamian et al., 2003; Jorgensen et al., 2009). Hearst et al. (2014a) engineered a PKA inhibitory polypeptide to prevent the formation of nuclear inclusions. The PKA inhibitory polypeptide (Synb1-ELP-PKI) is composed of a cell-penetrating peptide (Synb1), a heat responsive elastin-like peptide (ELP) carrier to increase peptide half-life, and a PKA inhibitory peptide (PKI). Using B05 mice, Synb1-ELP-PKI was delivered through the intraperitoneal or intranasal injection route. Both routes allowed the peptide to successfully cross the BBB and localize in the cerebellum. Mice showed decreased intranuclear inclusions and improved PC morphology. Motor function was not assessed (Hearst et al., 2014a; **Table 5**).

Hourez et al. (2011) found that aminopyridines might have positive neuroprotective and symptomatic effects for SCA 1. 3,4-diaminopyridine is an organic compound that blocks potassium channels and is used to treat neuronal dysfunction (Kirsch and Narahashi, 1978). Before SCA 1 symptoms present, B05 mice show reduced PC firing rate. Acute subcutaneous injection of 3,4-diaminopyridine in young B05 mice normalized the firing rate of PCs and improved motor function. Chronic subcutaneous injection, partially prevented PC atrophy. This effect was associated with increased brain-derived neurotrophic factor (BDNF), suggesting that protection against atrophy is possibly carried out by BDNF, which occurs secondary to the return of electrical activity (Hourez et al., 2011; **Table 5**). Adding to the argument that aminopyridines increase PC firing frequency, (Alviña and Khodakhah, 2010) reported that 4-aminopyridine restored pacemaking precision in the PCs in a mouse model of episodic ataxia 2 (Alviña and Khodakhah, 2010). A clinical trial of 4-aminopyridine (dalfampiridine) was completed in 2014. In a crossover study 20 patients with either SCA 1, 2, 3, or 6 received an oral dose of 4-aminopyridine for 4 weeks and 4 weeks of placebo with a 2 week washout period in between. One patient had adverse effects to the drug. Results showed that 4-aminopyridine did not significantly improve performance on the Timed 25 Feet Walking Test, the Scale of Assessment and Rating of Ataxia (SARA), or the Biomechanical Assessment of Gait–Stride Length (NCT01811706).

Other alternatives strategies that are less invasive, including whole body vibration (WBV), heat shock protein (HSP) stimulation, and oral doses of lithium, have also shown promising results and could be used alone or as an adjunct to other treatments. Kaut et al. investigated the effect of stochastic whole body vibration on SCA 1, 2, 3, and 6 patients in a double blind sham controlled study. WBV stimulates the neuromuscular system through vibration, and it has already shown to improve balance and mobility in patients with Parkinson's (Haas et al., 2006). WBV was applied on 4 sequent days, the treatment consisting of five stimulus trains of 60 s duration at a frequency of 6.5 Hz and 60 s resting time between stimuli. The sham group received the same treatment with a frequency of 1 Hz. Improvements in gait, posture, and speed of speech were seen but no response in limb kinetics and ataxia of speech was observed (Kaut et al., 2014). However, it is necessary to mention a Huang

TABLE 5 | Overview of other therapies for SCA 1.

	Treatment	Animal model	Route	Outcome
Cvetanovic et al., 2011	VEGF	154Q/2Q mice	Pharmacologic: intraventricular infusion Transgenic: gene over-expression	Improved pathological hallmarks and motor function
Hearst et al., 2014a	PKA inhibitory polypeptide (Synb1-ELP-PK)	B05 mice	Intraperitoneal/intranasal	Decreased intranucelar inclusions, improved PC morphology
Hourez et al., 2011	3,4-diaminopyridine	B05 mice	Subcutaneous injection	Normalized PC firing rate, reduced PC atrophy, improved motor function
Hearst et al., 2014b	Focused Laser Light Hyperthermia	B05 mice	Cerebellar	Hsp70 production, suppressed PC loss, improved motor function
Watase et al., 2002	Lithium	154Q/2Q	Dietary	Improved motor coordination, learning, and memory. Increased Dendritic branching in hippocampal pyramidal neurons
Perroud et al., 2013	Lithium	154/2Q	Dietary	Increased metabolic processes, specifically higher purine levels
Iizuka et al., 2015	Memantine	154Q/2Q	Dietary	Attenuated PC loss and vagus motor neuron loss. Extended life span and reduced weight loss

et al. (2014) review of WBV trials. The review states that there is insufficient evidence to support or negate if WBV can reduce symptoms in SCA among other diseases claiming more trials need to be performed with better methodological and reporting quality.

Hearst et al. (2014b) based on the neuroprotective role of chaperone HSPs known to modulate polyglutamine protein aggregation, explored the effects of focused laser light induced hyperthermia (HT) on HSP-mediated protection against ATXN1 toxicity in both cell culture model and transgenic mice. This study revealed that mild cerebellar HT stimulated the production of Hsp70 to a significant level and markedly suppressed the SCA 1 phenotype and PC loss as compared to sham-treated control animals (Hearst et al., 2014b). The nuclear inclusions in PCs stain positive for Hsp70 and Hsp40, ubiquitin and proteasomal subunits. Over expression of HDJ-2, an Hsp40 chaperone reduces protein aggregation (Cummings et al., 1998). Cummings et al. went on to find that overexpression of Hsp70 chaperone suppresses neuropathy and improves motor function in B05 mice (Cummings et al., 2001).

Lithium treatment has the potential to reduce SCA 1 symptoms in humans. A Watase et al. study showed that dietary lithium treatment resulted in improved motor coordination as well as learning and memory in 154Q/2Q mice. At 10 weeks of age, motor improvement was noted both in mice that received the treatment pre-symptomatically and post-symptomatically. Lithium treatment increased dendritic branching in mutant hippocampal pyramidal neurons (Watase et al., 2007). Perroud et al. also found that lithium treatment improved the motor coordination of 154Q/2Q mice. Mice receiving lithium exhibited increased metabolic processes, particularly higher purine levels. Perroud et al. propose that purine metabolites might have a neuroprotective effect (Perroud et al., 2013). Lithium is involved in a large number of cell processes; it is not clear what combination is alleviating the symptoms. A human phase I trial of oral lithium was completed in 2010; results have yet to be published (NCT00683943).

Memantine, a low-affinity non-competitive N-methyl-d-aspartate (NMDA) receptor antagonist is a possible drug. Iizuka et al. orally administered memantine to 154Q/2Q mice from 4 weeks old to death. Mice receiving the treatment lived longer and did not lose as much weight as typical 154Q/2Q mice. Mice receiving memantine had attenuated PC loss as well as motor neuron loss in the dorsal motor nucleus of the vagus. The study claims that these results exhibit that activation of extrasynaptic NMDA receptors lead to neuronal cell death in 154Q/2Q mice (Iizuka et al., 2015). However, the study fails to show the effect of memantine on SCA 1 symptoms is through its role as an NMDA antagonist. Memantine also affects the dopamine (Seeman et al., 2008), serotonin (Rammes et al., 2001), and acetyl choline receptors (Aracava et al., 2005) which would complicate its use as a SCA 1 therapy. Memantine has potential as a SCA 1 therapeutic but the mechanism of action needs to be better understood.

Glial cells have not received as much attention as neuronal pathology in SCA 1 studies, despite reports of gliosis in the brains of deceased SCA 1 patients (Genis et al., 1995; Gilman et al., 1996). In many neurological diseases, such as Amyotrophic Lateral Sclerosis and Parkinson's disease, astrocyte and microglia activation changes, including proinflammatory cytokine release, can reduce neuronal survival (Glass et al., 2010). Cvetanovic et al. observed hypertrophy of Bergmann glia, a sub-type of astrocyte that is located near Purkinje neurons, in 154Q/2Q mice using Glial Fibrillary Acidic Protein (GFAP). Hypertrophy was noticed in the presymptomatic period of the 154Q/2Q model at 8 weeks old, and the GFAP staining increased with disease progression. Cvetanovic et al. also observed hypertrophy of microglia cells in 154Q/2Q mice by staining for ionized calcium-binding adapter molecule 1 (Iba1). Like the Bergmann glia, microglia hypertrophy began at 8 weeks of age and increased with disease progression. Additionally, Cvetanovic et al. found glial activation occurs presymptomatically in B05 mice where only Purkinje neurons express ATXN1. Pro-inflammatory cytokine micro RNA levels increased alongside glial levels as well (Cvetanovic et al., 2015). Cvetanovic has recently received funding from the National Ataxia Foundation to test PLX3397, a drug that removes microglia from the brain without adverse effects in mice under laboratory conditions (Elmore et al., 2014), as a therapeutic.

TREATMENTS USED IN OTHER SCA TYPES

Two treatments currently being tested in other forms of SCA are worthy of mention, specifically Rhophylax, an IgG, and Dantrolene, a ryanodine-receptor inhibitor. Both therapies have the potential to be tested on SCA 1 as well.

It is believed that inflammation may contribute to neuronal dysfunction, although the pathophysiology is not known. Evert et al. (2001) found upregulation of mRNAs encoding metalloproteinase 2 (MMP-2), an endopeptidase matrix, the cytokine stromal cell-derived factor 1α (SDF1α), the transmembrane protein amyloid precursor protein, and the interleukin-1 receptor-related Fos-inducible transcript in SCA 3 mice. Immunohistochemical analysis of human SCA 3 brain tissue found increased expression of MMP-2 and amyloid β-protein (Aβ) in pontine neurons containing nuclear inclusions. Additionally, increased numbers of astrocytes and microglial cells were found in the pons of SCA 3 patients (Evert et al., 2001). In light of these results, a clinical trial is being initiated to administer intravenous immune globin (IVIG)- Rhophylax, an IgG, to SCA 1, 2, 3, 6, 10, and 11 patients to observe how the drug effects SCA symptoms as well as nerve and motor function (NCT02287064). In the pilot for the clinical trial, three patients received three courses of IVIG-Rhophylax at 2 grams/kilogram body weight over 5 days. Courses were 4 weeks apart. The patients in the pilot had SCA 3, SCA 5, or sporadic SCA. Results showed a 40% reduction in SARA total score and 10–20% average improvement in gait parameters. Patients improved the best after the third course and continued to improve until 28 days after the last infusion. Patients improvements declined by 56 days after the last infusion (Zesiewicz et al., 2014).

Calcium-mediated neurodegeneration has attracted considerable attention in the past couple of decades (Jimenez-Jimenez et al., 1996; Wojda et al., 2008); therefore a discussion on calcium-focused treatments for SCA 1 is warranted. Studies have shown SCA 1 model exhibiting down-regulation of proteins involved in PC calcium homeostasis, particularly Calbindin and Paravalbumin (Vig et al., 2000, 2001). Dantrolene has been tested on SCA 2 and SCA 3. Liu et al. found that mutant ataxin-2 facilitated inositol phosphate-induced Ca^{2+} release in cultured PC of a transgenic SCA 2 mouse model. Dantrolene blocked the Ca^{2+} release *in vitro* and, when given orally to mutant transgenic mice from 2 to 11 months old substantially reduced expression of SCA 2 (Liu et al., 2009). Chen et al. demonstrated that mutant ATXN3 associated with type 1 inositol 1,4,5-triphosphate receptor, an intracellular calcium release channel. They went on to demonstrate oral administration of dantrolene to SCA 3 transgenic mice stopped neuronal cell loss and improved motor performance, and stated dantrolene should be considered as a possible therapeutic for SCA 3 patients (Chen et al., 2008). Dantrolene should also be considered as a potential therapeutic for SCA 1.

HURDLES

At first glance, gene and cell therapies for SCA 1 seem to be straightforward. Gene therapy approaches involve the delivery of a transgene that can replace, silence, or inhibit the defective gene. Alternatively, the delivery of stem cells might replace the dying cell pool or provide a protective environment that would prevent these cells from dying. But in practice the process is more complex and a certain number of variables need to be controlled and optimized.

First, a route of delivery needs to be chosen. While peripheral administration (such as intravenous, intramuscular, or intranasal) sounds more appealing and less invasive, it raises several barriers. Higher dosages are needed to reach the same effect compared to a central delivery approach. Transduction of non-CNS tissues carries the risk of off-target effects. Finally, most gene therapy vectors lack the ability to cross the blood brain barrier.

Direct delivery to the CNS can be achieved via intraparenchymal injections to brain and spinal cord structures or via injections into the CSF (intrathecal or intraventricular). While these approaches offers the benefit of being more targeted, for SCA 1 a specific brain region may need to be chosen, such as deep cerebellar nuclei or cerebellar hemispheres. Additionally, surgical techniques need to be developed and optimized to be more reproducible and accurate. While these methods are more invasive, direct delivery of viral vectors and stem cells into the CNS have proven safe and effective (Marks et al., 2010; Gutierrez et al., 2015).

Concerning stem cells, it is also very important to determine the factors behind successful grafts. Many studies do not characterize graft survival or the factors that allow these cells to slow the rate of disease progression. The description of graft characteristics and features would help predict the outcomes and help choose the optimal cell type for type of injection and brain region receiving the injection.

CONCLUSION

A wide variety of therapies for SCA 1 are being investigated to preserve PCs and slow disease onset and progression. While stem cell therapies are the ones that have currently reached the clinical trial stage, recent progress in gene and protein delivery appear to be equally promising for SCA 1 treatment. Mouse models, particularly the 154Q/2Q mouse, provide a valuable model of the disease. However, the mechanism of action of polyQ-ATXN1 is not entirely understood and further research is needed to understand the disease process. Conceptually speaking, RNAi therapies, be they siRNA, shRNA, or miRNA-based, seem to be the most promising, since they deal directly with the root cause of the disease. All three RNAi options have been efficacious in SCA 1 models as well as models for other polyQ diseases. However, transducing a large majority of neurons throughout the brain remains a hurdle for gene therapy. Clinical trials will be necessary to determine which therapies or combinations of therapies will result in the best outcomes for patients.

AUTHOR CONTRIBUTIONS

JW is the primary author of the review. DO and AD edited the review and provided constructive criticism and approval. NB is an editor of the review and provided final approval.

ACKNOWLEDGMENTS

JW would like to thank the Boulis Lab and Emory University School of Medicine for their support in writing the review.

REFERENCES

Alvarez-Dolado, M., Pardal, R., Garcia-Verdugo, J. M., Fike, J. R., Lee, H. O., Pfeffer, K., et al. (2003). Fusion of bone-marrow-derived cells with Purkinje neurons, cardiomyocytes and hepatocytes. *Nature* 425, 968–973. doi: 10.1038/nature02069

Alviña, K., and Khodakhah, K. (2010). The therapeutic mode of action of 4-aminopyridine in cerebellar ataxia. *J. Neurosci.* 30, 7258–7268. doi: 10.1523/JNEUROSCI.3582-09.2010

Aracava, Y., Pereira, E. F., Maelicke, A., and Albuquerque, E. X. (2005). Memantine blocks alpha7* nicotinic acetylcholine receptors more potently than n-methyl-D-aspartate receptors in rat hippocampal neurons. *J. Pharmacol. Exp. Ther.* 312, 1195–1205. doi: 10.1124/jpet.104.077172

Bowman, A. B., Lam, Y. C., Jafar-Nejad, P., Chen, H. K., Richman, R., Samaco, R. C., et al. (2007). Duplication of Atxn1l suppresses SCA1 neuropathology by decreasing incorporation of polyglutamine-expanded ataxin-1 into native complexes. *Nat. Genet.* 39, 373–379. doi: 10.1038/ng1977

Bürk, K., Bösch, S., Globas, C., Zühlke, C., Daum, I., Klockgether, T., et al. (2001). Executive dysfunction in spinocerebellar ataxia type 1. *Eur. Neurol.* 46, 43–48. doi: 10.1159/000050755

Burright, E. N., Clark, H. B., Servadio, A., Matilla, T., Feddersen, R. M., Yunis, W. S., et al. (1995). SCA1 transgenic mice: a model for neurodegeneration caused by an expanded CAG trinucleotide repeat. *Cell* 82, 937–948. doi: 10.1016/0092-8674(95)90273-2

Chang, Y. K., Chen, M. H., Chiang, Y. H., Chen, Y. F., Ma, W. H., Tseng, C. Y., et al. (2011). Mesenchymal stem cell transplantation ameliorates motor function deterioration of spinocerebellar ataxia by rescuing cerebellar Purkinje cells. *J. Biomed. Sci.* 18:54. doi: 10.1186/1423-0127-18-54

Chen, H. K., Fernandez-Funez, P., Acevedo, S. F., Lam, Y. C., Kaytor, M. D., Fernandez, M. H., et al. (2003). Interaction of Akt-phosphorylated ataxin-1 with 14-3-3 mediates neurodegeneration in spinocerebellar ataxia type 1. *Cell* 113, 457–468. doi: 10.1016/S0092-8674(03)00349-0

Chen, K. A., Cruz, P. E., Lanuto, D. J., Flotte, T. R., Borchelt, D. R., Srivastava, A., et al. (2011). Cellular fusion for gene delivery to SCA1 affected Purkinje neurons. *Mol. Cell. Neurosci.* 47, 61–70. doi: 10.1016/j.mcn.2011.03.003

Chen, X., Tang, T. S., Tu, H., Nelson, O., Pook, M., Hammer, R., et al. (2008). Deranged calcium signaling and neurodegeneration in spinocerebellar ataxia type 3. *J. Neurosci.* 28, 12713–12724. doi: 10.1523/JNEUROSCI.3909-08.2008

Chintawar, S., Hourez, R., Ravella, A., Gall, D., Orduz, D., Rai, M., et al. (2009). Grafting neural precursor cells promotes functional recovery in an SCA1 mouse model. *J. Neurosci.* 29, 13126–13135. doi: 10.1523/JNEUROSCI.0647-09.2009

Clark, H. B., Burright, E. N., Yunis, W. S., Larson, S., Wilcox, C., Hartman, B., et al. (1997). Purkinje cell expression of a mutant allele of SCA1 in transgenic mice leads to disparate effects on motor behaviors, followed by a progressive cerebellar dysfunction and histological alterations. *J. Neurosci.* 17, 7385–7395.

Cummings, C. J., Mancini, M. A., Antalffy, B., DeFranco, D. B., Orr, H. T., and Zoghbi, H. Y. (1998). Chaperone suppression of aggregation and altered subcellular proteasome localization imply protein misfolding in SCA1. *Nat. Genet.* 19, 148–154. doi: 10.1038/502

Cummings, C. J., Sun, Y., Opal, P., Antalffy, B., Mestril, R., Orr, H. T., et al. (2001). Over-expression of inducible HSP70 chaperone suppresses neuropathology and improves motor function in SCA1 mice. *Hum. Mol. Genet.* 10, 1511–1518. doi: 10.1093/hmg/10.14.1511

Cvetanovic, M., Ingram, M., Orr, H., and Opal, P. (2015). Early activation of microglia and astrocytes in mouse models of spinocerebellar ataxia type 1. *Neuroscience* 289, 289–299. doi: 10.1016/j.neuroscience.2015.01.003

Cvetanovic, M., Patel, J. M., Marti, H. H., Kini, A. R., and Opal, P. (2011). Vascular endothelial growth factor ameliorates the ataxic phenotype in a mouse model of spinocerebellar ataxia type 1. *Nat. Med.* 17, 1445–1447. doi: 10.1038/nm.2494

Cvetanovic, M., Rooney, R. J., Garcia, J. J., Toporovskaya, N., Zoghbi, H. Y., and Opal, P. (2007). The role of LANP and ataxin 1 in E4F-mediated transcriptional repression. *EMBO Rep.* 8, 671–677. doi: 10.1038/sj.embor.7400983

Davidson, B. L., and Paulson, H. L. (2004). Molecular medicine for the brain: silencing of disease genes with RNA interference. *Lancet Neurol.* 3, 145–149. doi: 10.1016/S1474-4422(04)00678-7

de Chiara, C., Giannini, C., Adinolfi, S., de Boer, J., Guida, S., Ramos, A., et al. (2003). The AXH module: an independently folded domain common to ataxin-1 and HBP1. *FEBS Lett.* 551, 107–112. doi: 10.1016/S0014-5793(03)00818-4

Dongmei, H., Jing, L., Mei, X., Ling, Z., Hongmin, Y., Zhidong, W., et al. (2011). Clinical analysis of the treatment of spinocerebellar ataxia and multiple system atrophy-cerebellar type with umbilical cord mesenchymal stromal cells. *Cytotherapy* 13, 913–917. doi: 10.3109/14653249.2011.579958

Elmore, M. R., Najafi, A. R., Koike, M. A., Dagher, N. N., Spangenberg, E. E., Rice, R. A., et al. (2014). Colony-stimulating factor 1 receptor signaling is necessary for microglia viability, unmasking a microglia progenitor cell in the adult brain. *Neuron* 82, 380–397. doi: 10.1016/j.neuron.2014.02.040

Emamian, E. S., Kaytor, M. D., Duvick, L. A., Zu, T., Tousey, S. K., Zoghbi, H. Y., et al. (2003). Serine 776 of ataxin-1 is critical for polyglutamine-induced disease in SCA1 transgenic mice. *Neuron* 38, 375–387. doi: 10.1016/S0896-6273(03)00258-7

Evert, B. O., Vogt, I. R., Kindermann, C., Ozimek, L., de Vos, R. A. I., Brunt, E. R. P., et al. (2001). Inflammatory genes are upregulated in expanded ataxin-3-expressing cell lines and spinocerebellar ataxia type 3 brains. *J. Neurosci.* 21, 5389–5396.

Fernandez-Funez, P., Nino-Rosales, M. L., de Gouyon, B., She, W. C., Luchak, J. M., Martinez, P., et al. (2000). Identification of genes that modify ataxin-1-induced neurodegeneration. *Nature* 408, 101–106. doi: 10.1038/35040584

Gatchel, J. R., Watase, K., Thaller, C., Carson, J. P., Jafar-Nejad, P., Shaw, C., et al. (2008). The insulin-like growth factor pathway is altered in spinocerebellar ataxia type 1 and type 7. *Proc. Natl. Acad. Sci. U.S.A.* 105, 1291–1296. doi: 10.1073/pnas.0711257105

Genis, D., Matilla, T., Volpini, V., Rosell, J., Dávalos, A., Ferrer, I., et al. (1995). Clinical, neuropathologic, and genetic studies of a large spinocerebellar ataxia type 1 (SCA1) kindred: (CAG)n expansion and early premonitory signs and symptoms. *Neurology* 45, 24–30. doi: 10.1212/WNL.45.1.24

Gilman, S., Sima, A. A., Junck, L., Kluin, K. J., Koeppe, R. A., Lohman, M. E., et al. (1996). Spinocerebellar ataxia type 1 with multiple system degeneration and glial cytoplasmic inclusions. *Ann. Neurol.* 39, 241–255. doi: 10.1002/ana.410390214

Glass, C. K., Saijo, K., Winner, B., Marchetto, M. C., and Gage, F. H. (2010). Mechanisms underlying inflammation in neurodegeneration. *Cell* 140, 918–934. doi: 10.1016/j.cell.2010.02.016

Goold, R., Hubank, M., Hunt, A., Holton, J., Menon, R. P., Revesz, T., et al. (2007). Down-regulation of the dopamine receptor D2 in mice lacking ataxin 1. *Hum. Mol. Genet.* 16, 2122–2134. doi: 10.1093/hmg/ddm162

Grimm, D., Streetz, K. L., Jopling, C. L., Storm, T. A., Pandey, K., Davis, C. R., et al. (2006). Fatality in mice due to oversaturation of cellular microRNA/short hairpin RNA pathways. *Nature* 441, 537–541. doi: 10.1038/nature04791

Gutierrez, J., Moreton, C. L., Lamanna, J. J., Schapiro, R., Grin, N., Hurtig, C. V., et al. (2015). 203 Understanding cell migration after direct transplantation into the spinal cord: a tool to determine the optimal transplantation volume. *Neurosurgery* 62(Suppl. 1), 234. doi: 10.1227/01.neu.0000467124.38322.47

Haas, C. T., Turbanski, S., Kessler, K., and Schmidtbleicher, D. (2006). The effects of random whole-body-vibration on motor symptoms in Parkinson's disease. *NeuroRehabilitation* 21, 29–36. doi: 10.1007/3-540-36741-1_8

Harper, S. Q., Staber, P. D., He, X., Eliason, S. L., Martins, I. H., Mao, Q., et al. (2005). RNA interference improves motor and neuropathological abnormalities in a Huntington's disease mouse model. *Proc. Natl. Acad. Sci. U.S.A.* 102, 5820–5825. doi: 10.1073/pnas.0501507102

Hearst, S. M., Shao, Q., Lopez, M., Raucher, D., and Vig, P. J. (2014a). The design and delivery of a PKA inhibitory polypeptide to treat SCA1. *J. Neurochem.* 131, 101–114. doi: 10.1111/jnc.12782

Hearst, S. M., Shao, Q., Lopez, M., Raucher, D., and Vig, P. J. (2014b). Focused cerebellar laser light induced hyperthermia improves symptoms and pathology of polyglutamine disease SCA1 in a mouse model. *Cerebellum* 13, 596–606. doi: 10.1007/s12311-014-0576-1

Hong, S., Ka, S., Kim, S., Park, Y., and Kang, S. (2003). p80 coilin, a coiled body-specific protein, interacts with ataxin-1, the SCA1 gene product. *Biochim. Biophys. Acta* 1638, 35–42. doi: 10.1016/S0925-4439(03)00038-3

Hourez, R., Servais, L., Orduz, D., Gall, D., Millard, I., de Kerchove d'Exaerde, A., et al. (2011). Aminopyridines correct early dysfunction and delay neurodegeneration in a mouse model of spinocerebellar ataxia type 1. *J. Neurosci.* 31, 11795–11807. doi: 10.1523/JNEUROSCI.0905-11.2011

Huang, C.-C., Tseng, T.-L., Huang, W.-C., Chung, Y.-H., Chuang, H.-L., and Wu, J.-H. (2014). Whole-body vibration training effect on physical performance and obesity in mice. *Int. J. Med. Sci.* 11, 1218–1227. doi: 10.7150/ijms.9975

Iizuka, A., Nakamura, K., and Hirai, H. (2015). Long-term oral administration of the NMDA receptor antagonist memantine extends life span in spinocerebellar ataxia type 1 knock-in mice. *Neurosci. Lett.* 592, 37–41. doi: 10.1016/j.neulet.2015.02.055

Jayadev, S., and Bird, T. D. (2013). Hereditary ataxias: overview. *Genet. Med.* 15, 673–683. doi: 10.1038/gim.2013.28

Jimenez-Jimenez, F. J., García-Ruiz, P. J., and de Bustos, F. (1996). Calcium, neuronal death and neurological disease. *Rev. Neurol.* 24, 1199–1209.

Jin, J. L., Liu, Z., Lu, Z. J., Guan, D. N., Wang, C., Chen, Z. B., et al. (2013). Safety and efficacy of umbilical cord mesenchymal stem cell therapy in hereditary spinocerebellar ataxia. *Curr. Neurovasc. Res.* 10, 11–20. doi: 10.2174/156720213804805936

Jones, J., Jaramillo-Merchán, J., Bueno, C., Pastor, D., Viso-León, M., and Martinez, S. (2010). Mesenchymal stem cells rescue Purkinje cells and improve motor

functions in a mouse model of cerebellar ataxia. *Neurobiol. Dis.* 40, 415–423. doi: 10.1016/j.nbd.2010.07.001

Jorgensen, N. D., Andresen, J. M., Lagalwar, S., Armstrong, B., Stevens, S., Byam, C. E., et al. (2009). Phosphorylation of ATXN1 at Ser776 in the cerebellum. *J. Neurochem.* 110, 675–686. doi: 10.1111/j.1471-4159.2009.06164.x

Kang, S., and Hong, S. (2009). Molecular pathogenesis of spinocerebellar ataxia type 1 disease. *Mol. Cells* 27, 621–627. doi: 10.1007/s10059-009-0095-y

Kang, S., Jaworski, A., Ohshima, K., and Wells, R. D. (1995). Expansion and deletion of CTG repeats from human disease genes are determined by the direction of replication in *E. coli*. *Nat. Genet.* 10, 213–218. doi: 10.1038/ng0695-213

Karagianni, P., and Wong, J. (2007). HDAC3: taking the SMRT-N-CoRrect road to repression. *Oncogene* 26, 5439–5449. doi: 10.1038/sj.onc.1210612

Kaut, O., Jacobi, H., Coch, C., Prochnicki, A., Minnerop, M., Klockgether, T., et al. (2014). A randomized pilot study of stochastic vibration therapy in spinocerebellar ataxia. *Cerebellum* 13, 237–242. doi: 10.1007/s12311-013-0532-5

Keiser, M. S., Boudreau, R. L., and Davidson, B. L. (2014). Broad therapeutic benefit after RNAi expression vector delivery to deep cerebellar nuclei: implications for spinocerebellar ataxia type 1 therapy. *Mol. Ther.* 22, 588–595. doi: 10.1038/mt.2013.279

Keiser, M. S., Geoghegan, J. C., Boudreau, R. L., Lennox, K. A., and Davidson, B. L. (2013). RNAi or overexpression: alternative therapies for Spinocerebellar Ataxia Type 1. *Neurobiol. Dis.* 56, 6–13. doi: 10.1016/j.nbd.2013.04.003

Keiser, M. S., Kordower, J. H., Gonzalez-Alegre, P., and Davidson, B. L. (2015). Broad distribution of ataxin 1 silencing in rhesus cerebella for spinocerebellar ataxia type 1 therapy. *Brain* 138(Pt 12), 3555–3566. doi: 10.1093/brain/awv292

Kirsch, G. E., and Narahashi, T. (1978). 3,4-diaminopyridine. A potent new potassium channel blocker. *Biophys. J.* 22, 507–512. doi: 10.1016/S0006-3495(78)85503-9

Lam, J. K., Chow, M. Y., Zhang, Y., and Leung, S. W. (2015). siRNA versus miRNA as therapeutics for gene silencing. *Mol. Ther. Nucleic Acids* 4, e252. doi: 10.1038/mtna.2015.23

Lam, Y. C., Bowman, A. B., Jafar-Nejad, P., Lim, J., Richman, R., Fryer, J. D., et al. (2006). ATAXIN-1 interacts with the repressor Capicua in its native complex to cause SCA1 neuropathology. *Cell* 127, 1335–1347. doi: 10.1016/j.cell.2006.11.038

Lee, S., Hong, S., and Kang, S. (2008). The ubiquitin-conjugating enzyme UbcH6 regulates the transcriptional repression activity of the SCA1 gene product ataxin-1. *Biochem. Biophys. Res. Commun.* 372, 735–740. doi: 10.1016/j.bbrc.2008.05.125

Lee, Y., Samaco, R. C., Gatchel, J. R., Thaller, C., Orr, H. T., and Zoghbi, H. Y. (2008). miR-19, miR-101 and miR-130 co-regulate ATXN1 levels to potentially modulate SCA1 pathogenesis. *Nat. Neurosci.* 11, 1137–1139. doi: 10.1038/nn.2183

Lim, J., Crespo-Barreto, J., Jafar-Nejad, P., Bowman, A. B., Richman, R., Hill, D. E., et al. (2008). Opposing effects of polyglutamine expansion on native protein complexes contribute to SCA1. *Nature* 452, 713–718. doi: 10.1038/nature06731

Lin, X., Antalffy, B., Kang, D., Orr, H. T., and Zoghbi, H. Y. (2000). Polyglutamine expansion down-regulates specific neuronal genes before pathologic changes in SCA1. *Nat. Neurosci.* 3, 157–163. doi: 10.1038/72101

Liu, J., Tang, T. S., Tu, H., Nelson, O., Herndon, E., Huynh, D. P., et al. (2009). Deranged calcium signaling and neurodegeneration in spinocerebellar ataxia type 2. *J. Neurosci.* 29, 9148–9162. doi: 10.1523/JNEUROSCI.0660-09.2009

Marks, W. J. Jr., Bartus, R. T., Siffert, J., Davis, C. S., Lozano, A., Boulis, N., et al. (2010). Gene delivery of AAV2-neurturin for Parkinson's disease: a double-blind, randomised, controlled trial. *Lancet Neurol.* 9, 1164–1172. doi: 10.1016/S1474-4422(10)70254-4

Matilla, T., Volpini, V., Genis, D., Rosell, J., Corral, J., Davalos, A., et al. (1993). Presymptomatic analysis of spinocerebellar ataxia type 1 (SCA1) via the expansion of the SCA1 CAG-repeat in a large pedigree displaying anticipation and parental male bias. *Hum. Mol. Genet.* 2, 2123–2128. doi: 10.1093/hmg/2.12.2123

Matsuura, S., Shuvaev, A. N., Iizuka, A., Nakamura, K., and Hirai, H. (2014). Mesenchymal stem cells ameliorate cerebellar pathology in a mouse model of spinocerebellar ataxia type 1. *Cerebellum* 13, 323–330. doi: 10.1007/s12311-013-0536-1

Miller, V. M., Xia, H., Marrs, G. L., Gouvion, C. M., Lee, G., Davidson, B. L., et al. (2003). Allele-specific silencing of dominant disease genes. *Proc. Natl. Acad. Sci. U.S.A.* 100, 7195–7200. doi: 10.1073/pnas.1231012100

Monteys, A. M., Wilson, M. J., Boudreau, R. L., Spengler, R. M., and Davidson, B. L. (2015). Artificial miRNAs targeting mutant huntingtin show preferential silencing *in vitro* and *in vivo*. *Mol. Ther. Nucleic Acids* 4, e234. doi: 10.1038/mtna.2015.7

Oberdick, J., Smeyne, R. J., Mann, J. R., Zackson, S., and Morgan, J. I. (1990). A promoter that drives transgene expression in cerebellar Purkinje and retinal bipolar neurons. *Science* 248, 223–226. doi: 10.1126/science.2109351

Perroud, B., Jafar-Nejad, P., Wikoff, W. R., Gatchel, J. R., Wang, L., Barupal, D. K., et al. (2013). Pharmacometabolomic signature of ataxia SCA1 mouse model and lithium effects. *PLoS ONE* 8:e70610. doi: 10.1371/journal.pone.0070610

Ramachandran, P. S., Bhattarai, S., Singh, P., Boudreau, R. L., Thompson, S., Laspada, A. R., et al. (2014). RNA interference-based therapy for spinocerebellar ataxia type 7 retinal degeneration. *PLoS ONE* 9:e95362. doi: 10.1371/journal.pone.0095362

Rammes, G., Rupprecht, R., Ferrari, U., Zieglgansberger, W., and Parsons, C. G. (2001). The N-methyl-D-aspartate receptor channel blockers memantine, MRZ 2/579 and other amino-alkyl-cyclohexanes antagonise 5-HT(3) receptor currents in cultured HEK-293 and N1E-115 cell systems in a non-competitive manner. *Neurosci. Lett.* 306, 81–84. doi: 10.1016/S0304-3940(01)01872-9

Rodriguez-Lebron, E., Costa Mdo, C., Luna-Cancalon, K., Peron, T. M., Fischer, S., Boudreau, R. L., et al. (2013). Silencing mutant ATXN3 expression resolves molecular phenotypes in SCA3 transgenic mice. *Mol. Ther.* 21, 1909–1918. doi: 10.1038/mt.2013.152

Schols, L., Bauer, P., Schmidt, T., Schulte, T., and Riess, O. (2004). Autosomal dominant cerebellar ataxias: clinical features, genetics, and pathogenesis. *Lancet Neurol.* 3, 291–304. doi: 10.1016/S1474-4422(04)00737-9

Seeman, P., Caruso, C., and Lasaga, M. (2008). Memantine agonist action at dopamine D2High receptors. *Synapse* 62, 149–153. doi: 10.1002/syn.20472

Servadio, A., Koshy, B., Armstrong, D., Antalffy, B., Orr, H. T., and Zoghbi, H. Y. (1995). Expression analysis of the ataxin-1 protein in tissues from normal and spinocerebellar ataxia type 1 individuals. *Nat. Genet.* 10, 94–98. doi: 10.1038/ng0595-94

Subramony, S. H., and Ashizawa, T. (1993). "Spinocerebellar ataxia type 1," in *GeneReviews(R)*, eds R. A. Pagon, M. P. Adam, H. H. Ardinger, S. E. Wallace, A. Amemiya, L. J. H. Bean, T. D. Bird, C.-T. Fong, H. C. Mefford, R. J. H. Smith, and K. Stephens (Seattle, WA: University of Washington).

Vandaele, S., Nordquist, D. T., Feddersen, R. M., Tretjakoff, I., Peterson, A. C., and Orr, H. T. (1991). Purkinje cell protein-2 regulatory regions and transgene expression in cerebellar compartments. *Genes Dev.* 5, 1136–1148. doi: 10.1101/gad.5.7.1136

Venkatraman, A., Hu, Y. S., Didonna, A., Cvetanovic, M., Krbanjevic, A., Bilesimo, P., et al. (2014). The histone deacetylase HDAC3 is essential for Purkinje cell function, potentially complicating the use of HDAC inhibitors in SCA1. *Hum. Mol. Genet.* 23, 3733–3745. doi: 10.1093/hmg/ddu081

Vierra-Green, C. A., Orr, H. T., Zoghbi, H. Y., and Ferrington, D. A. (2005). Identification of a novel phosphorylation site in ataxin-1. *Biochim. Biophys. Acta* 1744, 11–18. doi: 10.1016/j.bbamcr.2004.10.012

Vig, P. J., Subramony, S. H., and McDaniel, D. O. (2001). Calcium homeostasis and spinocerebellar ataxia-1 (SCA-1). *Brain Res. Bull.* 56, 221–225. doi: 10.1016/S0361-9230(01)00595-0

Vig, P. J., Subramony, S. H., Qin, Z., McDaniel, D. O., and Fratkin, J. D. (2000). Relationship between ataxin-1 nuclear inclusions and Purkinje cell specific proteins in SCA-1 transgenic mice. *J. Neurol. Sci.* 174, 100–110. doi: 10.1016/S0022-510X(00)00262-8

Watase, K., Gatchel, J. R., Sun, Y., Emamian, E., Atkinson, R., Richman, R., et al. (2007). Lithium therapy improves neurological function and hippocampal dendritic arborization in a spinocerebellar ataxia type 1 mouse model. *PLoS Med.* 4:e182. doi: 10.1371/journal.pmed.0040182

Watase, K., Weeber, E. J., Xu, B., Antalffy, B., Yuva-Paylor, L., Hashimoto, K., et al. (2002). A long CAG repeat in the mouse Sca1 locus replicates SCA1 features and reveals the impact of protein solubility on selective

neurodegeneration. *Neuron* 34, 905–919. doi: 10.1016/S0896-6273(02)00733-X

Weimann, J. M., Charlton, C. A., Brazelton, T. R., Hackman, R. C., and Blau, H. M. (2003). Contribution of transplanted bone marrow cells to Purkinje neurons in human adult brains. *Proc. Natl. Acad. Sci. U.S.A.* 100, 2088–2093. doi: 10.1073/pnas.0337659100

Whaley, N. R., Fujioka, S., and Wszolek, Z. K. (2011). Autosomal dominant cerebellar ataxia type I: a review of the phenotypic and genotypic characteristics. *Orphanet J. Rare Dis.* 6:33. doi: 10.1186/1750-1172-6-33

Wojda, U., Salinska, E., and Kuznicki, J. (2008). Calcium ions in neuronal degeneration. *IUBMB Life* 60, 575–590. doi: 10.1002/iub.91

Xia, H., Mao, Q., Eliason, S. L., Harper, S. Q., Martins, I. H., Orr, H. T., et al. (2004). RNAi suppresses polyglutamine-induced neurodegeneration in a model of spinocerebellar ataxia. *Nat. Med.* 10, 816–820. doi: 10.1038/nm1076

Xia, H., Mao, Q., Paulson, H. L., and Davidson, B. L. (2002). siRNA-mediated gene silencing *in vitro* and *in vivo*. *Nat. Biotechnol.* 20, 1006–1010. doi: 10.1038/nbt739

Yang, S. H., Cheng, P. H., Banta, H., Piotrowska-Nitsche, K., Yang, J. J., Cheng, E. C., et al. (2008). Towards a transgenic model of Huntington's disease in a non-human primate. *Nature* 453, 921–924. doi: 10.1038/nature06975

Yue, S., Serra, H. G., Zoghbi, H. Y., and Orr, H. T. (2001). The spinocerebellar ataxia type 1 protein, ataxin-1, has RNA-binding activity that is inversely affected by the length of its polyglutamine tract. *Hum. Mol. Genet.* 10, 25–30. doi: 10.1093/hmg/10.1.25

Zesiewicz, T., Vu, T., Sullivan, K., Gooch, C., Jahan, I., Ward, C., et al. (2014). Treatment of Spinocerebellar Ataxia with Intravenous Immune Globulin (IVIG) (P6.052). *Neurology* 82(10 Suppl.).

Zoghbi, H. Y., Pollack, M. S., Lyons, L. A., Ferrell, R. E., Daiger, S. P., and Beaudet, A. L. (1988). Spinocerebellar ataxia: variable age of onset and linkage to human leukocyte antigen in a large kindred. *Ann. Neurol.* 23, 580–584. doi: 10.1002/ana.410230609

Conflict of Interest Statement: NB is a paid consultant for Agilis, MRI Interventions, Voyager, Oxford Biomedica, Q Therapeutics and Neuralstem Inc. He is a founder of Switch Bio Holdings and former employee of Above and Beyond LLC up to December 1st 2015.

The other authors declare that the research was conducted in the absence of any commercial or financial relationships that could be construed as a potential conflict of interest.

frontiers in Molecular Neuroscience

REVIEW
published: 07 December 2017
doi: 10.3389/fnmol.2017.00405

Motor Neuron Gene Therapy: Lessons from Spinal Muscular Atrophy for Amyotrophic Lateral Sclerosis

*Andrew P. Tosolini and James N. Sleigh**

Sobell Department of Motor Neuroscience and Movement Disorders, Institute of Neurology, University College London, London, United Kingdom

Spinal muscular atrophy (SMA) and amyotrophic lateral sclerosis (ALS) are severe nervous system diseases characterized by the degeneration of lower motor neurons. They share a number of additional pathological, cellular, and genetic parallels suggesting that mechanistic and clinical insights into one disorder may have value for the other. While there are currently no clinical ALS gene therapies, the splice-switching antisense oligonucleotide, nusinersen, was recently approved for SMA. This milestone was achieved through extensive pre-clinical research and patient trials, which together have spawned fundamental insights into motor neuron gene therapy. We have thus tried to distil key information garnered from SMA research, in the hope that it may stimulate a more directed approach to ALS gene therapy. Not only must the type of therapeutic (e.g., antisense oligonucleotide vs. viral vector) be sensibly selected, but considerable thought must be applied to the *where*, *which*, *what*, and *when* in order to enhance treatment benefit: to where (cell types and tissues) must the drug be delivered and how can this be best achieved? Which perturbed pathways must be corrected and can they be concurrently targeted? What dosing regime and concentration should be used? When should medication be administered? These questions are intuitive, but central to identifying and optimizing a successful gene therapy. Providing definitive solutions to these quandaries will be difficult, but clear thinking about therapeutic testing is necessary if we are to have the best chance of developing viable ALS gene therapies and improving upon early generation SMA treatments.

Keywords: adeno-associated virus (AAV), ALS, antisense oligonucleotide (ASO), motor neuron disease (MND), neurodegeneration, neurotrophic factor, SMA, survival motor neuron (SMN)

OPEN ACCESS

Edited by:
Michael J. Schmeisser, Universitätsklinikum Magdeburg, Germany

Reviewed by:
Patrick Weydt, University of Bonn, Germany
Jochen H. Weishaupt, Universitäts- und Rehabilitationskliniken Ulm, Germany

***Correspondence:**
James N. Sleigh
j.sleigh@ucl.ac.uk

Received: *19 September 2017*
Accepted: *21 November 2017*
Published: *07 December 2017*

Citation:
Tosolini AP and Sleigh JN (2017) Motor Neuron Gene Therapy: Lessons from Spinal Muscular Atrophy for Amyotrophic Lateral Sclerosis. Front. Mol. Neurosci. 10:405. doi: 10.3389/fnmol.2017.00405

Abbreviations: AAV, adeno-associated virus; ALS, amyotrophic lateral sclerosis; ASO, antisense oligonucleotide; BBB, blood-brain barrier; BDNF, brain-derived neurotrophic factor; BSCB, blood-spinal cord barrier; C9ORF72, chromosome 9 open reading frame 72; CNS, central nervous system; CNTF, ciliary-derived neurotrophic factor; CPP, cell-penetrating peptide; CSF, cerebrospinal fluid; EMA, European Medicines Agency; fALS, familial ALS; FDA, Food and Drug Administration; FTD, frontotemporal dementia; FUS, fused in sarcoma; HGF, hepatocyte growth factor; IGF-1, insulin-like growth factor; iPSC, induced pluripotent stem cell; ISS-N1, intronic splicing silencer N1; LMN, lower motor neuron; LV, lentivirus; MND, motor neuron disease; NMJ, neuromuscular junction; RNAi, RNA interference; sALS, sporadic ALS; scAAV, self-complementary AAV; SMA, spinal muscular atrophy; SMN, survival motor neuron; snRNA, small nuclear RNA; snRNP, small nuclear ribonucleoprotein; SOD1, superoxide dismutase 1; SSO, splice-switching oligonucleotide; TARDBP, transactive-region DNA binding protein; TLS, translocated in liposarcoma; UMN, upper motor neuron; VEGF, vascular endothelial growth factor.

INTRODUCTION

Spinal muscular atrophy and amyotrophic lateral sclerosis are two devastating neurological conditions with the common pathological hallmark of motor neuron degeneration, ultimately leading to muscle wasting and death. While etiology, age of onset, progression, and survival outcomes can drastically differ between the diseases, they share a number mechanistic parallels; thus, experimental and clinical insights into the one disorder may prove useful for the other.

It is an exciting time for the SMA community as the first treatment, an ASO gene therapy called nusinersen, was approved in the US by the FDA on 23rd December, 2016. Nusinersen subsequently received marketing authorisation in the EU from the EMA in June, 2017. This starkly contrasts with the situation for ALS, where clinically viable gene therapies are currently non-existent, while recent trials of chemically diverse drugs have failed to live up to expectations piqued by mouse experiments. Although there are numerous complications in treating ALS that do not pertain to SMA, a number of fundamental lessons have been learnt from the gamut of pre-clinical research and clinical trials of SMA gene therapies that could prove useful in galvanizing a targeted approach to ALS gene therapy design and development.

In this review, we will first provide introductions to SMA, ALS, and commonalities between the two, and follow this with an overview of gene therapies tested in clinical trials for both diseases. We use the term gene therapy to encompass both virus-mediated gene transfer and ASO gene targeting. Rather than provide an exhaustive review of all SMA and ALS gene therapy research, which has been collectively well covered (Federici and Boulis, 2012; Nizzardo et al., 2012; Mulcahy et al., 2014; Scarrott et al., 2015; Singh N.N. et al., 2017), we will then outline some of the major issues that SMA gene therapy has encountered, try to distil key, emergent concepts, and frame this in the context of ALS in order to provide possible future experimental directions.

DISEASES OF MOTOR NEURONS: GENETICS, CLASSIFICATIONS, AND MECHANISMS

Spinal Muscular Atrophy

Spinal muscular atrophy (SMA) is a monogenic neuromuscular disorder affecting ≈1 in 8,500–12,500 newborns, and is the most common genetic cause of infant mortality (Verhaart et al., 2017a,b). Patients present with severe muscle weakness and atrophy, predominantly in proximal (e.g., trunk) muscles, due to degeneration of LMNs of the spinal cord ventral horn. Pathology in additional cells and tissues can be observed in more severe manifestations of the disease, which has considerable implications for treatment (Hamilton and Gillingwater, 2013). SMA is caused by reduced levels of SMN protein (Lefebvre et al., 1995), which is found in the nucleus and cytoplasm of almost all cells, and plays a vital, canonical, housekeeping role in spliceosome assembly (Fischer et al., 1997; Liu et al., 1997; Pellizzoni et al., 2002), amongst other functions (Singh R.N. et al., 2017). Specifically, as part of the multi-protein SMN complex, SMN directs the efficient cytoplasmic assemblage of small nuclear RNAs (snRNAs) with Sm protein rings leading to the formation of small nuclear ribonucleoproteins (snRNPs) (Gruss et al., 2017). After nuclear-import, snRNPs function in the catalytic removal of introns from pre-mRNA transcripts in the process of splicing (Pellizzoni et al., 2002). Despite having a good understanding of this and other functions of SMN, the precise cause of the largely selective LMN death remains to be fully resolved. It is likely that a combination of multiple mechanisms account for this vulnerability, including mis-splicing of LMN-specific genes, SMN levels being lower in LMNs than other cell types, and disturbance of a possible non-canonical, LMN-specific SMN function (**Figure 1A**) (Tisdale and Pellizzoni, 2015; Jablonka and Sendtner, 2017; Tu et al., 2017).

Survival motor neuron is encoded by two almost identical genes, *SMN1* and its paralogue *SMN2* (**Figure 1B**) (Lefebvre et al., 1995). A single functioning *SMN1* allele produces sufficient protein for LMNs to remain healthy – as demonstrated by the ≈1 in 40–60 people with one functional copy of *SMN1* (i.e., SMA carriers) showing no clinical phenotype. However, due to a single nucleotide distinction (synonymous C-to-T alteration 6 nucleotides into exon 7), exon 7 of *SMN2* is aberrantly spliced ≈90% of the time (creating truncated, non-functional SMNΔ7 protein) and is therefore capable of producing only ≈10% of the full-length SMN made by *SMN1* (**Figure 1B**) (Lorson et al., 1999; Monani et al., 1999). Thus, when protein production from *SMN1* is impaired, as it is in SMA patients, *SMN2* can only partially compensate. SMN is highly conserved throughout evolution, permitting modeling of reduced SMN function in diverse organisms (Grice et al., 2011; Patten et al., 2014; Duque et al., 2015); however, all models naturally only possess an ortholog of *SMN1*, but not *SMN2*. To better mimic disease genetics, many transgenic mice have been engineered to express diminished SMN levels (Sleigh et al., 2011), the most frequently used being the SMNΔ7 mouse, which combines human *SMN2* and *SMNΔ7* transgenes on a null *Smn* background (Le et al., 2005). Relative genomic instability of the region (5q13) is believed to be the reason for the recent evolutionary duplication of the *SMN* locus (Rochette et al., 2001), and may also account for there being considerable variability in *SMN2* copy number within the population. The number of *SMN2* genes a patient with SMA possesses has important ramifications for disease severity, as more *SMN2* copies can produce more SMN, which correlates with diminished symptom severity (Lefebvre et al., 1997). Although not predictive at the individual level, in a population, *SMN2* copy number thus inversely correlates with SMA severity (McAndrew et al., 1997), which is categorised into four principal post-natal types (I-IV) based on age of onset and motor milestones achieved (Munsat and Davies, 1992).

Manifesting at or before 6 months and radically limiting life expectancy (<2 years), type I SMA (a.k.a. Werdnig-Hoffmann disease) is the most severe and frequently diagnosed form of SMA, and prevents children from ever being able to sit unaided. Infant death is usually caused by respiratory complications, although with specialized care, lifespan can be artificially

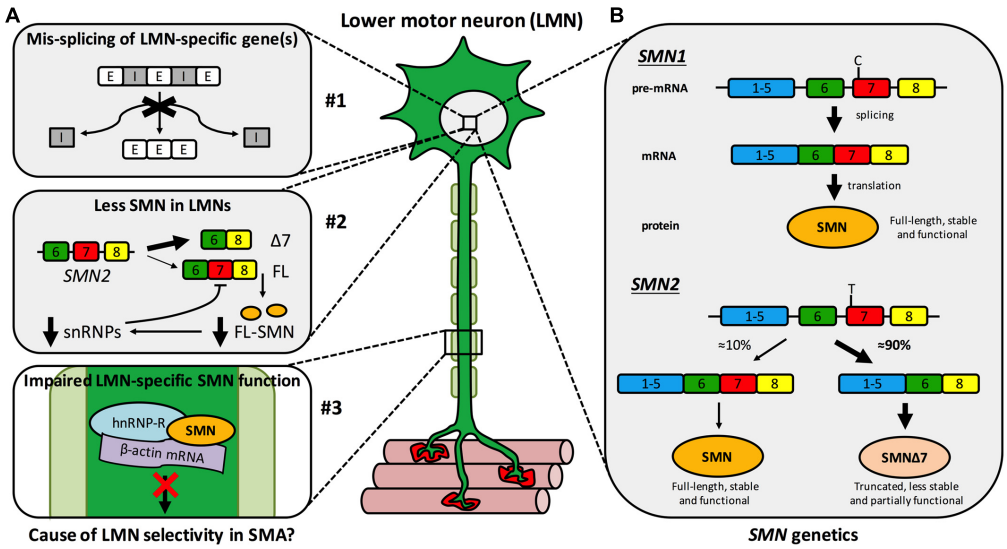

FIGURE 1 | Spinal muscular atrophy mechanisms and genetics. **(A)** Multiple hypothetical mechanisms have been suggested to cause or contribute to the selective LMN degeneration of SMA, the three most plausible of which are that: #1 SMN reduction impairs splicing fidelity of a LMN-specific gene(s). E, exon; I, intron; #2 less SMN is available in LMNs than other cells due to a negative feedback loop, more prominent in LMNs, in which low SMN levels impair further *SMN2* exon 7 inclusion (see **B**) exacerbating SMN reduction. Δ7, truncated *SMN* mRNA; FL, full-length *SMN* mRNA; FL-SMN, full-length SMN protein; snRNPs, small nuclear ribonucleoproteins; and #3 a non-canonical, LMN-specific function of SMN is perturbed, for instance anterograde axonal transport of mRNA. **(B)** A single copy of *SMN1* produces enough SMN protein for motor neurons to thrive and for SMA disease carriers to remain healthy. Due to a single base pair distinction (C-to-T transition in exon 7), exon 7 is mis-spliced out of ≈90% of *SMN2* transcripts, resulting in a truncated, less stable, and only partially functional protein. This figure has been adapted from *Neuromuscular Disorders*, 23, Sleigh et al., 2013 Spinal muscular atrophy at the crossroads of basic science and therapy, 96, Copyright (2013), with permission from Elsevier.

extended for long periods. Type II SMA (Intermediate/Dubowitz Syndrome) presents between 7 and 18 months, permits unaided sitting but not walking, and has survival probabilities of ≈93% and ≈52% at 20 and 40 years, respectively (Farrar et al., 2013). Type III SMA (Kugelberg-Welander disease) limits motor function and has an onset > 18 months, but before adolescence, while type IV SMA (adult-onset) typically manifests in the second or third decade of life with mild-to-moderate muscle weakness, but generally no respiratory issues.

Amyotrophic Lateral Sclerosis

With a lifetime risk of ≈1 in 400 (Alonso et al., 2009), ALS, also called MND and Lou Gehrig's disease, is a fatal, progressive, mostly adult-onset disorder of both LMNs and UMNs. Neurodegeneration is observed in the cortex, corticospinal tracts, brainstem, and spinal ventral horn neurons and is accompanied by neuroinflammation (Brown and Al-Chalabi, 2017). Starting focally and spreading, this causes major symptoms of muscle weakness and fasciculations with subsequent atrophy, leading to death usually through respiratory failure within 3 years of diagnosis (Chiò et al., 2009). ALS also shares neuropathological and genetic features with FTD (Morita et al., 2006; Neumann et al., 2006; Vance et al., 2006), with approximately half of ALS patients showing some level of cognitive impairment (Ringholz et al., 2005). This has led to ALS and FTD being considered as part of the same clinicopathological spectrum (Ling et al., 2013). ALS patients display considerable symptom heterogeneity inclusive of age, site of disease onset, the rate and pattern of spread, and relative LMN/UMN involvement (Kiernan et al., 2011). ALS can therefore be sub-categorized based on several clinical and neuropathological criteria (Al-Chalabi and Hardiman, 2013; Bäumer et al., 2014). Given this variability, the ALS diagnosis is challenging, particularly during early disease stages (Byrne et al., 2012). The mean time from first noticeable symptom to clinical diagnosis is consequently (≈1 year). Contributing to this delay, no diagnostic or prognostic biomarkers are yet in regular clinical use for ALS, which also impacts the assessment of therapeutic efficacy in patient trials (Rosenfeld and Strong, 2015). Nevertheless, a number of prospective biomarkers have recently been identified, including the neurotrophin receptor $p75^{NTR}$ extracellular domain in urine (Shepheard et al., 2017) and neurofilament chains in plasma (Lu et al., 2015) and CSF (Oeckl et al., 2016).

ALS has traditionally been classified into clinically indistinguishable sporadic (sALS) and familial (fALS) forms; sALS occurs without family history of the disease and represents the majority of cases (≈90%), whereas fALS contributes ≈10% of patients and is genetically inherited, predominantly in an autosomal, dominant fashion. The pathological and clinical variability of the disease has led to the idea that, in addition to being on a continuum with FTD, ALS itself may not be a single disorder, but a syndrome (Turner et al., 2013). Consistent with this, aberrations in over 25 genetic loci have been reproducibly linked with the ALS phenotype (Brown and Al-Chalabi, 2017), with new genes constantly being identified (Freischmidt et al., 2015; Brenner et al., 2016; Mackenzie et al., 2017). The four

most common mutations are large, intronic, hexanucleotide repeat (G_4C_2) expansions in *chromosome 9 open reading frame 72* (*C9orf72*) (DeJesus-Hernandez et al., 2011; Renton et al., 2011), and dominant mutations in *superoxide dismutase 1* (*SOD1*) (Rosen et al., 1993), *transactive-region DNA binding protein* (*TARDBP* encoding TDP-43) (Sreedharan et al., 2008), and *fused in sarcoma* (*FUS*, a.k.a. *translocated in liposarcoma*, *TLS*) (Kwiatkowski et al., 2009; Vance et al., 2009). Mutations in *C9orf72* are the most common genetic cause of ALS hitherto identified, accounting for ≈40% of fALS and ≈7% of sALS (in populations of European ancestry) (Renton et al., 2014). The exact function of the encoded protein remains unclear, but it appears that it may be important in membrane trafficking and autophagy (Nassif et al., 2017). Encoding a Cu/Zn dismutase enzyme that provides defense against toxic superoxide free radicals, *SOD1* was the first gene linked to ALS (Rosen et al., 1993), and its mutation is responsible for ≈12% and ≈1% of fALS and sALS patients, respectively (Renton et al., 2014). As a consequence of its early identification and the rapid generation of the $SOD1^{G93A}$ mouse model (Gurney et al., 1994), research into *SOD1* has shaped much of the ALS research landscape. Nevertheless, many other cellular and animal models are now available for different genetic forms of the disease (van Damme et al., 2017). *TARDBP* and *FUS* encode nucleic acid-binding proteins that predominantly reside in the nucleus, and are involved in multiple aspects of RNA processing, such as transcription and splicing. Mutations in these two genes each account for ≈4% of fALS and ≈1% of sALS patients (Renton et al., 2014). Despite significant progress in our understanding of the molecular pathogenesis linked to these four genes, it has not been fully resolved as to whether pathology is solely caused by a toxic gain-of-function or whether there are also loss-of-function effects (Lee et al., 2012; Bunton-Stasyshyn et al., 2015; Scekic-Zahirovic et al., 2016; Moens et al., 2017).

Causative genetic mutations have been identified in only ≈68% and ≈11% of fALS and sALS patients, respectively (Renton et al., 2014). This lack of an obvious genetic cause in most ALS patients, along with incomplete penetrance in several fALS pedigrees (Cirulli et al., 2015; Freischmidt et al., 2015), suggests that ALS may most frequently arise from additive effects of an assortment of predispositions and insults (Al-Chalabi and Hardiman, 2013). Indeed, rare variants in many other genes have been identified as ALS risk factors (van Rheenen et al., 2016), as have particular environmental stimuli (Martin et al., 2017a). Moreover, twin studies indicate that sALS heritability in the absence of a family history of the disease is still ≈60% (Al-Chalabi et al., 2010). Together, these data indicate that ALS may develop through a multi-step process in which aging is a critical component (Al-Chalabi et al., 2014), involving varying degrees of heritability and diverse, but inter-related, functional pathways that, upon dysregulation, yield motor neuron degeneration (Turner et al., 2013). This makes the strict fALS/sALS distinction an artificial dichotomy (Talbot, 2011), and presents obvious and considerable hurdles for the identification and development of viable therapeutic strategies for the disease.

Intrinsic motor neuron defects and non-cell autonomous toxicities in associated cell types (e.g., glia, interneurons) contribute to ALS (Ilieva et al., 2009; Ramírez-Jarquín et al., 2014; Puentes et al., 2016), but similar to SMA, the exact mechanisms underpinning motor neuron death, and their relative vulnerability-resistance axis (Nijssen et al., 2017), remain to be elucidated. Nevertheless, given the known functions of major ALS genes, altered RNA processing, nuclear protein mishandling/protein quality control, and impaired cytoskeletal dynamics appear to be three inter-related central themes (Bäumer et al., 2010; Brown and Al-Chalabi, 2017). Congruously, the vast majority of both sALS and fALS patients display cytoplasmic depositions of aggregated proteins, the main component of which is TDP-43 (Neumann et al., 2006), albeit with varied cellular distributions (Al-Sarraj et al., 2011). However, these inclusions conspicuously lack TDP-43 in *SOD1*-linked (Mackenzie et al., 2007) and *FUS*-linked (Vance et al., 2009) ALS. Additional defects in diverse cellular processes have been implicated in ALS including excitotoxicity, oxidative stress, altered oligodendrocyte function, axonal transport defects, mitochondrial malfunction, and neurotrophic factor deficits (reviewed in Kiernan et al., 2011; Taylor et al., 2016). It remains unclear as to which, if any, of these phenomena play a primary role in disease pathogenesis, rather than simply being non-specific consequences of a dysfunctional system. Moreover, it should be noted that most of these pathologies were identified using $SOD1^{G93A}$ mice, which have their limitations for modeling all forms of ALS (Kiernan et al., 2011; Turner et al., 2013). To overcome this, numerous transgenic mouse models of ALS have been developed (van Damme et al., 2017), and strict guidelines for their use in pre-clinical therapeutic trials have been created to limit irreproducibility (Ludolph et al., 2010).

SMA and ALS: A Common Mechanism?

SMA and ALS share a propensity for LMN degeneration leading to muscle wasting and atrophy. A number of key cellular and molecular parallels between the two diseases have also been reported (Cauchi, 2014; Gama-Carvalho et al., 2017; Hensel and Claus, 2017). The causative gene in SMA encodes a widely expressed, multi-functional protein important for fundamental cellular processes including pre-mRNA splicing (Fischer et al., 1997; Liu et al., 1997; Pellizzoni et al., 2002), transcription (Pellizzoni et al., 2001), and mRNA transport and stability (Rossoll et al., 2003; Zhang et al., 2003). While the importance of protein quality control to ALS should not be underestimated, some of the major genetic contributors to the disease, perhaps with the exception of C9ORF72, are also found ubiquitously and perform similar functions vital to RNA processing and maturation (Bäumer et al., 2010). For instance, both TDP-43 and FUS are involved in splicing (Zhou et al., 2002; Polymenidou et al., 2011) and transcription (Uranishi et al., 2001), and, along with SOD1, are thought to be important for the transport and stability of mRNA (Fujii and Takumi, 2005; Lu et al., 2007; Strong et al., 2007). Recently, dominant mutations in *T-cell restricted intracellular antigen 1* (*TIA1*), which is an RNA-binding protein involved in *SMN2* exon 7 splicing (Singh et al., 2011), were shown to play a causative role in ALS (Mackenzie et al., 2017), while *TIA1* knockout modifies phenotypes of mild male SMA mice (Howell et al., 2017). Furthermore, wild-type TDP-43 and FUS

interact with SMN (Wang I.-F. et al., 2002; Yamazaki et al., 2012; Groen et al., 2013; Sun et al., 2015), and all three proteins have been implicated in the formation of stress granules (Hua and Zhou, 2004; Andersson et al., 2008; Colombrita et al., 2009), as has C9ORF72 (Maharjan et al., 2017).

Comparable in structure to stress granules, Gemini of Cajal bodies (a.k.a. gems) are membrane-free, nuclear conglomerates of SMN and associated proteins (Liu and Dreyfuss, 1996), the number of which correlates with SMN availability and is thus inversely related to SMA severity (Lefebvre et al., 1997; Feng et al., 2005). Numerous studies have shown that gem distribution/number is also affected in SOD1-, FUS-, and TDP-43-associated ALS patient tissue, mice, and cellular models (Shan et al., 2010; Gertz et al., 2012; Kariya et al., 2012; Yamazaki et al., 2012; Ishihara et al., 2013; Tsuiji et al., 2013; Sun et al., 2015), although this pattern was not observed in sALS patient fibroblasts (Kariya et al., 2014b). Nonetheless, SMN protein levels are reduced in sALS patient spinal cords (Turner et al., 2014) and pre-symptomatically in SOD1^{G93A} mouse spinal cords, while a 50% reduction in SMN exacerbates the SOD1^{G93A} phenotype (Turner et al., 2009). Furthermore, one study showed that ALS patients on average possess fewer *SMN2* copies, while having one *SMN1* copy is associated with increased ALS susceptibility (Veldink et al., 2005), although this link is not straightforward (Blauw et al., 2012; Corcia et al., 2012; Wang X.-B. et al., 2014). Nevertheless, SMN upregulation protects against mutant SOD1-induced cell death in an immortalized motor neuronal cell line (NSC-34) (Zou et al., 2007), rescues mutant FUS-mediated axonal defects in primary cortical neurons (Groen et al., 2013), and can improve survival of iPSC-derived motor neurons differentiated from SOD1 and TDP-43 ALS patient fibroblasts (Rodriguez-Muela et al., 2017). Moreover, neuronal SMN overexpression aids motor neuron survival and delays symptom onset in SOD1^{G85A}, SOD1^{G93A}, and TDP-43^{A315T} mice (Kariya et al., 2012; Turner et al., 2014; Perera et al., 2016). Survival of both SOD1 models was unaffected, but female TDP-43 mice displayed a significant extension. SMN may in fact serve as a general survival factor for motor neurons, as it is required to facilitate neuromuscular regeneration post-sciatic nerve crush in adult mice (Kariya et al., 2014a). In addition, low SMN levels in healthy iPSC-derived motor neurons correlate with greater cell death, and SMN upregulation promotes increased survival of control motor, but not cortical, neurons (Rodriguez-Muela et al., 2017).

These commonalities between SMA and ALS suggest that a shared mechanism could underlie at least certain aspects of the two diseases. Perhaps the most likely cause of the link is sequestration of SMN and/or splicing factors into cytoplasmic inclusions by mutant ALS gene products, resulting in defective RNA homeostasis. Indeed, ALS-associated mutations in FUS can enhance its association with SMN and impinge upon its axonal localization (Groen et al., 2013; Sun et al., 2015). Additionally, mutant FUS and *C9orf72* expansion can affect splicing factor distribution (Gerbino et al., 2013; Lee et al., 2013; Mori et al., 2013; Yu et al., 2015; Reber et al., 2016), as can homozygous overexpression of human wild-type FUS in mice (Mirra et al., 2017). Widespread splicing defects are unlikely to account for the motor neuron selectivity observed in SMA (Bäumer et al., 2009); however, the early and specific mis-splicing of a few crucial motor neuron-expressed genes may be particularly relevant to disease pathogenesis (Zhang et al., 2013; Sleigh et al., 2014). Splicing impairments have also been reported in ALS models and patient tissue (Chabot and Shkreta, 2016; Conlon et al., 2016); it is thus plausible that early splicing perturbations in a common set of critical genes could explain some of the shared pathomechanisms of SMA and ALS. Indeed, considerable overlap in alternative splicing events between SMA models and human FUS-expressing mice were recently reported, including in a number of ALS-pertinent genes (Mirra et al., 2017). These discoveries and the mechanistic intersection of ALS with SMA, suggest that gene therapy strategies able to augment SMN levels may be beneficial to both fALS and sALS patients, perhaps not in isolation, but as part of a combinatorial approach.

CLINICAL GENE THERAPY FOR MOTOR NEURON DISEASES

SMA: SMN Restoration Is Key

The genetic lesion underlying SMA causes diminished SMN protein levels; in theory, treatment is thus simple – replenish SMN. Small molecule, *SMN2* splice-modifying drugs, such as RG7916 (Roche) and LMI070 (Novartis), that augment SMN and SMN-independent, neuroprotection strategies are being pursued (Scoto et al., 2017), but *SMN* gene therapies are currently proving more clinically promising. In the last decade, we have rapidly transitioned from several early ineffective SMA patient trials (Fuller et al., 2010), to the recent regulatory approval of nusinersen for the treatment of SMA types I-IV.

Nusinersen (a.k.a. Spinraza, IONIS-SMN$_{Rx}$, ISIS-SMN$_{Rx}$, ISIS 396443, and ASO-10-27) is an ASO developed through work of numerous laboratories and a collaboration between Biogen Idec and Ionis Pharmaceuticals (formerly Isis Pharmaceuticals). ASOs are short (15–25 nucleotides), synthetic, single-stranded DNA or RNA sequences that specifically bind to target pre-mRNA or mRNA sequences, impacting gene expression. ASOs that specifically modulate splicing are also called SSOs. Importantly for diseases affecting the nervous system, ASOs distribute widely when injected into the CSF, do not require carrier molecules, and have relatively long half-lives (Geary et al., 2015). Nusinersen, which is delivered via single intrathecal injections directly into the CSF (i.e., by lumbar puncture) (Chiriboga et al., 2016; Haché et al., 2016), is a 2′-*O*-(2-methoxyethyl) modified ASO complementary to the ISS-N1 found in intron 7 of *SMN2* pre-mRNA (Singh et al., 2006; Hua et al., 2008). Specific ASO/pre-mRNA hybridisation restricts exon 7 mis-splicing, thereby increasing the amount of functional SMN made by *SMN2* (**Figure 2A**). A considerable amount of work in SMA mice provided substantial evidence for *in vivo* efficacy of nusinersen (Singh N.N. et al., 2017), leading to a series of stratified clinical trials (Chiriboga et al., 2016; Finkel et al., 2016, 2017). A pre-specified interim analysis from a randomized, double-blind, sham procedure-controlled phase III trial in SMA type I patients called ENDEAR (ClinicalTrials.gov Identifier: NCT02193074),

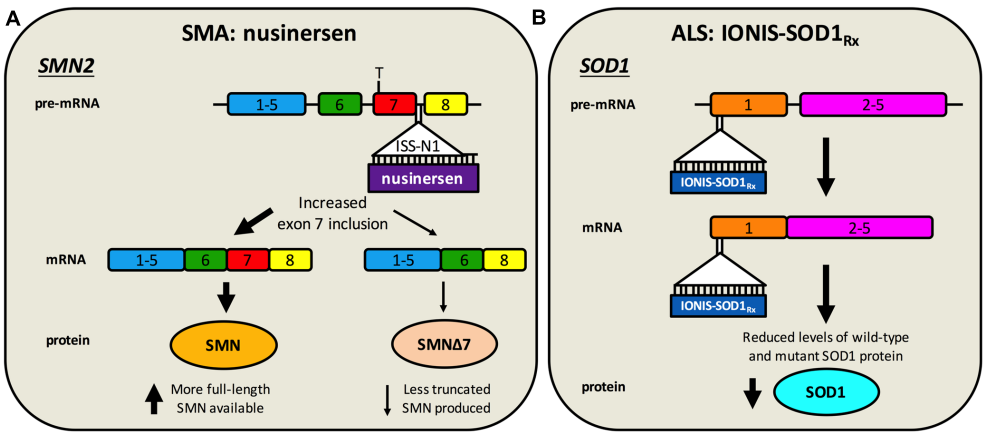

FIGURE 2 | Antisense oligonucleotide targeting of *SMN2* splicing and *SOD1* translation. **(A)** Nusinersen is a SSO complementary to an intronic sequence in *SMN2* called ISS-N1, which is the main inhibitory element for exon 7 splicing. Hybridisation of nusinersen to ISS-N1 within pre-mRNA causes more frequent inclusion of exon 7 in mature *SMN2* transcripts, leading to an increase in the production of full-length SMN protein. Nusinersen is FDA- and EMA- approved for the treatment of SMA. **(B)** IONIS-SOD1$_{Rx}$ specifically targets a 20 nucleotide-long sequence within exon 1 of *SOD1*, resulting in binding to both pre-mRNA and mature RNA causing inhibition of wild-type and mutant *SOD1* expression. ALS patients are currently being recruited for a phase Ib/IIa trial of IONIS-SOD1$_{Rx}$.

provided enough evidence in mid-2016 that nusinersen caused statistically significant improvements in motor function (Finkel et al., 2017), prompting submission to the FDA of the new drug application. Interim analyses from a second phase III trial with type II SMA patients called CHERISH (NCT02292537) and an open-label study in pre-symptomatic infants named NURTURE (NCT02386553) have also proven encouraging.

A second gene therapy called AVXS-101 (a.k.a. scAAV9.CB.SMN and ChariSMA), which delivers the *SMN1* gene using non-replicating self-complementary adeno-associated virus serotype 9 (scAAV9), has also shown significant pre-clinical potential (Mulcahy et al., 2014). A major advantage of this therapy over nusinersen is that AAV9 can cross the BBB in mice, cats, and non-human primates, permitting intravenous delivery (Duque et al., 2009; Foust et al., 2009; Samaranch et al., 2012). Moreover, AAV9 displays neuronal tropism and can mediate stable, long-term expression with a single administration, which is important given immunogenicity issues associated with viruses (Lorain et al., 2008). This contrasts with the multiple, invasive intrathecal injections of nusinersen, which can have adverse side effects (Haché et al., 2016). Marketed by AveXis, AVXS-101 has completed testing in type I SMA patients in an open-label, dose-escalation phase I clinical trial (NCT02122952). The treatment is safe and well tolerated, and caused improvements in survival, attainment of motor milestones, and motor function when compared with historical SMA type I cohorts (Mendell et al., 2017). Two further open-label phase III trials with type I patients in the US and EU are planned. *SMN1* expression is driven by a hybrid cytomegalovirus enhancer/chicken β-actin (CAG) promoter, and AVXS-101 is being injected intravenously.

ALS: A Gene Therapy on the Horizon?

No drugs are currently being tested in late-stage clinical trials for ALS, and until recently, the only FDA-/EMA-approved drug for the disease was the orally available Riluzole, which prolongs patient survival by ≈3 months (Bellingham, 2011). Riluzole can influence ion channel function, neurotransmission, and growth factor secretion, but inhibition of glutamate release from pre-synaptic nerve terminals counteracting motor neuron excitotoxicity appears to be the most disease-relevant benefit (Bellingham, 2011). In May 2017, the FDA surprisingly approved Edaravone (a.k.a. MCI-186 and Radicava), which is a free radical scavenger shown to modestly slow symptom progression in SOD1^{G93A} mice (Ito et al., 2008). In an open-label phase II study without comparator arm involving 19 ALS patients, intravenous administration of Edaravone was shown to be safe and reduce oxidative stress (Yoshino and Kimura, 2006); however, in a subsequent double-blind, placebo-controlled study, drug efficacy was not demonstrated (Abe et al., 2014). Nevertheless, a phase III trial with narrow inclusion criteria showed Edaravone modestly delayed disease progression in a limited subset of ALS patients (Writing Group and Edaravone (MCI-186) ALS 19 Study Group, 2017). Edaravone is unlikely to be effective in a wider ALS population and there is a sizeable administration burden, limiting excitement for the drug (Hardiman and van den Berg, 2017). Palliative care incorporating dietary and respiratory support, speech and language therapy, and specialist physiotherapy can also improve survival in ALS (Martin et al., 2017b), and provides arguably a greater benefit to quality of life than current pharmaceutical intervention (Hardiman et al., 2011).

In over 20 years since the approval of Riluzole, more than 20 additional compounds have been tested in over 50 randomized, controlled trials, involving in excess of 13,000 ALS patients, with little clinical success (Mitsumoto et al., 2014; Petrov et al., 2017). Consistent with ALS complexity, the tested drugs possess a broad range of proposed mechanisms of action, including anti-inflammation and anti-oxidation. Rather than targeting the underlying genetics, these compounds were trialled for their ability to support the ailing ALS nervous system and restrict the insidious progression of disease. These unsuccessful therapeutics

include three neurotrophic factors delivered as recombinant proteins - BDNF, CNTF, and insulin-like growth factor-1 (IGF-1) (Bartus and Johnson, 2017a). Also known as neurotrophins, neurotrophic factors are target-secreted (e.g., from muscles) proteins essential for the growth, development and survival of several nerve types, including motor neurons (Huang and Reichardt, 2001). Delivering neurotrophins has been pursued as a therapy for ALS because their expression can decline with time in models and patients (Krakora et al., 2012). While injection of recombinant proteins is not gene therapy *per se*, when adapted for delivery by viruses, these and other neurotrophic factors have shown promising results in pre-clinical ALS models (Henriques et al., 2010; Nizzardo et al., 2012) (**Table 1**). Additionally, intramuscular injections of plasmids encoding multiple isoforms of hepatocyte growth factor (HGF, drug named VM202) or a transcription factor able to increase expression of vascular endothelial growth factor (VEGF, drug named SB-509) have been trialled in ALS patients (Scarrott et al., 2015). Both plasmids had favorable safety profiles in phase I/II studies (VM202, NCT02039401 and SB-509, NCT00748501) (Sufit et al., 2017), but whether these drugs will be tested further remains unclear (Scarrott et al., 2015).

Without detailed knowledge of disease etiology and underlying cellular pathologies, neuroprotection is potentially the only viable method for tackling a complex syndrome like ALS. However, with increased understanding of gain- and loss-of-function mechanisms of genetic forms of ALS, a second category of knockdown gene therapies encompassing ASOs and RNAi has emerged. These have principally been tested in SOD1, but also C9ORF72, rodent models (**Table 2**). These oligonucleotide-mediated therapeutics are designed to specifically target and reduce levels of toxic, mutant proteins (e.g., C9ORF72, SOD1, TDP-43, FUS) and are showing promise in mice. While they may have a narrow applicability window due to small percentages of genetically determined ALS, given pathological commonalities, such as cytoplasmic TDP-43 sequestration (Neumann et al., 2006) and possible involvement of wild-type SOD1 misfolding in disease (Bosco et al., 2010), there is scope for broader application. Moreover, many sALS patients possess mutations in genes linked to fALS. Targeting the cause of disease in this manner is likely to have the greatest therapeutic impact, and obviates the requirement for co-treatment of multiple downstream pathways. The ASO IONIS-SOD1$_{Rx}$ (a.k.a. ISIS 333611 and BIIB067) targets both wild-type and mutant SOD1 mRNA for degradation (**Figure 2B**). Importantly for this strategy, *Sod1* knockout mice develop normally and do not show motor neuron loss, although their response to axonal injury is impaired (Reaume et al., 1996), and there is evidence that SOD1 loss-of-function may modify ALS severity (Saccon et al., 2013). IONIS-SOD1$_{Rx}$ administration into CSF of SOD1^{G93A} rats resulted in reduced SOD1 protein in spinal cord (Winer et al., 2013). IONIS-SOD1$_{Rx}$ was thus tested in 24 ALS patients in a randomized, placebo-controlled phase I trial (Miller et al., 2013). In this first-in-human clinical study of intrathecal ASO delivery, ≈12 h infusion of IONIS-SOD1$_{Rx}$ was shown to be safe and well tolerated. A phase Ib/IIa trial (NCT02623699) is currently recruiting ALS patients to further evaluate safety, tolerability, and pharmacokinetics of IONIS-SOD1$_{Rx}$.

SMA GENE THERAPY LESSONS FOR ALS

There are numerous possible intersecting explanations for the plethora of failed ALS clinical trials (Mitsumoto et al., 2014), not limited to (1) most pre-clinical research has been conducted in SOD1^{G93A} mice, which do not accurately model the entire ALS spectrum; (2) poor experimental design and execution of pre-clinical work (Scott et al., 2008); (3) focusing on mouse survival as an indicator of drug potential (Genç and Özdinler, 2014); (4) pharmacological issues such as insufficient dose or access/bioavailability to targeted tissue; (5) timing of intervention (Benatar, 2007); (6) patient heterogeneity, poor trial stratification, and scarcity of biomarkers; and (7) incomplete understanding of disease mechanism(s).

Similar difficulties have, at least partially, been overcome by the SMA research community in order for nusinersen to receive regulatory approval. Being a monogenic condition, treating SMA is undoubtedly simpler than the challenge posed by the broad-ranging heterogeneity of ALS. Nonetheless, the clinical approval of nusinersen was a significant milestone not just for SMA, but gene therapy as a whole. That is not to say that the job is complete for SMA, as the clinical response to nusinersen is wide-ranging and includes non-responders (Finkel et al., 2017). However, over the last decade, a great deal has been learnt from the pre-clinical development of SMA gene therapies and the clinical trials of nusinersen and AVXS-101. Given the clinical and mechanistic overlap between the diseases, these lessons learned from SMA may be useful for ALS, particularly when considering the array of gene therapies pre-clinically tested in ALS rodent models (**Tables 1**, **2**) and thus likely to be in the clinical drug pipeline. We have therefore summarised this information to emphasize some key points for ALS gene therapy development.

Careful Therapeutic Targeting Is Required

A clear understanding of where a therapy is needed is mandatory for clinical success. SMA is primarily a LMN disorder; however, in severe cases, pervasive pathology has been reported. For instance, congenital heart problems (Rudnik-Schöneborn et al., 2008), bone complications (Khatri et al., 2008), and vascular defects (Somers et al., 2016) are known to occur in some type I SMA patients. Cell intrinsic SMN depletion causes similar and additional pathologies in mice (Hamilton and Gillingwater, 2013). A sliding scale of vulnerability to SMN reduction has therefore been suggested; at one end, LMNs are the first cell type disturbed by diminished SMN, and as levels are decreased further, more cell types and tissues become affected (Sleigh et al., 2011). This appears to be the case in mouse models, but may be sub-clinical in the majority of SMA patients, as non-motor neuronal involvement is less common. Nevertheless, concerns persist that treating SMA patients with nusinersen, which is delivered directly to the CSF to target LMNs, may alter disease trajectory and reveal

TABLE 1 | Virus-mediated, neuroprotection gene therapies tested in animal models of ALS.

Delivery	Virus-promoter-transgene	Age at injection	Major findings	Animal model	Reference
GDNF					
T/p: MPCs into GC	Rv-PGK1-GDNF (*ex vivo*)	P42	Preserved MN size/number and muscle weight, resulting in improved motor function and extended survival.	$SOD1^{G93A}$ mouse	Mohajeri et al., 1999
I/M: GC, PS, Q, TA	Ad-CMV-GDNF	P5–7	Preserved MNs, improved motor function, delayed disease onset, and extended survival. No significant benefit in CMAP.	$SOD1^{G93A}$ mouse	Acsadi et al., 2002
I/M: GC, TB	AAV2-CMV-GDNF	P56	Delayed disease onset, reduced muscle atrophy, preserved MNs, improved motor function, and extended survival.	$SOD1^{G93A}$ mouse	Wang L.-J. et al., 2002
T/p: hNPCs into lumbar SC	LV-PGK1-GDNF (*ex vivo*)	P100	Robust GDNF expression at end-stage and upregulation of ChAT in the ventral horn, but no significant changes in disease observed.	$SOD1^{G93A}$ rat	Klein et al., 2005
T/p: hMSCs into DT, TA, TB	LV-PGK1-GDNF (*ex vivo*)	P80 (F)	Control and GDNF hMSCs improved NMJ innervation and preserved MNs. GDNF hMSCs extended survival.	$SOD1^{G93A}$ rat strains	Suzuki et al., 2008
T/p: MPCs into GC	CMV-GDNF, -VEGF, -IGF-1, and/or -BDNF (*ex vivo*)	P90/P104 /P118	Combined MPC delivery synergistically delayed disease onset, improved motor function and NMJ innervation, and extended survival.	$SOD1^{G93A}$ mouse	Dadon-Nachum et al., 2015
I/V: tail	AAV9-CAG-GDNF	∼P25	Brain, SC, and limb-muscle GDNF expression. Preserved MNs, increased weight gain and motor function in FL, but not HL.	$SOD1^{G93A}$ rat	Thomsen et al., 2017
IGF-1					
I/M: InC, Q	AAV2-CMV-IFG-1, or -GDNF	P60/P90	IGF-1 delayed disease onset and rate of disease progression, even when delivered symptomatically (P90). GDNF only delayed disease onset.	$SOD1^{G93A}$ mouse	Kaspar et al., 2003
I/S: lumbar	AAV2-CAG-IGF-1	P60	Preserved MNs and improved motor function, but no difference in microgliosis. Delayed disease onset and extended survival in M.	$SOD1^{G93A}$ mouse	Lepore et al., 2007
I/C	AAV1-, or AAV2-CMV-IGF-1	P88–90	Preserved MNs, improved motor function, reduced astrogliosis/microgliosis, and extended survival. AAV1 caused better cervical MN preservation, but there was no survival difference between serotypes.	$SOD1^{G93A}$ mouse	Dodge et al., 2008
I/S: cervical	AAV2-CAG-IGF-1	P80	Preserved MNs. Improved motor function in M. No change in disease onset, disease progression, or survival.	$SOD1^{G93A}$ rat	Franz et al., 2009
I/CV	AAV4-CMV-IGF-1, and/or -VEGF-165	P80–90	Individually, both improved motor function, and extended survival. No additive effect of combined treatment.	$SOD1^{G93A}$ mouse	Dodge et al., 2010
I/M: InC, Q	AAV9-CAG-IGF-2	P80	Preserved MNs, improved motor function, induced nerve regeneration, and extended survival.	$SOD1^{G93A}$ mouse	Allodi et al., 2016
I/M: GC, InC, TA, TB	LV-αCAR-CMV-IGF-1 (MN-specific), or LV-VSV-G-CMV-IGF-1 (muscle-specific)	P28	MN-specific: preserved MNs, improved motor function, delayed disease onset, and extended survival. Muscle-specific: delayed disease onset and improved motor function, but not as well as MN-specific. Gender differences observed.	$SOD1^{G93A}$ mouse	Eleftheriadou et al., 2016
I/M – Ab, FL, HL, InC, Ma	scAAV9-CMV-IGF-1	P60/P90	Delayed disease onset, preserved MNs, improved motor function, and extended survival.	$SOD1^{G93A}$ mouse	Lin et al., 2016
VEGF					
I/M: D, F, GC, InC, T	LV(EIAV)-VEGF-165, or GDNF	P21/P90	VEGF-165 delayed disease onset, reserved MNs, and extended survival, even when delivered symptomatically (P90). GDNF had little impact on disease phenotypes.	$SOD1^{G93A}$ mouse	Azzouz et al., 2004b
I/C, I/CV, or I/V: jugular	ssAAV1-PGK1-VEGF, or scAAV9-PGK1-VEGF	P2/P49	I/C resulted in high VEGF expression along entire SC. No VEGF treatment impacted the disease course.	*LIX1*$^{-/-}$ cat	Bucher et al., 2013

(Continued)

TABLE 1 | Continued

Delivery	Virus-promoter-transgene	Age at injection	Major findings	Animal model	Reference
T/p: hMSCs into DT, TA, TB	LV-PGK1-VEGF-165, -BDNF, -GDNF, -IGF-1 or -GDNF/-VEGF-165 (*ex vivo*)	P90 (F)	VEGF-165 and GDNF preserved MNs, improved NMJ innervation, and extended survival in isolation, with additive improvements in NMJ innervation and survival when co-delivered.	$SOD1^{G93A}$ rat	Krakora et al., 2013
I/T	Pseudotyped scAAV9-CMV-VEGF-165	P90	Preserved MNs, improved motor function, reduced microgliosis, and extended survival.	$SOD1^{G93A}$ mouse	Wang et al., 2016
Other					
I/M: DT, GC, TB	Ad-RSV-NT-3 alone or with -CNTF	P3–5	NT3 improved motor function, reduced axonal degeneration, induced muscle re-innervation, and extended survival. CNTF addition provided additive effects.	*pmn* mouse	Haase et al., 1997, 1998
I/S: lumbar	rAAV-CMV-Bcl-2	P35	Bcl-2 delayed disease onset, preserved MNs, and improved CMAP.	$SOD1^{G93A}$ mouse	Azzouz et al., 2000
I/M: DT, GC, TB	Ad-RSV-CT-1	P3–5	CT-1 delayed disease onset, weight loss, CMAP decline, and axonal degeneration, improved motor function and muscle weight, and extended survival.	$SOD1^{G93A}$ mouse	Bordet et al., 2001
I/S: lumbar, or I/M: DT, GC	rAAV1/2-CBA-G-CSF	P70 (F)	I/C delayed disease onset, preserved MNs and NMJs, improved motor function and axon regeneration post-nerve crush, and extended survival. I/M increased plasma G-CSF levels, but failed to transduce MNs.	$SOD1^{G93A}$ mouse	Henriques et al., 2011
I/M: D, F, HL, InC, T	AAV6-CMV-PRDX3, or -NRF2	P29–31	Neither PRDX3 or NRF2 impacted disease. Poor CNS transduction may have been the cause.	$SOD1^{G93A}$mouse	Nanou et al., 2013
I/S: lumbar	rAAV2/1-CAG-IL-10	P1	IL-10 did not impact disease onset, but extended survival. Altered immune system genes in CNS at end-stage.	$SOD1^{G93A}$mouse	Ayers et al., 2015
I/C and I/M: GC	LV-CMV-EEAT2, -GDH2, and/or -NRF2	P65	Individual EAAT2, GDH2, and NRF2 treatments all preserved MNs, but combination therapy also delayed disease onset, improved motor function and body weight, and extended survival.	$SOD1^{G93A}$mouse	Benkler et al., 2016
I/M: GC	AAV1-CMV-NRG1	P56/P84	NRG1 improved GC but not TA CMAP, preserved NMJs, but not axons or MNs, and increased collateral NMJ sprouting. Had no impact on motor function or disease onset. Effects were reduced when treated later.	$SOD1^{G93A}$mouse	Mancuso et al., 2016
I/V: tail	AAV9-CMV-DOK7	P90 (M)	DOK7 increased NMJ size and innervation, reduced muscle atrophy, and extended survival, without preserving MNs.	$SOD1^{G93A}$mouse	Miyoshi et al., 2017
I/T	ssAAV9-CMV-DAO	P90	>2-fold increase in lumbar SC DAO levels. Preserved MNs and axons, reduced microgliosis, and delayed muscle atrophy. Extended survival of F.	$SOD1^{G93A}$mouse	Wang et al., 2017

In the Delivery column, the mode of delivery (hMSC, human mesenchymal stem cell; hNPC, human neural progenitor cell; I/C, intracerebral; I/CV, intracerbroventricular; I/M, intramuscular; I/S, intraspinal; I/T, intrathecal; I/V, intravenous; MPC, muscle progenitor cell; SC, spinal cord; T/p, transplant) is followed by details of site of injection (Ab, abdominal; D, diaphragm; DT, dorsal trunk; F, facial; FL, forelimb; GC, gastrocnemius; HL, hindlimb; InC, intercostal; Ma, masseter; PS, paraspinal; Q, quadriceps; T, tongue; TA, tibialis anterior; TB, triceps brachii). In the Virus-promoter-transgene column, information on the viral vector (Ad, adenovirus; AAV, adeno-associated virus; EIAV, Rabies-G pseudotyped lentiviral-vector; LV, lentivirus; r, recombinant; Rv, retrovirus; sc, self-complementary; ss, single-stranded), gene promoter (CAG, hybrid cytomegalovirus enhancer/chicken β-actin; CBA, chicken β-actin; CMV, cytomegalovirus; PGK1, phosphoglycerate kinase 1; RSV, rous sarcoma virus; VSV-G, Vesicular Stomatitis Virus glycoprotein), and gene of interest (αCAR, coxsackievirus and adenovirus receptor; BDNF, brain-derived neurotrophic factor; Bcl-2, B-cell lymphoma-2; CNTF, ciliary neurotrophic factor; CT-1, cardiotrophin-1; DAO, D-amino acid oxidase; DOK7, docking protein 7; EAAT2, excitatory amino acid transporter 2; G-CSF, granulocyte-colony stimulating factor; GDH2, glutamate-dehydrogenase 2; GDNF, glial-derived neurotrophic factor; IGF-1/2, insulin-like growth factor 1/2; IL-10, interleukin-10; NRF2, nuclear factor erythroid 2-related factor 2; NRG1, Neuroregulin-1; NT-3, neurotrophin-3; PRDX3, peroxiredoxin 3; VEGF, vascular endothelial growth factor) is provided. Acronyms used in additional columns: ChAT, choline acetyltransferase; CMAP, compound muscle action potential; CNS, central nervous system; LIX, limb-expression 1; F, females only; M, males only; MN, motor neuron; NMJ, neuromuscular junction; P, postnatal day; pmn, progressive motor neuronopathy; SOD1, superoxide dismutase 1.

TABLE 2 | Knockdown strategy gene therapies tested in animal models of ALS.

Delivery	Therapeutic	Targeted gene	Treatment age	Major findings	Animal model	Reference
Repeated I/P	ASO	*p75*^{NTR}	Starting at P60 (F)	p75^{NTR} levels reduced in lumbar SC, kidneys, and MNs. Delayed disease onset and extended survival, but did not impact disease progression.	SOD1^{G93A} mouse	Turner et al., 2003
Repeated I/P	ASO	*GluR3*	Starting at P50	Delayed disease onset and extended survival, despite lack of GluR3 reduction in the lumbar SC.	SOD1^{G93A} mouse	Rembach et al., 2004
I/M: HL	AAV2-CMV-siRNA	*SOD1*	P45	SOD1 levels reduced in MNs, and motor function improved.	SOD1^{G93A} mouse	Miller et al., 2005
I/M: D, F, HL, InC, T	LV(EIAV)-CMV-shRNA	*SOD1*	P7	SOD1 levels reduced in MNs. Delayed disease onset, preserved MNs, improved motor function, and extended survival.	SOD1^{G93A} mouse	Ralph et al., 2005
I/S: lumbar	LV-PGK1-shRNA	*SOD1*	P40	SOD1 levels reduced in MNs and glial cells. Delayed disease onset, preserved MNs and axons, and improved motor function and CMAP.	SOD1^{G93A} mouse	Raoul et al., 2005
Repeated I/P, or continuous I/CV inf.	ASO	*SOD1*	P65	SOD1 levels reduced in brain and SC by I/CV infusion. Slowed disease progression and extended survival, but did not affect disease onset.	SOD1^{G93A} rat	Smith et al., 2006
Continuous I/T inf.	siRNA	*FasR*	P90	FasR levels reduced in SC. Preserved MNs and axons, improved motor function, and extended survival.	SOD1^{G93A} mouse	Locatelli et al., 2007
I/M: GC, or I/V: tail	rAAV6-H1-shRNA	*SOD1*	P42	I/M delivery targeted MNs and reduced SOD1 mRNA/protein in GC. I/V delivery reduced SOD1 levels in muscle, heart, and liver, and to a lesser extent in SC, but not brain. Disease onset and progression unaffected.	SOD1^{G93A} mouse	Towne et al., 2008
Continuous I/T inf.	siRNA	*SOD1*	≈P85 (M)	SOD1 levels reduced in SC. Delayed disease onset and extended survival.	SOD1^{G93A} mouse	Wang et al., 2008
SN, or I/M: GC	rAd-, or AAV2-U6-shRNA	*SOD1*	P94	Nerve injection more efficient than I/M at MN delivery. rAd reduced SOD1 levels in MNs, slowed disease progression, and extended survival. rAAV2 did not confer any benefit.	SOD1^{G93A} mouse	Wu et al., 2009
I/M: F, FL, HL, InC, T, TC	rAAV6-H1-shRNA	*SOD1*	P1/P5/P15	SOD1 levels reduced in muscles and MNs. Preserved MNs, NMJs, and axon, reduced muscle atrophy, but did not impact neuroinflammation or disease progression.	SOD1^{G93A} mouse	Towne et al., 2011
I/V: tail (P21), or temporal (P1)	AAV9-CAG-shRNA	*SOD1*	P1-2/P21/P85	P1 injections caused greater reduction than P21 in SOD1 levels in SC, due to more efficient MN transduction. Injections at all ages improved motor function, increased muscle mass, and extended survival, but only P1 delayed disease onset.	SOD1^{G93A} mouse; SOD1^{G37R} mouse	Foust et al., 2013
Repeated I/P	ASO	*AChE*	P35/P84	Treatment at P35 preserved MNs and extended survival, but later delivery had no impact.	SOD1^{G93A} mouse	Gotkine et al., 2013
I/CV: continuous inf.	ASO	*miR-155*	P60	ASO incorporated into brain and SC, and miR-155 target genes impacted. Disease progression slowed and survival extended, but disease onset unaffected.	SOD1^{G93A} mouse	Koval et al., 2013
I/T	AAV2/1-CMV-scFvD3H5	*SOD1*	P45	Sustained expression was observed in MNs. Delayed disease onset, preserved MNs and axons, improved motor function, reduced	SOD1^{G93A} mouse	Patel et al., 2014
I/C	AAV9-H1-shRNA	*SOD1*	P70	SOD1 levels reduced in cortex, but not MNs. Delayed disease onset, preserved MNs and NMJs, improved motor function in hindlimbs, and extended survival.	SOD1^{G93A} rat	Thomsen et al., 2014
I/T	rAAVrh10-CAG-amiR	*SOD1*	P55–60 (F)	SOD1 levels reduced in SC and MNs. Slowed disease progression and extended survival, but disease onset unaffected.	SOD1^{G93A} mouse	Wang H. et al., 2014

(Continued)

TABLE 2 | Continued

Delivery	Therapeutic	Targeted gene	Treatment age	Major findings	Animal model	Reference
I/M: GC (P2), or I/CV (P2), or I/T (P35)	AAV6-CMV-miR, and/or AAV9-gfaABC$_1$D-miR, or AAV9-CMV-miR	*SOD1*	P2/P35	I/M (AAV6) delivery reduced SOD1 levels in GC. I/CV delivery resulted in MN (AAV6) and astrocyte (AAV9-gfaABC$_1$D) targeting. Both I/CV treatments preserved MNs, and NMJs, improved motor function, decreased muscle atrophy, and extended survival. There was no additive effect. I/T (gfaABC$_1$D and CMV) at P35 improved CMAP and motor function, but only CMV preserved MNs and NMJs. Survival was unaffected by I/T.	SOD1^{G93A} mouse	Dirren et al., 2015
I/V: tail	rAAVrh10-U6-miR, or CBA-miR	*SOD1*	P50-68	U6 delayed disease onset and extended survival, while CBA delayed disease progression and extended survival. The effects of U6 were marginally better than CBA. U6 also preserved MNs and improved motor function.	SOD1^{G93A} mouse	Borel et al., 2016
I/CV	ASO	*C9ORF72*	≈P90/≈P180	Different ASOs decreased repeat-containing C9ORF72 RNA levels in cortex and SC, sense foci in cortex, and poly(GP) and poly(GA) peptides at both time points. Behavioral deficits were alleviated when treated at ≈P180.	*C9ORF72* BAC transgenic mouse (C9^{405B})	Jiang et al., 2016
I/CV (P0), or I/P (P0, P3, and P6), or I/CV and I/V (P85)	MO	*S0D1*	P0/P3/P6/P85	SOD1 levels reduced in CNS via all routes. I/CV and I/V combination preserved MNs and axons, improved motor function, reduced microgliosis, and extended survival.	SOD1^{G93A} mouse	Nizzardo et al., 2016
I/CV	AAV9-CAG-amiR	*S0D1*	P1	*SOD1* mRNA levels reduced in CNS, muscle, and heart. Preserved MNs, NMJs and axons, delayed SC inflammation, improved motor function and extended survival.	SOD1^{G93A} mouse	Stoica et al., 2016
I/CV	ASO	*Atxn2*	P1	*Atxn2*, but not *TDP-43*, mRNA levels reduced in brain. Improved motor function and extended survival.	*TDP-43*$^{Tg/Tg}$ mouse	Becker et al., 2017
I/CV and I/V: temporal (P1), or I/CV and I/V: temporal and/or RbS (P50), or I/S: lumbar (P50)	scAAVrh10-U7-ASO	*S0D1*	P1/P50	All paradigms reduced SOD1 levels in SC. Delayed disease onset and progression, improved motor function, and extended survival at both time points. Neonatal delivery preserved MNs, NMJs, and myofibres, and reduced microgliosis.	SOD1^{G93A} mouse	Biferi et al., 2017
I/V: tail (P21), or temporal (P1)	scAAV9-CAG-shRNA	*S0D1*	P1/P21	Greater MN transduction at P1, shifting to astrocyte tropism at P21, with both reducing SOD1 levels in SC. Both treatments delayed disease onset, improved motor function, and extended survival, but amelioration was better at P1. Genetic suppression of NF-κB in microglia resulted in additive phenotypic improvements.	SOD1^{G93A} mouse	Frakes et al., 2017
I/T	rAAVrh10-CAG-amiR	*S0D1*	P30	Slow and fast injection protocols resulted in different transduction patterns. Both protocols preserved axons, delayed disease onset, and extended survival. Slow injection produced greater phenotypic improvements.	SOD1^{G93A} mouse	Li et al., 2017

In the Delivery column, the mode of delivery (I/C, intracerebral; I/CV, intracerbroventricular; I/M, intramuscular; I/P, intraperitoneal; I/S, intraspinal; I/T, intrathecal; I/V, intravenous; SN, sciatic nerve) is followed by details of site of injection (D, diaphragm; F, facial; FL, forelimb; GC, gastrocnemius; HL, hindlimb; InC, intercostal; inf., infusion; P, postnatal day; RbS, retrobulbar sinus; T, tongue; TC, thoracic cavity). In the Therapeutic column, information on the type of therapeutic is provided (Ad, adenovirus; AAV, adeno-associated virus; amiR, artificial microRNA; ASO, antisense oligonucleotide; EIAV, Rabies-G pseudotyped lentiviral-vector; LV, lentivirus; miR, microRNA; MO, morpholino oligonucleotide; r, recombinant; sc, self-complementary; scFvD3H5, a secretable single-chain fragment variable (scFv) antibody composed of heavy and light chain regions of D3H5 monoclonal antibody that binds specifically to misfolded SOD1; shRNA, short hairpin RNA; siRNA, small interfering RNA; ss, single-stranded), along with details on promoter usage (CAG, hybrid cytomegalovirus enhancer/chicken β-actin; CBA, chicken β-actin; CMV, cytomegalovirus; gfaABC$_1$D, minimal glial fibrillary acidic protein; H1, H1 RNA polymerase III; PGK1, phosphoglycerate kinase 1). Additional acronyms used in other columns include: AChE, acetylcholinesterase; Atxn2, ataxin-2; BAC, bacterial artificial chromosome; CMAP, compound muscle action potential; F, females only; FasR, Fas receptor; GluR3, glutamate receptor subunit 3; M, males only; MN, motor neuron; NMJ, neuromuscular junction; p75^{NTR}, p75-neurotrophin receptor; SC, spinal cord; SOD1, superoxide dismutase 1; Tg, transgene.

novel pathologies caused by chronic SMN deficiency outside the CNS (Tizzano and Finkel, 2017).

There is thus discussion, for both ASOs and viruses, as to which single delivery route provides the best therapeutic outcome for SMA (Hua et al., 2011; Glascock et al., 2012b; Porensky et al., 2012; Nizzardo et al., 2014; Zhou et al., 2015). Major determinants of this are the BBB and the BSCB, which not only restrict access of systemically delivered therapies to the brain and spinal cord, but can also confine drugs within the CNS when directly administered. Targeting therapies to NMJs for uptake and retrograde transport along motor axons can circumvent these barriers (Tosolini et al., 2013; Mohan et al., 2014; Tosolini and Morris, 2016), but this is compromised by denervation. Nonetheless, once inside the CNS, ASOs are able to distribute widely (Rigo et al., 2014). Accordingly, intracerebroventricular injection of SMN ASOs results in robust SMN upregulation in the CNS (Hua et al., 2010; Passini et al., 2011; Porensky et al., 2012; Rigo et al., 2014), while intravenous or subcutaneous administration triggers a more systemic increase outside the CNS (Hua et al., 2011; Keil et al., 2014). Viral vectors are better than ASOs at overcoming BBB permeability problems (Foust et al., 2010; Valori et al., 2010; Dominguez et al., 2011; Meyer et al., 2015), but distinctions in therapeutic outcome between routes still apply (Glascock et al., 2012a,b). In addition, modifying the delivery speed of intrathecal injections can alter AAV tropism; slower injections (i.e., over 8 min) result in preferential transduction of the spinal cord, whereas faster injections (i.e., over 30 s) preferably transduce the brain and peripheral tissue (Li et al., 2017). Notwithstanding, there remains little doubt that using multiple injection modes to provide body-wide SMN augmentation provides the best phenotypic rescue in SMA mice (Nizzardo et al., 2014; Osman et al., 2014), while limiting the onset of delayed, non-neuronal pathologies such as tail necrosis (Foust et al., 2010; Dominguez et al., 2011). The importance of careful therapeutic targeting of SMN to all required cells has been confirmed using numerous transgenic mice where SMN has been overexpressed in SMA models in a tissue-specific fashion (Gogliotti et al., 2012; Martinez et al., 2012).

Cautious selection of administration route is not the only way to affect the voyage of gene therapy through the body. A number of additional therapy-dependent tactics can be employed to optimize delivery. Despite limited packaging capacity (≈4.5 kb for single-stranded and ≈2.4 kb for self-complementary AAV), AAV has become the most promising vector for gene delivery in neurological disease; it establishes stable nuclear episomes, thus reducing the risk of integrating into the host genome and causing insertional mutagenesis, it can transduce both dividing and non-mitotic cells, and it maintains exogenous gene expression for extended periods (Murlidharan et al., 2014). With approximately twice the capacity of AAV, LV has also been employed as a proof-of-concept vector in pre-clinical models of SMA (Azzouz et al., 2004a) and ALS (**Tables 1**, **2**); however, given that LV can randomly insert into the host genome, there are major safety issues associated with its clinical application (Imbert et al., 2017). The advantages of AAV led to scAAV9 being chosen for *SMN1* delivery in the AveXis gene therapy, AVXS-101. AAV serotypes possess divergent capsid proteins that bind to distinct host cell surface receptors and co-receptors, thereby determining the cells a virus can transduce (i.e., the tropism) and how efficiently it can spread (Murlidharan et al., 2014). Multiple AAV serotypes have been used in SMA mice (Foust et al., 2010; Passini et al., 2010; Tsai et al., 2012), but serotype 9 was selected for AVXS-101 because of its comparatively strong tropism toward LMNs throughout the spinal cord in a range of species (Foust et al., 2009; Bevan et al., 2011; Federici et al., 2012). While numerous AAV serotypes and administration routes have also been tested in ALS mice (**Tables 1**, **2**), it remains unclear which serotype will prove to be most effective. AAV9 and AAVrh10 are good candidates, but natural and engineered serotypes have recently been identified with improved tropism toward ALS-pertinent tissues (Deverman et al., 2016; Chan et al., 2017). Viral transgene expression can also be restricted using promoters with selective and defined expression patterns (Kügler, 2016). Combining knowledge of viral tropism with promoter selectivity thus provides a potential method for exquisite, cell type-specific targeting (von Jonquieres et al., 2013). Disease state (Chen et al., 2012) and age (Foust et al., 2009; Tosolini and Morris, 2016) also impact viral tropism, likely through alterations in host cell receptor availability, while promoter usage likewise changes with pathology and time; hence, it will be vital to test permutations of virus serotype/promoter in relevant pre-clinical models of ALS throughout all stages of disease.

Unlike AAV, ASOs do not readily penetrate tissues, while their cellular uptake and transition to the nucleus, their site of action, is limited. Indeed, it is estimated that <1% of ASOs reach their desired target, as the majority distribute to unwanted organs such as the liver (Godfrey et al., 2017). This mandates repeated therapeutic injections that can cause adverse events (Haché et al., 2016) and toxic ASO accumulation (Godfrey et al., 2017). Consequently, several chemical modifications to the ASO phosphate backbone have been tested and shown to improve safety and pharmacological properties (Evers et al., 2015). Moreover, a number of drug distribution systems compatible with systemic delivery are being developed that enhance ASO transport to disease-pertinent tissues and therefore ease administration and reduce the required dose. These ASO vectorisation strategies can be divided into (1) viral approaches that use harmless, non-replicating viruses, such as AAV, and (2) non-viral strategies that utilise different positively charged molecules such as lipids or peptides (Lehto et al., 2012). Viruses present immunogenicity issues and are not suitable for all nucleic acid-based molecules; nevertheless, to aid cellular targeting and cytoplasm-to-nucleus transport, viral vectors have been engineered to encode modified snRNAs that incorporate specific ASO sequences. Once inside target cells, these ASOs are imported into the nucleus where they accumulate as part of snRNPs (Imbert et al., 2017). When packaged into viral vectors, snRNAs containing ASOs targeting *SMN2* have shown potential for SMA (Meyer et al., 2009; Dal Mas et al., 2015; Odermatt et al., 2016). As has the non-viral approach of conjugating ASOs to CPPs (Hammond et al., 2016; Shabanpoor et al., 2017). CPPs are 5–30 amino acid long, positively charged peptides that transport various macromolecules across cell membranes (Lehto et al., 2012). Highlighting the significance of therapeutic

targeting, intravenous injection of an *SMN2* SSO conjugated to a CNS-targeting CPP caused the greatest extension in SMA mouse survival reported to date – from 12 to 456 days compared to only 54 days for the "naked" oligonucleotide (Hammond et al., 2016). Importantly, these CPP-oligonucleotides are capable of delivery to the CNS of both neonatal and adult mice (Hammond et al., 2016; Shabanpoor et al., 2017); however, the safety, tolerability, and pharmacokinetics of CPP-conjugated ASOs are yet to be tested in additional organisms.

AAV and LV have separately been combined with RNAi-based strategies for SOD1 knockdown (**Table 2**), but only recently have ASO vectorisation strategies been tried in ALS models. Compared with non-encapsulated oligonucleotides, loading *SOD1*-specific ASOs into lipid particles caused a much greater reduction in SOD1 protein in HEK293 cells (Chen et al., 2017). Moreover, direct intravascular delivery of non-ASO-loaded nanoparticles resulted in brain accumulation in wild-type zebrafish, indicating promise for future work in ALS mice (Chen et al., 2017). *SOD1* pre-mRNA-targeting ASOs were also embedded in modified snRNAs and engineered into AAVrh10, which was then co-injected into the blood and brain of $SOD1^{G93A}$ mice either at birth or pre-symptomatically at 50 days (Biferi et al., 2017). The ASO skips *SOD1* exon 2 generating a premature stop codon, which resulted in ≈70% reduction of SOD1 protein levels in the spinal cord 112 days post-perinatal administration. The gene therapy caused vast improvements in neuromuscular function, restricted weight loss, and, when given early, resulted in the greatest $SOD1^{G93A}$ survival extension yet reported to ≈250 days (Biferi et al., 2017).

Amyotrophic lateral sclerosis patients and models do not show the same cell and tissue vulnerability-resistance continuum as SMA; however, it is clear that pathology is not limited to LMNs and UMNs, probably contributing to the gamut of unsuccessful ALS clinical trials (Bartus and Johnson, 2017a). Indeed, the ALS/FTD clinicopathological overlap (Morita et al., 2006; Neumann et al., 2006; Vance et al., 2006) has been replicated in ALS mice, indicating the importance of cortical cells and synapses to the disease (Fogarty et al., 2015, 2016). Furthermore, the non-cell autonomous toxicities emanating from cells such as microglia (Puentes et al., 2016), and the prion-like cell-to-cell spread of pathological aggregates, also indicate that targeting therapies to motor neurons as well as additional cells and tissues is likely to be required in order to generate meaningful improvements in ALS prognosis. Indeed, disease onset and mortality are delayed in mutant SOD1 mice when microglial activation is pharmacologically restricted prior to disease onset (Kriz et al., 2002; van den Bosch et al., 2002), while disease progression is slowed in mutant SOD1 mice in which SOD1 is removed from microglia, oligodendrocytes, or astrocytes (Boillée et al., 2006; Yamanaka et al., 2008; Kang et al., 2013). Moreover, expression of mutant SOD1 in motor neurons alone is insufficient to fully recapitulate the mutant SOD1 mouse phenotype (Lino et al., 2002; Pramatarova et al., 2001), while deletion of *SOD1* from motor neurons and interneurons of SOD1 mutant mice only delays disease onset (Wang et al., 2009).

Spinal muscular atrophy research has highlighted the importance of comparing different therapy injection sites and testing novel technologies to improve targeting of therapeutics not only to the required tissues, but also to the correct resident cells and subcellular locations. Viral targeting of rapidly dividing cells affected by ALS (e.g., astrocytes), subtleties in motor neuron subtype vulnerability (Nijssen et al., 2017), along with the indication that different subcellular motor neuron compartments, such as the NMJ, may require differential support and treatment (Moloney et al., 2014), add to the complexity of the challenge ahead. It is therefore imperative that during ALS therapy design, careful consideration is given to what cells and tissues need to be targeted and how exactly this can be most effectively achieved.

Combinatorial Treatment Is Key

It is conceivable that carefully crafted gene therapy combinations targeting multiple disease mechanisms could provide additive effects in MNDs. Indeed, AAV1-follistatin treatment significantly boosted muscle and body weight of SMA mice suboptimally dosed with *SMN2* ASO (Feng et al., 2016), while in isolation, follistatin upregulation or myostatin reduction have little effect (Sumner et al., 2009; Rindt et al., 2012). Co-delivery of recombinant follistatin with an *SMN2*-inducing compound also resulted in a small additive enhancement in motor function, but not survival (Harris and Butchbach, 2015). Similarly, genetic upregulation of SMA modifier plastin 3 has no effect on untreated SMA mouse lifespan (Ackermann et al., 2013), but can drastically improve survival in ASO-dosed animals (Hosseinibarkooie et al., 2016). A range of other pathological mechanisms could be concomitantly targeted in SMA (Bowerman et al., 2017). Combinations of drugs directed at just the SMN pathway have also proven more effective than individual treatments (Kwon et al., 2011; Liu et al., 2013), while the impact of ASOs targeting *SMN2* has been enhanced by co-treatment with a compound (Osman et al., 2017), co-targeting the *SMN2*-repressing long non-coding RNA, *SMN-AS1*, for ASO-mediated knockdown (d'Ydewalle et al., 2017; Woo et al., 2017), and co-masking additional negative *SMN2* splicing elements (Pao et al., 2013). Furthermore, a holistic approach to treatment appears to be important, as providing nutritional support to SMA mice can advance therapeutic efficacy (Narver et al., 2008; Butchbach et al., 2014).

These SMA studies suggest that previously unsuccessful therapeutics may provide additive benefits when used in combination, highlighting the importance of simultaneously treating multiple disease pathways. Given the pathology observed in ALS, it will also be vital to co-modify pathways in different cell types. To facilitate this, viral vectors engineered with selective promoters could be united with CPP-conjugated ASOs in order to synergistically target multiple genes in related and independent pathways across distinct and highly specific cell populations. This was recently confirmed in mutant $SOD1^{G93A}$ mice by concomitantly targeting distinct disease mechanisms in motor neurons, astrocytes and microglia (Frakes et al., 2017). In isolation, genetic suppression of the NF-κB pathway in

microglia or shRNA-mediated knockdown of *SOD1* in motor neurons and astrocytes via systemic AAV9 administration resulted in similar improvements in survival, disease onset, and progression of mutant SOD1 mice. However, the combined targeting of these two pathomechanisms across three major cell types resulted in an additive amelioration in all assessed phenotypes. The median mutant lifespan was expanded from 137 to 188 days with a maximum survival of 204 days, which is one of the best extensions reported to date (Frakes et al., 2017). In a separate study, joint lentiviral targeting of three distinct disease pathways aiming to reduce excitotoxicity resulted in a synergistic neuroprotective effect in $SOD1^{G93A}$ mice (Benkler et al., 2016), while simultaneous delivery of multiple neurotrophic factors can also induce modest additive effects over individual therapies (Haase et al., 1997; Krakora et al., 2013; Dadon-Nachum et al., 2015), although not consistently (Dodge et al., 2010). Like SMA, it is thus clear that prognosis can be improved in ALS models by attempting a multifaceted gene therapy approach. It is somewhat surprising that there have not yet been any published studies that test concurrent delivery of neuroprotective and knockdown strategies *in vivo* for ALS. ASO-mediated depletion of toxic mutant proteins is likely to be most critical in ALS, and should be joined with a gamut of neuroprotective accessory therapies such as neurotrophic factors (Henriques et al., 2010), SMN upregulation (e.g., via nusinersen or AVXS-101) (Kariya et al., 2012; Turner et al., 2014), and preservation of NMJ innervation (Miyoshi et al., 2017), in order to determine the most efficacious drug combinations.

Consider Dose Number and Drug Concentrations

In addition to delivering gene therapies to the intended cellular and subcellular site(s), effectors must be expressed/released at a therapeutically viable concentration. Providing multiple *SMN2* ASO doses results in greater phenotypic amelioration in SMA mice (Hua et al., 2011; Zhou et al., 2015; Hammond et al., 2016), while increased concentrations of ASOs or AAVs have a similar positive effect (Meyer et al., 2015; Hammond et al., 2016; Hosseinibarkooie et al., 2016). These results unsurprisingly indicate that delivering greater quantities of therapy, results in higher SMN upregulation, and therefore a better phenotypic rescue of SMA mice. There will inevitably be a point at which SMN overexpression becomes detrimental to cells; however, two-fold genetic overexpression of *SMN* in the nervous system of control mice appears to be safe (Turner et al., 2014; Perera et al., 2016). Nevertheless, this may not be the case for all genes (Denovan-Wright et al., 2008), and thus care must be taken when artificially increasing protein abundance, especially considering that secreted proteins can elicit autocrine and paracrine effects (Baumgartner and Shine, 1997).

Caution must also be exercised with target gene reduction strategies as there may be disparate, time-dependent consequences between protein reduction below a physiological threshold and complete absence (Rossi et al., 2015). That being said, toxicities associated with ASO or AAV accumulation are likely to arise before viability is perturbed by excessive modulation of a gene. Hence, there is a fine balance between administering sufficient gene therapy to ensure correct targeting in effective quantities without causing systemic toxic accumulation and adverse side effects. Upon intravenous injection, ASOs accumulate in the liver, kidneys, and lymph nodes, amongst other places, and can cause hybridisation-independent toxicities (Godfrey et al., 2017), while AAVs can become similarly enriched (Zincarelli et al., 2008). The methods to enhance delivery to disease-susceptible cells and tissues discussed above (e.g., ASO-CPP conjugation) will undoubtedly aid in this battle, and should be optimized in ALS mice, along with ASO chemistries, to enrich the appropriately targeted therapeutic load. Moreover, multiple ASO doses and increasing concentrations of gene therapies must be tested in relevant models to identify the most effective and safe therapeutic regimes. Due to the immune response, repeated AAV dosing is not practical (although immunomodulation is an option) (Lorain et al., 2008), but ASOs can be administered at multiple time points. However, ASO concentration must also be optimized to escape host immune responses (Wang et al., 2008). It should also be remembered that once an AAV has been delivered, relatively little can be done to regulate transgene expression, but ASOs can be neutralized by sequestration using complimentary decoy ASOs (Rigo et al., 2014; Hua et al., 2015).

Therapeutic Timing Is Critical

As disease progresses, the number of impacted proteins and processes will likely increase as a result of time as pathways diverge from the initial cause of pathology. This provides a rationale for why selectively targeting individual disease pathways toward the end of a cascade may provide only limited benefit. Moreover, the greater the duration over which a disease develops, the more anatomical, circuit, and cellular damage will ensue leading to greater loss-of-function and thus a more significant challenge of recovery (Ramírez-Jarquín et al., 2014; Bartus and Johnson, 2017b). For example, early NMJ denervation followed by LMN die-back will severely, if not totally, restrict the ability of the LMN to respond to extracellular neurotrophic signaling. The successful treatment of any disorder is thus more likely to occur when a therapy is administered during early pathogenesis rather than at later time points and, in particular, at disease end stage. Whilst intuitive, this highlights the importance of earlier diagnosis, especially for ALS.

Indeed, the earlier SMN levels are augmented in SMA mice via *SMN* gene therapy, the better the therapeutic outcome (Foust et al., 2010; Hua et al., 2010, 2011; Porensky et al., 2012; Bogdanik et al., 2015; Zhou et al., 2015). Age-dependent differences in BBB permeability, neuropil density, and cell tropisms may contribute (Foust et al., 2009, 2010); however, the early temporal requirement for SMN has been corroborated using mice with inducible *SMN* alleles (Le et al., 2011; Lutz et al., 2011; Kariya et al., 2014a), and is consistent with

human and mouse *SMN* being most highly expressed in the CNS perinatally (Jablonka and Sendtner, 2017), and the most common and severe form of SMA (type I) manifesting before 6 months of age. Accordingly, artificially reducing SMN levels in young adult mice has fewer repercussions than when SMN is diminished at earlier time points (Le et al., 2011; Kariya et al., 2014a). All of this suggests that there is a therapeutic window of opportunity during early development in which *SMN* gene therapy is likely to have the greatest chance of success. One study indicates that in mice, the postnatal window of highest SMN requirement coincides with neuromuscular maturation, and that NMJ disruption causes SMN upregulation in motor neurons (Kariya et al., 2014a). Accordingly, nusinersen is being tested in the open-label NURTURE trial in pre-symptomatic newborns genetically diagnosed with SMA. Interim analyses appear promising, and when complete are likely to provide compelling evidence of the importance of treating SMA as early as possible. It is perhaps for this reason, that a number of small molecule drugs that have proven useful in SMA mice dosed from birth, have failed in clinical trials in which patients are treated post-symptom onset (Fuller et al., 2010). Nevertheless, post-symptomatic restoration of SMN using an inducible allele has been shown to reverse overt neuromuscular pathology and significantly improve SMA mouse lifespan (Lutz et al., 2011). This was corroborated using systemic administration of *SMN2*-targeting ASOs in a mild SMA mouse model (Bogdanik et al., 2015), and in SMA mice sub-optimally dosed with a small molecule *SMN2* splice-modifying drug and subsequently re-treated with the same compound or AAV1-follistatin gene therapy (Feng et al., 2016).

Early therapeutic interventions in mutant SOD1 mice also often result in greater impact on disease. For example, pre-symptomatic injection of VEGF-expressing LV into SOD1^{G93A} mouse muscles resulted in greater delay in disease onset and progression compared to injection at paralysis onset (Azzouz et al., 2004b). The same is true for AAV-mediated IGF-1 delivery (Kaspar et al., 2003) and SOD1 silencing (Foust et al., 2013; Biferi et al., 2017), and recombinant VEGF injections into the brain of mutant SOD1 rats (Storkebaum et al., 2005). Significantly, these studies show, like in SMA, that survival of mutant SOD1 rodents can be extended even when therapies are delivered post-symptomatically. There is also evidence to indicate that treatment during the perinatal stage (e.g., postnatal day 1, P1) can cause even greater improvements in SOD1^{G93A} lifespan (Foust et al., 2013; Biferi et al., 2017), perhaps due in part to sub-clinical embryonic/perinatal defects (van Zundert et al., 2012) and differential age-dependent gene therapy tropism (Foust et al., 2009); however, testing intervention timing in these models needs to be therapeutically appropriate, as ALS is an adult-onset neurodegenerative disease currently with no biomarkers. The pre-symptomatic treatment of fALS patients with a known ALS-causing genetic mutation is a possibility, in the same vein as SMA patients in the NURTURE trial of nusinersen, but treatment in humans at an age akin to P1 is highly unlikely. Nevertheless, perinatal therapy administration paradigms provide useful proof-of-concept information, and are invaluable in gene therapy optimisation.

Amyotrophic lateral sclerosis greatly impacts the neuromuscular system and its proteome, which could cause disease-specific, time-constrained alterations that affect therapeutic efficacy; for instance, viral tropism could be impacted through differential receptor expression (Tosolini and Morris, 2016). Rodent work indicates that there is likely to be an optimal period for ALS therapy delivery, but with a broader therapeutic window, in which disease progression can at least be slowed, if not halted or even partially reversed. It is therefore paramount that potential therapeutics are tested at a range of time points in ALS rodents and in large animals including non-human primates in order to improve therapeutic timing strategy.

CONCLUSION

Typified by extensive heterogeneity, the ALS disease spectrum poses a daunting challenge for developing effective treatments. This diversity, along with numerous other factors, has resulted in an overabundance of unsuccessful clinical trials. Many of these involved compounds targeting likely secondary pathogenic pathways with only limited therapeutic potential. However, over the last two decades, gene therapy using ASOs or viral vectors have emerged as the most promising strategy for treating nervous system disorders. The predominantly LMN disease SMA has benefited from this burgeoning field, with the recent regulatory approval of the ASO nusinersen. Through developing ASO- and virus-mediated drugs for SMA, much has been learnt about gene therapy design and development that could help to alleviate the impact of other MNDs. Pre-clinical SMA research has made it clear that gene therapies must be efficiently delivered to pertinent sites of pathology, at concentrations within the therapeutic range, and at appropriate times in order to increase the chances of success. Tantamount to this is the parallel modification of multiple disease pathways across cell and tissue types. Similar conclusions are also beginning to emerge from pre-clinical ALS models. It is thus by no coincidence that the greatest amelioration of the SOD1^{G93A} mouse phenotype to date was driven by the combined targeting of two pathomechanisms across multiple cell types, and the dual-administration of an AAV-guided *SOD1*-specific ASO into the blood and brain. Given the current lack of diagnostic and prognostic biomarkers for ALS and reliance upon the SOD1^{G93A} mouse, successful translation to patients will be tricky. Nevertheless, by considering issues outlined in this review and thinking clearly about treatment logistics, a viable ALS gene therapy is unlikely to be far from the clinic.

AUTHOR CONTRIBUTIONS

APT and JNS wrote the manuscript, and have approved submission of this work.

FUNDING

This work was funded by a Wellcome Trust Sir Henry Wellcome Postdoctoral Fellowship [103191/A/13/Z to JNS], and a postdoctoral position [APT] supported by a Wellcome Trust Senior Investigator Award [107116/Z/15/Z] to Giampietro Schiavo (Institute of Neurology, University College London).

ACKNOWLEDGMENTS

This paper is dedicated to the memory of Paul Victor Tosolini, who, like all those living with ALS, showed endless courage and never gave up. The authors would like to thank Nicol Birsa, Pietro Fratta, and Giampietro Schiavo (Institute of Neurology, University College London) for critical reading of the manuscript.

REFERENCES

Abe, K., Itoyama, Y., Sobue, G., Tsuji, S., Aoki, M., Doyu, M., et al. (2014). Confirmatory double-blind, parallel-group, placebo-controlled study of efficacy and safety of edaravone (MCI-186) in amyotrophic lateral sclerosis patients. *Amyotroph. Lateral Scler. Frontotemporal Degener.* 15, 610–617. doi: 10.3109/21678421.2014.959024

Ackermann, B., Kröber, S., Torres-Benito, L., Borgmann, A., Peters, M., Hosseini Barkooie, S. M., et al. (2013). Plastin 3 ameliorates spinal muscular atrophy via delayed axon pruning and improves neuromuscular junction functionality. *Hum. Mol. Genet.* 22, 1328–1347. doi: 10.1093/hmg/dds540

Acsadi, G., Anguelov, R. A., Yang, H., Toth, G., Thomas, R., Jani, A., et al. (2002). Increased survival and function of SOD1 mice after glial cell-derived neurotrophic factor gene therapy. *Hum. Gene Ther.* 13, 1047–1059. doi: 10.1089/104303402753812458

Al-Chalabi, A., Calvo, A., Chio, A., Colville, S., Ellis, C. M., Hardiman, O., et al. (2014). Analysis of amyotrophic lateral sclerosis as a multistep process: a population-based modelling study. *Lancet Neurol.* 13, 1108–1113. doi: 10.1016/S1474-4422(14)70219-4

Al-Chalabi, A., Fang, F., Hanby, M. F., Leigh, P. N., Shaw, C. E., Ye, W., et al. (2010). An estimate of amyotrophic lateral sclerosis heritability using twin data. *J. Neurol. Neurosurg. Psychiatr.* 81, 1324–1326. doi: 10.1136/jnnp.2010.207464

Al-Chalabi, A., and Hardiman, O. (2013). The epidemiology of ALS: a conspiracy of genes, environment and time. *Nat. Rev. Neurol.* 9, 617–628. doi: 10.1038/nrneurol.2013.203

Allodi, I., Comley, L., Nichterwitz, S., Nizzardo, M., Simone, C., Benitez, J. A., et al. (2016). Differential neuronal vulnerability identifies IGF-2 as a protective factor in ALS. *Sci. Rep.* 6:25960. doi: 10.1038/srep25960

Alonso, A., Logroscino, G., Jick, S. S., and Hernán, M. A. (2009). Incidence and lifetime risk of motor neuron disease in the United Kingdom: a population-based study. *Eur. J. Neurol.* 16, 745–751. doi: 10.1111/j.1468-1331.2009.02586.x

Al-Sarraj, S., King, A., Troakes, C., Smith, B., Maekawa, S., Bodi, I., et al. (2011). p62 positive, TDP-43 negative, neuronal cytoplasmic and intranuclear inclusions in the cerebellum and hippocampus define the pathology of *C9orf72*-linked FTLD and MND/ALS. *Acta Neuropathol.* 122, 691–702. doi: 10.1007/s00401-011-0911-2

Andersson, M. K., Ståhlberg, A., Arvidsson, Y., Olofsson, A., Semb, H., Stenman, G., et al. (2008). The multifunctional FUS, EWS and TAF15 proto-oncoproteins show cell type-specific expression patterns and involvement in cell spreading and stress response. *BMC Cell Biol.* 9:37. doi: 10.1186/1471-2121-9-37

Ayers, J. I., Fromholt, S., Sinyavskaya, O., Siemienski, Z., Rosario, A. M., Li, A., et al. (2015). Widespread and efficient transduction of spinal cord and brain following neonatal AAV injection and potential disease modifying effect in ALS mice. *Mol. Ther.* 23, 53–62. doi: 10.1038/mt.2014.180

Azzouz, M., Hottinger, A., Paterna, J. C., Zurn, A. D., Aebischer, P., and Büeler, H. (2000). Increased motoneuron survival and improved neuromuscular function in transgenic ALS mice after intraspinal injection of an adeno-associated virus encoding Bcl-2. *Hum. Mol. Genet.* 9, 803–811. doi: 10.1093/hmg/9.5.803

Azzouz, M., Le, T., Ralph, G. S., Walmsley, L., Monani, U. R., Lee, D. C. P., et al. (2004a). Lentivector-mediated SMN replacement in a mouse model of spinal muscular atrophy. *J. Clin. Invest.* 114, 1726–1731.

Azzouz, M., Ralph, G. S., Storkebaum, E., Walmsley, L. E., Mitrophanous, K. A., Kingsman, S. M., et al. (2004b). VEGF delivery with retrogradely transported lentivector prolongs survival in a mouse ALS model. *Nature* 429, 413–417.

Bartus, R. T., and Johnson, E. M. (2017a). Clinical tests of neurotrophic factors for human neurodegenerative diseases, part 1: where have we been and what have we learned? *Neurobiol. Dis.* 97, 156–168. doi: 10.1016/j.nbd.2016.03.027

Bartus, R. T., and Johnson, E. M. (2017b). Clinical tests of neurotrophic factors for human neurodegenerative diseases, part 2: where do we stand and where must we go next? *Neurobiol. Dis.* 97, 169–178. doi: 10.1016/j.nbd.2016.03.026

Bäumer, D., Ansorge, O., Almeida, M., and Talbot, K. (2010). The role of RNA processing in the pathogenesis of motor neuron degeneration. *Expert Rev. Mol. Med.* 12:e21. doi: 10.1017/S1462399410001523

Bäumer, D., Lee, S., Nicholson, G., Davies, J. L., Parkinson, N. J., Murray, L. M., et al. (2009). Alternative splicing events are a late feature of pathology in a mouse model of spinal muscular atrophy. *PLOS Genet.* 5:e1000773. doi: 10.1371/journal.pgen.1000773

Bäumer, D., Talbot, K., and Turner, M. R. (2014). Advances in motor neurone disease. *J. R. Soc. Med.* 107, 14–21. doi: 10.1177/0141076813511451

Baumgartner, B. J., and Shine, H. D. (1997). Targeted transduction of CNS neurons with adenoviral vectors carrying neurotrophic factor genes confers neuroprotection that exceeds the transduced population. *J. Neurosci.* 17, 6504–6511.

Becker, L. A., Huang, B., Bieri, G., Ma, R., Knowles, D. A., Jafar-Nejad, P., et al. (2017). Therapeutic reduction of ataxin-2 extends lifespan and reduces pathology in TDP-43 mice. *Nature* 544, 367–371. doi: 10.1038/nature22038

Bellingham, M. C. (2011). A review of the neural mechanisms of action and clinical efficiency of riluzole in treating amyotrophic lateral sclerosis: what have we learned in the last decade? *CNS Neurosci. Ther.* 17, 4–31. doi: 10.1111/j.1755-5949.2009.00116.x

Benatar, M. (2007). Lost in translation: treatment trials in the SOD1 mouse and in human ALS. *Neurobiol. Dis.* 26, 1–13. doi: 10.1016/j.nbd.2006.12.015

Benkler, C., Barhum, Y., Ben-Zur, T., and Offen, D. (2016). Multifactorial gene therapy enhancing the glutamate uptake system and reducing oxidative stress delays symptom onset and prolongs survival in the SOD1-G93A ALS mouse model. *J. Mol. Neurosci.* 58, 46–58. doi: 10.1007/s12031-015-0695-2

Bevan, A. K., Duque, S., Foust, K. D., Morales, P. R., Braun, L., Schmelzer, L., et al. (2011). Systemic gene delivery in large species for targeting spinal cord, brain, and peripheral tissues for pediatric disorders. *Mol. Ther.* 19, 1971–1980. doi: 10.1038/mt.2011.157

Biferi, M. G., Cohen-Tannoudji, M., Cappelletto, A., Giroux, B., Roda, M., Astord, S., et al. (2017). A new AAV10-U7-mediated gene therapy prolongs survival and restores function in an ALS mouse model. *Mol. Ther.* 25, 2038–2052. doi: 10.1016/j.ymthe.2017.05.017

Blauw, H. M., Barnes, C. P., van Vught, P. W. J., van Rheenen, W., Verheul, M., Cuppen, E., et al. (2012). SMN1 gene duplications are associated with sporadic ALS. *Neurology* 78, 776–780. doi: 10.1212/WNL.0b013e318249f697

Bogdanik, L. P., Osborne, M. A., Davis, C., Martin, W. P., Austin, A., Rigo, F., et al. (2015). Systemic, postsymptomatic antisense oligonucleotide rescues motor unit maturation delay in a new mouse model for type II/III spinal muscular atrophy. *Proc. Natl. Acad. Sci. U.S.A.* 112, E5863–E5872. doi: 10.1073/pnas.1509758112

Boillée, S., Yamanaka, K., Lobsiger, C. S., Copeland, N. G., Jenkins, N. A., Kassiotis, G., et al. (2006). Onset and progression in inherited ALS determined by motor neurons and microglia. *Science* 312, 1389–1392. doi: 10.1126/science.1123511

Bordet, T., Lesbordes, J. C., Rouhani, S., Castelnau-Ptakhine, L., Schmalbruch, H., Haase, G., et al. (2001). Protective effects of cardiotrophin-1 adenoviral gene

transfer on neuromuscular degeneration in transgenic ALS mice. *Hum. Mol. Genet.* 10, 1925–1933. doi: 10.1093/hmg/10.18.1925

Borel, F., Gernoux, G., Cardozo, B., Metterville, J. P., Toro Cabreja, G. C., Song, L., et al. (2016). Therapeutic rAAVrh10 mediated SOD1 silencing in adult SOD1G93A mice and nonhuman primates. *Hum. Gene Ther.* 27, 19–31. doi: 10.1089/hum.2015.122

Bosco, D. A., Morfini, G., Karabacak, N. M., Song, Y., Gros-Louis, F., Pasinelli, P., et al. (2010). Wild-type and mutant SOD1 share an aberrant conformation and a common pathogenic pathway in ALS. *Nat. Neurosci.* 13, 1396–1403. doi: 10.1038/nn.2660

Bowerman, M., Becker, C. G., Yáñez-Muñoz, R. J., Ning, K., Wood, M. J. A., Gillingwater, T. H., et al. (2017). Therapeutic strategies for spinal muscular atrophy: SMN and beyond. *Dis. Model. Mech.* 10, 943–954. doi: 10.1242/dmm.030148

Brenner, D., Müller, K., Wieland, T., Weydt, P., Böhm, S., Lulé, D., et al. (2016). NEK1 mutations in familial amyotrophic lateral sclerosis. *Brain* 139:e28. doi: 10.1093/brain/aww033

Brown, R. H., and Al-Chalabi, A. (2017). Amyotrophic lateral sclerosis. *N. Engl. J. Med.* 377, 162–172. doi: 10.1056/NEJMra1603471

Bucher, T., Colle, M.-A., Wakeling, E., Dubreil, L., Fyfe, J., Briot-Nivard, D., et al. (2013). scAAV9 intracisternal delivery results in efficient gene transfer to the central nervous system of a feline model of motor neuron disease. *Hum. Gene Ther.* 24, 670–682. doi: 10.1089/hum.2012.218

Bunton-Stasyshyn, R. K. A., Saccon, R. A., Fratta, P., and Fisher, E. M. C. (2015). SOD1 function and its implications for amyotrophic lateral sclerosis pathology: new and renascent themes. *Neuroscientist* 21, 519–529. doi: 10.1177/1073858414561795

Butchbach, M. E. R., Singh, J., Gurney, M. E., and Burghes, A. H. M. (2014). The effect of diet on the protective action of D156844 observed in spinal muscular atrophy mice. *Exp. Neurol.* 256, 1–6. doi: 10.1016/j.expneurol.2014.03.005

Byrne, S., Elamin, M., Bede, P., and Hardiman, O. (2012). Absence of consensus in diagnostic criteria for familial neurodegenerative diseases. *J. Neurol. Neurosurg. Psychiatr.* 83, 365–367. doi: 10.1136/jnnp-2011-301530

Cauchi, R. J. (2014). Gem depletion: amyotrophic lateral sclerosis and spinal muscular atrophy crossover. *CNS Neurosci. Ther.* 20, 574–581. doi: 10.1111/cns.12242

Chabot, B., and Shkreta, L. (2016). Defective control of pre-messenger RNA splicing in human disease. *J. Cell Biol.* 212, 13–27. doi: 10.1083/jcb.201510032

Chan, K. Y., Jang, M. J., Yoo, B. B., Greenbaum, A., Ravi, N., Wu, W.-L., et al. (2017). Engineered AAVs for efficient noninvasive gene delivery to the central and peripheral nervous systems. *Nat. Neurosci.* 20, 1172–1179. doi: 10.1038/nn.4593

Chen, L., Watson, C., Morsch, M., Cole, N. J., Chung, R. S., Saunders, D. N., et al. (2017). Improving the delivery of SOD1 antisense oligonucleotides to motor neurons using calcium phosphate-lipid nanoparticles. *Front. Neurosci.* 11:476. doi: 10.3389/fnins.2017.00476

Chen, Y. H., Claflin, K., Geoghegan, J. C., and Davidson, B. L. (2012). Sialic acid deposition impairs the utility of AAV9, but not peptide-modified AAVs for brain gene therapy in a mouse model of lysosomal storage disease. *Mol. Ther.* 20, 1393–1399. doi: 10.1038/mt.2012.100

Chiò, A., Logroscino, G., Hardiman, O., Swingler, R., Mitchell, D., Beghi, E., et al. (2009). Prognostic factors in ALS: a critical review. *Amyotroph. Lateral Scler.* 10, 310–323. doi: 10.3109/17482960802566824

Chiriboga, C. A., Swoboda, K. J., Darras, B. T., Iannaccone, S. T., Montes, J., De Vivo, D. C., et al. (2016). Results from a phase 1 study of nusinersen (ISIS-SMNRx) in children with spinal muscular atrophy. *Neurology* 86, 890–897. doi: 10.1212/WNL.0000000000002445

Cirulli, E. T., Lasseigne, B. N., Petrovski, S., Sapp, P. C., Dion, P. A., Leblond, C. S., et al. (2015). Exome sequencing in amyotrophic lateral sclerosis identifies risk genes and pathways. *Science* 347, 1436–1441. doi: 10.1126/science.aaa3650

Colombrita, C., Zennaro, E., Fallini, C., Weber, M., Sommacal, A., Buratti, E., et al. (2009). TDP-43 is recruited to stress granules in conditions of oxidative insult. *J. Neurochem.* 111, 1051–1061. doi: 10.1111/j.1471-4159.2009.06383.x

Conlon, E. G., Lu, L., Sharma, A., Yamazaki, T., Tang, T., Shneider, N. A., et al. (2016). The *C9ORF72* GGGGCC expansion forms RNA G-quadruplex inclusions and sequesters hnRNP H to disrupt splicing in ALS brains. *Elife* 5:e17820. doi: 10.7554/eLife.17820

Corcia, P., Ingre, C., Blasco, H., Press, R., Praline, J., Antar, C., et al. (2012). Homozygous SMN2 deletion is a protective factor in the Swedish ALS population. *Eur. J. Hum. Genet.* 20, 588–591. doi: 10.1038/ejhg.2011.255

Dadon-Nachum, M., Ben-Yaacov, K., Ben-Zur, T., Barhum, Y., Yaffe, D., Perlson, E., et al. (2015). Transplanted modified muscle progenitor cells expressing a mixture of neurotrophic factors delay disease onset and enhance survival in the SOD1 mouse model of ALS. *J. Mol. Neurosci.* 55, 788–797. doi: 10.1007/s12031-014-0426-0

Dal Mas, A., Rogalska, M. E., Bussani, E., and Pagani, F. (2015). Improvement of SMN2 pre-mRNA processing mediated by exon-specific U1 small nuclear RNA. *Am. J. Hum. Genet.* 96, 93–103. doi: 10.1016/j.ajhg.2014.12.009

DeJesus-Hernandez, M., Mackenzie, I. R., Boeve, B. F., Boxer, A. L., Baker, M., Rutherford, N. J., et al. (2011). Expanded GGGGCC hexanucleotide repeat in noncoding region of *C9ORF72* causes chromosome 9p-linked FTD and ALS. *Neuron* 72, 245–256. doi: 10.1016/j.neuron.2011.09.011

Denovan-Wright, E. M., Attis, M., Rodriguez-Lebron, E., and Mandel, R. J. (2008). Sustained striatal ciliary neurotrophic factor expression negatively affects behavior and gene expression in normal and R6/1 mice. *J. Neurosci. Res.* 86, 1748–1757. doi: 10.1002/jnr.21636

Deverman, B. E., Pravdo, P. L., Simpson, B. P., Kumar, S. R., Chan, K. Y., Banerjee, A., et al. (2016). Cre-dependent selection yields AAV variants for widespread gene transfer to the adult brain. *Nat. Biotechnol.* 34, 204–209. doi: 10.1038/nbt.3440

Dirren, E., Aebischer, J., Rochat, C., Towne, C., Schneider, B. L., and Aebischer, P. (2015). SOD1 silencing in motoneurons or glia rescues neuromuscular function in ALS mice. *Ann. Clin. Transl. Neurol.* 2, 167–184. doi: 10.1002/acn3.162

Dodge, J. C., Haidet, A. M., Yang, W., Passini, M. A., Hester, M., Clarke, J., et al. (2008). Delivery of AAV-IGF-1 to the CNS extends survival in ALS mice through modification of aberrant glial cell activity. *Mol. Ther.* 16, 1056–1064. doi: 10.1038/mt.2008.60

Dodge, J. C., Treleaven, C. M., Fidler, J. A., Hester, M., Haidet, A., Handy, C., et al. (2010). AAV4-mediated expression of IGF-1 and VEGF within cellular components of the ventricular system improves survival outcome in familial ALS mice. *Mol. Ther.* 18, 2075–2084. doi: 10.1038/mt.2010.206

Dominguez, E., Marais, T., Chatauret, N., Benkhelifa-Ziyyat, S., Duque, S., Ravassard, P., et al. (2011). Intravenous scAAV9 delivery of a codon-optimized SMN1 sequence rescues SMA mice. *Hum. Mol. Genet.* 20, 681–693. doi: 10.1093/hmg/ddq514

Duque, S., Joussemet, B., Riviere, C., Marais, T., Dubreil, L., Douar, A.-M., et al. (2009). Intravenous administration of self-complementary AAV9 enables transgene delivery to adult motor neurons. *Mol. Ther.* 17, 1187–1196. doi: 10.1038/mt.2009.71

Duque, S. I., Arnold, W. D., Odermatt, P., Li, X., Porensky, P. N., Schmelzer, L., et al. (2015). A large animal model of spinal muscular atrophy and correction of phenotype. *Ann. Neurol.* 77, 399–414. doi: 10.1002/ana.24332

d'Ydewalle, C., Ramos, D. M., Pyles, N. J., Ng, S.-Y., Gorz, M., Pilato, C. M., et al. (2017). The antisense transcript SMN-AS1 regulates SMN expression and is a novel therapeutic target for spinal muscular atrophy. *Neuron* 93, 66–79. doi: 10.1016/j.neuron.2016.11.033

Eleftheriadou, I., Manolaras, I., Irvine, E. E., Dieringer, M., Trabalza, A., and Mazarakis, N. D. (2016). αCAR IGF-1 vector targeting of motor neurons ameliorates disease progression in ALS mice. *Ann. Clin. Transl. Neurol.* 3, 752–768. doi: 10.1002/acn3.335

Evers, M. M., Toonen, L. J. A., and van Roon-Mom, W. M. C. (2015). Antisense oligonucleotides in therapy for neurodegenerative disorders. *Adv. Drug Deliv. Rev.* 87, 90–103. doi: 10.1016/j.addr.2015.03.008

Farrar, M. A., Vucic, S., Johnston, H. M., du Sart, D., and Kiernan, M. C. (2013). Pathophysiological insights derived by natural history and motor function of spinal muscular atrophy. *J. Pediatr.* 162, 155–159. doi: 10.1016/j.jpeds.2012.05.067

Federici, T., and Boulis, N. M. (2012). Gene therapy for amyotrophic lateral sclerosis. *Neurobiol. Dis.* 48, 236–242. doi: 10.1016/j.nbd.2011.08.018

Federici, T., Taub, J. S., Baum, G. R., Gray, S. J., Grieger, J. C., Matthews, K. A., et al. (2012). Robust spinal motor neuron transduction following intrathecal delivery of AAV9 in pigs. *Gene Ther.* 19, 852–859. doi: 10.1038/gt.2011.130

Feng, W., Gubitz, A. K., Wan, L., Battle, D. J., Dostie, J., Golembe, T. J., et al. (2005). Gemins modulate the expression and activity of the SMN complex. *Hum. Mol. Genet.* 14, 1605–1611. doi: 10.1093/hmg/ddi168

Feng, Z., Ling, K. K. Y., Zhao, X., Zhou, C., Karp, G., Welch, E. M., et al. (2016). Pharmacologically induced mouse model of adult spinal muscular atrophy to evaluate effectiveness of therapeutics after disease onset. *Hum. Mol. Genet.* 25, 964–975. doi: 10.1093/hmg/ddv629

Finkel, R. S., Chiriboga, C. A., Vajsar, J., Day, J. W., Montes, J., De Vivo, D. C., et al. (2016). Treatment of infantile-onset spinal muscular atrophy with nusinersen: a phase 2, open-label, dose-escalation study. *Lancet* 388, 3017–3026. doi: 10.1016/S0140-6736(16)31408-8

Finkel, R. S., Mercuri, E., Darras, B. T., Connolly, A. M., Kuntz, N. L., Kirschner, J., et al. (2017). Nusinersen versus sham control in infantile-onset spinal muscular atrophy. *N. Engl. J. Med.* 377, 1723–1732. doi: 10.1056/NEJMoa1702752

Fischer, U., Liu, Q., and Dreyfuss, G. (1997). The SMN-SIP1 complex has an essential role in spliceosomal snRNP biogenesis. *Cell* 90, 1023–1029.

Fogarty, M. J., Klenowski, P. M., Lee, J. D., Drieberg-Thompson, J. R., Bartlett, S. E., Ngo, S. T., et al. (2016). Cortical synaptic and dendritic spine abnormalities in a presymptomatic TDP-43 model of amyotrophic lateral sclerosis. *Sci. Rep.* 6:37968. doi: 10.1038/srep37968

Fogarty, M. J., Noakes, P. G., and Bellingham, M. C. (2015). Motor cortex layer V pyramidal neurons exhibit dendritic regression, spine loss, and increased synaptic excitation in the presymptomatic hSOD1G93A mouse model of amyotrophic lateral sclerosis. *J. Neurosci.* 35, 643–647. doi: 10.1523/JNEUROSCI.3483-14.2015

Foust, K. D., Nurre, E., Montgomery, C. L., Hernandez, A., Chan, C. M., and Kaspar, B. K. (2009). Intravascular AAV9 preferentially targets neonatal neurons and adult astrocytes. *Nat. Biotechnol.* 27, 59–65. doi: 10.1038/nbt.1515

Foust, K. D., Salazar, D. L., Likhite, S., Ferraiuolo, L., Ditsworth, D., Ilieva, H., et al. (2013). Therapeutic AAV9-mediated suppression of mutant SOD1 slows disease progression and extends survival in models of inherited ALS. *Mol. Ther.* 21, 2148–2159. doi: 10.1038/mt.2013.211

Foust, K. D., Wang, X., McGovern, V. L., Braun, L., Bevan, A. K., Haidet, A. M., et al. (2010). Rescue of the spinal muscular atrophy phenotype in a mouse model by early postnatal delivery of SMN. *Nat. Biotechnol.* 28, 271–274. doi: 10.1038/nbt.1610

Frakes, A. E., Braun, L., Ferraiuolo, L., Guttridge, D. C., and Kaspar, B. K. (2017). Additive amelioration of ALS by co-targeting independent pathogenic mechanisms. *Ann. Clin. Transl. Neurol.* 4, 76–86. doi: 10.1002/acn3.375

Franz, C. K., Federici, T., Yang, J., Backus, C., Oh, S. S., Teng, Q., et al. (2009). Intraspinal cord delivery of IGF-I mediated by adeno-associated virus 2 is neuroprotective in a rat model of familial ALS. *Neurobiol. Dis.* 33, 473–481. doi: 10.1016/j.nbd.2008.12.003

Freischmidt, A., Wieland, T., Richter, B., Ruf, W., Schaeffer, V., Müller, K., et al. (2015). Haploinsufficiency of TBK1 causes familial ALS and fronto-temporal dementia. *Nat. Neurosci.* 18, 631–636. doi: 10.1038/nn.4000

Fujii, R., and Takumi, T. (2005). TLS facilitates transport of mRNA encoding an actin-stabilizing protein to dendritic spines. *J. Cell Sci.* 118, 5755–5765. doi: 10.1242/jcs.02692

Fuller, H. R., Barišić, M., Šešo-Šimić, Đ., Špeljko, T., Morris, G. E., and Šimić, G. (2010). Treatment strategies for spinal muscular atrophy. *Transl. Neurosci.* 1, 308–321. doi: 10.2478/v10134-010-0045-4

Gama-Carvalho, M., Garcia-Vaquero, L. M., Pinto, R. F., Besse, F., Weis, J., Voigt, A., et al. (2017). Linking amyotrophic lateral sclerosis and spinal muscular atrophy through RNA-transcriptome homeostasis: a genomics perspective. *J. Neurochem.* 141, 12–30. doi: 10.1111/jnc.13945

Geary, R. S., Norris, D., Yu, R., and Bennett, C. F. (2015). Pharmacokinetics, biodistribution and cell uptake of antisense oligonucleotides. *Adv. Drug Deliv. Rev.* 87, 46–51. doi: 10.1016/j.addr.2015.01.008

Genç, B., and Özdinler, P. H. (2014). Moving forward in clinical trials for ALS: motor neurons lead the way please. *Drug Discov. Today* 19, 441–449. doi: 10.1016/j.drudis.2013.10.014

Gerbino, V., Carrì, M. T., Cozzolino, M., and Achsel, T. (2013). Mislocalised FUS mutants stall spliceosomal snRNPs in the cytoplasm. *Neurobiol. Dis.* 55, 120–128. doi: 10.1016/j.nbd.2013.03.003

Gertz, B., Wong, M., and Martin, L. J. (2012). Nuclear localization of human SOD1 and mutant SOD1-specific disruption of survival motor neuron protein complex in transgenic amyotrophic lateral sclerosis mice. *J. Neuropathol. Exp. Neurol.* 71, 162–177. doi: 10.1097/NEN.0b013e318244b635

Glascock, J. J., Osman, E. Y., Wetz, M. J., Krogman, M. M., Shababi, M., and Lorson, C. L. (2012a). Decreasing disease severity in symptomatic, Smn−/−;SMN2+/+, spinal muscular atrophy mice following scAAV9-SMN delivery. *Hum. Gene Ther.* 23, 330–335. doi: 10.1089/hum.2011.166

Glascock, J. J., Shababi, M., Wetz, M. J., Krogman, M. M., and Lorson, C. L. (2012b). Direct central nervous system delivery provides enhanced protection following vector mediated gene replacement in a severe model of spinal muscular atrophy. *Biochem. Biophys. Res. Commun.* 417, 376–381. doi: 10.1016/j.bbrc.2011.11.121

Godfrey, C., Desviat, L. R., Smedsrød, B., Piétri-Rouxel, F., Denti, M. A., Disterer, P., et al. (2017). Delivery is key: lessons learnt from developing splice-switching antisense therapies. *EMBO Mol Med* 9, 545–557. doi: 10.15252/emmm.201607199

Gogliotti, R. G., Quinlan, K. A., Barlow, C. B., Heier, C. R., Heckman, C. J., and Didonato, C. J. (2012). Motor neuron rescue in spinal muscular atrophy mice demonstrates that sensory-motor defects are a consequence, not a cause, of motor neuron dysfunction. *J. Neurosci.* 32, 3818–3829. doi: 10.1523/JNEUROSCI.5775-11.2012

Gotkine, M., Rozenstein, L., Einstein, O., Abramsky, O., Argov, Z., and Rosenmann, H. (2013). Presymptomatic treatment with acetylcholinesterase antisense oligonucleotides prolongs survival in ALS (G93A-SOD1) mice. *Biomed. Res. Int.* 2013:845345. doi: 10.1155/2013/845345

Grice, S. J., Sleigh, J. N., Liu, J.-L., and Sattelle, D. B. (2011). Invertebrate models of spinal muscular atrophy: insights into mechanisms and potential therapeutics. *Bioessays* 33, 956–965. doi: 10.1002/bies.201100082

Groen, E. J. N., Fumoto, K., Blokhuis, A. M., Engelen-Lee, J., Zhou, Y., van den Heuvel, D. M. A., et al. (2013). ALS-associated mutations in FUS disrupt the axonal distribution and function of SMN. *Hum. Mol. Genet.* 22, 3690–3704. doi: 10.1093/hmg/ddt222

Gruss, O. J., Meduri, R., Schilling, M., and Fischer, U. (2017). UsnRNP biogenesis: mechanisms and regulation. *Chromosoma* 126, 577–593. doi: 10.1007/s00412-017-0637-6

Gurney, M. E., Pu, H., Chiu, A. Y., Dal Canto, M. C., Polchow, C. Y., Alexander, D. D., et al. (1994). Motor neuron degeneration in mice that express a human Cu,Zn superoxide dismutase mutation. *Science* 264, 1772–1775. doi: 10.1126/science.8209258

Haase, G., Kennel, P., Pettmann, B., Vigne, E., Akli, S., Revah, F., et al. (1997). Gene therapy of murine motor neuron disease using adenoviral vectors for neurotrophic factors. *Nat. Med.* 3, 429–436. doi: 10.1038/nm0497-429

Haase, G., Pettmann, B., Vigne, E., Castelnau-Ptakhine, L., Schmalbruch, H., and Kahn, A. (1998). Adenovirus-mediated transfer of the neurotrophin-3 gene into skeletal muscle of pmn mice: therapeutic effects and mechanisms of action. *J. Neurol. Sci.* 160(Suppl. 1), S97–S105. doi: 10.1016/S0022-510X(98)00207-X

Haché, M., Swoboda, K. J., Sethna, N., Farrow-Gillespie, A., Khandji, A., Xia, S., et al. (2016). Intrathecal injections in children with spinal muscular atrophy: nusinersen clinical trial experience. *J. Child Neurol.* 31, 899–906. doi: 10.1177/0883073815627882

Hamilton, G., and Gillingwater, T. H. (2013). Spinal muscular atrophy: going beyond the motor neuron. *Trends Mol. Med.* 19, 40–50. doi: 10.1016/j.molmed.2012.11.002

Hammond, S. M., Hazell, G., Shabanpoor, F., Saleh, A. F., Bowerman, M., Sleigh, J. N., et al. (2016). Systemic peptide-mediated oligonucleotide therapy improves long-term survival in spinal muscular atrophy. *Proc. Natl. Acad. Sci. U.S.A.* 113, 10962–10967. doi: 10.1073/pnas.1605731113

Hardiman, O., and van den Berg, L. H. (2017). Edaravone: a new treatment for ALS on the horizon? *Lancet Neurol.* 16, 490–491. doi: 10.1016/S1474-4422(17)30163-1

Hardiman, O., van den Berg, L. H., and Kiernan, M. C. (2011). Clinical diagnosis and management of amyotrophic lateral sclerosis. *Nat. Rev. Neurol.* 7, 639–649. doi: 10.1038/nrneurol.2011.153

Harris, A. W., and Butchbach, M. E. R. (2015). The effect of the DcpS inhibitor D156844 on the protective action of follistatin in mice with spinal muscular atrophy. *Neuromuscul. Disord.* 25, 699–705. doi: 10.1016/j.nmd.2015.05.008

Henriques, A., Pitzer, C., Dittgen, T., Klugmann, M., Dupuis, L., and Schneider, A. (2011). CNS-targeted viral delivery of G-CSF in an animal model for ALS: improved efficacy and preservation of the neuromuscular unit. *Mol. Ther.* 19, 284–292. doi: 10.1038/mt.2010.271

Henriques, A., Pitzer, C., and Schneider, A. (2010). Neurotrophic growth factors for the treatment of amyotrophic lateral sclerosis: where do we stand? *Front. Neurosci.* 4:32. doi: 10.3389/fnins.2010.00032

Hensel, N., and Claus, P. (2017). The actin cytoskeleton in SMA and ALS: how does it contribute to motoneuron degeneration? *Neuroscientist* doi: 10.1177/1073858417705059 [Epub ahead of print].

Hosseinibarkooie, S., Peters, M., Torres-Benito, L., Rastetter, R. H., Hupperich, K., Hoffmann, A., et al. (2016). The power of human protective modifiers: PLS3 and CORO1C unravel impaired endocytosis in spinal muscular atrophy and rescue SMA phenotype. *Am. J. Hum. Genet.* 99, 647–665. doi: 10.1016/j.ajhg.2016.07.014

Howell, M. D., Ottesen, E. W., Singh, N. N., Anderson, R. L., Seo, J., Sivanesan, S., et al. (2017). TIA1 is a gender-specific disease modifier of a mild mouse model of spinal muscular atrophy. *Sci. Rep.* 7:7183. doi: 10.1038/s41598-017-07468-2

Hua, Y., Liu, Y. H., Sahashi, K., Rigo, F., Bennett, C. F., and Krainer, A. R. (2015). Motor neuron cell-nonautonomous rescue of spinal muscular atrophy phenotypes in mild and severe transgenic mouse models. *Genes Dev.* 29, 288–297. doi: 10.1101/gad.256644.114

Hua, Y., Sahashi, K., Hung, G., Rigo, F., Passini, M. A., Bennett, C. F., et al. (2010). Antisense correction of SMN2 splicing in the CNS rescues necrosis in a type III SMA mouse model. *Genes Dev.* 24, 1634–1644. doi: 10.1101/gad.1941310

Hua, Y., Sahashi, K., Rigo, F., Hung, G., Horev, G., Bennett, C. F., et al. (2011). Peripheral SMN restoration is essential for long-term rescue of a severe spinal muscular atrophy mouse model. *Nature* 478, 123–126. doi: 10.1038/nature10485

Hua, Y., Vickers, T. A., Okunola, H. L., Bennett, C. F., and Krainer, A. R. (2008). Antisense masking of an hnRNP A1/A2 intronic splicing silencer corrects SMN2 splicing in transgenic mice. *Am. J. Hum. Genet.* 82, 834–848. doi: 10.1016/j.ajhg.2008.01.014

Hua, Y., and Zhou, J. (2004). Survival motor neuron protein facilitates assembly of stress granules. *FEBS Lett.* 572, 69–74. doi: 10.1016/j.febslet.2004.07.010

Huang, E. J., and Reichardt, L. F. (2001). Neurotrophins: roles in neuronal development and function. *Annu. Rev. Neurosci.* 24, 677–736. doi: 10.1146/annurev.neuro.24.1.677

Ilieva, H., Polymenidou, M., and Cleveland, D. W. (2009). Non-cell autonomous toxicity in neurodegenerative disorders: ALS and beyond. *J. Cell Biol.* 187, 761–772. doi: 10.1083/jcb.200908164

Imbert, M., Dias-Florencio, G., and Goyenvalle, A. (2017). Viral Vector-Mediated Antisense therapy for genetic diseases. *Genes* 8:E51. doi: 10.3390/genes8020051

Ishihara, T., Ariizumi, Y., Shiga, A., Kato, T., Tan, C.-F., Sato, T., et al. (2013). Decreased number of Gemini of coiled bodies and U12 snRNA level in amyotrophic lateral sclerosis. *Hum. Mol. Genet.* 22, 4136–4147. doi: 10.1093/hmg/ddt262

Ito, H., Wate, R., Zhang, J., Ohnishi, S., Kaneko, S., Ito, H., et al. (2008). Treatment with edaravone, initiated at symptom onset, slows motor decline and decreases SOD1 deposition in ALS mice. *Exp. Neurol.* 213, 448–455. doi: 10.1016/j.expneurol.2008.07.017

Jablonka, S., and Sendtner, M. (2017). Developmental regulation of SMN expression: pathophysiological implications and perspectives for therapy development in spinal muscular atrophy. *Gene Ther.* 24, 506–513. doi: 10.1038/gt.2017.46

Jiang, J., Zhu, Q., Gendron, T. F., Saberi, S., McAlonis-Downes, M., Seelman, A., et al. (2016). Gain of toxicity from ALS/FTD-linked repeat expansions in *C9ORF72* is alleviated by antisense oligonucleotides targeting GGGGCC-containing RNAs. *Neuron* 90, 535–550. doi: 10.1016/j.neuron.2016.04.006

Kang, S. H., Li, Y., Fukaya, M., Lorenzini, I., Cleveland, D. W., Ostrow, L. W., et al. (2013). Degeneration and impaired regeneration of gray matter oligodendrocytes in amyotrophic lateral sclerosis. *Nat. Neurosci.* 16, 571–579. doi: 10.1038/nn.3357

Kariya, S., Obis, T., Garone, C., Akay, T., Sera, F., Iwata, S., et al. (2014a). Requirement of enhanced Survival Motoneuron protein imposed during neuromuscular junction maturation. *J. Clin. Invest.* 124, 785–800. doi: 10.1172/JCI72017

Kariya, S., Re, D. B., Jacquier, A., Nelson, K., Przedborski, S., and Monani, U. R. (2012). Mutant superoxide dismutase 1 (SOD1), a cause of amyotrophic lateral sclerosis, disrupts the recruitment of SMN, the spinal muscular atrophy protein to nuclear Cajal bodies. *Hum. Mol. Genet.* 21, 3421–3434. doi: 10.1093/hmg/dds174

Kariya, S., Sampson, J. B., Northrop, L. E., Luccarelli, C. M., Naini, A. B., Re, D. B., et al. (2014b). Nuclear localization of SMN and FUS is not altered in fibroblasts from patients with sporadic ALS. *Amyotroph. Lateral Scler. Frontotemporal Degener.* 15, 581–587. doi: 10.3109/21678421.2014.907319

Kaspar, B. K., Lladó, J., Sherkat, N., Rothstein, J. D., and Gage, F. H. (2003). Retrograde viral delivery of IGF-1 prolongs survival in a mouse ALS model. *Science* 301, 839–842. doi: 10.1126/science.1086137

Keil, J. M., Seo, J., Howell, M. D., Hsu, W. H., Singh, R. N., and DiDonato, C. J. (2014). A short antisense oligonucleotide ameliorates symptoms of severe mouse models of spinal muscular atrophy. *Mol. Ther. Nucleic Acids* 3:e174. doi: 10.1038/mtna.2014.23

Khatri, I. A., Chaudhry, U. S., Seikaly, M. G., Browne, R. H., and Iannaccone, S. T. (2008). Low bone mineral density in spinal muscular atrophy. *J .Clin. Neuromuscul. Dis.* 10, 11–17. doi: 10.1097/CND.0b013e318183e0fa

Kiernan, M. C., Vucic, S., Cheah, B. C., Turner, M. R., Eisen, A., Hardiman, O., et al. (2011). Amyotrophic lateral sclerosis. *Lancet* 377, 942–955. doi: 10.1016/S0140-6736(10)61156-7

Klein, S. M., Behrstock, S., McHugh, J., Hoffmann, K., Wallace, K., Suzuki, M., et al. (2005). GDNF delivery using human neural progenitor cells in a rat model of ALS. *Hum. Gene Ther.* 16, 509–521. doi: 10.1089/hum.2005.16.509

Koval, E. D., Shaner, C., Zhang, P., du Maine, X., Fischer, K., Tay, J., et al. (2013). Method for widespread microRNA-155 inhibition prolongs survival in ALS-model mice. *Hum. Mol. Genet.* 22, 4127–4135. doi: 10.1093/hmg/ddt261

Krakora, D., Macrander, C., and Suzuki, M. (2012). Neuromuscular junction protection for the potential treatment of amyotrophic lateral sclerosis. *Neurol. Res. Int.* 2012:379657. doi: 10.1155/2012/379657

Krakora, D., Mulcrone, P., Meyer, M., Lewis, C., Bernau, K., Gowing, G., et al. (2013). Synergistic effects of GDNF and VEGF on lifespan and disease progression in a familial ALS rat model. *Mol. Ther.* 21, 1602–1610. doi: 10.1038/mt.2013.108

Kriz, J., Nguyen, M. D., and Julien, J.-P. (2002). Minocycline slows disease progression in a mouse model of amyotrophic lateral sclerosis. *Neurobiol. Dis.* 10, 268–278. doi: 10.1006/nbdi.2002.0487

Kügler, S. (2016). Tissue-specific promoters in the CNS. *Methods Mol. Biol.* 1382, 81–91. doi: 10.1007/978-1-4939-3271-9_6

Kwiatkowski, T. J., Bosco, D. A., Leclerc, A. L., Tamrazian, E., Vanderburg, C. R., Russ, C., et al. (2009). Mutations in the FUS/TLS gene on chromosome 16 cause familial amyotrophic lateral sclerosis. *Science* 323, 1205–1208. doi: 10.1126/science.1166066

Kwon, D. Y., Motley, W. W., Fischbeck, K. H., and Burnett, B. G. (2011). Increasing expression and decreasing degradation of SMN ameliorate the spinal muscular atrophy phenotype in mice. *Hum. Mol. Genet.* 20, 3667–3677. doi: 10.1093/hmg/ddr288

Le, T. T., McGovern, V. L., Alwine, I. E., Wang, X., Massoni-Laporte, A., Rich, M. M., et al. (2011). Temporal requirement for high SMN expression in SMA mice. *Hum. Mol. Genet.* 20, 3578–3591. doi: 10.1093/hmg/ddr275

Le, T. T., Pham, L. T., Butchbach, M. E. R., Zhang, H. L., Monani, U. R., Coovert, D. D., et al. (2005). SMNΔ7, the major product of the centromeric survival motor neuron (SMN2) gene, extends survival in mice with spinal muscular atrophy and associates with full-length SMN. *Hum. Mol. Genet.* 14, 845–857. doi: 10.1093/hmg/ddi078

Lee, E. B., Lee, V. M.-Y., and Trojanowski, J. Q. (2012). Gains or losses: molecular mechanisms of TDP43-mediated neurodegeneration. *Nat. Rev. Neurosci.* 13, 38–50.

Lee, Y.-B., Chen, H.-J., Peres, J. N., Gomez-Deza, J., Attig, J., Stalekar, M., et al. (2013). Hexanucleotide repeats in ALS/FTD form length-dependent RNA foci, sequester RNA binding proteins, and are neurotoxic. *Cell Rep.* 5, 1178–1186. doi: 10.1016/j.celrep.2013.10.049

Lefebvre, S., Bürglen, L., Reboullet, S., Clermont, O., Burlet, P., Viollet, L., et al. (1995). Identification and characterization of a spinal muscular atrophy-determining gene. *Cell* 80, 155–165. doi: 10.1016/0092-8674(95)90460-3

Lefebvre, S., Burlet, P., Liu, Q., Bertrandy, S., Clermont, O., Munnich, A., et al. (1997). Correlation between severity and SMN protein level in spinal muscular atrophy. *Nat. Genet.* 16, 265–269. doi: 10.1038/ng0797-265

Lehto, T., Kurrikoff, K., and Langel, Ü. (2012). Cell-penetrating peptides for the delivery of nucleic acids. *Expert Opin. Drug Deliv.* 9, 823–836. doi: 10.1517/17425247.2012.689285

Lepore, A. C., Haenggeli, C., Gasmi, M., Bishop, K. M., Bartus, R. T., Maragakis, N. J., et al. (2007). Intraparenchymal spinal cord delivery of adeno-associated

virus IGF-1 is protective in the SOD1G93A model of ALS. *Brain Res.* 1185, 256–265. doi: 10.1016/j.brainres.2007.09.034

Li, D., Liu, C., Yang, C., Wang, D., Wu, D., Qi, Y., et al. (2017). Slow intrathecal injection of rAAVrh10 enhances its transduction of spinal cord and therapeutic efficacy in a mutant SOD1 model of ALS. *Neuroscience* 365, 192–205. doi: 10.1016/j.neuroscience.2017.10.001

Lin, H., Hu, H., Duan, W., Liu, Y., Tan, G., Li, Z., et al. (2016). Intramuscular delivery of scAAV9-hIGF1 prolongs survival in the hSOD1G93A ALS mouse model via upregulation of D-amino acid oxidase. *Mol. Neurobiol.* (in press). doi: 10.1007/s12035-016-0335-z

Ling, S.-C., Polymenidou, M., and Cleveland, D. W. (2013). Converging mechanisms in ALS and FTD: disrupted RNA and protein homeostasis. *Neuron* 79, 416–438. doi: 10.1016/j.neuron.2013.07.033

Lino, M. M., Schneider, C., and Caroni, P. (2002). Accumulation of SOD1 mutants in postnatal motoneurons does not cause motoneuron pathology or motoneuron disease. *J. Neurosci.* 22, 4825–4832.

Liu, H.-C., Ting, C.-H., Wen, H.-L., Tsai, L.-K., Hsieh-Li, H.-M., Li, H., et al. (2013). Sodium vanadate combined with L-ascorbic acid delays disease progression, enhances motor performance, and ameliorates muscle atrophy and weakness in mice with spinal muscular atrophy. *BMC Med.* 11:38. doi: 10.1186/1741-7015-11-38

Liu, Q., and Dreyfuss, G. (1996). A novel nuclear structure containing the survival of motor neurons protein. *EMBO J.* 15, 3555–3565.

Liu, Q., Fischer, U., Wang, F., and Dreyfuss, G. (1997). The spinal muscular atrophy disease gene product, SMN, and its associated protein SIP1 are in a complex with spliceosomal snRNP proteins. *Cell* 90, 1013–1021. doi: 10.1016/S0092-8674(00)80367-0

Locatelli, F., Corti, S., Papadimitriou, D., Fortunato, F., Del Bo, R., Donadoni, C., et al. (2007). Fas small interfering RNA reduces motoneuron death in amyotrophic lateral sclerosis mice. *Ann. Neurol.* 62, 81–92. doi: 10.1002/ana.21152

Lorain, S., Gross, D.-A., Goyenvalle, A., Danos, O., Davoust, J., and Garcia, L. (2008). Transient immunomodulation allows repeated injections of AAV1 and correction of muscular dystrophy in multiple muscles. *Mol. Ther.* 16, 541–547. doi: 10.1038/sj.mt.6300377

Lorson, C. L., Hahnen, E., Androphy, E. J., and Wirth, B. (1999). A single nucleotide in the SMN gene regulates splicing and is responsible for spinal muscular atrophy. *Proc. Natl. Acad. Sci. U.S.A.* 96, 6307–6311. doi: 10.1073/pnas.96.11.6307

Lu, C.-H., Macdonald-Wallis, C., Gray, E., Pearce, N., Petzold, A., Norgren, N., et al. (2015). Neurofilament light chain: a prognostic biomarker in amyotrophic lateral sclerosis. *Neurology* 84, 2247–2257. doi: 10.1212/WNL.0000000000001642

Lu, L., Zheng, L., Viera, L., Suswam, E., Li, Y., Li, X., et al. (2007). Mutant Cu/Zn-superoxide dismutase associated with amyotrophic lateral sclerosis destabilizes vascular endothelial growth factor mRNA and downregulates its expression. *J. Neurosci.* 27, 7929–7938. doi: 10.1523/JNEUROSCI.1877-07.2007

Ludolph, A. C., Bendotti, C., Blaugrund, E., Chio, A., Greensmith, L., Loeffler, J.-P., et al. (2010). Guidelines for preclinical animal research in ALS/MND: a consensus meeting. *Amyotroph. Lateral Scler.* 11, 38–45. doi: 10.3109/17482960903545334

Lutz, C. M., Kariya, S., Patruni, S., Osborne, M. A., Liu, D., Henderson, C. E., et al. (2011). Postsymptomatic restoration of SMN rescues the disease phenotype in a mouse model of severe spinal muscular atrophy. *J. Clin. Invest.* 121, 3029–3041. doi: 10.1172/JCI57291

Mackenzie, I. R., Nicholson, A. M., Sarkar, M., Messing, J., Purice, M. D., Pottier, C., et al. (2017). TIA1 mutations in amyotrophic lateral sclerosis and frontotemporal dementia promote phase separation and alter stress granule dynamics. *Neuron* 95, 808–816.e9. doi: 10.1016/j.neuron.2017.07.025

Mackenzie, I. R. A., Bigio, E. H., Ince, P. G., Geser, F., Neumann, M., Cairns, N. J., et al. (2007). Pathological TDP-43 distinguishes sporadic amyotrophic lateral sclerosis from amyotrophic lateral sclerosis with SOD1 mutations. *Ann. Neurol.* 61, 427–434. doi: 10.1002/ana.21147

Maharjan, N., Künzli, C., Buthey, K., and Saxena, S. (2017). *C9ORF72* regulates stress granule formation and its deficiency impairs stress granule assembly, hypersensitizing cells to stress. *Mol. Neurobiol.* 54, 3062–3077. doi: 10.1007/s12035-016-9850-1

Mancuso, R., Martínez-Muriana, A., Leiva, T., Gregorio, D., Ariza, L., Morell, M., et al. (2016). Neuregulin-1 promotes functional improvement by enhancing collateral sprouting in SOD1G93A ALS mice and after partial muscle denervation. *Neurobiol. Dis.* 95, 168–178. doi: 10.1016/j.nbd.2016.07.023

Martin, S., Al Khleifat, A., and Al-Chalabi, A. (2017a). What causes amyotrophic lateral sclerosis? *F1000Res.* 6:371. doi: 10.12688/f1000research.10476.1

Martin, S., Trevor-Jones, E., Khan, S., Shaw, K., Marchment, D., Kulka, A., et al. (2017b). The benefit of evolving multidisciplinary care in ALS: a diagnostic cohort survival comparison. *Amyotroph. Lateral Scler. Frontotemporal Degener.* 18, 569–575. doi: 10.1080/21678421.2017.1349151

Martinez, T. L., Kong, L., Wang, X., Osborne, M. A., Crowder, M. E., van Meerbeke, J. P., et al. (2012). Survival motor neuron protein in motor neurons determines synaptic integrity in spinal muscular atrophy. *J. Neurosci.* 32, 8703–8715. doi: 10.1523/JNEUROSCI.0204-12.2012

McAndrew, P. E., Parsons, D. W., Simard, L. R., Rochette, C., Ray, P. N., Mendell, J. R., et al. (1997). Identification of proximal spinal muscular atrophy carriers and patients by analysis of SMNT and SMNC gene copy number. *Am. J. Hum. Genet.* 60, 1411–1422. doi: 10.1086/515465

Mendell, J. R., Al-Zaidy, S., Shell, R., Arnold, W. D., Rodino-Klapac, L. R., Prior, T. W., et al. (2017). Single-dose gene-replacement therapy for spinal muscular atrophy. *N. Engl. J. Med.* 377, 1713–1722. doi: 10.1056/NEJMoa1706198

Meyer, K., Ferraiuolo, L., Schmelzer, L., Braun, L., McGovern, V., Likhite, S., et al. (2015). Improving single injection CSF delivery of AAV9-mediated gene therapy for SMA: a dose-response study in mice and nonhuman primates. *Mol. Ther.* 23, 477–487. doi: 10.1038/mt.2014.210

Meyer, K., Marquis, J., Trüb, J., Nlend Nlend, R., Verp, S., Ruepp, M.-D., et al. (2009). Rescue of a severe mouse model for spinal muscular atrophy by U7 snRNA-mediated splicing modulation. *Hum. Mol. Genet.* 18, 546–555. doi: 10.1093/hmg/ddn382

Miller, T. M., Kaspar, B. K., Kops, G. J., Yamanaka, K., Christian, L. J., Gage, F. H., et al. (2005). Virus-delivered small RNA silencing sustains strength in amyotrophic lateral sclerosis. *Ann. Neurol.* 57, 773–776. doi: 10.1002/ana.20453

Miller, T. M., Pestronk, A., David, W., Rothstein, J., Simpson, E., Appel, S. H., et al. (2013). An antisense oligonucleotide against SOD1 delivered intrathecally for patients with SOD1 familial amyotrophic lateral sclerosis: a phase 1, randomised, first-in-man study. *Lancet Neurol.* 12, 435–442. doi: 10.1016/S1474-4422(13)70061-9

Mirra, A., Rossi, S., Scaricamazza, S., Di Salvio, M., Salvatori, I., Valle, C., et al. (2017). Functional interaction between FUS and SMN underlies SMA-like splicing changes in wild-type hFUS mice. *Sci. Rep.* 7:2033. doi: 10.1038/s41598-017-02195-0

Mitsumoto, H., Brooks, B. R., and Silani, V. (2014). Clinical trials in amyotrophic lateral sclerosis: why so many negative trials and how can trials be improved? *Lancet Neurol.* 13, 1127–1138. doi: 10.1016/S1474-4422(14)70129-2

Miyoshi, S., Tezuka, T., Arimura, S., Tomono, T., Okada, T., and Yamanashi, Y. (2017). DOK7 gene therapy enhances motor activity and life span in ALS model mice. *EMBO Mol. Med.* 9, 880–889. doi: 10.15252/emmm.201607298

Moens, T. G., Partridge, L., and Isaacs, A. M. (2017). Genetic models of *C9orf72*: what is toxic? *Curr. Opin. Genet. Dev.* 44, 92–101. doi: 10.1016/j.gde.2017.01.006

Mohajeri, M. H., Figlewicz, D. A., and Bohn, M. C. (1999). Intramuscular grafts of myoblasts genetically modified to secrete glial cell line-derived neurotrophic factor prevent motoneuron loss and disease progression in a mouse model of familial amyotrophic lateral sclerosis. *Hum. Gene Ther.* 10, 1853–1866. doi: 10.1089/10430349950017536

Mohan, R., Tosolini, A. P., and Morris, R. (2014). Targeting the motor end plates in the mouse hindlimb gives access to a greater number of spinal cord motor neurons: an approach to maximize retrograde transport. *Neuroscience* 274, 318–330. doi: 10.1016/j.neuroscience.2014.05.045

Moloney, E. B., de Winter, F., and Verhaagen, J. (2014). ALS as a distal axonopathy: molecular mechanisms affecting neuromuscular junction stability in the presymptomatic stages of the disease. *Front. Neurosci.* 8:252. doi: 10.3389/fnins.2014.00252

Monani, U. R., Lorson, C. L., Parsons, D. W., Prior, T. W., Androphy, E. J., Burghes, A. H., et al. (1999). A single nucleotide difference that alters splicing patterns distinguishes the SMA gene SMN1 from the copy gene SMN2. *Hum. Mol. Genet.* 8, 1177–1183. doi: 10.1093/hmg/8.7.1177

Mori, K., Lammich, S., Mackenzie, I. R. A., Forné, I., Zilow, S., Kretzschmar, H., et al. (2013). hnRNP A3 binds to GGGGCC repeats and is a constituent of p62-positive/TDP43-negative inclusions in the hippocampus of patients with *C9orf72* mutations. *Acta Neuropathol.* 125, 413–423. doi: 10.1007/s00401-013-1088-7

Morita, M., Al-Chalabi, A., Andersen, P. M., Hosler, B., Sapp, P., Englund, E., et al. (2006). A locus on chromosome 9p confers susceptibility to ALS and frontotemporal dementia. *Neurology* 66, 839–844. doi: 10.1212/01.wnl.0000200048.53766.b4

Mulcahy, P. J., Iremonger, K., Karyka, E., Herranz-Martn, S., Shum, K.-T., Tam, J. K. V., et al. (2014). Gene therapy: a promising approach to treating spinal muscular atrophy. *Hum. Gene Ther.* 25, 575–586. doi: 10.1089/hum.2013.186

Munsat, T. L., and Davies, K. E. (1992). International SMA consortium meeting. (26-28 June 1992, Bonn, Germany). *Neuromuscul. Disord.* 2, 423–428. doi: 10.1016/S0960-8966(06)80015-5

Murlidharan, G., Samulski, R. J., and Asokan, A. (2014). Biology of adeno-associated viral vectors in the central nervous system. *Front. Mol. Neurosci.* 7:76. doi: 10.3389/fnmol.2014.00076

Nanou, A., Higginbottom, A., Valori, C. F., Wyles, M., Ning, K., Shaw, P., et al. (2013). Viral delivery of antioxidant genes as a therapeutic strategy in experimental models of amyotrophic lateral sclerosis. *Mol. Ther.* 21, 1486–1496. doi: 10.1038/mt.2013.115

Narver, H. L., Kong, L., Burnett, B. G., Choe, D. W., Bosch-Marcé, M., Taye, A. A., et al. (2008). Sustained improvement of spinal muscular atrophy mice treated with trichostatin A plus nutrition. *Ann. Neurol.* 64, 465–470. doi: 10.1002/ana.21449

Nassif, M., Woehlbier, U., and Manque, P. A. (2017). The enigmatic role of *C9ORF72* in autophagy. *Front. Neurosci.* 11:442. doi: 10.3389/fnins.2017.00442

Neumann, M., Sampathu, D. M., Kwong, L. K., Truax, A. C., Micsenyi, M. C., Chou, T. T., et al. (2006). Ubiquitinated TDP-43 in frontotemporal lobar degeneration and amyotrophic lateral sclerosis. *Science* 314, 130–133. doi: 10.1126/science.1134108

Nijssen, J., Comley, L. H., and Hedlund, E. (2017). Motor neuron vulnerability and resistance in amyotrophic lateral sclerosis. *Acta Neuropathol.* 133, 863–885. doi: 10.1007/s00401-017-1708-8

Nizzardo, M., Simone, C., Falcone, M., Riboldi, G., Rizzo, F., Magri, F., et al. (2012). Research advances in gene therapy approaches for the treatment of amyotrophic lateral sclerosis. *Cell Mol. Life. Sci.* 69, 1641–1650. doi: 10.1007/s00018-011-0881-5

Nizzardo, M., Simone, C., Rizzo, F., Ulzi, G., Ramirez, A., Rizzuti, M., et al. (2016). Morpholino-mediated SOD1 reduction ameliorates an amyotrophic lateral sclerosis disease phenotype. *Sci. Rep.* 6:21301. doi: 10.1038/srep21301

Nizzardo, M., Simone, C., Salani, S., Ruepp, M.-D., Rizzo, F., Ruggieri, M., et al. (2014). Effect of combined systemic and local morpholino treatment on the spinal muscular atrophy Δ7 mouse model phenotype. *Clin. Ther.* 36, 340–356.e5. doi: 10.1016/j.clinthera.2014.02.004

Odermatt, P., Trüb, J., Furrer, L., Fricker, R., Marti, A., and Schümperli, D. (2016). Somatic therapy of a mouse SMA model with a U7 snRNA gene correcting SMN2 splicing. *Mol. Ther.* 24, 1797–1805. doi: 10.1038/mt.2016.152

Oeckl, P., Jardel, C., Salachas, F., Lamari, F., Andersen, P. M., Bowser, R., et al. (2016). Multicenter validation of CSF neurofilaments as diagnostic biomarkers for ALS. *Amyotroph. Lateral Scler. Frontotemporal. Degener.* 17, 404–413. doi: 10.3109/21678421.2016.1167913

Osman, E. Y., Miller, M. R., Robbins, K. L., Lombardi, A. M., Atkinson, A. K., Brehm, A. J., et al. (2014). Morpholino antisense oligonucleotides targeting intronic repressor Element1 improve phenotype in SMA mouse models. *Hum. Mol. Genet.* 23, 4832–4845. doi: 10.1093/hmg/ddu198

Osman, E. Y., Washington, C. W., Simon, M. E., Megiddo, D., Greif, H., and Lorson, C. L. (2017). Analysis of azithromycin monohydrate as a single or a combinatorial therapy in a mouse model of severe spinal muscular atrophy. *J. Neuromuscul. Dis.* 4, 237–249. doi: 10.3233/JND-170230

Pao, P. W., Wee, K. B., Yee, W. C., and Pramono, Z. A. D. (2013). Dual masking of specific negative splicing regulatory elements resulted in maximal exon 7 inclusion of SMN2 gene. *Mol. Ther.* 22, 854–861. doi: 10.1038/mt.2013.276

Passini, M. A., Bu, J., Richards, A. M., Kinnecom, C., Sardi, S. P., Stanek, L. M., et al. (2011). Antisense oligonucleotides delivered to the mouse CNS ameliorate symptoms of severe spinal muscular atrophy. *Sci. Transl. Med.* 3:72ra18. doi: 10.1126/scitranslmed.3001777

Passini, M. A., Bu, J., Roskelley, E. M., Richards, A. M., Sardi, S. P., O'Riordan, C. R., et al. (2010). CNS-targeted gene therapy improves survival and motor function in a mouse model of spinal muscular atrophy. *J. Clin. Invest.* 120, 1253–1264. doi: 10.1172/JCI41615

Patel, P., Kriz, J., Gravel, M., Soucy, G., Bareil, C., Gravel, C., et al. (2014). Adeno-associated virus-mediated delivery of a recombinant single-chain antibody against misfolded superoxide dismutase for treatment of amyotrophic lateral sclerosis. *Mol. Ther.* 22, 498–510. doi: 10.1038/mt.2013.239

Patten, S. A., Armstrong, G. A. B., Lissouba, A., Kabashi, E., Parker, J. A., and Drapeau, P. (2014). Fishing for causes and cures of motor neuron disorders. *Dis. Model. Mech.* 7, 799–809. doi: 10.1242/dmm.015719

Pellizzoni, L., Charroux, B., Rappsilber, J., Mann, M., and Dreyfuss, G. (2001). A functional interaction between the survival motor neuron complex and RNA polymerase II. *J. Cell Biol.* 152, 75–85. doi: 10.1083/jcb.152.1.75

Pellizzoni, L., Yong, J., and Dreyfuss, G. (2002). Essential role for the SMN complex in the specificity of snRNP assembly. *Science* 298, 1775–1779. doi: 10.1126/science.1074962

Perera, N. D., Sheean, R. K., Crouch, P. J., White, A. R., Horne, M. K., and Turner, B. J. (2016). Enhancing survival motor neuron expression extends lifespan and attenuates neurodegeneration in mutant TDP-43 mice. *Hum. Mol. Genet.* 25, 4080–4093. doi: 10.1093/hmg/ddw247

Petrov, D., Mansfield, C., Moussy, A., and Hermine, O. (2017). ALS clinical trials review: 20 years of failure. Are we any closer to registering a new treatment? *Front. Aging Neurosci.* 9:68. doi: 10.3389/fnagi.2017.00068

Polymenidou, M., Lagier-Tourenne, C., Hutt, K. R., Huelga, S. C., Moran, J., Liang, T. Y., et al. (2011). Long pre-mRNA depletion and RNA missplicing contribute to neuronal vulnerability from loss of TDP-43. *Nat. Neurosci.* 14, 459–468. doi: 10.1038/nn.2779

Porensky, P. N., Mitrpant, C., McGovern, V. L., Bevan, A. K., Foust, K. D., Kaspar, B. K., et al. (2012). A single administration of morpholino antisense oligomer rescues spinal muscular atrophy in mouse. *Hum. Mol. Genet.* 21, 1625–1638. doi: 10.1093/hmg/ddr600

Pramatarova, A., Laganière, J., Roussel, J., Brisebois, K., and Rouleau, G. A. (2001). Neuron-specific expression of mutant superoxide dismutase 1 in transgenic mice does not lead to motor impairment. *J. Neurosci.* 21, 3369–3374.

Puentes, F., Malaspina, A., van Noort, J. M., and Amor, S. (2016). Non-neuronal cells in ALS: role of glial, immune cells and blood-CNS barriers. *Brain Pathol.* 26, 248–257. doi: 10.1111/bpa.12352

Ralph, G. S., Radcliffe, P. A., Day, D. M., Carthy, J. M., Leroux, M. A., Lee, D. C. P., et al. (2005). Silencing mutant SOD1 using RNAi protects against neurodegeneration and extends survival in an ALS model. *Nat. Med.* 11, 429–433.

Ramírez-Jarquín, U. N., Lazo-Gómez, R., Tovar-Y-Romo, L. B., and Tapia, R. (2014). Spinal inhibitory circuits and their role in motor neuron degeneration. *Neuropharmacology* 82, 101–107. doi: 10.1016/j.neuropharm.2013.10.003

Raoul, C., Abbas-Terki, T., Bensadoun, J.-C., Guillot, S., Haase, G., Szulc, J., et al. (2005). Lentiviral-mediated silencing of SOD1 through RNA interference retards disease onset and progression in a mouse model of ALS. *Nat. Med.* 11, 423–428.

Reaume, A. G., Elliott, J. L., Hoffman, E. K., Kowall, N. W., Ferrante, R. J., Siwek, D. F., et al. (1996). Motor neurons in Cu/Zn superoxide dismutase-deficient mice develop normally but exhibit enhanced cell death after axonal injury. *Nat. Genet.* 13, 43–47.

Reber, S., Stettler, J., Filosa, G., Colombo, M., Jutzi, D., Lenzken, S. C., et al. (2016). Minor intron splicing is regulated by FUS and affected by ALS-associated FUS mutants. *EMBO J.* 35, 1504–1521. doi: 10.15252/embj.201593791

Rembach, A., Turner, B. J., Bruce, S., Cheah, I. K., Scott, R. L., Lopes, E. C., et al. (2004). Antisense peptide nucleic acid targeting GluR3 delays disease onset and progression in the SOD1 G93A mouse model of familial ALS. *J. Neurosci. Res.* 77, 573–582.

Renton, A. E., Chiò, A., and Traynor, B. J. (2014). State of play in amyotrophic lateral sclerosis genetics. *Nat. Neurosci.* 17, 17–23. doi: 10.1038/nn.3584

Renton, A. E., Majounie, E., Waite, A., Simón-Sánchez, J., Rollinson, S., Gibbs, J. R., et al. (2011). A hexanucleotide repeat expansion in *C9ORF72* is the cause of chromosome 9p21-linked ALS-FTD. *Neuron* 72, 257–268. doi: 10.1016/j.neuron.2011.09.010

Rigo, F., Chun, S. J., Norris, D. A., Hung, G., Lee, S., Matson, J., et al. (2014). Pharmacology of a central nervous system delivered 2′-O-methoxyethyl-modified survival of motor neuron splicing oligonucleotide in mice and nonhuman primates. *J. Pharmacol. Exp. Ther.* 350, 46–55. doi: 10.1124/jpet.113.212407

Rindt, H., Buckley, D. M., Vale, S. M., Krogman, M., Rose, F. F., Garcia, M. L., et al. (2012). Transgenic inactivation of murine myostatin does not decrease the severity of disease in a model of Spinal Muscular Atrophy. *Neuromuscul. Disord.* 22, 277–285. doi: 10.1016/j.nmd.2011.10.012

Ringholz, G. M., Appel, S. H., Bradshaw, M., Cooke, N. A., Mosnik, D. M., and Schulz, P. E. (2005). Prevalence and patterns of cognitive impairment in sporadic ALS. *Neurology* 65, 586–590.

Rochette, C. F., Gilbert, N., and Simard, L. R. (2001). SMN gene duplication and the emergence of the SMN2 gene occurred in distinct hominids: SMN2 is unique to Homo sapiens. *Hum. Genet.* 108, 255–266.

Rodriguez-Muela, N., Litterman, N. K., Norabuena, E. M., Mull, J. L., Galazo, M. J., Sun, C., et al. (2017). Single-cell analysis of SMN reveals its broader role in neuromuscular disease. *Cell Rep.* 18, 1484–1498. doi: 10.1016/j.celrep.2017.01.035

Rosen, D. R., Siddique, T., Patterson, D., Figlewicz, D. A., Sapp, P., Hentati, A., et al. (1993). Mutations in Cu/Zn superoxide dismutase gene are associated with familial amyotrophic lateral sclerosis. *Nature* 362, 59–62.

Rosenfeld, J., and Strong, M. J. (2015). Challenges in the understanding and treatment of amyotrophic lateral sclerosis/motor neuron disease. *Neurotherapeutics* 12, 317–325. doi: 10.1007/s13311-014-0332-8

Rossi, A., Kontarakis, Z., Gerri, C., Nolte, H., Hölper, S., Krüger, M., et al. (2015). Genetic compensation induced by deleterious mutations but not gene knockdowns. *Nature* 524, 230–233. doi: 10.1038/nature14580

Rossoll, W., Jablonka, S., Andreassi, C., Kröning, A.-K., Karle, K., Monani, U. R., et al. (2003). Smn, the spinal muscular atrophy-determining gene product, modulates axon growth and localization of beta-actin mRNA in growth cones of motoneurons. *J. Cell Biol.* 163, 801–812.

Rudnik-Schöneborn, S., Heller, R., Berg, C., Betzler, C., Grimm, T., Eggermann, T., et al. (2008). Congenital heart disease is a feature of severe infantile spinal muscular atrophy. *J. Med. Genet.* 45, 635–638. doi: 10.1136/jmg.2008.057950

Saccon, R. A., Bunton-Stasyshyn, R. K. A., Fisher, E. M. C., and Fratta, P. (2013). Is SOD1 loss of function involved in amyotrophic lateral sclerosis? *Brain* 136, 2342–2358. doi: 10.1093/brain/awt097

Samaranch, L., Salegio, E. A., San Sebastian, W., Kells, A. P., Foust, K. D., Bringas, J. R., et al. (2012). Adeno-associated virus serotype 9 transduction in the central nervous system of nonhuman primates. *Hum. Gene Ther.* 23, 382–389. doi: 10.1089/hum.2011.200

Scarrott, J. M., Herranz-Martín, S., Alrafiah, A. R., Shaw, P. J., and Azzouz, M. (2015). Current developments in gene therapy for amyotrophic lateral sclerosis. *Expert Opin. Biol. Ther.* 15, 935–947. doi: 10.1517/14712598.2015.1044894

Scekic-Zahirovic, J., Sendscheid, O., El Oussini, H., Jambeau, M., Sun, Y., Mersmann, S., et al. (2016). Toxic gain of function from mutant FUS protein is crucial to trigger cell autonomous motor neuron loss. *EMBO J.* 35, 1077–1097. doi: 10.15252/embj.201592559

Scoto, M., Finkel, R. S., Mercuri, E., and Muntoni, F. (2017). Therapeutic approaches for spinal muscular atrophy (SMA). *Gene Ther.* 24, 514–519. doi: 10.1038/gt.2017.45

Scott, S., Kranz, J. E., Cole, J., Lincecum, J. M., Thompson, K., Kelly, N., et al. (2008). Design, power, and interpretation of studies in the standard murine model of ALS. *Amyotroph. Lateral Scler.* 9, 4–15. doi: 10.1080/17482960701856300

Shabanpoor, F., Hammond, S. M., Abendroth, F., Hazell, G., Wood, M. J. A., and Gait, M. J. (2017). Identification of a peptide for systemic brain delivery of a morpholino oligonucleotide in mouse models of spinal muscular atrophy. *Nucleic Acid Ther.* 27, 130–143. doi: 10.1089/nat.2016.0652

Shan, X., Chiang, P.-M., Price, D. L., and Wong, P. C. (2010). Altered distributions of Gemini of coiled bodies and mitochondria in motor neurons of TDP-43 transgenic mice. *Proc. Natl. Acad. Sci. U.S.A.* 107, 16325–16330. doi: 10.1073/pnas.1003459107

Shepheard, S. R., Wuu, J., Cardoso, M., Wiklendt, L., Dinning, P. G., Chataway, T., et al. (2017). Urinary p75ECD: a prognostic, disease progression, and pharmacodynamic biomarker in ALS. *Neurology* 88, 1137–1143. doi: 10.1212/WNL.0000000000003741

Singh, N. K., Singh, N. N., Androphy, E. J., and Singh, R. N. (2006). Splicing of a critical exon of human survival motor neuron is regulated by a unique silencer element located in the last intron. *Mol. Cell. Biol.* 26, 1333–1346.

Singh, N. N., Howell, M. D., Androphy, E. J., and Singh, R. N. (2017). How the discovery of ISS-N1 led to the first medical therapy for spinal muscular atrophy. *Gene Ther.* 24, 520–526. doi: 10.1038/gt.2017.34

Singh, N. N., Seo, J., Ottesen, E. W., Shishimorova, M., Bhattacharya, D., and Singh, R. N. (2011). TIA1 prevents skipping of a critical exon associated with spinal muscular atrophy. *Mol. Cell. Biol.* 31, 935–954. doi: 10.1128/MCB.00945-10

Singh, R. N., Howell, M. D., Ottesen, E. W., and Singh, N. N. (2017). Diverse role of survival motor neuron protein. *Biochim. Biophys. Acta* 1860, 299–315.

Sleigh, J. N., Barreiro-Iglesias, A., Oliver, P. L., Biba, A., Becker, T., Davies, K. E., et al. (2014). Chondrolectin affects cell survival and neuronal outgrowth in *in vitro* and *in vivo* models of spinal muscular atrophy. *Hum. Mol. Genet.* 23, 855–869. doi: 10.1093/hmg/ddt477

Sleigh, J. N., Gillingwater, T. H., and Talbot, K. (2011). The contribution of mouse models to understanding the pathogenesis of spinal muscular atrophy. *Dis. Model. Mech.* 4, 457–467. doi: 10.1242/dmm.007245

Sleigh, J. N., Grice, S. J., Davies, K. E., and Talbot, K. (2013). Spinal muscular atrophy at the crossroads of basic science and therapy. *Neuromuscul. Disord.* 23:96.

Smith, R. A., Miller, T. M., Yamanaka, K., Monia, B. P., Condon, T. P., Hung, G., et al. (2006). Antisense oligonucleotide therapy for neurodegenerative disease. *J. Clin. Invest.* 116, 2290–2296.

Somers, E., Lees, R. D., Hoban, K., Sleigh, J. N., Zhou, H., Muntoni, F., et al. (2016). Vascular defects and spinal cord hypoxia in spinal muscular atrophy. *Ann. Neurol.* 79, 217–230. doi: 10.1002/ana.24549

Sreedharan, J., Blair, I. P., Tripathi, V. B., Hu, X., Vance, C., Rogelj, B., et al. (2008). TDP-43 mutations in familial and sporadic amyotrophic lateral sclerosis. *Science* 319, 1668–1672. doi: 10.1126/science.1154584

Stoica, L., Todeasa, S. H., Cabrera, G. T., Salameh, J. S., ElMallah, M. K., Mueller, C., et al. (2016). Adeno-associated virus-delivered artificial microRNA extends survival and delays paralysis in an amyotrophic lateral sclerosis mouse model. *Ann. Neurol.* 79, 687–700. doi: 10.1002/ana.24618

Storkebaum, E., Lambrechts, D., Dewerchin, M., Moreno-Murciano, M.-P., Appelmans, S., Oh, H., et al. (2005). Treatment of motoneuron degeneration by intracerebroventricular delivery of VEGF in a rat model of ALS. *Nat. Neurosci.* 8, 85–92.

Strong, M. J., Volkening, K., Hammond, R., Yang, W., Strong, W., Leystra-Lantz, C., et al. (2007). TDP43 is a human low molecular weight neurofilament (hNFL) mRNA-binding protein. *Mol. Cell. Neurosci.* 35, 320–327.

Sufit, R. L., Ajroud-Driss, S., Casey, P., and Kessler, J. A. (2017). Open label study to assess the safety of VM202 in subjects with amyotrophic lateral sclerosis. *Amyotroph. Lateral Scler. Frontotemporal Degener.* 18, 269–278. doi: 10.1080/21678421.2016.1259334

Sumner, C. J., Wee, C. D., Warsing, L. C., Choe, D. W., Ng, A. S., Lutz, C., et al. (2009). Inhibition of myostatin does not ameliorate disease features of severe spinal muscular atrophy mice. *Hum. Mol. Genet.* 18, 3145–3152. doi: 10.1093/hmg/ddp253

Sun, S., Ling, S.-C., Qiu, J., Albuquerque, C. P., Zhou, Y., Tokunaga, S., et al. (2015). ALS-causative mutations in FUS/TLS confer gain and loss of function by altered association with SMN and U1-snRNP. *Nat. Commun.* 6:6171. doi: 10.1038/ncomms7171

Suzuki, M., McHugh, J., Tork, C., Shelley, B., Hayes, A., Bellantuono, I., et al. (2008). Direct muscle delivery of GDNF with human mesenchymal stem cells improves motor neuron survival and function in a rat model of familial ALS. *Mol. Ther.* 16, 2002–2010. doi: 10.1038/mt.2008.197

Talbot, K. (2011). Familial versus sporadic amyotrophic lateral sclerosis–a false dichotomy? *Brain* 134, 3429–3431.

Taylor, J. P., Brown, R. H., and Cleveland, D. W. (2016). Decoding ALS: from genes to mechanism. *Nature* 539, 197–206. doi: 10.1038/nature20413

Thomsen, G. M., Alkaslasi, M., Vit, J. P., Lawless, G., Godoy, M., Gowing, G., et al. (2017). Systemic injection of AAV9-GDNF provides modest functional improvements in the SOD1G93A ALS rat but has adverse side effects. *Gene Ther.* 24, 245–252. doi: 10.1038/gt.2017.9

Thomsen, G. M., Gowing, G., Latter, J., Chen, M., Vit, J.-P., Staggenborg, K., et al. (2014). Delayed disease onset and extended survival in the SOD1G93A rat model of amyotrophic lateral sclerosis after suppression of mutant SOD1 in the

motor cortex. *J. Neurosci.* 34, 15587–15600. doi: 10.1523/JNEUROSCI.2037-14.2014

Tisdale, S., and Pellizzoni, L. (2015). Disease mechanisms and therapeutic approaches in spinal muscular atrophy. *J. Neurosci.* 35, 8691–8700. doi: 10.1523/JNEUROSCI.0417-15.2015

Tizzano, E. F., and Finkel, R. S. (2017). Spinal muscular atrophy: a changing phenotype beyond the clinical trials. *Neuromuscul. Disord.* 27, 883–889. doi: 10.1016/j.nmd.2017.05.011

Tosolini, A. P., Mohan, R., and Morris, R. (2013). Targeting the full length of the motor end plate regions in the mouse forelimb increases the uptake of fluoro-gold into corresponding spinal cord motor neurons. *Front. Neurol.* 4:58. doi: 10.3389/fneur.2013.00058

Tosolini, A. P., and Morris, R. (2016). Targeting motor end plates for delivery of adenoviruses: an approach to maximize uptake and transduction of spinal cord motor neurons. *Sci. Rep.* 6:33058. doi: 10.1038/srep33058

Towne, C., Raoul, C., Schneider, B. L., and Aebischer, P. (2008). Systemic AAV6 delivery mediating RNA interference against SOD1: neuromuscular transduction does not alter disease progression in fALS mice. *Mol. Ther.* 16, 1018–1025. doi: 10.1038/mt.2008.73

Towne, C., Setola, V., Schneider, B. L., and Aebischer, P. (2011). Neuroprotection by gene therapy targeting mutant SOD1 in individual pools of motor neurons does not translate into therapeutic benefit in fALS mice. *Mol. Ther.* 19, 274–283. doi: 10.1038/mt.2010.260

Tsai, L.-K., Chen, Y.-C., Cheng, W.-C., Ting, C.-H., Dodge, J. C., Hwu, W.-L., et al. (2012). IGF-1 delivery to CNS attenuates motor neuron cell death but does not improve motor function in type III SMA mice. *Neurobiol. Dis.* 45, 272–279. doi: 10.1016/j.nbd.2011.06.021

Tsuiji, H., Iguchi, Y., Furuya, A., Kataoka, A., Hatsuta, H., Atsuta, N., et al. (2013). Spliceosome integrity is defective in the motor neuron diseases ALS and SMA. *EMBO Mol. Med.* 5, 221–234. doi: 10.1002/emmm.201202303

Tu, W.-Y., Simpson, J. E., Highley, J. R., and Heath, P. R. (2017). Spinal muscular atrophy: factors that modulate motor neurone vulnerability. *Neurobiol. Dis.* 102, 11–20. doi: 10.1016/j.nbd.2017.01.011

Turner, B. J., Alfazema, N., Sheean, R. K., Sleigh, J. N., Davies, K. E., Horne, M. K., et al. (2014). Overexpression of survival motor neuron improves neuromuscular function and motor neuron survival in mutant SOD1 mice. *Neurobiol. Aging* 35, 906–915. doi: 10.1016/j.neurobiolaging.2013.09.030

Turner, B. J., Cheah, I. K., Macfarlane, K. J., Lopes, E. C., Petratos, S., Langford, S. J., et al. (2003). Antisense peptide nucleic acid-mediated knockdown of the p75 neurotrophin receptor delays motor neuron disease in mutant SOD1 transgenic mice. *J. Neurochem.* 87, 752–763. doi: 10.1046/j.1471-4159.2003.02053.x

Turner, B. J., Parkinson, N. J., Davies, K. E., and Talbot, K. (2009). Survival motor neuron deficiency enhances progression in an amyotrophic lateral sclerosis mouse model. *Neurobiol. Dis.* 34, 511–517. doi: 10.1016/j.nbd.2009.03.005

Turner, M. R., Hardiman, O., Benatar, M., Brooks, B. R., Chio, A., de Carvalho, M., et al. (2013). Controversies and priorities in amyotrophic lateral sclerosis. *Lancet Neurol.* 12, 310–322. doi: 10.1016/S1474-4422(13)70036-X

Uranishi, H., Tetsuka, T., Yamashita, M., Asamitsu, K., Shimizu, M., Itoh, M., et al. (2001). Involvement of the pro-oncoprotein TLS (translocated in liposarcoma) in nuclear factor-kappa B p65-mediated transcription as a coactivator. *J. Biol. Chem.* 276, 13395–13401. doi: 10.1074/jbc.M011176200

Valori, C. F., Ning, K., Wyles, M., Mead, R. J., Grierson, A. J., Shaw, P. J., et al. (2010). Systemic delivery of scAAV9 expressing SMN prolongs survival in a model of spinal muscular atrophy. *Sci. Transl. Med.* 2:35ra42. doi: 10.1126/scitranslmed.3000830

van Damme, P., Robberecht, W., and van den Bosch, L. (2017). Modelling amyotrophic lateral sclerosis: progress and possibilities. *Dis. Model. Mech.* 10, 537–549. doi: 10.1242/dmm.029058

van den Bosch, L., Tilkin, P., Lemmens, G., and Robberecht, W. (2002). Minocycline delays disease onset and mortality in a transgenic model of ALS. *Neuroreport* 13, 1067–1070. doi: 10.1097/00001756-200206120-00018

van Rheenen, W., Shatunov, A., Dekker, A. M., McLaughlin, R. L., Diekstra, F. P., Pulit, S. L., et al. (2016). Genome-wide association analyses identify new risk variants and the genetic architecture of amyotrophic lateral sclerosis. *Nat. Genet.* 48, 1043–1048. doi: 10.1038/ng.3622

van Zundert, B., Izaurieta, P., Fritz, E., and Alvarez, F. J. (2012). Early pathogenesis in the adult-onset neurodegenerative disease amyotrophic lateral sclerosis. *J. Cell. Biochem.* 113, 3301–3312. doi: 10.1002/jcb.24234

Vance, C., Al-Chalabi, A., Ruddy, D., Smith, B. N., Hu, X., Sreedharan, J., et al. (2006). Familial amyotrophic lateral sclerosis with frontotemporal dementia is linked to a locus on chromosome 9p13.2-21.3. *Brain* 129, 868–876. doi: 10.1093/brain/awl030

Vance, C., Rogelj, B., Hortobágyi, T., De Vos, K. J., Nishimura, A. L., Sreedharan, J., et al. (2009). Mutations in FUS, an RNA processing protein, cause familial amyotrophic lateral sclerosis type 6. *Science* 323, 1208–1211. doi: 10.1126/science.1165942

Veldink, J. H., Kalmijn, S., van der Hout, A. H., Lemmink, H. H., Groeneveld, G. J., Lummen, C., et al. (2005). SMN genotypes producing less SMN protein increase susceptibility to and severity of sporadic ALS. *Neurology* 65, 820–825. doi: 10.1212/01.wnl.0000174472.03292.dd

Verhaart, I. E. C., Robertson, A., Leary, R., McMacken, G., König, K., Kirschner, J., et al. (2017a). A multi-source approach to determine SMA incidence and research ready population. *J. Neurol.* 264, 1465–1473. doi: 10.1007/s00415-017-8549-1

Verhaart, I. E. C., Robertson, A., Wilson, I. J., Aartsma-Rus, A., Cameron, S., Jones, C. C., et al. (2017b). Prevalence, incidence and carrier frequency of 5q-linked spinal muscular atrophy - a literature review. *Orphanet. J. Rare Dis.* 12:124. doi: 10.1186/s13023-017-0671-8

von Jonquieres, G., Mersmann, N., Klugmann, C. B., Harasta, A. E., Lutz, B., Teahan, O., et al. (2013). Glial promoter selectivity following AAV-delivery to the immature brain. *PLOS ONE* 8:e65646. doi: 10.1371/journal.pone.0065646

Wang, H., Ghosh, A., Baigude, H., Yang, C.-S., Qiu, L., Xia, X., et al. (2008). Therapeutic gene silencing delivered by a chemically modified small interfering RNA against mutant SOD1 slows amyotrophic lateral sclerosis progression. *J. Biol. Chem.* 283, 15845–15852. doi: 10.1074/jbc.M800834200

Wang, H., Yang, B., Qiu, L., Yang, C., Kramer, J., Su, Q., et al. (2014). Widespread spinal cord transduction by intrathecal injection of rAAV delivers efficacious RNAi therapy for amyotrophic lateral sclerosis. *Hum. Mol. Genet.* 23, 668–681. doi: 10.1093/hmg/ddt454

Wang, I.-F., Reddy, N. M., and Shen, C.-K. J. (2002). Higher order arrangement of the eukaryotic nuclear bodies. *Proc. Natl. Acad. Sci. U.S.A.* 99, 13583–13588. doi: 10.1073/pnas.212483099

Wang, L.-J., Lu, Y.-Y., Muramatsu, S., Ikeguchi, K., Fujimoto, K., Okada, T., et al. (2002). Neuroprotective effects of glial cell line-derived neurotrophic factor mediated by an adeno-associated virus vector in a transgenic animal model of amyotrophic lateral sclerosis. *J. Neurosci.* 22, 6920–6928.

Wang, L., Sharma, K., Grisotti, G., and Roos, R. P. (2009). The effect of mutant SOD1 dismutase activity on non-cell autonomous degeneration in familial amyotrophic lateral sclerosis. *Neurobiol. Dis.* 35, 234–240. doi: 10.1016/j.nbd.2009.05.002

Wang, W., Duan, W., Wang, Y., Wen, D., Liu, Y., Li, Z., et al. (2017). Intrathecal delivery of ssAAV9-DAO extends survival in SOD1G93A ALS mice. *Neurochem. Res.* 42, 986–996. doi: 10.1007/s11064-016-2131-6

Wang, X.-B., Cui, N.-H., Gao, J.-J., Qiu, X.-P., and Zheng, F. (2014). SMN1 duplications contribute to sporadic amyotrophic lateral sclerosis susceptibility: evidence from a meta-analysis. *J. Neurol. Sci.* 340, 63–68. doi: 10.1016/j.jns.2014.02.026

Wang, Y., Duan, W., Wang, W., Di Wen, Liu, Y., Liu, Y., et al. (2016). scAAV9-VEGF prolongs the survival of transgenic ALS mice by promoting activation of M2 microglia and the PI3K/Akt pathway. *Brain Res.* 1648(Pt A), 1–10. doi: 10.1016/j.brainres.2016.06.043

Winer, L., Srinivasan, D., Chun, S., Lacomis, D., Jaffa, M., Fagan, A., et al. (2013). SOD1 in cerebral spinal fluid as a pharmacodynamic marker for antisense oligonucleotide therapy. *JAMA Neurol.* 70, 201–207. doi: 10.1001/jamaneurol.2013.593

Woo, C. J., Maier, V. K., Davey, R., Brennan, J., Li, G., Brothers, J., et al. (2017). Gene activation of SMN by selective disruption of lncRNA-mediated recruitment of PRC2 for the treatment of spinal muscular atrophy. *Proc. Natl. Acad. Sci. U.S.A.* 114, E1509–E1518. doi: 10.1073/pnas.1616521114

Writing Group and Edaravone (MCI-186) ALS 19 Study Group (2017). Safety, and efficacy of edaravone in well defined patients with amyotrophic lateral sclerosis: a randomised, double-blind, placebo-controlled trial. *Lancet Neurol.* 16, 505–512. doi: 10.1016/S1474-4422(17)30115-1

Wu, R., Wang, H., Xia, X., Zhou, H., Liu, C., Castro, M., et al. (2009). Nerve injection of viral vectors efficiently transfers transgenes into motor neurons

and delivers RNAi therapy against ALS. *Antioxid. Redox. Signal.* 11, 1523–1534. doi: 10.1089/ARS.2009.2618

Yamanaka, K., Chun, S. J., Boillee, S., Fujimori-Tonou, N., Yamashita, H., Gutmann, D. H., et al. (2008). Astrocytes as determinants of disease progression in inherited amyotrophic lateral sclerosis. *Nat. Neurosci.* 11, 251–253. doi: 10.1038/nn2047

Yamazaki, T., Chen, S., Yu, Y., Yan, B., Haertlein, T. C., Carrasco, M. A., et al. (2012). FUS-SMN protein interactions link the motor neuron diseases ALS and SMA. *Cell Rep.* 2, 799–806. doi: 10.1016/j.celrep.2012.08.025

Yoshino, H., and Kimura, A. (2006). Investigation of the therapeutic effects of edaravone, a free radical scavenger, on amyotrophic lateral sclerosis (Phase II study). *Amyotroph. Lateral Scler.* 7, 241–245. doi: 10.1080/17482960600881870

Yu, Y., Chi, B., Xia, W., Gangopadhyay, J., Yamazaki, T., Winkelbauer-Hurt, M. E., et al. (2015). U1 snRNP is mislocalized in ALS patient fibroblasts bearing NLS mutations in FUS and is required for motor neuron outgrowth in zebrafish. *Nucleic Acids Res.* 43, 3208–3218. doi: 10.1093/nar/gkv157

Zhang, H. L., Pan, F., Hong, D., Shenoy, S. M., Singer, R. H., and Bassell, G. J. (2003). Active transport of the survival motor neuron protein and the role of exon-7 in cytoplasmic localization. *J. Neurosci.* 23, 6627–6637.

Zhang, Z., Pinto, A. M., Wan, L., Wang, W., Berg, M. G., Oliva, I., et al. (2013). Dysregulation of synaptogenesis genes antecedes motor neuron pathology in spinal muscular atrophy. *Proc. Natl. Acad. Sci. U.S.A.* 110, 19348–19353. doi: 10.1073/pnas.1319280110

Zhou, H., Meng, J., Marrosu, E., Janghra, N., Morgan, J., and Muntoni, F. (2015). Repeated low doses of morpholino antisense oligomer: an intermediate mouse model of spinal muscular atrophy to explore the window of therapeutic response. *Hum. Mol. Genet.* 24, 6265–6277. doi: 10.1093/hmg/ddv329

Zhou, Z., Licklider, L. J., Gygi, S. P., and Reed, R. (2002). Comprehensive proteomic analysis of the human spliceosome. *Nature* 419, 182–185. doi: 10.1038/nature01031

Zincarelli, C., Soltys, S., Rengo, G., and Rabinowitz, J. E. (2008). Analysis of AAV serotypes 1-9 mediated gene expression and tropism in mice after systemic injection. *Mol. Ther.* 16, 1073–1080. doi: 10.1038/mt.2008.76

Zou, T., Ilangovan, R., Yu, F., Xu, Z., and Zhou, J. (2007). SMN protects cells against mutant SOD1 toxicity by increasing chaperone activity. *Biochem. Biophys. Res. Commun.* 364, 850–855. doi: 10.1016/j.bbrc.2007.10.096

Conflict of Interest Statement: The authors declare that the research was conducted in the absence of any commercial or financial relationships that could be construed as a potential conflict of interest.

frontiers in Molecular Neuroscience

MINI REVIEW
published: 24 May 2016
doi: 10.3389/fnmol.2016.00034

Evaluation of Gene Therapy as an Intervention Strategy to Treat Brain Injury from Stroke

Amanda J. Craig and Gary D. Housley*

Translational Neuroscience Facility & Department of Physiology, School of Medical Sciences, University of New South Wales, Sydney, NSW, Australia

Stroke is a leading cause of death and disability, with a lack of treatments available to prevent cell death, regenerate damaged cells and pathways, or promote neurogenesis. The extended period of hours to weeks over which tissue damage continues to occur makes this disorder a candidate for gene therapy. This review highlights the development of gene therapy in the area of stroke, with the evolution of viral administration, in experimental stroke models, from pre-injury to clinically relevant timeframes of hours to days post-stroke. The putative therapeutic proteins being examined include anti-apoptotic, pro-survival, anti-inflammatory, and guidance proteins, targeting multiple pathways within the complex pathology, with promising results. The balance of findings from animal models suggests that gene therapy provides a viable translational platform for treatment of ischemic brain injury arising from stroke.

Keywords: ischemia, viral vector, protein expression, AAV, adeno, herpes simplex virus, lentivirus

OPEN ACCESS

Edited by:
George Smith,
Lewis Katz School of Medicine at Temple University, USA

Reviewed by:
Muzamil Ahmad,
Indian Institute of Integrative Medicine, India
Nicole Déglon,
Lausanne University Hospital, Switzerland
Stefan Momma,
University Hospital Frankfurt, Germany

****Correspondence:***
Amanda J. Craig
a.craig@unsw.edu.au

Received: *31 January 2016*
Accepted: *06 May 2016*
Published: *24 May 2016*

Citation:
Craig AJ and Housley GD (2016) Evaluation of Gene Therapy as an Intervention Strategy to Treat Brain Injury from Stroke. Front. Mol. Neurosci. 9:34. doi: 10.3389/fnmol.2016.00034

STOKE: PREVALENCE AND TREATMENT OPTIONS

This review considers the opportunity that gene therapy targeting neuroprotective protein expression in the brain may lend to development of novel treatments for stroke. Stroke is a leading cause of death throughout the world, and in Australia, stroke is the leading cause of severe disability; one in five people die within 1 month of their first infarct and one in three die within a year. About 88% of stroke survivors live at home and most have a disability (Banks et al., 2010; Thrift et al., 2014; Mozaffarian et al., 2015). These statistics reflect the need to develop therapeutics for stroke, whether being an ischemic event, or a hemorrhagic stroke, as there are currently limited clinical treatment options, rehabilitation often frustrates expectation, and the aging population will further exacerbate the health burden from stroke-induced brain injury.

The current treatments for acute ischemic strokes [accounting for ~87% of strokes (Mozaffarian et al., 2015)] are the intravenous administration of recombinant tissue plasminogen activator (rtPA) to enzymatically digest the thrombi, endovascular therapy to mechanically remove the large proximal clots, or a combination of both treatment regimes, with the aim to restore blood flow to the hypoperfused area. However, the proportion of stroke patients that satisfy the criteria to undergo treatment is low. Approximately 94% of patients are ineligible for treatment with rtPA (de Los Rios la Rosa et al., 2012; Madsen et al., 2015), due to diminishing benefit and increased risk when administrating rtPA more than 4.5 h after the ischemic event, in addition to exclusion criteria which includes those patients >80 years, taking anticoagulants, with a history of previous strokes in the last 3 months, those with severe or mild strokes, or lacking a penumbral region (de Los Rios la Rosa et al., 2012; Emberson et al., 2014; Saver et al., 2015). Moreover, the effectiveness

of rtPA is limited; only ∼10% of patients have a better outcome with treatment, with the site and nature of the occlusion appearing to be a factor in efficacy (Paciaroni et al., 2012; Emberson et al., 2014). Hence this approach addresses <1% of stroke incidences. There are conflicting reports of clinical outcomes following endovascular therapy, with trials indicating mechanical thrombectomy provides benefit when not coupled with rtPA, the lack of benefit of endovascular therapy with tPA, or that endovascular therapy improves patient outcomes when undertaken following tPA treatment (Broderick et al., 2013; Paciaroni et al., 2015; Saver et al., 2015). In addition to the low eligibility rate to receive treatment following acute ischemic stroke, reperfusion may result in ischemia–reperfusion injury or subsequent hemorrhage (Paciaroni et al., 2012; Emberson et al., 2014).

To date, there are no therapeutic interventions available to inhibit neuronal cell death, or to facilitate regeneration or neurogenesis following a neuronal injury. Research into the cellular and molecular events following an ischemic event in the brain provide a key resource for evaluation of putative therapeutics (Dirnagl et al., 1999; Moskowitz et al., 2010). Of particular interest is a range of endogenous proteins whose expression is up-regulated by stroke-induced brain ischemia, where manipulation of expression may contribute to neuroprotection, neuroregeneration, or neurogenesis. Clinically, it is essential that the manipulation of the expression profile of these proteins is matched to the therapeutic time window following stroke; for example, targeting necrosis, which occurs in the minutes following neuronal injury, may be practically unachievable, whereas manipulation of proteins that have anti-apoptotic or anti-inflammatory properties presents a far more realistic timeframe of therapy-delivery in the hours or days following a stroke (**Figure 1**).

CONSIDERATIONS AROUND GENE THERAPY PLATFORMS

When undertaking gene therapy, in addition to the success of the treatment being dependent upon the gene target, consideration of the time of delivery in relation to the stroke onset, site of delivery, cell transduction, and onset and duration of gene expression are also critical considerations.

Protein Synthesis

An advantage of gene delivery as a tool for administration of a therapeutic intervention in a disorder with on-going and delayed cell death is the persistence of synthesis of the therapeutic protein over a prolonged period of time (Hallek and Wendtner, 1996); thereby diminishing the need for repeated

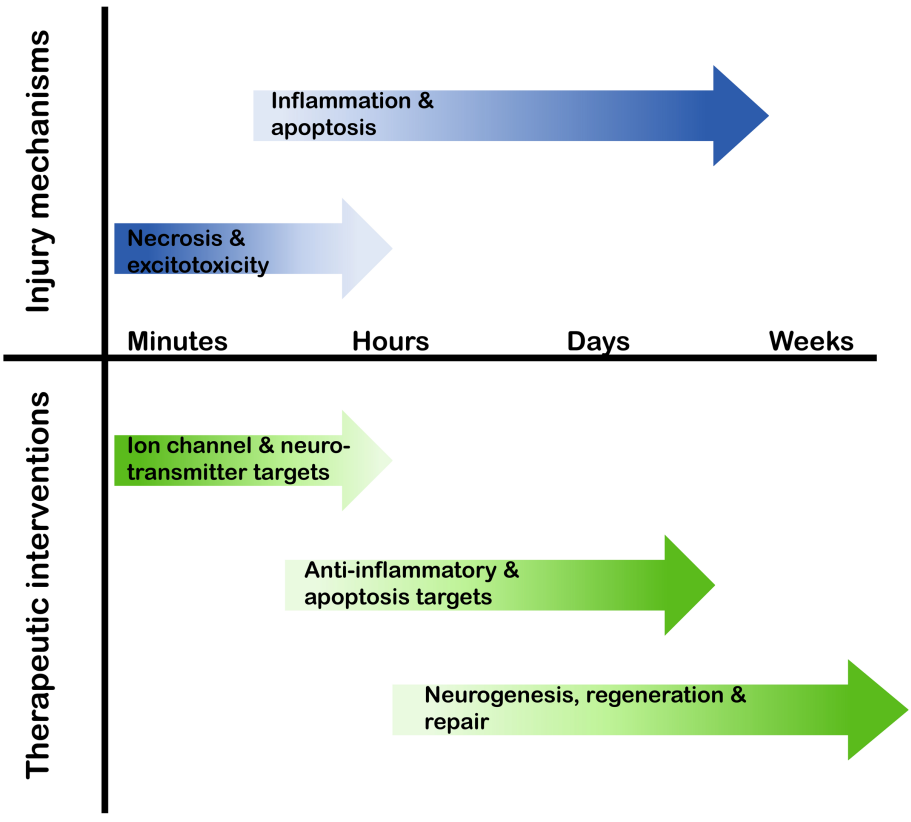

FIGURE 1 | Therapeutic target timeline following a stroke. In the minutes to weeks following a stroke the cellular and molecular pathways that are activated alter, therefore the potential therapeutic targets and possible interventional approaches need to align with this temporal profile.

and/or frequent pharmaceutical interventions. In the context of this review, the long-term expression of therapeutic proteins has been demonstrated in rodent models of stroke (**Table 1**), with proteins evident at 7 weeks following ischemia, with an administration time-point of 3–5 weeks prior to injury, totaling 12 weeks of protein expression (Andsberg et al., 2002; Arvidsson et al., 2003).

Conversely, the reliance of host-mediated protein synthesis of the viral-encoded sequences, following an ischemic event, may be compromised, and, therefore, result in diminished putative therapeutic efficacy, due to the inherent reduction in protein synthesis associated with the brain injury (Kleihues and Hossmann, 1971). Specific to gene delivery, Lawrence et al. (1997) demonstrated herpes simplex virus (HSV)-mediated expression increased at 12 h following ischemia in ischemic tissue; however non-ischemic tissue had increased expression, to a greater extent, as early as 8 h post-ischemia. These data not only highlight a delay in peak protein expression, but also a reduction in the extent of expression with the ischemic brain injury (Lawrence et al., 1997).

Delivery Site

Down-regulation of protein synthesis can be overcome, in part, by viral delivery into a non-affected region of the brain, or to the peri-infarct area, as opposed to the ischemic area (Zhao et al., 2003; Matlik et al., 2014). This approach not only overcomes potential synthesis suppression, but delivery to striatal peri-infarct regions of the brain, post-ischemia, has shown to be an effective means of viral distribution, with viral particles hypothesized to travel toward white matter tracts during the period of edema (Matlik et al., 2014). There is also evidence of virally derived proteins in brain regions remote of the initial viral delivery site (Hermann et al., 2001b). Alternatively, viral delivery into sites remote of the brain, such as a stroke-affected limb may promote corticospinal axonal sprouting in the spinal cord from the less affected hemisphere driven by the viral expression of neurotrophin-3 (Duricki et al., 2016). This could present as an alternative approach to the problem of inhibition of axonal re-growth in areas with astrocytic scarring. In contrast, studies have also shown increased striatal neuronal loss following post-ischemia anterograde delivery of GDNF. Whether this result is due to the delivery mode, the protein being expressed, the relative time of expression, or a combination of all of these, as well as additional factors is yet to be determined (Arvidsson et al., 2003).

An alternative approach to overcome the time-delay of protein expression is to express the viral-derived proteins in stem cells, which are then transplanted by intracerebroventricular injection (Watanabe et al., 2004; Chen et al., 2016). This method has resulted in reduced infarct volume and increased behavioral outcomes and may be a viable adjunct to gene delivery, with clinical trials of stem cell therapy in stroke patients already well established (Jeong et al., 2014).

Viral Vectors

The design of the viral vector is an important component in gene delivery, ensuring that the virus is not pathogenic or induces neurotoxicity, targeted cell-specific delivery can be facilitated or alternatively the vector can be developed for broad transduction, and gene expression duration can be appropriately modulated. The desired expression profile of the protein should be considered in terms of expression instigation, duration, and efficacy. The four most commonly used viral vectors are HSV type-1 (Bloom et al., 1995; Carpenter and Stevens, 1996), adenovirus (Ad; Akli et al., 1993), recombinant adeno-associated virus (rAAV; Hallek and Wendtner, 1996), and lentivirus (Naldini et al., 1996). Each have their own innate attributes and deficiencies, which must be considered in relation to the size of the gene sequence to be inserted, the target cell population, and the protein expression profile. In addition to the innate variations between viral vector system, viral serotypes will also affect the target cell specificity and protein expression (Davidson et al., 2000; von Jonquieres et al., 2013, 2016). As noted below, HSV vector-mediated expression has been reported with a few hours (Hoehn et al., 2003), whereas other commonly used viral vectors exhibit expression profiles that take days or weeks to establish (Mason et al., 2010). Further alterations in the expression profile of the protein of interest can be driven with capsid modifications, as well as the promoter used to drive gene expression, which can bias glial versus neuronal expression, and the potential to incorporate gene cassette control elements (von Jonquieres et al., 2013, 2016). The broad consideration of technical development of gene therapy platforms for clinical applications, including non-viral modalities, and use of gene regulatory strategies such as shRNA are outside of the scope of this review, which is a perspective on the opportunity and exemplar prospective gene targets.

THERAPEUTIC PROTEIN CANDIDATES FOR STROKE TREATMENTS

Bcl-2 Family

In terms of a gene-delivered therapy following stroke, the anti-apoptotic proteins within the B-cell lymphoma-2 (Bcl-2) family, including Bcl-2 itself, Bcl-extra long (Bcl-XL), and Bcl-2-like 2 (Bcl-2l2 or Bcl-w), are an obvious therapeutic choice due to their intrinsic role in modulating apoptosis and neurogenesis (Czabotar et al., 2014). Evidence of the neuroprotective capabilities of Bcl-2 has been demonstrated in a variety of injury models, with roles including modulation of intracellular Ca^{2+} concentration (Zhong et al., 1993; Murphy and Fiskum, 1999), reducing reactive oxygen species (Kane et al., 1993), and inhibiting the translocation of apoptosis-inducing factor (Zhao et al., 2004), all of which are prevalent following stroke. Furthermore, transgenic mice experiments have shown that over-expression of Bcl-2 provides neuroprotection following ischemia (Kitagawa et al., 1998). In addition, the over-expression of Bcl-2 induces neurogenesis following ischemic injury (Lei et al., 2012).

The therapeutic effectiveness of Bcl-2 anti-apoptotic proteins, expressed from viral vectors including HSV (Linnik et al., 1995; Lawrence et al., 1997; Yenari et al., 2001), Ad (Kilic et al., 2002), rAAV (Sun et al., 2003), and lentivirus (Wong et al., 2005) has been demonstrated in middle cerebral artery occlusion (MCAO) and bilateral common carotid artery (CCA) occlusion models of

stroke in rodents, as well as a model of excitotoxicity (**Table 1**). The administration of the viral vector ranged from 3 weeks pre-ischemic insult to 4 h post-ischemia, which provide proof-of-principle data, but are sub-optimal for clinical translation. The most promising studies utilized administration of a HSV-Bcl-2 construct at 30 and 90 min following MCAO, with significant neuroprotection achieved (Lawrence et al., 1997; Yenari et al., 2001). Disappointingly, there was a lack of neuroprotection

TABLE 1 | Viral gene delivery in animal models of stroke.

Protein	Viral vector	Administration (pre-/post-injury)	Stroke model	Neuroprotective	Reference
Bcl-XL	Ad	7 days pre-	Mouse; 30 min or 2 h MCAO	Yes	Kilic et al., 2002
Bcl-2	Lentivirus	3 weeks pre-	Rat; NMDA in hippocampus	Yes	Wong et al., 2005
	HSV	24 h pre-	Rat; permanent MCAO	Yes	Linnik et al., 1995
	HSV	30 mins post-	Rat; 1 h MCAO	Yes	Lawrence et al., 1997
	HSV	1.5 h post-	Rat; 1 h MCAO	Yes	Yenari et al., 2001
	HSV	4 h post-	Rat; 1 h MCAO	No	Lawrence et al., 1997
Bcl-w	rAAV	3 weeks pre-	Rat; 1.5 h MCAO	Yes	Sun et al., 2003
BDNF	rAAV	4–5 weeks pre-	Rat; 30 min MCAO	Yes	Andsberg et al., 2002
	rAAV	14 days pre-	Rat; various MCAO models	Yes	Zhang et al., 2011
CDNF	rAAV	2 days post-	Rat; 1 h bilateral CCA and right MCAO	No	Matlik et al., 2014
CNTF	Ad	7 days pre-	Mouse; 30 min MCAO	Yes	Hermann et al., 2001b
GDNF	Lentivirus	3 weeks pre-	Rat NMDA to hippocampus	Yes	Wong et al., 2005
	Ad	7 days pre-	Mouse; 30 min MCAO	Yes	Hermann et al., 2001a,b
	HSV	4 days pre- and	Rat; 1 h MCAO	Yes	Harvey et al., 2003
	HSV	3 days post-	Rat; 1 h MCAO	No, but behavioral improvement	Harvey et al., 2003
	Ad	During and	Rat; 1.5 h MCAO	Yes	Zhang et al., 2002
	Ad	1 h post-	Rat; 1.5 h MCAO	No	Zhang et al., 2002
	rAAV	During	Rat; 1.5 h bilateral CCA and right MCAO	Yes	Tsai et al., 2000, 2006
HB-EGF	rAAV	6–7 days post-	Rat; 80 min MCAO	No, but functional recovery with neurogenesis and angiogenesis	Sugiura et al., 2005
NGF	rAAV	4–5 weeks pre-	Rat; 30 min MCAO	Yes	Andsberg et al., 2002
NT3	rAAV	24 h post-	Rat; endothelin-1	No, but improved behavioral and sensory outcomes	Duricki et al., 2016
HSP-27	HSV	3 days pre-	Rat; 30 min MCAO	Yes	Badin et al., 2006
	HSV	30 mins post-	Rat; 30 min MCAO	Yes	Badin et al., 2009
HSP-70	HSV	3 days pre-	Rat; 30 min MCAO	No	Badin et al., 2006
	HSV	30 mins post-	Rat; 30 min MCAO	No	Badin et al., 2009
HSP-72	HSV	24 h pre-	Rat; 1 h MCAO	Yes	Yenari et al., 1998
	HSV	17 h pre-	Rat; 8 min bilateral CCA	Yes	Kelly et al., 2002
	HSV	0.5 and 2 h post-	Rat; 1 h MCAO	Yes	Hoehn et al., 2001
	HSV	5 h post-	Rat; 1 h MCAO	No	Hoehn et al., 2001
Gpx	HSV	12 h pre-	Rat; 1 h MCAO	Yes	Hoehn et al., 2003
		2 and 5 h post-	Rat; 1 h MCAO	Yes	Hoehn et al., 2003
CXCL12 (SDF-1α)	Ad	3 days pre- and	Rat; 1.5 h MCAO	Yes	Yoo et al., 2012
	Ad	7 days post-	Rat; 1.5 h MCAO	Yes	Yoo et al., 2012
	rAAV	7 days post -	Mouse; permanent MCAO	Protects myelin sheath	Li et al., 2015
	rAAV	7 days post-	Mouse; permanent MCAO	Yes	Li et al., 2014
IL-1 receptor antagonist	rAAV	During	Rat; 1.5 h bilateral CCA and right MCAO	Yes	Tsai et al., 2003
Netrin-1	rAAV	1 day post-	Rat; 1 h bilateral CCA and left MCAO	No, but increased vascularisation and improved behavior	Sun et al., 2011

The efficacy of gene therapy as a treatment option following stroke, to facilitate the expression of various proteins, has been assessed in several animal models of stroke with the administration of viral vectors tested both pre- and post-ischemia. Outcomes of neuroprotection varied between infarct volume and neuronal cell counts. Ad, adenovirus; rAAV, recombinant adeno-associated virus; BDNF, brain derived neurotrophic factor; CCA, common carotid artery; CDNF, cerebral dopamine neurotrophic factor; CNTF, ciliary neurotrophic factor; CXCL – CXC chemokine ligand; GDNF, glial cell-derived neurotrophic factor; Gpx, glutathione peroxidase; HB-EGF, heparin-binding epidermal growth factor-like growth factor; HSP, heat shock protein; HSV, herpes simplex virus; MCAO, middle cerebral artery occlusion; NMDA, N-methyl D-aspartate; NT, neurotrophin; SDF, stromal cell-derived factor.

afforded at the 4 h post-ischemic administration time-point, which is postulated to be due to decreased protein synthesis following ischemia (Lawrence et al., 1997).

Heat Shock Proteins

The heat shock proteins (HSP) are stress-related proteins with chaperone properties. Of particular interest are the HSP-70 family, comprising of the constitutive HSP-70 and the homologous inducible HSP-72, which are up-regulated following cerebral ischemia (Brea et al., 2015). The over-expression of HSP-72 proteins in transgenic mice has provided evidence of the neuroprotective role following cerebral ischemia (Xu et al., 2011). In addition, the smaller HSP-27 (also known as HSP-25), similarly, provides neuroprotection following ischemia, when over-expressed in a transgenic mouse model (van der Weerd et al., 2010). The success of the HSPs in providing neuroprotection when transduced has been varied (**Table 1**), with studies finding neuroprotection evident with HSV-HSP-72 delivery 3 days pre-insult to 2 h post-insult, but not when administered 5 h post-ischemia (Yenari et al., 1998; Hoehn et al., 2001; Kelly et al., 2002). Conversely, HSP-70 did not confer neuroprotection when administered 3 days pre- or 30 min post-ischemia, while HSP-27 did with similar administration and injury models (Badin et al., 2006, 2009). These differences may, in part, be due to the method in which neuroprotection is measured, with studies varying from counts of transduced surviving striatal neurons to infarct volume analysis following magnetic resonance imaging (Kelly et al., 2002; Badin et al., 2009). Additionally, the neuroprotective effect of HSP-72 may lie not only with its innate role in protein chaperoning, but also in the induction of Bcl-2 expression, possibly enhancing the neuroprotective effect following ischemia (Lawrence et al., 1997).

Antioxidant Enzymes

Antioxidant enzymes, such as superoxide dismutase (SOD), catalase, and glutathione peroxidase (Gpx), are postulated to reduce brain damage incurred due to increases in reactive oxygen species following stroke. Transgenic animal studies have shown that over-expression, or deficiencies, of antioxidant enzymes affects the outcome following stroke (Murakami et al., 1997; Chan et al., 1998; Kawase et al., 1999). Gene delivery of Gpx both pre- and up to 5 h post-MCAO conferred neuroprotection, in conjunction with an increase in Bcl-2 (**Table 1**). It is proposed that the neuroprotective effect seen with administering the gene therapy at 5 h post-ischemia may be attributed to both the benefit of the antioxidant action, as well as the anti-apoptotic properties of Bcl-2, accounting in part for why the Bcl-2 administration alone was not neuroprotective when administered 4 h post-ischemia (Hoehn et al., 2001). The HSV construct was reported to drive Gpx expression at 4–6 h post-administration, which indicates the therapeutic time window for the Gpx action was 9–11 h post-MCAO, in the rat model. This is in line with the belief that complex pathologies such as stroke will require therapeutic agents to target multiple pathways for inhibition and/or activation to be truly efficacious (Moretti et al., 2015).

Neurotrophins

Neurotrophins have a role in the regulation of neuronal tissue development and repair, promoting survival, differentiation, and maintenance in physiological and pathological conditions. Neurotrophin gene cassettes, therefore, offer broad potential for therapy following stroke (Lindholm et al., 2007; Machalinski, 2014; Otsuka et al., 2016). Experimentally, various *in vitro* and *in vivo* ischemic injury models have been utilized to demonstrate the neuroprotective efficacy of neurotrophins, including brain-derived neurotrophic factor (BDNF; Zhang and Pardridge, 2001; Otsuka et al., 2016), glial cell-derived neurotrophic factor (GDNF; Yuan et al., 2013), and nerve growth factor (NGF; Semkova and Krieglstein, 1999; Tabakman et al., 2005). This has been further translated to delivery of gene cassettes for the recombinant neurotrophic factors, including BDNF (Andsberg et al., 2002; Zhang et al., 2011), GDNF (Tsai et al., 2000, 2006; Hermann et al., 2001a,b; Zhang et al., 2002; Harvey et al., 2003; Wong et al., 2005), ciliary neurotrophic factor (CNTF; Hermann et al., 2001a), and cerebral dopamine neurotrophic factor (CDNF; Matlik et al., 2014). These gene therapy agents have been shown to provide neuroprotection with viral vector delivery, including HSV, Ad, and rAAV, in MCAO models of stroke in rodents (**Table 1**). When the viral vectors were administered either pre-ischemia, during, or up to 1 h following ischemia, the infarct volume was significantly reduced, as was caspase-3 expression (Hermann et al., 2001a,b; Zhang et al., 2002; Harvey et al., 2003; Matlik et al., 2014). Further increasing the therapeutic window to 6–7 days post-injury, with the administration of heparin-binding epidermal growth factor-like growth factor (HB-EGF; Sugiura et al., 2005), did not provide the same reduction in infarct volume. This outcome may be expected considering the timeline of neuropathological pathways activated in relation to therapy administration time. However, there was an increase in angiogenesis and improved functional recovery, modulated by the gene delivery of HB-EGF. As clinical outcomes in humans are not measured in terms of infarct volumes but rather as an improvement of motor function and cognition, these results in animal models are encouraging for translation of the gene targets, demonstrating a positive outcome coupled with a clinically relevant administration timeframe. Therapeutic targets for the neurotrophin signaling cascade may be very broad, including the neurotrophins themselves, the corresponding tropomyosin-related kinase (Trk) receptors (also referred to as receptor tyrosine kinases), and potentially second messenger-coupled effectors such as ion channels modulated downstream of phospholipase Cγ activation.

Chemokines

Chemokines are inflammatory mediators that are up-regulated following stroke, with a role in recruiting leukocytes to the area of damage in the brain. The resulting inflammation in the brain can increase the severity of the stroke, or conversely the recruited phagocytes aid in cellular debris clearance, or a combination of both (García-Berrocoso et al., 2014). The expression of the chemokine CXCL-12, otherwise known as stromal cell-derived factor-1 (SDF-1), is constitutively expressed in the

brain, with increased expression occurring following ischemia (Wang et al., 2012). Studies modulating endogenous CXCL-12 following stroke provide contrasting results. The inhibition of CXCL-12 with the receptor CXCR4, by delivery of receptor antagonist during the acute post-ischemic time period, improved behavioral recovery and reduced infarct volumes (Ruscher et al., 2013). Similarly, rAAV gene delivery of the IL-1 receptor antagonist reduced infarct volume (**Table 1**) (Tsai et al., 2003). However, in a study with forced limb use following stroke, the administration of the CXCR4 antagonist resulted in a deficit in recovery with worse motor and cognitive outcomes (Zhao et al., 2015). Gene delivery studies have provided evidence of the benefit of CXCL-12 following stroke. Adenoviral or rAAV gene delivery of CXCL-12 into mice and rats, administered from 3 days pre-ischemia to 7 days post-ischemia reduced brain atrophy, maintained myelin sheath integrity, increased oligodendrocyte progenitor cell proliferation and migration, and the promotion of angiogenesis (Yoo et al., 2012; Li et al., 2014, 2015). Further contrast is seen in clinical studies, with a positive correlation between increased serum CXCL-12 levels and poor outcome in stroke patients in a Chinese cohort, but increases in CXCL-12 serum levels in patients transplanted with autologous mesenchymal stem cells correlating to improved outcome (Lee et al., 2010; Liu et al., 2015; Cheng et al., 2016).

Guidance Proteins

In contrast to therapeutic proteins targeting neuroprotection, gene therapy can also be utilized to express proteins to aid in regeneration. Netrins are axon and cell guidance proteins, that are expressed both during neural development and in the mature nervous system in physiological conditions, with up-regulation of expression occurring in the peri-infarct region 14 days following ischemia (Moore et al., 2007; Tsuchiya et al., 2007). Gene delivery of netrin-1 with rAAV, 1 day following ischemia, resulted in an increase in peri-infarct vascularisation and immature neuronal migration. Despite the lack in reduction of infarct volume, there was an improvement in post-stroke locomotor activity, motor asymmetry, and exploratory behavior (Sun et al., 2011).

CONCLUSION

Stroke is a complex pathology with a multitude of biochemical, cellular, and molecular pathways instigated differentially over time, providing a challenge to target therapeutically, while also providing multiple opportunities for intervention. The aim for stroke researchers to develop therapeutics that will increase survival probability of patients, as well as improve cognitive and behavioral recovery, whilst ensuring therapeutic delivery within a clinically relevant timeframe is challenging. However, enhancing the expression of endogenous proteins or facilitating expression in areas most susceptible to damage, by gene delivery, provides promise, with progress being made in both the therapeutic window for delivery and an expanding range of potential protein targets. The use of these therapies in conjunction with the currently available treatments, such as rtPA or mechanical clot removal, is an additional area of research to be explored. Despite the promising progress, further research will need to be undertaken before these therapies reach clinical trials, as the regulatory challenges for gene therapy trials are particularly arduous.

AUTHOR CONTRIBUTIONS

The authors listed have made substantial, direct and intellectual contributions to the work, and approved it for publication.

REFERENCES

Akli, S., Caillaud, C., Vigne, E., Stratford-Perricaudet, L. D., Poenaru, L., Perricaudet, M., et al. (1993). Transfer of a foreign gene into the brain using adenovirus vectors. *Nat. Genet.* 3, 224–228. doi: 10.1038/ng0393-224

Andsberg, G., Kokaia, Z., Klein, R. L., Muzyczka, N., Lindvall, O., and Mandel, R. J. (2002). Neuropathological and behavioral consequences of adeno-associated viral vector-mediated continuous intrastriatal neurotrophin delivery in a focal ischemia model in rats. *Neurobiol. Dis.* 9, 187–204. doi: 10.1006/nbdi.2001.0456

Arvidsson, A., Kirik, D., Lundberg, C., Mandel, R. J., Andsberg, G., Kokaia, Z., et al. (2003). Elevated GDNF levels following viral vector-mediated gene transfer can increase neuronal death after stroke in rats. *Neurobiol. Dis.* 14, 542–556. doi: 10.1016/j.nbd.2003.08.002

Badin, R. A., Lythgoe, M. F., van der Weerd, L., Thomas, D. L., Gadian, D. G., and Latchman, D. S. (2006). Neuroprotective effects of virally delivered HSPs in experimental stroke. *J. Cereb. Blood Flow Metab.* 26, 371–381. doi: 10.1038/sj.jcbfm.9600190

Badin, R. A., Modo, M., Cheetham, M., Thomas, D. L., Gadian, D. G., Latchman, D. S., et al. (2009). Protective effect of post-ischaemic viral delivery of heat shock proteins in vivo. *J. Cereb. Blood Flow Metab.* 29, 254–263. doi: 10.1038/jcbfm.2008.106

Banks, P., Franks, N. P., and Dickinson, R. (2010). Competitive inhibition at the glycine site of the N-methyl-D-aspartate receptor mediates xenon neuroprotection against hypoxia-ischemia. *Anesthesiology* 112, 614–622. doi: 10.1097/ALN.0b013e3181cea398

Bloom, D. C., Maidment, N. T., Tan, A., Dissette, V. B., Feldman, L. T., and Stevens, J. G. (1995). Long-term expression of a reporter gene from latent herpes simplex virus in the rat hippocampus. *Brain Res. Mol. Brain Res.* 31, 48–60. doi: 10.1016/0169-328x(95)00031-m

Brea, D., Agulla, J., Staes, A., Gevaert, K., Campos, F., Sobrino, T., et al. (2015). Study of protein expresion in peri-infarct tissue after cerebral ischemia. *Sci. Rep.* 5:12030. doi: 10.1038/srep12030

Broderick, J. P., Palesch, Y. Y., Demchuk, A. M., Yeatts, S. D., Khatri, P., Hill, M. D., et al. (2013). Endovascular therapy after intravenous t-PA versus t-PA alone for stroke. *N. Engl. J. Med.* 368, 893–903. doi: 10.1056/NEJMoa1214300

Carpenter, D. E., and Stevens, J. G. (1996). Long-term expression of a foreign gene from a unique position in the latent herpes simplex virus genome. *Hum. Gene Ther.* 7, 1447–1454. doi: 10.1089/hum.1996.7.12-1447

Chan, P. H., Kawase, M., Murakami, K., Chen, S. F., Li, Y., Calagui, B., et al. (1998). Overexpression of SOD1 in transgenic rats protects vulnerable neurons against ischemic damage after global cerebral ischemia and reperfusion. *J. Neurosci.* 18, 8292–8299.

Chen, B., Zhang, F., Li, Q.-Y., Gong, A., and Lan, Q. (2016). Protective effect of Ad-VEGF-Bone mesenchymal stem cells on cerebral infarction. *Turk. Neurosurg.* 26, 8–15. doi: 10.5137/1019-5149.jtn.11488-14.3

Cheng, X., Lian, Y., Ma, Y., Xie, N., and Wu, C. (2016). Elevated serum levels of CXC Chemokine Ligand-12 are associated with unfavorable functional outcome and mortality at 6-month follow-up in chinese patients with acute ischemic stroke. *Mol. Neurobiol.* doi: 10.1007/s12035-015-9645-9 [Epub ahead of print].

Czabotar, P. E., Lessene, G., Strasser, A., and Adams, J. M. (2014). Control of apoptosis by the BCL-2 protein family: implications for physiology and therapy. *Nat. Rev. Mol. Cell Biol.* 15, 49–63. doi: 10.1038/nrm3722

Davidson, B. L., Stein, C. S., Heth, J. A., Martins, I., Kotin, R. M., Derksen, T. A., et al. (2000). Recombinant adeno-associated virus type 2, 4, and 5 vectors: transduction of variant cell types and regions in the mammalian central nervous system. *Proc. Natl. Acad. Sci. U.S.A.* 97, 3428–3432. doi: 10.1073/pnas.050581197

de Los Rios la Rosa, F., Khoury, J., Kissela, B. M., Flaherty, M. L., Alwell, K., Moomaw, C. J., et al. (2012). Eligibility for intravenous recombinant tissue-type plasminogen activator within a population: the effect of the european cooperative acute stroke study (ECASS) III trial. *Stroke* 43, 1591–1595. doi: 10.1161/strokeaha.111.645986

Dirnagl, U., Iadecola, C., and Moskowitz, M. A. (1999). Pathobiology of ischaemic stroke: an integrated view. *Trends Neurosci.* 22, 391–397. doi: 10.1016/S0166-2236(99)01401-0

Duricki, D. A., Hutson, T. H., Kathe, C., Soleman, S., Gonzalez-Carter, D., Petruska, J. C., et al. (2016). Delayed intramuscular human neurotrophin-3 improves recovery in adult and elderly rats after stroke. *Brain* 139, 259–275. doi: 10.1093/brain/awv341

Emberson, J., Lees, K. R., Lyden, P., Blackwell, L., Albers, G., Bluhmki, E., et al. (2014). Effect of treatment delay, age, and stroke severity on the effects of intravenous thrombolysis with alteplase for acute ischaemic stroke: a meta-analysis of individual patient data from randomised trials. *Lancet* 384, 1929–1935. doi: 10.1016/s0140-6736(14)60584-5

García-Berrocoso, T., Giralt, D., Llombart, V., Bustamante, A., Penalba, A., Flores, A., et al. (2014). Chemokines after human ischemic stroke: from neurovascular unit to blood using protein arrays. *Transl. Proteom.* 3, 1–9. doi: 10.1016/j.trprot.2014.03.001

Hallek, M., and Wendtner, C. M. (1996). Recombinant adeno-associated virus (rAAV) vectors for somatic gene therapy: recent advances and potential clinical applications. *Cytokines Mol. Ther.* 2, 69–79.

Harvey, B. K., Chang, C. F., Chiang, Y. H., Bowers, W. J., Morales, M., Hoffer, B. J., et al. (2003). HSV amplicon delivery of glial cell line-derived neurotrophic factor is neuroprotective against ischemic injury. *Exp. Neurol.* 183, 47–55. doi: 10.1016/S0014-4886(03)00080-3

Hermann, D. M., Kilic, E., Kugler, S., Isenmann, S., and Bahr, M. (2001a). Adenovirus-mediated GDNF and CNTF pretreatment protects against striatal injury following transient middle cerebral artery occlusion in mice. *Neurobiol. Dis.* 8, 655–666. doi: 10.1006/nbdi.2001.0399

Hermann, D. M., Kilic, E., Kugler, S., Isenmann, S., and Bahr, M. (2001b). Adenovirus-mediated glial cell line-derived neurotrophic factor (GDNF) expression protects against subsequent cortical cold injury in rats. *Neurobiol. Dis.* 8, 964–973. doi: 10.1006/nbdi.2001.0448

Hoehn, B., Ringer, T. M., Xu, L., Giffard, R. G., Sapolsky, R. M., Steinberg, G. K., et al. (2001). Overexpression of HSP72 after induction of experimental stroke protects neurons from ischemic damage. *J. Cereb. Blood Flow Metab.* 21, 1303–1309. doi: 10.1097/00004647-200111000-00006

Hoehn, B., Yenari, M. A., Sapolsky, R. M., and Steinberg, G. K. (2003). Glutathione peroxidase overexpression inhibits cytochrome c release and proapoptotic mediators to protect neurons from experimental stroke. *Stroke* 34, 2489–2494. doi: 10.1161/01.str.0000091268.25816.19

Jeong, H., Yim, H. W., Cho, Y.-S., Kim, Y.-I., Jeong, S.-N., Kim, H.-B., et al. (2014). Efficacy and safety of stem cell therapies for patients with stroke: a systematic review and single arm meta-analysis. *Int. J. Stem Cells* 7, 63–69. doi: 10.15283/ijsc.2014.7.2.63

Kane, D., Sarafian, T., Anton, R., Hahn, H., Gralla, E., Valentine, J., et al. (1993). Bcl-2 inhibition of neural death: decreased generation of reactive oxygen species. *Science* 262, 1274–1277. doi: 10.1126/science.8235659

Kawase, M., Murakami, K., Fujimura, M., Morita-Fujimura, Y., Gasche, Y., Kondo, T., et al. (1999). Exacerbation of delayed cell injury after transient global ischemia in mutant mice with CuZn superoxide dismutase deficiency. *Stroke* 30, 1962–1968. doi: 10.1161/01.str.30.9.1962

Kelly, S., Zhang, Z., Zhao, H., Xu, L., Giffard, R., Sapolsky, R., et al. (2002). Gene transfer of HSP72 protects cornu ammonis 1 region of the hippocampus neurons from global ischemia: influence of Bcl-2. *Ann. Neurol.* 52, 160–167. doi: 10.1002/ana.10264

Kilic, E., Hermann, D. M., Kügler, S., Kilic, U., Holzmüller, H., Schmeer, C., et al. (2002). Adenovirus-mediated Bcl-X(L) expression using a neuron-specific synapsin-1 promoter protects against disseminated neuronal injury and brain infarction following focal cerebral ischemia in mice. *Neurobiol. Dis.* 11, 275–284. doi: 10.1006/nbdi.2002.0552

Kitagawa, K., Matsumoto, M., Tsujimoto, Y., Ohtsuki, T., Kuwabara, K., Matsushita, K., et al. (1998). Amelioration of hippocampal neuronal damage after global ischemia by neuronal overexpression of BCL-2 in transgenic mice. *Stroke* 29, 2616–2621. doi: 10.1161/01.str.29.12.2616

Kleihues, P., and Hossmann, K. (1971). Protein synthesis in the cat brain after prolonged cerebral ischemia. *Brain Res.* 35, 409–418. doi: 10.1016/0006-8993(71)90484-7

Lawrence, M. S., McLaughlin, J. R., Sun, G. H., Ho, D. Y., McIntosh, L., Kunis, D. M., et al. (1997). Herpes simplex viral vectors expressing Bcl-2 are neuroprotective when delivered after a stroke. *J. Cereb. Blood Flow Metab.* 17, 740–744. doi: 10.1097/00004647-199707000-00003

Lee, J., Hong, J., Moon, G., Lee, P., Ahn, Y., and Bang, O. (2010). A long-term follow-up study of intravenous autologous mesenchymal stem cell transplantation in patients with ischemic stroke. *Stem cells* 28, 1099–1106. doi: 10.1002/stem.430

Lei, Z., Liu, F., Zhang, L., Huang, Y., and Sun, F. (2012). Bcl-2 increases stroke-induced striatal neurogenesis in adult brains by inhibiting BMP-4 function via activation of beta-catenin signaling. *Neurochem. Int.* 61, 34–42. doi: 10.1016/j.neuint.2012.04.004

Li, Y., Huang, J., He, X., Tang, G., Tang, Y. H., Liu, Y., et al. (2014). Postacute stromal cell-derived factor-1alpha expression promotes neurovascular recovery in ischemic mice. *Stroke* 45, 1822–1829. doi: 10.1161/strokeaha.114.005078

Li, Y., Tang, G., Liu, Y., He, X., Huang, J., Lin, X., et al. (2015). CXCL12 gene therapy ameliorates ischemia-induced white matter injury in mouse brain. *Stem Cells Transl. Med.* 4, 1122–1130. doi: 10.5966/sctm.2015-0074

Lindholm, P., Voutilainen, M. H., Lauren, J., Peranen, J., Leppanen, V.-M., Andressoo, J.-O., et al. (2007). Novel neurotrophic factor CDNF protects and rescues midbrain dopamine neurons in vivo. *Nature* 448, 73–77. doi: 10.1038/nature05957

Linnik, M. D., Zahos, P., Geschwind, M. D., and Federoff, H. J. (1995). Expression of bcl-2 from a defective herpes simplex virus-1 vector limits neuronal death in focal cerebral ischemia. *Stroke* 26, 1670–1674: discussion 5. doi: 10.1161/01.str.26.9.1670

Liu, P., Xiang, J.-W., and Jin, S.-X. (2015). Serum CXCL12 levels are associated with stroke severity and lesion volumes in stroke patients. *Neurolog. Res.* 37, 853–858. doi: 10.1179/1743132815Y.0000000063

Machalinski, B. (2014). Tissue regeneration in stroke: cellular and trophic mechanisms. *Expert Rev. Neurotherapeutics* 14, 959–969. doi: 10.1586/14737175.2014.939172

Madsen, T. E., Khoury, J. C., Alwell, K. A., Moomaw, C. J., Kissela, B. M., De Los Rios La Rosa, F., et al. (2015). Analysis of tissue plasminogen activator eligibility by sex in the Greater Cincinnati/Northern Kentucky stroke study. *Stroke* 46, 717–721. doi: 10.1161/strokeaha.114.006737

Mason, M. R. J., Ehlert, E. M. E., Eggers, R., Pool, C. W., Hermening, S., Huseinovic, A., et al. (2010). Comparison of AAV serotypes for gene delivery to dorsal root ganglion neurons. *Mol. Ther.* 18, 715–724. doi: 10.1038/mt.2010.19

Matlik, K., Abo-Ramadan, U., Harvey, B. K., Arumae, U., and Airavaara, M. (2014). AAV-mediated targeting of gene expression to the peri-infarct region in rat cortical stroke model. *J. Neurosci. Methods* 236, 107–113. doi: 10.1016/j.jneumeth.2014.08.014

Moore, S., Tessier-Lavigne, M., and Kennedy, T. (2007). Netrins and their receptors. *Adv. Exp. Med. Biol.* 621, 17–31. doi: 10.1007/978-0-387-76715-4_2

Moretti, A., Ferrari, F., and Villa, R. F. (2015). Neuroprotection for ischaemic stroke: current status and challenges. *Pharmacol. Ther.* 146, 23–34. doi: 10.1016/j.pharmthera.2014.09.003

Moskowitz, M. A., Lo, E. H., and Iadecola, C. (2010). The science of stroke: mechanisms in search of treatments. *Neuron* 67, 181–198. doi: 10.1016/j.neuron.2010.07.002

Mozaffarian, D., Benjamin, E. J., Go, A. S., Arnett, D. K., Blaha, M. J., Cushman, M., et al. (2015). Heart disease and stroke statistics—2015 update: a report from the american heart association. *Circulation* 131, e29–e322. doi: 10.1161/cir.0000000000000152

Murakami, K., Kondo, T., Epstein, C. J., and Chan, P. H. (1997). Overexpression of CuZn-Superoxide dismutase reduces hippocampal injury after global ischemia in transgenic mice. *Stroke* 28, 1797–1804. doi: 10.1161/01.str.28.9.1797

Murphy, A., and Fiskum, G. (1999). Bcl-2 and Ca(2+)-mediated mitochondrial dysfunction in neural cell death. *Biochem. Soc. Symp.* 66, 33–41. doi: 10.1042/bss0660033

Naldini, L., Blömer, U., Gallay, P., Ory, D., Mulligan, R., Gage, F. H., et al. (1996). In vivo gene delivery and stable transduction of nondividing cells by a lentiviral vector. *Science* 272, 263–267. doi: 10.1126/science.272.5259.263

Otsuka, S., Sakakima, H., Sumizono, M., Takada, S., Terashi, T., and Yoshida, Y. (2016). The neuroprotective effects of preconditioning exercise on brain damage and neurotrophic factors after focal brain ischemia in rats. *Behav. Brain Res.* 303, 9–18. doi: 10.1016/j.bbr.2016.01.049

Paciaroni, M., Balucani, C., Agnelli, G., Caso, V., Silvestrelli, G., Grotta, J. C., et al. (2012). Systemic thrombolysis in patients with acute ischemic stroke and internal carotid ARtery occlusion: the ICARO study. *Stroke* 43, 125–130. doi: 10.1161/strokeaha.111.630624

Paciaroni, M., Inzitari, D., Agnelli, G., Caso, V., Balucani, C., Grotta, J. C., et al. (2015). Intravenous thrombolysis or endovascular therapy for acute ischemic stroke associated with cervical internal carotid artery occlusion: the ICARO-3 study. *J. Neurol.* 262, 459–468. doi: 10.1007/s00415-014-7550-1

Ruscher, K., Kuric, E., Liu, Y., Walter, H. L., Issazadeh-Navikas, S., Englund, E., et al. (2013). Inhibition of CXCL12 signaling attenuates the postischemic immune response and improves functional recovery after stroke. *J. Cereb. Blood Flow Metab.* 33, 1225–1234. doi: 10.1038/jcbfm.2013.71

Saver, J. L., Goyal, M., Bonafe, A., Diener, H. C., Levy, E. I., Pereira, V. M., et al. (2015). Stent-retriever thrombectomy after intravenous t-PA vs. t-PA alone in stroke. *N. Engl. J. Med.* 372, 2285–2295. doi: 10.1056/NEJMoa1415061

Semkova, I., and Krieglstein, J. (1999). Neuroprotection mediated via neurotrophic factors and induction of neurotrophic factors. *Brain Res. Rev.* 30, 176–188. doi: 10.1016/S0165-0173(99)00013-2

Sugiura, S., Kitagawa, K., Tanaka, S., Todo, K., Omura-Matsuoka, E., Sasaki, T., et al. (2005). Adenovirus-mediated gene transfer of heparin-binding epidermal growth factor-like growth factor enhances neurogenesis and angiogenesis after focal cerebral ischemia in rats. *Stroke* 36, 859–864. doi: 10.1161/01.str.0000158905.22871.95

Sun, H., Le, T., Chang, T. T. J., Habib, A., Wu, S., Shen, F., et al. (2011). AAV-mediated netrin-1 overexpression increases peri-infarct blood vessel density and improves motor function recovery after experimental stroke. *Neurobiol. Dis.* 44, 73–83. doi: 10.1016/j.nbd.2011.06.006

Sun, Y., Jin, K., Clark, K. R., Peel, A., Mao, X. O., Chang, Q., et al. (2003). Adeno-associated virus-mediated delivery of BCL-w gene improves outcome after transient focal cerebral ischemia. *Gene Ther.* 10, 115–122. doi: 10.1038/sj.gt.3301868

Tabakman, R., Jiang, H., Shahar, I., Arien-Zakay, H., Levine, R., and Lazarovici, P. (2005). Neuroprotection by NGF in the PC12 in vitro OGD model: involvement of mitogen-activated protein kinases and gene expression. *Ann. N. Y. Acad. Sci.* 1053, 84–96. doi: 10.1196/annals.1344.008

Thrift, A. G., Cadilhac, D. A., Thayabaranathan, T., Howard, G., Howard, V. J., Rothwell, P. M., et al. (2014). Global stroke statistics. *Int. J. Stroke* 9, 6–18. doi: 10.1111/ijs.12245

Tsai, T., Chen, S., Xiao, X., Chiang, Y., Lin, S., Kuo, S., et al. (2003). Gene treatment of cerebral stroke by rAAV vector delivering IL-1ra in a rat model. *Neuroreport* 14, 803–807. doi: 10.1097/01.wnr.0000065732.03340.b5

Tsai, T. H., Chen, S. L., Chiang, Y. H., Lin, S. Z., Ma, H. I., Kuo, S. W., et al. (2000). Recombinant adeno-associated virus vector expressing glial cell line-derived neurotrophic factor reduces ischemia-induced damage. *Exp. Neurol.* 166, 266–275. doi: 10.1006/exnr.2000.7505

Tsai, T. H., Chen, S. L., Xiao, X., Chiang, Y. H., and Tsao, Y. P. (2006). Gene therapy of focal cerebral ischemia using defective recombinant adeno-associated virus vectors. *Front. Biosci.* 11, 2061–2070. doi: 10.2741/1948

Tsuchiya, A., Hayashi, T., Deguchi, K., Sehara, Y., Yamashita, T., Zhang, H., et al. (2007). Expression of netrin-1 and its receptors DCC and neogenin in rat brain after ischemia. *Brain Res.* 1159, 1–7. doi: 10.1016/j.brainres.2006.12.096

van der Weerd, L., Tariq Akbar, M., Aron Badin, R., Valentim, L. M., Thomas, D. L., Wells, D. J., et al. (2010). Overexpression of heat shock protein 27 reduces cortical damage after cerebral ischemia. *J. Cereb. Blood Flow Metab.* 30, 849–856. doi: 10.1038/jcbfm.2009.249

von Jonquieres, G., Fröhlich, D., Klugmann, C. B., Wen, X., Harasta, A. E., Ramkumar, R., et al. (2016). Recombinant human myelin-associated glycoprotein promoter drives selective AAV-Mediated transgene expression in oligodendrocytes. *Front. Mol. Neurosci.* 9:13. doi: 10.3389/fnmol.2016.00013

von Jonquieres, G., Mersmann, N., Klugmann, C. B., Harasta, A. E., Lutz, B., Teahan, O., et al. (2013). Glial promoter selectivity following AAV-delivery to the immature brain. *PLoS One* 8:e65646. doi: 10.1371/journal.pone.0065646

Wang, Y., Huang, J., Li, Y., and Yang, G. (2012). Roles of chemokine CXCL12 and its receptors in ischemic stroke. *Curr. Drug Targets* 13, 166–172. doi: 10.2174/138945012799201603

Watanabe, T., Okuda, Y., Nonoguchi, N., Zhao, M. Z., Kajimoto, Y., Furutama, D., et al. (2004). Postischemic intraventricular administration of FGF-2 expressing adenoviral vectors improves neurologic outcome and reduces infarct volume after transient focal cerebral ischemia in rats. *J. Cereb. Blood Flow Metab.* 24, 1205–1213. doi: 10.1097/01.wcb.0000136525.75839.41

Wong, L.-F., Ralph, G. S., Walmsley, L. E., Bienemann, A. S., Parham, S., Kingsman, S. M., et al. (2005). Lentiviral-mediated delivery of Bcl-2 or GDNF protects against excitotoxicity in the rat hippocampus. *Mol. Ther.* 11, 89–95. doi: 10.1016/j.ymthe.2004.08.026

Xu, L., Xiong, X., Ouyang, Y., Barreto, G., and Giffard, R. (2011). Heat shock protein 72 (Hsp72) improves long term recovery after focal cerebral ischemia in mice. *Neurosci. Lett.* 488, 279–282. doi: 10.1016/j.neulet.2010.11.047

Yenari, M. A., Dumas, T. C., Sapolsky, R. M., and Steinberg, G. K. (2001). Gene therapy for treatment of cerebral ischemia using defective herpes simplex viral vectors. *Ann. N. Y. Acad. Sci.* 939, 340–357. doi: 10.1111/j.1749-6632.2001.tb03643.x

Yenari, M. A., Fink, S. L., Sun, G. H., Chang, L. K., Patel, M. K., Kunis, D. M., et al. (1998). Gene therapy with HSP72 is neuroprotective in rat models of stroke and epilepsy. *Ann. Neurol.* 44, 584–591. doi: 10.1002/ana.410440403

Yoo, J., Seo, J., Eom, J., and Hwang, D. (2012). Effects of stromal cell-derived factor 1alpha delivered at different phases of transient focal ischemia in rats. *Neuroscience* 209, 171–186. doi: 10.1016/j.neuroscience.2012.02.031

Yuan, M., Wen, S., Yang, C., Pang, Y., Gao, X., Liu, X., et al. (2013). Transplantation of neural stem cells overexpressing glial cell line-derived neurotrophic factor enhances Akt and Erk1/2 signaling and neurogenesis in rats after stroke. *Chin. Med. J.* 126, 1302–1309.

Zhang, J., Yu, Z., Yu, Z., Yang, Z., Zhao, H., Liu, L., et al. (2011). rAAV-mediated delivery of brain-derived neurotrophic factor promotes neurite outgrowth and protects neurodegeneration in focal ischemic model. *Int. J. Clin. Exp. Pathol.* 4, 496–504.

Zhang, W. R., Sato, K., Iwai, M., Nagano, I., Manabe, Y., and Abe, K. (2002). Therapeutic time window of adenovirus-mediated GDNF gene transfer after transient middle cerebral artery occlusion in rat. *Brain Res.* 947, 140–145. doi: 10.1016/S0006-8993(02)02923-2

Zhang, Y., and Pardridge, W. M. (2001). Neuroprotection in transient focal brain ischemia after delayed intravenous administration of brain-derived neurotrophic factor conjugated to a blood-brain barrier drug targeting system. *Stroke* 32, 1378–1384. doi: 10.1161/01.str.32.6.1378

Zhao, H., Yenari, M., Cheng, D., Barreto-Chang, O., Sapolsky, R., and Steinberg, G. (2004). Bcl-2 transfection via herpes simplex virus blocks apoptosis-inducing factor translocation after focal ischemia in the rat. *J. Cereb. Blood Flow Metab.* 24, 681–692. doi: 10.1097/01.wcb.0000127161.89708.a5

Zhao, H., Yenari, M. A., Cheng, D., Sapolsky, R. M., and Steinberg, G. K. (2003). Bcl-2 overexpression protects against neuron loss within the ischemic margin following experimental stroke and inhibits cytochrome c translocation and caspase-3 activity. *J. Neurochem.* 85, 1026–1036. doi: 10.1046/j.1471-4159.2003.01756.x

Zhao, S., Qu, H., Zhao, Y., Xiao, T., Zhao, M., Li, Y., et al. (2015). CXCR4 antagonist AMD3100 reverses the neurogenesis and behavioral recovery promoted by forced limb-use in stroke rats. *Restor. Neurol. Neurosci.* 33, 809–821. doi: 10.3233/rnn-150515

Zhong, L. T., Sarafian, T., Kane, D. J., Charles, A. C., Mah, S. P., Edwards, R. H., et al. (1993). bcl-2 inhibits death of central neural cells induced by multiple agents. *Proc. Natl. Acad. Sci. U.S.A.* 90, 4533–4537. doi: 10.1073/pnas.90.10.4533

Conflict of Interest Statement: The authors declare that the research was conducted in the absence of any commercial or financial relationships that could be construed as a potential conflict of interest.

frontiers in Molecular Neuroscience

MINI REVIEW
published: 02 August 2016
doi: 10.3389/fnmol.2016.00056

Adeno Associated Viral Vector Delivered RNAi for Gene Therapy of SOD1 Amyotrophic Lateral Sclerosis

Lorelei Stoica[1,2]* *and Miguel Sena-Esteves*[1,2]

[1] Gene Therapy Center, University of Massachusetts Medical School, Worcester, MA, USA, [2] Department of Neurology, University of Massachusetts Medical School, Worcester, MA, USA

Amyotrophic Lateral Sclerosis (ALS) is a fatal neurodegenerative disease caused by progressive loss of upper and lower motor neurons. Mutations in superoxide dismutase 1 (*SOD1*) are a leading cause of ALS, responsible for up to 20% of familial cases. Although the exact mechanism by which mutant SOD1 causes disease remains unknown, multiple studies have shown that reduction of the mutant species leads to delayed disease onset and extension of lifespan of animal models. This makes SOD1 an ideal target for gene therapy coupling adeno associated virus vector (AAV) gene delivery with RNAi molecules. In this review we summarize the studies done thus far attempting to decrease *SOD1* gene expression, using AAV vectors as delivery tools, and RNAi as therapeutic molecules. Current hurdles to be overcome, such as the need for widespread gene delivery through the entire central nervous system (CNS), are discussed. Continued efforts to improve current AAV delivery methods and capsids will accelerate the application of these therapeutics to the clinic.

Keywords: AAV vectors, superoxide dismutase, ALS, RNAi, gene therapy

OPEN ACCESS

Edited by:
Andrew Paul Tosolini,
University College of London, UK

Reviewed by:
Subhabrata Sanyal,
Biogen, USA
Laura Ferraiuolo,
University of Sheffield, UK

***Correspondence:**
Lorelei Stoica
lorelei.stoica@umassmed.edu

Received: *23 May 2016*
Accepted: *04 July 2016*
Published: *02 August 2016*

Citation:
Stoica L and Sena-Esteves M (2016) Adeno Associated Viral Vector Delivered RNAi for Gene Therapy of SOD1 Amyotrophic Lateral Sclerosis. Front. Mol. Neurosci. 9:56. doi: 10.3389/fnmol.2016.00056

INTRODUCTION

Amyotrophic lateral sclerosis (ALS) is a progressive neuromuscular disorder, resulting in loss of upper and lower motor neurons, leading to paralysis, and death within 3–5 years after diagnosis (Orsini et al., 2015). Mutations in super oxide dismutase 1 (*SOD1*) are responsible for over 20% of familial, or inherited, ALS cases (Renton et al., 2014). Since its discovery as the first ALS causative gene over 20 years ago, *SOD1* has been extensively studied (Rosen et al., 1993). Although the exact mechanism of disease has not been elucidated, *in vitro* and *in vivo* studies have shown that mutations in SOD1 lead to misfolding and aggregation of the mutant protein species (Rakhit and Chakrabartty, 2006; Peters et al., 2015b). Additionally, as SOD1 knockout mice do not develop a paralysis phenotype (Reaume et al., 1996), nor do all SOD1 mutations cause a complete loss of dismutase function, and enzymatically inactive mutant SOD1 still causes motor neuron disease (Borchelt et al., 1994; Wang et al., 2002), it is widely accepted that mutant SOD1 acts through a toxic gain of function mechanism.

A common therapeutic approach for gain of function diseases is reduction of the toxic gene product. Loss of *Sod1* in mice does not lead to paralysis or motor neuron loss. Additionally, there is no survival benefit in expressing mutant human *SOD1* in the presence of mouse *Sod1* compared to *Sod1* null background (Bruijn et al., 1998). This would imply that SOD1 reduction is likely to be a safe therapeutic approach. However, there does appears to be increased motor neuron vulnerability

in response to stress and injury in both *Sod1*$^{-/-}$ and *Sod1*$^{+/-}$ mice (Reaume et al., 1996; Saccon et al., 2013). While this suggests a potential effect due to SOD1 loss of function, complete knockout mouse models are not accurate representation of gene reduction strategies, such as RNAi. In the *Sod1*$^{-/-}$ mouse, the enzyme is absent from embryonic development, while an RNAi approach would reduce, but not completely eliminate (see below), the levels of an already existing protein. Nevertheless, since the *Sod1*$^{+/-}$ mouse does have a mild phenotype, ideal therapies would be allelic specific, reducing only the mutant gene product. Meanwhile, future clinical trials could consider supplementation with SOD1 enzyme replacement therapy.

Gene therapy for familial ALS has made substantial headway in recent years, especially as the number of preclinical studies and clinical trials using RNAi therapies and AAV vectors have increased rapidly (Borel et al., 2014). Multiple studies have approached SOD1-ALS treatment through the use of AAV delivered RNAi in both mouse and rat models of ALS, as well as target engagement and safety studies in normal monkeys. Although the studies have had various degrees of success, they have consistently shown AAV-RNAi to be a viable therapeutic approach.

REDUCTION OF *SOD1* IS NECESSARY IN BOTH NEURONS AND ASTROCYTES

Some of the initial work aimed at assessing the therapeutic potential of reducing mutant SOD1 expression used transgenic mouse models. The most widely used mouse model is the SOD1^{G93A} mouse, which contains multiple copies of the mutated human *SOD1* gene. This mouse reproduces the patient phenotype, including the progressive loss of motor neurons and development of hind limb paralysis. The first study (Saito et al., 2005) crossed mice constitutively expressing an anti-*SOD1* siRNA transgene with SOD1^{G93A} mice, and the double transgenic mice showed no signs of disease. In the study, *SOD1* expression was reduced in all cells, presumably from the first stages of embryonic development. Additionally, the shRNA used was not specific for human *SOD1* but also reduced mouse *Sod1* expression. The absence of a phenotype associated with loss of SOD1 activity in these mice supports the notion that non-allele specific silencing of SOD1 is likely to be safe in humans. A parallel study (Boillee et al., 2006) used conditional knock-out mice where the mutant *SOD1* transgene was flanked by loxP sites. These mice were crossed with other transgenic mice expressing Cre under neuronal or microglial/macrophage promoters, leading to cell type-specific excision of *SOD1*. Both mouse lines displayed an increase in survival, but elimination of *SOD1* in neurons delayed onset, while in glia it slowed disease progression. These two studies in transgenic animals highlighted early on that although motor neurons are selectively vulnerable in ALS, targeting non-neuronal cells is likely crucial to fully treat the disease.

The first gene therapy studies for SOD1-ALS focused on viral vector delivered RNAi molecules to spinal cord motor neurons. The largest increase in lifespan in a SOD mouse model was documented for an approach based on intramuscular injections of a lentivirus encoding a shRNA against *SOD1*. The vector was delivered at postnatal day 7 by direct injection into multiple muscle groups, resulting in a survival increase of 77%, due to a delay in disease onset; suggesting it was successful in silencing SOD1 expression in motor neurons. The muscles injected included the hindlimb, to target lower motor neurons; as well as the facial, tongue, and intercostal muscles, since ALS has not only mobility, but feeding and respiratory deficits as well. While these results were promising, the large number of injections required made clinical translation challenging. It is interesting to note that the researchers chose injections into muscle to take advantage of the retrograde transport capabilities of the (equine infectious anemia virus) EIAV lentivirus vector pseudotyped with the Rabies G envelope glycoprotein, and specifically target the innervating neurons. Thus, it is not surprising that while disease onset was delayed, the length of disease duration was not increased further supporting the notion that motor neurons are mediators of disease onset, but progression is also dependent on expression of mutant SOD1 in glia (Ralph et al., 2005). Another study used a lentivirus to deliver an shRNA through bilateral injection into the lumbar spinal cord, in 40-day-old SOD1^{G93A} mice. This injection approach was successful in targeting motor neurons in the lumbar spinal cord. However, there was no increase in lifespan, despite a 60% improvement in motor neuron survival (Raoul et al., 2005). These outcomes further emphasize the importance of targeting multiple cell types throughout the spinal cord.

Widespread transduction is likely necessary to completely prevent cell autonomous and non-autonomous toxic mechanisms from triggering a cascade of events that ultimately lead to complete loss of motor function. Reduction of mutant *SOD1* in motor neurons and glia, and possibly also muscle, has been shown to be critical to prevent disease manifestation. The presence of *SOD1* in non-neuronal cells is important for disease progression and multiple studies have shown that motor neurons are selectively vulnerable to astrocyte-mediated toxicity (Julien, 2007). Studies in different SOD1 mouse models have shown that reduction of *SOD1* specifically in astrocytes leads to an increase in survival (Boillee et al., 2006; Yamanaka et al., 2008). Additionally, astrocytes from SOD1 mice are toxic to motor neurons, both *in vivo* and *in vitro* (Nagai et al., 2007; Di Giorgio et al., 2008; Haidet-Phillips et al., 2011). An increase in astrocytosis is also associated with *SOD1* astrocyte driven disease progression. A recent study aimed to definitively answer the question as to whether neurons or astrocytes alone can be therapeutic targets using a gene transfer approach. AAV vectors encoding *SOD1*-specific artificial microRNAs (amiRNAs) under cell specific promoters were infused into the lateral ventricles of neonate SOD1 mice (Dirren et al., 2015). An AAV6 vector carrying the cytomegalovirus (CMV) promoter (shown to have strong propensity to transduce motor neurons with this type of serotype and delivery method Dirren et al., 2014) extended survival by 26% while an AAV9 vector carrying a GFAP glial promoter increased survival by 14%. Unfortunately, the combined injection of both AAV vectors showed no additional benefit, and fell short of the large increase

in lifespan documented with the intravenous delivery of AAVs encoding shRNA or amiRNA under ubiquitous promoters. However, this could be due to the need to half the dose of both vectors for combined infusion, in order to maintain the same injection volume. Studies are also underway testing a single bicistronic AAV vector where the therapeutic artificial miRNA is expressed from both the neuronal synapsin 1 and glial GFAP promoters. The bicistronic AAV vector appears to have superior therapeutic effect based on motor performance compared to AAV vectors targeting a single cell type (Bobela-Aebischer et al., 2016).

THERAPEUTIC SUCCESS OF SYSTEMIC AAV-RNAI DELIVERY IS AGE DEPENDENT

The discovery that AAV9 is capable of crossing the blood brain barrier after systemic administration opened a new avenue for development of a gene therapy approach capable of tackling ALS in a global manner (Foust et al., 2009). The first AAV9 based study used an H1 promoter driven shRNA (Foust et al., 2013) and reported a 39% increase in median survival when delivered to SOD1 mice at postnatal day 1 (P1), and 30% when delivered at postnatal day 21 (P21). The spinal cord transduction profile of AAV9 injected systemically changes from motor neurons in neonates to mostly glia in older animals (Foust et al., 2009). Consistently P1 injections led to transduction of more motor neurons (64%) than glia (34%), while it was the reverse for P21 injection with transduction of fewer motor neurons (8%) than glia (54%). The degree of SOD1 protein reduction in the spinal cord was also age dependent with 60% for P1, but only by 45% after P21 injection. In this study, mice were also injected at 85 days of age, when disease symptoms are starting to manifest, leading to a 23% increase in survival. These results raise the question of how late in disease progression is an AAV-RNAi intervention likely to have a therapeutic effect. This has been further confirmed by a recent study (Borel et al., 2016), which also used an intravenous infusion, of AAVrh10, to deliver an artificial microRNA specific to *SOD1*. Mice were treated at 56–68 days, when early signs of disease are already apparent at the molecular and biochemical levels. Testing therapeutic efficacy in early symptomatic adult mice is more relevant compared to neonatal or P21 interventions since ALS patients are diagnosed as adults and often at early stages of disease progression. Treatment with AAVrh10-amiRNA reduced *SOD1* mRNA in transduced cells and increased lifespan by 21%, an outcome similar to the previous treatment initiated at 85 days of age. Since AAV9 (and AAVrh10) target mostly glia after an postnatal day 1 intravenous infusion (Zhang et al., 2011; Yang et al., 2014), it is clear that SOD1 reduction in glial alone is not sufficient, as shown in previous studies with conditional knock-out SOD1 mice (Boillee et al., 2006), and it is likely that more motor neurons need to be transduced to achieve greater therapeutic efficacy. Thus, while an intravenous infusion is the easiest delivery method, current AAV vectors are not efficient enough at crossing the blood brain barrier in adult mice to transduce the majority of cells in the CNS.

UPPER MOTOR NEURONS, AS WELL AS MUSCLE, PLAY A ROLE IN DISEASE PROGRESSION

It has been hypothesized that ALS is caused by a "dying back" mechanism, where degeneration starts in muscle, travels up the axons to the spinal cord motor neurons and then to the cortical layer V motor neurons in the brain. AAV6 has been shown to efficiently transduce skeletal muscle as well as undergo retrograde transport to motor neurons after intramuscular injection (Kaspar et al., 2003; Gregorevic et al., 2004). Thus, several studies used AAV6 to deliver an *SOD1*-specific shRNA in SOD1 mice, to reduce the mutant protein in muscle as well as in the central nervous system (CNS). In the first study, adult SOD1 mice received an intravenous infusion of AAV6-shRNA vector resulting in 50% reduction in SOD1 protein in skeletal muscle. However, <5% of motor neurons were transduced, and there was no apparent reduction in SOD1 levels in the spinal cord (Towne et al., 2008). In a subsequent study (Towne et al., 2011), AAV6-shRNA was injected directly into multiple muscle groups in neonate SOD1 mice, similar to the EIAV lentivirus study, but there was no change in survival. This was surprising as there was efficient retrograde transport of AAV6 to motor neurons as evidenced by the >50% reduction of *SOD1* mRNA level in transduced cells. This discrepancy is potentially due to the lower number of motor neurons transduced in the AAV6 study compared to the EIAV lentivirus study (40% vs. >50% in the lumbar spinal cord, respectively), or differences in shRNA efficacy. In a separate experiment, an shRNA against *SOD1* was delivered by intramuscular injection of a lentivirus vector pseudotyped with the vesicular stomatitis virus glycoprotein (VSV-G) not capable of retrograde transport, or an AAV2 vector capable of retrograde transport. Both vectors reduced SOD1 protein levels in skeletal muscle, but the improvement in motor function was seen solely in the AAV2 treated SOD1 mouse (Miller et al., 2006). However, partial reduction of mutant *SOD1* in muscle using the Cre-Lox system had no effect on survival (Miller et al., 2006), and expression of mutant *SOD1* in muscle alone led to motor impairment caused by alterations in neuromuscular junction (Jaarsma et al., 2008; Wong and Martin, 2010).

Recently, more attention has been given to the potential role of cortical layer V (upper) motor neuron degeneration in the disease phenotype. Ozdinler et al. (2011) showed that layer V cortical motor neurons also undergo degeneration in $SOD1^{G93A}$ mice, an observation that reproduces the neuropathological findings in the brain of ALS patients (Saberi et al., 2015). Thomsen et al. (2014) demonstrated the importance of this neuronal population in disease progression and as a key therapeutic target: multiple injections of an AAV-H1-shRNA vector covering the motor cortex of SOD1 rats led to a 20-day extension in survival with no evidence of spinal cord transduction. Moreover, this study also raised questions regarding the hypothesis that ALS is caused by a "dying back" mechanism—that disease and degeneration starts in muscle, travels up to the motor neurons of the spinal cord and eventually to those in the brain. Since suppression of the

misfolded SOD1 protein in motor cortex resulted in a therapeutic benefit, it is possible that disease starts concomitantly at all levels of the CNS, albeit perhaps with varying kinetics for different susceptible neuronal populations.

WIDESPREAD DELIVERY THROUGHOUT THE CNS REMAINS CHALLENGING IN MOUSE MODELS

AAV9 is highly effective for transduction of spinal cord motor neurons, in an age dependent manner, but it remains relatively ineffective for widespread neuronal gene transfer in the brain by systemic delivery. An alternative approach to achieve broader neuronal transduction in the CNS is to infuse AAV vectors into the lateral ventricles of neonatal mice. Stoica et al., performed a proof-of-concept experiment using an AAV9 vector encoding a CBA promoter-driven artificial microRNA specific to human *SOD1*, delivered into the brain lateral ventricles of SOD1^{G93A} mice at post natal day 1 (Stoica et al., 2016). This type of infusion leads to gene expression in cortical and spinal cord motor neurons (Broekman et al., 2006; Chakrabarty et al., 2013; McLean et al., 2014), as well as non-neuronal cells and peripheral muscle. As a result this study reported the longest extension in lifespan to date using AAV mediated RNAi. Interestingly, treated SOD1^{G93A} mice did not die from the typical onset of paralysis, but instead from rapid body weight loss accompanied by a progressively hunched kyphotic posture. A previous study testing the therapeutic efficacy of an AAV6-amiRNA vector delivered by the same route to neonate SOD1^{G93A} mice reported development of similar symptoms unrelated to paralysis (Dirren et al., 2015). The authors of the AAV9 CBA-amiRNA study postulated the cause of death to be a previously undetected respiratory phenotype, similar to the respiratory impairment developed by ALS patients. Indeed, the reported respiratory phenotype in the ALS mice was not fully corrected by AAV treatment, making this a plausible hypothesis to explain the demise of treated mice. It is important to note that although treated mice survived longer with no visible motor impairment, there was evidence of neuronal loss at euthanasia. It is possible that the neurons involved in respiration—in the medulla, cervical, and thoracic spinal cord—were lost in these mice, explaining the observed decrease in respiratory response. Additionally, since this was a neonatal treatment, the therapeutic artificial microRNA would have been lost from post-natally dividing cells in the spinal cord, such as astrocytes. Thus, although this delivery approach was able to achieve widespread transduction, it is still not an accurate representation of the transduction achievable in the clinic as the distribution profile of AAV9 via cerebral spinal fluid (CSF) infusion routes is considerably more restricted in adult animals.

The next step for this therapeutic approach is the translation into adult animals, and larger mammals. The most accessible way to deliver AAVs into the CSF is through intrathecal (IT) infusion into the lumbar spinal cord. This injection route leads to effective transduction of spinal cord motor neurons in adult non-human primates, but the percentage of transduced neurons in the brain remains limited. Studies using intrathecal infusions of AAV vectors in mice reported variable reproducibility, and limited vector spread to distal spinal cord regions and to the brain (Snyder et al., 2011). Wang et al. (2014) performed IT injections of an AAVrh10 vector encoding an artificial miRNA against SOD1 into the lumbar spinal cord of adult SOD1^{G93A} mice. This resulted in an 11% average increase in survival and a direct correlation between survival and the level of transduction of the spinal cord. Patel et al. performed IT injections of an AAV1 encoding a single chain antibody against misfolded SOD1 and reported a 28% increase in survival of treated SOD1^{G93A} mice. However, survival was highly variable among treated animals, which directly correlated with antibody titers in the spinal cord (Patel et al., 2014). This highlights the still unsolved problem of widespread AAV delivery to motor neurons in adult mice. Multiple studies have shown effective transduction of both motor neurons and astrocytes in non-human primates after CSF infusion (Bevan et al., 2011; Samaranch et al., 2013; Passini et al., 2014). Presently it is unclear whether the differences in transduction profiles between mice and larger species is due to intrinsic differential tropism across species or technical challenges associated with intrathecal delivery in mice due to their small size. Nevertheless, Meyer at al. has recently shown that holding a non-human primate in the Trendelenburg position following an IT injection enhances AAV9 spread throughout the spinal cord and into the brain (Meyer et al., 2015). This type of injection is also feasible in the clinic, making this delivery technique relevant for clinical translation.

SUMMARY

Multiple studies have used AAVs to deliver therapeutic RNAi molecules (**Table 1**), but none reached the widespread gene transfer in CNS and periphery thought to be necessary to achieve transformative outcomes. Intravenous infusion of AAV9 in neonatal mice, such as in transduce peripheral muscle and mainly motor neurons in the spinal cord, but not in the cortex; while intravenous infusions in adults transduce mainly glial in the spinal cord. Lumbar intrathecal AAV injections in adult mice transduce local motor neurons in the spinal cord, but few if any in the cortex. Additionally, this type of delivery method has significant inter-animal variability. Intramuscular injections using vectors able to undergo retrograde transport transduce motor neurons, but only those neurons innervating the injected muscles. Lastly, neonatal intraventricular injections achieve widespread transduction of cortical and spinal cord motor neurons, as well as peripheral muscle, but gene expression is lost from dividing cells, such as astrocytes, which are known determinants of disease progression. Additionally, SOD1 reduction in upper or lower motor neurons alone is beneficial but not sufficient to substantially affect the course of disease progression. The many studies discussed here have clearly proven the potential of AAV-RNAi gene therapy for treating SOD1-ALS, and this approach is now also being applied to

TABLE 1 | Preclinical viral vector mediated RNAi therapeutics for SOD1-ALS.

Animal model	Vector	Promoter	RNAi species (miR backbone)	Age at delivery	Total dose	Delivery method	Survival benefit	Study
SOD1^{G93A} /B6/SJL mouse	VSV-G lentivirus	H1	shRNA	P40	180 ng of p24 antigen	IT, bilateral	None	Raoul et al., 2005
SOD1^{G93A} /B6/SJL mouse	Rabies-G EIAV lentivirus	H1	shRNA	P7	8.4E7−1.2E8 tu	IM, multiple muscle groups	77%	Ralph et al., 2005
SOD1^{G93A} /B6/SJL mouse	AAV6	H1	shRNA	P42	2E11 vg	IV	none	Towne et al., 2008
SOD1^{G93A} /B6/SJL mouse	AAV6	H1	shRNA	P1–P5, P15	3.7E8 tu	IM, multiple muscle groups	none	Towne et al., 2011
SOD1^{G93A} /B6/SJL mouse	AAV9	H1	shRNA	P1	5E11 vg	IV	39%	Foust et al., 2013
				P21	2E12 vg	IV	30%	
				P85	3E12 vg	IV	23%	
loxSOD1^{G37R} mouse				P215	3E12 vg	IV	22%	
SOD1^{G93A} /FVB/NJ mouse	AAVrh10	CBA	amiR (miR30a)	65	2.4e10 vg	IT	11%	Wang et al., 2014
SOD1^{G93A} /rat	AAV9	H1	shRNA	P70	1.6E11 vg	IC (motor cortex)	12%	Thomsen et al., 2014
SOD1^{G93A} /B6 mouse	AAV6	CMV	amiR (mir155)	P2	1.6E11 vg	ICV	26%	Dirren et al., 2015
	AAV9	GFAP	amiR (mir155)	P2	6.8E11 vg	ICV	14%	
	AAV6+AAV9	CMV/GFAP	amiR (mir155)	P2	8E10/3.4E10 vg	ICV	10%	
	AAV9	CMV	amiR (mir155)	P35	2.4E12 vg	IT	None	
	AAV9	GFAP	amiR (mir155)	P35	2.4E12 vg	IT	None	
SOD1^{G93A} /B6/SJL mouse	AAVrh10	CB	amiR (mir155) × 2	P56−68	2E11 vg	IV	20%	Borel et al., 2016
		U6	amiR (miR155)	P56−68	2E11 vg	IV	21%	
SOD1^{G93A} /B6/SJL mouse	AAV9	CBA	amiR (mir155) × 2	P1	1E11 vg	ICV	50%	Stoica et al., 2016

SOD1, superoxide dismutase 1; AAV, adeno associated viral vectors; VSV, vesicular stomatitis virus; IT, intrathecal; IM, intramuscular; IV, intravenous; IC, intracranial; ICV, intracerebral ventricular; P, postnatal day; tu, transducting units; vg, vector genomes.

other ALS causative genes (Peters et al., 2015a), but more potent delivery vehicles are still needed to simultaneously target all disease-relevant CNS populations in adults. The recent improvements in injection techniques as well as development of engineered AAV capsids with vastly improved CNS transduction efficiency in adult animals are quickly paving the way to the emergence of potential transformative therapies for ALS and other neurodegenerative diseases (Choudhury et al., 2016; Deverman et al., 2016).

AUTHOR CONTRIBUTIONS

LS drafted the initial manuscript, and edited it into the final version. MSE edited the manuscript.

REFERENCES

Bevan, A. K., Duque, S., Foust, K. D., Morales, P. R., Braun, L., Schmelzer, L., et al. (2011). Systemic gene delivery in large species for targeting spinal cord, brain, and peripheral tissues for pediatric disorders. *Mol. Ther.* 19, 1971–1980. doi: 10.1038/mt.2011.157

Bobela-Aebischer, J., Bernard-Marissal, N., Aebischer, P., and Schneider, B. (2016). *Use of a Bicistronic Vector to Silence SOD1 in Motoneurons and Astrocytes for the Treatment of Familial Amyotrophic Lateral Sclerosis.* Washington, DC: American Society for Gene and Cell Therapy. Poster #190.

Boillee, S., Yamanaka, K., Lobsiger, C. S., Copeland, N. G., Jenkins, N. A., Kassiotis, G., et al. (2006). Onset and progression in inherited ALS determined by motor neurons and microglia. *Science* 312, 1389–1392. doi: 10.1126/science.1123511

Borchelt, D. R., Lee, M. K., Slunt, H. S., Guarnieri, M., Xu, Z. S., Wong, P. C., et al. (1994). Superoxide dismutase 1 with mutations linked to familial amyotrophic lateral sclerosis possesses significant activity. *Proc. Natl. Acad. Sci. U.S.A.* 91, 8292–8296. doi: 10.1073/pnas.91.17.8292

Borel, F., Gernoux, G., Cardozo, B., Metterville, J. P., Toro Cabreja, G. C., Song, L., et al. (2016). Therapeutic rAAVrh10 mediated SOD1 silencing in adult SOD1(G93A) mice and nonhuman primates. *Hum. Gene Ther.* 27, 19–31. doi: 10.1089/hum.2015.122

Borel, F., Kay, M. A., and Mueller, C. (2014). Recombinant AAV as a platform for translating the therapeutic potential of RNA interference. *Mol. Ther.* 22, 692–701. doi: 10.1038/mt.2013.285

Broekman, M. L., Comer, L. A., Hyman, B. T., and Sena-Esteves, M. (2006). Adeno-associated virus vectors serotyped with AAV8 capsid are more efficient than AAV-1 or -2 serotypes for widespread gene delivery to the neonatal mouse brain. *Neuroscience* 138, 501–510. doi: 10.1016/j.neuroscience.2005.11.057

Bruijn, L. I., Houseweart, M. K., Kato, S., Anderson, K. L., Anderson, S. D., Ohama, E., et al. (1998). Aggregation and motor neuron toxicity of an ALS-linked SOD1 mutant independent from wild-type SOD1. *Science* 281, 1851–1854. doi: 10.1126/science.281.5384.1851

Chakrabarty, P., Rosario, A., Cruz, P., Siemienski, Z., Ceballos-Diaz, C., Crosby, K., et al. (2013). Capsid serotype and timing of injection determines AAV transduction in the neonatal mice brain. *PLoS ONE* 8:e67680. doi: 10.1371/journal.pone.0067680

Choudhury, S. R., Harris, A. F., Cabral, D. J., Keeler, A. M., Sapp, E., Ferreira, J. S., et al. (2016). Widespread central nervous system gene transfer and silencing after systemic delivery of novel AAV-AS vector. *Mol. Ther.* 24, 726–735. doi: 10.1038/mt.2015.231

Deverman, B. E., Pravdo, P. L., Simpson, B. P., Kumar, S. R., Chan, K. Y., Banerjee, A., et al. (2016). Cre-dependent selection yields AAV variants for widespread gene transfer to the adult brain. *Nat. Biotechnol.* 34, 204–209. doi: 10.1038/nbt.3440

Di Giorgio, F. P., Boulting, G. L., Bobrowicz, S., and Eggan, K. C. (2008). Human embryonic stem cell-derived motor neurons are sensitive to the toxic effect of glial cells carrying an ALS-causing mutation. *Cell Stem Cell* 3, 637–648. doi: 10.1016/j.stem.2008.09.017

Dirren, E., Aebischer, J., Rochat, C., Towne, C., Schneider, B. L., and Aebischer, P. (2015). SOD1 silencing in motoneurons or glia rescues neuromuscular function in ALS mice. *Ann. Clin. Transl. Neurol.* 2, 167–184. doi: 10.1002/acn3.162

Dirren, E., Towne, C. L., Setola, V., Redmond, D. E. Jr., Schneider, B. L., and Aebischer, P. (2014). Intracerebroventricular injection of adeno-associated virus 6 and 9 vectors for cell type-specific transgene expression in the spinal cord. *Hum. Gene Ther.* 25, 109–120. doi: 10.1089/hum.2013.021

Foust, K. D., Nurre, E., Montgomery, C. L., Hernandez, A., Chan, C. M., and Kaspar, B. K. (2009). Intravascular AAV9 preferentially targets neonatal neurons and adult astrocytes. *Nat. Biotechnol.* 27, 59–65. doi: 10.1038/nbt.1515

Foust, K. D., Salazar, D. L., Likhite, S., Ferraiuolo, L., Ditsworth, D., Ilieva, H., et al. (2013). Therapeutic AAV9-mediated suppression of mutant SOD1 slows disease progression and extends survival in models of inherited ALS. *Mol. Ther.* 21, 2148–2159. doi: 10.1038/mt.2013.211

Gregorevic, P., Blankinship, M. J., Allen, J. M., Crawford, R. W., Meuse, L., Miller, D. G., et al. (2004). Systemic delivery of genes to striated muscles using adeno-associated viral vectors. *Nat. Med.* 10, 828–834. doi: 10.1038/nm1085

Haidet-Phillips, A. M., Hester, M. E., Miranda, C. J., Meyer, K., Braun, L., Frakes, A., et al. (2011). Astrocytes from familial and sporadic ALS patients are toxic to motor neurons. *Nat. Biotechnol.* 29, 824–828. doi: 10.1038/nbt.1957

Jaarsma, D., Teuling, E., Haasdijk, E. D., De Zeeuw, C. I., and Hoogenraad, C. C. (2008). Neuron-specific expression of mutant superoxide dismutase is sufficient to induce amyotrophic lateral sclerosis in transgenic mice. *J. Neurosci.* 28, 2075–2088. doi: 10.1523/JNEUROSCI.5258-07.2008

Julien, J. P. (2007). ALS: astrocytes move in as deadly neighbors. *Nat. Neurosci.* 10, 535–537. doi: 10.1038/nn0507-535

Kaspar, B. K., Llado, J., Sherkat, N., Rothstein, J. D., and Gage, F. H. (2003). Retrograde viral delivery of IGF-1 prolongs survival in a mouse ALS model. *Science* 301, 839–842. doi: 10.1126/science.1086137

McLean, J. R., Smith, G. A., Rocha, E. M., Hayes, M. A., Beagan, J. A., Hallett, P. J., et al. (2014). Widespread neuron-specific transgene expression in brain and spinal cord following synapsin promoter-driven AAV9 neonatal intracerebroventricular injection. *Neurosci. Lett.* 576, 73–78. doi: 10.1016/j.neulet.2014.05.044

Meyer, K., Ferraiuolo, L., Schmelzer, L., Braun, L., McGovern, V., Likhite, S., et al. (2015). Improving single injection CSF delivery of AAV9-mediated gene therapy for SMA: a dose-response study in mice and nonhuman primates. *Mol. Ther.* 23, 477–487. doi: 10.1038/mt.2014.210

Miller, T. M., Kim, S. H., Yamanaka, K., Hester, M., Umapathi, P., Arnson, H., et al. (2006). Gene transfer demonstrates that muscle is not a primary target for non-cell-autonomous toxicity in familial amyotrophic lateral sclerosis. *Proc. Natl. Acad. Sci. U.S.A.* 103, 19546–19551. doi: 10.1073/pnas.0609411103

Nagai, M., Re, D. B., Nagata, T., Chalazonitis, A., Jessell, T. M., Wichterle, H., et al. (2007). Astrocytes expressing ALS-linked mutated SOD1 release factors selectively toxic to motor neurons. *Nat. Neurosci.* 10, 615–622. doi: 10.1038/nn1876

Orsini, M., Oliveira, A. B., Nascimento, O. J., Reis, C. H., Leite, M. A., de Souza, J. A., et al. (2015). Amyotrophic lateral sclerosis: new perpectives and update. *Neurol. Int.* 7:5885. doi: 10.4081/ni.2015.5885

Ozdinler, P. H., Benn, S., Yamamoto, T. H., Guzel, M., Brown, R. H. Jr., and Macklis, J. D. (2011). Corticospinal motor neurons and related subcerebral projection neurons undergo early and specific neurodegeneration in hSOD1G(9)(3)A transgenic ALS mice. *J. Neurosci.* 31, 4166–4177. doi: 10.1523/JNEUROSCI.4184-10.2011

Passini, M. A., Bu, J., Richards, A. M., Treleaven, C. M., Sullivan, J. A., O'Riordan, C. R., et al. (2014). Translational fidelity of intrathecal delivery of self-complementary AAV9-survival motor neuron 1 for spinal muscular atrophy. *Hum. Gene Ther.* 25, 619–630. doi: 10.1089/hum.2014.011

Patel, P., Kriz, J., Gravel, M., Soucy, G., Bareil, C., Gravel, C., et al. (2014). Adeno-associated virus-mediated delivery of a recombinant single-chain antibody against misfolded superoxide dismutase for treatment of amyotrophic lateral sclerosis. *Mol. Ther.* 22, 498–510. doi: 10.1038/mt.2013.239

Peters, O. M., Cabrera, G. T., Tran, H., Gendron, T. F., McKeon, J. E., Metterville, J., et al. (2015a). Human C9ORF72 hexanucleotide expansion reproduces RNA foci and dipeptide repeat proteins but not neurodegeneration in BAC transgenic mice. *Neuron* 88, 902–909. doi: 10.1016/j.neuron.2015.11.018

Peters, O. M., Ghasemi, M., and Brown, R. H. Jr. (2015b). Emerging mechanisms of molecular pathology in ALS. *J. Clin. Invest.* 125, 1767–1779. doi: 10.1172/JCI71601

Rakhit, R., and Chakrabartty, A. (2006). Structure, folding, and misfolding of Cu, Zn superoxide dismutase in amyotrophic lateral sclerosis. *Biochim. Biophys. Acta* 1762, 1025–1037. doi: 10.1016/j.bbadis.2006.05.004

Ralph, G. S., Radcliffe, P. A., Day, D. M., Carthy, J. M., Leroux, M. A., Lee, D. C., et al. (2005). Silencing mutant SOD1 using RNAi protects against neurodegeneration and extends survival in an ALS model. *Nat. Med.* 11, 429–433. doi: 10.1038/nm1205

Raoul, C., Abbas-Terki, T., Bensadoun, J. C., Guillot, S., Haase, G., Szulc, J., et al. (2005). Lentiviral-mediated silencing of SOD1 through RNA interference retards disease onset and progression in a mouse model of ALS. *Nat. Med.* 11, 423–428. doi: 10.1038/nm1207

Reaume, A. G., Elliott, J. L., Hoffman, E. K., Kowall, N. W., Ferrante, R. J., Siwek, D. F., et al. (1996). Motor neurons in Cu/Zn superoxide dismutase-deficient mice develop normally but exhibit enhanced cell death after axonal injury. *Nat. Genet.* 13, 43–47. doi: 10.1038/ng0596-43

Renton, A. E., Chio, A., and Traynor, B. J. (2014). State of play in amyotrophic lateral sclerosis genetics. *Nat. Neurosci.* 17, 17–23. doi: 10.1038/nn.3584

Rosen, D. R., Siddique, T., Patterson, D., Figlewicz, D. A., Sapp, P., Hentati, A., et al. (1993). Mutations in Cu/Zn superoxide dismutase gene are associated with familial amyotrophic lateral sclerosis. *Nature* 362, 59–62. doi: 10.1038/362059a0

Saberi, S., Stauffer, J. E., Schulte, D. J., and Ravits, J. (2015). Neuropathology of amyotrophic lateral sclerosis and its variants. *Neurol. Clin.* 33, 855–876. doi: 10.1016/j.ncl.2015.07.012

Saccon, R. A., Bunton-Stasyshyn, R. K., Fisher, E. M., and Fratta, P. (2013). Is SOD1 loss of function involved in amyotrophic lateral sclerosis? *Brain* 136, 2342–2358. doi: 10.1093/brain/awt097

Saito, Y., Yokota, T., Mitani, T., Ito, K., Anzai, M., Miyagishi, M., et al. (2005). Transgenic small interfering RNA halts amyotrophic lateral sclerosis in a mouse model. *J. Biol. Chem.* 280, 42826–42830. doi: 10.1074/jbc.M507685200

Samaranch, L., Salegio, E. A., San Sebastian, W., Kells, A. P., Bringas, J. R., Forsayeth, J., et al. (2013). Strong cortical and spinal cord transduction after AAV7 and AAV9 delivery into the cerebrospinal fluid of nonhuman primates. *Hum. Gene Ther.* 24, 526–532. doi: 10.1089/hum.2013.005

Snyder, B. R., Gray, S. J., Quach, E. T., Huang, J. W., Leung, C. H., Samulski, R. J., et al. (2011). Comparison of adeno-associated viral vector serotypes for spinal cord and motor neuron gene delivery. *Hum. Gene Ther.* 22, 1129–1135. doi: 10.1089/hum.2011.008

Stoica, L., Todeasa, S. H., Cabrera, G. T., Salameh, J. S., ElMallah, M. K., Mueller, C., et al. (2016). Adeno-associated virus-delivered artificial microRNA extends survival and delays paralysis in an amyotrophic lateral sclerosis mouse model. *Ann. Neurol.* 79, 687–700. doi: 10.1002/ana.24618

Thomsen, G. M., Gowing, G., Latter, J., Chen, M., Vit, J. P., Staggenborg, K., et al. (2014). Delayed disease onset and extended survival in the SOD1G93A rat model of amyotrophic lateral sclerosis after suppression of mutant SOD1 in the motor cortex. *J. Neurosci.* 34, 15587–15600. doi: 10.1523/JNEUROSCI.2037-14.2014

Towne, C., Raoul, C., Schneider, B. L., and Aebischer, P. (2008). Systemic AAV6 delivery mediating RNA interference against SOD1: neuromuscular transduction does not alter disease progression in fALS mice. *Mol. Ther.* 16, 1018–1025. doi: 10.1038/mt.2008.73

Towne, C., Setola, V., Schneider, B. L., and Aebischer, P. (2011). Neuroprotection by gene therapy targeting mutant SOD1 in individual pools of motor neurons does not translate into therapeutic benefit in fALS mice. *Mol. Ther.* 19, 274–283. doi: 10.1038/mt.2010.260

Wang, H., Yang, B., Qiu, L., Yang, C., Kramer, J., Su, Q., et al. (2014). Widespread spinal cord transduction by intrathecal injection of rAAV delivers efficacious RNAi therapy for amyotrophic lateral sclerosis. *Hum. Mol. Genet.* 23, 668–681. doi: 10.1093/hmg/ddt454

Wang, J., Xu, G., Gonzales, V., Coonfield, M., Fromholt, D., Copeland, N. G., et al. (2002). Fibrillar inclusions and motor neuron degeneration in transgenic mice expressing superoxide dismutase 1 with a disrupted copper-binding site. *Neurobiol. Dis.* 10, 128–138. doi: 10.1006/nbdi.2002.0498

Wong, M., and Martin, L. J. (2010). Skeletal muscle-restricted expression of human SOD1 causes motor neuron degeneration in transgenic mice. *Hum. Mol. Genet.* 19, 2284–2302. doi: 10.1093/hmg/ddq106

Yamanaka, K., Chun, S. J., Boillee, S., Fujimori-Tonou, N., Yamashita, H., Gutmann, D. H., et al. (2008). Astrocytes as determinants of disease progression in inherited amyotrophic lateral sclerosis. *Nat. Neurosci.* 11, 251–253. doi: 10.1038/nn2047

Yang, B., Li, S., Wang, H., Guo, Y., Gessler, D. J., Cao, C., et al. (2014). Global CNS transduction of adult mice by intravenously delivered rAAVrh.8 and rAAVrh.10 and nonhuman primates by rAAVrh.10. *Mol. Ther.* 22, 1299–1309. doi: 10.1038/mt.2014.68

Zhang, H., Yang, B., Mu, X., Ahmed, S. S., Su, Q., He, R., et al. (2011). Several rAAV vectors efficiently cross the blood-brain barrier and transduce neurons and astrocytes in the neonatal mouse central nervous system. *Mol. Ther.* 19, 1440–1448. doi: 10.1038/mt.2011.98

Conflict of Interest Statement: The authors declare that the research was conducted in the absence of any commercial or financial relationships that could be construed as a potential conflict of interest.

frontiers in Molecular Neuroscience

MINI REVIEW
published: 28 April 2016
doi: 10.3389/fnmol.2016.00030

CRISPR/Cas9: Implications for Modeling and Therapy of Neurodegenerative Diseases

Weili Yang[1], *Zhuchi Tu*[1], *Qiang Sun*[1] *and Xiao-Jiang Li*[1,2]*

[1] *Institute of Genetics and Developmental Biology, Chinese Academy of Sciences, Beijing, China,* [2] *Department of Human Genetics, Emory University School of Medicine, Atlanta, GA, USA*

CRISPR/Cas9 is now used widely to genetically modify the genomes of various species. The ability of CRISPR/Cas9 to delete DNA sequences and correct DNA mutations opens up a new avenue to treat genetic diseases that are caused by DNA mutations. In this review, we describe the advantages of using CRISPR/Cas9 to engineer genomic DNAs in animal embryos, as well as in specific regions or cell types in the brain. We also discuss how to apply CRISPR/Cas9 to establish animal models of neurodegenerative diseases, such as Parkinson's and Huntington's disease (HD), and to treat these disorders that are caused by genetic mutations.

Keywords: CRISPR/Cas9, neurodegenerative diseases, animal models

THE DEVELOPMENT AND APPLICATION OF CRISPR/Cas9

CRISPR/Cas9, a recent addition to our tools for genome editing, has led to a revolution in biological research. CRISPR was originally reported as a set of short repeats located downstream of the iap gene in *E. coli* (Ishino et al., 1987). As more similar repeat elements were reported over years, Mojica et al. (2000) termed it as Short Regularly Spaced Repeats (SRSR). Jansen et al. (2002) then reported that several clusters of signature CRISPR-associated (Cas) genes were well conserved and typically adjacent to the repeat elements. Later, a series of studies uncovered the efficient antiviral defense mechanism of the CRISPR system (Jansen et al., 2002; Barrangou et al., 2007; Brouns et al., 2008; Karginov and Hannon, 2010). In this system, the non-coding CRISPR array is transcribed and cleaved within direct repeats into short crRNAs containing individual spacer sequences, which direct the nuclease Cas9 to targeted sequences of genomic DNA. The nuclease Cas9 then cuts both strands of DNA precisely, and the damaged DNA is repaired via non-homologous end joining (NHEJ) or homology-directed repair (HDR), thereby resulting in gene disruptions and inactivation of the targeted gene. Jinek et al. (2012) fused a crRNA containing the targeting guide sequence to a tracrRNA, called a single guide RNA (gRNA), to facilitate DNA cleavage by CRISPR/Cas9. CRISPR/Cas9 has now been used for genome editing in a variety of species (Hsu et al., 2014; Sander and Joung, 2014), especially in non-human primates that do not have embryonic stem cells for genomic manipulation (Niu et al., 2014; Chen et al., 2015) and human tripronuclear (3PN) zygotes (Liang et al., 2015).

Another powerful application of the CRISPR/Cas9 system is based on its ability to target many genomic loci simultaneously for studying gene function on a global scale (Koike-Yusa et al., 2014; Shalem et al., 2014; Zhou et al., 2014) which is certainly an advantage over RNAi and its limitations, such as low efficiency and specificity in genome-scale screens. Based on the DNA binding property of CRISPR/Cas9, researchers have also developed catalytically dead Cas9 (dCas9) to act as transcriptional or epigenetic regulators (Larson et al., 2013; Qi et al., 2013)

OPEN ACCESS

Edited by:
George Smith, Temple University School of Medicine, USA

Reviewed by:
Nicole Déglon, Lausanne University Hospital (CHUV), Switzerland
Nicholas D. Mazarakis, Imperial College London, UK

***Correspondence:**
Xiao-Jiang Li
xli2@emory.edu

Received: *17 March 2016*
Accepted: *15 April 2016*
Published: *28 April 2016*

Citation:
Yang W, Tu Z, Sun Q and Li X-J (2016) CRISPR/Cas9: Implications for Modeling and Therapy of Neurodegenerative Diseases. Front. Mol. Neurosci. 9:30. doi: 10.3389/fnmol.2016.00030

or to couple Cas9 to fluorescence as DNA-binding reporters for live imaging (Chen et al., 2014).

The power of CRISPR/Cas9 to edit the genome holds great promise for treating human diseases caused by genetic DNA mutations. Recently, the UK Human Fertilization and Embryology Authority (HFEA) granted scientists in London permission to genetically edit human embryos within the range of research ethics (Callaway, 2016). Although there are still social and ethical issues that remain to be resolved, it is clear we must consider how to use CRISPR/Cas9 to treat human diseases in the future. In this review, we will focus on the application of CRISPR/Cas9 to animal models of neurodegenerative diseases.

USE OF CRISPR/Cas9 TO GENERATE ANIMAL MODELS OF NEURODEGENERATIVE DISEASES

Neurodegenerative diseases, such as Parkinson's disease (PD) and Huntington's disease (HD), share common features: namely, the age-dependent accumulation of misfolded proteins and selective neurodegeneration. For example, in PD, the presence of cytoplasmic misfolded proteins, termed Lewy bodies, which contain ubiquitinated alpha-synuclein, parkin, synphilin, and neurofilaments, are the pathological hallmark of this disease in patient brains. In the brains of HD patients, on the other hand, there are aggregates or inclusions formed in an age-dependent manner by mutant huntingtin with an expanded polyQ tract (Li and Li, 2011).

Animal models are highly valuable and have been used extensively to investigate neurological disorders and to find therapeutic targets for them. Because many neurodegenerative diseases can be caused by genetic DNA mutations, the ability of CRISPR/Cas9 to directly target any gene in one or two alleles of the embryonic genome opens up a new avenue for using this new technology to generate animal models of neurodegenerative diseases. The traditional gene targeting technology made it difficult to establish large animal models of human diseases due to the lack of embryonic stem cell lines. Since large animals are closer to humans, their disease models may more faithfully mimic the clinical symptoms of patients and are important for exploring the mechanisms and treatment of both neuropsychiatric disorders and age-related neurodegenerative diseases. For example, because the loss of function of the Parkin and Pink1 genes can cause PD, CRISPR/Cas9-mediated mutations can mimic knockout of the Parkin and/or Pink1 gene. CRISPR/Cas9 was found to functionally disrupt the dystrophin gene in founder monkeys and causes the same muscle atrophy phenotype seen in patients (Chen et al., 2015). Thus, when both alleles are mutated by CIRSPR/Cas9, the complete loss of Parkin or Pink1 will mimic the genetic mutations in PD patients. Also, because CRISPR/Cas9 can target multiple genes in the same cells, deletion of the Parkin and Pink1 genes will allow for studies of synergistic effects of loss of these important genes. Indeed, CRISPR/Cas9 has been used to generate pig models of PD by targeting the genes for Parkin, Pink1 and DJ1 (Zhou et al., 2015; Wang et al., 2016).

In addition to genome editing in germline cells, CRISPR/Cas9 can efficiently target genes in somatic tissues, such as neurons in the brain (Incontro et al., 2014; Platt et al., 2014; Straub et al., 2014; Swiech et al., 2015; Heidenreich and Zhang, 2016; Walters et al., 2016). In PD patients, a progressive loss of dopaminergic neurons in the substantia nigra is a key pathological feature. Thus, gRNAs and Cas9 can be delivered to the substantia nigra of animal brains by a viral system to investigate the effect of Parkin or Pink1 loss in adult brains. This approach is particularly useful for investigating the age-related neuropathology in PD.

Also, Cas9-mediated knock-in mutations within the genome can help generate animal models of those neurodegenerative diseases caused by a gain of toxicity of mutant proteins. For example, PD can be caused by mutations in α-synuclein, and HD is caused by polyQ expansion in huntingtin. Co-injection of Cas9/gRNAs with exogenous donor fragments carrying mutant sequences can replace the endogenous gene with mutant DNAs, thus creating animal models carrying the mutated sequences in the endogenous genes.

CRISPR/Cas9-MEDIATED TREATMENT OF GENETIC DISEASES

The animal models created by CRISPR/Cas9 normally carry mutations in endogenous genes and therefore provide better models to mimic human diseases than transgenic animals that express mutant genes under exogenous promoters. These new animal models will be highly valuable for identifying therapies using drugs or chemicals. Although CRSIPR/Cas9 has been used widely in the generation of a variety of cellular or animal models of human diseases, it is particularly important that we develop CRISPR/Cas9 as a therapeutic tool for treating human diseases. For example, CRISPR/Cas9 can be used to correct the causative gene mutations in monogenic recessive disorders or to inactivate the mutated allele in dominant-negative disorders to achieve therapeutic benefits. Recently, three groups independently reported that CRISPR/Cas9 was able to snip out a faulty exon of the dystrophin gene to generate a shortened but functional version of dystrophin to treat mice with muscular dystrophy (Long et al., 2016; Nelson et al., 2016; Tabebordbar et al., 2016). Although the mature muscle cells of adults lack the ability for cell division and have different DNA repair machinery than dividing cells, CRISPR/Cas9 gene editing can occur in skeletal muscle to functionally repair DNA mutations. In addition, CRISPR/Cas9 was used to correct the mutant Crygc gene that causes cataracts in zygotes from mice via HDR with an endogenous WT allele (Wu et al., 2013). All these findings suggest that CRISPR/Cas9 can modify the genome in any type of cell.

For neurodegenerative diseases, CRISPR/Cas9 can also be a powerful tool to eliminate the expression of mutant genes and therefore can alleviate the neuropathology caused by DNA mutations. For example, HD is caused by polyQ expansion in huntingtin, and selective targeting of the mutant huntingtin gene

via CRISPR/Cas9 can be done in specific types of vulnerable neurons in the brain. Similarly, for transgenic PD animal models that express mutant α-synuclein, CRISPR/Cas9 can be designed to deplete the expression of mutant genes via NHEJ, which can lead to gene inactivation, in dopaminergic neurons. Furthermore, the ability of CRISPR/Cas9 to replace the mutant gene via HDR with normal DNA sequences can also lead to the genetic correction of DNA mutations in HD and PD animal models. Although the efficiency of such gene replacement is low at present, the rapidly developing CRISPR/Cas9 system offers a promising approach to generate knock-in models of human diseases.

CHALLENGES FOR CRISPR/Cas9

Despite the power of CRISPR/Cas9 for genome editing, there are still many challenges to be overcome when applying it to generate and treat animal models of human diseases. Because genome editing by CRISPR/Cas9 relies on approximately 23 base pair matches (Hsu et al., 2014), possible off-target effects have been considered an important issue. However, some studies reported that Cas9 could tolerate mismatches, depending on their distribution and number (Hsu et al., 2013; Mali et al., 2013; Fu et al., 2014). Also, a lower Cas9 concentration can decrease the off-target effect at the expense of on-target efficiency (Hsu et al., 2013). Thus, using specific gRNAs and appropriate Cas9 concentrations should minimize the off-targets and increase the specificity of CRSIPR/Cas9-mediated gene targeting.

The second issue with CRISPR/Cas9 is mosaic mutations, which may result from the prolonged expression of Cas9 after cell division or may be due to a slow rate of cleavage by Cas9 nuclease. Alternatively, differential DNA repair and non-homozygous recombination activities in zygotes and divided embryonic cells can also influence genetic mutation rates and mosaicism. Direct delivery of Cas9 protein into cells has also been tried and showed high target efficiency, but still resulted in mosaic mutations (Kim et al., 2014; Sung et al., 2014). Precise control of Cas9 nuclease expression at the transcriptional and translational levels in zygotes may reduce mosaic mutations.

Another challenge for CRISPR/Cas9 is the low rate of homologous recombination. Generally, HDR takes place in the synthesis (S) and the premitotic (G2) phases (Heyer et al., 2010), whereas NHEJ occurs in the growth 1 (G1) and the mitotic (M) phases (Daley and Sung, 2014). Although CRISPR/Cas9-mediated indel mutations via NHEJ have high efficiency, the HDR rate is relatively low. Suppression of NHEJ key molecules is found to increase the HDR rate by CRISPR/Cas9 (Chu et al., 2015; Maruyama et al., 2015). Further evolution of the CRISPR/Cas9 system to increase targeting specificity and efficiency is expected to improve the knock-in rate and the application of this genetic engineering tool to treat neurodegenerative diseases in the future.

AUTHOR CONTRIBUTIONS

WY, ZT, QS and X-JL wrote the review.

ACKNOWLEDGMENTS

This work was supported by the National Key Basic Research Program of China (2012CBA01304), a National Natural Science Foundation of China (NSFC) grant (91332206), National Institutes of Health grants (NS041669, AG019206), and the State Key Laboratory of Molecular Developmental Biology, China. We thank Cheryl Strauss for critical reading of this manuscript.

REFERENCES

Barrangou, R., Fremaux, C., Deveau, H., Richards, M., Boyaval, P., Moineau, S., et al. (2007). CRISPR provides acquired resistance against viruses in prokaryotes. *Science* 315, 1709–1712. doi: 10.1126/science.1138140

Brouns, S. J. J., Jore, M. M., Lundgren, M., Westra, E. R., Slijkhuis, R. J. H., Snijders, A. P. L., et al. (2008). Small CRISPR RNAs guide antiviral defense in prokaryotes. *Science* 321, 960–964. doi: 10.1126/science.1159689

Callaway, E. (2016). UK scientists gain licence to edit genes in human embryos. *Nature* 530:18. doi: 10.1038/nature.2016.19270

Chen, B. H., Gilbert, L. A., Cimini, B. A., Schnitzbauer, J., Zhang, W., Li, G. W., et al. (2014). Dynamic imaging of genomic loci in living human cells by an optimized CRISPR/cas system. *Cell* 155, 1479–1491. doi: 10.1016/j.cell.2013.12.001

Chen, Y., Zheng, Y., Kang, Y., Yang, W., Niu, Y., Guo, X., et al. (2015). Functional disruption of the dystrophin gene in rhesus monkey using CRISPR/Cas9. *Hum. Mol. Genet.* 24, 3764–3774. doi: 10.1093/hmg/ddv120

Chu, V. T., Weber, T., Wefers, B., Wurst, W., Sander, S., Rajewsky, K., et al. (2015). Increasing the efficiency of homology-directed repair for CRISPR-Cas9-induced precise gene editing in mammalian cells. *Nat. Biotechnol.* 33, 543–548. doi: 10.1038/nbt.3198

Daley, J. M., and Sung, P. (2014). 53BP1, BRCA1 and the choice between recombination and end joining at DNA double-strand breaks. *Mol. Cell. Biol.* 34, 1380–1388. doi: 10.1128/MCB.01639-13

Fu, Y., Sander, J. D., Reyon, D., Cascio, V. M., and Joung, J. K. (2014). Improving CRISPR-Cas nuclease specificity using truncated guide RNAs. *Nat. Biotechnol.* 32, 279–284. doi: 10.1038/nbt.2808

Heidenreich, M., and Zhang, F. (2016). Applications of CRISPR-Cas systems in neuroscience. *Nat. Rev. Neurosci.* 17, 36–44. doi: 10.1038/nrn.2015.2

Heyer, W. D., Ehmsen, K. T., and Liu, J. (2010). Regulation of homologous recombination in eukaryotes. *Annu. Rev. Genet.* 44, 113–139. doi: 10.1146/annurev-genet-051710-150955

Hsu, P. D., Lander, E. S., and Zhang, F. (2014). Development and applications of CRISPR-Cas9 for genome engineering. *Cell* 157, 1262–1278. doi: 10.1016/j.cell.2014.05.010

Hsu, P. D., Scott, D. A., Weinstein, J. A., Ran, F. A., Konermann, S., Agarwala, V., et al. (2013). DNA targeting specificity of RNA-guided Cas9 nucleases. *Nat. Biotechnol.* 31, 827–832. doi: 10.1038/nbt.2647

Incontro, S., Asensio, C. S., Edwards, R. H., and Nicoll, R. A. (2014). Efficient, complete deletion of synaptic proteins using CRISPR. *Neuron* 83, 1051–1057. doi: 10.1016/j.neuron.2014.07.043

Ishino, Y., Shinagawa, H., Makino, K., Amemura, M., and Nakata, A. (1987). Nucleotide sequence of the iap gene, responsible for alkaline phosphatase isozyme conversion in Escherichia coli and identification of the gene product. *J. Bacteriol.* 169, 5429–5433.

Jansen, R., van Embden, J. D. A., Gaastra, W., and Schouls, L. M. (2002). Identification of genes that are associated with DNA repeats in prokaryotes. *Mol. Microbiol.* 43, 1565–1575. doi: 10.1046/j.1365-2958.2002.02839.x

Jinek, M., Chylinski, K., Fonfara, I., Hauer, M., Doudna, J. A., and Charpentier, E. (2012). A programmable dual-RNA-guided DNA endonuclease in adaptive bacterial immunity. *Science* 337, 816–821. doi: 10.1126/science.1225829

Karginov, F. V., and Hannon, G. J. (2010). The CRISPR system: small RNA-guided defense in bacteria and archaea. *Mol. Cell* 37, 7–19. doi: 10.1016/j.molcel.2009.12.033

Kim, S., Kim, D., Cho, S. W., Kim, J., and Kim, J. S. (2014). Highly efficient RNA-guided genome editing in human cells via delivery of purified Cas9 ribonucleoproteins. *Genome Res.* 24, 1012–1019. doi: 10.1101/gr.171322.113

Koike-Yusa, H., Li, Y. L., Tan, E. P., Velasco-Herrera, M. D., and Yusa, K. (2014). Genome-wide recessive genetic screening in mammalian cells with a lentiviral CRISPR-guide RNA library. *Nat. Biotechnol.* 32, 267–273. doi: 10.1038/nbt.2800

Larson, M. H., Gilbert, L. A., Wang, X. W., Lim, W. A., Weissman, J. S., and Qi, L. S. (2013). CRISPR interference (CRISPRi) for sequence-specific control of gene expression. *Nat. Protoc.* 8, 2180–2196. doi: 10.1038/nprot.2013.132

Li, X. J., and Li, S. H. (2011). Proteasomal dysfunction in aging and Huntington disease. *Neurobiol. Dis.* 43, 4–8. doi: 10.1016/j.nbd.2010.11.018

Liang, P., Xu, Y., Zhang, X., Ding, C., Huang, R., Zhang, Z., et al. (2015). CRISPR/Cas9-mediated gene editing in human tripronuclear zygotes. *Protein Cell* 6, 363–372. doi: 10.1007/s13238-015-0153-5

Long, C., Amoasii, L., Mireault, A. A., McAnally, J. R., Li, H., Sanchez-Ortiz, E., et al. (2016). Postnatal genome editing partially restores dystrophin expression in a mouse model of muscular dystrophy. *Science* 351, 400–403. doi: 10.1126/science.aad5725

Mali, P., Esvelt, K. M., and Church, G. M. (2013). Cas9 as a versatile tool for engineering biology. *Nat. Methods* 10, 957–963. doi: 10.1038/nmeth.2649

Maruyama, T., Dougan, S. K., Truttmann, M. C., Bilate, A. M., Ingram, J. R., and Ploegh, H. L. (2015). Increasing the efficiency of precise genome editing with CRISPR-Cas9 by inhibition of nonhomologous end joining. *Nat. Biotechnol.* 33, 538–542. doi: 10.1038/nbt.3190

Mojica, F. J., Díez-Villaseñor, C., Soria, E., and Juez, G. (2000). Biological significance of a family of regularly spaced repeats in the genomes of Archaea, Bacteria and mitochondria. *Mol. Microbiol.* 36, 244–246. doi: 10.1046/j.1365-2958.2000.01838.x

Nelson, C. E., Hakim, C. H., Ousterout, D. G., Thakore, P. I., Moreb, E. A., Castellanos Rivera, R. M., et al. (2016). *In vivo* genome editing improves muscle function in a mouse model of Duchenne muscular dystrophy. *Science* 351, 403–407. doi: 10.1126/science.aad5143

Niu, Y., Shen, B., Cui, Y., Chen, Y., Wang, J., Wang, L., et al. (2014). Generation of gene-modified cynomolgus monkey via Cas9/RNA-mediated gene targeting in one-cell embryos. *Cell* 156, 836–843. doi: 10.1016/j.cell.2014.01.027

Platt, R. J., Chen, S. D., Zhou, Y., Yim, M. J., Swiech, L., Kempton, H. R., et al. (2014). CRISPR-Cas9 knockin mice for genome editing and cancer modeling. *Cell* 159, 440–455. doi: 10.1016/j.cell.2014.09.014

Qi, L. S., Larson, M. H., Gilbert, L. A., Doudna, J. A., Weissman, J. S., Arkin, A. P., et al. (2013). Repurposing CRISPR as an RNA-guided platform for sequence-specific control of gene expression. *Cell* 152, 1173–1183. doi: 10.1016/j.cell.2013.02.022

Sander, J. D., and Joung, J. K. (2014). CRISPR-Cas systems for editing, regulating and targeting genomes. *Nat. Biotechnol.* 32, 347–355. doi: 10.1038/nbt.2842

Shalem, O., Sanjana, N. E., Hartenian, E., Shi, X., Scott, D. A., Mikkelsen, T. S., et al. (2014). Genome-scale CRISPR-Cas9 knockout screening in human cells. *Science* 343, 84–87. doi: 10.1126/science.1247005

Straub, C., Granger, A. J., Saulnier, J. L., and Sabatini, B. L. (2014). CRISPR/Cas9-mediated gene knock-down in post-mitotic neurons. *PLoS One* 9:e105584. doi: 10.1371/journal.pone.0105584

Sung, Y. H., Kim, J. M., Kim, H. T., Lee, J., Jeon, J., Jin, Y., et al. (2014). Highly efficient gene knockout in mice and zebrafish with RNA-guided endonucleases. *Genome Res.* 24, 125–131. doi: 10.1101/gr.163394.113

Swiech, L., Heidenreich, M., Banerjee, A., Habib, N., Li, Y., Trombetta, J., et al. (2015). *In vivo* interrogation of gene function in the mammalian brain using CRISPR-Cas9. *Nat. Biotechnol.* 33, 102–106. doi: 10.1038/nbt.3055

Tabebordbar, M., Zhu, K., Cheng, J. K., Chew, W. L., Widrick, J. J., Yan, W. X., et al. (2016). *In vivo* gene editing in dystrophic mouse muscle and muscle stem cells. *Science* 351, 407–411. doi: 10.1126/science.aad5177

Walters, B. J., Azam, A. B., Gillon, C. J., Josselyn, S. A., and Zovkic, I. B. (2016). Advanced *in vivo* use of CRISPR/Cas9 and anti-sense DNA inhibition for gene manipulation in the brain. *Front. Genet.* 6:362. doi: 10.3389/fgene.2015.00362

Wang, X., Cao, C., Huang, J., Yao, J., Hai, T., Zheng, Q., et al. (2016). One-step generation of triple gene-targeted pigs using CRISPR/Cas9 system. *Sci. Rep.* 6:20620. doi: 10.1038/srep20620

Wu, Y., Liang, D., Wang, Y., Bai, M., Tang, W., Bao, S., et al. (2013). Correction of a genetic disease in mouse via use of CRISPR-Cas9. *Cell Stem Cell* 13, 659–662. doi: 10.1016/j.stem.2013.10.016

Zhou, X., Xin, J., Fan, N., Zou, Q., Huang, J., Ouyang, Z., et al. (2015). Generation of CRISPR/Cas9-mediated gene-targeted pigs via somatic cell nuclear transfer. *Cell. Mol. Life Sci.* 72, 1175–1184. doi: 10.1007/s00018-014-1744-7

Zhou, Y. X., Zhu, S. Y., Cai, C. Z., Yuan, P. F., Li, C. M., Huang, Y. Y., et al. (2014). High-throughput screening of a CRISPR/Cas9 library for functional genomics in human cells. *Nature* 509, 487–491. doi: 10.1038/nature13166

Conflict of Interest Statement: The authors declare that the research was conducted in the absence of any commercial or financial relationships that could be construed as a potential conflict of interest.

frontiers in Molecular Neuroscience

HYPOTHESIS AND THEORY
published: 15 July 2015
doi: 10.3389/fnmol.2015.00032

Gene therapy and peripheral nerve repair: a perspective

Stefan A. Hoyng[1,2], *Fred de Winter*[1,2], *Martijn R. Tannemaat*[1,3], *Bas Blits*[4], *Martijn J. A. Malessy*[1,2] *and Joost Verhaagen*[1,5]*

[1] Department of Neuroregeneration, Netherlands Institute for Neuroscience, Amsterdam, Netherlands, [2] Department of Neurosurgery, Leiden University Medical Center, Leiden, Netherlands, [3] Department of Neurology, Leiden University Medical Center, Leiden, Netherlands, [4] UniQure, Amsterdam, Netherlands, [5] Center for Neurogenomics and Cognition Research, Neuroscience Campus Amsterdam, Amsterdam, Netherlands

Clinical phase I/II studies have demonstrated the safety of gene therapy for a variety of central nervous system disorders, including Canavan's, Parkinson's (PD) and Alzheimer's disease (AD), retinal diseases and pain. The majority of gene therapy studies in the CNS have used adeno-associated viral vectors (AAV) and the first AAV-based therapeutic, a vector encoding lipoprotein lipase, is now marketed in Europe under the name Glybera. These remarkable advances may become relevant to translational research on gene therapy to promote peripheral nervous system (PNS) repair. This short review first summarizes the results of gene therapy in animal models for peripheral nerve repair. Secondly, we identify key areas of future research in the domain of PNS-gene therapy. Finally, a perspective is provided on the path to clinical translation of PNS-gene therapy for traumatic nerve injuries. In the latter section we discuss the route and mode of delivery of the vector to human patients, the efficacy and safety of the vector, and the choice of the patient population for a first possible proof-of-concept clinical study.

Keywords: gene therapy, adeno-associated viral vector, lentiviral vector, neurosurgery, Schwann cell

OPEN ACCESS

Edited by:
Andrew Paul Tosolini, University of New South Wales, Australia

Reviewed by:
Claudia Grothe, Hannover Medical School, Germany
Assumpcio Bosch, Universitat Autonoma de Barcelona, Spain

***Correspondence:**
Joost Verhaagen, Department of Neuroregeneration, Netherlands Institute for Neuroscience, Meibergdreef 47, 1105 BA Amsterdam, Netherlands
j.verhaagen@nin.knaw.nl

Received: *19 May 2015*
Accepted: *01 July 2015*
Published: *15 July 2015*

Citation:
Hoyng SA, de Winter F, Tannemaat MR, Blits B, Malessy MJA and Verhaagen J (2015) Gene therapy and peripheral nerve repair: a perspective. Front. Mol. Neurosci. 8:32. doi: 10.3389/fnmol.2015.00032

Gene Therapy in Animal Models for PNS Injury

The peripheral nervous system (PNS) consists of primary sensory neurons in the dorsal root ganglia and motor neurons in the ventral horn of the spinal cord (**Figure 1**). Most peripheral nerves contain axons of sensory and motor neurons and patients who sustain an injury experience loss of sensory and motor function. In patients regeneration of injured peripheral axons does occur but is almost never complete. This is due to the low velocity of axon growth, the deterioration of pro-regenerative Schwann cells in the distal nerve stump following longer periods of denervation, and the misrouting of regrowing axons (Brushart, 2011; Allodi et al., 2012). Nerve regeneration is studied in well-defined rodent models of nerve injury. A widely used model is transection of the sciatic nerve of the rat followed by end-to-end repair of the nerve stumps or implantation of an autograft or artificial nerve guide to bridge the gap between the stumps. In this model axons reinnervate the end organs within weeks to months. Cervical or lumbar spinal root avulsions followed by reimplantation of the roots are much more severe injuries (Eggers et al., 2010; Chu et al., 2012). Following cervical lesions it can take up to 12 weeks before the first axons reinnervate target cells, whereas a significant proportion of axons will stall in the nerve and never reach the end organ. In the lumbar root avulsion model functional recovery is minimal and it is therefore

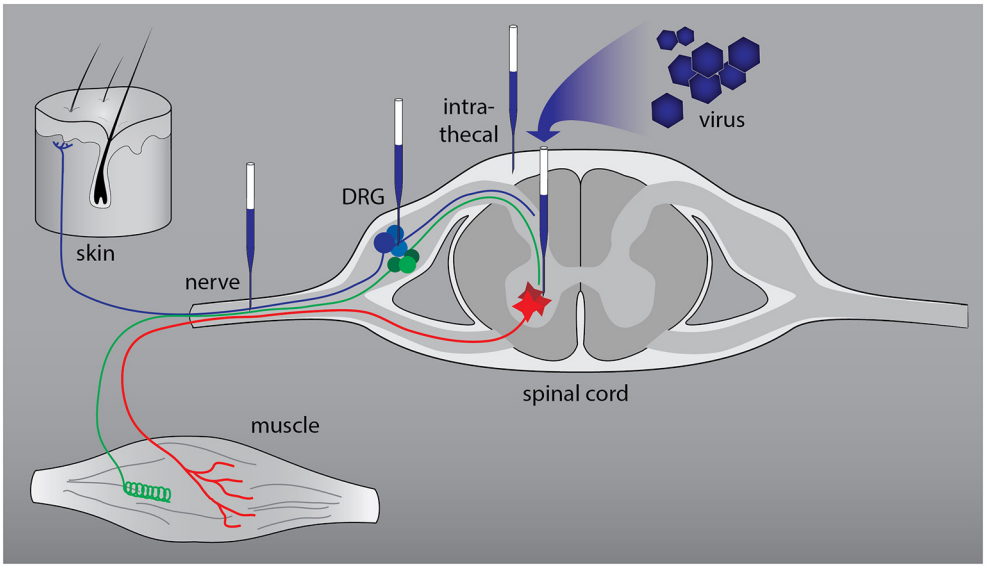

FIGURE 1 | Anatomical relationships in the peripheral nervous system (PNS) and sites of viral vector-mediated gene delivery. The PNS consists of primary sensory neurons (blue and green: nociceptive and proprioceptive neurons) in the dorsal root ganglia (DRG) and motor neurons (red) in the ventral horn of the spinal cord. The axons form a mixed nerve that innervates the skin and muscle. Successful gene delivery to primary sensory and motor neurons and to Schwann cells, the resident glia cells of peripheral nerves, has been reported with various viral vectors. To target primary sensory and motor neurons two routes of delivery have been used successfully: direct intraganglionic or intraspinal injection and intrathecal (IT) delivery. Injection of a viral vector in the nerve stump distal to the lesion or in a nerve graft that bridges the lesion results in transduction of Schwann cells.

one of the best possible mimics of chronic denervation in human patients with proximal lesions.

Surgical repair of peripheral nerves has reached its optimal refinement. Recovery of function as a result of surgical repair has significantly improved but remains limited. Novel adjuvant therapeutic strategies to promote axon regeneration in the injured peripheral nerve are needed to further improve recovery of function. One of these strategies is gene therapy. Successful gene delivery to primary sensory and motor neurons and to Schwann cells, the resident glia cells of peripheral nerves, has been reported with various viral vectors (Haastert-Talini, 2011; Mason et al., 2011). Herpes simplex viral vectors attracted early interest because of their natural tropism for sensory neurons (Geller and Breakefield, 1988; Glorioso and Fink, 2009). Adeno-associated viral vectors (AAV) vectors have become popular as gene delivery agents for neurons of the PNS for several reasons. AAV have a low risk of insertional mutagenesis and immunogenicity, they lack endogenous viral genes, can be produced at high titer and at clinical grade (Salmon et al., 2014; Felberbaum, 2015; Hastie and Samulski, 2015). There are at least 12 vector serotypes, and a number of AAV variants engineered by e.g., viral evolution, which display distinct transduction profiles (Kotterman and Schaffer, 2014). AAV5 is the serotype of choice for rat sensory neurons (Mason et al., 2010), whereas AAV2, 6, 9 and rh10 efficiently target spinal motor neurons (Peel et al., 1997; Blits et al., 2004; Snyder et al., 2011; Homs et al., 2014; Hordeaux et al., 2015). AAV vectors have been used to study the effects of a variety of genes on regeneration of the central branch of sensory neurons (Andrews et al., 2009; Bareyre et al., 2011; Parikh et al., 2011) and on the survival of motor neurons (Blits et al., 2004; Homs et al., 2014; Pajenda et al., 2014; Hordeaux et al., 2015).

Schwann cells are central to the success of peripheral nerve regeneration. However, the unique pro-regenerative properties of these cells fade away after longer periods of denervation. Most gene therapy studies used lentiviral vectors to promote the therapeutic potential of Schwann cells transplanted in artificial nerve guides or in nerve sheets (Haastert et al., 2006; Li et al., 2006; Shakhbazau et al., 2012; Godinho et al., 2013; Santosa et al., 2013) of Schwann cells in autografts (Hoyng et al., 2014a), of Schwann cells present in damaged nerves distal to an injury (Tannemaat et al., 2008; Esaki et al., 2011) or in spinal roots reimplanted in the spinal cord (Eggers et al., 2008). Increased expression of neurotrophic factors is one of the key events observed following peripheral nerve injury. Neurotrophic factor gene therapy stimulated axon regeneration (Mason et al., 2011), myelination (Haastert et al., 2006, 2008; Homs et al., 2011) and facilitated the return of compound motor action potentials (Allodi et al., 2014). Moreover, nerve growth factor (NGF)-gene therapy was used to promote directional growth of sensory axons (Hu et al., 2010). Unexpectedly, however, persistent expression of NGF or glial cell line-derived neurotrophic factor (GDNF) did cause excessive, modality specific axon growth and trapping at the site of expression thereby prohibiting distal growth of axons toward the skin or muscle (Tannemaat et al., 2008; Santosa et al., 2013; Hoyng et al., 2014a). On the one hand, these observations highlight the unprecedented potency of neurotrophic factors. On the other hand they underscore

the need to control the dose and timing of these therapeutic proteins. In the next section three key future areas of research will be discussed, including the optimization of the transduction of Schwann cells, development of gene switches to control the timing of transgene expression, and the need to better understand the biology of the pro-regenerative properties of Schwann cells.

Key Areas of Future Research

AAV is gaining increasing acceptance as a clinical gene delivery platform (Hastie and Samulski, 2015). However, in animal studies PNS-gene therapy to enhance the performance of Schwann cells largely relied on lentiviral vector or adenoviral vector-mediated gene delivery (Mason et al., 2011), with the exception of one recent study that used AAV (Homs et al., 2011). Lentiviral vectors integrate their genetic information into the host cell genome, whereas transgene expression via adenoviral vectors rapidly declines as a result of immune-mediated toxicity (Hermens and Verhaagen, 1997; Dijkhuizen et al., 1998). Although the overall risk of lentiviral vector-associated insertional mutagenesis is low (De Palma et al., 2005; Montini et al., 2006), lentiviral vectors could potentially be harmful for the transduced cells. Surprisingly, very little information is available on the transduction of Schwann cells with AAV vectors (Homs et al., 2011). A recent comparative study of nine AAV serotypes and lentiviral vectors shows that optimal transduction of rat and human Schwann cells is achieved by different serotypes. Rat nerve segments could be genetically modified equally well by a set of four AAV vectors (AAV1, 5, 7, 9), whereas AAV2 was superior in human nerve segments (Hoyng et al., 2015; **Figure 2**). Transduction with lentiviral vectors was, however, superior to the best AAV vectors. Thus, a *first key area of future research* would be to further optimize gene delivery to Schwann cells, either by identifying newly engineered AAV vectors with an improved tropism for Schwann cells (Kotterman and Schaffer, 2014), or by testing lentiviral vectors with an improved safety profile, e.g., non-integrating lentiviral vectors (Yáñez-Muñoz et al., 2006; Cesana et al., 2014). *In vivo* electroporation of expression plasmids in Schwann cells could be an alternative to viral vector-directed gene delivery (Aspalter et al., 2009; Pereira Lopes et al., 2013). Plasmid-mediated gene transfer is a straight forward procedure, however, the strong electrical currents required for the electroporation, the relatively low transduction rate, and short-lived expression of the therapeutic gene indicate that *in vivo* plasmid-based gene transfer will have limited utility.

A *second area of key future research* concerns the creation of a safe regulatable gene therapy vector. In the context of PNS-gene therapy this is essential for two reasons. First, persistent expression of certain growth factors leads to local trapping of axons (discussed above). Second, continued growth factor expression may have unacceptable side-effects, e.g., Nerve growth factor (NGF) may induce hypersensitivity (Verge et al., 2014). The criteria for regulated vector-based therapeutic gene expression are that: (1) it can be induced by a small molecule that is safe; (2) it can be turned off effectively by withdrawal of the inducer whereas "leaky" expression should be minimal and preferably undetectable; and (3) the transactivator protein (TA) that is employed should be non-immunogenic and well-tolerated. The prototypical system for regulating gene expression involves a TA that binds to a promoter in the presence of doxycycline. However, the TA is a bacterial protein and is therefore a permanent immunological target (Markusic and Seppen, 2010). Clinical use of analogous systems using alternative TAs is precluded for the same reason. Viruses have evolved several strategies to escape immune surveillance (Zaldumbide and Hoeben, 2008). We took advantage of the long Gly-Ala repeat (GAr) domain of Epstein Barr virus (Yin et al., 2003) to generate an immunologically inert version of the TA. This idea was based on the observation that Schwann cells which express a foreign protein (e.g., green fluorescent protein, GFP) are cleared from the nerve by an immune response. This does not happen when these proteins are fused to GAr (Ossevoort et al., 2006; Hendriks et al., 2007). We fused GAr to TA and showed that GAr-TA retains its sensitivity to doxorubicin (dox). This system has been used to turn GDNF expression "on" and "off" in rat sciatic nerve. The GAr-TA system is several fold less "leaky" compared to the TA protein. GAr-TA displays strongly reduced immunogenicity in a bioassay for antigenic peptide generation. Therefore, the GAr-TA system fulfills many of the criteria for safe regulatable gene expression (Hoyng et al., 2014b). However, GAr-TA requires doxycycline concentrations that are 40-fold higher than clinically acceptable levels. Therefore, current studies focus on testing newer versions of the TA (Das et al., 2008) and shorter

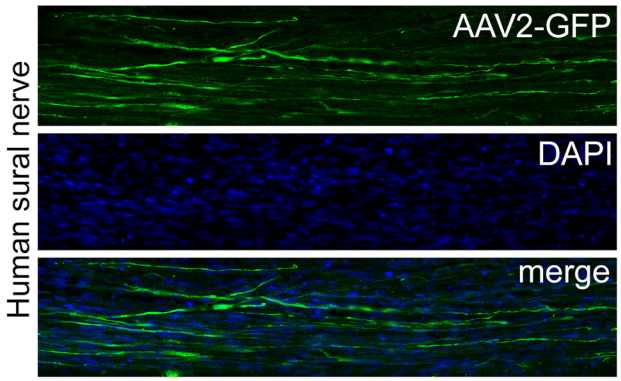

FIGURE 2 | AAV2-mediated transduction of a human sural nerve segment. Surplus human nerve material was obtained from the operation room and anonymized as stated in the code of conduct for responsible use of human tissue and medical research (Federa, 2011). Nine AAV serotypes were compared for their transduction efficiency by injecting 1.85×10^{10} gc/cm nerve and culturing the nerve segments for 14 days. After 14 days nerve segments were immersion fixed with paraformaldehyde and 20 μm sections were prepared. The upper panel show a section through a human sural nerve stained for GFP. The middle panel shows the same image stained for the nuclear stain Hoechst and the lower panel shows the merged images of the two panels. AAV2 transduced numerous cells that display the typical longitudinal shape of Schwann cells and this serotype was superior to all other serotypes tested. More details on this study can be found in Hoyng et al. (2015).

GAr tags which may have improved doxycycline sensitivity. Another complication that may occur is that the continuous presence of the immune-inert TA in cells may induce unwanted effects. Therefore efforts are ongoing to regulate therapeutic and TA gene expression simultaneously. Apart from ligand (i.e., doxcycyline) regulated promoters, promoters induced by physiological stimuli associated with neural injury may emerge as tools to restrict transgene expression to the post-lesion period (Jazwa et al., 2013). The glia fibrillary acidic protein (GFAP)-promoter is an example of an injury induced promotor that has been used in transgenic mice to turn on gene expression in a diseased peripheral nerve (Keller et al., 2009). However GFAP continues to be expressed in non-myelinating Schwann cells in an intact nerve which would result in some level of persistent transgene expression after nerve regeneration has been completed.

Optimization of gene delivery to Schwann cells and the creation of safe regulatable gene therapy vectors are biotechnological challenges. A *third area of future research* concerns the gathering of fundamental biological know-how on the cellular and molecular properties of Schwann cells in a regenerating nerve. A nerve injury induces major, tightly coordinated changes in gene expression in Schwann cells in the distal nerve. Together with the typical alignment of Schwann cells in pathways for growing axons, this creates a unique environment for successful regeneration. The signals that transform stable Schwann cells into the specialized repair cells in an injured nerve are not clearly understood and it is not known why Schwann cells gradually lose their pro-regenerative properties after longer times of denervation (Gordon et al., 2011). Moreover, growing evidence indicates the existence of Schwann cells with distinct phenotypes preferentially supporting either motor or sensory neuron regeneration (Wright et al., 2014) which is relevant to direct growing axons to their correct target cells.

To develop new strategies to stimulate axon regeneration, an analysis of the mechanisms that underlie the pro-regenerative properties of Schwann cells is needed. Conditional knock-out of the gene for the transcription factor c-Jun in Schwann cells has a negative impact on axon regeneration and results in simultaneous down-regulation of multiple pro-regenerative proteins in Schwann cells in an injured nerve (Arthur-Farraj et al., 2012). Neurotrophic factor expression in Schwann cells can be enhanced by overexpression of c-Jun (Huang et al., 2015). C-Jun appears to be one, of perhaps a small set, of central transcriptional "master switches" which, in a cooperative manner, control the pro-regenerative phenotype of Schwann cells (Hung et al., 2015). If, in future experiments, the key regulatory complex of transcription factors are identified, these genes would be prime targets for Schwann cell gene therapy. "Transcriptional reprogramming" of Schwann cells is fundamentally different from PNS-gene therapy with a vector encoding a single neurotrophic factor because this would result in an elaborate repertoire of molecular changes (Huang et al., 2015), which would be particularly beneficial during the intermediate and later phases of the regeneration process when the ability of Schwann cells to support axonal outgrowth deteriorates (Gordon et al., 2011). The identification of the transcriptional "master switches" and studies on their combinatorial role in determining the repair-properties of Schwann cells may also shed new light on the occurrence of specific "motor" and "sensory" specific Schwann cells (Wright et al., 2014).

Path to a Clinical Study

The preclinical issues discussed above require several more years of systematic research in rodents. A clinical study to promote PNS regeneration by gene therapy is therefore currently hypothetical. However, the rapidly growing clinical experience with gene therapy for other neurological diseases and the steady advances in preclinical PNS-gene therapy support the conception of a framework for a future clinical study. The development of a PNS-gene therapy study will benefit particularly from experience with gene therapy for pain and neuromuscular diseases. In these disorders the sensory (pain) and motor neurons and muscle cells (neuromuscular disorders) are the primary target cells (Pleticha et al., 2014a; Cheever et al., 2015). Gene therapy for traumatic nerve injury has to include methods for safe gene transfer to the nerve Schwann cells as well. The following three topics need careful consideration in the context of preclinical-to-clinical translation of PNS-gene therapy and will be discussed below: (1) the route and mode of delivery of the vector; (2) the efficacy and safety of the vector; and (3) the choice of the patient population.

Route and Mode of Delivery of the Vector

Pleticha and colleagues presented a roadmap for the preclinical evaluation of AAV-based genetic modification of dorsal root ganglia (DRG) for clinical trials on pain (Pleticha et al., 2014a). This roadmap covers the essential preclinical steps needed to realize safe AAV-mediated targeting of primary sensory neurons in human patients. The human DRG is approximately 50 times larger than the rat DRG (Shen et al., 2006). The rat motor neuron pool that supplies the nerves that innervate the forepaw (equivalent to the brachial plexus in humans) spreads over 0.5 cm of cervical cord, whereas the motor neuron pool innervating the brachial plexus in humans spans at least 10 cm of the spinal cord. The longest rat peripheral nerve, the sciatic nerve, is approximately 12 cm long while the nerves that innervate the human arm measure 80–100 cm. Therefore, translating gene therapy to the PNS of humans poses specific challenges with respect to the route and mode of delivery of the vector because of the diverging anatomical dimensions of the rodent and human PNS (Pleticha et al., 2014a).

To target primary sensory and motor neurons two routes of delivery have successfully been used: direct intraganglionic or intraspinal injection and intrathecal (IT) delivery. In the rat a single intraganglionic injection of an AAV vector results in efficient transduction of sensory neurons with very little if any spread of the vector to other locations (Mason et al., 2010). In contrast, IT delivery results in transduction of sensory and spinal motor neurons and other

non-neuronal cell types (Snyder et al., 2011). In humans, lumbar puncture is a relatively safe and standard technique to approach the cerebrospinal fluid and it would be feasible to deliver a vector to human DRGs and spinal motor neurons via this route. AAV vectors were delivered to the cat, the pig and to non-human primates using a lumbar puncture technique (Bucher et al., 2013; Gray et al., 2013; Pleticha et al., 2013; Samaranch et al., 2013; Dirren et al., 2014; Passini et al., 2014). If expression of a transgene in areas outside the DRG is not desirable, direct injection would be a requirement. Convection enhanced delivery (CED) relies on enhanced extracellular transport of a solution infused in tissue over an extended period of time (typically ranging from 20 min to 2 h, Krauze et al., 2005a,b) and results in equal tissue distribution of the infusate. Minimally invasive intra-ganglionic gene transfer by CT-guided percutaneous injection and CED of AAV1 in lumbar DRGs of the pig resulted in 33% transduction of DRG neurons (Pleticha et al., 2014c).

Gene transfer to the injury-repair site of a human peripheral nerve will require a method to deliver a vector to a sural nerve graft inserted to connect the proximal and distal stump or to the nerve distal to the repair site. In rats, when relying on diffusion of the viral vector during a single manually guided 1–2 µl injection, the vector spreads in a nerve graft or in a nerve stump distal to a repair site over several millimeters (Tannemaat et al., 2008; Hoyng et al., 2014a). Four injections placed at 5–8 mm distances from each other resulted in the transduction of a 4–5 cm long segment of rat sciatic nerve (Eggers et al., 2013). This injection technique results in rather unequal transduction of Schwann cells, with "hot spots" containing many transduced cells, and areas with no or very little transduced cells. CED carries macromolecules (such as Gadolinium-labeled Albumine for direct monitoring of the infusion process) over a distance of 1 cm in a rat nerve (Pleticha et al., 2014b) and over distances of 2.7–3.5 cm in a nerve of a non-human primate (Ratliff and Oldfield, 2001; Chen et al., 2011). Importantly, and in contrast to manual injection of small volumes of vector solution, CED resulted in an equal distribution of the infusate over the nerve. Future studies have to test whether CED of a viral vector to an injured nerve of a larger animal is a feasible option. Taken together, gene therapy for traumatic nerve injuries will benefit significantly from the encouraging observations in larger animals which show that the neuroanatomical dimensions do not preclude efficient gene delivery to the human PNS.

Safety and Efficacy of the Vector

Rigorous toxicity, and serological and cellular immune assessments have been performed for AAV1, AAV2, AAV5 AAV8 and AAVrh10. These serotypes have been used in clinical trials for lipoprotein lipase deficiency (LPLD; AAV-1; Scott, 2015), Canavan disease, PD and AD (AAV-2; Leone et al., 2000, 2012; Kaplitt et al., 2007; Richardson et al., 2011; Bartus et al., 2013; Rafii et al., 2014), liver mediated diseases (AAV5; Grosios and Pañeda, 2013), San Fillipo B (AAV5, AAVrh10; Tardieu et al., 2014)[1] and Hemeophilia B (AAV-5, AAV-8; Nathwani et al., 2014). Although most humans have natural occurring neutralizing antibodies against AAV and treatment with AAV usually results in enhanced levels of these antibodies, this occurred without detectable pathological effects (Salmon et al., 2014). Screening of patients following application of an AAV-1 vector to skeletal muscle resulted in seropositivity for AAV1 (Ferreira et al., 2014; Salmon et al., 2014). Antibodies which develop after the administration of AAV1 would not interfere with the therapeutic effect as the AAV vector has already delivered its therapeutic cargo. However, preexisting antibodies may interfere significantly with the transduction process as has been shown in some studies (Samaranch et al., 2013), whereas neutralizing antibodies had no effect on gene delivery with AAV after intraparenchymal or IT injection in other studies (Gray et al., 2013).

Transduction differences between different serotypes in rat, larger animals and human complicates the choice of the vector for preclinical-to-clinical translation. The use of primary human tissue, either biopsy material or autopsy tissue, may prove to be critical in determining the optimal serotype for human patients. In our hands, cultured human peripheral nerve segments, obtained as left-over tissue from the operation theater after nerve repair surgery, were transducible by lentiviral vectors (Tannemaat et al., 2007), whereas AAV-serotype testing showed that AAV2 was superior to eight other common serotypes investigated (Hoyng et al., 2015; **Figure 2**). To date, AAV2 has been used in several clinical trials and, together with AAV1, is one of the best characterized serotypes. AAV2 outperforms other serotypes in human nerve segments and is therefore currently the leading vector for a clinical study that aims at enhancing the therapeutic potential of Schwann cells in a human peripheral nerve.

The Choice of the Patient Population

Animal models will provide information about the efficacy and safety of the delivery technique, the vector and the transgene. However, the predictive value of animal studies is limited and eventually a study on a small number of human subjects with a PNS-lesion will be a necessary step in the translation process (Cheever et al., 2015). An early gene therapy study for AD enrolled eight patients (Tuszynski et al., 2005). This study was too small to demonstrate efficacy, but showed that the gene therapy procedure was feasible and well-tolerated. The transgene was NGF, a growth factor relevant in the context of PNS-gene therapy. NGF expression was detectable in post-mortem brain tissue of a subject that died of causes unrelated to the gene delivery procedure. This shows that a small clinical study can be highly informative and may form the basis of a larger randomized gene therapy trial (Cheever et al., 2015).

Nerve injury is a heterogeneous condition, ranging from brachial plexus injuries to distal injuries of the digital

[1]http://www.uniqure.com/news/182/182/Clinical-trial-launched-to-treat-Sanfilippo-B-syndrome-using-gene-therapy.html

nerves that innervate the hand. Established guidelines on the design of clinical trials for the evaluation of novel treatments for nerve injury do not (yet) exist. Previous trials to test experimental treatments to promote nerve regeneration involved patients that sustained very different types of injuries. A recent successful clinical trial on the beneficial effect of electrical stimulation was performed on patients with complete transection injury of the digital nerve (Wong et al., 2015). An advantage of this study population is its relative homogeneity. Although a clinically meaningful degree of regeneration occurs spontaneously in these patients, enhanced sensory reinnervation was detectable following a short period of per-operative electrical stimulation. A follow-up trial with electrical stimulation as adjuvant treatment to surgical repair in patients with a severe brachial plexus injury, a severe lesion that causes serious dysfunction of the arm with prospects of only limited functional recovery of biceps function, is currently underway.[2] Thus, although electrical stimulation is a straight-forward procedure shown to be effective and safe in animals (Al-Majed et al., 2000; Brushart et al., 2005; Gordon et al., 2008, 2010; Haastert-Talini et al., 2011), tolerability and efficacy were first studied in a patient population that sustained a lesion with relatively moderate medical consequences before translating the procedure to lesions associated with long-lasting disability. A similarly cautious and phased translational path for PNS-gene therapy is mandatory.

[2]www.clinicaltrials.gov

Gene therapy for neurotrophic factors was well-tolerated in Alzheimer's (NGF; Rafii et al., 2014) and Parkinson's disease (Neurturin; Bartus et al., 2013) patients. In contrast to neurotrophic factor gene therapy in the brain, neurotrophic factor gene delivery to an injured peripheral nerve is not without risk, as it may induce uncontrolled growth of axons, hypersensitivity and unwanted changes in Schwann cells (Mason et al., 2011). As discussed above, animal studies must first provide robust experimental evidence showing that control over the dose and the timing of viral vector-derived neurotrophic factor expression is effective, before gene therapy in a small group of patients with a nerve lesion can be undertaken. A gene therapy study in patients with a digital nerve injury, as performed for electrical stimulation, may reveal potential unwanted effects, and monitoring benefit is possible with the current battery of sensory tests (Wong et al., 2015). The vector, preferably an immune-inert regulatable AAV vector encoding NGF (a growth factor with stimulatory effects on sensory fibers) would be delivered to the denervated digital nerve by CED or by multiple injections along the 6–10 cm long digital nerve immediately following end-to-end repair. While this pilot study could be important in demonstrating safety and tolerability of PNS gene therapy, the therapeutic benefit of gene therapy for digital nerve injury patients is probably limited as this nerve displays a significant degree of spontaneous regeneration. Patients with a brachial plexus injury, a lesion which has a permanent negative impact, are a target group where gene therapeutic intervention could develop into a genuine adjuvant regenerative treatment strategy to further promote repair after neurosurgical intervention.

References

Allodi, I., Mecollari, V., González-Pérez, F., Eggers, R., Hoyng, S., Verhaagen, J., et al. (2014). Schwann cells transduced with a lentiviral vector encoding Fgf-2 promote motor neuron regeneration following sciatic nerve injury. *Glia* 62, 1736–1746. doi: 10.1002/glia.22712

Allodi, I., Udina, E., and Navarro, X. (2012). Specificity of peripheral nerve regeneration: interactions at the axon level. *Prog. Neurobiol.* 98, 16–37. doi: 10.1016/j.pneurobio.2012.05.005

Al-Majed, A. A., Brushart, T. M., and Gordon, T. (2000). Electrical stimulation accelerates and increases expression of BDNF and trkB mRNA in regenerating rat femoral motoneurons. *Eur. J. Neurosci.* 12, 4381–4390. doi: 10.1111/j.1460-9568.2000.01341.x

Andrews, M. R., Czvitkovich, S., Dassie, E., Vogelaar, C. F., Faissner, A., Blits, B., et al. (2009). Alpha9 integrin promotes neurite outgrowth on tenascin-C and enhances sensory axon regeneration. *J. Neurosci.* 29, 5546–5557. doi: 10.1523/jneurosci.0759-09.2009

Arthur-Farraj, P. J., Latouche, M., Wilton, D. K., Quintes, S., Chabrol, E., Banerjee, A., et al. (2012). c-Jun reprograms Schwann cells of injured nerves to generate a repair cell essential for regeneration. *Neuron* 75, 633–647. doi: 10.1016/j.neuron.2012.06.021

Aspalter, M., Vyas, A., Feiner, J., Griffin, J., Brushart, T., and Redett, R. (2009). Modification of Schwann cell gene expression by electroporation *in vivo*. *J. Neurosci. Methods* 176, 96–103. doi: 10.1016/j.jneumeth.2008.08.035

Bareyre, F. M., Garzorz, N., Lang, C., Misgeld, T., Büning, H., and Kerschensteiner, M. (2011). *In vivo* imaging reveals a phase-specific role of STAT3 during central and peripheral nervous system axon regeneration. *Proc. Natl. Acad. Sci. U S A* 108, 6282–6287. doi: 10.1073/pnas.1015239108

Bartus, R. T., Baumann, T. L., Siffert, J., Herzog, C. D., Alterman, R., Boulis, N., et al. (2013). Safety/feasibility of targeting the substantia nigra with AAV2-neurturin in Parkinson patients. *Neurology* 80, 1698–1701. doi: 10.1212/wnl.0b013e3182904faa

Blits, B., Carlstedt, T. P., Ruitenberg, M. J., de Winter, F., Hermens, W. T., Dijkhuizen, P. A., et al. (2004). Rescue and sprouting of motoneurons following ventral root avulsion and reimplantation combined with intraspinal adeno-associated viral vector-mediated expression of glial cell line-derived neurotrophic factor or brain-derived neurotrophic factor. *Exp. Neurol.* 189, 303–316. doi: 10.1016/j.expneurol.2004.05.014

Brushart, T. M. (2011). *Nerve Repair*. New York: Oxford University Press.

Brushart, T. M., Jari, R., Verge, V., Rohde, C., and Gordon, T. (2005). Electrical stimulation restores the specificity of sensory axon regeneration. *Exp. Neurol.* 194, 221–229. doi: 10.1016/j.expneurol.2005.02.007

Bucher, T., Colle, M. A., Wakeling, E., Dubreil, L., Fyfe, J., Briot-Nivard, D., et al. (2013). scAAV9 intracisternal delivery results in efficient gene transfer to the central nervous system of a feline model of motor neuron disease. *Hum. Gene Ther.* 24, 670–682. doi: 10.1089/hum.2012.218

Cesana, D., Ranzani, M., Volpin, M., Bartholomae, C., Duros, C., Artus, A., et al. (2014). Uncovering and dissecting the genotoxicity of self-inactivating lentiviral vectors *in vivo*. *Mol. Ther.* 22, 774–785. doi: 10.1038/mt.2014.3

Cheever, T. R., Berkley, D., Braun, S., Brown, R. H., Byrne, B. J., Chamberlain, J. S., et al. (2015). Perspectives on best practices for gene therapy programs. *Hum. Gene Ther.* 26, 127–133. doi: 10.1089/hum.2014.147

Chen, X., Astary, G. W., Mareci, T. H., and Sarntinoranont, M. (2011). *In vivo* contrast-enhanced MR imaging of direct infusion into rat peripheral nerves. *Ann. Biomed. Eng.* 39, 2823–2834. doi: 10.1007/s10439-011-0362-x

Chu, T. H., Wang, L., Guo, A., Chan, V. W., Wong, C. W., and Wu, W. (2012). GDNF-treated acellular nerve graft promotes motoneuron axon regeneration after implantation into cervical root avulsed spinal cord.

Neuropathol. Appl. Neurobiol. 38, 681–695. doi: 10.1111/j.1365-2990.2012.01253.x

Das, A. T., Klaver, B., Centlivre, M., Harwig, A., Ooms, M., Page, M., et al. (2008). Optimization of the doxycycline-dependent simian immunodeficiency virus through *in vitro* evolution. *Retrovirology* 5:44. doi: 10.1186/1742-4690-5-44

De Palma, M., Montini, E., Santoni de Sio, F. R., Benedicenti, F., Gentile, A., Medico, E., et al. (2005). Promoter trapping reveals significant differences in integration site selection between MLV and HIV vectors in primary hematopoietic cells. *Blood* 105, 2307–2315. doi: 10.1182/blood-2004-03-0798

Dijkhuizen, P. A., Pasterkamp, R. J., Hermens, W. T., de Winter, F., Giger, R. J., and Verhaagen, J. (1998). Adenoviral vector-mediated gene delivery to injured rat peripheral nerve. *J. Neurotrauma* 15, 387–397. doi: 10.1089/neu.1998.15.387

Dirren, E., Towne, C. L., Setola, V., Redmond, D. E. Jr., Schneider, B. L., and Aebischer, P. (2014). Intracerebroventricular injection of adeno-associated virus 6 and 9 vectors for cell type-specific transgene expression in the spinal cord. *Hum. Gene Ther.* 25, 109–120. doi: 10.1089/hum.2013.021

Eggers, R., de Winter, F., Hoyng, S. A., Roet, K. C., Ehlert, E. M., Malessy, M. J., et al. (2013). Lentiviral vector-mediated gradients of GDNF in the injured peripheral nerve: effects on nerve coil formation, Schwann cell maturation and myelination. *PLoS One* 8:e71076. doi: 10.1371/journal.pone.0071076

Eggers, R., Hendriks, W. T., Tannemaat, M. R., van Heerikhuize, J. J., Pool, C. W., Carlstedt, T. P., et al. (2008). Neuroregenerative effects of lentiviral vector-mediated GDNF expression in reimplanted ventral roots. *Mol. Cell. Neurosci.* 39, 105–117. doi: 10.1016/j.mcn.2008.05.018

Eggers, R., Tannemaat, M. R., Ehlert, E. M., and Verhaagen, J. (2010). A spatio-temporal analysis of motoneuron survival, axonal regeneration and neurotrophic factor expression after lumbar ventral root avulsion and implantation. *Exp. Neurol.* 223, 207–220. doi: 10.1016/j.expneurol.2009.07.021

Esaki, S., Kitoh, J., Katsumi, S., Goshima, F., Kimura, H., Safwat, M., et al. (2011). Hepatocyte growth factor incorporated into herpes simplex virus vector accelerates facial nerve regeneration after crush injury. *Gene Ther.* 18, 1063–1069. doi: 10.1038/gt.2011.57

Federa. (2011). Human tissue and medical research: code of conduct for responsible use. Available online at: http://www.federa.org/

Felberbaum, R. S. (2015). The baculovirus expression vector system: a commercial manufacturing platform for viral vaccines and gene therapy vectors. *Biotechnol. J.* 10, 702–714. doi: 10.1002/biot.201400438

Ferreira, V., Petry, H., and Salmon, F. (2014). Immune responses to AAV-vectors, the glybera example from bench to bedside. *Front. Immunol.* 5:82. doi: 10.3389/fimmu.2014.00082

Geller, A. I., and Breakefield, X. O. (1988). A defective HSV-1 vector expresses Escherichia coli beta-galactosidase in cultured peripheral neurons. *Science* 241, 1667–1669. doi: 10.1126/science.2843986

Glorioso, J. C., and Fink, D. J. (2009). Herpes vector-mediated gene transfer in the treatment of chronic pain. *Mol. Ther.* 17, 13–18. doi: 10.1038/mt.2008.213

Godinho, M. J., Teh, L., Pollett, M. A., Goodman, D., Hodgetts, S. I., Sweetman, I., et al. (2013). Immunohistochemical, ultrastructural and functional analysis of axonal regeneration through peripheral nerve grafts containing Schwann cells expressing BDNF, CNTF or NT3. *PLoS One* 8:e69987. doi: 10.1371/journal.pone.0069987

Gordon, T., Amirjani, N., Edwards, D. C., and Chan, K. M. (2010). Brief post-surgical electrical stimulation accelerates axon regeneration and muscle reinnervation without affecting the functional measures in carpal tunnel syndrome patients. *Exp. Neurol.* 223, 192–202. doi: 10.1016/j.expneurol.2009.09.020

Gordon, T., Brushart, T. M., and Chan, K. M. (2008). Augmenting nerve regeneration with electrical stimulation. *Neurol. Res.* 30, 1012–1022. doi: 10.1179/174313208x362488

Gordon, T., Tyreman, N., and Raji, M. A. (2011). The basis for diminished functional recovery after delayed peripheral nerve repair. *J. Neurosci.* 31, 5325–5334. doi: 10.1523/jneurosci.6156-10.2011

Gray, S. J., Nagabhushan Kalburgi, S., McCown, T. J., and Jude Samulski, R. (2013). Global CNS gene delivery and evasion of anti-AAV-neutralizing antibodies by intrathecal AAV administration in non-human primates. *Gene Ther.* 20, 450–459. doi: 10.1038/gt.2012.101

Grosios, K., and Pañeda, A. (2013). Gene therapy for AIP. *Pan European Networks: Science and Technology.* Available online at: www.paneuropeannetworks.com

Haastert, K., Lipokatic, E., Fischer, M., Timmer, M., and Grothe, C. (2006). Differentially promoted peripheral nerve regeneration by grafted Schwann cells over-expressing different FGF-2 isoforms. *Neurobiol. Dis.* 21, 138–153. doi: 10.1016/j.nbd.2005.06.020

Haastert, K., Ying, Z., Grothe, C., and Gómez-Pinilla, F. (2008). The effects of FGF-2 gene therapy combined with voluntary exercise on axonal regeneration across peripheral nerve gaps. *Neurosci. Lett.* 443, 179–183. doi: 10.1016/j.neulet.2008.07.087

Haastert-Talini, K. (2011). Gene therapy approaches for neuroregeneration. *Curr. Gene Ther.* 11:74. doi: 10.2174/156652311794940809

Haastert-Talini, K., Schmitte, R., Korte, N., Klode, D., Ratzka, A., and Grothe, C. (2011). Electrical stimulation accelerates axonal and functional peripheral nerve regeneration across long gaps. *J. Neurotrauma* 28, 661–674. doi: 10.1089/neu.2010.1637

Hastie, E., and Samulski, R. J. (2015). Adeno-associated virus at 50: a golden anniversary of discovery, research and gene therapy success-a personal perspective. *Hum. Gene Ther.* 26, 257–265. doi: 10.1089/hum.2015.025

Hendriks, W. T., Eggers, R., Carlstedt, T. P., Zaldumbide, A., Tannemaat, M. R., Fallaux, F. J., et al. (2007). Lentiviral vector-mediated reporter gene expression in avulsed spinal ventral root is short-term, but is prolonged using an immune "stealth" transgene. *Restor. Neurol. Neurosci.* 25, 585–599.

Hermens, W. T., and Verhaagen, J. (1997). Adenoviral vector-mediated gene expression in the nervous system of immunocompetent Wistar and T cell-deficient nude rats: preferential survival of transduced astroglial cells in nude rats. *Hum. Gene Ther.* 8, 1049–1063. doi: 10.1089/hum.1997.8.9-1049

Homs, J., Ariza, L., Pagès, G., Udina, E., Navarro, X., Chillón, M., et al. (2011). Schwann cell targeting via intrasciatic injection of AAV8 as gene therapy strategy for peripheral nerve regeneration. *Gene Ther.* 18, 622–630. doi: 10.1038/gt.2011.7

Homs, J., Pagès, G., Ariza, L., Casas, C., Chillón, M., Navarro, X., et al. (2014). Intrathecal administration of IGF-I by AAVrh10 improves sensory and motor deficits in a mouse model of diabetic neuropathy. *Mol. Ther. Methods Clin. Dev.* 1:7. doi: 10.1038/mtm.2013.7

Hordeaux, J., Dubreil, L., Deniaud, J., Iacobelli, F., Moreau, S., Ledevin, M., et al. (2015). Efficient central nervous system AAVrh10-mediated intrathecal gene transfer in adult and neonate rats. *Gene Ther.* 22, 316–324. doi: 10.1038/gt.2014.121

Hoyng, S. A., De Winter, F., Gnavi, S., de Boer, R., Boon, L. I., Korvers, L. M., et al. (2014a). A comparative morphological, electrophysiological and functional analysis of axon regeneration through peripheral nerve autografts genetically modified to overexpress BDNF, CNTF, GDNF, NGF, NT3 or VEGF. *Exp. Neurol.* 261, 578–593. doi: 10.1016/j.expneurol.2014.08.002

Hoyng, S. A., Gnavi, S., de Winter, F., Eggers, R., Ozawa, T., Zaldumbide, A., et al. (2014b). Developing a potentially immunologically inert tetracycline-regulatable viral vector for gene therapy in the peripheral nerve. *Gene Ther.* 21, 549–557. doi: 10.1038/gt.2014.22

Hoyng, S. A., De Winter, F., Gnavi, S., van Egmond, L., Attwell, C., Tannemaat, M. R., et al. (2015). Gene delivery to rat and human Schwann cells and nerve segments: a comparison of AAV 1 to 9 and lentiviral vectors. *Gene Ther.* doi: 10.1038/gt.2015.47 [Epub ahead of print].

Hu, X., Cai, J., Yang, J., and Smith, G. M. (2010). Sensory axon targeting is increased by NGF gene therapy within the lesioned adult femoral nerve. *Exp. Neurol.* 223, 153–165. doi: 10.1016/j.expneurol.2009.08.025

Huang, L., Quan, X., Liu, Z., Ma, T., Wu, Y., Ge, J., et al. (2015). c-Jun gene-modified schwann cells: upregulating multiple neurotrophic factors and promoting neurite outgrowth. *Tissue Eng. Part A* 21, 1409–1421. doi: 10.1089/ten.tea.2014.0416

Hung, H. A., Sun, G., Keles, S., and Svaren, J. (2015). Dynamic regulation of Schwann cell enhancers after peripheral nerve injury. *J. Biol. Chem.* 290, 6937–6950. doi: 10.1074/jbc.m114.622878

Jazwa, A., Florczyk, U., Jozkowicz, A., and Dulak, J. (2013). Gene therapy on demand: site specific regulation of gene therapy. *Gene* 525, 229–238. doi: 10.1016/j.gene.2013.03.093

Kaplitt, M. G., Feigin, A., Tang, C., Fitzsimons, H. L., Mattis, P., Lawlor, P. A., et al. (2007). Safety and tolerability of gene therapy with an adeno-associated virus (AAV) borne GAD gene for Parkinson's disease: an open label, phase I trial. *Lancet* 369, 2097–2105. doi: 10.1016/s0140-6736(07)60982-9

Keller, A. F., Gravel, M., and Kriz, J. (2009). Live imaging of amyotrophic lateral sclerosis pathogenesis: disease onset is characterized by marked induction of GFAP in Schwann cells. *Glia* 57, 1130–1142. doi: 10.1002/glia.20836

Kotterman, M. A., and Schaffer, D. V. (2014). Engineering adeno-associated viruses for clinical gene therapy. *Nat. Rev. Genet.* 15, 445–451. doi: 10.1038/nrg3742

Krauze, M. T., Mcknight, T. R., Yamashita, Y., Bringas, J., Noble, C. O., Saito, R., et al. (2005a). Real-time visualization and characterization of liposomal delivery into the monkey brain by magnetic resonance imaging. *Brain Res. Brain Res. Protoc.* 16, 20–26. doi: 10.1016/j.brainresprot.2005.08.003

Krauze, M. T., Saito, R., Noble, C., Bringas, J., Forsayeth, J., Mcknight, T. R., et al. (2005b). Effects of the perivascular space on convection-enhanced delivery of liposomes in primate putamen. *Exp. Neurol.* 196, 104–111. doi: 10.1016/j.expneurol.2005.07.009

Leone, P., Janson, C. G., Bilaniuk, L., Wang, Z., Sorgi, F., Huang, L., et al. (2000). Aspartoacylase gene transfer to the mammalian central nervous system with therapeutic implications for Canavan disease. *Ann. Neurol.* 48, 27–38. doi: 10.1002/1531-8249(200007)48:1<27::aid-ana6>3.0.co;2-6

Leone, P., Shera, D., Mcphee, S. W., Francis, J. S., Kolodny, E. H., Bilaniuk, L. T., et al. (2012). Long-term follow-up after gene therapy for canavan disease. *Sci. Transl. Med.* 4:165ra163. doi: 10.1126/scitranslmed.3003454

Li, Q., Ping, P., Jiang, H., and Liu, K. (2006). Nerve conduit filled with GDNF gene-modified Schwann cells enhances regeneration of the peripheral nerve. *Microsurgery* 26, 116–121. doi: 10.1002/micr.20192

Markusic, D., and Seppen, J. (2010). Doxycycline regulated lentiviral vectors. *Methods Mol. Biol.* 614, 69–76. doi: 10.1007/978-1-60761-533-0_4

Mason, M. R., Ehlert, E. M., Eggers, R., Pool, C. W., Hermening, S., Huseinovic, A., et al. (2010). Comparison of AAV serotypes for gene delivery to dorsal root ganglion neurons. *Mol. Ther.* 18, 715–724. doi: 10.1038/mt.2010.19

Mason, M. R., Tannemaat, M. R., Malessy, M. J., and Verhaagen, J. (2011). Gene therapy for the peripheral nervous system: a strategy to repair the injured nerve? *Curr. Gene Ther.* 11, 75–89. doi: 10.2174/156652311794940764

Montini, E., Cesana, D., Schmidt, M., Sanvito, F., Ponzoni, M., Bartholomae, C., et al. (2006). Hematopoietic stem cell gene transfer in a tumor-prone mouse model uncovers low genotoxicity of lentiviral vector integration. *Nat. Biotechnol.* 24, 687–696. doi: 10.1038/nbt1216

Nathwani, A. C., Reiss, U. M., Tuddenham, E. G., Rosales, C., Chowdary, P., Mcintosh, J., et al. (2014). Long-term safety and efficacy of factor IX gene therapy in hemophilia B. *N. Engl. J. Med.* 371, 1994–2004. doi: 10.1056/NEJMoa1407309

Ossevoort, M., Zaldumbide, A., Cramer, S. J., Van Der Voort, E. I., Toes, R. E., and Hoeben, R. C. (2006). Characterization of an immuno 'stealth' derivative of the herpes simplex virus thymidine-kinase gene. *Cancer Gene Ther.* 13, 584–591. doi: 10.1038/sj.cgt.7700925

Pajenda, G., Hercher, D., Marton, G., Pajer, K., Feichtinger, G. A., Maleth, J., et al. (2014). Spatiotemporally limited BDNF and GDNF overexpression rescues motoneurons destined to die and induces elongative axon growth. *Exp. Neurol.* 261, 367–376. doi: 10.1016/j.expneurol.2014.05.019

Parikh, P., Hao, Y., Hosseinkhani, M., Patil, S. B., Huntley, G. W., Tessier-Lavigne, M., et al. (2011). Regeneration of axons in injured spinal cord by activation of bone morphogenetic protein/Smad1 signaling pathway in adult neurons. *Proc. Natl. Acad. Sci. U S A* 108, E99–107. doi: 10.1073/pnas.1100426108

Passini, M. A., Bu, J., Richards, A. M., Treleaven, C. M., Sullivan, J. A., O'riordan, C. R., et al. (2014). Translational fidelity of intrathecal delivery of self-complementary AAV9-survival motor neuron 1 for spinal muscular atrophy. *Hum. Gene Ther.* 25, 619–630. doi: 10.1089/hum.2014.011

Peel, A. L., Zolotukhin, S., Schrimsher, G. W., Muzyczka, N., and Reier, P. J. (1997). Efficient transduction of green fluorescent protein in spinal cord neurons using adeno-associated virus vectors containing cell type-specific promoters. *Gene Ther.* 4, 16–24. doi: 10.1038/sj.gt.3300358

Pereira Lopes, F. R., Martin, P. K., Frattini, F., Biancalana, A., Almeida, F. M., Tomaz, M. A., et al. (2013). Double gene therapy with granulocyte colony-stimulating factor and vascular endothelial growth factor acts synergistically to improve nerve regeneration and functional outcome after sciatic nerve injury in mice. *Neuroscience* 230, 184–197. doi: 10.1016/j.neuroscience.2012.10.025

Pleticha, J., Heilmann, L. F., Evans, C. H., Asokan, A., Samulski, R. J., and Beutler, A. S. (2014a). Preclinical toxicity evaluation of AAV for pain: evidence from human AAV studies and from the pharmacology of analgesic drugs. *Mol. Pain* 10:54. doi: 10.1186/1744-8069-10-54

Pleticha, J., Jeng-Singh, C., Rezek, R., Zaibak, M., and Beutler, A. S. (2014b). Intraneural convection enhanced delivery of AAVrh20 for targeting primary sensory neurons. *Mol. Cell. Neurosci.* 60, 72–80. doi: 10.1016/j.mcn.2014.04.004

Pleticha, J., Maus, T. P., Christner, J. A., Marsh, M. P., Lee, K. H., Hooten, W. M., et al. (2014c). Minimally invasive convection-enhanced delivery of biologics into dorsal root ganglia: validation in the pig model and prospective modeling in humans. Technical note. *J. Neurosurg.* 121, 851–858. doi: 10.3171/2014.6.jns132364

Pleticha, J., Maus, T. P., Jeng-Singh, C., Marsh, M. P., Al-Saiegh, F., Christner, J. A., et al. (2013). Pig lumbar spine anatomy and imaging-guided lateral lumbar puncture: a new large animal model for intrathecal drug delivery. *J. Neurosci. Methods* 216, 10–15. doi: 10.1016/j.jneumeth.2013.03.006

Rafii, M. S., Baumann, T. L., Bakay, R. A., Ostrove, J. M., Siffert, J., Fleisher, A. S., et al. (2014). A phase1 study of stereotactic gene delivery of AAV2-NGF for Alzheimer's disease. *Alzheimers Dement.* 10, 571–581. doi: 10.1016/j.jalz.2013.09.004

Ratliff, J. K., and Oldfield, E. H. (2001). Convection-enhanced delivery in intact and lesioned peripheral nerve. *J. Neurosurg.* 95, 1001–1011. doi: 10.3171/jns.2001.95.6.1001

Richardson, R. M., Kells, A. P., Rosenbluth, K. H., Salegio, E. A., Fiandaca, M. S., Larson, P. S., et al. (2011). Interventional MRI-guided putaminal delivery of AAV2-GDNF for a planned clinical trial in Parkinson's disease. *Mol. Ther.* 19, 1048–1057. doi: 10.1038/mt.2011.11

Salmon, F., Grosios, K., and Petry, H. (2014). Safety profile of recombinant adeno-associated viral vectors: focus on alipogene tiparvovec (Glybera(R)). *Expert Rev. Clin. Pharmacol.* 7, 53–65. doi: 10.1586/17512433.2014.852065

Samaranch, L., Salegio, E. A., San Sebastian, W., Kells, A. P., Bringas, J. R., Forsayeth, J., et al. (2013). Strong cortical and spinal cord transduction after AAV7 and AAV9 delivery into the cerebrospinal fluid of nonhuman primates. *Hum. Gene Ther.* 24, 526–532. doi: 10.1089/hum.2013.005

Santosa, K. B., Jesuraj, N. J., Viader, A., Macewan, M., Newton, P., Hunter, D. A., et al. (2013). Nerve allografts supplemented with schwann cells overexpressing glial-cell-line-derived neurotrophic factor. *Muscle Nerve* 47, 213–223. doi: 10.1002/mus.23490

Scott, L. J. (2015). Alipogene tiparvovec: a review of its use in adults with familial lipoprotein lipase deficiency. *Drugs* 75, 175–182. doi: 10.1007/s40265-014-0339-9

Shakhbazau, A., Kawasoe, J., Hoyng, S. A., Kumar, R., Van, M. J., Verhaagen, J., et al. (2012). Early regenerative effects of NGF-transduced Schwann cells in peripheral nerve repair. *Mol. Cell. Neurosci.* 50, 103–112. doi: 10.1016/j.mcn.2012.04.004

Shen, J., Wang, H. Y., Chen, J. Y., and Liang, B. L. (2006). Morphologic analysis of normal human lumbar dorsal root ganglion by 3D MR imaging. *AJNR Am. J. Neuroradiol.* 27, 2098–2103.

Snyder, B. R., Gray, S. J., Quach, E. T., Huang, J. W., Leung, C. H., Samulski, R. J., et al. (2011). Comparison of adeno-associated viral vector serotypes for spinal cord and motor neuron gene delivery. *Hum. Gene Ther.* 22, 1129–1135. doi: 10.1089/hum.2011.008

Tannemaat, M. R., Boer, G. J., Verhaagen, J., and Malessy, M. J. (2007). Genetic modification of human sural nerve segments by a lentiviral vector encoding nerve growth factor. *Neurosurgery* 61, 1286–1294. doi: 10.1227/01.neu.0000306108.78044.a2

Tannemaat, M. R., Eggers, R., Hendriks, W. T., De Ruiter, G. C., Van Heerikhuize, J. J., Pool, C. W., et al. (2008). Differential effects of lentiviral vector-mediated overexpression of nerve growth factor and glial cell line-derived neurotrophic factor on regenerating sensory and motor axons in the transected peripheral nerve. *Eur. J. Neurosci.* 28, 1467–1479. doi: 10.1111/j.1460-9568.2008.06452.x

Tardieu, M., Zerah, M., Husson, B., De Bournonville, S., Deiva, K., Adamsbaum, C., et al. (2014). Intracerebral administration of adeno-associated viral vector serotype rh.10 carrying human SGSH and SUMF1 cDNAs in children with mucopolysaccharidosis type IIIA disease: results of a phase I/II trial. *Hum. Gene Ther.* 25, 506–516. doi: 10.1089/hum.2013.238

Tuszynski, M. H., Thal, L., Pay, M., Salmon, D. P., U, H. S., Bakay, R., et al. (2005). A phase 1 clinical trial of nerve growth factor gene therapy for Alzheimer disease. *Nat. Med.* 11, 551–555. doi: 10.1038/nm1239

Verge, V. M., Andreassen, C. S., Arnason, T. G., and Andersen, H. (2014). Mechanisms of disease: role of neurotrophins in diabetes and diabetic neuropathy. *Handb. Clin. Neurol.* 126, 443–460. doi: 10.1016/B978-0-444-53480-4.00032-1

Wong, J. N., Olson, J. L., Morhart, M. J., and Chan, K. M. (2015). Electrical stimulation enhances sensory recovery: a randomized control trial. *Ann. Neurol.* 77, 996–1006. doi: 10.1002/ana.24397

Wright, M. C., Mi, R., Connor, E., Reed, N., Vyas, A., Alspalter, M., et al. (2014). Novel roles for osteopontin and clusterin in peripheral motor and sensory axon regeneration. *J. Neurosci.* 34, 1689–1700. doi: 10.1523/jneurosci.3822-13.2014

Yáñez-Muñoz, R. J., Balaggan, K. S., Macneil, A., Howe, S. J., Schmidt, M., Smith, A. J., et al. (2006). Effective gene therapy with nonintegrating lentiviral vectors. *Nat. Med.* 12, 348–353. doi: 10.3410/f.1007629.373945

Yin, Y., Manoury, B., and Fåhraeus, R. (2003). Self-inhibition of synthesis and antigen presentation by Epstein-Barr virus-encoded EBNA1. *Science* 301, 1371–1374. doi: 10.1126/science.1088902

Zaldumbide, A., and Hoeben, R. C. (2008). How not to be seen: immune-evasion strategies in gene therapy. *Gene Ther.* 15, 239–246. doi: 10.1038/sj.gt.3303082

Conflict of Interest Statement: The authors declare that the research was conducted in the absence of any commercial or financial relationships that could be construed as a potential conflict of interest.

Advantages of publishing in Frontiers

OPEN ACCESS
Articles are free to read, for greatest visibility

COLLABORATIVE PEER-REVIEW
Designed to be rigorous – yet also collaborative, fair and constructive

FAST PUBLICATION
Average 85 days from submission to publication (across all journals)

COPYRIGHT TO AUTHORS
No limit to article distribution and re-use

TRANSPARENT
Editors and reviewers acknowledged by name on published articles

SUPPORT
By our Swiss-based editorial team

IMPACT METRICS
Advanced metrics track your article's impact

GLOBAL SPREAD
5'100'000+ monthly article views and downloads

LOOP RESEARCH NETWORK
Our network increases readership for your article

Frontiers
EPFL Innovation Park, Building I • 1015 Lausanne • Switzerland
Tel +41 21 510 17 00 • Fax +41 21 510 17 01 • info@frontiersin.org
www.frontiersin.org

Find us on